

**LATERAL-TORSIONAL BUCKLING OF HAUNCHED MEMBERS IN PORTAL
FRAMES: AN ASSESSMENT OF BS 5950: PART 1.**

**A thesis submitted for
the degree of
DOCTOR OF PHILOSOPHY
by**

SYED MANSUR BIN SYED JUNID

**Department of Civil Engineering
University of Salford**

April 1992

**LATERAL-TORSIONAL BUCKLING OF HAUNCHED MEMBERS IN PORTAL
FRAMES: AN ASSESSMENT OF BS 5950: PART 1.**

TABLE OF CONTENTS

Declaration	i
Abstract	ii
The Author	iv
Acknowledgements	v
List of Figures	vi
List of Tables	xiii
List of Symbols	xvi
List of Photographs	xvii
	Page
CHAPTER 1	
1.0 Introduction	
1.1 General	1
1.2 Review of Some Research Work and Tests on Portal Frames	6
1.3 Research on Portal Frames at University of Salford	14
1.4 Contribution of the Author in the Project	16
1.5 The Scope of the Thesis	18
CHAPTER 2	
2.0 Full Scale Test on a 24m Portal Frame	
2.1 Introduction	24
2.2 Description of Portal Frame 3	25
2.3 Design of Frame 3	27
2.4 The Test Assembly	33
2.5 Test and Behaviour of Frame 3	39
2.6 The Bending Tests	46
2.7 Summary and Conclusion	50

CHAPTER 3

3.0 Literature Review of the Lateral-Torsional Buckling of Tapered Members

3.1 Introduction	74
3.2 Historical Background to the Study of Tapered Member	75
3.3 Review of Available Methods to Analyse the Lateral Buckling of Tapered I-Beams	99
3.4 Summary and Conclusions	110

CHAPTER 4

4.0 The Finite Element Formulation and the SPACE Computer Programme

4.1 General	113
4.2 The Finite Element Formulation	115
4.3 The Computer Programme	129

CHAPTER 5

5.0 Verification of the "SPACE" Finite Element Computer Programme in the Analysis of Non-Uniform Members

5.1 Introduction	144
5.2 Beam with Rectangular Cross-section	145
5.3 Lateral-Torsional Buckling of Tapered I-Beams and Cantilevers	150
5.4 Lateral Buckling of Tapered I-Section Beam-Columns	162
5.5 Summary and Conclusion	170

CHAPTER 6

6.0 Design for Lateral-Torsional Buckling to BS 5950: Part 1.

6.1 Introduction	189
6.2 Theoretical Basis of Design for Elastic Lateral-Torsional Buckling of Beams	190

6.3 Design Approach for Lateral-Torsional Buckling	198
CHAPTER 7	
7.0 Assessment of the Lateral Stability Clauses in BS 5950	
7.1 Introduction	246
7.2 Assessment 1: General Clause for Lateral Buckling of Prismatic Members	247
7.3 Assessment 2: The General Clauses for Lateral Stability Of Unrestrained Non-Uniform member	253
7.4 Assessment 3: The Assessment of Appendix G	256
7.5 Conclusions	265
CHAPTER 8	
8.0 Amendments to Appendix G and Clause 5.5.3.5. of BS 5950:Part 1	
8.1 Introduction	298
8.2 Elastic and Plastic Stability of Prismatic Members	299
8.3 Elastic and Plastic Stability of Non-Uniform Members	306
8.4 Amendment to Clause 5.5.3.5	318
8.5 Conclusions	322
CHAPTER 9	
9.0 Conclusions	
9.1 Summary of Research	349
9.2 Suggested Further Studies	353
References	355
Appendix 1	367
Appendix 2	373
Appendix 3	
Appendix 3.1	414

Appendix 3.2	417
Appendix 3.3	420
Appendix 3.4	423
Appendix 3.5	426
Appendix 3.6	431
Appendix 3.7	435
Appendix 3.8	445
Appendix 4	452
Appendix 5	457

DECLARATION

None of the material in this Thesis has been submitted in support of an application for any other degree or qualification of this or other University or Institute of Learning.

SYED MANSUR BIN SYED JUNID

APRIL 1992

ABSTRACT

The research described in this thesis, relates mainly to the current method of design of steel portal frame structures. The study is divided into two major parts, first being the full-scale test on a 24 metre span frame and the second deals with the problems of lateral-torsional buckling in the haunch region of the frame.

Detailed accounts of the full-scale testing on the 24 metre span frame and the experimental results are given. Supplementary tests on beams cut out from the tested frame in order to establish the strain-hardening factor are also presented.

A literature survey on the published material pertinent to the lateral torsional-buckling of a tapered member was undertaken. Different methods of treatment for the elastic stability of tapered members and any evidence from previous research in this area were reviewed.

Details of an appropriate finite element and the corresponding computer programme are given. This section describes the assumptions and the Finite Element formulations adopted in the computer programme. The earlier work on this analysis dealt only with prismatic members and this was extended to solve tapered sections. Therefore, a full calibration of the finite element formulation for a tapered member was carried out.

The stability clauses in BS 5950 are introduced systematically. Theoretical work which leads to the formulation of the clauses in Appendix G is also described. These stability clauses were assessed by the analysis of selected prismatic and tapered members using the finite element formulation. From this assessment some modifications to the clauses are proposed. The results of the modified clauses are compared with those given by the finite element analysis and the original clauses. Lastly, the modified clauses are checked with the results of the portal frame tested, to confirm its validity.

This study leads to the proposal for some amendments in the clauses in Appendix G and Clause 5.5.3.5. of BS 5950.

The Author

After graduating in 1977 from Cranfield Institute of Technology, Bedford, England, with an Engineering Degree, the author returned to Malaysia and joined the Universiti Pertanian Malaysia, as a Tutor. A year later he continued his studies at the University of Salford and undertook research on Stressed Skin Design under the supervision of Professor J.M Davies. He received a degree of Master of Science, from Salford University in 1980 and was later appointed a Lecturer at the Faculty of Engineering in Universiti Pertanian Malaysia. While serving the University, he was also attached with the Malaysia International Consultants for two and a half years as a Structural Engineer. This attachment gave him the opportunity to be involved in the design work undertaken by the Firm. Since October 1988, he has returned to Salford University to pursue the degree of Ph.D under the sponsorship of the Association of Commonwealth Universities.

ACKNOWLEDGEMENTS

I would like to thank Professor J.M. Davies for providing supervision, encouragement and valuable advice throughout the project. I also wish to express my thanks to Dr. Philip Leach, for his help during the initial stage of the computing work. My thanks are also due to the staff of the Heavy Structures Laboratory for their invaluable assistance.

I am greatly indebted to The Association of Commonwealth Universities and Universiti Pertanian Malaysia for their sponsorships, and to the British Council who was responsible for the welfare of myself and my family, while in England.

My main thanks, however, are reserved for my wife Latifah, and my children for all their support, patience and understanding, which has made this work possible.

LIST OF FIGURES

Chapter 1

- 1.1 A Typical Modern Portal Frame Construction
- 1.2 The Cambridge Test Frame
- 1.3 The Lehigh Test Frame
- 1.4 The Imperial College Tapered Frame Test
- 1.5 The Bradford Frame Test

Chapter 2

- 2.1 Detail Drawing for the 24 metres Span Frame
- 2.2 Detail of the Standard Bracing Cleat
- 2.3 An Artist's Impression of the Test Rig
- 2.4 Articulated Gable Frame
- 2.5 Column Base Detail
- 2.6 Detail of Loading System
- 2.7 General Layout of the Timber Frames on the Roof
- 2.8 Experimental Results - Frame 3
- 2.9 Member Instability - Frame 3
- 2.10 Experimental and Theoretical Load/Deflection Curve for Frame 3
- 2.11 Experimental Bending Moment Diagram Near Working Load Compared with the Theoretical Solution
- 2.12 Experimental Bending Moment Diagram Near Collapse
- 2.13 Computed Experimental Bending Moment - Column 1 and 2
- 2.14 Load/Stress Curves for the Strain-Gauges at C
- 2.15 Load/Stress Curves for the Strain-Gauges at R
- 2.16 Collapse Mechanisms for Frame 3
- 2.17 Different Material Stress/Strain Curve
- 2.18 Plastic Hinge and Plastic Zone Concept
- 2.19 Arrangement of Bending Tests

- 2.20 Load/Deflection Curve for Beam Specimen Cut from Rafter of Frame 3
- 2.21 Load/Deflection Curve of Beam Specimen Cut from Column of Frame 3

Chapter 3

- 3.1 Simply Supported Tapered I-Beam Analysed by Kittipornchai (3.19)
- 3.2 Shape of the Buckled Beam
- 3.3 The Seven Degree-of-Freedom 2-Noded Beam Element
- 3.4 Loading Presumed by Lee, Morrell and Ketter (3.20)

Chapter 4

- 4.1 Warping of Doubly Symmetry I-Beam
- 4.2 Torsion with Restrained Warping
- 4.3 The Prismatic Member
- 4.4 Torsional Flexural Displacement of Point m
- 4.5 Normal and Tangential Displacements
- 4.6 Element End Forces
- 4.7 Bending M_y
- 4.8 Bending M_z
- 4.9 Standard Southwell Plot
- 4.10 Modified Southwell Plot
- 4.11 The Inner Iteration Procedure
- 4.12 Flow Diagram of the Computer Program
- 4.13 The Flow Chart of the Computer Operations to Find the Value of Δ_{cr} at a Given Load Factor
- 4.14 The Flow Chart of the Prediction of λ_{cr} from the Modified Southwell Plot
- 4.15 Joint Connecting Part of Structure
- 4.16 Imaginary Connections after Eliminating Joint t

Chapter 5

- 5.1 Stepped Representation of a Tapered Beam
- 5.2 Lateral Buckling of Narrow Rectangular Tapered Beam
- 5.3 Comparison Between Lee (5.1) and Finite Element Method
- 5.4 Beam and Loading Considered by Massey (5.2)
- 5.5 Comparison Between Massey (5.2) and Finite Element Method
- 5.6 Simply Supported Beam with Double Taper
- 5.7 Comparison of Brown (5.3) and Finite Element Method
- 5.8 Taper Beam with Flange Breadth Curtailed
- 5.9 Deflected Shape of Buckled Beam Considered by Kittipornchai and Trahir (5.5)
- 5.10 Properties of Beam used in Analysis for P_{cr}
- 5.11 Comparison of Results of Analysis Between Kittipornchai (5.5), Kerensky (5.4) and the Finite Element Method
- 5.12 Tapered I-Cantilever
- 5.13 Section Properties of Tapered I-Cantilever
- 5.14 Comparison of Results of Analysis of Brown (5.3), Nethercot (5.6) and the Finite Element Method
- 5.15 I-Cantilever with Flange Breadth Taper
- 5.16 Comparison of Results of Analysis by Nethercot and the Finite Element Method
- 5.17 Section Properties of Tapered I-Cantilever
- 5.18 Comparison of Results of Analysis by Karabalis and the Finite Element Method
- 5.19 Tapered I-Section Beam-Column
- 5.20 Fixed-Pinned Tapered Beam-Column
- 5.21 Comparison of Results of Culver's Finite Difference (5.8) with Finite Element Method ; $d_2/d_1=2$
- 5.22 Comparison of Results of Culver's Finite Difference (5.8) with Finite Element Method ; $d_2/d_1=1.8$
- 5.23 Comparison of Results of Culver's Finite Difference (5.8) with Finite Element Method ; $d_2/d_1=1.5$

- 5.24 Comparison of Results of Culver's Finite Difference (5.8) with Finite Element Method ; $d_2/d_1=1.3$
- 5.25 Pinned-Pinned Tapered Beam-Column
- 5.26 Comparison of Results of Culver's Finite Difference (5.8) with Finite Element Method ; $d_2/d_1=2$
- 5.27 Comparison of Results of Culver's Finite Difference (5.8) with Finite Element Method ; $d_2/d_1=1.8$
- 5.28 Comparison of Results of Culver's Finite Difference (5.8) with Finite Element Method ; $d_2/d_1=1.5$
- 5.29 Comparison of Results of Culver's Finite Difference (5.8) with Finite Element Method ; $d_2/d_1=1.3$

Chapter 6

- 6.1 Buckling of a Simply Supported I-Beam
- 6.2 Buckling of a Beam with a Central Concentrated Load
- 6.3 I-Beam with Central Transverse Load
- 6.4 Effect of Level of Loading on Beam Stability
- 6.5 Buckling of Cantilever and Simply Supported Beams Under Uniform Moment
- 6.6 Lateral Deflection and Twist of a Beam with Equal End Moments
- 6.7 Behaviour of Real Beams
- 6.8 Lateral-Torsional Buckling Strength of Grade 55 Steel
- 6.9 Test Results for Hot Rolled Beams
- 6.10 Comparison of lower Bound Strength Approximations for Uniform Bending
- 6.11 Typical stability Curve - Unrestrained Member
- 6.12 Bending Moment Distribution in A Portal Frame (A Typical Example with Haunch)
- 6.13 Restrained Member Subject to Linear Moment Gradient
- 6.14 Critical Slenderness Ratio of Restrained Universal Beam Sections

- 6.15 Lateral Buckling of Tapered and Haunch Beam
- 6.16 Out of Plane Behaviour of Restrained I-Beam Under Uniform Moment
- 6.17 Typical stability Curve - Restrained Member
- 6.18 Two-Flanged Haunched Rafter
- 6.19 Limiting Length L_t

Chapter 7

- 7.1 Graph for Universal Beam Size 203x133xUB30 (D/T=21)
- 7.2 Graph for Universal Beam Size 254x102xUB28 (D/T=26)
- 7.3 Graph for Universal Beam Size 305x102xUB25 (D/T=45)
- 7.4 Graph for Universal Beam Size 406x140xUB46 (D/T=36)
- 7.5 Graph for Universal Beam Size 457x191xUB98 (D/T=24)
- 7.6 Graph for Universal Beam Size 203x133xUB30 (D/T=21)
Results of Analysis, Moment Ratio $\beta=0.5$ and $\beta=-0.5$
- 7.7 Graph for Universal Beam Size 254x102xUB28 (D/T=26)
Results of Analysis, Moment Ratio $\beta=0.5$ and $\beta=-0.5$
- 7.8 Graph for Universal Beam Size 305x102xUB25 (D/T=45)
Results of Analysis, Moment Ratio $\beta=0.5$ and $\beta=-0.5$
- 7.9 Graph for Universal Beam Size 406x140xUB46 (D/T=36)
Results of Analysis, Moment Ratio $\beta=0.5$ and $\beta=-0.5$
- 7.10 Graph for Universal Beam Size 457x191xUB98 (D/T=24)
Results of Analysis, Moment Ratio $\beta=0.5$ and $\beta=-0.5$
- 7.11 Graph for Universal Beam Size 203x133xUB30 (D/T=21)
Results of Analysis, Destabilising Transverse Load
- 7.12 Graph for Universal Beam Size 254x102xUB28 (D/T=26)
Results of Analysis, Destabilising Transverse Load
- 7.13 Graph for Universal Beam Size 305x102xUB25 (D/T=45)
Results of Analysis, Destabilising Transverse Load
- 7.14 Graph for Universal Beam Size 406x140xUB46 (D/T=36)
Results of Analysis, Destabilising Transverse Load
- 7.15 Graph for Universal Beam Size 457x191xUB98 (D/T=24)
Results of Analysis, Destabilising Transverse Load
- 7.16 Graph for Universal Beam Size 203x133xUB30 (D/T=21)
Cantilever with Destabilising Transverse Load

- 7.17 Graph for Universal Beam Size 254x102xUB28 ($D/T=26$) Cantilever with Destabilising Transverse Load
- 7.18 Graph for Universal Beam Size 305x102xUB25 ($D/T=45$) Cantilever with Destabilising Transverse Load
- 7.19 Graph for Universal Beam Size 406x140xUB46 ($D/T=36$) Cantilever with Destabilising Transverse Load
- 7.20 Graph for Universal Beam Size 457x191xUB98 ($D/T=24$) Cantilever with Destabilising Transverse Load
- 7.21A Results of Analysis of Tapered Beam, Base section 203x133xUB30 $r=(D_2/D_1)=3$
- 7.21B Results of Analysis of Tapered Beam, Base section 203x133xUB30 $r=(D_2/D_1)=2$
- 7.22A Results of Analysis of Tapered Beam, Base section 254x102xUB28 $r=(D_2/D_1)=3$
- 7.22B Results of Analysis of Tapered Beam, Base section 254x102xUB28 $r=(D_2/D_1)=2$
- 7.23A Results of Analysis of Tapered Beam, Base section 254x146xUB43 $r=(D_2/D_1)=3$
- 7.23B Results of Analysis of Tapered Beam, Base section 254x146xUB43 $r=(D_2/D_1)=2$
- 7.24A Results of Analysis of Tapered Beam, Base section 457x152xUB82 $r=(D_2/D_1)=3$
- 7.24B Results of Analysis of Tapered Beam, Base section 457x152xUB82 $r=(D_2/D_1)=2$
- 7.25A Results of Analysis of Tapered Beam, Base section 457x191xUB98 $r=(D_2/D_1)=3$
- 7.25B Results of Analysis of Tapered Beam, Base section 457x191xUB98 $r=(D_2/D_1)=2$
- 7.26 Beam with Tension Flange Restrained
- 7.27 Results of Prismatic Member with Moment Gradient ($\beta=0.5$)
- 7.28 A Model of Haunched Beam and the Bending Moment Diagram
- 7.29A Results of Analysis of Tapered Beam, Top Flange Restrained, Base Section 203x133xUB30, $r=(D_2/D_1)=3$
- 7.29B Results of Analysis of Tapered Beam, Top Flange Restrained, Base Section 203x133xUB30, $r=(D_2/D_1)=2$
- 7.30A Results of Analysis of Tapered Beam, Top Flange Restrained, Base Section 254x102xUB28, $r=(D_2/D_1)=3$

- 7.30B Results of Analysis of Tapered Beam, Top Flange
Restrained, Base Section 254x102xUB28, $r=(D2/D1)=2$
- 7.31A Results of Analysis of Tapered Beam, Top Flange
Restrained, Base Section 254x146xUB43, $r=(D2/D1)=3$
- 7.31B Results of Analysis of Tapered Beam, Top Flange
Restrained, Base Section 254x146xUB43, $r=(D2/D1)=2$
- 7.32A Results of Analysis of Tapered Beam, Top Flange
Restrained, Base Section 457x152xUB82, $r=(D2/D1)=3$
- 7.32B Results of Analysis of Tapered Beam, Top Flange
Restrained, Base Section 457x152xUB82, $r=(D2/D1)=2$
- 7.33A Results of Analysis of Tapered Beam, Top Flange
Restrained, Base Section 457x191xUB98, $r=(D2/D1)=3$
- 7.33B Results of Analysis of Tapered Beam, Top Flange
Restrained, Base Section 457x191xUB98, $r=(D2/D1)=2$

LIST OF TABLES

Chapter 2

- 2.1 Main Parameter of Frame 3
- 2.2 (A) Member and Material Properties of Frame 3
(Properties of Columns)
- 2.2 (B) Member and Material Properties of Frame 3
(Properties of Rafters)
- 2.3 Bending Tests Results

Chapter 5

- 5.1 Results of Analysis by Lee and F.E.M.
- 5.2 Properties of Beam and Results of Analysis
- 5.3 Results of Analysis of Simply Supported Double
Taper I-Beam
- 5.4 Results of Analysis of Flange Breadth Taper I-Beam
- 5.5 Results of Analysis of Tapered I-Cantilever
- 5.6 Results of Analysis of Flange Breadth Taper I-
Cantilever
- 5.7 Comparison of Results of Various Finite Element
Formulations

Chapter 6

- 6.1 Various Cases for Member Between Restraints in BS
5950: Part 1
- 6.2 Equivalent Uniform Moment Factors, m , for Simply
Supported Beams

Chapter 7

- 7.1 Properties of Universal Beams Used in the
Assessment for the General Clause in the Design for
Elastic Stability of Prismatic Member
- 7.2 Geometry of Haunched Members
- 7.3 Results of Analysis for Lateral Stability of
Haunched Members
- 7.4 Data for Prismatic Members used in the Calculation
for Appendix G

- 7.5 Results of Analysis of Prismatic Member by Appendix G and Finite Element Method
- 7.6 Results of Analysis of Haunched Member by the Method of Appendix G
- 7.7 Results of Analysis of Haunched Member by the Method of Clause 5.5.3.5 of BS 5950
- 7.8 Results of Analysis for Plastic Stability for Haunched Members to Appendix G: BS 5950

Chapter 8

- 8.1 Results of Numerical Analysis for Elastic Stability of Prismatic Members by Ammendment to Appendix G (By Introducing ELR Factor)
- 8.2 Results of Numerical Analysis of Prismatic Beam for Plastic Stability by Ammendment to Appendix G (By Introducing the ELR Factor)
- 8.3 Results of Numerical Analysis of Prismatic Beam for Plastic Stability to Appendix G (By Including the ELR Factor)
- 8.4 Results of Analysis by Increasing the Allowable Buckling Stress in Expression G.2.(a).2 of Appendix G
- 8.5 Comparison of Percentage Error/Percentage Safety Reserve for Various Ammendments to Appendix G
- 8.6 Stresses at the Critical Section when Analysed by Increasing the Allowable Buckling Stress in Expression G.2.(a).2 in Appendix G by Expression $F/A + M/S_x < (P_b + P_y)/2$
- 8.7 Stresses at the Critical Section when Analysed by Increasing the Allowable Buckling Stress in Expression G.2.(a).2 in Appendix G by Expression $F/A + M/S_x < 1.11P_b$
- 8.8 Stresses at the Critical Section when Analysed by Increasing the Allowable Buckling Stress in Expression G.2.(a).2 in Appendix G by Expression $F/A + M/S_x < 1.25P_b$
- 8.9 Stresses at the Critical Section when Analysed by Increasing the Allowable Buckling Stress in Expression G.2.(a).2 in Appendix G by Expression $F/A + M/S_x < 1.66P_b$

- 8.10 Results of Analysis of Haunched Member by Modification of the Limiting Length Expression in Clause 5.5.3.5 of BS 5950. The New Expression is;

$$L_t = \{K1 r_y X\} / \sqrt{\{q(72 X^2 - 10^4)\}}$$
- 8.11 Results of Analysis of Haunched Member by Modification of the Limiting Length Expression in Clause 5.5.3.5 of BS 5950. The New Expression is;

$$L_t = f\{K1 r_y X\} / \sqrt{\{q(72 X^2 - 10^4)\}}$$

 Where $f = 1, 1.1, 1.15, 1.2$ and 1.25
- 8.12 Percentage Error/Safety Reserve to the Results of Analysis of Haunched Member by Modification of the Limiting Length Expression in Clause 5.5.3.5 of BS 5950 to Results of Analysis by F.E.M
- 8.13 Results of Analysis for Plastic Stability for Haunched members by Including the ELR factor in Expression for L_k in Appendix G
- 8.14 Percentage Error/Reserve of Safety for Plastic Stability for Haunched Members by Including ELR Factor in Expression for L_k in Appendix G
- 8.15 Results of Analysis for Elastic Stability for Haunched Members by L_k Values from Horne, Shakir-Khalil and Akhtar (6.29) and Followed Appendix G
- 8.16 Results of Analysis for Elastic Stability for Haunched Members by L_k Values from Horne, Shakir-Khalil and Akhtar (6.29) and Followed Horne's Method
- 8.17 Results of Analysis of Haunch of Frame 3 by the Modified Expressions
- 8.17 Results of Analysis of Haunch of Frame 3 by the Clause 5.5.3.5 and the Expressions 8.11 and 8.12

LIST OF SYMBOLS

Unless otherwise specified within the thesis, the symbols that appear in the text are defined as follows:

A	Cross-sectional Area
a	Distance of centroid of uniform I-beam from axis of restraint
a ₁	Distance of nearer flange of haunched beam from axis of restraint
B	Flexural rigidity about minor axis EI_y
b	Width of flange of I-beam
C	St. Venant torsional rigidity GJ
c	Factor for tapered and haunched beams
D	Overall depth of I-section
d	distance between centroids of flanges of I-section
d ₁ , d ₂	minimum and maximum values of d respectively for tapered and haunched beams
E	Young's Modulus of Elasticity
f ₁	$2a_1 + d_1$
f_y	yield stress
G	Shear Modulus of Elasticity
I_x, I_y	Major and Minor Second Moments of Area respectively
J	St. Venant torsional constant
k ₁	torsional restraint per unit length per unit angle of twist
k	factor for tapered and haunched beam
L	Length of Beam
L_{cr}, L_m	Elastic critical and limiting length for plastic design respectively of a uniform beam under uniform moment
M	bending moment about major axis

M_y	major axis moment at first yield
M_{y1}, M_{y2}	minimum and maximum values of M_y respectively for tapered and haunched beams
M_p	plastic moment of resistance about major axis
q	ratio of tapered to total length of haunched beam
q'	ratio of uniform to total length of haunch beam, (i.e., $1-q$)
r	ratio of end depths d_2/d_1 of tapered and haunch beams
r_y	minor axis radius of gyration
S_x	Plastic section modulus about major axis
t_f, t_w	flange and web thickness respectively of I-beam
u_o, u_c, u_r	lateral displacement of outstand flange, centroid and restrained flange respectively
Z_x, Z_y	plastic section modulus about major and minor axis respectively
z	distance of section from origin
α	angle of taper of beam
β	ratio of greater to smaller end moment for linearly varying bending moment distribution
Γ	warping resistance of beam about axis of restraint
ϕ	angle of twist about axis of restraint
ϕ_o	initial angle of twist about axis of restraint
ϕ_{co}	initial central angle of twist about axis of restraint

LIST OF PHOTOGRAPHS

- Plate 2.1 Assembly of the Test Frame Prior to Sheeting
- Plate 2.2 The General View of the Assembly During the Test
- Plate 2.3 Internal View Showing the Loading Arrangement
- Plate 2.4 Detail of Haunch Failed by Lateral-Torsional
Buckling

CHAPTER 1

1.0 Introduction

1.1. General

1.1.1. The Steel Portal Frame.

The steel portal frame structure is probably the most frequently designed structure in the United Kingdom. It has become the natural choice for most single story factory or warehouse buildings and is also used in other structures ranging from small agricultural buildings to sports halls with spans of 50 metres or more. This is because steel portal frame structures offer a practical and economical solution in providing a large, clear, uninterrupted space under cover and are therefore suitable for multipurpose use.

The modern portal frame construction, as shown in figure 1.1 is made up of universal beams, bolted together to make a frame. It is normal practice to provide haunches at the eaves and apex connections to accommodate the large moments that occur at these locations. Bolted connections are always preferred due to practical considerations especially transportation and ease of erection at the site. There have also been many other developments resulting in the modern portal frame structure being built with different types of structural elements, such as cold formed purlins, roofing

and various types of connections. These together with new materials are being incorporated in the whole structural system and influence the behaviour of the structure. It would be unjustified therefore, to assume that the behaviour of the modern portal frame structure, with its various features, is entirely dependent on its main frame only.

1.1.2. Brief History of Steel Portal Frame Design and Development

1.1.2.1 The Evolution of Steel as Structural Material

The use of metal as structural material began with cast-iron used on a (30m) arch span which was built in England in 1777 - 1779 (1.1). Several cast-iron bridges were built during the period 1780 - 1820, mostly arch-shaped with girders consisting of individual cast-iron pieces forming bars or trusses. Cast-iron was also used for chain links on suspension bridges until about 1840.

Wrought-iron began replacing cast-iron soon after 1840, the earliest important example being the Britannia Bridge over the Menai Straits in Wales which was built in 1846 - 1850. This was a tubular girder bridge having spans of 70 - 140 - 140 - 70 metres, which was made from wrought-iron plates and angles.

The process of rolling various shapes was developing as cast-iron and wrought-iron received wider usage. Bars were rolled on an industrial scale beginning about 1780. The rolling of rails began about 1820 and was extended to I-shapes by the 1870s.

As the production methods and technology improved, in particular with the Bessemer Process (1855), more iron ore products were being used as building materials. Since 1890, steel has replaced wrought-iron as the principal metallic building material. Today, steel having a yield stress ranging from 165 to 690 N/mm² is available in various forms for structural uses.

1.1.2.2. Development of Portal Frame Construction

The development of steel portal frame construction goes hand in hand with the progress and development in the material itself, (i.e, from the cast-iron era to wrought-iron and then to the rolled steel era), and has brought rapid development to the portal frame construction that we know today.

The earliest portal frame built was dated back to approximately 1880. The frame was built with moulded cast-iron and incorporated sculpture in the columns and in the haunches. It had dimensions of 15 feet span, 10 feet

high at eaves and 15 feet high at the ridge. The stability of the structure was achieved by pseudo-rigid joints. However, this type of construction was not adequate for large span buildings, and in those days, larger spans were achieved by incorporating the same type of column with triangulated trusses.

In the early part of the 20th century, the riveted frame became popular especially in the USA where they were used as small railway bridges. In this type of construction, the frames are pieced together from different "panels". Each of the panels is shaped and splices are riveted to them. The panels are joined to the adjacent ones through the splices and connected by rivets to obtain the structural continuity of the frame. Because of this, a massive amount of splices and rivets are required in the construction. Later, with the use of carbon steel as the material of construction, the designers were able to build similar frames with larger spans.

Further development took place in 1930, with the introduction of electric arc welding for connections in the structures. This has led to the downfall of popularity of riveted joints in portal frame construction. The use of electric arc welding has enabled designers to improve the structural continuity and get aesthetic benefits, as well as the ability to build larger span buildings.

None the less, this technique of construction had its disadvantages. Usually, the entire frame was manufactured in the workshop where good quality control of the welded joints could be achieved. However, as the length became larger, the designers had to opt to introduce site welding of joints. Since it was difficult to control the quality and obtain a satisfactory standard of welded joints at site, several solutions were sought in order to establish a compromise. This could well mark the beginning of today's portal frame construction, when features like systems of rivets with splices, and bolts with end plates were introduced into the structures together with the welded connections.

It has to be mentioned that the design philosophy that was adopted by the designers in those days was that of "the working stress design". The main objective was to maintain the working stress within the elastic limit of the material. The 1950s however, marked the introduction of a new design philosophy known as "plastic theory". Since the late 1950s, most steel portal frames have been designed by the plastic design concept. This is because it was evident that the application of plastic design produced lighter and more economical structures than similar rigid frames designed by elastic theory.

In plastic design, it is assumed that the structure is capable of reaching its ultimate strength by the formation of "plastic hinges" without premature failure occurring.

However, as the span of the beams increases and as the structure becomes more slender, the problem of instability may become the main design concern. It is therefore very important for the relevant code of practice to provide proper guidance for preventing premature instability.

1.2. Review of Some Research Work and Tests on Portal Frames

Research in portal frame construction can be traced back more than fifty years. Perhaps the most notable early research on portal frame design was conducted in Bristol by Baker and Roderick (1936) who carried out several tests on small portal frames. These tests, despite their scale and simplicity, helped to confirm the findings of earlier research by Maier-Leibnitz (1927) in Germany (1.2). The work by Maier-Leibnitz stipulated that the collapse load of a simple beam structure depends on its full plastic moment, however Baker and Roderick extended the work to cover the collapse of rigid frames.

Their report published in 1938 (1.3) described in detail their investigations on portal frame stability and the tests confirmed their finding that the strength of a rigid frame depends on the plastic moment capacity of its members provided that premature failure was prevented. This report became the first document describing an experimental investigation into the plastic collapse of rigid frames.

The work at Bristol led Baker to realise the potential of what came to be known as the limit state design philosophy. One aspect of this method is commonly known as "plastic design". In 1943, Baker and Roderick embarked on a very important research programme, involving both experimental and theoretical work, which lasted for more than ten years. Further tests on pitched roof portal frames were carried out but this time at Cambridge and with larger frames. The tests at Cambridge (1.4) conducted in the early 1950s can be considered as the first full scale tests on portal frames. These tests investigated the development of plastic hinges in a real frame and the eventual failure of the frame as a collapse "mechanism". The frame, as shown in figure 1.2, was loaded with a vertical point load at the apex and a horizontal side load at one eaves' point. Results of the tests conducted show good correlation with the theoretical predictions that were based on manual calculations, thus confirming the validity of the plastic theory.

In these investigations however, the frames were stiffer and there was less risk of member instability than there is in current construction. This was because, in those days, the purlins were made of hot rolled sections, and the member sections were the same size throughout. The members were also relatively compact and fully welded. Furthermore, the column bases were idealised as fixed bases or connected to piled foundations. Nevertheless, they observed signs of member instability towards the end of each test after the

formation of a collapse mechanism.

Around the same period, similar work was carried out in the USA, notably by Beedle (1.5) at Lehigh University and Greenberg & Prager (1.7) at Brown University, Providence. A series of full scale tests to failure was conducted at Lehigh using larger scale frames compared to the Cambridge tests. An example of the test arrangement for a rectangular frame is shown in figure 1.3. However, the tests were set up so that in-plane load was applied to the frame and, with the prevention of out-of-plane movement, the complete collapse mechanism was achieved before ultimate failure. These tests therefore, in view of current portal frame construction, do not simulate the real behaviour of portal frames in modern buildings.

The effort required to simulate the actual loading conditions on portal frames showed clearly in 1953 and 1954. This was when Baker, Eickhoff and Roscoe carried out full scale tests (1.8, 1.9) on three pairs of north light type portal frames. In these tests the loading patterns were more in accordance with the actual practice and four point loads were used to simulate the vertically distributed load. The frames were built up on piled foundations in order to introduce more realistic base conditions.

The effect of strain-hardening on the collapse load of a rigid frame was investigated by Vickery (1.10) in Sydney,

Australia in 1960. Tests on both miniature and full scale pitched roof portal frames were conducted. Satisfactory agreement between observed and theoretical results were obtained for the two full-scale tests. This shows that the approximate analysis proposed by Vickery could allow a rapid and reasonably accurate estimate of the influence of deformation and strain-hardening on the collapse behaviour of rigid frames.

An investigation to study the effect of gross distortion on portal frame behaviour was conducted by Charlton (1.11) in 1960. He conducted a full scale test on a pair of pitched roof portal frames with short stanchions. He used four point loading and predicted the collapse mechanism by simple plastic theory. He also conducted tests on beam specimens cut from an undeformed portion of the rafter after the test in order to investigate the plastic characteristics of the section. He concluded from the test results that the reason for the increased value of the load at collapse was due to the effect of strain-hardening.

A series of full-scale tests on pitched roof portal frames incorporating tapered members was carried out by Vickery (1.12) in 1962. These tapered members were prepared from standard R.S.Js by cutting diagonally along the web, turning the pieces end for end and rejoining by welding along the cut edge. In this study he investigated the advantages of using tapered members in portal frames and also studied the

behaviour of tapered frames at collapse as compared with rectangular frames. He concluded that the use of tapered members could result in considerable economy in material. However, many problems with regard to instability had to be solved.

Bates, Bryan and El-Dakhakhni (1965) reported their full scale tests (1.13) on a pitched roof portal frame shed. The shed, had a 46 m span and was about 100 m long. Directed by Bryan, they studied the stiffening effect of cladding and roof sheeting on the frame. Tests were conducted during various stages of construction of the shed and the results show the remarkable influence of the sheeting on the deflections and on the bending moments.

Horne and Chin (1966), (1.14) investigated the use of high tensile steel (to BS 968) in the plastic design of portal frames. In this investigation, they carried out tests on four pitched roof portal frames. The results of the tests were compared with two theoretical models that were developed by Davies (1.15) and Chin (1.16) and also with some design charts they themselves produced in B.C.S.A. publication no: 29 (1.17). Since the digital computer was already available then, the two theoretical models that consider second order deformation and strain-hardening required calculation using computers. The conclusion derived in their investigation was that the use of high strength steel helped to increase the strength. However, the

deflections were also increased due to the reduced stiffness of the members.

The effect of secondary structural elements on the overall stability of portal frames was also investigated at the University of Canterbury in New Zealand (1.18). This took place when a new welded-steel portal frame laboratory wing at the University was under construction. Measurements of the stresses induced in the main structural members were made during different stages of construction and after the completion of the building. The investigation also compared the experimental stress distribution with the theoretical stress distribution obtained by elastic computer analysis. Good correlation was obtained between the measured and theoretical stress distributions for the bare frame. However, at the stage of construction when the roof was put in place, considerable interaction between the portal frames and other elements of the building was evident.

Four full-scale tests on 12 metre span portal frames made of built-up sections were reported by Halasz and Ivanyi (1978) (1.19). These tests were conducted as part of the general investigation undertaken for the preparation of a new version of the Hungarian steel specification for plastic design. As one purpose of these tests was to find appropriate measures to exclude premature lateral torsional buckling, various types of restraints were used on the frames at various stages of loading. Tests were conducted by

loading the frames using a spreader beam technique that allowed the jacks to follow the frame in sway, and side loading was applied using a tension rod connected to the strong floor. These tests are interesting in the sense that they constituted the first attempt to test non-tapered, up to date portal frames. These tests confirmed the importance of the positional restraints since they do have influence on the failure load of the frame.

A massive testing programme involving the testing of 30 frames between 21m and 30m span was initiated in 1980 under the direction of Dowling (1.20, 1.21 and 1.22) at Imperial College, London. The portal frames were made of tapered members fabricated from welded steel plates as shown in figure 1.4. The design philosophy of this form of construction is radically different from that of the hot-rolled I-section portal frame. The test programme was sponsored by Ward Bros (Sherburn) Ltd. and was devoted to the development of their "ATLAS SYSTEM". Since economical aspects were one of the priorities of the project, much of the research was directed in this perspective. Information about the details of the tests are inadequate, probably due to commercial interests. However, it seems that, provided adequate bracing was incorporated in the design, the overall response of the frames was good. The economy achieved is also impressive, with the claim that this method of fabrication can save up to 30% of weight compared with conventional hot-rolled construction.

The most recent test on a full scale portal frame was reported in 1986 when Elvidge (1.23) tested a pitched roof portal frame with haunches at Bradford University. The frame tested was 14m span, 3 metres high at the eaves and had a 10° roof slope. It was fabricated from Universal Beam sections and constructed with bolted end plate connections and pinned bases. The set up of the test is shown in figure 1.5, where it is shown how another identical frame was constructed and placed next to the test frame. Purlins and cross-bracing members made up of light gauge steel sections were connected to both of the frames in order to restrain the test frame. Prior to the final test to destruction, physical tests were performed in the elastic range to obtain load-deflection curves under different loading regimes. In the final test it was observed that the frame collapsed after several plastic hinges had formed. It was found that the collapse load of the frame was 20% greater than that predicted by rigid plastic analysis. This according to the author was due to the omission of several factors from the analysis including the actual value of yield stress and the strain hardening parameter. This test appears to be the only test that is in line with current industrial practice.

From this brief review of previous work on portal frames, it becomes evident that there is little experimental data available on the performance of the modern portal frame. Consequently, there is an urgent need for new experimental data to be collected using realistic structures.

1.3. Research on Portal Frames at University of Salford

A major research project was carried out by The Universities of Salford and Manchester in which the behaviour of steel portal frames up to failure was investigated. In this project, three full scale portal frame tests were conducted at Salford University under the direction of Professor J.M. Davies while a finite element analysis programme was developed at Manchester University led by Dr. L.J. Morris. Supplementary studies were also conducted and they include second-order elastic-plastic frame analysis, the effect of connection flexibility and a detailed study of the elastic-stability clauses of the current British Code, BS 5950. Part 1.

The main aim of this research project is to provide valuable information on the true behaviour of the modern portal frame. Earlier, full scale tests conducted by Professor J.F. Baker at Cambridge decades ago led to the inclusion of plastic design in the British Standard. Since then, there have been many developments in the design and construction of steel structures. Many of these developments directly affect portal frame construction, whose apparent simplicity conceals some practical design problems that were not covered by the earlier tests. This project is aimed at fulfilling the urgent requirement for tests on full-scale portal frames of modern construction in order to investigate the real behaviour of these structures.

It is only very recently that the necessary computer power and numerical methods of analysis have become available so that the full non-linear, three dimensional analytical problem can be attempted. Previous research work on portal frames had indicated that the finite element method was able to simulate the behaviour of parts of a frame with reasonable success. The mathematical model, however reliable and proven, cannot be developed without the aid of comparable test results, and these were not available at the commencement of the project. Therefore, the joint research project is approaching the problem experimentally and also analytically. In broad terms, that is to say that the results of the tests at Salford are being used to calibrate the finite element programme at Manchester.

The work at Salford involved the testing of two structures of 12 metres span and a third of 24 metres span. The frames were heavily instrumented in order to collect as much data as possible and, because of that, they had to be carried out indoors. The structural laboratory at Salford offers excellent facilities for testing such a large assembly and very few other laboratories in the U.K. are capable of work on this scale.

This project was initiated in late 1985 and is jointly funded by the Science and Engineering Research Council (SERC) and several commercial sponsors amounting to over £100,000 in total.

1.4. Contribution of the Author in the Project

The author joined the research team in Salford in 1988 when the full-scale test on the 24 metre span frame was just starting. He spent the first few months working with the rest of the team to carry out the full-scale test on the frame. After the completion of the test, the author conducted a series of bending tests on beam specimens cut from the unyielded part of the rafter and column members of the 24 metre frame. The objective of these bending tests was to obtain the strain-hardening characteristics of each of the frame elements so that this information could be considered in the elastic-plastic analysis.

During the full-scale frame test it was found that the problem of lateral torsional buckling especially at the haunch region was indeed very serious. The frame that was designed according to the code BS 5950: Part 1 (1.24) failed prematurely by lateral-torsional buckling in the haunch region of the rafter. This code provides clauses for the design of tapered steel members including portal frame haunches. At the vicinity of the haunch in modern portal frame constructions are purlins and sheeting that, as a system, can produce a fairly complete positional restraint at those points. The code BS 5950 provides a method of design for this situation notably in clauses in Appendix G of the code. However, this provision has proved to be complicated to apply especially with the introduction of

several new parameters. The problem is augmented by the many checks to be performed and this has made the use of the computer inevitable. The results of analysis of the actual conditions at collapse showed that Appendix G had predicted the failure by lateral-torsional buckling at a lower load. It was also shown that the actual bending stress at collapse at the most critical point of the haunch was 1.75 times the allowable buckling stress. This led to the conclusion that Appendix G had provided an over-safe design.

A parametric study was therefore undertaken, using the "SPACE" Finite Element computer programme that is described in chapter 4, to investigate the problem of lateral-torsional buckling in tapered members, particularly in the haunched region of a portal frame. This study allows the various design recommendations given in the steel code BS 5950 pertaining to lateral-torsional buckling to be assessed in relation to the overall performance of the portal frame. The clauses in Appendix G of the code and its alternative "Clause 5.5.3.5." were studied in detail. Recommendations for some amendments to the clauses in BS 5950 are suggested.

The "SPACE" Finite Element computer programme that was used in the analysis of the tapered member was developed by Nemir (1.25). This is a new finite element formulation that is superior to the one developed by Barsoum and Gallagher (1.24) in the sense that it contains new terms representing the bimoment influence and is valid for any cross-section

shape. However, when the author obtained the computer programme, it was in six different versions that contained many changes from the original described in Nemir's thesis. Since no authentic programme was available, the author had to make corrections to the programme and because of that it was thought that the programme had to be verified again.

In so far as the numerical work is concerned, Nemir had worked on prismatic members only. The author has extended the work to cover tapered members and members with restraint to one flange.

1.5. The Scope of the Thesis

The research described in this thesis is divided into two major parts, the first one being the full-scale test on the 24 span frame. The second part deals with details of the problems of lateral-torsional buckling in the haunch region. In this second part the provision for lateral-torsional buckling in the code of practice is scrutinised.

In chapter two, a detailed account of the full-scale testing of the 24 metre span frame and the experimental results are given. Design calculations of the frame in accordance with BS 5950 for the design of the frame are also given. Supplementary tests on beams cut from the tested frame in order to establish the strain-hardening factor (k) are also presented in this chapter.

In chapter 3, a literature review of the lateral-torsional buckling of tapered members is given. Particular attention to tapered members is given because a proper treatment on this subject is required to verify the (SPACE) Finite Element computer programme. The SPACE Finite Element computer program is then used as a tool for the analysis of the elastic buckling problems in this project. Various alternative methods of treatment for the elastic stability of tapered members are studied in detail.

Chapter 4 of the thesis, presents the details of the SPACE Finite Element programme. It describes the assumptions and the Finite Element formulations adopted by Nemir in the computer programme.

In chapter 5, details of the verification of the SPACE Finite Element program are given. Only verification using tapered members is given in this chapter, whereas verification for prismatic members is given in the Appendix 2.

In chapter 6, the stability clauses in BS 5950: Part 1 are introduced systematically. The stability clauses for prismatic and non-uniform members are described in detail. Theoretical work which leads to the formulation of the clauses in Appendix G is also given. This chapter also describes Clause 5.5.3.5 that is an alternative to Appendix G provided within BS 5950.

Chapter 7 assesses the stability clauses by means of the SPACE Finite Element program. Several prismatic beams and haunched beams fabricated from Universal beam sections are analysed and the results compared with the provisions of the stability clauses.

In chapter 8, the stability clauses in Appendix G and Clause 5.5.3.5 are scrutinised further. Both the cases of Elastic and Plastic Stability are checked and some modifications to these clauses proposed and then analysed. The results of these analyses are compared to the results of analysis by the original clauses and the Finite Element method. This study leads to the proposal for some amendments to be made in the clauses in Appendix G and Clause 5.5.3.5.

Finally, conclusions are drawn with suggestions for further research work in chapter 9.

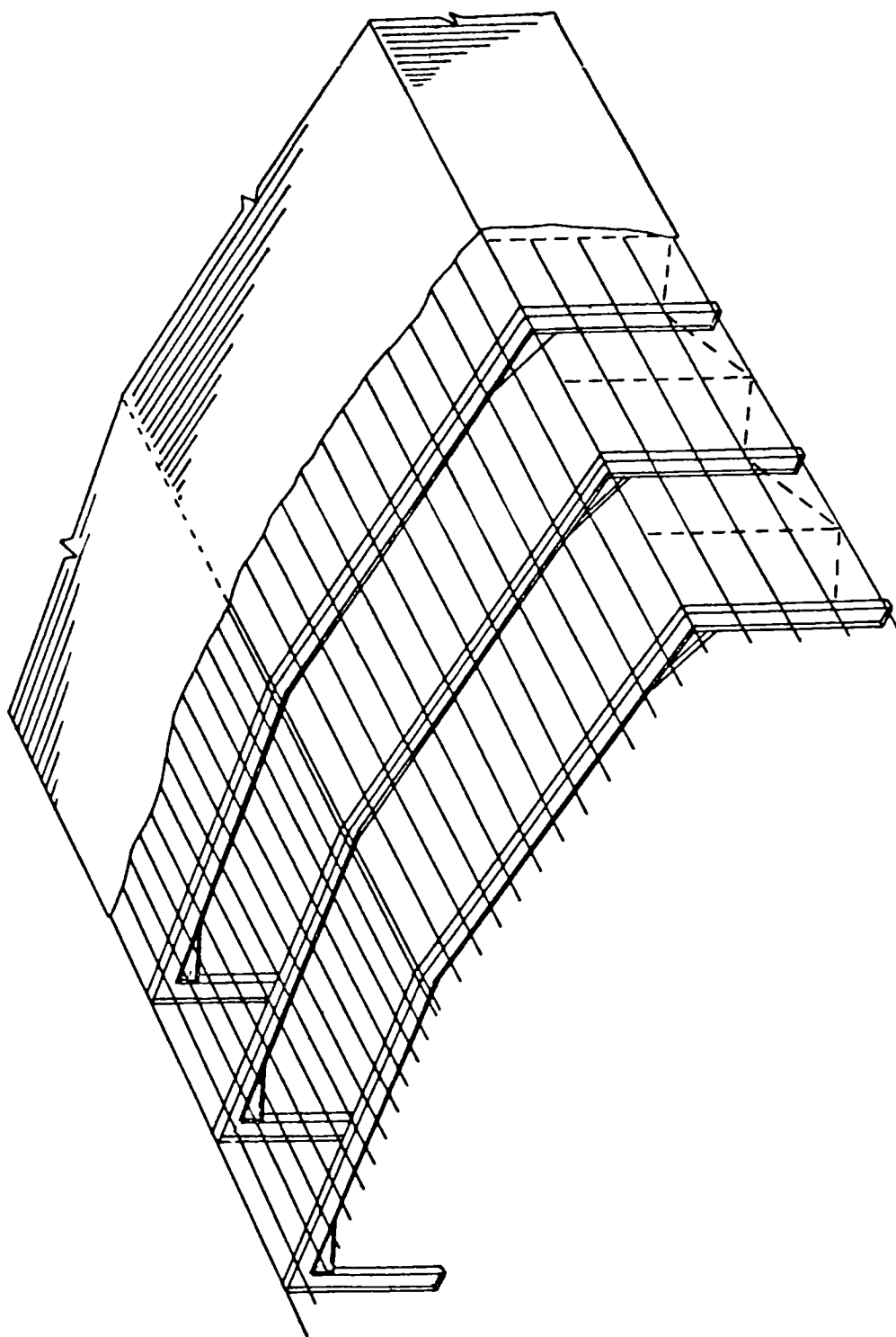


Figure 1.1 A Typical Modern Portal Frame Construction

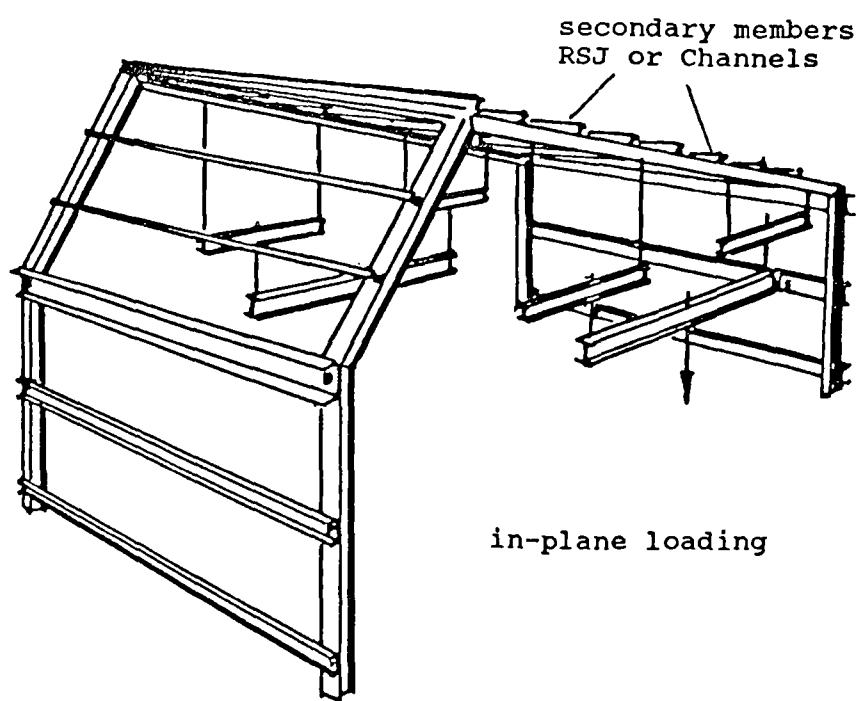


Figure 1.2 The Cambridge Test Frame

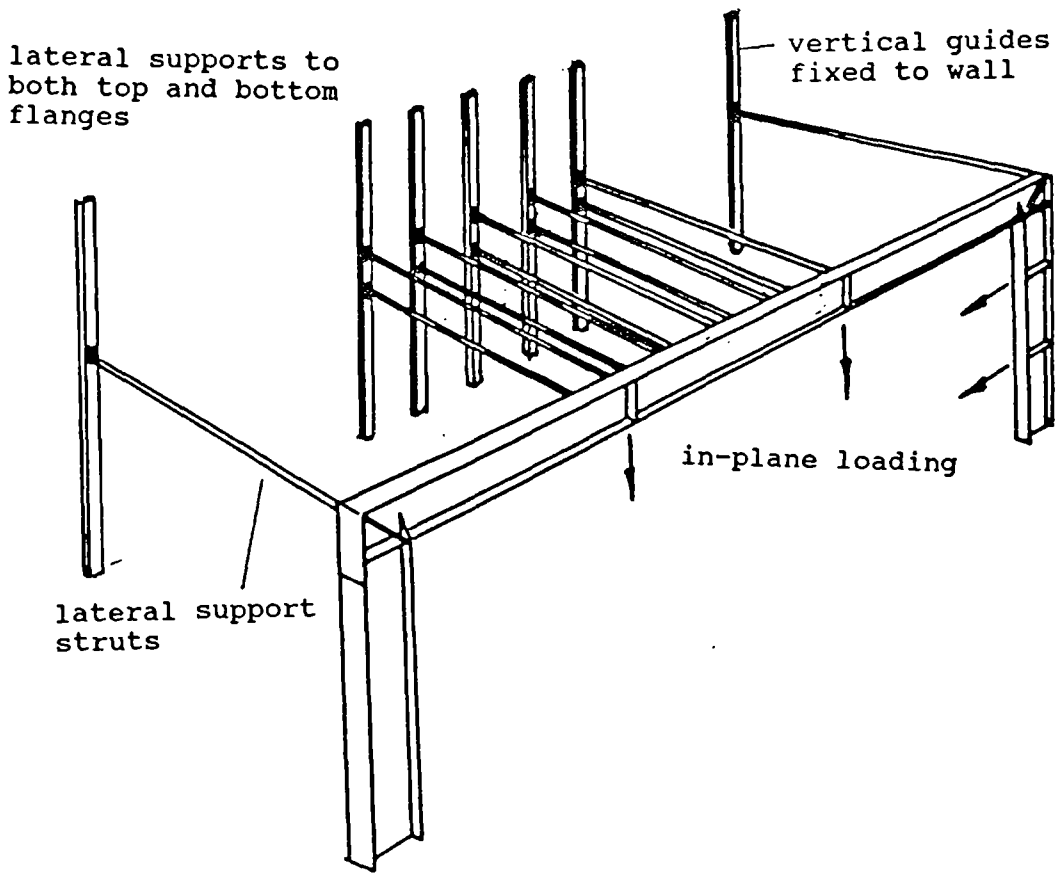


Figure 1.3 The Lehigh Test Frame

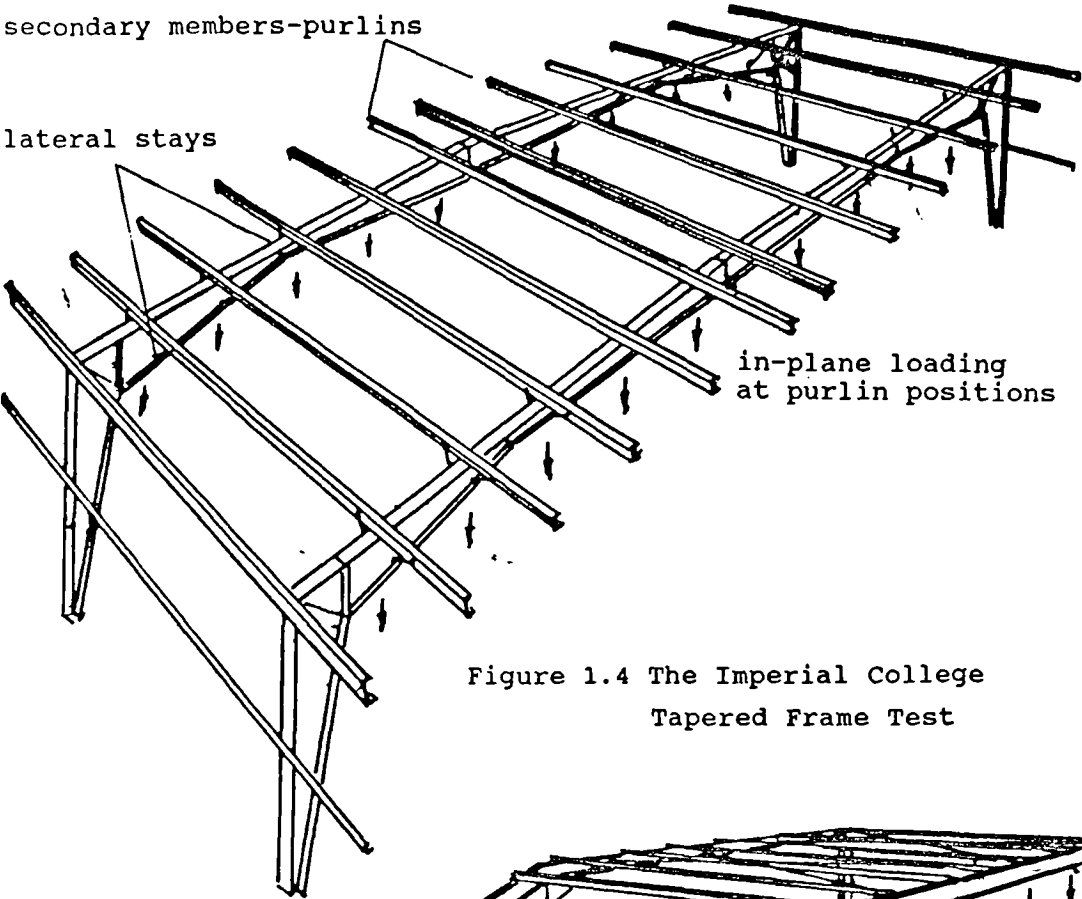


Figure 1.4 The Imperial College
Tapered Frame Test

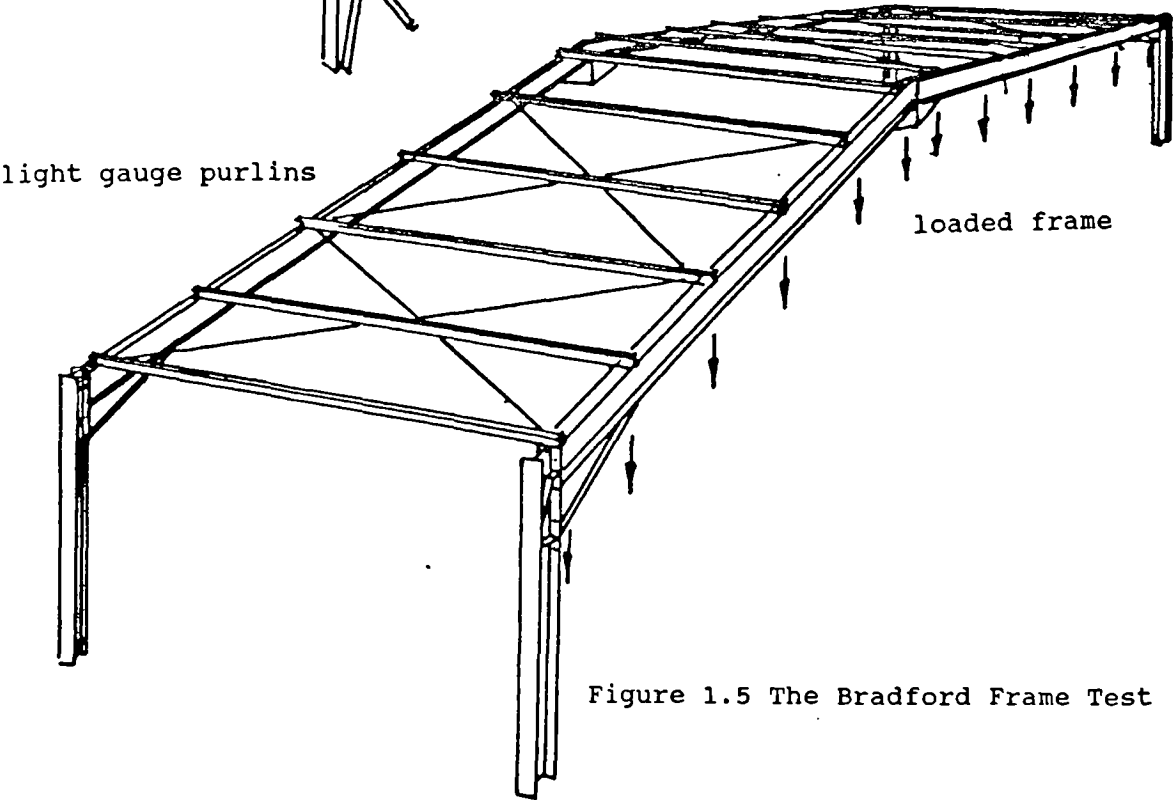


Figure 1.5 The Bradford Frame Test

CHAPTER 2

2.0. Full Scale Test on a 24m Portal Frame

2.1. Introduction

The behaviour of a portal frame in a building can only be studied in detail if tests on complete structures, including secondary members, purlins, bracing, lateral restraints and cladding are conducted. The technique used to apply the loading is also very important and must simulate the real conditions.

The work described in this chapter forms part of a research programme in which the behaviour of steel portal frames up to failure was investigated in considerable detail. In the experimental part of the project, 3 full-scale portal frame structures in a three-dimensional test assembly were tested in the structures laboratory of the University of Salford. The frames tested were;

Frame 1. (span = 12m)

Frame 2. (span = 12m) Agricultural building,

Frame 3. (span = 24m) Industrial building.

Since the author was only involved in the testing of frame 3, this chapter will describe the details of this particular test. The design of the frame, details of the test assembly, test procedures and results of the test are discussed. Descriptions of the tests on all of the frames are also

available in other references (2.1, 2.2, 2.3, and 2.4).

2.2. Description of Portal Frame 3

2.2.1 General Description

The basic arrangement of portal frame 3 is shown in figure 2.1. It has a span of 24 metres and a roof slope of 6.56° . This frame was designed in accordance with BS 5950: Part 1 (2.5) by the fabricator and was fabricated in a standard workshop by a standard contractor. The frame was identical to those fabricated by the manufacturer for normal construction. The frame was designed on the assumption that the bases were pinned and the loading pattern was uniformly distributed vertical load. Table 2.1 gives details of the loading assumptions and the dimensions of the frame.

In figure 2.1, it is shown that the rafter was made up of a Universal Beam UB 356x127x33, incorporating a long shallow haunch. The two haunches were fabricated by cutting a section of the Universal Beam diagonally along the web and welding along the bottom rafter flange. At the larger end, the eaves connection was made by welding the resulting haunch onto an end plate. The column was a Universal Beam type UB 406x178x54 with a base plate of 425x230x15mm. This was in line with the current practice allowing the use of different section sizes for column and rafter members. The roof sheeting consisted of steel sheet type R.M.F. RS 3255.

This sheet profile was chosen in order to avoid sheeting failure during the test. The purlins were cold formed light gauge steel Zed sections of the type METSEC 20218, with sleeves. A similar section of purlin with circular solid cross bracing (16mm diameter) was provided to ensure stability at the eaves. The standard bracing cleats shown in figure 2.2 were used on this frame.

2.2.2 Member and Material Properties of the Frame

The steel used for the fabrication of the frame was an A43 grade to BS 4360 with a nominal yield stress of 275 N/mm^2 . However, in order to investigate the real behaviour of the frame the actual member and material properties of the frame must be known. Previous research into member instability (2.6) had shown the importance of detailed measurement of geometric and material imperfections if accurate theoretical behaviour was to be estimated.

A lot of supplementary experimental work and accurate measurement was therefore necessary in this project. These included the accurate measurement of cross-sections and lack of straightness of individual members and the measurement of stress-strain characteristics from coupon tensile tests obtained from different locations in the cross-section. The measured material and dimensional properties of the test members are tabulated in table 2.2(A) and 2.2(B).

Details of bending tests on lengths of the unyielded material cut from the frame and the results are described in section 2.7.

2.3 Design of Frame 3

2.3.1 Design Procedures in Accordance With BS 5950: Part 1

British Standard BS 5950: Part 1 entitled "The Structural use of Steelwork in Building", deals with the design in simple and continuous construction using hot rolled sections. Portal frame design is specifically covered in section 5.5 of the code. In the code, steel portal frames can be designed using either the elastic and plastic methods of analysis.

The design procedures for portal frames provided by this code are very rigorous and comprehensive. A study of the design procedure shows that the code always refers to general clauses or conditions before the detailed aspects of the design are considered. For instance in the case of plastic design of portal frames (i.e clause 5.5.3.1), reference is made to the clause in section 5.3 that deals with plastic design in general.

Important aspects of the design of portal frames include the stability of the frame and stability of the members. In the

case of the frame stability, treatment of in-plane stability are considered for both cases of sway stability and snap through stability. These are given in clauses 5.5.3.2 and 5.5.3.3 respectively. Two alternative methods of design are given in clause 5.5.3.2 to deal with sway stability.

In the case of member instability, it is important that the general requirements for all members of the frame must first be emphasized. These are;

- (1) The load capacity of any member's cross-section must comply with the conditions given in clauses 4.8.2 and 4.8.3.2(b)
- (2) Plasticity should not occur in the haunch length. It is important that the haunch portion remains completely elastic, otherwise instability becomes a problem.
- (3) The bending moment at the end of the haunch should be less than 0.85 times the full plastic moment of the rafter. The value of 0.85 adopted is the approximate ratio between the elastic modulus Z_e and the plastic modulus Z_p . The moment at the haunch/rafter intersection should be less or equal to $0.85 M_p$, in order to avoid yielding of the extreme fibres of the section.

Reliable stability of members is only possible if a number of practices are adhered to. The code specifies that restraints should be provided where plastic hinges form or not further than $D/2$ from the plastic hinge position (where

D is the depth of the member). In addition, the code also provides the following guidance :

- (1) Purlins provide intermediate lateral restraint to the outer (tension) flange.
- (2) Fly braces provide torsional restraint at specific locations. These members are to be designed to resist a couple derived from the lever arm equal to depth between centroids of flanges and a force equal to not less than 1% of the maximum factored compression flange force of the restrained member.
- (3) When the purlins and their connections are capable of providing torsional restraint to the top flange of the rafter, it can be assumed that a virtual torsional restraint is present at the point of contraflexure.

The code of practice distinguishes two types of length between lateral restraints, namely 'restrained' and the 'unrestrained' lengths. The design checks for lateral stability are carried out in terms of critical lengths of member between restraints. The following critical lengths are used in BS 5950: Part 1;

L_e = Effective length for calculations according to Section four of the code. (This covers the cases of unrestrained length with no plastic hinge formation for both prismatic and tapered members).

L_m = Maximum distance from plastic hinge restraint to adjacent restraint. (This covers the cases of

unrestrained length with plastic hinge formation for both prismatic and tapered members -

Clause 5.3.5)

L_t = Maximum distance between compression flange restraints. (This covers the cases of members with restraints positioned on the tension flange for both prismatic and tapered members with and without plastic hinge formation - Clause 5.5.3.5 or Appendix G).

2.3.2 Detailed Design of the Frame

The details of the frame are as shown in figure 2.1. The design was based on gravity load condition i.e., snow + dead load. Both the geometries of the frame and the applied loading were symmetrical about the apex. The frame had a span of 24 m and the rafter slope was 6.56° . The column height was 4 m from the column base to the intersection of rafter/column. The frame was designed assuming pinned bases.

The haunch length was 2.4 m from the inner column flange to the end of the haunch, i.e., 10% of the span. The haunch region was detailed so that the ends of the inclined haunch flanges at the haunch rafter intersection had not been welded to the rafter. Also the column head panel had a web stiffener of about 80% of the depth of the column web at the compression zone. There were also small stiffeners in the

tension flange welded to the inner column flange. Details of these are shown in figure 2.1.

There were 14 lines of purlins which spanned 5 m between the gable frames and the test frame. These purlins distributed the vertical load applied to the test and gable frames while providing lateral restraints to the outer flange of the rafter. The outer flanges of the columns of the test frame and the gable frames were connected together by means of three rows of sheeting rails. Lateral stays (fly braces) were also provided to the frame at locations shown in figure 2.1.

2.3.3 Design Checks

The original design of the portal frame assumed a steel yield strength of 275 N/mm^2 and nominal sectional properties. A design check was conducted using the properties of the members from tables 2.2(A) and 2.2(B) on the basis of simple elastic and plastic analyses. Details of the design of the frame in accordance with BS 5950: Part 1 are given in Appendix 1.

A check on member properties shows that the capacity of column web for shear moment, M_{sh} was 325 kNm. This value was greater than the nominal plastic moment of the column ($M_{pc}=288 \text{ kNm}$), so that the plastic hinge would form first.

The reason for this was that the use of a deep haunch to provide a large lever arm had the effect of reducing the shear stress to acceptable limits. The nominal capacity of the rafter was $M_{pr}=148$ kNm, but considering the purlin spacing of 1.795 metres and the stress reduction factor of 0.80 at the apex region, the moment resistance in that vicinity was 115 kNm.

Stability of individual members namely the column and the haunch region were also checked. By making use of Clause 5.5.3.5(a) in BS 5950: Part 1, the required distance between full lateral restraints L_t was calculated to be equal to 2.962 m. Since the maximum length between lateral restraints in the column (Figure 2.8) was 2.0 m, then this length of column should remain stable.

A check on the stability of the haunch region was also conducted by means of Appendix G and Clause 5.5.3.5. of the design code. Based on the nominal yield strength of 275 kN/mm² and the ultimate design load of 1.5 kN/m², the calculation by the method of Appendix G shows that the haunch should fail by lateral-torsional buckling at a lower load. A check by clause 5.5.3.5 shows that the maximum allowable length of the haunch was 1.577 m, but the design provided 2.408 m. This shows that there was a strong possibility that premature failure by member instability in the haunch region could develop before the development of the collapse mechanism. However, the complete collapse

mechanism would occur at an ultimate design load of 1.5 kN/m^2 (or 7.52 kN/m), by the formation of plastic hinges at the haunch rafter/junction and in the rafter at the purlin adjacent to the apex. The design check conducted shows the existence of some deficiencies in the design of frame 3. Some of the rules on member stability were not followed in accordance with BS 5950.

2.4 The Test Assembly

2.4.1 Details of Test Assembly

It has been stated earlier that the tests on full scale frames carried out in the past gave little experimental data to deal with modern portal frame construction. This is especially true for tests that subject the frame to in-plane applied load. Consequently, the decision was taken at the planning stage that the tests must simulate as realistically as possible, the actual conditions to which a portal frame could be subjected. In the actual situation, "snow" loading is applied through the sheeting and thence via the purlins to the frame. These secondary members not only apply the load but also offer restraint against lateral-torsional buckling of the frame members.

The requirement of simulating these conditions leads to the development of a 3-dimensional test assembly. That is the

only way that a realistic degree of structural interaction between the secondary members and the main frame can be reproduced. Meanwhile, the effect of any stressed-skin action (2.7) within the plane of the roofing must not induce any unknown restraint to the frame. Furthermore, it was also necessary to design the complete test assembly to fit the available area of strong floor in the structures laboratory.

Figure 2.3 shows the details of the test rig. It consisted of three frames with the central test frame connected at rafter level by cold-formed purlins to the two "gable" frames. The gable frame members were chosen to be stiffer and stronger than the test frames. They were designed to incorporate suitable extension pieces within the rafter so that the span could be increased from the original 12m to 24m. This degree of flexibility was required so that after the first two tests on 12m span frames the assembly could then be used to test this 24m span frame. Lateral movement of the gable frames was restrained by bracing them back to the stanchions of the laboratory walls.

The effect of stressed-skin action must be eliminated since this study is not directed to that particular aspect of the behaviour. Therefore it was decided that the gable frames must be made to follow the movements of the test frame. This required that the joints in the gable frame should be pinned and the associated column bases had knife-edge supports. The effect is that the gable frame could behave like a rigid

link mechanism as shown in figure 2.4a. With this arrangement, any movement of the test frame could be reproduced by the gable frame. The vertical movement of the apices of the gable frames was controlled using hydraulic push-pull jacks. Figure 2.4b shows the jack positioned underneath the base support of the central posts. The spread of the eaves, including the sway movement of the gable frame was controlled by a horizontal push-pull jack positioned near the top of one outer post (see figure 2.4c). Thus, two jacks that were operated manually, controlled the shape of each articulated gable frame at any stage of the loading regime. At each load increment, the nodal deflections of the test frame were measured and the articulated gable frames were then adjusted until their corresponding deflections coincided with those of the test frame.

The column base system of the test frame was designed to provide the same rigidity as a typical foundation and also to allow the measurement of forces transmitted to the foundation by the structure. The arrangement of the column base is shown in figure 2.5 and is made up of a highly reinforced concrete slab, to which the column base is anchored using two holding down (HD) bolts. This arrangement represents the "pinned" base condition in practice. Each base was supported on three load cells arranged in a pattern so that the vertical load and any moments induced into the base about the two major axes could be measured. In addition, a horizontal load cell was positioned to measure

any horizontal force exerted by the base and to prevent any significant horizontal movement. By placing a set of linear needle roller bearings under each vertical load cell, any horizontal movement of the base should not have had any effect on the operation of these load cells.

2.4.2. The Roof Loading System

A realistic condition of loading applied to the roof sheeting is uniformly distributed load simulating snow or wind load. One method of testing that would allow this condition is to apply load using sandbags. However, for practical reasons, this method is difficult to apply for a large structure. It was therefore decided to adopt the spreader beam technique, that had been successfully used by Bryan and Davies (2.7, 2.8) and Lawson (2.9) for the full scale testing of buildings of stressed-skin design at Salford University.

In this system of loading, the uniformly distributed load was approximated by a large number of point loads applied to the sheeting via a series of timber spreaders. The load was supplied to the timber spreaders by hydraulic jacks anchored to the strong floor, using a system of beams and hangers. Details of the loading system and the general layout of the timber spreaders is shown in figures 2.6 and 2.7 respectively. Each spreader applied six points locally to

the sheeting. A total of 96 points were controlled by each jack giving a total of 576 load points for the whole test arrangement. The maximum test capacity of the system was 2 kN/m². This loading capacity plus the self weight of the frame, purlins and sheeting and the weight of the loading system itself was sufficient to ensure failure of the test frame.

The actual load being transferred from the sheeting into the test frame could not be assumed to be directly related to the applied load. This is because the relative stiffnesses of the various components making up the test assembly would determine the magnitude of the actual load being imposed on the test frame. Furthermore, the precise distribution of load on the frame could not be readily assessed by simple analysis, and it was later found that the distribution was varying during the test. That was why the arrangement of the four load cells per concrete base was necessary, as it would allow the actual load acting on the test frame to be measured.

2.4.3. Instrumentation of the Test Frame

It has been the philosophy of this research project to be able to collect information concerning the behaviour of the frame during the test as thoroughly as possible. This information regarding the test frame was essential for both

direct interpretation of the frame's behaviour and the calibration of the mathematical model developed at Manchester. Measurement of the member and material properties of the frame was discussed in section 2.3. This section describes the method in which data was collected during the test.

To control the several parameters involved, many measurement points were defined on the test rig. The measuring devices used were electrical resistance strain-gauges, electrical displacement transducers, electronic load-cells and inclinometer or rotation gauges. 250 strain-gauges, 20 transducers and 8 load cells were used to instrument the frame. Because of the large number of measurements that needed to be recorded, a sophisticated data logging system with interlinked computers was used to collect and analyse the test data.

Three microcomputers were used as the basis of the data logging system. These three microcomputers had the capability of recording all the strain-gauge readings as well as the measurements from 20 linear displacement transducers and 8 load cells.

This data processing system was backed up by a PDP computer linked to the PRIME mainframe computer. The purpose of this set up was to produce test data in graphical form as quickly as possible using a programme "TRACADERO" (2.4) written by

P. Engel, another member of the research team. This enabled complete sets of graphs depicting the variation of the recorded measurements against load to be available within 24 hours of the completion of the test. Furthermore, this system also ensured that a permanent and accurate record of the measured results at any stage of the loading regime could be made. This system can also make direct conversion of some of the recorded parameters into a more useful form. For example, linear strain can be converted into bending moments, enabling the behaviour of the frame to be quickly checked.

The strain-gauges were positioned in a symmetrical pattern on either side of the ridge. This enabled the exact bending moment distributions of the frame to be recorded, even if the behaviour became unsymmetrical during testing. When detailed examination at certain sections was required, such as at the haunch regions, they were required to be fully strain-gauged. Even the bolts in the end plate connection at the eaves and the HD bolts at the bases of the test frame were strain-gauged in order to obtain information regarding the development and magnitude of loads in the different bolts. Rotation gauges were also used to obtain information regarding the relative rotations in the eaves' connection zones.

In addition, some regions of the frame were coated with brittle lacquer prior to the test so that some visual

observations could be made. This was most effective particularly with regard to the onset and spread of plasticity.

2.5 Test and Behaviour of Frame 3

2.5.1 The Full-Scale Test

After the setting up of the test frame the whole test rig was then squared and levelled in order to avoid initial deflections prior to the test. The loading system was then constructed, after that the test rig was levelled a second time in order to compensate for the deflections due to the loading system.

The analysis of the test results was first carried out by performing a linear regression on the three first experimental points that allowed extrapolation in order to obtain the origin of the curves. The loading on the roof was gradually applied and the increments were determined taking into account the true load recorded by the load-cells. Considering the true value of the yield stress of the members of the frame, the elastic limit of loading was assessed to be $1.3 \times$ the working load. Since the loading system represented $0.6 \times$ the working load the possible amplitude of loading in the elastic range was 0.58 kN/m^2 .

In the first loading session the frame was loaded up to $1.312 \times$ the working load in six increments. At each increment the nodal displacements of the gable frames were adjusted in order to release any stressed skin action. This procedure, with a waiting period of 15 minutes after every adjustment was followed throughout the test. At the end of this first loading session a transducer measurement at the apex showed a residual vertical deflection of 10 mm. A second loading session was conducted in five increments in which the frame was loaded to $1.370 \times$ working load. A further 8 mm residual vertical deflection was recorded at the apex. These values may be compared with the maximum apex deflection of 185 mm noted during the two tests.

After these two loading sessions, the frame was loaded in increments until the stage at which the last increment caused the initiation of elastic member instability in one of the haunch regions. Immediately after the application of the final increment, there appeared to be no effect. However, after a few minutes the whole of the haunch region failed suddenly by lateral-torsional instability. The test was then terminated immediately in order not to cause any further damage to the test assembly. The collapse of the frame took place at the load factor of 1.668. The resulting load-apex deflection characteristic of the test is shown in figure 2.8 and the distorted shape of the haunch is illustrated in figure 2.9. Details of all the results of the test can be found in reference (2.4).

2.5.2 The Load-Deflection Curves

The deflections of the frame during the test were recorded by means of transducers located at various points on the frame. Since the deflection at the apex was characteristic of the behaviour of the frame and the magnitude of this displacement was relatively large, it has been used to compare the various theoretical analyses. The experimental load deflection curve at this point is shown in figure 2.10 together with 4 theoretical curves obtained using a powerful computer program written by Davies (2.11). In the theoretical analyses, the actual measured geometrical and material properties of the member were used in the input data of the programme.

The four analyses were computed using the following hypothesis:

Curve 1: Elastic-Plastic Analysis.

This curve is the result of analysis using the first order elastic-plastic analysis with an average yield stress σ_y equal to 300 N/mm²

Curve 2: Elastic-Plastic Analysis with P- Δ Effects.

This curve is the result of a second order elastic plastic analysis where the geometrical non-linearity is additionally considered.

Curve 3: Full Second Order Elastic-Plastic Analysis.

This curve is the result of a second order analysis for both the geometry and the material. Strain-

hardening is introduced into discrete plastic hinges using the formulae derived by Davies (2.12).

Curve 4: Analysis with Base Fixity.

This curve is the result of introducing semi-fixity at the column bases. These base fixities were determined using the bending/rotation relationship at the base recorded during the test.

2.5.3 Bending Moment Distribution in the Frame

The experimental bending moment diagram was obtained by means of computation of the strain-gauge readings. This was done directly by the computer programme "TROCADERO" mentioned earlier. Using this approach two different computations were conducted. The first was the calculation of the bending moment by considering only the readings given by the strain-gauges situated at mid-flange. The second was the calculation of the bending moment by fitting a straight line to the three readings on each flange and then interpolating for the strains at mid-flange. Details of this methodology is given in reference (2.4).

The bending moment distributions for frame 3 are shown in figures 2.11 and 2.12. The bending moment diagram in figure 2.11 shows a comparison between the theoretical solutions obtained with the model producing the curve 4 in figure 2.10

at a load factor close to the working load. It can be seen that both the experimental and the theoretical values agree reasonably well. The same comparison is made in the bending moment diagram shown in figure 2.12 but with load factor very close to the collapse load. It shows again that the experimental and theoretical values agree reasonably well. This confirms that the control of the load applied to the frame using the load-cells gives good results and also proves that the computer modelling is accurate.

The experimental bending moment can also be evaluated by considering the plots of load/bending relationship at the sections which have been strain-gauged. In the tests the strain-gauges were positioned at selected places including those where plastic hinges were likely to occur. This enabled the analysis of the rate of increase of the bending moment at a specific sections to be checked and the non-linear behaviour at potential plastic hinges to be detected. In figure 2.13, the bending moment computed from the strain-gauge readings illustrates the behaviour of the frame. It can be seen that the load/bending curves remain linear until the penultimate increment when suddenly the curves of the bending moment at sections C and R (i.e, the top section of each column) show a non-linear rise. This change of slope at sections C and R indicates the on-set of plasticity occurring in those sections at a load factor of about $\lambda=1.64$. In figures 2.14 and 2.15 where the load/stress curves of the relevant strain-gauges are shown, this same

phenomenon can also be observed.

2.5.4 The Frame's Sway Mechanisms

It could be argued that because of the formation of the two plastic hinges at the top of the column the frame failed by a "sway mechanism". In this case however, the frame was symmetrical with a symmetrical loading and the direction of rotation of one of the plastic hinges in the "sway mechanism" was in the opposite sense to the bending moment producing the hinge. Consequently sway movement cannot take place without one of the hinges unloading and thus becoming locked. Therefore the "sway mechanism" is "false" in this case.

This problem of false mechanisms is quite difficult to tackle in a computer analysis. Davies (2.13) pointed out the problem demonstrating that a false mechanism occurring in an elastic-plastic analysis could result in a wrong estimation of the collapse load. In this present case the two plastic hinges were formed mathematically at the same time, thus the determinant of the stiffness matrix becomes zero. Unless corrected this causes the analysis to terminate at the wrong collapse load. The correct mechanisms for the case of Frame 3 and some "false" mechanisms are shown in figure 2.16.

2.6 The Bending Tests

2.6.1 The Effects of Strain-Hardening

The simple theory of plasticity assumes that the material is perfectly plastic. This assumption ignores the elastic deformation, in which, when the yield stress is attained the deformation follows a regime of pure plastic flow, as shown in figure 2.17. In reality, when the strain ϵ_s in figure 2.17 is reached, the extreme fibre stresses start to increase and thus the theoretical value of the plastic moment at the plastic hinge is exceeded. This phenomenon is called strain-hardening and it is present in mild steel and is even enhanced in high tensile steel.

The effect of strain-hardening in relation to instability was first given by Horne (2.10), in which he introduced a method termed the "rigid-plastic-rigid" theory. In this approach, the plastic hinges could be augmented by the concept of a plastic zone (see figure 2.18), where the spread of plasticity is a direct consequence of strain-hardening. Thus, when the strain-hardening takes place, the collapse load in the particular case of a simply supported beam is increased. Horne presented expressions relating the strain-hardening effects in terms of the extra virtual work done by the hinge.

Horne's model of strain-hardening however, does not provide

any information regarding the collapse load of the structure. The method is qualitative and indicates only the stability of the load deflection curve at collapse. Davies (2.12, 2.13) extended the model proposed by Horne by developing a theory suitable for inclusion in the stiffness matrix method. This method is powerful and made strain-hardening applicable to a wide range of steel structures. In this method, the elastic and the plastic components of the curvature and deflection are kept separate. Thus, the theory can be applied in any elastic-plastic problem, where the plastic hinges are assumed to be discrete with linear strain-hardening properties. In Davies's approach the plastic moment at the i^{th} hinge (M_{pi}) could be substituted by an equivalent moment M_{hi} including the effect of strain-hardening.

$$M_{Hi} = \pm (M_p)_i - \left(\frac{EI}{kh} \right)_i \theta_{Hi} \dots \dots \dots (2.1)$$

where;

E = Modulus of Elasticity (N/mm^2)

k = Strain-hardening parameter (values between 8 and 20)

M_p = Plastic moment of the section (kNm)

θ_{hi} = Current rotation of hinge i (radian)

h = The equivalent cantilever of hinge, which is obtained by plotting the tangent in an equivalent cantilever diagram from the section of maximum bending moment.

In the above expressions, the values of strain-hardening parameter, k , are invariably obtained from bending tests. It then followed that at a given plastic hinge i the

modification to the corresponding term in the global stiffness matrix of the structure (2.13) is;

$$Y_{3m+i, .3m+i} = Y_{3m+i, .3m+i} \left(\frac{EI}{kh} \right)_i \dots \dots (2.2)$$

Therefore in the well known matrix equation of the stiffness matrix method $\{\delta\} = [Y_s]^{-1} \{P\}$, the stiffness matrix $[Y_s]$ will be substituted by a modified stiffness matrix $[Y_s]'$ which incorporates modifications to the leading diagonal terms corresponding to plastic hinges.

2.6.2 The Bending Tests on Beam Specimens

Bending tests were carried out on unyielded beam specimens cut from the rafter and column members of the frame when the full-scale test was completed. In this case, 5 bending tests on simply supported beams loaded with a single point load up to failure were conducted. Of the 5 beam specimens tested, 4 were cut from the rafter section and 1 from the column section. The tests were carried out using a 500 kN Denison universal testing machine. The specimens were tested in accordance with the procedure given in reference (2.4).

Figure 2.19 shows the arrangement of the beam specimen on the test rig. Beam specimens were placed on top of the test rig on a specially fabricated simple support system. The support also provided side restraint and the whole system

could be adjusted to cater for the different lengths of specimen. With the use of timber packings and roller-bearings, the ends of the specimens were prevented from longitudinal torsional displacement. Lateral-torsional buckling was also prevented at the centre of the beam by a similar arrangement in order to ensure that failure of the beam was delayed until long after the full plastic moment was reached. Nine dial gauges were positioned at the region in the centre and both ends of the specimens (*figure 2.19*) in order to record the deflections and movement of the specimen during the test.

The specimens were first loaded up to about 60% of the calculated failure load in increments of 10 kN and then unloaded in the same manner. During this process, the readings of the dial gauges were taken. This procedure was carried out in order to allow 'bedding in' in the system. The specimens were then loaded again in the same load increments and dial gauge readings were taken. A plot of load-deflection was also made during the test. At the point when the load deflection graphs showed the first non-linear behaviour, the creep observation procedures were carried out. At this point a load increment of 5 kN was applied, and the readings of the dial gauges were taken immediately and at intervals of 2, 8, 12 and 20 minutes before the next incremental load was applied. This procedures were followed until failure occurred.

2.6.3 Results of the Bending Tests

Table 2.3 summarises the results of the bending tests and figures 2.20 and 2.21 show the moment deflection curves of one of the rafters and the column section tested. The strain-hardening parameter k was obtained using Davies' (2.12) theory by the following expression;

$$k = \frac{1}{3} \left(\frac{w}{\Delta} \right) \left(\frac{\Delta'}{w'} \right) \dots \dots \dots (2.3)$$

where;

k is the strain-hardening parameter

w is load within the elastic range (kN)

Δ is the corresponding elastic deflection (mm)

w' is load within the plastic range (kN)

Δ' is the corresponding plastic deflection (mm)

The values of these variables are obtained from the load/deflection curves drawn for a particular beam test.

2.7 Summary and Conclusion

A full-scale test on a 24 m span pitched roof portal frame made of hot rolled steel sections was conducted. The frame was loaded uniformly using a total of 96 hangers connected to the timber frames spreading the load over an array of 576 discrete points. After the construction of the loading system, the frame was gradually loaded up to collapse by means of six hydraulic jacks.

Checks on the design of the frame show some poor design features which could be eliminated by using the design code meticulously. The column was designed satisfactorily for both elastic and plastic criteria. In the case of the rafter, the member length adjacent to the plastic hinge near to the ridge was more than twice the permitted value L_m . The rafter was also found to be unstable in the elastic part of the rafter. This is not the only aspect of the design rule which was not observed in the design. In the haunch region of the frame, a check using Appendix G and Clause 5.5.3.5 showed that it was unstable at the collapse load. Consequently, the frame failed by lateral-torsional buckling at one of the haunches at a load factor of 1.668.

The behaviour of the frame was closely monitored by means of the instrumentation provided during the test. The bending moment distribution on the frame was investigated in detail. The comparison made between the experimentally determined moments and those based on the best mathematical solution was good at all levels. The theoretical elastic-plastic plane frame analysis has proved to be accurate enough to predict satisfactorily the load/deflection curve and the collapse load of the structure.

An interesting aspect of this test is the manner in which the haunch failed by lateral-torsional buckling as predicted by Appendix G and Clause 5.5.3.5. of BS 5950. Although superficially this prediction was proved correct, in actual

fact the calculations show that the failure should have occurred at a much lower load. Based on this finding, it can be said that there is a certain amount of "over-design" in the Appendix G. The rest of this thesis sets to study the problem of lateral-torsional buckling at the haunch region and to investigate Appendix G in more detail.

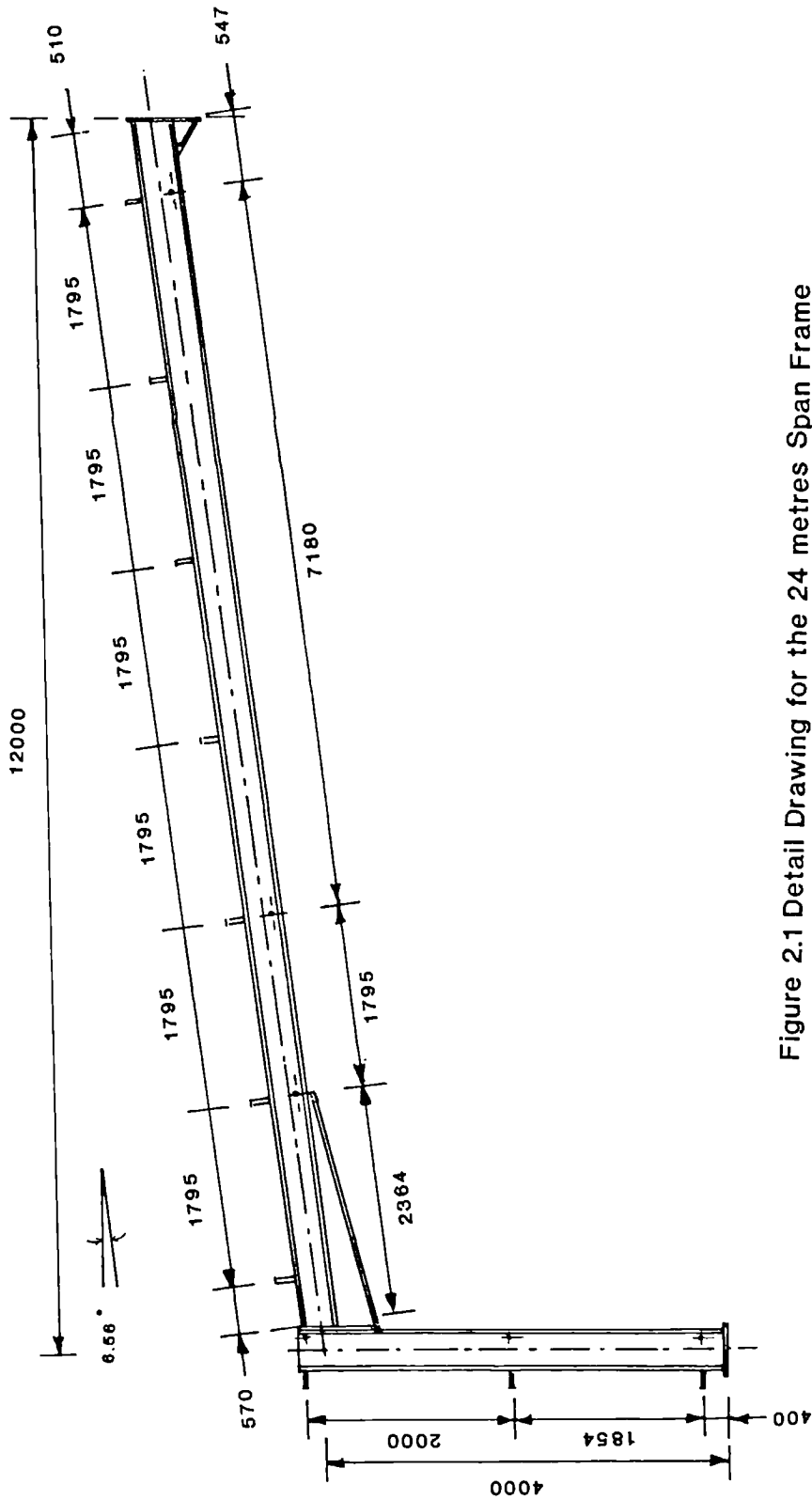


Figure 2.1 Detail Drawing for the 24 metres Span Frame
.....Continued

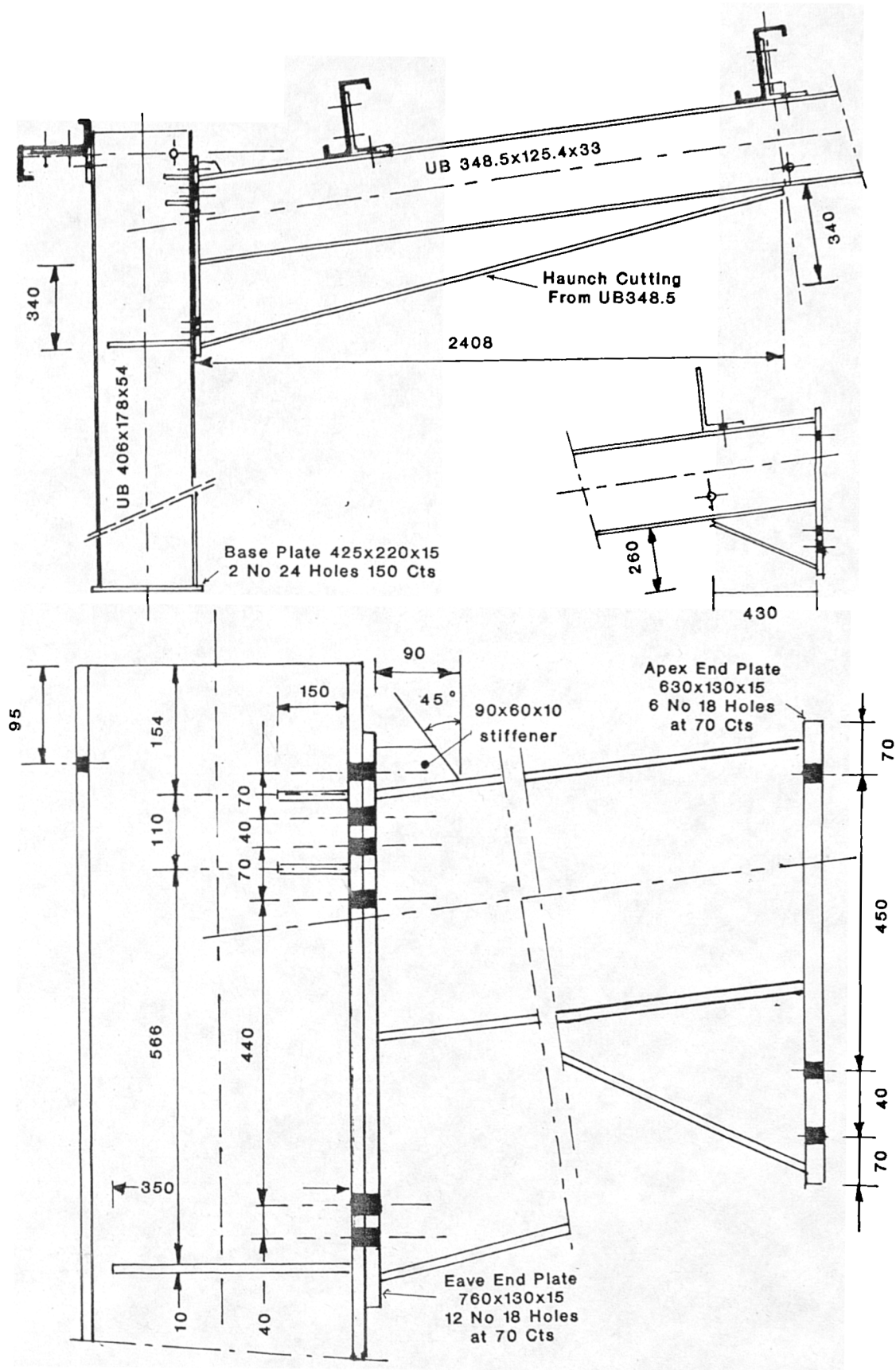


Figure 2.1 Continued: Detail of the Connections

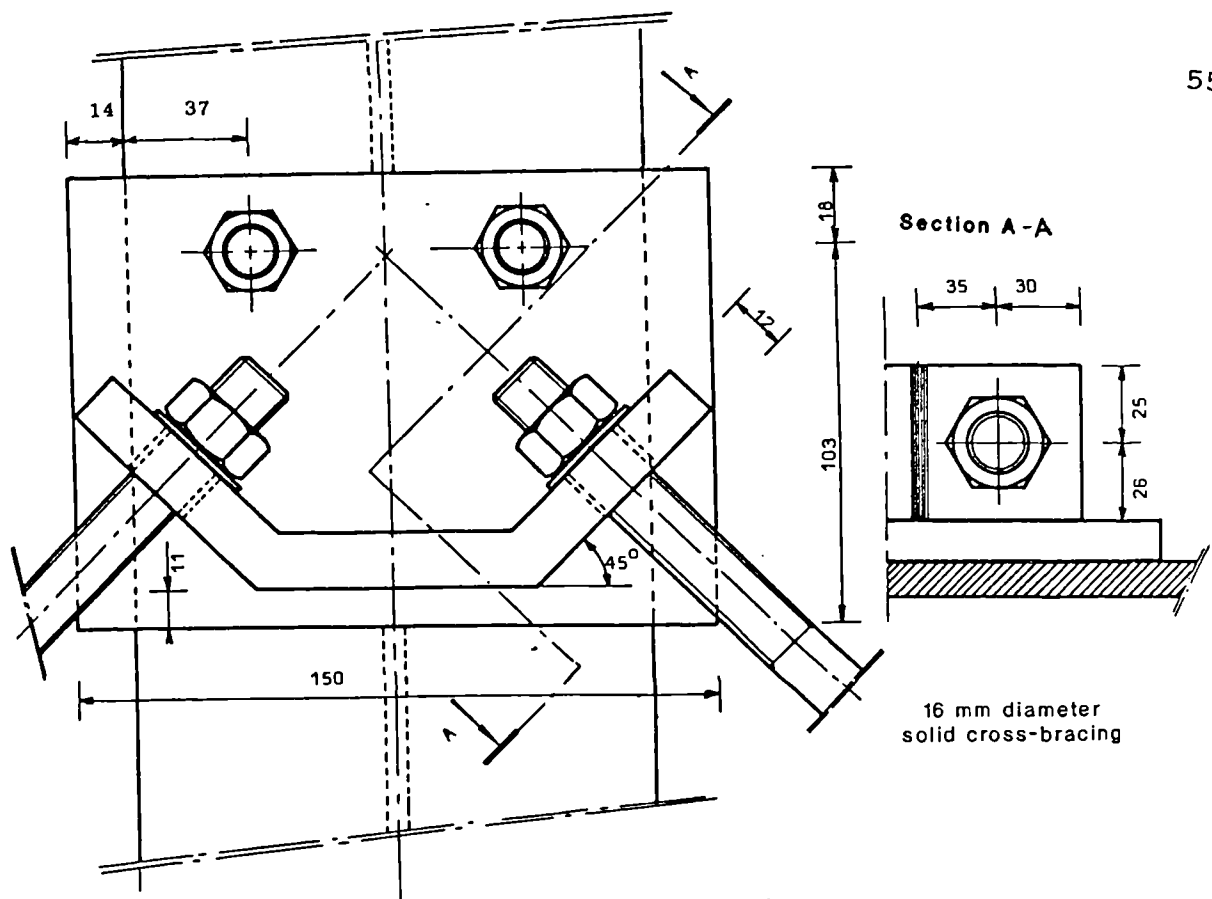


Figure 2.2 Detail of the Standard Bracing Cleat

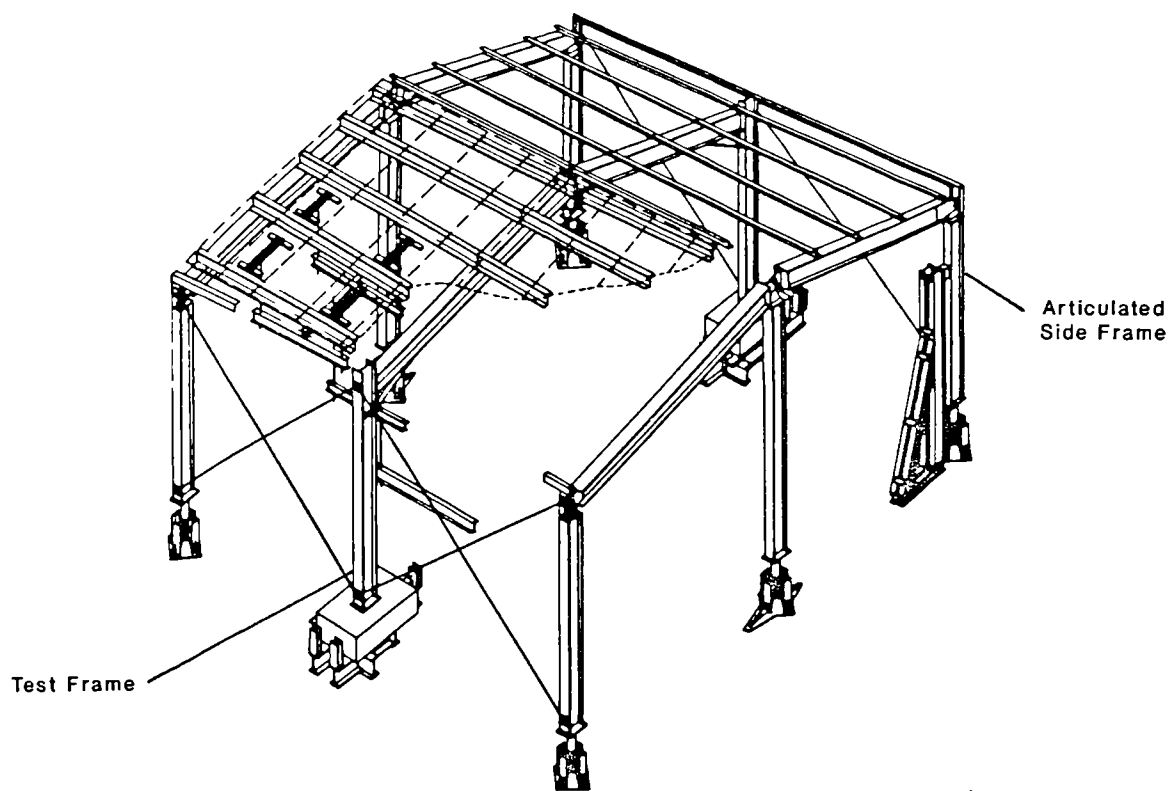


Figure 2.3 An Artist's Impression of the Test Rig

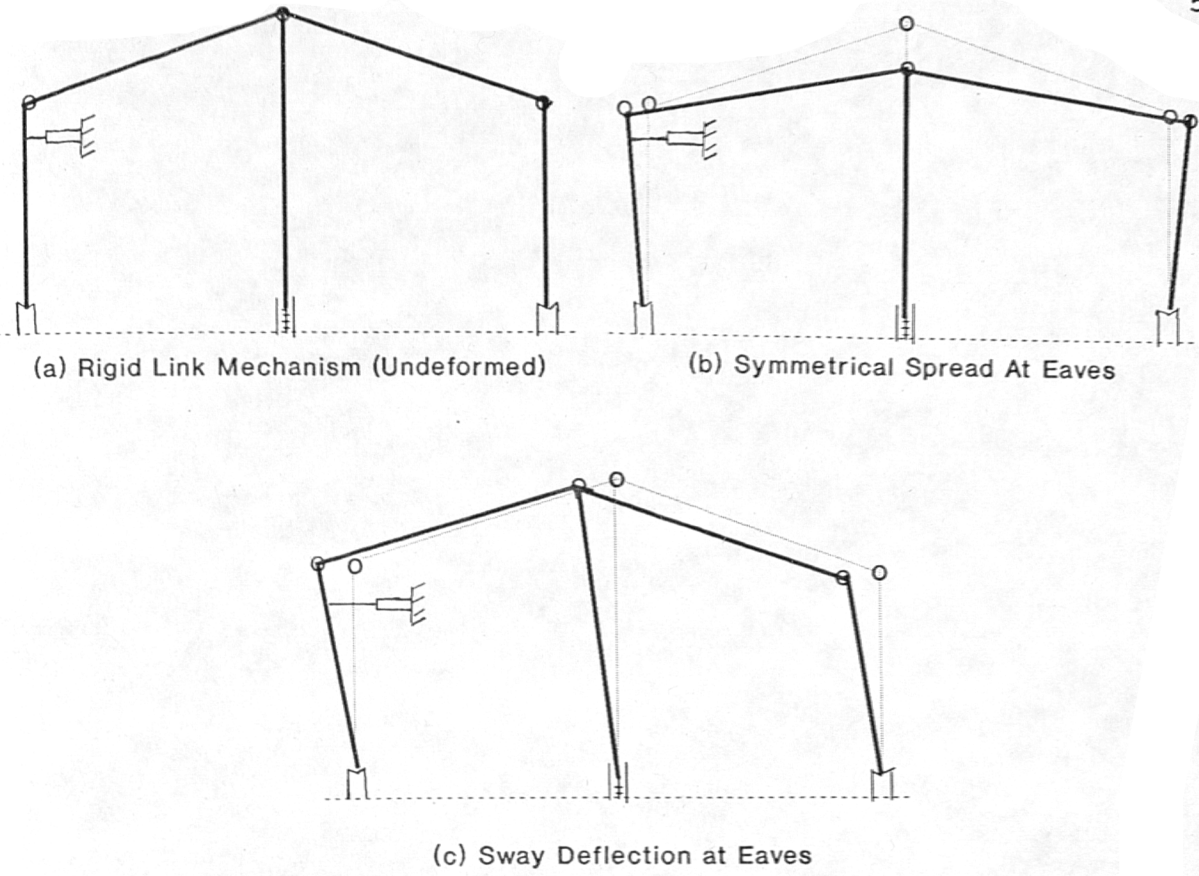


Figure 2.4 Articulated Gable Frame

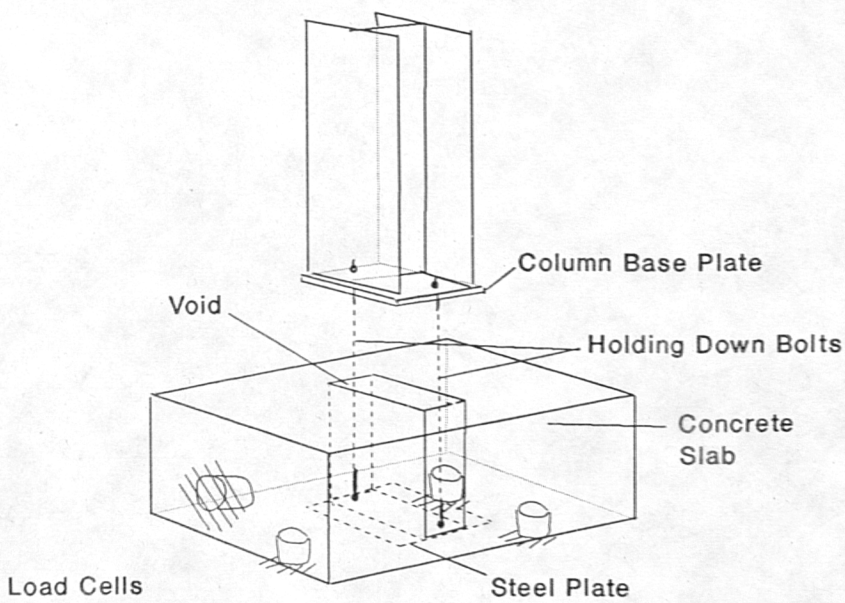


Figure 2.5 Column Base Detail

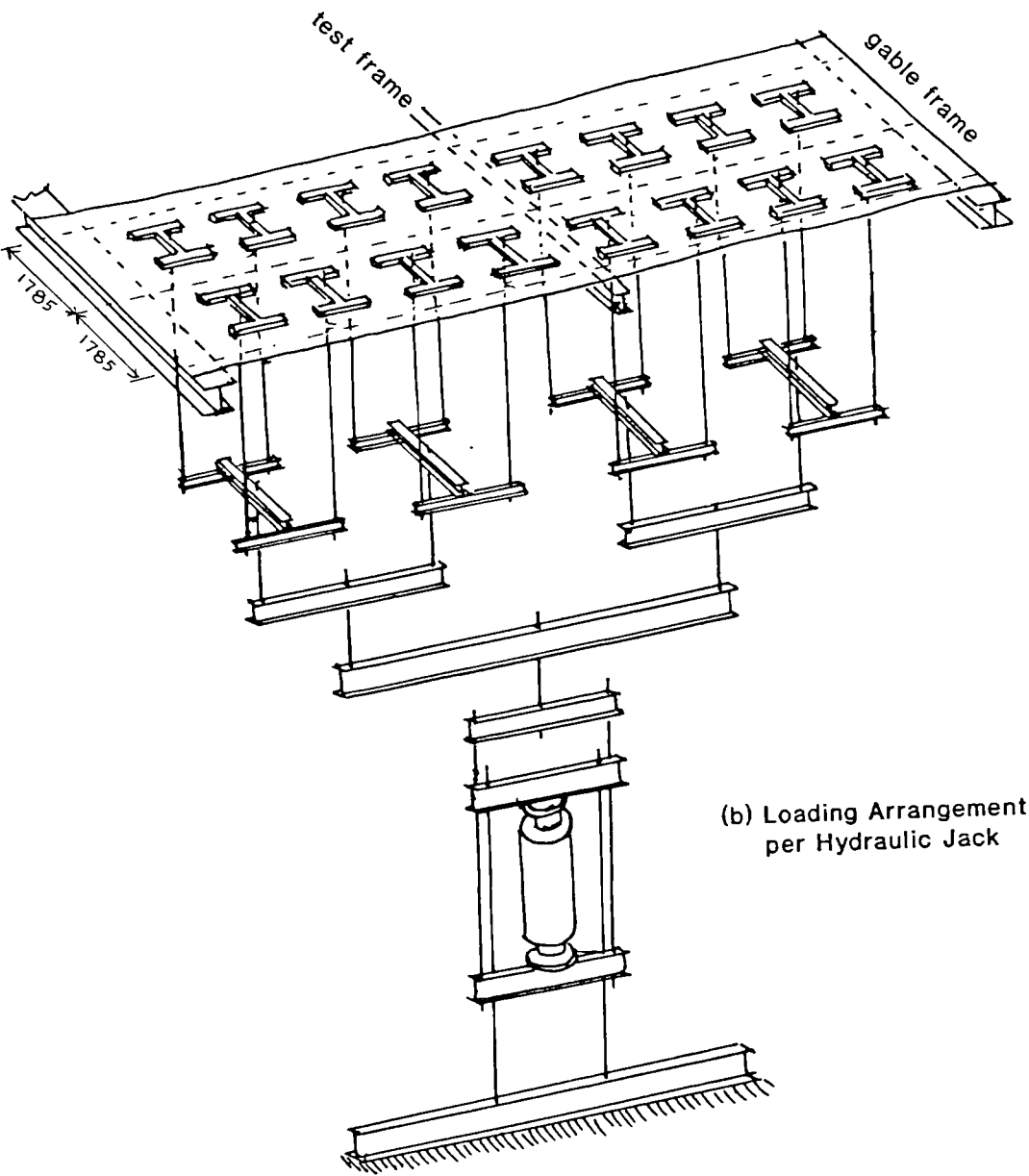
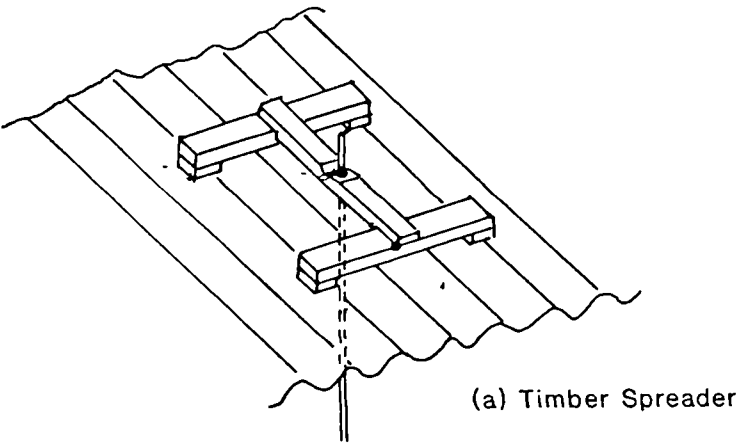


Figure 2.6 Detail of Loading System

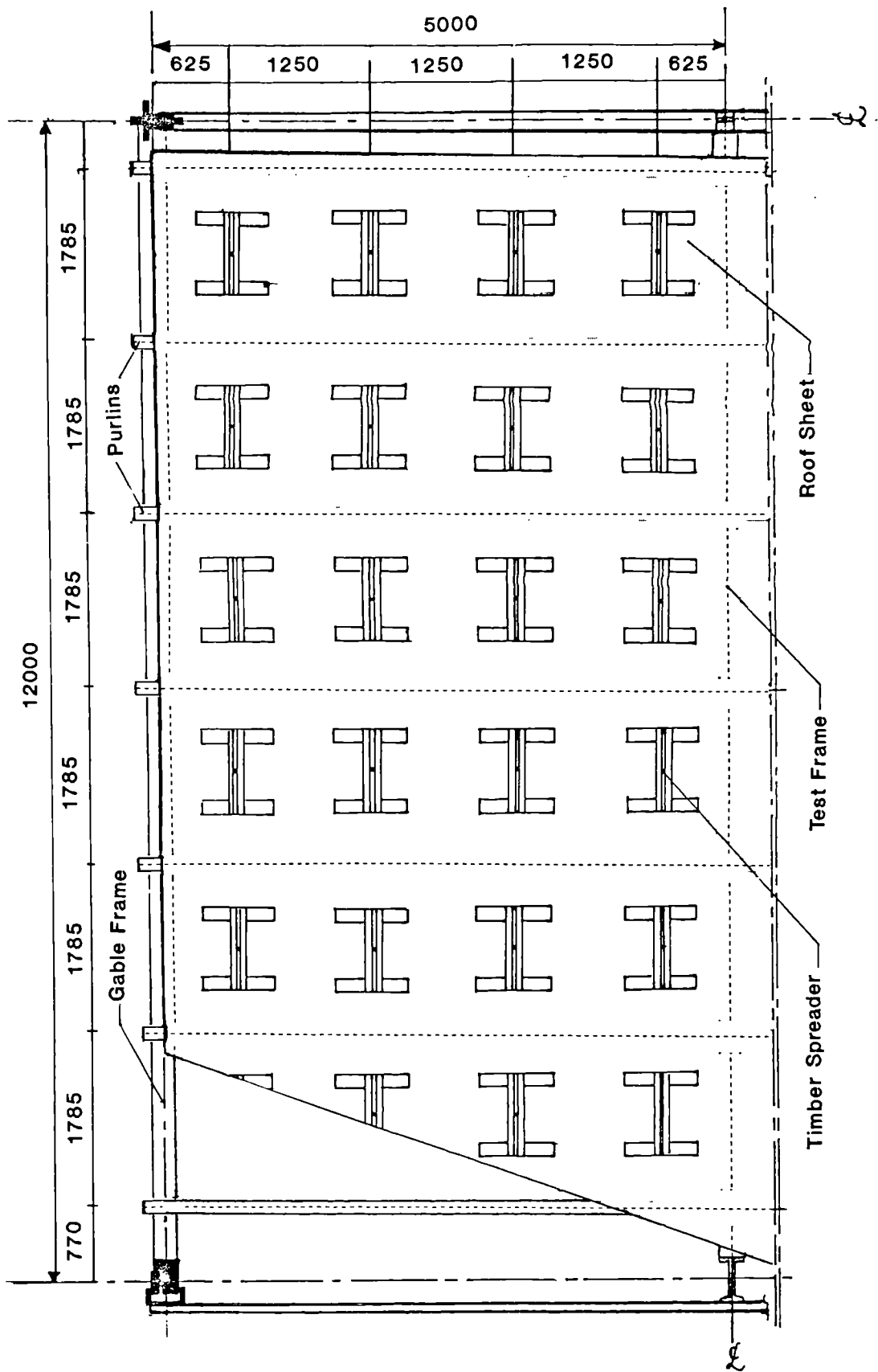


Figure 2.7 General Layout of the Timber Spreader on the Roof

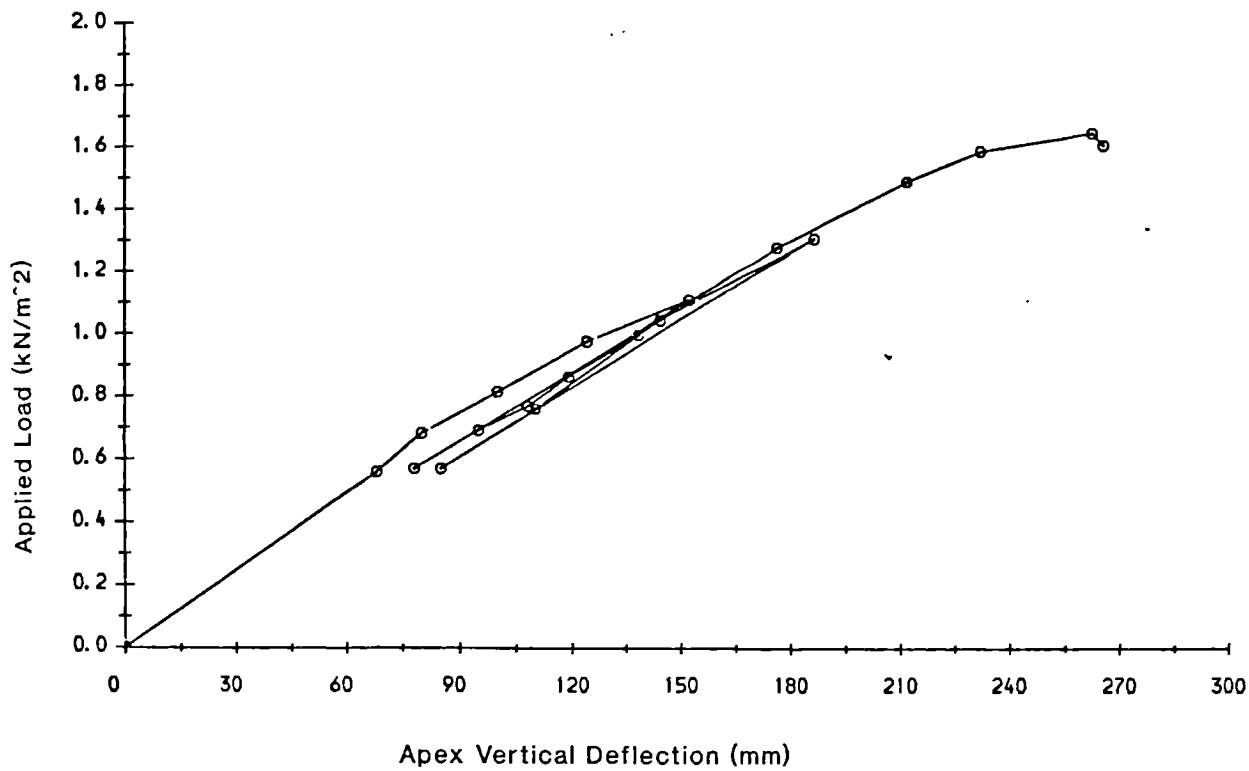


Figure 2.8 Experimental Result -Frame 3

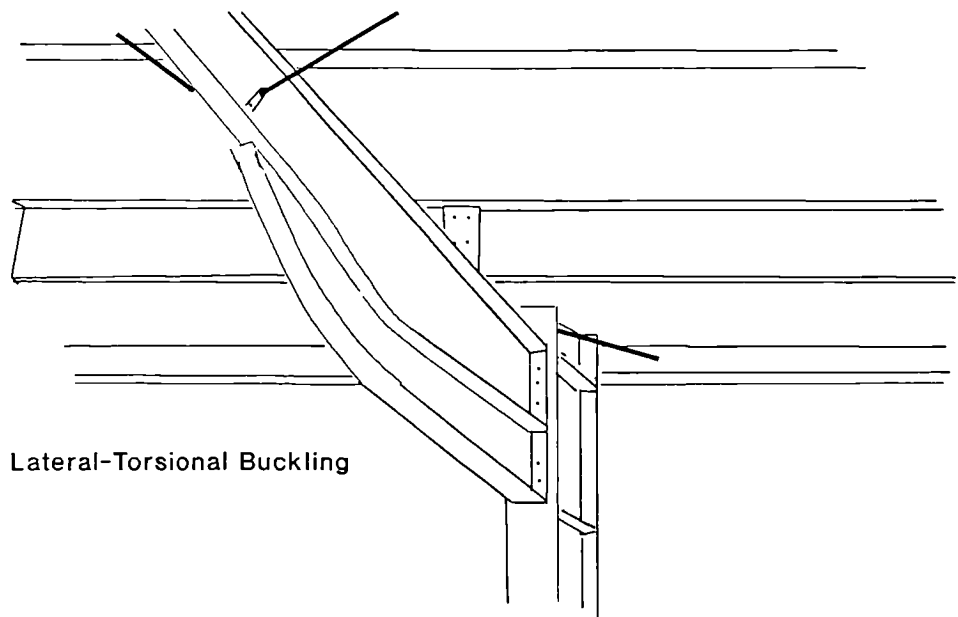


Figure 2.9 Member Instability - Frame 3

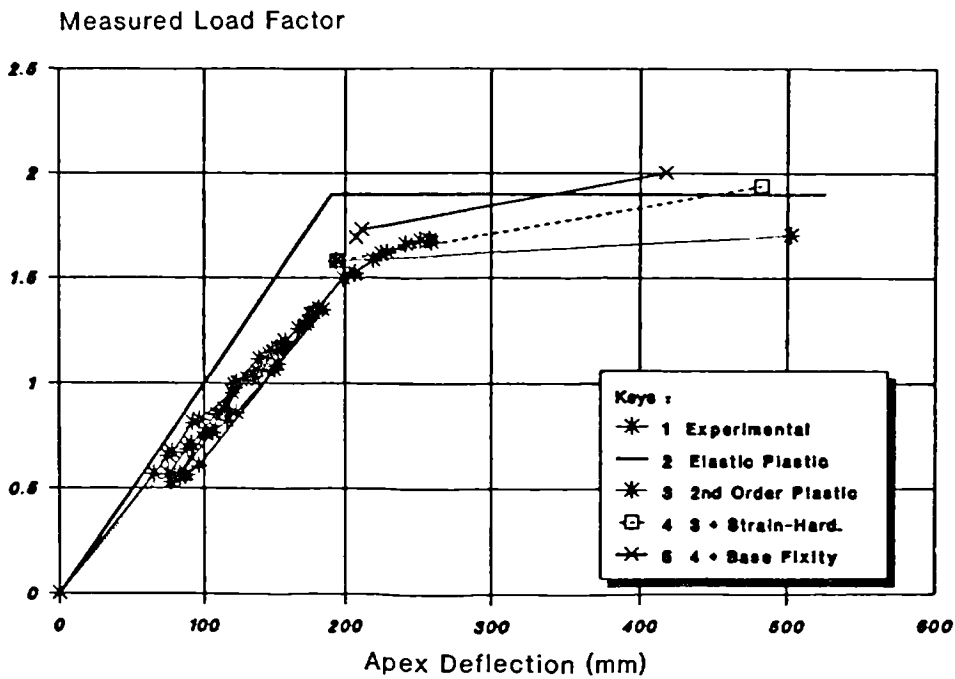


Figure 2.10 Experimental and Theoretical Load/Deflection Curve For Frame 3

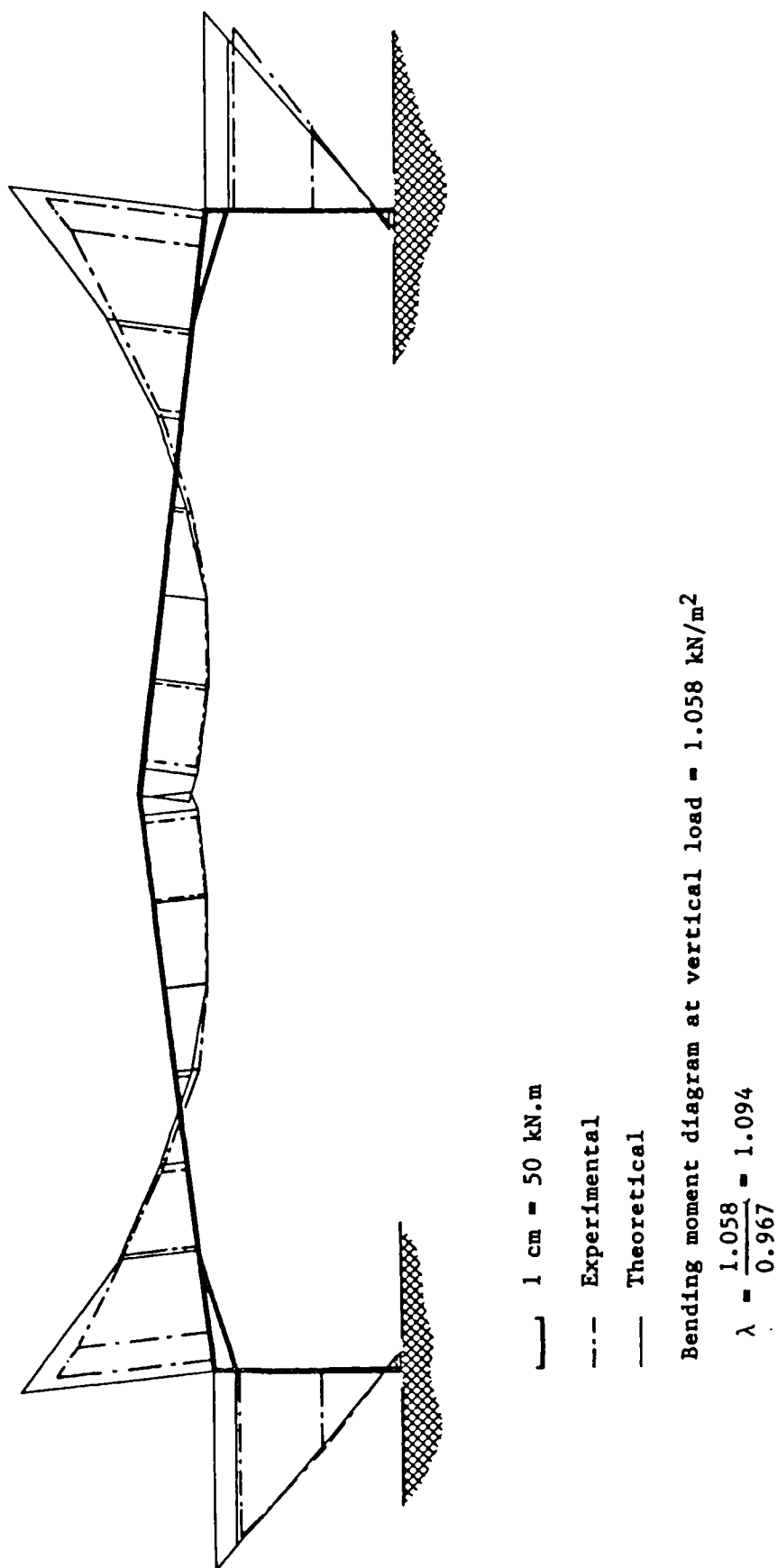
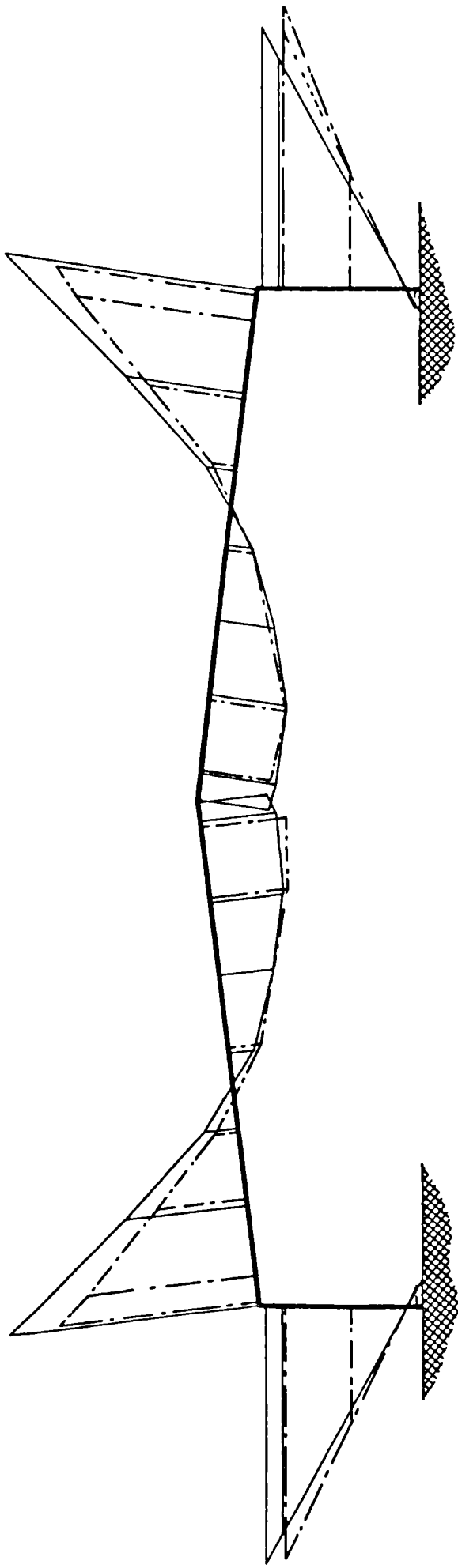


Figure 2.11 Experimental Bending Moment Diagram Near Working Load Compared With the Theoretical Solution



1 cm = 50 kN.m

Experimental

Theoretical

Bending moment diagram at vertical load = 1.586 kN/m²

$$\lambda = \frac{1.586}{0.967} = 1.64$$

Figure 2.12 Experimental Bending Moment Diagram
Near Collapse

Bending Moments

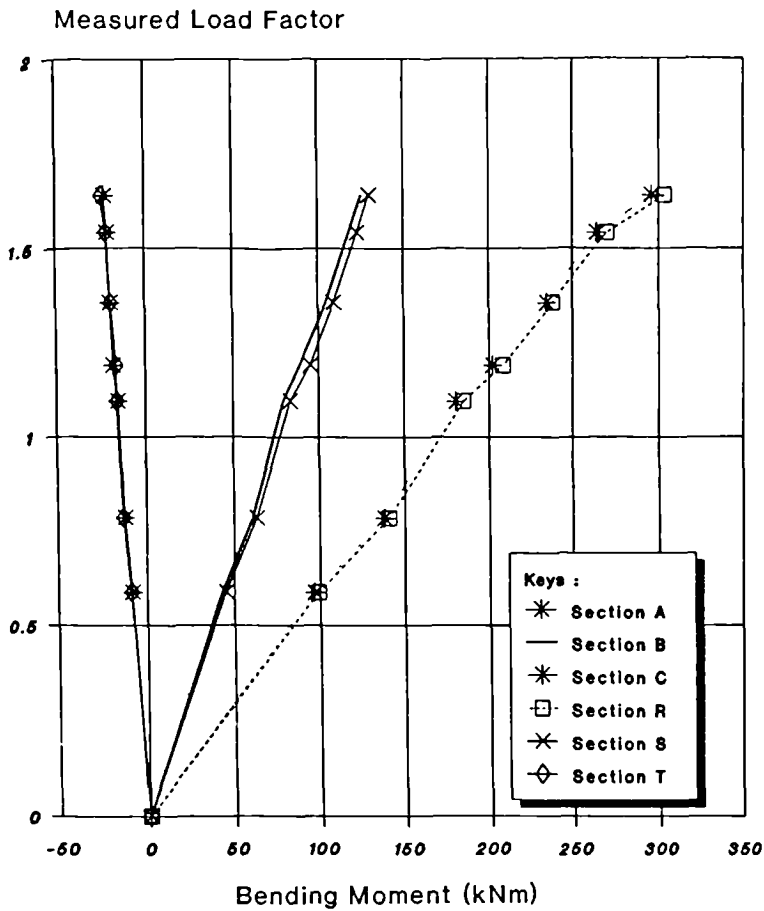


Figure 2.13 Computed Experimental Bending Moment - Column 1 and 2

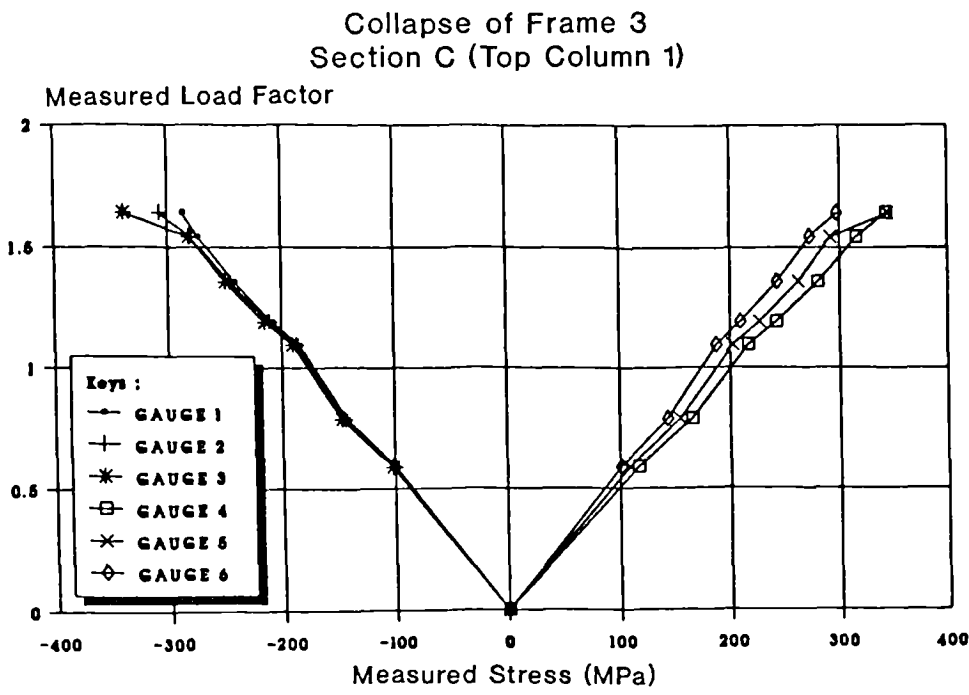


Figure 2.14 Load/Stress Curves for the Strain-Gauges at C

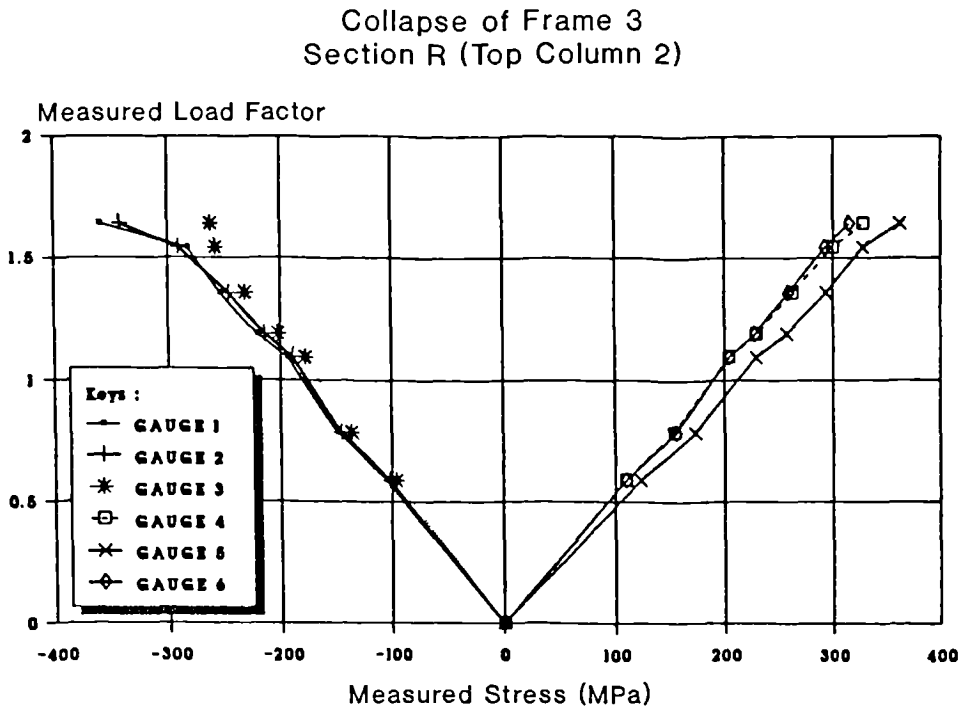
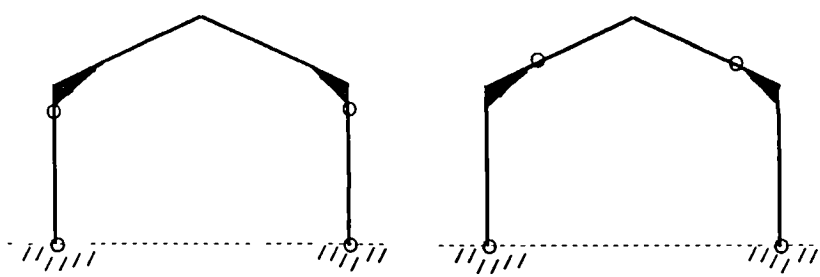
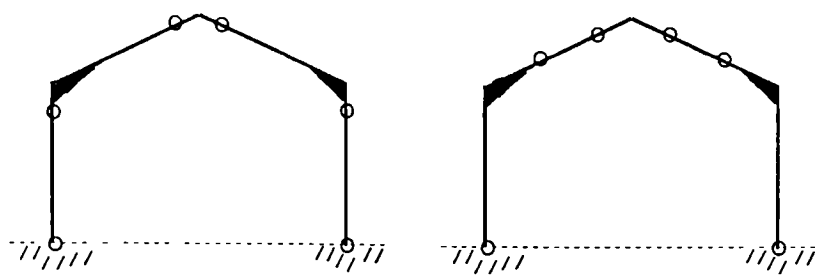


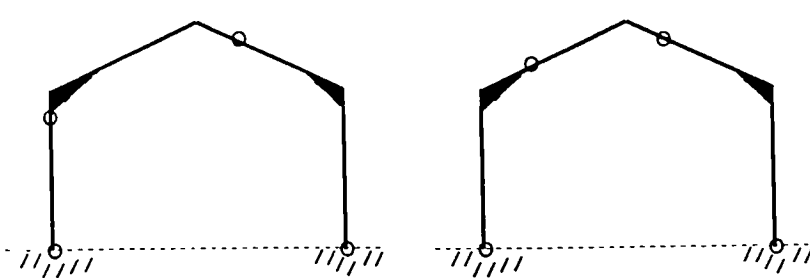
Figure 2.15 Load/Stress Curves for the Strain Gauges at R



(a) False Mechanisms in Pinned-Base Portal Frames



(b) Correct (Overcomplete) Collapse Mechanisms



(c) Correct Complete Mechanisms

Figure 2.16 Collapse Mechanisms for Frame 3

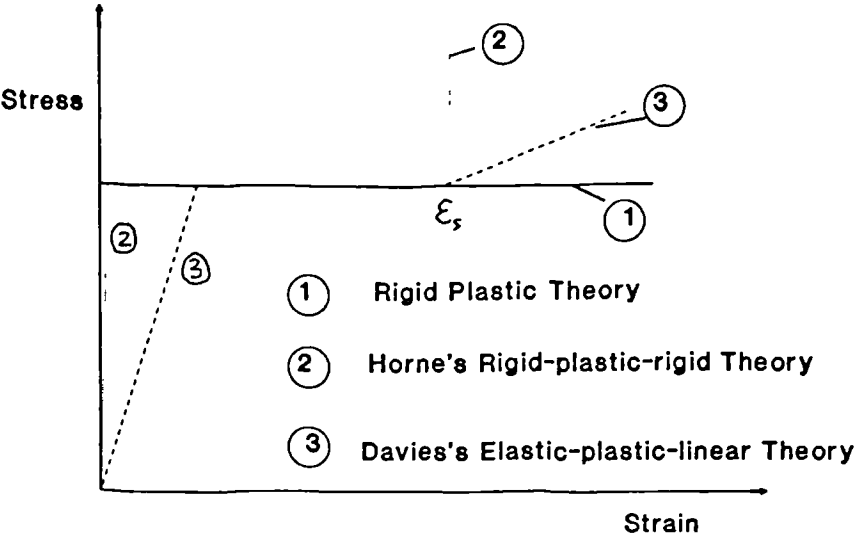


Figure 2.17 Different Material Stress/Strain Curves

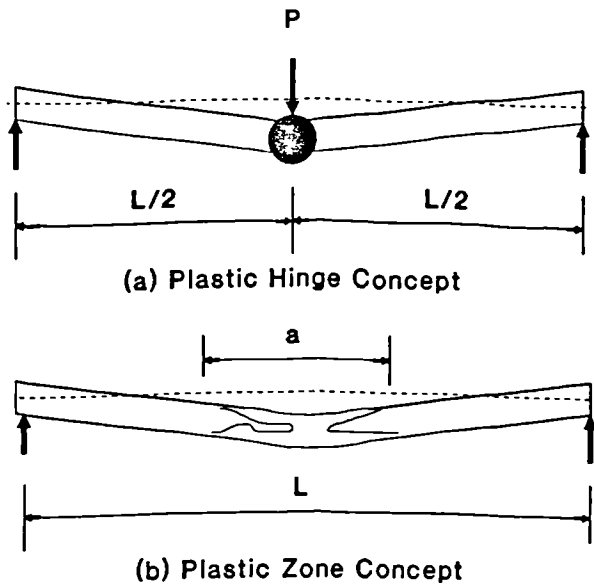


Figure 2.18 Plastic Hinge and Plastic Zone Concept

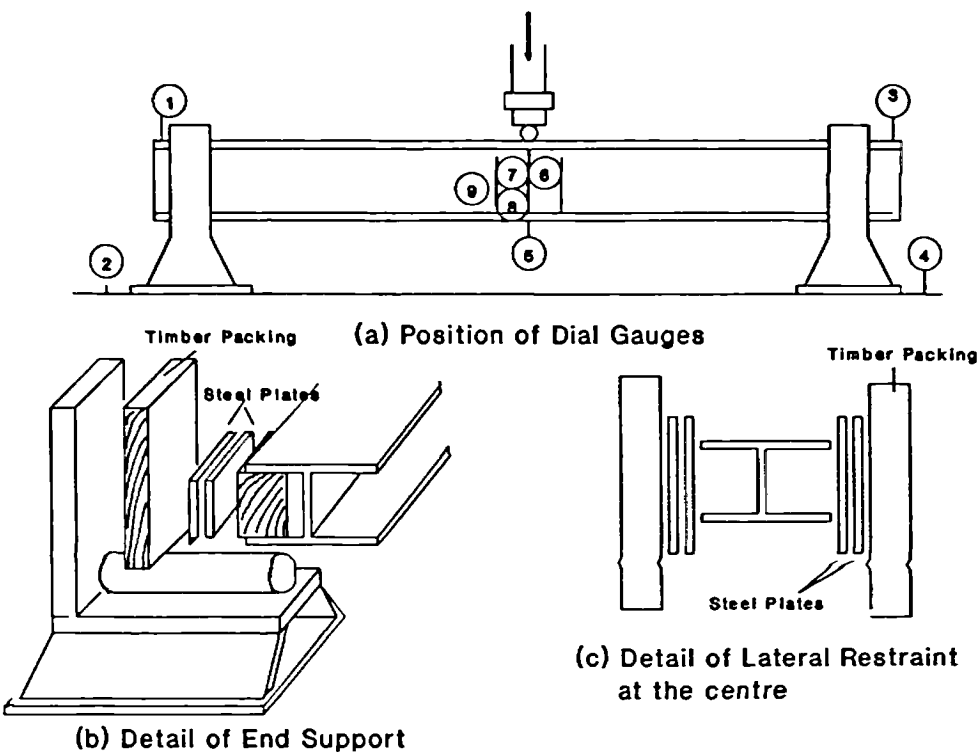


Figure 2.19 Arrangement of Bending Tests

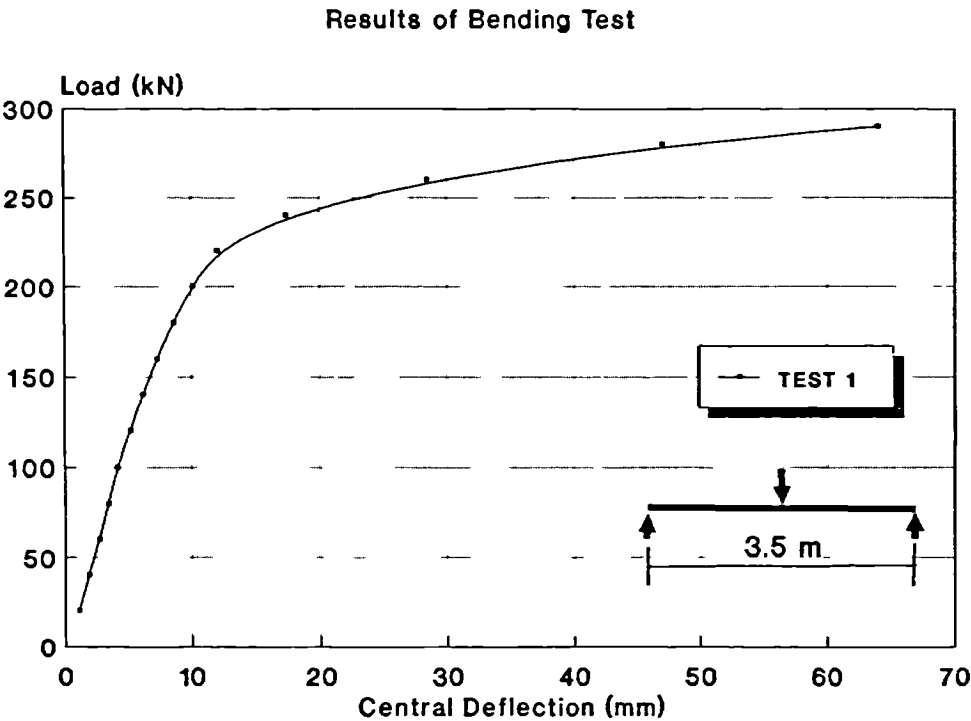


Figure 2.20 Load/Deflection Curve For Beam Specimen Cut From Rafter of Frame 3

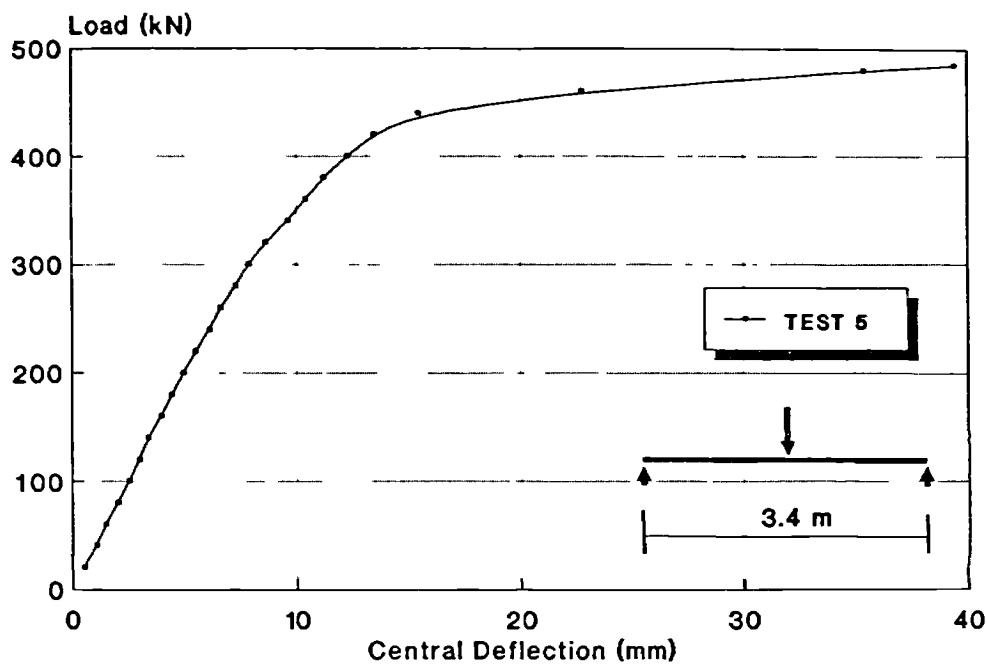


Figure 2.21 Load/Deflection Curve of Beam Specimen Cut From Column of Frame 3

Table 2.1 MAIN PARAMETER OF FRAME 3

Parameter	Frame 3
Span at column center line	24.00 (m)
Height at eaves intersection	4.00 (m)
Roof slope (degree)	6.56°
H apex / H eaves (ratio)	1.349
Bay spacing	5.00 (m)
Purlin spacing	1.795 (m)
Stanchion type	UB 406x178x54
Rafter type	UB 348x125x33
Self-weight	0.217 kN/mm ²
Super load	0.750 kN/mm ²
Dead load factor	1.40
Live load factor	1.60
Mean, Dead load + Live load factor	1.55
Factored Dead + Live load	7.519 kN/m
Uniformly Distributed Load, Lamda = 1	0.967 kN/mm ²

TABLE 2.2 (A) MEMBER AND MATERIAL PROPERTIES OF FRAME 3
(PROPERTIES OF COLUMNS)

PROPERTIES		LEFT COLUMN	RIGHT COLUMN
TOP FLANGE	WIDTH	177.2 mm	177.1 mm
	THICKNESS	10.6 mm	10.5 mm
	YIELD STRESS	298 N/mm ²	298 N/mm ²
	ULTIMATE STRESS	508 N/mm ²	508 N/mm ²
	YOUNG'S MODULUS	210000 N/mm ²	210000 N/mm ²
	E/E _s	60	60
	ϵ_p/ϵ_y	10	10
BOTTOM FLANGE	WIDTH	178.1 mm	177.7 mm
	THICKNESS	10.9 mm	10.9 mm
	YIELD STRESS	294 N/mm ²	294 N/mm ²
	ULTIMATE STRESS	488 N/mm ²	488 N/mm ²
	YOUNG'S MODULUS	200000 N/mm ²	200000 N/mm ²
	E/E _s	40	40
	ϵ_p/ϵ_y	11	11
WEB	WIDTH	407.0 mm	407.2 mm
	THICKNESS	7.8 mm	7.7 mm
	YIELD STRESS	333 N/mm ²	333 N/mm ²
	ULTIMATE STRESS	540 N/mm ²	540 N/mm ²
	YOUNG'S MODULUS	207800 N/mm ²	207800 N/mm ²
	E/E _s	52	52
	ϵ_p/ϵ_y	12	12

TABLE 2.2 (B) MEMBER AND MATERIAL PROPERTIES OF FRAME 3
(PROPERTIES OF RAFTERS)

PROPERTIES		LEFT RAFTER	RIGHT RAFTER
TOP FLANGE	WIDTH	125.1 mm	125.1 mm
	THICKNESS	8.4 mm	8.2 mm
	YIELD STRESS	298 N/mm ²	298 N/mm ²
	ULTIMATE STRESS	507 N/mm ²	507 N/mm ²
	YOUNG'S MODULUS	195500 N/mm ²	195500 N/mm ²
	E/E _s	40	40
	ϵ_p / ϵ_y	6	6
BOTTOM FLANGE	WIDTH	126.3 mm	125.7 mm
	THICKNESS	8.5 mm	8.5 mm
	YIELD STRESS	295 N/mm ²	295 N/mm ²
	ULTIMATE STRESS	500 N/mm ²	500 N/mm ²
	YOUNG'S MODULUS	195500 N/mm ²	195500 N/mm ²
	E/E _s	45	45
	ϵ_p / ϵ_y	10	10
WEB	WIDTH	352.3 mm	352.0 mm
	THICKNESS	6.5 mm	6.5 mm
	YIELD STRESS	325 N/mm ²	325 N/mm ²
	ULTIMATE STRESS	511 N/mm ²	511 N/mm ²
	YOUNG'S MODULUS	206500 N/mm ²	206500 N/mm ²
	E/E _s	45	45
	ϵ_p / ϵ_y	10	10

TABLE 2.3 BENDING TESTS RESULTS

Test	BEAM SPECIMEN	BEAM'S IDENTITY	SPAN (m)	MAX LOAD (kN)	STRAIN-HARD'NG FACTOR k	Mp (kNm)
1	RAFTER 348.5x125xUB33	L	3.0	290	14.24	186.8
2	RAFTER 348.5x125xUB33	STR-GAUGE 58,59,60	3.0	254	14.64	166.5
3	FAFTER 348.5x125xUB33	STR-GAUGE 64,65,66	2.5	320	15.75	175
4	RAFTER 348.5x125xUB33	STR-GAUGE 86,87,88	2.5	332	15.06	186.3
5	COLUMN 406x178xUB54	STR-GAUGE 6,7,8	3.4	485	7.49	375

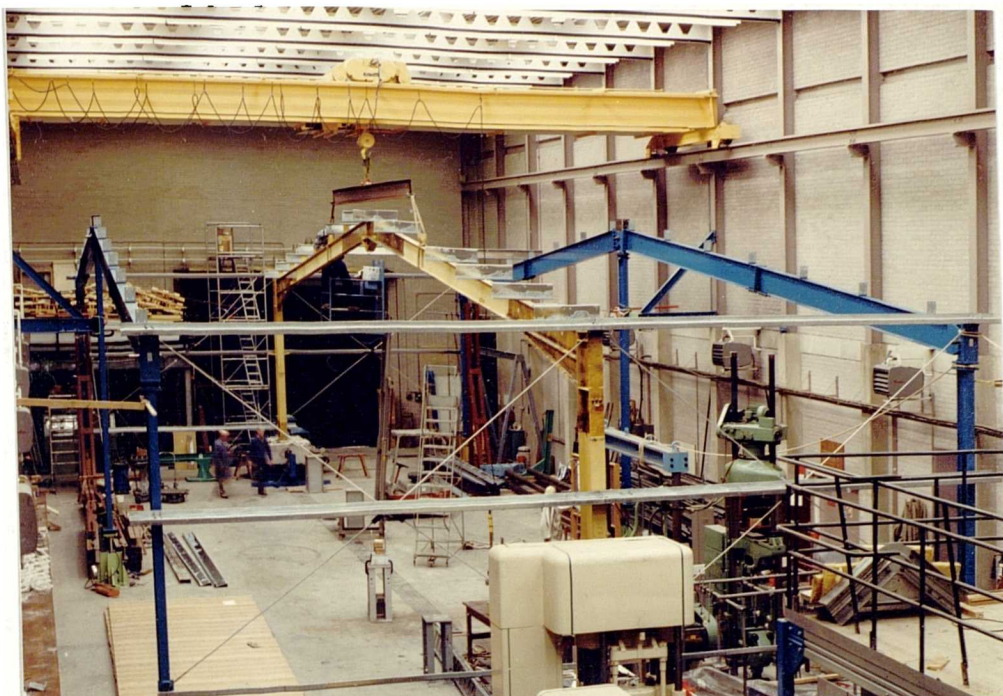


Plate 2.1 Assembly of the Test Frame Prior to Sheeting

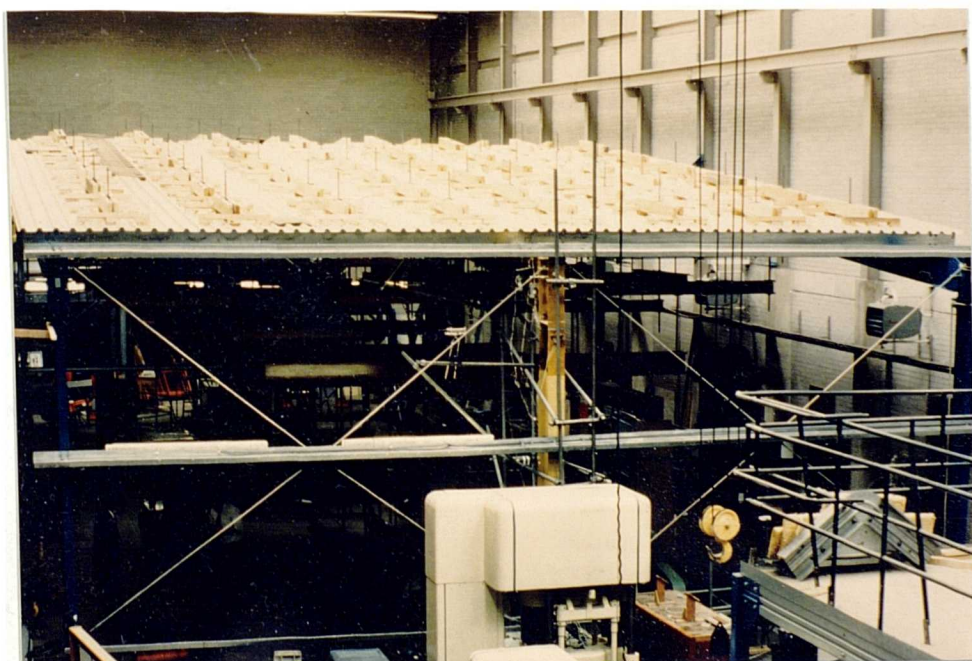


Plate 2.2 The General View of the Assembly During Testing



Plate 2.3 Internal View Showing the Loading Arrangement

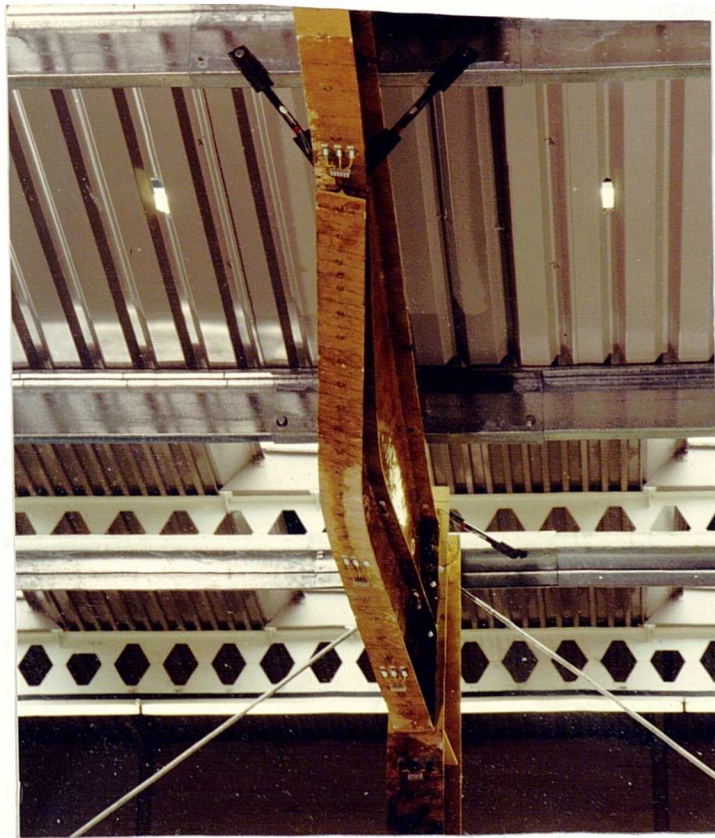


Plate 2.4 Detail of the Haunch Failed by Lateral-Torsional Buckling

CHAPTER 3

3.0 Literature Review of the Lateral-Torsional Buckling of Tapered Members.

3.1 Introduction.

In the design of steel portal frame structures, greater economy can be achieved if member sections in the regions of low bending moment are reduced. In order to achieve this, the members may be tapered or haunched in order to suit the bending moment distributions. The aim in that exercise is to vary the cross-section so that a more uniform stress is obtained along the members.

However, economy in the design can only be fully realised if the strength of the member is governed by the full plastic moment capacity of the section. In most cases, especially for members with I-section, the tendency is for lateral-torsional buckling to occur before the full plastic moment is significant if the lateral support is not adequate. This problem of premature failure can become particularly acute with the use of deep sections. This typically arises in the haunch region of the modern portal frame. At the deep part of the haunch, often the web may have a depth to thickness ratio several times the value for a standard I-section. Hence, stability of the rafter and column with respect to lateral-torsional buckling is

frequently a ruling factor in the design of portal frame structures. This has been shown by the results of the full-scale test on Frame 3, when the frame failed by lateral-torsional buckling at the haunch. Therefore it is important to derive efficient solutions to the lateral-torsional buckling problems involved so that the design capacity of these members can easily be determined.

The design rules provided by the codes are often based on theoretical and experimental findings. It is important therefore to understand the behaviour of the structures undergoing lateral-torsional buckling in order to address the problems in design stage. In this chapter a review of the theoretical studies of the problem of lateral-torsional buckling of tapered members is presented. It is divided into two parts namely;

- (i) The historical background to the study of tapered members, and
- (ii) Review of various methods used to analyse lateral-torsional buckling of tapered I-beams.

3.2 Historical Background to the Study of Tapered Member.

The elastic-flexural-torsional buckling of prismatic I-sections under transverse loading has been examined and documented since the early work of Timoshenko (3.1). Research in this area includes simply supported beams,

cantilevers, and continuous beams (3.2, 3.3). Subsequently, comprehensive treatments of this subject are available in a number of texts (3.4, 3.5, 3.6, 3.7).

However, the stability of tapered members has been less well studied and a limited number of investigations to study the corresponding behaviour of tapered I-sections have been made. The literature search conducted as part of the present investigation revealed that the work on tapered members can be traced back to 1908, when Timoshenko (3.1) studied the buckling of bars of varying cross-section. In 1917, Morley (3.8) studied the critical loads of long tapering struts. In the late 1920s, Dinnik (3.9) presented a method of design for columns of varying cross sections. This was followed in the 1930s by Nakagawa (3.10) who studied the buckling of columns with tapering parts. Little progress in this area of study seems to have prevailed during 1940s but it gathered momentum again in the 1950s. The outbreak of the Second World War could be the reason for the interruption of this study in the 1940s. For more detailed consideration, the study of tapered members can conveniently be divided into four areas namely, beams, columns, beam-columns and frames. These are considered in the following sections.

3.2.1 Previous Studies of Tapered Beams.

In 1952 Boley and Zimnoch (3.11) reported their

investigations of the application of a numerical method that they had developed for the problem of the lateral buckling of tapered members. They found the analysis by either differential equations or energy considerations proposed by Timoshenko (3.1) for uniform members to be difficult to apply to tapered members. The approach that they adopted was to make use of influence coefficients to derive a set of simultaneous linear algebraic equations and, from these, the buckling load was calculated. This method was used in a number of examples for both uniform and tapered cantilever beams with various loading conditions. Satisfactory results were obtained in all examples when six degrees of freedom were used and they concluded that the buckling load calculated by this procedure are on the safe side.

In 1956, Lee (3.12) reported an analysis which he had made of tapered I-beams in non-uniform torsion. In his analysis, he considered a tapered I-beam to consist of three tapered plates of rectangular cross section with the two flanges subjected to both bending and torsion. In this case the web was assumed to take only part of the Saint Venant Torsion. In his analysis of the tapered plates he found that, for small values of the angle of taper, the expression for longitudinal stress coincided with that given by the elementary beam formula. Similarly the moment-curvature relationship along the centre line could be closely approximated by the elementary beam formula. He also verified through experiments that the variation of the angle

of twist agreed almost exactly with that determined by the modified Saint Venant torsional relationship for members under uniform torsion. His analysis of the tapered I-beam was based on those two considerations.

In his analysis, Lee first established the condition for rotational equilibrium which is the summation of the Saint Venant torque, the sum of the x-components of the bending moments in the flanges and the shear couple developed by the bending in the flanges. Since he considered the tapered I-beam as an aggregate of the three tapered plates he could then use the relevant expressions to determine the components of the rotational equilibrium and thus he established the differential equation for torsion. He then used a power series to solve this differential equation.

In 1959, Krefeld, Butler and Anderson (3.13) reported their investigation of the formulation of criteria predicting the load carrying capacity of steel cantilever beams having tapered flanges and webs. Their work essentially narrowed down to the experimental determination of the critical stresses at which such beams buckle elastically. They conducted tests on beams having both I and channel sections, with various dimensions, span lengths and degrees of taper. They also conducted load tests on straight untapered beams. An empirical relationship for predicting the load capacity of the tapered cantilever beam was obtained by comparing the load producing elastic buckling of a tapered beam, with that of a straight beam having the same section at the support.

The ratio of capacities, called a "reduction factor," was expressed as a function of the support dimensions and the degree of taper. Their investigation established this empirically-derived "reduction factor" for tapered cantilever beams which permitted prediction of the critical elastic-buckling stress at the support for beams with any taper, when the critical stress for an untapered beam having the same support section is known.

In the same year, Lee (3.14) studied the case of elastic lateral buckling of a tapered rectangular beam subjected to pure bending in its plane. He approached the critical moment and the corresponding angular rotation expressions by considering the familiar equilibrium method used in stability analysis. He derived differential equations to determine the longitudinal deformation of the beam based on the moment-curvature and torque-rotation relationships for tapered rectangular plates (3.12). These equations were found to be similar to the analogous system of equations for a beam of constant cross section (3.7) except for the variation of the flexural rigidities and the torsional rigidity to account for the tapering along the member. Homogeneous linear equations were established and solved for the boundary conditions before arriving at the results.

Venkayya (3.15), in 1961 investigated the stability of an I-beam whose depth increased parabolically from the centre. He considered cases of beams loaded by central concentrated

loads or uniformly distributed loads. He allowed for the effect of continuity with adjacent beams and restraining moments in the same way as Austin, Yegian, and Tung (3.16). In his analysis, he made some simplifying assumptions about the variation of the torsional rigidity and tabulated his solutions obtained by the Ritz variational technique.

In 1966, Butler (3.17) presented results of an experimental investigation which studied the influence of lateral and torsional bracing on the elastic buckling strength of tip loaded, tapered, cantilever I-beams. The results of these tests provided some empirical information on bracing requirements.

Lee and Szabo (3.18), in 1967 derived a differential equation of torsion for a tapered I-beam. They derived the differential equation starting from first principles and taking into account Saint Venant's torsion, warping, and secondary torsional stiffnesses. They also showed that the well-known differential equation of torsion developed by Timoshenko (3.7) is a special case of this differential equation. The boundary conditions of the mathematical problem were established for some practical cases. They obtained an analytical solution for a uniformly loaded, linearly tapered, cantilever I-beam and found that the results given by this solution were in close agreement with those obtained by finite difference methods. They also obtained a number of finite difference solutions for both

prismatic and tapered I-beams subjected to a variety of end constraints.

In 1972, Kittipornchai and Trahair (3.19) reported the findings of their studies on the elastic buckling of tapered I-beams considering the effects of transverse loads and their points of application in relation to the shear centres. They developed a general method of analysis which can be applied to the elastic buckling of any tapered I-beam with any type of loading. They then used this method to study the effect of tapering flange widths, flange thicknesses, and web depths on the theoretical elastic critical loads of simply supported I-beams. Experimental investigations conducted on beams with flange width or thickness taper or web-depth taper gave results in reasonable agreement with the theoretical predictions.

In the same year Lee, Morrell and Ketter (3.20) developed buckling solutions for linearly web-tapered beams with idealised simple supports. By using the Rayleigh-Ritz method they formed the total potential energy equation accounting for the sloping flange resistance and the critical moment. The displacements were approximated by polynomial series.

In 1974, Lee and Morrell (3.21) improved the allowable bending stress equation proposed in their earlier work (3.20) for web tapered beams by incorporating the total resistance to lateral buckling and the restraining effects

of adjacent spans. They investigated the design approximation for the allowable critical stress suggested by the Column Research Council Guide to Compression Members (3.5) for a simply supported beam and proposed a new equation for allowable bending stress that included relevant parameters for tapered members. They used the finite element method to investigate the restraining effects of adjacent beams. They noted that the finite element solutions were more accurate and that the Raleigh-Ritz method was potentially unsafe.

The work on tapered members was continued by Horne, Shakir-Khalil and Akhtar (3.22). In 1979, they reported an investigation on the elastic critical behaviour of tapered and haunched I-beams restrained at intervals on a longitudinal axis near the tension flange, causing buckling to occur by twisting about the restrained axis. They proposed approximate formulae for estimating the critical loads of haunched members subjected to arbitrary bending moment distribution and justified it by reference to examples for which accurate solutions had previously been obtained. They also extended this approximate treatment to the derivation of the maximum permissible slenderness ratio appropriate to haunched rafters, laterally supported on the top flange by purlins, when the rafter is assumed to contain a plastic hinge at the end of the tapered part.

They conducted tests on tapered and haunched beams (3.23),

supported at intervals along the tension flange in order to check the ability for the beams to undergo plastic deformation without significant reduction in the moment of resistance. The beams were designed to be near the limiting slenderness judged to be satisfactory for this purpose on a theoretical basis. In the test program, three tapered and eight haunched beams were tested to check the validity of the method they had suggested (3.22) for determining the maximum permissible unbraced length of an inelastic beam. The tapered beams were subjected to unequal end moments and were provided at the end with supports which satisfied the boundary conditions generally assumed in theoretical analysis. The haunched beams were tested as cantilevers loaded at the shallower end which was laterally braced, and the support at the deeper end represented the condition at the column-rafter joint of a pitched portal frame. All of the test beams were provided with discrete point lateral restraint along the tension flange, corresponding to the form of restraints against lateral movement provided in practice by roof purlins. The results of the tests conducted indicated that the theoretical approach adopted was satisfactory.

Brown (3.24) in 1981 studied the lateral-torsional buckling behaviour of tapered beams of both simply supported and cantilever form. He determined the critical loads using the finite difference method. In his study he also paid particular attention to the location (with respect to the

centroid) of the transverse load. In his analysis he derived the displacement equations for a buckled I-section and worked out the buckling strain equations. From energy considerations he developed the equations for the total change in the potential energy. A series of differential equations were developed and approximated using finite differences leading to a matrix eigenvalue equation of quadratic form. Using the direct solution (3.24) of the quadratic characteristic equation, the effects of load placed either above or below the centroid were also included. The problem was then solved by a conventional eigenvalue program.

In 1988, Bradford (3.25) examined the proposals of the British and Australian limit states design codes for the instability limit state of tapered I-beams. He pointed out that the provisions of the codes were based on a limited analysis of only a few geometrical and loading conditions and are therefore approximate. In his study, he used the finite element method that he had developed earlier (3.26) to derive parametric solutions for the elastic lateral buckling of tapered beams. This method was shown to be accurate and to converge rapidly. He then proposed a method of design, based on inelastic buckling, which transformed the accurate elastic solutions into member strengths. He worked out an example and demonstrated that little additional effort is required to use the accurate design curves than is needed in the codes.

3.2.2 Previous Studies of Tapered Columns

Gatewood (3.27) in 1954 presented curves for the buckling coefficient for columns of variable cross section for all taper ratios and for variations of the moment of inertia between constant and sixth power. He also presented curves for the lateral buckling coefficients of cantilever beams with the same variations as for the column case and gave interaction curves for buckling coefficient under combined lateral and compression loads on the beam.

In 1962, Gere and Carter (3.28) presented formulae and graphs for the determination of elastic critical buckling loads of uniformly tapered columns having different values of the end depth ratio and shape factors for columns with pinned ends, fixed-free ends, fixed-pinned and fixed ends. In their study, they first defined the shape factor and this can be found readily when the dimensions of the end cross-section of the column are known. For columns with wide flanged shape i.e I-section, or closed box sections, it was found that the shape factor tended to be between $n=2.1$ and $n=2.6$ for all columns of realistic cross-sectional proportions and taper.

They considered various methods for determining the theoretical buckling loads of columns including solutions of the differential equation of the deflection curve and the

method of successive approximation of the deflection curve (3.7). They carried out the successive-approximation calculations on a computer.

The general solution of the differential equation of the deflection curve of a slightly bent, ideal column was obtained in terms of Bessel functions. After applying the appropriate boundary conditions, these provided a means of obtaining an equation for critical buckling load. Most of these solutions were highly transcendental and must be solved by trial-and-error or iterative methods. They solved all of the cases under consideration using such methods (in combination with successive-approximation calculations) thus providing duplicate sets of numerical results that were used in plotting the graphs of the buckling load. Critical elastic buckling loads for uniformly tapered columns having various end conditions may be obtained directly from the graphs plotted.

In 1963, Butler and Anderson (3.29) presented the results of their tests to determine the elastic buckling strength of tapered steel I-beams under pure axial thrust and under combined bending and thrust. The results of their pure thrust tests showed excellent agreement with Nakagawa's theoretical solution (3.10) for the elastic buckling of tapered columns appropriate to the test conditions and specimens employed.

In 1984, Olowokere (3.30) reported his numerical work on the development of the lateral-torsional buckling load equation for linearly tapered I-section members with unequal flange areas. He used a finite element method to solve the equations. Solutions were obtained for different flange area ratios and taper ratios. These solutions were used to develop an interaction relationship for tapered unequal flanged steel structural columns subjected to both axial and bending stresses. In order to check the accuracy of the results obtained, some special cases were considered and compared with the AISC design formulae. From the comparison it was shown that the results from the study underestimated the load carrying capacity of the member, although there was an adequate comparison for practical purposes.

Emorpoulos in 1986 (3.31) examined the case of tapered bars axially compressed by concentrated loads applied at various locations along their axes. On the basis of linear stability analysis he derived the buckling equations of axially compressed tapered bars. The axial compressive loads were concentrated and applied at several points on the centre-line of the bar. The law of stiffness variation which he used covers mainly members of steel structures and is also valid for I-sections.

From the buckling equations, the determination of the critical loads of the bars was achieved. He derived three sets of equations for three different boundary conditions.

By solving the critical buckling equation, dimensionless critical loads were evaluated as functions of the parameters for all the three cases considered. Graphs of the dimensionless critical load against the aforementioned parameters were also plotted. From this study, he concluded that for every combination of parameters considered and for all of the support conditions examined, estimates of the critical load of an axially loaded tapered bar can easily be made.

Most recently, in 1989, Williams and Aston (3.32) presented curves that enabled buckling loads to be found for tapered columns with a uniform compressive axial force applied over the length L or over all except BL of their length, where BL is a length measured from the smaller end. These curves covered six combinations of end conditions; with $r=0.05$ and 1 , $B=0$ and 0.9 , and $h=2, 3$, and 4 . Where, r is the ratio of the second moment of area at the smaller end to the second moment of area at the larger end and h is the power which governs how the second moment of area varies along the length of the column.

Their evaluation of the accuracy of the method, which uses the curves to obtain lower bound approximations to the critical load factor c for a stepped distribution of axial force, shows that, for the majority of practical problems, the error will be below 10%. However, even if the error is larger, it will always be on the safe side and so will only

cause loss of economy, not loss of safety.

3.2.3 Previous Studies of Tapered Beam-Column.

The work of Butler and Anderson (3.29) in 1963 which determined the elastic buckling strength of tapered steel I-beams under combined bending and stress had led to the establishment of a bending-thrust interaction curve for tapered I-beam-columns. This curve was essentially independent of the amount of taper. The results gave good agreement with other theoretical results (3.33) obtained for beams of uniform cross-section.

In 1968, Culver and Preg (3.34) investigated the behaviour of tapered beam-columns with unequal end moments. They derived differential equations for determining the critical combinations of axial load and end moments for tapered WF beam-columns. This derivation was based on an equilibrium analysis of the buckled deflected shape of the beam column. They evaluated the critical end moments for tapered beams and the critical load for tapered columns by the method of finite differences. These critical moments and loads can be used in an interaction formula which can then be solved for the critical load and moment combination for beam-columns.

The experimental work by Krefeld, Butler and Anderson (3.29, 3.13) was extended by Prawell, Morrell and Lee (3.35) to

include the effect of axial inclination of cantilevered beam-columns and the effect of intermediate lateral restraints on simply supported beams. Their report, which was published in 1974 summarized the results of an experimental program to determine the bending and buckling strength of several linearly tapered members whose cross-sectional dimensions were similar to those found in practice. In that research program they also attempted to find information relating to the effect of the fabrication process, namely the behaviour of members made of oxygen cut plates and shear cut plates.

As an integral part of the project, an analytical procedure to predict the inplane behaviour of tapered beam-columns was also developed. The major effort of this part was the development of families of moment curvature curves for tapered members. With the availability of these curves, the bending deformation could be obtained by a simple double integration process. A computer program was also developed to compute the beam-column deformation by a step by step integration of the moment curvature relationship. The results of the tests indicated that the procedure used in the fabrication process of a tapered member has a decisive effect upon the elastic response of the member. Members cut using the oxygen flame appear to have a higher inelastic lateral buckling strength. The results also pointed out that local buckling in the compression flange near the end of the member generally led directly to failure. The larger the

angle of taper, the more pronounced was the local buckling effect. The analytical procedure developed satisfactorily predicted the inplane bending behaviour of the tapered member up to the point at which buckling occurred.

In 1980, Salter, Anderson and May (3.36) reported a test program conducted to test web-tapered steel columns which were subjected to axial load and major axis bending moment. They tested eight members each being half to one-third full size web-tapered I-section column specimens fabricated from plate by welding. In the tests the specimens were subjected to compressive axial load together with a major axis moment applied at the deep end of each member. No applied moment or rotational restraint was provided about either principal axis at the shallow end. These conditions represent those arising in the column of a pinned based portal frame, for which the ratio of the end moments is zero. In the tests, full rotational freedom was allowed at the deep end of each of the test columns. However, twisting and warping were prevented at both ends as joint details in tapered frames usually include endplates that approximate to such restraints. The ends of the columns were also held against sway about both principal axes. The parameters that varied in the tests were angle of taper, the ratio of axial load to the Euler load, member length and the position of intermediate restraints.

The results of the tests conducted showed that the five

columns without intermediate restraint failed by lateral or lateral-torsional inelastic buckling. These results show reasonable agreement with the computed failure load given by a biaxial non-linear elasto-plastic analysis program (3.37) which was originally written for a uniform member. From the analyses of the results they also pointed that the load capacity given by BS 449 and the then Draft British Limit State Standard were on the conservative side.

In 1984, Shiomi and Kurata (3.38) reported their numerical analysis and experimental investigation into the ultimate strength of tapered beam-columns in order to obtain information concerning practical design formulae. An interaction formula for the ultimate strength of tapered I-shaped and box-shaped beam-columns was presented for use in practical design. Tapered members subjected to axial compression force or bending moment were analysed by a non-linear inelastic computer program using the transfer matrix method. An equivalent length factor was then developed in order to permit the extension of an empirical interaction equation for prismatic beam-columns to tapered beam-columns using a statistical technique.

Their numerical analysis was performed based on the following idealisations:

- 1) The tapered member was divided into 30 segments, and each segment was assumed to have a uniform cross-section and to be subjected to uniform

moment.

- 2) The perfectly elastic stress-strain curve was used as a stress-strain relationship and strain hardening was neglected.
- 3) The flexural rigidity and warping rigidity of the segments were estimated using the *tangent modulus* theory and torsional rigidity was estimated by plastic flow theory.
- 4) The pattern of residual stress distribution was idealised from actual measurements.

They separately studied the cases of centrally loaded tapered columns and tapered beams with end moments applied at the larger end.

For the case of centrally-loaded, tapered columns, they derived the conditional equation for inelastic buckling and found it to have a similar form to that for elastic buckling. The buckling strength of the member was obtained from this equation. They conducted analyses on a large number of specimens that were chosen by considering the combination of the slenderness ratio L/r about the x axis based on the smaller end section and the ratio of the member depth at both ends. For the case of tapered beams with end moments applied at the larger end, they used the differential equation proposed by Galambos (3.6) in order to express the lateral torsional buckling of a segment subjected to uniform bending moment. From the solution the necessary function can be arranged in a matrix form. The

conditional equation for buckling can then be expressed. The critical moment for inelastic buckling was obtained in the same way as for the column. Again, a large number of specimens were chosen for this computer analysis in a similar way as for the column.

From the numerical results, the equivalent length factor was determined by a statistical method in order to substitute a prismatic member for a tapered one. They worked out the equivalent length for both tapered beams and columns. They also extended the work in order to study the interaction formula for the ultimate strength of the prismatic beam-column, subjected to thrust and moments acting at both ends. They found that the formula remains applicable since the tapered beam-column can be transformed to an equivalent beam-column.

In their experimental studies they tested 24 full size I-section beam-column specimens. Each of the specimens was fabricated by double fillet welding of the flange plates along the edges of web plate.

Their load deflection curves indicated that under smaller loads the location of the maximum deflection coincided with that obtained using elastic calculation. Under larger loads, however, the maximum deflection occurred at a point deviated from the centre of the member towards the smaller end.

A comparison of the test results with the results from the equivalent beam-column equation showed that the scattering of test points was not very great and this led to the conclusion that the equation provided a safe estimate of the lower bound to the test results.

In 1988, Bradford and Cuk (3.26) presented a finite element method of analysis that is capable of making accurate predictions of the elastic buckling load of tapered, monosymmetric I-section beam-columns. The finite element method that they presented was superior to the use of uniform elements, in that it correctly caters for the effects of non-uniformity. This was achieved by abandoning the usual shear centre and centroidal axis system in the development of the line element. The element used a convenient and arbitrary Cartesian axis system passing through the mid-height of the web as the reference axis for lateral displacement and twists. The stiffness and stability matrices were easily calculated by making the assumption of an arbitrary axis of twist. The accuracy of the method was shown by comparison with independent solutions. It converged rapidly when compared with a finite element representation that used uniform elements. Furthermore very few elements were required to obtain an accurate solution. They concluded that the tapered element may therefore be employed to study parametrically the stability of tapered beams, columns and beam-columns.

3.2.4 Previous Studies of Portal Frames with Tapered and Haunched Members

Chapter 1 of this thesis reviewed some of the experimental research on portal frame structures carried out in the past fifty years. However, the specific subject of portal frames with tapered and haunched members was not thoroughly dealt with. This section covers some of the work which was mentioned in that review.

Perhaps the first full scale test on a tapered portal frame was that conducted by Leeming and Redshaw (3.39) in 1939. However, their test was not directly applicable to low rise buildings but to portal frame bridges. The test was carried out on portal frame girders for the Kiddington Canal Bridge in Oxfordshire, with the objective of finding out how far the thrust, stresses and deflections observed agreed with those calculated in the course of the design. They tested two portal frame girders simultaneously. These were positioned horizontally on greased rails, foot to foot, and bolted together with a tie plate between the base plates. The results of their tests showed some agreement with the calculated values. However, they observed higher compressive stresses in the region around the knee than calculated, even when curved bar theory was used. They concluded that the method of design which was based on Mohr's theorem could be used with some confidence but called for more work to study the problem of stress concentration around the knee.

It was described that the work on portal frames in the early days concentrated on the elastic behaviour of the structure and therefore no conclusion can be made regarding the collapse behaviour. The work on portal frame structures shifted in another direction in the early 1940s and early 1950s when research at Cambridge led by Baker (3.40, 3.41, 3.42) concentrated on the plastic range of behaviour and the collapse mechanisms of the frames. Miniature frames with fixed bases were often used in these studies. This work led to the successful development of the plastic design method.

In 1977, Just (3.43) formulated stiffness matrices which he used in the analysis of tapered beams and which he later used to solve pitched portal frames composed of tapering thin I-sections subjected to point loads. Instead of adopting the then common approach to the study of tapering beams, which considered the member to be approximately equivalent to a number of prismatic portions, he used the exact stiffness matrices in his analyses. This was made possible because the matrices, which do not depend on subdivision for their accuracy, could be obtained since the variation of the transverse and axial displacements can be expressed exactly. These displacement functions are dependent on the second moment of area and the cross-sectional area of the section. He also gave the expressions for the geometrical properties for both the thin and thick classes of box or I-sections. In order to obtain these matrices, the displacement function must be expressed in

terms of the geometry of the section and this consideration led to the general formulation of the exact stiffness matrices for linear elastic analysis. He verified the accuracy of the elements produced by comparing the analyses of two propped cantilevers of tapering I-section with a number of convergence solutions. To demonstrate the power and versatility of the approach the matrices were then used to solve a pitched portal frame structure composed of tapering thin I-sections subjected to point loads. The frame that was analysed had a span of 24 m with height to eaves of 24m and height of the ridge from eaves of 5m. The breadth of the sections was 300 mm while the depth varied from a minimum of 400 mm to a maximum of 1200 mm. The web and flange thicknesses were 15 mm, thus the section was classified as thin.

The frame was analysed under two loading configurations namely :

- (1) A vertical point load of 100 kN at the crown, and
- (2) A lateral point load of the same magnitude at an eaves point.

A five-joint analysis was carried out using the matrix derived for the thick section, that derived for thin sections and the approximate matrix obtained from the superposition of two solid sections. In addition, each member of the frame was considered to be of constant depth, and a solution obtained for the resulting prismatic frame.

The results obtained for both the thin and thick class of section were almost identical and the values obtained from the approximate matrix by superposition were also fairly accurate, while larger difference occurred when the members were considered to be prismatic.

In 1979, Al-Sarraff (3.44) reported his investigation of the elastic instability of frames with uniformly tapered members. He developed modified stability functions for uniformly tapered beam-columns having wide flanges, box sections and other cross-sectional shapes and tabulated the results for different values of axial parameters, end depth ratios and shape factors. From these tables rapid predictions of the elastic critical loads of structures with non-prismatic members can be calculated. He demonstrated this by solving two numerical examples of frames with tapered members.

In 1983, Fraser (3.45) reported a parametric study of the buckling of tapered members and haunched member frames. These were both rectangular and pitched roofed. His approach was to develop formulae that would allow the conversion of the non-uniform frame into an equivalent uniform frame with the same buckling load. In this study, he only considered completely symmetrical frames with pinned or fixed bases.

The equivalent frame was visualised as retaining the same geometry as the real non-uniform frame by substituting a

uniform section for the non-uniform section. He presented conversion formulae for four types of frames. They were as follows:

- (1) Tapered member frame - fixed base
- (2) Tapered member frame - pinned base
- (3) Haunched member frame - fixed base
- (4) Haunched member frame - pinned base

He demonstrated the application by considering two numerical examples one of the examples gave a result comparable with that obtained using the AISC method (3.33).

3.3 Review of Available Methods to Analyse the Lateral Buckling of Tapered I-Beams

3.3.1 General

The buckling solutions previously obtained for tapered I-beams and beam-columns have been numerical. The methods that have been used are the Finite Integral Method, the Finite Element Method, the Finite Difference Method and a Power Series Method. In this section, the available flexural torsional buckling methods of analyses mentioned are summarised and one is chosen for further study.

3.3.2 Solutions by Finite Integral Method

The finite integral method is an approximate technique for solving complex differential equations. The method is based on considering the differential equation as an integral equation in the highest derivative of the dependent variable $f(x)$. The length l of the beam is divided into a number of equal parts n of length b , where $b=l/n$. The integral equation is then replaced by a finite number of homogeneous equations one for each point. The dependent variable $f(x)$ and its lower derivatives are replaced by a combination of the values of highest derivatives of $f(x)$.

The application of this method in the study of buckling of a tapered I-beam can be illustrated by the work of Kitipornchai and Trahair (3.19). They considered a case of a beam as shown in figure 3.1, where a central concentrated load P is applied at a distance ' \bar{a} ' above the shear centre. The ends of the beam are free to rotate about the major and minor axes, but are restrained against rotation about the longitudinal axis, so that the angle of twist remains zero at the ends. The cross sections of the beam at the end are free to warp.

The governing differential equations for buckling of the beam were obtained by considering the deflected shape shown in figure 3.2. A computer program was then prepared to solve the differential equations for the critical load parameter

γ by using finite integral solutions.

In the finite integral method, it is assumed that the variation of the dependent function 'f' is approximately parabolic with 'x' so that a parabola $f=ax^2 + bx + c$ can be fitted to three adjacent values f_i, f_{i+1}, f_{i+2} of f. Assuming the corresponding values x_i, x_{i+1}, x_{i+2} of x are equally spaced so that $x_{i+2} - x_{i+1} = x_{i+1} - x_i = L$ the interval size, then the expressions for a, b and c can be obtained in terms of f and x. The integral f was then derived from the approximating parabola by Simpson's rule. Thus if the integral I of the function f is defined by;

$$I_i = \int_0^{ih} f dx \dots \dots \dots (3.1)$$

this can be approximated by matrix equation;

$$[I] = \frac{h}{2} \cdot [N] \cdot [f] \dots \dots \dots (3.2)$$

where [I] is the vector $[I_0, I_1, I_2, \dots, I_n]$, [f] is the vector $[f_0, f_1, f_2, \dots, f_n]$, and the integral operator N is a square matrix of size $n+1$.

The function I, like f, may be approximated by a series of parabolas so that the second integral m of function f defined by

$$m_j = \int_0^{jh} I \cdot dx \dots = \int_0^{jh} \int_0^x f \cdot dx \cdot dx \dots \dots \dots (3.3)$$

can be approximated by

$$[m] = \frac{h^3}{144} [N] \cdot [N] \cdot [f] \dots \dots \dots (3.4)$$

Hence by employing this technique an approximate solution can be obtained.

3.3.3 Solutions by the Finite Element Method

Presently, the most widely used numerical methods for statically analysing structures with non-uniform beams is the finite element method. Nethercot (3.46), Karabalis and Beskos (3.47) and Bradford (3.25, 3.26)^{*} have used this method to solve buckling problems of tapered beams. Since the first application of finite element analysis, many different elements have been developed to predict realistically the physical behaviour of material, elements, components and structures. In this section, only the "beam" element (figure 3.3) is considered and therefore all discussions are directed to this type of element. Nemir (3.48) studied the stability of thin-walled steel structures by this finite element method and developed a formulation which can also be used for lateral-torsional buckling of tapered beams. This finite element formulation which was an advancement of the work of Barsoum and Gallagher (3.49) was originally based on Vlasov's concept (3.50) on the general behaviour of thin-walled members. It is valid for any cross-sectional shape and since it also includes new terms representing the bimoment influence, therefore it is valid for sections with no axes of symmetry. This formulation

which is used in the study of tapered I-beams in this thesis is discussed in chapter 4.

In the finite element method, a tapered member is broken into a number of uniform beam elements (stepped representation) with known stiffnesses, which are superimposed to produce the stiffness of the member. A set of displacements is used to describe approximately the deformed state of the structure in terms of the displacements at the nodal points. The solution is then formulated for each typified unit and then combined to obtain the solution for the whole beam.

In the conventional analysis of an elastic linear structure by the finite element method, the energy concept is often used to derive the first order stiffness matrix of the element. The energy concept can also be employed in elastic buckling problems to establish the second order load displacement relationship. In elastic buckling problems, the conventional linear stiffness matrix $[K_e]$ is supplemented by another matrix $[K_g]$ called geometric (stability) matrix. This matrix represents the elastic effect of the applied loads on the buckling deformations.

For a condition of stable equilibrium, where the load factor is of a value less than its critical value, the element stiffness equation given by the first variation of the potential energy expression becomes;

$$\{P\} = [K_E] \cdot \{\Delta\} + [K_G] \cdot \{\Delta\} \dots \dots \dots (3.5)$$

in which $\{\Delta\}$ is the nodal displacement vector. Equation 3.5 represents the second order behaviour of the element.

In elastic stability problems it is usually assumed that pre-buckling deformations have taken place and that the analysis is being conducted at a near buckling state. Equation 3.5 can be then modified to,

$$\{dP\} = ([K_E] + [K_G]) \cdot \{d\Delta\} \dots \dots \dots (3.6)$$

in which, $\{d\Delta\}$ is the matrix of vanishing small increments of the displacements and $\{dP\}$ is the matrix of corresponding forces.

At the critical load, more than one equilibrium state is possible and the deformation of the structure corresponding to a given load factor can reach infinite values for arbitrarily small load increments. Thus at the buckling stage equation 3.6 becomes,

$$[K_E] + \lambda_c [K_G] \cdot \{d\Delta\} = 0 \dots \dots \dots (3.7)$$

where $\{d\Delta\}$ represents the buckling deformations and λ_c is an instability parameter (i.e., eigenvalue).

The analysis begins with a chosen value of the applied load from which the individual element end forces are calculated through a pre-buckling analysis. These end forces can then be used to formulate the geometric matrix $[K_G]$. The critical

load is equal to the instability parameter λ_c times the chosen value of the load factor. The instability problem then becomes an eigenvalue problem of finding the instability parameter λ_c from the non-trivial solution of equation 3.7. Such a solution exists when,

$$|K_E| + \lambda_c |K_G| = 0 \dots \dots \dots (3.8)$$

in which, $|K_E|$ and $|K_G|$ are the two determinants corresponding to the stiffness matrices $[K_E]$ and $[K_G]$ respectively.

3.3.4 Solutions by the Finite Difference Method

The finite difference method is yet another approximate method for solving complex differential equations. This method can be applied to stability problems to give approximate values for buckling loads. The method is based on replacing the differential equation, which is applicable over a certain range of an independent variable x , by a finite number of algebraic equations, one for each of a number of points within the range of x . At each point, the differential operators of the dependent function $f(x)$ are represented by finite difference approximations which can be given as combinations of the value of $f(x)$ of neighbouring points, assuming some polynomial shape for the $f(x)$ values. The boundary conditions of the differential equations are represented in the same way. The solution of the resulting

homogenous equations gives the desired unknowns of the problem.

The application of the method to buckling problems for tapered beams can be illustrated by the work of Brown (3.24). He studied the cases of tapered beams and cantilevers and obtained the solutions of the differential equations using the finite difference method. The eigenvalue equation of structural stability for a doubly symmetric I-section was developed by displacement functions and energy considerations.

The differential equation obtained from the exercise was approximated by using central finite differences (3.51), leading to a matrix eigenvalue equation of the form;

$$[C] \cdot \{\beta\} - p \cdot [\beta] \cdot \{\beta\} - p^2 \cdot [A] \cdot \{\beta\} = 0 \dots \dots \dots (3.9)$$

This equation is of quadratic form and therefore does not lend itself to the normal eigenvalue extraction techniques. It may, however be solved by the introduction (3.37) of;

$$\{\bar{\beta}\} = p \cdot \{\beta\} \dots \dots \dots (3.10)$$

Pre-multiplying equation 3.9 by $|A|^{-1}$ and combining equation 3.9 and 3.10 results in the equation;

$$\begin{bmatrix} [0] & [I] \\ [A]^{-1} [C] & -[A]^{-1} [\beta] \end{bmatrix} \begin{Bmatrix} \{\beta\} \\ \{\bar{\beta}\} \end{Bmatrix} = p \cdot \begin{Bmatrix} \{\beta\} \\ \{\bar{\beta}\} \end{Bmatrix} \dots \dots \dots (3.11)$$

from which eigenvalues can be extracted using any conventional eigenvalue program.

3.3.5 Solutions by Power Series Method

Lee, Morrell and Ketter (3.20) examined the use of the power series method to solve some problems of tapered I-sections. They considered a doubly symmetric tapered I-section for the general analysis. From consideration of the deformation parameter, they established the equation for virtual displacement of the beam, satisfying the prescribed geometrical boundary conditions for the beam in question. Assuming that the bending rigidity of the member about the Y axis was constant, the bending component of the first variation in the strain energy was established. The expression for non-uniform torsion was also established. It contains two sets of terms representing the flange bending strain energies due to warping and the pure torsional strain energy.

Given the specified linear variation in depth of the member, the first variation component of the non-uniform torsional strain energy was established. Considering the case of loading shown in figure 3.4 and relating the moment by a non-dimensional parameter, the equation of the external work done during the virtual displacement was established.

To obtain a solution to the inplane deformational and lateral stability behaviour of tapered members, the above mentioned equation could be used to establish the differential equation and the appropriate boundary

conditions. However, due to the complicated non-geometrical boundary conditions that are required to handle the torsion problem, and also because of the many difficulties that frequently are encountered when attempting to obtain direct solutions for these types of differential equations, Rayleigh-Ritz procedures are normally used to solve these equations.

3.3.6 The Selection of Method of Analysis

Four methods of analysis for buckling of tapered members have been summarised in the previous sections. Except for the finite element method, the other three methods provide solutions by means of approximate techniques for solving complex differential equations of the actual physical system.

In the finite element method a modified structural system consisting of discrete (finite) elements is substituted for the actual continuum and thus, the approximation is of a physical nature. Furthermore, there needs to be no approximation in the mathematical analysis of this substitute system. By intelligent modelling, various parameters of tapered members can be substituted for the actual physical ones and a wide range of studies can be carried out. Different properties of materials can also be incorporated in the modelling thus, rendering it into a very

versatile and powerful tool for the analysis.

3.4 Summary and Conclusions.

This chapter has reviewed previous work relating to the stability of tapered members. Whereas some experimental work has been reported, most the work is theoretical/numerical in nature.

The available methods of analysis for lateral-torsional buckling of tapered members have also been reviewed with a particular interest in the finite element method. This method appears to be suitable for the study undertaken in this thesis. Previously this method was confined to mainframe computer systems using some commercial Finite Element packages. However, the method can now be easily available on a PC-based system and proved to be cost effective for both the hardware and software.

In the next chapter, the finite element formulation and the computer program that is used in this study is described.

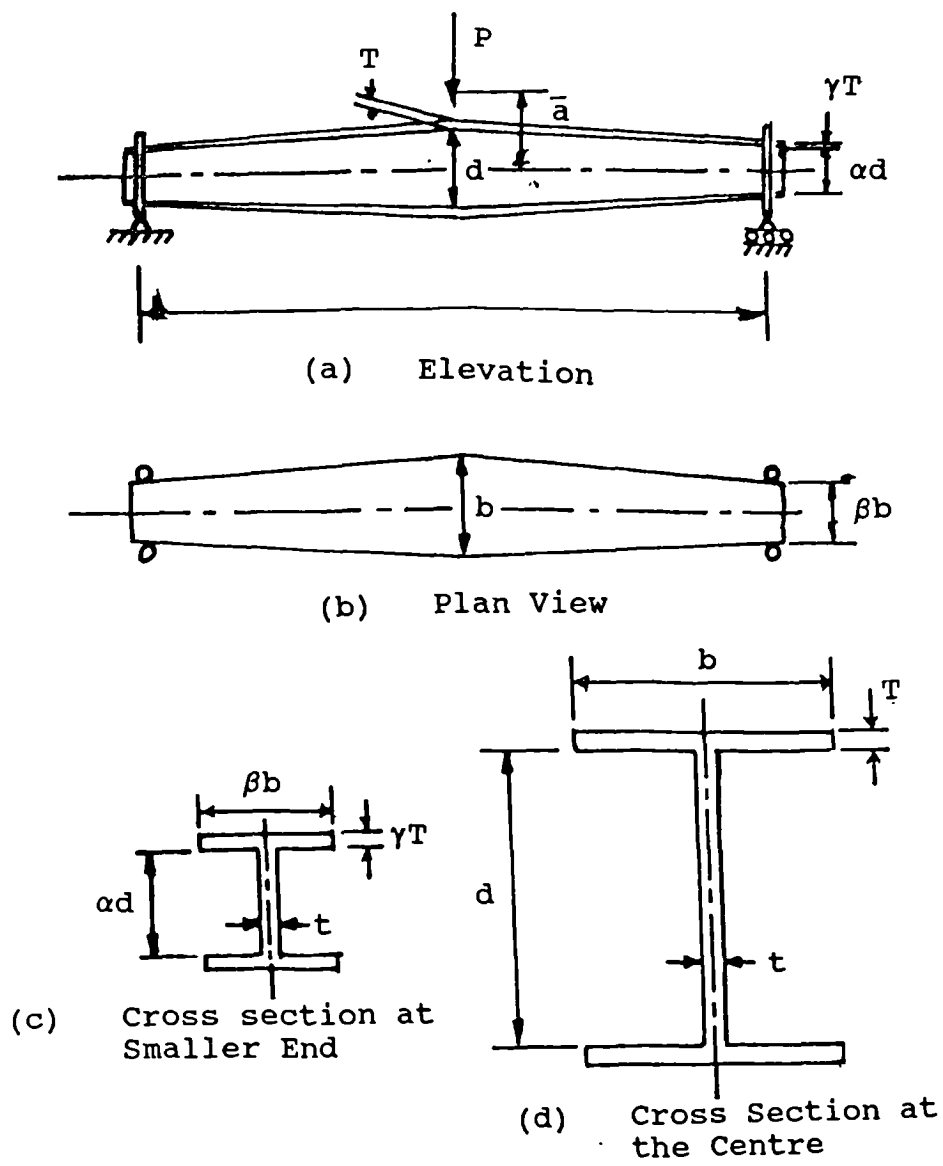


Figure 3.1 Simply Supported Tapered I-beam
Analysed by Kitipornchai (3.19)

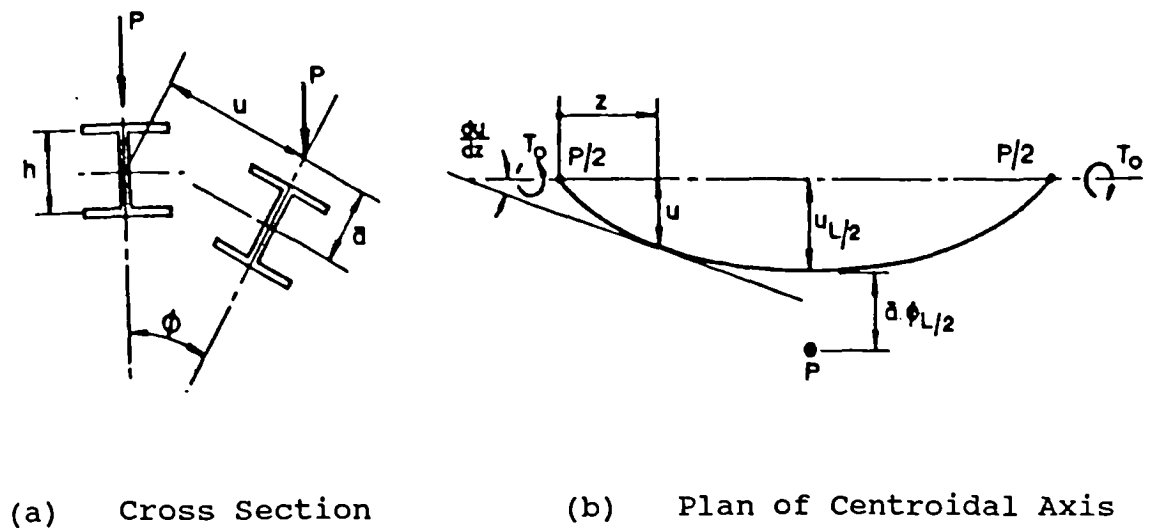


Figure 3.2 Shape of the Buckled Beam

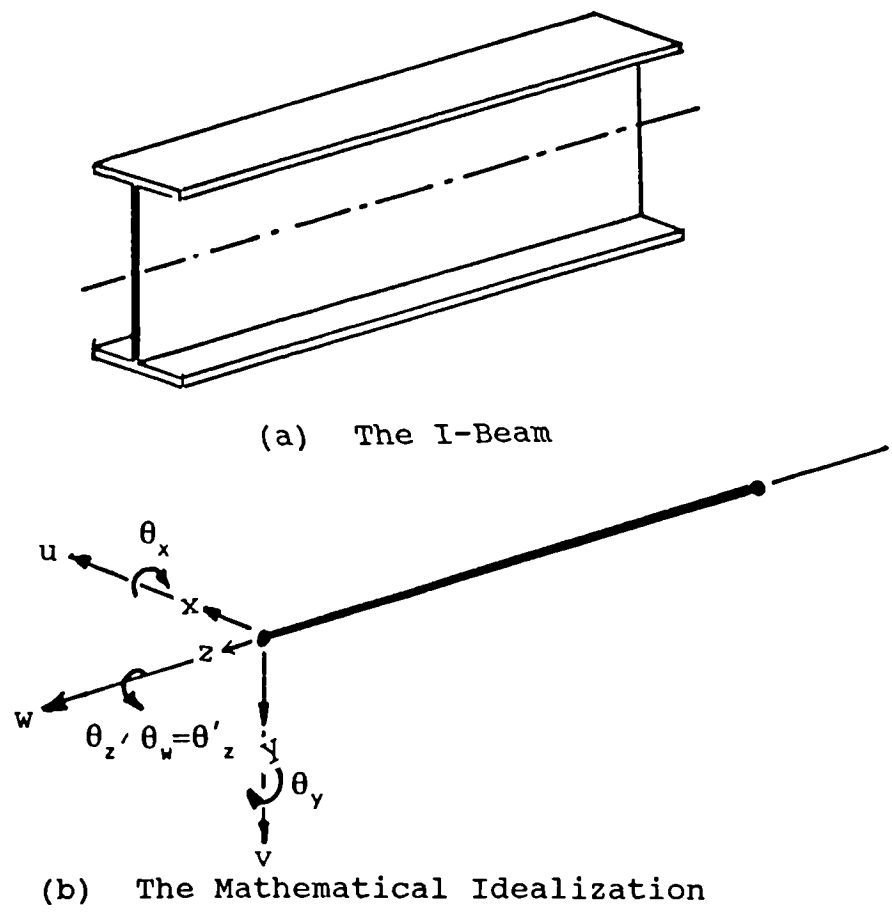


Figure 3.3 The 7 Degree-of-freedom 2-noded Beam Element

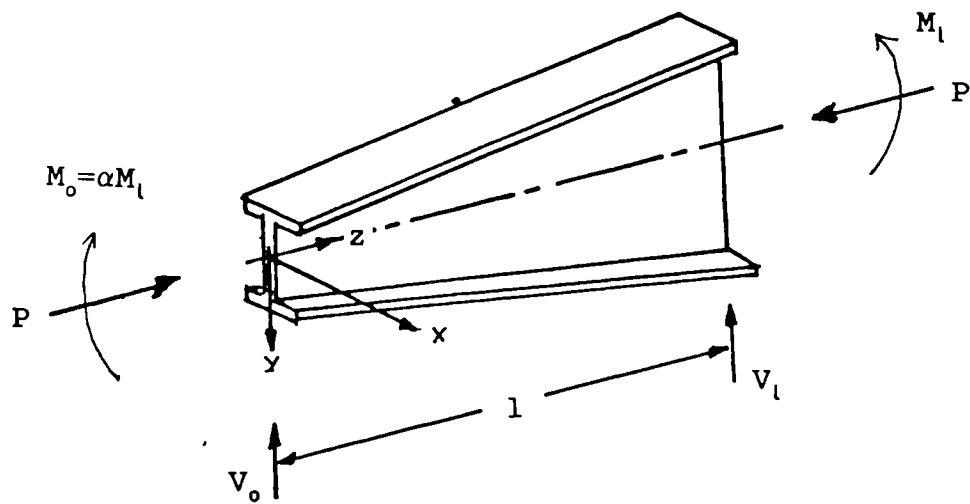


Figure 3.4 Loading Presumed by Lee, Morell and Ketter (3.20)

CHAPTER 4

4.0 The Finite Element Formulation and the SPACE Computer Programme

4.1 General

The basic formulation of the finite element method in structural analysis has been widely publicised, with many applications (4.1, 4.2, 4.3). The use of the finite element method to solve lateral buckling problems has been actively pursued for the last twenty years. Barsoum and Gallagher (4.4) and Powell and Klinger (4.5) developed one-dimensional line elements assuming the coincidence of the axis of twist with the shear centre which is parallel to the centroidal axis. They derived the stiffness matrices in the finite element formulation for torsional and lateral-torsional instability analysis based on an approximate representation of the flexural and torsional displacement of the member. The stiffness matrix $[K_E]$ and the geometric matrix $[K_G]$ were derived using the energy concept. The validity and adequacy of this approximate formulation for structural behaviour was measured by comparative analyses of problems for which exact or highly accurate solutions had been derived by alternative means. The formulation derived was able to provide solutions for a variety of problems and the results showed excellent agreement with the exact solution for both prismatic beams and columns. The same procedure was then followed by many

researchers to analyse the elastic torsional flexural buckling of continuous beams (4.5, 4.6), unbraced and braced portal frames (4.7) and one bay symmetrical frames loaded at the tops of the columns (4.6). A similar uniform element was also used by Nethercot (4.8) to study the lateral-torsional buckling of tapered members.

The finite element presented by Barsoum and Gallagher however lacked generality and consistency. These formulations are applicable only to members with doubly symmetrical cross-sections. Furthermore the effect of external bimoments, which may be very important in, for instance, the light gauge steel members, has not been considered. In view of this situation Nemir (4.9), presented a new finite element formulation that was based on Vlasov's concept (4.10) of the general behaviour of thin-walled members. This formulation which was based on uniform line element is also valid for any cross-sectional shape. Since it includes new terms representing the bimoment influence for sections with no axes of symmetry, this formulation is considered to be superior to the one developed by Barsoum and Gallagher.

In this thesis, the finite element formulation that was presented by Nemir (4.9) has been used in the numerical analysis conducted. This chapter describes this finite element and the corresponding computer program called the SPACE finite element program.

4.2 The Finite Element Formulation

4.2.1 Basic Assumptions

The development of this finite element formulation for the elastic three dimensional buckling behaviour of thin-walled members was based on the theory of torsional-flexural behaviour as described by Vlasov (4.10). Vlasov showed that self-balancing longitudinal forces applied to cross sections of a thin-walled beam-column member can distort the cross-section. The warping of the cross section by either longitudinal or transverse load applied eccentric to the shear centre can cause normal stresses in the cross-section. The generalised force corresponding to this effect is called a "bimoment".

In the analysis presented, it was assumed that, at the moment of buckling, the structure passes from a torsional-flexural equilibrium state to another torsional-flexural equilibrium but critical state. The bimoment stresses are included as the fourth term to be added to the conventional three terms of the equation of normal stresses.

In the derivation of the elastic matrix and the geometric matrix describing the behaviour of the element, the energy concept was used. The derivation of these matrices was based on the small deformation theory. Pre-buckling deformations were considered as very small, in comparison to the buckling

deformations and so their effects were neglected.

4.2.2 Bimoment Mechanism of Buckling of I-section Beams

A thin-walled member exhibits warping displacements when it is twisted by a uniform torque. If the flanges at the end cross-sections have no longitudinal restraints, warping is the same for all cross-sections. In this case the only stresses produced are the shearing stresses at each cross-section of the member. Figure 4.1 shows warping of the cross-section of a twisted I-beam. The behaviour is one in which plane sections do not remain plane, only the web remains plane while the flanges rotate bodily in two opposite directions.

If some longitudinal restraint is applied to the flanges at any cross-section, or if the torque varies along the length of the member, the flanges will be forced to take up a curvature in the longitudinal direction. Figure 4.2 shows a cantilever beam twisted by a concentrated torque 'T' applied at the free end. The curvature of the flanges varies along the member and the flanges appear to be subjected to two equal, but opposite bending moments, acting in their own plane. This combination of the two bending moments induced in the flanges as the result of the non-uniform torque is a bimoment. The longitudinal stresses caused by the bimoment can be very large and must be considered in the analysis.

The bimoment caused by either an eccentric longitudinal force or by a non-uniform torsion (fig 4.2) is given by the expression,

$$B = \overline{M}_f \cdot h \dots \dots \dots (4.1)$$

where B is the bimoment, M_f is the flange in-plane bending moment, and h is the distance between centroids of the two flanges. In terms of the normal stress σ_x in the cross-section, the bimoment 'B' can also be given by,

$$B = \int_A \sigma_x \cdot \bar{\omega} dA \dots \dots \dots (4.2)$$

in which $\bar{\omega}$ is the sectorial co-ordinate.

If the bimoment B_x acting at a given cross-section ($x = \text{constant}$) is known, the longitudinal normal stresses σ_x caused by this bimoment can be evaluated from the expression,

$$\sigma_x = \frac{B_x \cdot \bar{\omega}}{I_\omega} \dots \dots \dots (4.3)$$

in which, I_ω is the warping constant of the cross section.

4.2.3 The Strain Energy

Consider a prismatic element with an arbitrary chosen cross-section shown in figure 4.3. From figures 4.4 and 4.5, the longitudinal displacement u_m at an arbitrary point 'm' can be given by,

$$u_m = u - w'z - v'y - \theta'_x \bar{\omega} \dots \dots \dots (4.4)$$

where, u is the average longitudinal displacement of the cross-section (the longitudinal displacement caused by central thrust), and $\bar{\omega}$ is the sectorial co-ordinate with respect to the sectorial origin. The longitudinal normal strain can be expressed by the equation,

$$\epsilon_m = u' - \omega''z - v''y - \theta''_x \bar{\omega} \dots \dots \dots (4.5)$$

The total strain energy U_s for the element is the sum of strain energy due to normal stresses U_1 and strain energy due to shear stresses U_2 and is given by;

$$U_s = \frac{1}{2} \int_0^1 (EAu'^2 + EI_y w'^2 + EI_z v'^2 + EI_\omega \theta_x'^2 + GJ\theta_x'^2) dx \dots \dots \dots (4.6)$$

4.2.4 The Potential of Applied Load

The general expression of the normal stresses σ_x acting on the cross-section $x=\text{constant}$ in the precritical state is,

$$\sigma_x = -\frac{P_x}{A} - \frac{M_y}{I_y} \cdot z - \frac{M_z}{I_z} \cdot y + \frac{B}{I_\omega} \cdot \bar{\omega} \dots \dots \dots (4.7)$$

in which, P_x is the axial thrust, M_y and M_z are the two bending moments about the principal axes oy and oz respectively, and B is the bimoment.

The shear stress τ is given by;

$$\tau = \frac{M_y'}{tI_y} \cdot S_y + \frac{M_z'}{tI_z} \cdot S_z - \frac{B'}{tI_w} \cdot S_w \dots \dots \dots (4.8)$$

where t is the thickness of the cross-section at the point where τ is considered. M_y' , M_z' and B' are the first derivatives of the bending moments M_y and M_z and the bimoment B . S_y and S_z are the static moments of the considered part of the cross-section about oy and oz axes and S_w is the sectorial static moment of the same part. The static moments of area are given by,

$$\begin{aligned} S_y &= \int_0^s t \cdot y \cdot ds \\ S_z &= \int_0^s t \cdot z \cdot ds \dots \dots \dots (4.9) \\ S_w &= \int_0^s t \cdot w \cdot ds \end{aligned}$$

The transition of the element from the stable equilibrium state to the critical state is associated with the appearance of the critical deformations. At the critical state, the effect of the initial normal stresses σ_x acting on the deformed cross section can be presented by three fictitious loads. They are, the fictitious distributed loads in y and z directions and fictitious distributed torque about the shear centre's longitudinal axis. The potential of the applied load V_l is the sum of the potentials of these three fictitious loads. This potential can be obtained from the expressions;

$$\begin{aligned}
V_T = V_1 + V_2 + V_3 = \frac{1}{2} \left[\int_0^l P_x (-w \cdot w'' - v \cdot v'' - y_o (w \cdot \theta_x'' + \theta_x \cdot w'')) \right. \\
+ z_o (v \theta_x'' + \theta_x \cdot v'') - i_o^2 \theta_x \theta_x'' \\
- M_y (\theta_{xv}'' + v \theta_{xv}' + B_y \theta_x \theta_x'') \\
- M_y (2 \theta_x' v + B_y \theta_x \theta_x') - M_y \theta_x v \\
+ M_z (\theta_{xw}'' + w \theta_{xw}' - B_z \theta_x \theta_x'') \\
M_z' (2 \theta_x' w - B_z \theta_x \theta_x') + M_z' \theta_{xw} \\
\left. B B_\omega \theta_x \theta_x'' + B' B_\omega \theta_x \theta_x' \right] dx \quad \dots\dots (4.10)
\end{aligned}$$

in which, i_o is the polar radius of gyration about shear centre.

4.2.5 Potential Energy in Terms of the External Joint Load

Consider figure 4.6 which shows each end of the element being subjected to the action of seven forces. These forces are the bending moments M_y and M_z , the shearing forces Q_y and Q_z , twisting moment M_x , Bimoment B , and Axial force P_x . The subscript shows the position of the loads at ends 1 or 2.

The average bending moment M_y in the element as shown in figure 4.7 can be written as;

$$M_y = \frac{1}{2} (M_{y1} - M_{y2}) + \frac{1}{2} Q_{z1} x + \frac{1}{2} Q_{z2} (l - x) + P_x e_z \dots\dots\dots (4.11)$$

The average bending moment M_z as shown in figure 4.8 is;

$$M_z = \frac{1}{2} (M_{z1} - M_{z2}) + \frac{1}{2} Q_{y1} x + \frac{1}{2} Q_{y2} (1-x) + P_x e_y \dots \dots \dots (4.12)$$

By considering $\theta_x v'' = v \theta_x''$ and $\theta_x w'' = w \theta_x''$ and substituting for the end forces from equation 4.11 and 4.12 and their derivatives, the applied load becomes;

$$\begin{aligned} V_T = & \frac{1}{2} P_x \int_0^1 (-v \cdot v'' - w \cdot w'' - 2 C_z \cdot v'' \theta_x + 2 C_y \cdot w'' \theta_x - C_o \cdot \theta_x \cdot \theta_x'') dx \\ & - \frac{1}{4} \int_0^1 (M_{y1} - M_{y2} + Q_{z1} x + Q_{z2} (1-x)) (2 v'' \theta_x + \beta_y \theta_x \theta_x'') dx \\ & + \frac{1}{4} \int_0^1 (M_{z1} - M_{z2} + Q_{y1} x + Q_{y2} (1-x)) (2 w'' \theta_x - \beta_z \theta_x \theta_x'') dx \\ & - \frac{1}{4} \int_0^1 (Q_{z1} - Q_{z2}) (2 \theta_x' v + \beta_y \theta_x' \theta_x) dx \\ & + \frac{1}{4} \int_0^1 (Q_{y1} - Q_{y2}) (2 \theta_x' w - \beta_z \theta_x' \theta_x) dx \\ & + \frac{1}{2} \beta_w \int_0^1 (B \theta_x \theta_x'' + B' \theta_x' \theta_x) dx \end{aligned} \dots \dots (4.13)$$

where $C_y = (e_y - y_o)$, $C_z = (e_z - z_o)$ and $C_o = i_o^2 + e_y \beta_y + e_z \beta_z$.

4.2.6 Derivation of the Element Matrices

The derivation of the element matrices requires a suitable functional representation of the displaced behaviour of the element. The general form of each displacement function is given by;

$$\delta = d_i \cdot \Delta_i \dots \dots \dots (4.14)$$

in which, δ is the displacement component, d_i is the shape

function which often takes the form of polynomials of coordinates x and Δ_i is a set of nodal displacements.

By considering the shape function and the displacement components of an axial and flexural behaviour of the element, the expression of the total strain energy in equation 4.6 can be written as;

$$U_s = \frac{1}{2} \int_v \{\epsilon\}^T [D] \{\epsilon\} dv \dots \dots \dots (4.15)$$

in which, $\{\epsilon\}$ is the strain vector, $\{\epsilon\}^T$ is the transposé of the strain vector and $[D]$ is the matrix representing the generalised Hookean constant.

Substituting for the strain ϵ from equation 4.14 the strain energy U_s becomes;

$$U_s = \{\Delta_i\}^T [K_E] \{\Delta_i\} \dots \dots \dots (4.16)$$

where, $[K_E]$ is the element stiffness matrix which can be evaluated from the integration,

$$[K_E] = \frac{1}{2} \int_v \{d_i\}^T [D] \{d_i\} dv \dots \dots \dots (4.17)$$

Following the same procedure, the potential of the applied load V can be written by the expression;

$$V = -\{\Delta_i\}^T [K_G] \{\Delta_i\} \dots \dots \dots (4.18)$$

in which $[K_G]$ is the element geometric matrix which can be

written as

$$[K_G] = \int_v \{d_i\}^T [P] \{d_i\} dv \dots \dots \dots (4.19)$$

where, [P] is the matrix of the applied external loads. The total potential energy U_p of the element is then given by the expression,

$$U_p = \{\Delta_i\}^T [K_E] + [K_G] \{\Delta_i\} \dots \dots \dots (4.20)$$

Applying Castigliano's first theorem, the element stiffness equation becomes,

$$\{P\} = [K_E] + [K_G] \{\Delta_i\} \dots \dots \dots (4.21)$$

The condition of elastic instability is when the buckling load of the second variation of the total potential energy of the system is equal to zero. This condition leads to an expression for the buckling criterion which is given by,

$$|\overline{K_E}| + \lambda |\overline{K_G}| = 0 \dots \dots \dots (4.22)$$

in which $|\overline{K_E}|$ is the determinant of the stiffness matrix, $[K_E]$, $|\overline{K_G}|$ is the determinant of the geometric matrix $[K_G]$, and λ is the instability parameter (eigenvalue).

4.2.6.1 Stiffness Matrix

By substituting for the derivatives of the shape functions d_i in equation 4.17 and integrating with respect to the volume of the element V the elastic stiffness matrix can be given by;

$$[K_E] = \begin{bmatrix} u_1 & v_1 & w_1 & \theta_{x1} & \phi_1 & \psi_1 & X_1 & u_2 & v_2 & w_2 & \theta_{x2} & \phi_2 & \psi_2 & X_2 \\ a_{11} & & & & & & & & & & & & & \\ & a_{22} & & & & & & & & & & & & \\ & & a_{33} & & & & & & & & & & & \\ & & & a_{44} & & & & & & & & & & \\ & & & & a_{55} & & & & & & & & & \\ & & & & & a_{66} & & & & & & & & \\ & & & & & & a_{77} & & & & & & & \\ b_{11} & & & & & & & c_{11} & & & & & & \\ & b_{22} & & & & & & & c_{22} & & & & & \\ & & b_{33} & & & & & & & c_{33} & & & & \\ & & & b_{35} & & & & & & & c_{44} & & & \\ & & & & b_{44} & & & & & & & c_{55} & & \\ & & & & & b_{47} & & & & & & & c_{66} & \\ & & & & & & b_{55} & & & & & & & c_{77} \\ & & & & & & & b_{66} & & & & & & \\ & & & & & & & & b_{77} & & & & & \\ & & & & & & & & & b_{74} & & & & \\ & & & & & & & & & & b_{74} & & & \\ & & & & & & & & & & & b_{74} & & \\ & & & & & & & & & & & & b_{74} & \\ & & & & & & & & & & & & & b_{74} \end{bmatrix} \dots\dots\dots (4.23)$$

where,

$$\begin{aligned}
a_{11} &= \frac{EA}{l} \dots \dots \dots b_{11} = -a_{11} \dots \dots c_{11} = a_{11} \\
&\cdot \\
a_{22} &= \frac{12EI_z}{l^3} \dots \dots \dots b_{22} = -a_{22} \dots \dots c_{22} = a_{22} \\
&\cdot \\
a_{33} &= \frac{12EI_y}{l^3} \dots \dots \dots b_{33} = -a_{33} \dots \dots c_{33} = a_{33} \\
&\cdot \\
a_{44} &= \frac{1.2GJ}{l} + \frac{12EI_w}{l^3} \dots \dots b_{44} = -a_{44} \dots \dots c_{44} = a_{44} \\
&\cdot \\
a_{55} &= \frac{4EI_y}{l} \dots \dots \dots b_{55} = \frac{2EI_y}{l} \dots \dots c_{55} = a_{55} \\
&\cdot \\
a_{66} &= \frac{4EI_z}{l} \dots \dots \dots b_{66} = \frac{2EI_z}{l} \dots \dots c_{66} = a_{66} \dots \dots (4.24) \\
&\cdot \\
a_{77} &= \frac{2GJl}{15} + \frac{4EI_w}{l} \dots \dots b_{77} = -\frac{GJl}{30} + 2\frac{EI_w}{l} \dots \dots c_{77} = a_{77} \\
&\cdot \\
a_{53} &= -\frac{6EI_y}{l^2} \dots \dots \dots b_{53} = a_{53} \dots \dots \dots c_{53} = -a_{53} \\
&\cdot \\
a_{62} &= -\frac{6EI_z}{l^2} \dots \dots \dots b_{62} = a_{62} \dots \dots \dots c_{62} = -a_{62} \\
&\cdot \\
a_{74} &= -\frac{GJ}{10} - \frac{6EI_w}{l^2} \dots \dots \dots b_{74} = a_{74} \dots \dots \dots c_{74} = -a_{74} \\
&\cdot \\
b_{35} &= -b_{35} \dots \dots \dots b_{26} = -b_{26} \dots \dots \dots b_{47} = -b_{74}
\end{aligned}$$

4.2.6.2 Geometric Matrix

By substituting for the derivatives of the shape factor d_i and the external end forces in equation 4.19 and integrating with respect to the volume of the element v the geometric stiffness matrix can be given by;

$$[K_G] = \begin{bmatrix} u_1 & v_1 & w_1 & \theta_{x1} & \phi_1 & \psi_1 & X_1 & u_2 & v_2 & w_2 & \theta_{x2} & \phi_2 & \psi_2 & X_2 \\ & d_{22} & & & & & & & & & & & & \\ & & d_{33} & & & & & & & & & & & \\ & d_{42} & d_{43} & d_{44} & & & & & & & & & & \\ & & d_{53} & d_{54} & d_{55} & & & & & & & & & \\ & d_{62} & & d_{64} & & d_{66} & & & & & & & & \\ & d_{72} & d_{73} & d_{74} & & & d_{77} & & & & & & & \\ & e_{22} & & e_{24} & & e_{26} & e_{27} & & f_{22} & & & & & \\ & & e_{33} & e_{34} & e_{35} & & e_{37} & & & f_{33} & & & & \\ & e_{42} & e_{43} & e_{44} & e_{45} & e_{46} & e_{47} & & f_{42} & f_{43} & f_{44} & & & \\ & & e_{53} & e_{54} & e_{55} & & e_{57} & & & f_{53} & f_{54} & f_{55} & & \\ & e_{62} & & e_{64} & & e_{66} & e_{67} & & f_{62} & & f_{64} & & f_{66} & \\ & e_{72} & e_{73} & e_{74} & e_{75} & e_{76} & e_{77} & & f_{72} & f_{73} & f_{74} & f_{75} & f_{76} & f_{77} \end{bmatrix} \quad . (4.25)$$

Details of the expressions in this matrix are given in Appendix 5.

In comparison with the geometric matrix presented by Barsoum and Gallagher (4.4), or that derived by Tebedge (4.6), or those presented by Powell (4.5), the above Geometric Matrix includes more terms. These matrices can be used to analyse members having monosymmetric cross-sections since they include the geometric characteristics that reflect the effect of monosymmetry on the buckling behaviour of the member. The effect of bimoment caused by the external load is also included. By making use of a transformation matrix given in equation 3.59 of reference (4.9), the formulation can also be used for a three dimensional buckling analysis.

4.2.7 Prediction of the Buckling Load (Buckling Criterion)

The following equation gives the second-order behaviour of a framed structure having n joints.

$$\{F_n\} = [K_{ee}] + [K_{gg}] \{\Delta_n\} \dots \dots \dots (4.26)$$

where, $\{F_n\}$ is the column vector of the external loads acting at the joints of the frame, $[K_{ee}]$ is the overall elastic stiffness matrix of the frame, $[K_{gg}]$ is the overall geometric matrix, and $\{\Delta_n\}$ is the joint displacement vector. The term $[K_{ee}] + [K_{gg}]$ which represents the second order matrix of the structure can be obtained from the transformation operation,

$$[K_{ee}] + [K_{gg}] = \sum_n^{i=1} [\bar{t}_i]^T [K_E] + [K_G] [\bar{t}_i] \dots \dots \dots (4.27)$$

in which, $[K_E]$ and $[K_G]$ are the member stiffness and geometric matrices in the local co-ordinate system, $[t_i]$ and $[t_i]^T$ are the member transformation matrix and its transpose.

In an elastic stability analysis, the applied load on the structure is regarded as a fixed loading pattern multiplied by some factor λ . The critical load F_{cr} can be defined as the load F multiplied by the smallest value of λ at which the displacements of the structure become indeterminate (bifurcation of equilibrium).

4.2.8 Solution for the Elastic Critical Load

The solution for the above problem is given by,

$$|\overline{K}_{ee}| + \lambda |\overline{K}_{gg}| = 0 \dots \dots \dots (4.28)$$

in which, $|\overline{K}_{ee}|$ and $|\overline{K}_{gg}|$ are the determinants of the stiffness and geometric matrices respectively.

Equation 4.28 is similar to the general eigenvalue equation, thus it can be treated as an eigenvalue problem and the critical load found as the lowest eigenvalue. The buckling load can also be predicted from the load displacement curve. This method is based on performing a second-order analysis of the structure and predicting the critical load from the load-displacement relationship. A suitable prediction routine can be based on the Southwell method. This method was first used to estimate the Euler buckling load of a real column using the load-deflection plot from a non-destructive test. It was later refined and applied by many investigators to predict the buckling loads for different types of buckling problems. The equation for the critical load can be written by;

$$P_{cr} \cdot \frac{\delta}{P} = \delta + \overline{v}_1 \dots \dots \dots (4.29)$$

Equation 4.29 describes the standard Southwell plot which is shown in figure 4.9. The critical buckling load P_{cr} can be calculated from the slope of the plot.

Figure 4.10 shows an alternative representation of equation

4.9. This plot is known as the modified Southwell plot. The plot represents a linear relationship between P/δ and P . The critical load P_{cr} is given by the intercept with the P axis, while the inverse slope gives v_1 .

The modified Southwell plot is used in the Finite Element computer programme to predict the buckling load from a second order analysis.

4.3. The Computer Programme

The main routines of the SPACE Finite Element computer programme used in this thesis were already developed by Davies (4.11). Nemir (4.9) modified the computer program to include the geometric matrix presented earlier. He also included the transformation matrix for three dimensional problems.

The computer programme can be used for the following types of analysis:

- (a) Conventional elastic analysis of framed structures with a maximum of seven degrees of freedom at each joint
- (b) Second-order torsional-flexural analysis of framed structures.
- (c) Torsional-flexural buckling analysis of framed structures.

4.3.1. The Input Data

The data to run the computer programme is presented in batch mode (as opposed to interactive mode) and the basic format for a job is independent of the type of problem under consideration. The basic format is shown in Appendix 2, in which tables of particular parts of the data are presented schematically by two rows of spaces and single quantities by a single row of spaces. All data is fixed format and the particular task to be undertaken is determined by the integer value of "Mode" in line 2.

The preparation of the data in the input file involves the translation of the properties of the member and its loading into logical numerical form. This is done in order that it can be understood by the computer. It is vital that all the data for a given job is presented in consistent units. These units can be, for instance, (i) Tons and inches, (ii) Kips and inches, or (iii) kN and centimetres.

The input data for a given problem consists of the following:

- (1) **Joints:** Each joint of the structure, including the supports, has to be numbered and identified by its co-ordinates with respect to the adopted global system of co-ordinates. Degrees of freedom must also be given according to the restraining conditions at the joint.

- (2) **Members:** The members connected by the joints are divided into groups according to their elastic and cross-sectional properties. Each member is identified by four integer numbers. The first refers to the group of the members, the second and third identify the two end joints of the member. The fourth number specifies a third joint chosen to define the principal plane of the member.
- (3) **Loads:** The applied loads are identified in the data sheet by the number of loaded joints, the direction at which the load is applied and by the value of the load. The direction of the load is specified by an integer between 1 and 6.

4.3.2 Programme Subroutine

The flow chart of the computer programme is shown in figure 4.12. The programme consists of the following sub-routines,

- | | |
|----------------------|---------------------------|
| (a) Main subroutine | (d) Subroutine BARS |
| (b) Subroutine MAPP | (e) Subroutine SOLVE, and |
| (c) Subroutine SPACE | (f) Subroutine STORE. |

The main sub-routine contains the basic organisation and the

interaction process to calculate the elastic critical load using the modified Southwell plot.

The procedure of calculating the torsional-flexural buckling load for a given structure starts by applying a small value of the load factor. Then, solving for the displacements, the largest component of the deflection can be identified. An infinitesimal value of the load can then be applied at the critical joint in the critical direction to start the buckling displacements.

The instability problem is linearized by carrying out a doubly interactive process. At each load level the singularity of the determinant $[K_{ee}] + \lambda[K_{gg}]$ is checked. At each load level, also, an inner iteration is performed to find out the correct value of the displacement. This operation is carried out by solving repeatedly the second order equation for the displacements. It stops when the percentage difference between the two consecutive values of the critical displacement is less than the adopted value for the tolerance. This step is shown in figure 4.11.

Figure 4.13 shows the flow chart of the inner iteration technique to calculate the correct value of the critical displacement Δ_{cr} of a given value of the load factor. The prediction of the critical load factor λ_{cr} using the modified Southwell plot is illustrated by the flow chart in figure 4.14. The procedure continues until the percentage

difference between two consecutive predictions of λ_{cr} becomes less than the tolerance (0.0005).

The method used to solve the linear matrix equation is based on making use of the sparse nature of the stiffness matrices and operating on the non-zero elements only. This method has the advantage because the exact size of each submatrix generated storage is evaluated before the actual solution starts. This helps in the planning for the storage reserve. The basic theory of the method will now be explained in more detail.

The load displacement relationship for an elastic structure having n joints can be described by the stiffness equation, $F=K.\delta$. This equation can be expanded and re-written as:

$$\begin{bmatrix} F_1 \\ F_2 \\ \vdots \\ F_n \end{bmatrix} = \begin{bmatrix} K_{11} & K_{12} & \dots & K_{1n} \\ K_{21} & K_{22} & \dots & K_{2n} \\ \vdots & \vdots & & \vdots \\ K_{n1} & K_{n2} & \dots & K_{nn} \end{bmatrix} \cdot \begin{bmatrix} \delta_1 \\ \delta_2 \\ \vdots \\ \delta_n \end{bmatrix} \dots\dots\dots (4.30)$$

where, the individual K terms are submatrix associated with the n joints of the structure.

For the part of the structure which is shown in figure 4.15, the submatrix equation of this part is given by,

$$\begin{bmatrix} F_b \\ F_c \\ F_d \\ F_e \\ F_t \end{bmatrix} = \begin{bmatrix} K_{bb} & & & & K_{bt} \\ & K_{cc} & & & K_{ct} \\ & & K_{dd} & & K_{dt} \\ & & & K_{ee} & K_{et} \\ K_{tb} & K_{tc} & K_{td} & K_{te} & K_{tt} \end{bmatrix} \cdot \begin{bmatrix} \delta_b \\ \delta_c \\ \delta_d \\ \delta_e \\ \delta_t \end{bmatrix} \dots\dots\dots (4.31)$$

where, the K submatrices of the above equation are of a size depending on the number of degrees of freedom of the joints. Equation 4.30 can be re-written in a partitioned form as follows;

$$\begin{bmatrix} F_a \\ F_t \end{bmatrix} = \begin{bmatrix} K_{aa} & K_{at} \\ K_{ta} & K_{tt} \end{bmatrix} \cdot \begin{bmatrix} \delta_a \\ \delta_t \end{bmatrix} \dots\dots\dots (4.32)$$

By eliminating joint t from the analysis (figure 4.16) the following relationships are obtained,

$$K_{aa}^* = K_{aa} - K_{at} \cdot K_{tt}^{-1} \cdot K_{ta} \dots\dots\dots (4.33)$$

$$F_a^* = F_a - K_{at} \cdot K_{tt}^{-1} \cdot F_t \dots\dots\dots (4.34)$$

After calculating δ_a , δ_t can be evaluated by substituting for δ_a in equation 4.31. By repeating the application of equation 4.32 and 4.33 the number of joints in the analysis reduces until for the last joint the displacement can be calculated from the following equation,

$$\delta_n = K_{nn}^{*-1} F_n^* \dots\dots\dots (4.35)$$

The sparse matrix K_{aa} is replaced by the dense matrix K_{aa}^* . As the stiffness matrix is symmetrical, K_{at} is the transposé of

K_{ta} so that it is sufficient to store only one of them. The elimination equations (equation 4.33 and 4.34) show that it is only necessary to store the two matrices K_{tt}^{-1} and K_{ta} (or their product).

The solution starts with a simple operation to establish a list of the joints at the near optimum order of elimination together with the joint connections which will be created during the solution. The order of elimination and the connection list do not include the joints with no degree of freedom.

The elimination order is performed by selecting, at each stage, to eliminate next the joint, or one of the joints, with the lowest sum of degrees of freedom for the joints to which it is connected. The connection list is contained in a two-dimensional integer array, MAP. The number of degrees of freedom for a given joint m is specified in a one dimensional array JS. Another array NM, is used to specify the sum of the number of the degrees of freedom of the joints connected to joint m . The integer array JDF is used to specify, in a binary form, the active degrees of freedom at each joint. During the preliminary mapping the solution process continues updating the array MAP and NM up to the last joint of the structure.

The subroutine SPACE includes the formulation of the elastic stiffness matrix and the transformation matrix given by

Jennings and Majid (4.12). It can be used for first-order analysis of framed structures provided that six degrees of freedom are considered at each joint.

The subroutine BARS includes the formulation of the elastic stiffness and geometric matrices for the second order and stability analysis of thin-walled structures. It also contains the formulation of the transformation matrix, which was discussed earlier, for performing a three dimensional stability analysis of frames.

The addresses of the stiffness and load matrix elements are stored in two linear arrays in the working store, namely ADDR, and WADDR respectively. Having completed the mapping operation, the complete stiffness matrix for the structure is built up, member by member, in the form of submatrices which are entered at the appropriate addresses. The solution then proceeds by eliminating the joints one at a time according to the previously arranged elimination list using equation 4.33 and 4.34. During the elimination process, stiffness terms of the form K_{tt}^{-1} and $K_{at} \cdot K_{tt}^{-1}$ and the modified load submatrices F_a^* , are written up to the backing store. These terms are required for the evaluation of the joint displacements and member forces.

The joint displacements and member forces are evaluated using equation 4.34 and 4.35. These calculations are performed using the subroutine SOLVE.

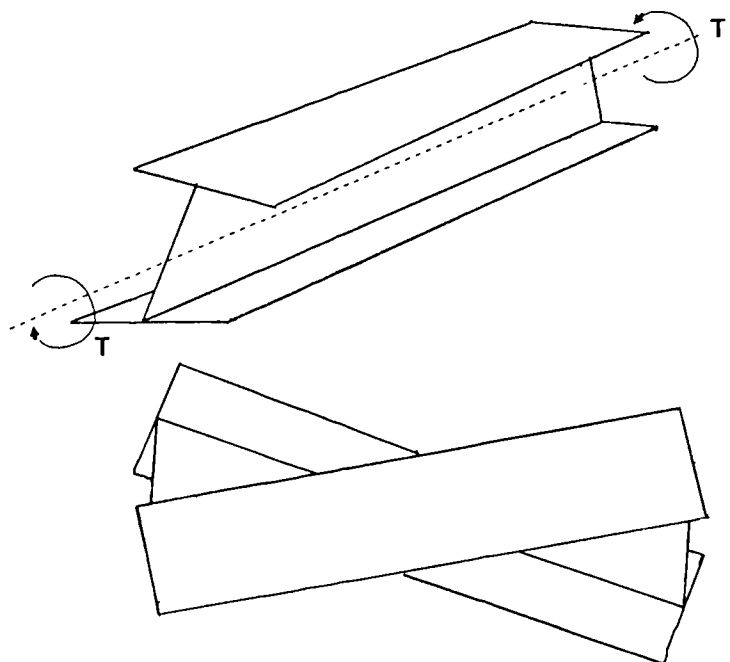


Figure 4.1 Warping of Doubly Symmetry I-Beam

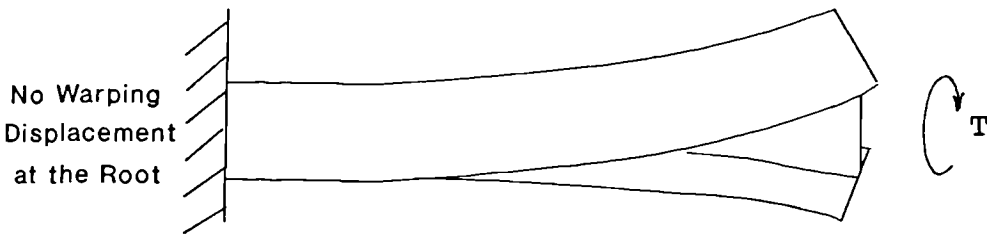


Figure 4.2 Torsion with Restrained Warping

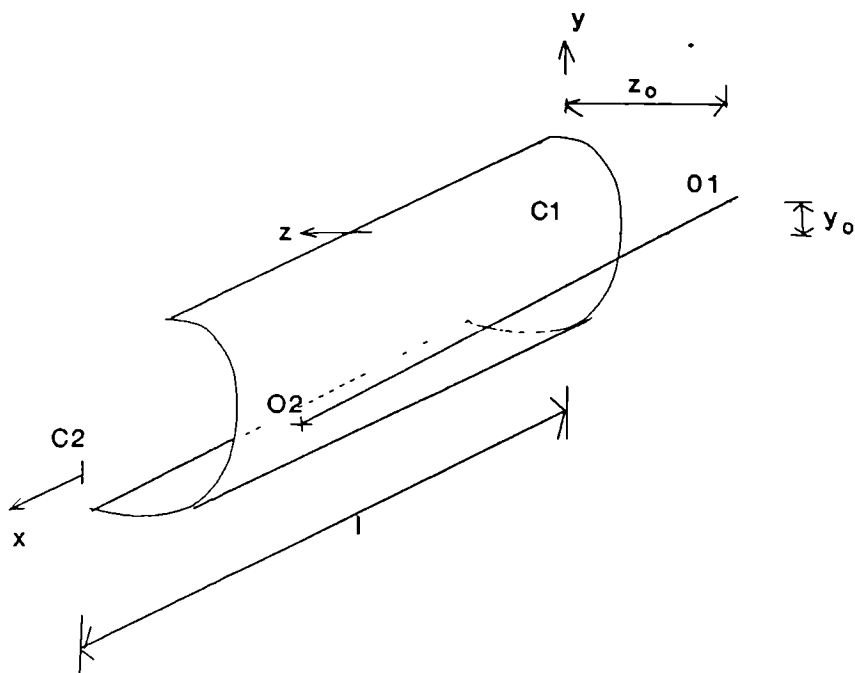


Figure 4.3 The Prismatic Member

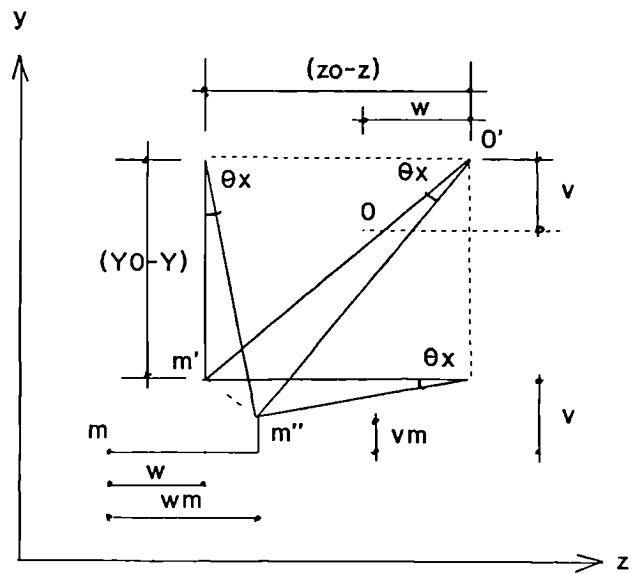


Figure 4.4 Torsional Flexural Displacement of Point m

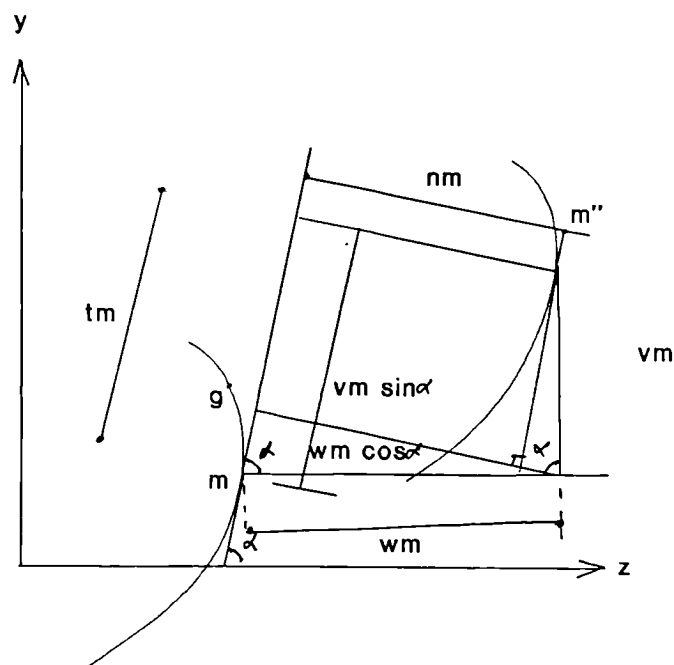


Figure 4.5 Normal and Tangential Displacements

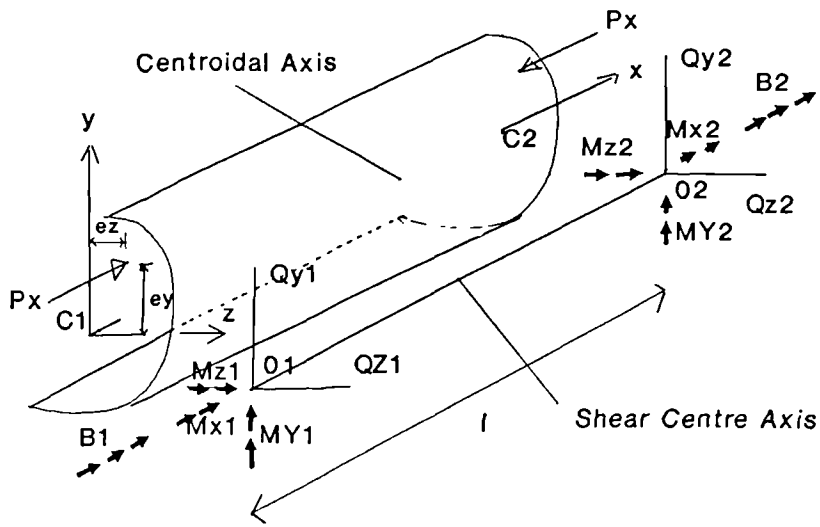


Figure 4.6 Element End Forces

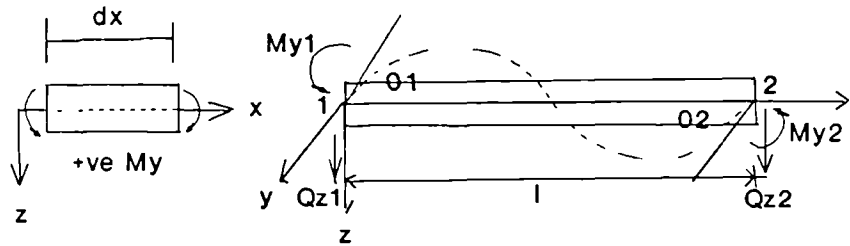


Figure 4.7 Bending M_y

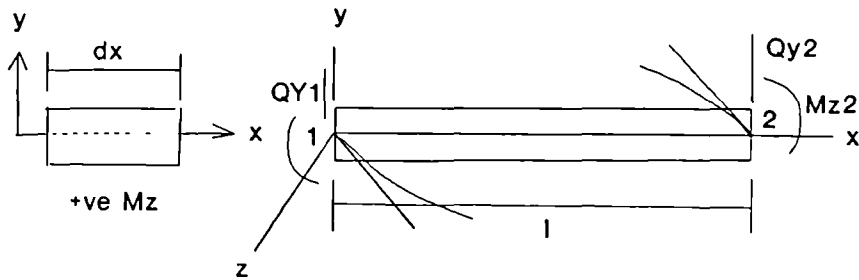


Figure 4.8 Bending M_z

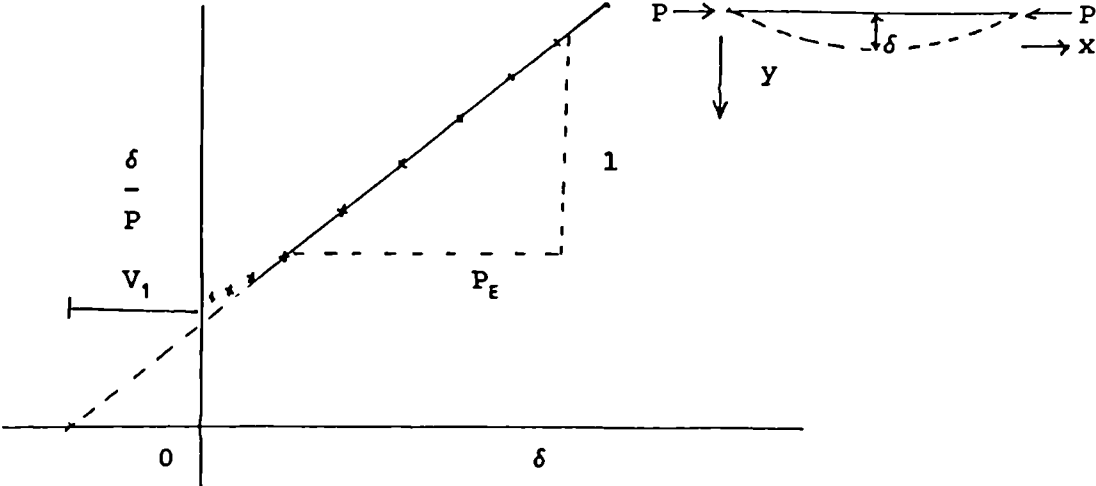


Figure 4.9 Standard Southwell Plot

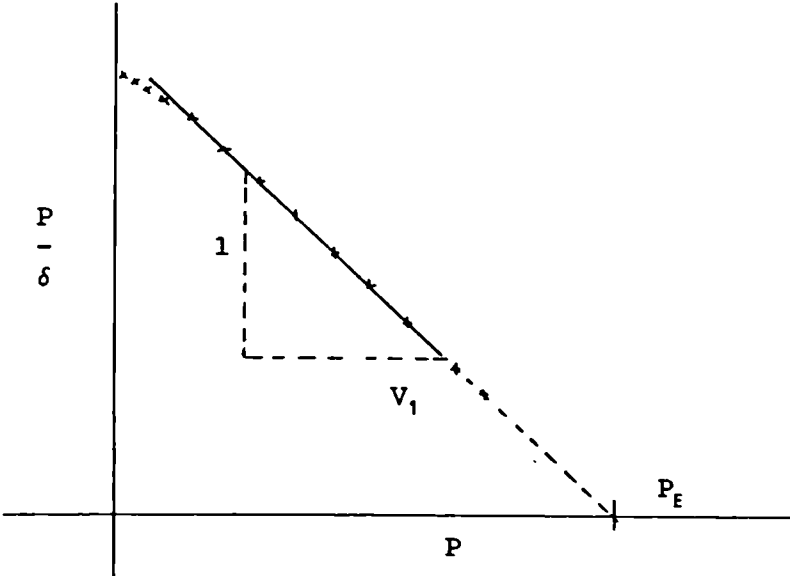


Figure 4.10 Modified Southwell Plot

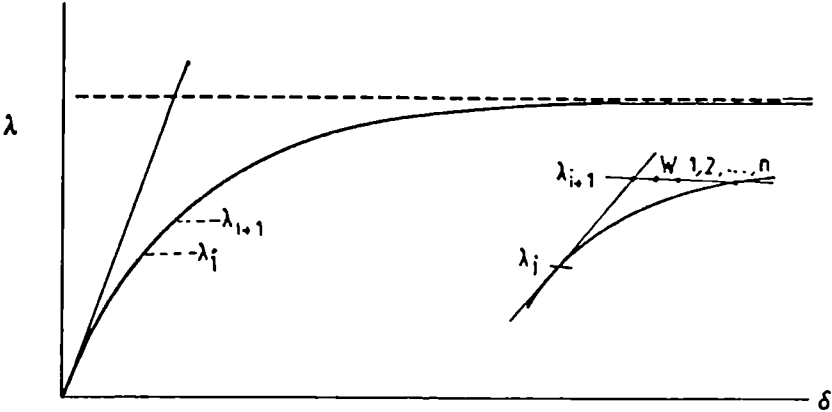


Figure 4.11 The Inner Iteration Procedure

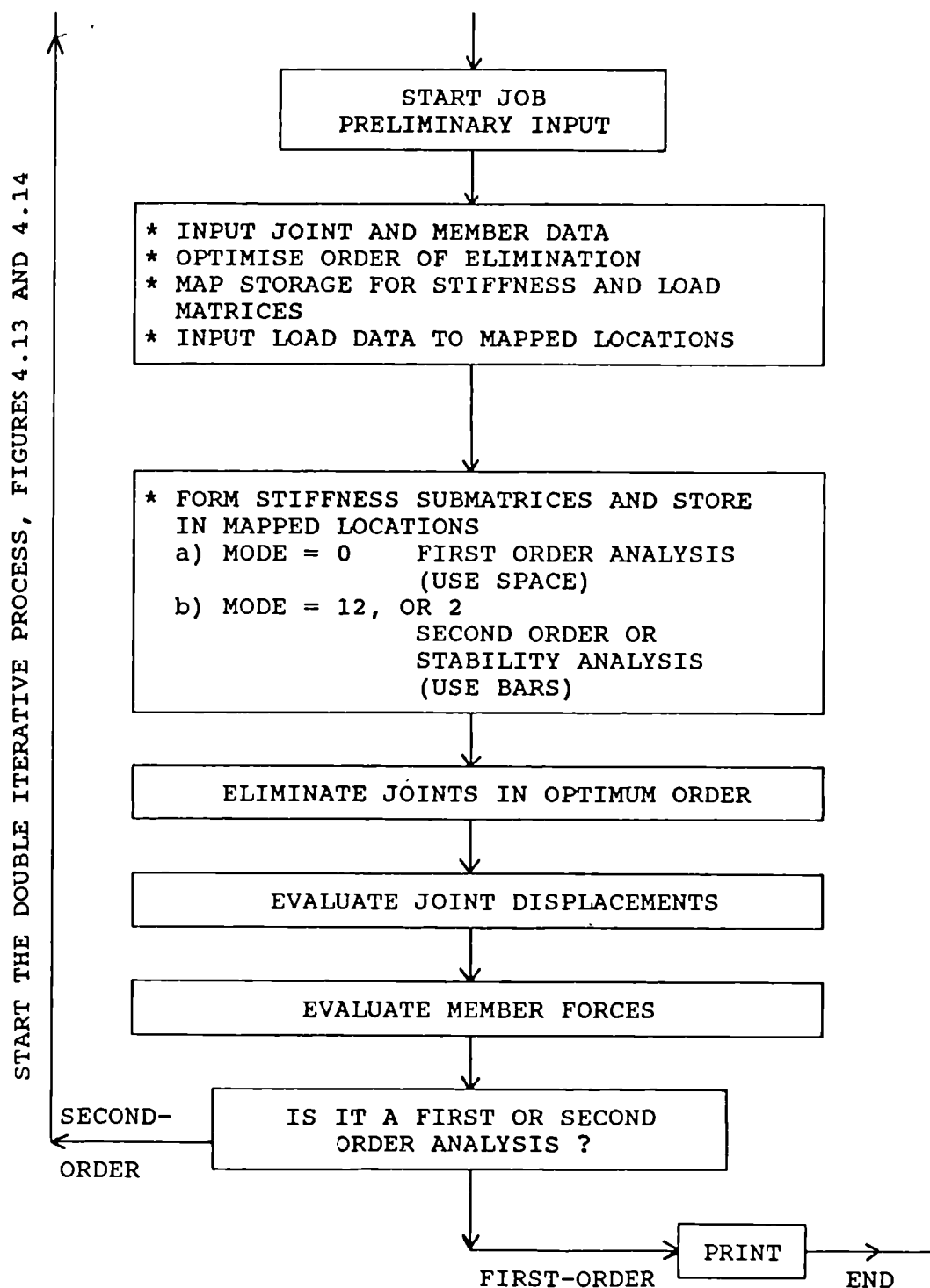


Figure 4.12 Flow diagram of the computer program

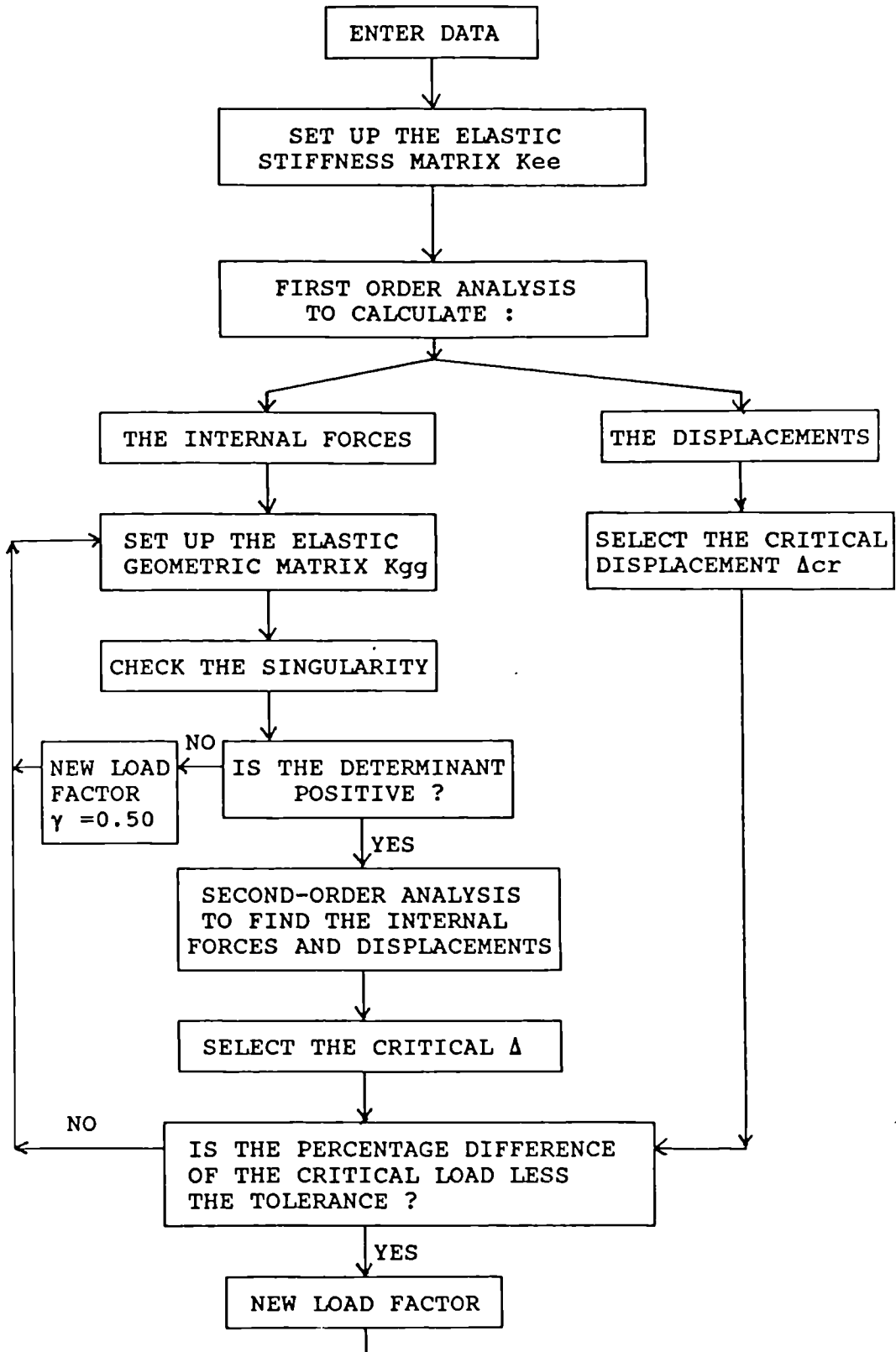


Figure 4.13 The flow chart of the computer operations to find the value of Δ_{cr} at a given load factor.

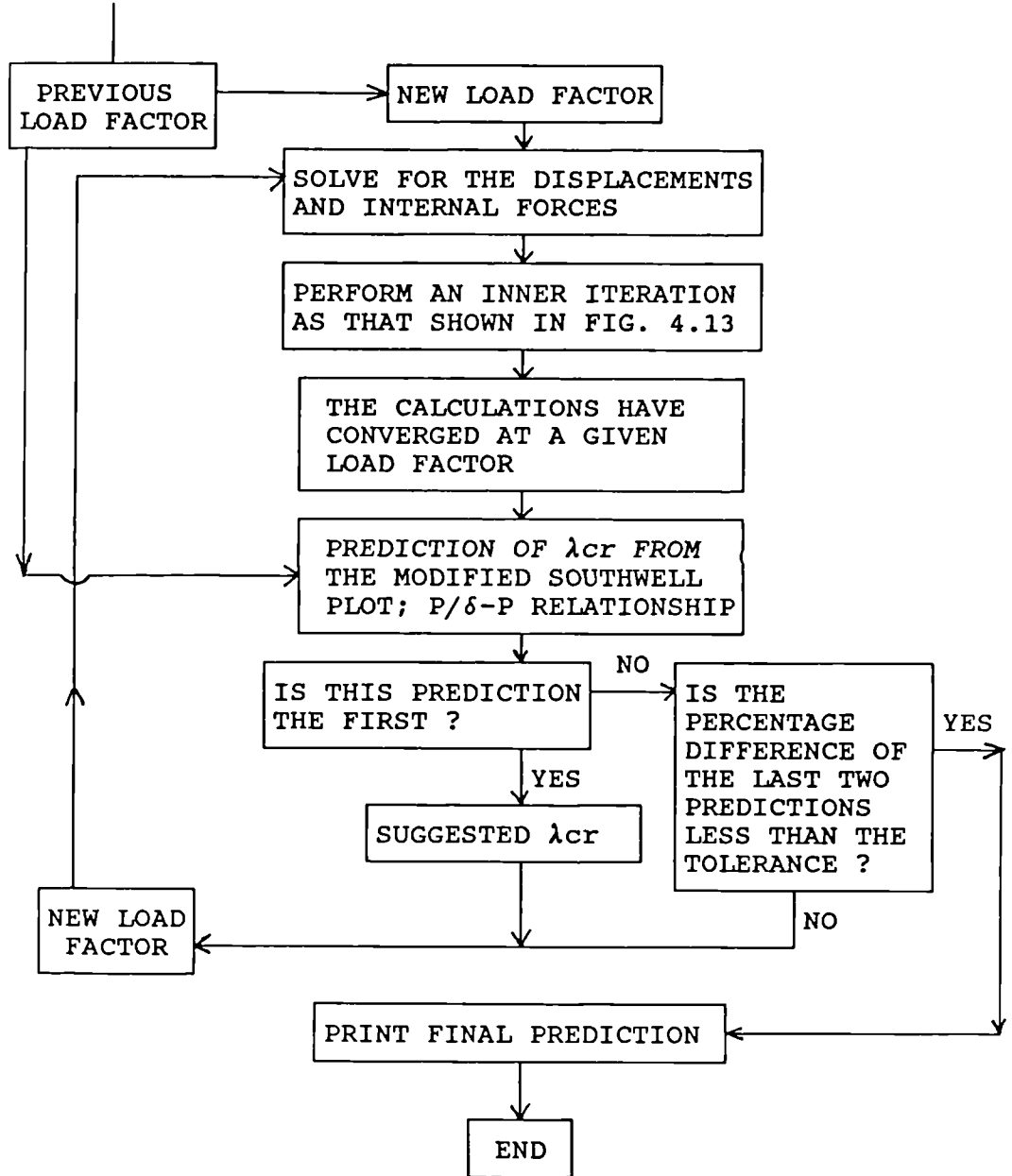


Figure 4.14 The flow chart of the prediction of λ_{cr} from the modified Southwell plot.

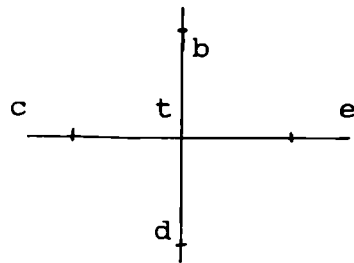


Figure 4.15 Joint connecting part of structure

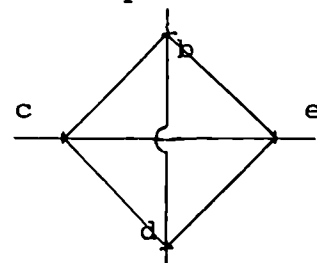


Figure 4.16 Imaginary connections after eliminating joint t

CHAPTER 5

5.0 Verification of the "SPACE" Finite Element Computer Programme for the Analysis of Non-Uniform Members

5.1 Introduction

The Finite Element formulation and the "SPACE" Finite Element computer programme used in the numerical analysis in this thesis were discussed in Chapter 4. Appendix 2 of this thesis reports on the initial verification of the computer programme by conducting numerical tests on prismatic members. It was first proved that the Finite Element formulation was valid in solving most of the conventional lateral-torsional buckling problems for prismatic members. Rapid convergence was achieved even with the use of 4-elements but the accuracy of the solution was greatly enhanced by the use of an 8-element model. However, the Finite Element formulation had not been verified for lateral-torsional buckling of tapered members.

In this chapter, the Finite Element formulation is verified by the analysis of various cases of tapered beams and cantilevers. Since this Finite Element formulation was based on a prismatic beam or line element, modelling of tapered members was achieved by a stepped representation. This procedure by which the tapered member was approximated by a series of uniform elements is shown in figure 5.1. The

geometrical properties of each element, such as the moment of inertia, area etc., were chosen at the centre of the element.

The verification starts with the analysis of some cases of narrow rectangular sections and is then followed by I-section members. The results of the Finite Element analysis were compared with the results of other available accurate methods of analysis of tapered members. The case of tapered beam-columns is considered later in this chapter.

In all of the cases considered, the values of E , Young's Modulus and G , the Shear Modulus used were 210 kN/mm^2 and 80.5 kN/mm^2 respectively, unless otherwise stated. In the Finite Element analysis a 10-element model was used since earlier verification of the program had shown that this number of elements was sufficient to achieve accurate results.

5.2 Beams with Rectangular Cross-Section

5.2.1 Simply Supported Tapered, Narrow Rectangular Beam

Lee (5.1) studied the case of the elastic buckling of tapered narrow rectangular beams subjected to pure bending. He considered a simply supported tapered beam under simple

lateral restraint at the ends as shown in figure 5.2. At a certain critical value of the applied moment M the beam buckles laterally.

This critical moment M_{cr} , which is the minimum value of M necessary to keep the beam in equilibrium in a slightly buckled form was given by Lee as;

$$M_{cr} = \frac{\delta}{\log_e(1+\delta)} \frac{\pi \sqrt{B_0 C_0}}{l} \dots \dots \dots (5.1)$$

where B_0 , C_0 and $(1+\delta)$ are the flexural and torsional rigidities at the origin of the beams and the ratios of the depth at the two ends of the beams. The flexural and torsional rigidities are given as, $B_0 = (hb^3/12)E$ and $C_0 = (hb^3/12)G$ respectively.

In this study, a beam with 300 cm. length, $h=15$ cm., and different cases of depth ratios, $\delta=1, 0.8, 0.6, 0.4$ and 0.2 was considered. Equation (5.1) was used to calculate the critical moments for the cases mentioned above.

The beam was also analysed using the "SPACE" Finite Element computer programme. In this case, the boundary condition was that the beam was simply supported with torsional displacement prevented at both ends.

The results of the analysis are presented in table 5.1 and figure 5.3. These results show that there is a close agreement between the results of the analysis by equation

(5.1) and the Finite Element formulation. However, the Finite Element formulation gave prediction of slightly underestimated values of the critical moments compared to equation (5.1). This was true for all cases except for the case when $\delta=1$ in which the Finite Element method gave slightly over-estimated results. The actual error band was -2.9% to 0.85%.

From these results it can be said that the Finite Element formulation was able to predict accurately the critical buckling moment for a narrow rectangular tapered beam.

5.2.2 Simply Supported Narrow Rectangular Double Tapered Beam

Massey (5.2) studied the case of the lateral stability of a narrow rectangular double tapered beam. He considered the beam shown in figure 5.4 which is simply supported at each end in the vertical and horizontal planes, but the end supports prevent rotation about the longitudinal axis.

Since the beam is narrow, the vertical rigidity is large compared with the lateral rigidity. The lateral rigidity B and the torsional rigidity C are assumed to vary linearly but independently from each end to the centre of the span about which the beam is symmetrical. Hence for, $0 \leq z \leq L/2$;

$$Bz=B+azB.....(5.2)$$

and

$$Cz=C+bzC.....(5.3)$$

where B and C are the rigidities at z=0 and it is assumed that warping rigidity C_w has negligible effect since in this case $CL^2/C_w > 300$.

The equation of equilibrium was established by Massey for the above conditions as;

$$(B+azB) u''=\frac{Pz\phi}{2}.....(5.4)$$

$$(C+bzC) \phi=-\frac{Pzu'}{2}-\frac{P(\delta-u)}{2}.....(5.5)$$

where δ is the midspan lateral deflection and the primes denote differentiation with respect to z.

Differentiation of equation 5.5 and substituting, gave the following equation;

$$\phi''(1+bz+az+abz^2)+\phi'(b+abz)+\frac{k^2z^2\phi}{4L^4}=0.....(5.6)$$

where,

$$k^2=\frac{P^2.L^4}{BC}.....(5.7)$$

The approximate solution for equation 5.6 for a range of values can then be worked out. This gave the values of k expressed to the first decimal place for values of α and β ranging from 0.25 to 10. In this case, α is defined as the ratio of the lateral rigidity at either end and β as the

similar ratio for torsional rigidity. By making use of the values of k for a particular problem within the range of the analysis, the value of critical load P , was calculated.

In this present analysis, beams with 3000 mm length, depth at the centre of the beam equal to 300 mm and thickness of 25 mm, and with the taper ratio taken as 1, 1.5, 2, 3, 4 and 6 for both α and β were considered. The values of critical load were calculated for the cases under consideration using equation 5.7 and values of k from the table or graph in reference (5.2).

The beams were also analysed by the Finite Element method and the boundary conditions were simply supported with torsional restraints in the longitudinal direction at both ends. An initial load of 10 kN was applied at the top of the centre of the span.

The results of the analysis are shown in table 5.2 and figure 5.5. It shows that there is a close agreement between both the analysis by the method of Massey and the Finite Element Formulation. However as shown in table 5.2, the Finite Element Method gave a slightly higher prediction of the critical load by a margin of 1.2% to 2.3%.

These results indicate that the Finite Element formulation used in this Finite Element computer programme gave an accurate prediction of critical buckling load for the case

of the simply supported narrow rectangular tapered beam which was considered.

5.3 Lateral-Torsional Buckling of Tapered I-Beams and Cantilevers

5.3.1 Simply Supported Tapered I-Beam

5.3.1.1 Double Taper I-Beam

Figure 5.6, shows a simply supported double tapered I-beam loaded by central concentrated load P acting at the top flange. Brown (5.3) used the finite difference method to solve the differential equation for the stability of the member.

The equation for critical load is given as;

$$P_{cr} = \frac{\gamma_1 \sqrt{EI_{y0} GK_o}}{L^2} \dots \dots \dots (5.8)$$

or

$$Q_{cr} = \frac{\gamma_2 \sqrt{EI_{y0} GK_o}}{L^3} \dots \dots \dots (5.9)$$

where γ_1 is a non-dimensional critical load parameter, I_{y0} is the moment of inertia of the deepest section and K_o is the Saint Venant's torsion constant at the deepest section. The

boundary conditions at $z=0$ and $z=L$ were, $u = u'' = \beta = \beta'' = 0$. The values of critical loads for cases where only the beam depth varies, the flange width and thickness and the web thickness remaining constant, were obtained. In his analysis, Brown used the section that was an idealised I-section with a maximum depth of 610 mm. Flange width and thickness were 152 mm and 13 mm respectively and the web thickness was 9.5 mm.

A table of coefficient γ_1 , for critical midspan concentrated load for a 6.10 m span simply supported beam, for the case of load applied at the top flange, the centroid and the bottom flange are presented in table 1 of reference (5.3). The table gave the coefficient γ_1 , for the taper ratio α equal to 0.167, 0.333, 0.5, 0.667, 0.833 and 1. (i.e., α =ratio of depth of shallow end to depth at midspan.)

The critical load was calculated for the above beam for the case where the load was applied at the centroid by equation 5.8, with the values of γ_1 , from table 1 of reference (5.3) for the cases of taper ratio mentioned.

The beam was also analysed for the critical load by Finite Element method. The boundary conditions imposed were simply supported at the ends and torsionally restrained but free to warp.

The results of the two analyses are shown in table 5.3 and

figure 5.7. These show that the results are in close agreement with each other. The difference of the two results varies from 3.75% with $\alpha=0.167$, to 0.04% with $\alpha=0.5$ and increase again to 1.63% when $\alpha=1$. The graphs in figure 5.7 intercept at a value of $\alpha=0.55$. Therefore the present analysis shows the validity of the Finite Element formulation in solving centrally loaded double tapered I-beams.

5.3.1.2 Flange Breadth Tapered I-Beams

Kerensky, Flint and Brown (5.4) studied the case of a simply supported flange breadth tapered I-beam with load applied at the centroid. Figure 5.8 shows the beam with uniform flange thickness but the breadth curtailed linearly from B to VB , V being the ratio of the minimum flange area to the maximum flange area.

Consider that the beam has a span L , and is subjected to a load P at the shear centre of mid span. The support conditions were simply supported i.e., there is no restraint to bending action, but with rotation of the end sections about the longitudinal axis prevented. The load was assumed to be free to move laterally during buckling, remaining parallel to the y axis.

When the critical value of P is reached, the system remains

in a state of equilibrium defined by the condition that the total potential energy of the system is stationary. This means that it does not vary with small displacements of the beam. In this situation the critical load may be defined by;

$$\Delta (U+V) = \int_0^L \left[GK(\theta')^2 + C(\theta'')^2 + P_p [\theta]_{pL}^2 - \frac{\gamma M_x^2 \theta^2}{EI_y} - \alpha M_x (\theta')^2 \right] dz \dots (5.10)$$

The neutral equilibrium equation 5.10 is satisfied if;

$$\int_0^{L/2} \left[GK_2 (\theta')^2 + \frac{Eh^2}{4} I_{yz} (\theta'')^2 - \frac{\gamma P^2}{4EI_{yz}} z^2 \theta^2 \right] dz = 0 \dots \dots \dots (5.11)$$

where the origin is taken at one support.

In this case the lateral second moment of area and the torsion constant may be expressed as ;

$$I_{yz} = I_y [v + 2(1+v)z/L]^3 \dots \dots \dots (5.12)$$

$$K_2 = \frac{K}{n} [(n-1) + 2(1-v)z/l + v] \dots \dots \dots (5.13)$$

By employing equation 5.11 and integrating the last function graphically, a solution in the form of equation 5.14 was obtained.

$$P_{crit} = \frac{4\pi\alpha}{L^2} \sqrt{EI_y GK} \sqrt{1 + \frac{\beta\pi^2 EI_y h^2}{4GKL^2}} \dots \dots \dots (5.14)$$

Values of the coefficients for α and β for this case are found in figure 9 of reference (5.4).

Kitipornchai and Trahair (5.5) used the finite integral method to predict the lateral buckling of the flange breadth tapered I-beam shown in figure 5.8. Assuming the same support conditions as Kerensky, Flint and Brown (5.4), and by considering the deflected shape given in figure 5.9, they obtained the governing differential equation for buckling of the beam using the following equations,

$$\begin{aligned}\gamma_2 &= \frac{P_c L^2}{\sqrt{(EI_y GJ)_{L/2}}} \\ K^2 &= \pi^2 \left(\frac{EI_w}{GJ L^2} \right)_{L/2} \\ U &= \frac{u \sqrt{(EI_y)_{L/2}}}{\gamma_2 L} \dots \dots \dots (5.15) \\ \phi &= \phi \sqrt{(GJ)_{L/2}} \\ Z &= z L \\ \Lambda &= \lambda L\end{aligned}$$

The differential equations of minor axis flexure and torsion become;

$$\frac{d^2 v}{dz^2} = -\frac{1}{k_1} \frac{\phi z}{2} \dots \dots \dots (5.16)$$

and

$$\begin{aligned}\left[1 + \frac{K^2}{\pi} \left(\frac{3}{2} \Lambda^2 \frac{k_s}{k_s} - \Lambda \frac{1}{k_2} \frac{dk_3}{dz} \right) \right] \frac{d\phi}{dz} - \frac{1}{k_2} \frac{dk_3}{dz} \frac{K^2}{\pi^2} \frac{d^2 \phi}{dz^2} - \frac{k_3}{k_2} \frac{K^2}{\pi^2} \frac{d^3 \phi}{dz^3} \\ = \frac{\gamma_2^2}{2k_2} \left[U_{L/2} - U + z \frac{dU}{dz} \right] + \frac{\gamma_2 K}{2\pi} \frac{1}{k_2} \frac{2\bar{a}}{h_L/2} \phi_{L/2}\end{aligned} \dots (5.17)$$

respectively, where

$$\begin{aligned} k_1(z) &= \frac{EI_y(z)}{EI_y(L/2)} \\ k_2(z) &= \frac{GJ(z)}{GJ(L/2)} \dots\dots\dots (5.18) \\ k_3(z) &= \frac{EI_w(z)}{EI_w(L/2)} \end{aligned}$$

The boundary conditions for equation 5.16 and 5.17 are

$$\begin{aligned} z=0, \\ \phi=U=\frac{d^2\phi}{dz^2}+\Lambda_0\frac{d\phi}{dz}=0 \\ z=\frac{1}{2}, \dots\dots\dots (5.19) \\ \frac{d\phi}{dz}=\frac{dU}{dz}=0 \end{aligned}$$

By using the finite integral method of solution, the critical load parameter γ_l was obtained from equations 5.16, 5.17 and 5.18. This was done with the help of a computer programme written in the Algol language.

An aluminium beam with the dimensions shown in figure 5.10 was analysed for the critical load for taper ratios equal to 0.2, 0.4, 0.6, 0.8 and 1 by Kerensky, Flint and Brown's method and by Kitipornchai and Trahair's finite integral method. The values of Young's modulus and Shear modulus used in the analysis were 64 kN/mm², and 26 kN/mm² respectively.

The same analysis was made for the above beam by using the Finite Element formulation that is being verified. The boundary conditions were simply supported at the ends with torsion restrained in the longitudinal direction but the ends were free to warp. The beam was loaded with a

concentrated load at the centroid.

The results of the three different methods of analysis are shown in figure 5.11 and Table 5.4. It can be seen in Table 5.4 that all the results show a similar pattern. However the Finite Element Method predicted lower elastic critical loads when the taper ratio is less than 0.8. The Finite Element Method on the other hand predicted higher values of critical load when compared to the other two method of analysis at taper ratios more than 0.8 but less than 1. An interesting feature of the graph in figure 5.11 is that at the taper ratio of 0.8, all the three analyses gave results in very close agreement with each other. Furthermore, both Kerensky, Flint and Brown, and Kitipornchai and Trahir's method appear to be in agreement with each other in all the predictions of the critical load. It can therefore be said that the Finite Element formulation of the SPACE programme can predict the critical load for the beam under consideration, however it tends to give a more conservative prediction at the lower taper ratios.

5.3.2 Lateral Buckling of Tapered I-Cantilever

5.3.2.1 Web Depth Taper

The case of lateral buckling of tapered I-cantilevers loaded at the end, as shown in figure 5.12, was investigated by

Brown (5.3) and Nethercot (5.6). Brown used the same method described in section 5.3.1 to arrive at equation 5.8 that was also used for this specific tapered I-cantilever. The values of γ_1 used for this case were tabulated (Table 3) in reference (5.3). The boundary conditions at $z=0$, were

$$u=u'=\beta=\beta'=0 \dots\dots\dots (5.20)$$

and at the free end, $z=L$, were

$$u''=(EIu'')'=\beta''=\beta'''=0 \dots\dots\dots (5.21)$$

Nethercot (5.6) proposed the use of a reduction formula (equation 5.22) to predict the critical moment for lateral buckling of the tapered cantilevers shown in figure 5.12. The critical moment equation for this case is;

$$M_{cr} = \frac{\gamma_e}{L} \sqrt{(EI_y GJ)} \dots\dots\dots (5.22)$$

where M_{cr} = maximum moment in the beam i.e., moment at the root.

EI_y = minor flexural rigidity

GJ = Torsional rigidity

L = span

γ_e = Lateral coefficient

He obtained the value of γ_e for various cases of tapered cantilever using the Finite Element formulation for lateral buckling first introduced by Barsoum and Ghallenger. His results include the case of depth taper, flange breadth taper and flange thickness taper. The values of γ_e were tabulated (Table 1c) in reference (5.6) for three different

positions of loading, namely end load at the top flange, centroid and at the bottom flange.

A cantilever beam with a length $L=6100$ mm and with the section properties at the root shown in figure 5.13, were analysed for values of critical load at the centroid of the free end for different taper ratios of 0.167, 0.333, 0.5, 0.667, 0.835 and 1. The beam was analysed by both Brown's method and Nethercot's reduction formula.

In the analysis by the Finite Element method the ends of the beam were modelled to be completely fixed at one end while the other end was free. Vertical load was applied at the centroid of the free end.

The results of the these analyses are presented in figure 5.14 and table 5.5. It shows that each of the methods produced a straight line almost parallel to each other. By comparison, the prediction of Nethercot's method gave higher values, followed by Brown's, while the Finite Element formulation predicted lower values. These types of results were consistent throughout the analyses.

It can be said that the Finite Element formulation in the SPACE Finite Element computer programme is valid in predicting the values of critical load of a Web tapered I-cantilever with sufficient accuracy.

5.3.2.2 I-Cantilever with Flange Breadth Taper

Nethercot (5.6) also analysed the case of an I-cantilever with the flange breadth taper shown in figure 5.15. The critical moment M_{cr} was also predicted by using equation 5.22, but making use of the values of γ_e tabulated in table 1a of reference 5.5.

The beam in figure 5.15 with $L=4000$ mm, $t_f=8.5$ mm, $b_{fo}=125.4$ mm, $t_w=5.9$ mm and $d_o=360$ mm was analysed for lateral torsional buckling using Nethercot's method. The analysis was carried out for flange breadth taper ratios v of 0.2, 0.4, 0.6, 0.8 and 1.

In the Finite Element analyses conducted the beam were modelled to be completely fixed at one end while the other end was free. Vertical load was applied at the centroid of the free end.

The results of the two methods of analysis are shown in figure 5.16 and table 5.6. It shows that the results of both analyses agree with each other at taper ratio $v=0.6$, however below the value of this ratio the Finite Element formulation gave slightly higher values. At higher value of the taper ratio, Nethercot's prediction gave slightly higher results.

It can be said that the Finite Element formulation in the SPACE computer programme is able to predict fairly

accurately, the critical lateral buckling load for an I-cantilever with flange breadth taper, loaded at the centroid of the end.

5.3.2.3 Taper I-Cantilever by Other Finite Element Formulations

Karabalis and Beskos (5.7) proposed a Finite Element methodology for the static, free flexural vibration and stability analyses of linear elastic plane structures consisting of tapered beams. The method was based on the development of flexural stiffness, axial stiffness, geometric stiffness and consistent mass matrices for a beam element of constant width and linearly varying depth.

They conducted parametric studies to test numerically the accuracy of the Finite Element formulation that they presented. Stability analysis was conducted on a linearly tapered cantilever beam of constant width and of I-section. The geometric and material characteristic of the cantilever beam are as shown in figure 5.17. The depth of the support was kept constant at 50.8 mm, while the depth at the free end was of the values of 25.4, 12.7 and 10.16 mm to produce taper ratios d_2/d_1 of, 2, 4 and 5 respectively.

In their analysis of the stability problems of the cantilever beam shown in figure 5.17, they compared the

results of the analysis using their formulation ($S_{ij}^*-N^*$) with that of ($G_{ij}-N$) and ($S_{ij}-N$), where S_{ij}^* , G_{ij} and S_{ij} were stiffness coefficients for linearly tapered elements, general tapered elements and uniform elements respectively, while N and N^* stand for geometric stiffness coefficients for uniform elements and for linearly tapered elements respectively (5.7).

The I-Cantilever under consideration was also analysed for elastic stability by the Finite Element Formulation that is being verified. For this purpose of comparison, a taper ratio $d_2/d_1=5.0$ was analysed. The boundary conditions were completely fixed at one end while the other end was free. Vertical load was applied at the centroid of the free end.

The results of the analysis by the SPACE Finite Element formulation are compared with those obtained by Karabalis and Beskos. The results of these stability analyses are as shown in figure 5.18 and table 5.7. Figure 5.18 shows that while all the results computed by Karabalis and Beskos converge to a critical load in the region of 24 kN, the SPACE Finite Element Formulation converges to a load of around 28.0 kN. It can also be seen that an 8-element model was required for the SPACE Finite Element Formulation whereas the others converged sufficiently using 5 or 6 elements.

Therefore it can be said that the SPACE Finite Element

Formulation gave less conservative results when compared to the Finite Element formulations by Karabalis and Beskos. However, it also shows that the SPACE Finite Element formulation converges with sufficient accuracy for this tapered member using only 8 elements.

5.4 Lateral Buckling of Tapered I-Section Beam-Columns

5.4.1 Governing Equation for Buckling Of Beam-Columns

Culver and Preg (5.8) studied the case of the beam-column shown in figure 5.19 and derived the critical combinations of axial load and end moment. The beam column under consideration was subjected to an axial load P and moment M applied in the $y - z$ plane. When the load was applied, the beam-column initially deflected in the $y - z$ plane. Upon reaching a certain critical combination of P and M , however, *bifurcation of equilibrium became possible* and lateral torsional buckling occurred.

Culver and Preg, formulated the differential equation for determining the critical loads by using Vlasov's method (5.9) for a beam-column of uniform cross-section. They modified it to account for the variation of cross sectional properties along the length of the member.

Denoting by u , v and ϕ , the deflections of the buckled beam-

column configuration in the x and y directions and the angle of twist about the shear centre respectively, the equilibrium conditions of the beam can be derived as ;

$$E[I_x(z) v'''] = q_y \dots \dots \dots (5.23)$$

$$E[I_y(z) u'''] = q_x \dots \dots \dots (5.24)$$

$$E[I_w(z) \phi'''] + 4E \left[\frac{I_w(z)}{z^2} \phi' \right]' - G[K_T(z) \phi'] = m \dots \dots \dots (5.25)$$

Equations 5.23 and 5.24 were the familiar beam equations according to Bernoulli-Euler Theory whilst equation 5.25 was obtained by converting Lee's (5.10) equation for non-uniform torsion of tapered beams to the notation now used. In these equations, q_x and q_y equals to the magnitudes of additional transverse load per unit length induced during buckling. These loads were the results from the projection of stresses acting on the infinitesimal element $dz=1$, in the pre-buckled state onto the same element in the buckled state.

The normal stresses at any cross section of the pre-buckled beam-column can be represented as ;

$$\sigma(z) = -\frac{P}{A(z)} - \frac{M_x(z) y(z)}{I_x(z)} \dots \dots \dots (5.26)$$

$$M_x(z) = M_2 \left[(1-\eta) \left(\frac{z-a}{L} \right) + \eta \right] \dots \dots \dots (5.27)$$

It was assumed that the angle of taper α was small when using equation 5.26. Using this normal stress equation (5.26 and 5.27), and following Vlasov's procedure, the expression for additional transverse loads and torque was established as;

$$Q_x = -Pu'' + M_2 \left[(1-\eta) \left(\frac{z-a}{L} \right) + \eta \right] \eta'' + 2 \frac{M_2}{L} [(1-\eta)] \eta' \dots \dots \dots (5.28)$$

$$Q_y = -Pv'' \dots \dots \dots (5.29)$$

$$m = +M_2 \left[(1-\eta) \left(\frac{z-a}{L} \right) + \eta \right] u'' - \frac{PI_p(z)}{A(z)} \phi'' \dots \dots \dots (5.30)$$

The differential equation which governs the elastic deformation behaviour of the beam-column can then be established by equations 5.23, 5.24, 5.25, 5.28, 5.29 and 5.30, and it becomes ;

$$E[I_x(z) v'''] + Pv'' = 0 \dots \dots \dots (5.31)$$

$$E[I_y(z) u'''] + Pu'' - M_2 \left[(1-\eta) \left(\frac{z-a}{L} \right) + \eta \right] \phi'' - M_2 \left[\frac{2(1-\eta)}{L} \right] \phi' = 0 \dots \dots (5.32)$$

$$E[I_x(z) \phi'''] + 4E \left[\frac{I_x(z)}{z^2} \phi' \right]' - G[K_T(z) \phi']' \frac{PI_p(z)}{A(z)} \phi'' + E \left[\frac{I_p(z)}{A(z)} \right]' \phi' - M_2 \left[(1-\eta) \left(\frac{z-a}{L} \right) + \eta \right] u'' = 0 \dots \dots \dots (5.33)$$

These equations were solved by finite difference method using the appropriate boundary conditions as follows;

For pinned end,

$$u = u'' = \phi = z\phi' + 2\phi' = 0 \dots \dots \dots (5.34)$$

For fixed end,

$$u = u' = \phi = \phi' = 0 \dots \dots \dots (5.35)$$

In order to obtain a solution for the above expressions applicable to a broad class of problems, the equation was non-dimensionalised using the critical load and moment for uniform beam-columns. This results in a more useful form of expression of the critical loads for tapered beam-columns.

Using the energy approach, the critical combination of the axial load P and end moments $M_2=M$, $M_1=\eta M$, for the tapered beam-column can be given as

$$\left[1 - \frac{P}{P_y^*}\right] \cdot \left[1 - \frac{P}{P_T^*}\right] = \left[\frac{M}{M_{cr}^*}\right] \dots \dots \dots (5.36)$$

In equation 5.36, P_y^* , P_T^* , and M_{cr}^* are the Euler buckling loads and the critical moment under no thrust for a tapered column. In order to use the interaction equation (i.e. equation 5.36), to find the critical combination of axial load P and end moment M , for a particular tapered beam-column, it was first necessary to evaluate P_y^* , P_T^* , and M_{cr}^* for the same column. These values have been solved by the finite difference method and presented in tables and graphs in reference 5.8. Four types of combinations of end conditions namely, pinned-pinned ends, pinned-fixed ends, fixed-fixed ends and fixed-pinned ends were considered.

5.4.2 Analysis of Tapered Beam-Columns

Two cases of beams with two different boundary conditions were studied in this section in order to compare the results of the analysis by Culver's method and that of the SPACE Finite Element formulation. The two cases were as follows;

5.4.2.1 Case of a Tapered Beam-Column with the Small End Pinned and the Large End Fixed

The tapered beam-column under consideration is shown in figure 5.20. It is subjected to an axial load of P kN and an applied moment M at the larger end which caused lateral-torsional buckling. The beam was supported by a roller at the smaller end while the large end was fixed. Four cases of this beam-column were studied for the taper parameters $d_2/d_1=2, 1.8, 1.5$ and 1.3 . In all the cases considered, Culver's method was used to calculate the critical moment applied at the larger end when a known axial load was applied at the smaller end. The procedure was first to establish the critical loads for an untapered section based on the section properties of the large end. From the table in reference 5.8 the critical loads and moments for the untapered section were determined. From these values the critical values for tapered beam-columns were obtained. Inserting the critical values obtained, and the known axial load, in the interaction equation (equation 5.36), the critical value of end moment can be calculated.

The same four cases of beam-column, were analysed by the SPACE Finite Element formulation. Two sets of results were obtained for each case, namely by modelling with 10-elements and 20-elements. This was done to check the convergence and the accuracy of the results as affected by the number of elements used in the model.

Figures 5.21, 5.22, 5.23 and 5.24 show the results of the analysis for different values of the taper parameter, i.e, $d_2/d_1=2, 1.8, 1.5$ and 1.3 respectively. Figure 5.21 shows that the curves were almost parallel. However, Culver's curve gave a smaller predicted critical moment for the same axial load when compared with the Finite Element curves. Furthermore, the results of the 20-element analysis in the Finite Element method gave more critical results than the 10-element cases.

Figure 5.22 shows the results for the case of a taper parameter $d_2/d_1=1.8$. The predictions of critical moment by Culver were higher for axial load below 80 kN when compared to the prediction of Finite Element method. However, above this value of axial load, the Finite Element method predicted higher value of critical moment. It can be said that close agreement between Culver's and the Finite Element Method was achieved between the axial load range of 50 kN to 100kN.

Figure 5.23 shows the results of analysis for the case of a taper parameter $d_2/d_1=1.5$. The results are similar to those in figure 5.22. However, in this case the difference between the gradient of Culver's curve and that of the F.E.M. curves was even greater. It was also observed that the difference in the value of critical moment between Culver's and the Finite Element method appeared to be greater at low value of axial load.

Figure 5.24 shows the results of analysis for the case of a taper parameter $d_2/d_1=1.3$. It can be seen that the results are in same form as those of the previous case. However, in this case the Finite Element method shows a higher value of critical moment for values of axial load below 180 kN. Above this value of axial load the Culver's curve gave higher critical moment.

It can be said therefore, that for the case of tapered beam-column with small-end pinned, and large-end fixed, the SPACE Finite Element formulation was able to predict good and fairly accurate critical loading.

5.4.2.2 The Case of Tapered Beam-Column with Pinned-Pinned-Ends

The tapered beam-column under consideration is shown in figure 5.25. It is subjected to an axial load P kN and a moment M applied at the larger end. The beam is supported by a pin joint at the large end and roller at the small end.

This case was investigated in a similar manner to the case in the previous section in which tapered parameters of $d_2/d_1=2, 1.8, 1.5$ and 1.3 were considered. Analyses were conducted by Culver's Method and the Finite Element Method using 10-and 20-element models. However, in this case the boundary conditions for the Finite Element model were that

no torsional restraint was provided at both ends but longitudinal movement was imposed at the large end.

The results of the analyses are shown in figures 5.26, 5.27, 5.28 and 5.29. Figure 5.26 shows the results of the analysis for the case of taper parameter $d_2/d_1=2$. It can be seen that Culver's curve had a steeper gradient than the Finite Element curves. Similar curves were observed for the other three cases considered. It also appeared that the *differences in the value of critical moments* between Culver's and the Finite Element method were greater at lower value of axial load.

Therefore, it can be deduced that for the case of tapered beam-columns with both ends pinned, the SPACE Finite Element formulation was able to give fairly accurate results for elastic buckling. It appears that in all the cases considered, the Finite Element method gave lower values of critical moment than Culver's method. It can also be seen that the value of critical moment at axial load P , increases with the increase in the value of the taper parameter.

Comparing the case of fixed-pinned in section 5.4.2.1 with that of the pinned-pinned end in this section, it has been shown that the case of pinned-pinned end gave a much lower critical moment for the same axial load than the fixed-pinned end cases.

5.5 Summary and Conclusion

An assessment of the Finite Element Formulation described in chapter 4 and used in the SPACE Finite Element computer program was carried out against published theoretical evidence for tapered members. This present assessment was done by modelling selected specimens from the literature and showing whether or not the Finite Element model could simulate accurately the behaviour associated with elastic buckling of the specimen.

Consideration was first given to narrow, tapered rectangular cross-section beams. This was followed by tapered I-section beams and cantilevers. An investigation was also conducted in this section to check the convergence of the SPACE Finite Element formulation with other selected Finite Element formulations. Tapered beam-columns were treated at the end of the chapter.

It was shown in section 5.2. that the elastic buckling of a tapered, narrow beam with rectangular cross-section could be predicted very accurately. A double taper model was also considered and its ability to analyse different types of taper conditions was demonstrated.

Lateral-torsional buckling of tapered I-beams and cantilevers was treated in section 5.3. Again, comparisons of the theoretical results and the Finite Element models

produced very good agreement. However, the Finite Element model tends to produce slightly more conservative predictions especially at lower taper ratios.

Investigation on the convergence of the Finite Element Formulation in the case of I-cantilevers revealed that an 8-element model was required to achieve accurate results for tapered members. The convergence for the case of beam-columns showed that 20-element models achieve more accurate results than the 10-elements.

Fairly accurate results were obtained for the case of tapered beam-columns. Modelling in this case was more crucial in deciding the results since the accurate factor must first be established for the axial load and the end moment.

The Finite Element formulation being verified appeared capable of predicting accurately the elastic buckling behaviour of tapered members. The investigation into the behaviour of modern portal frame construction, particularly the results of testing of Frame 3 showed the importance of checking for lateral-torsional buckling in the haunch area. The following chapters deal in detail with the design aspects for lateral-torsional buckling. This Finite Element Formulation is used to analyse lateral-torsional buckling problems at the haunch section of the modern portal frame.

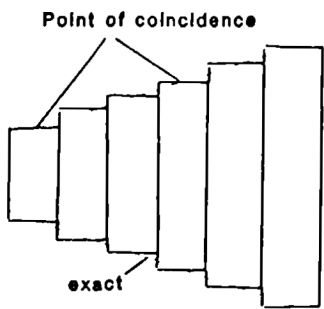


Figure 5.1 Stepped Representation of a Tapered Beam

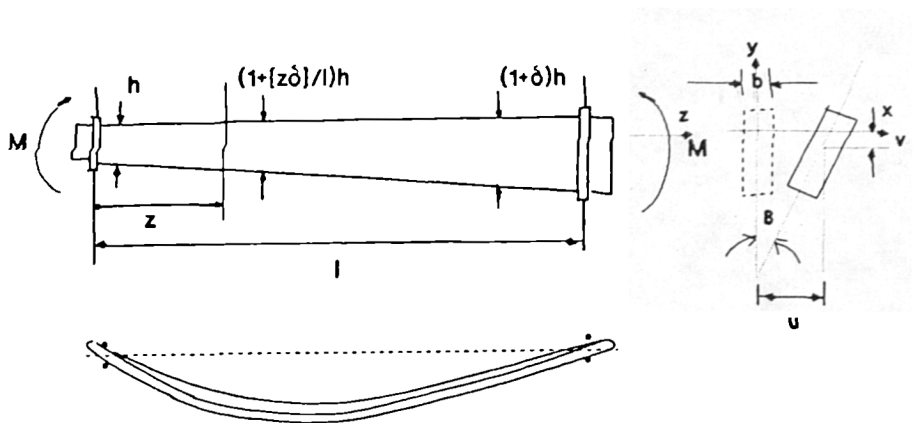


Figure 5.2 Lateral Buckling of Narrow Rectangular Tapered Beam

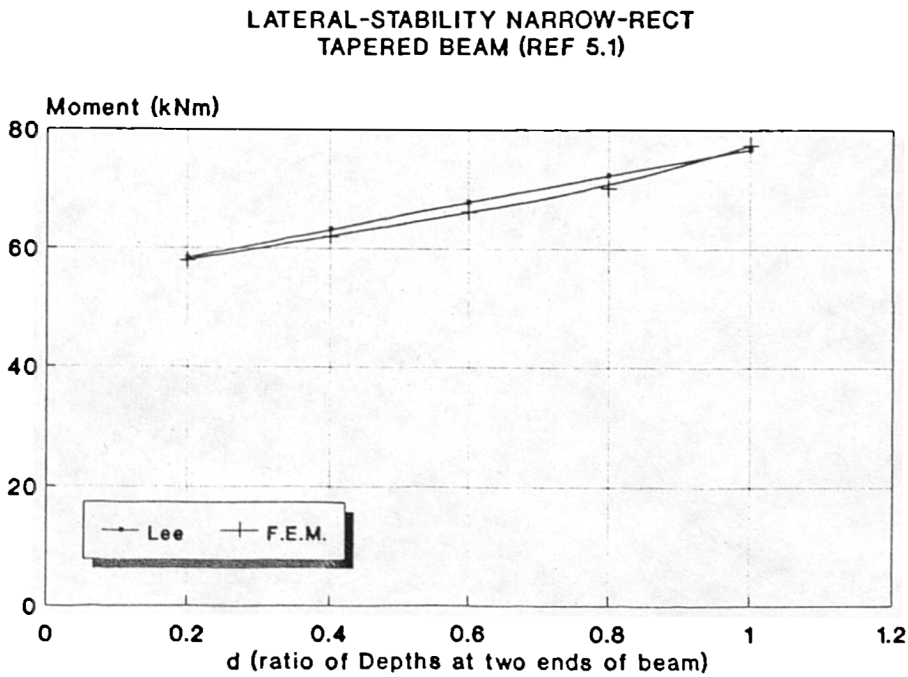


Figure 5.3 Comparison between Lee (5.1) and Finite Element Method

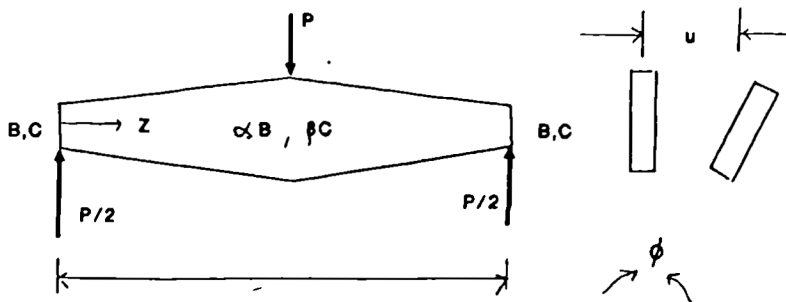


Figure 5.4 Beam and the Loading Considered by Massey (5.2)

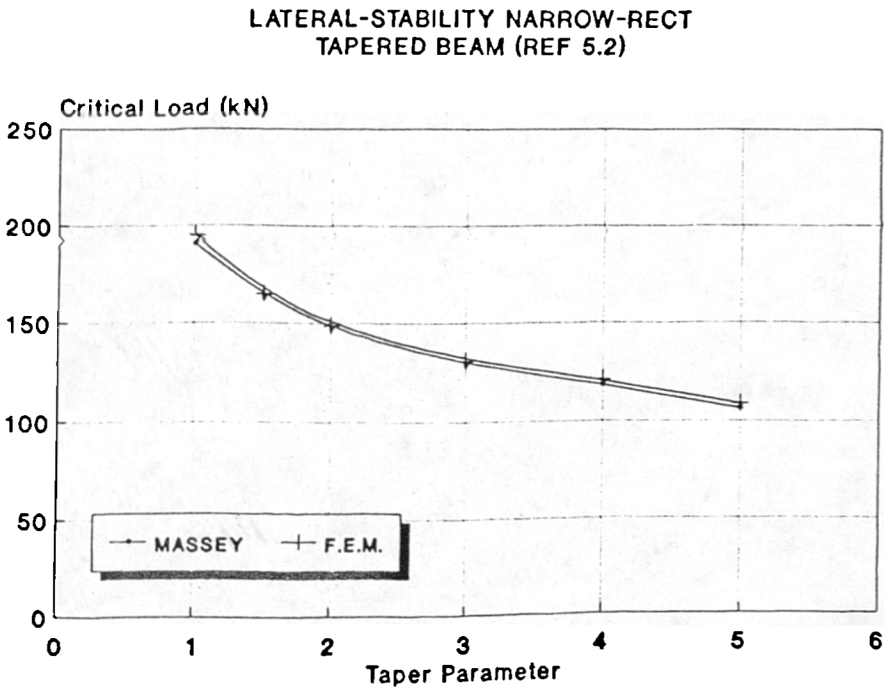


Figure 5.5 Comparison between Massey and Finite Element Method

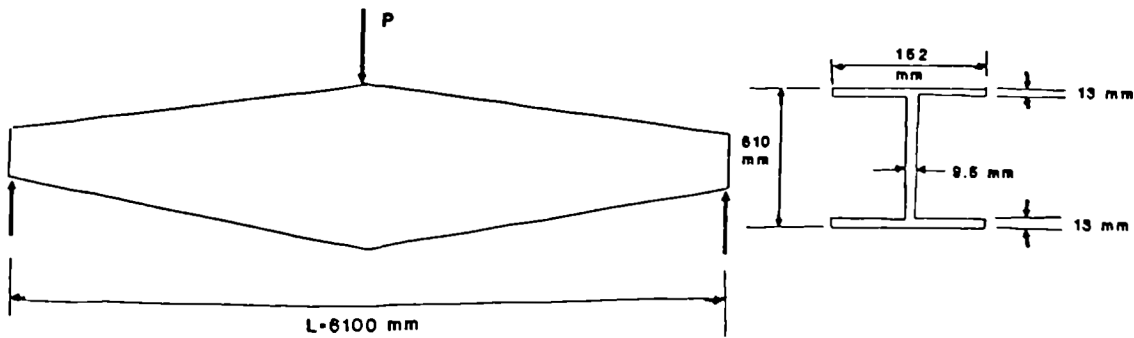


Figure 5.6 Simply Supported Beam with Double Taper

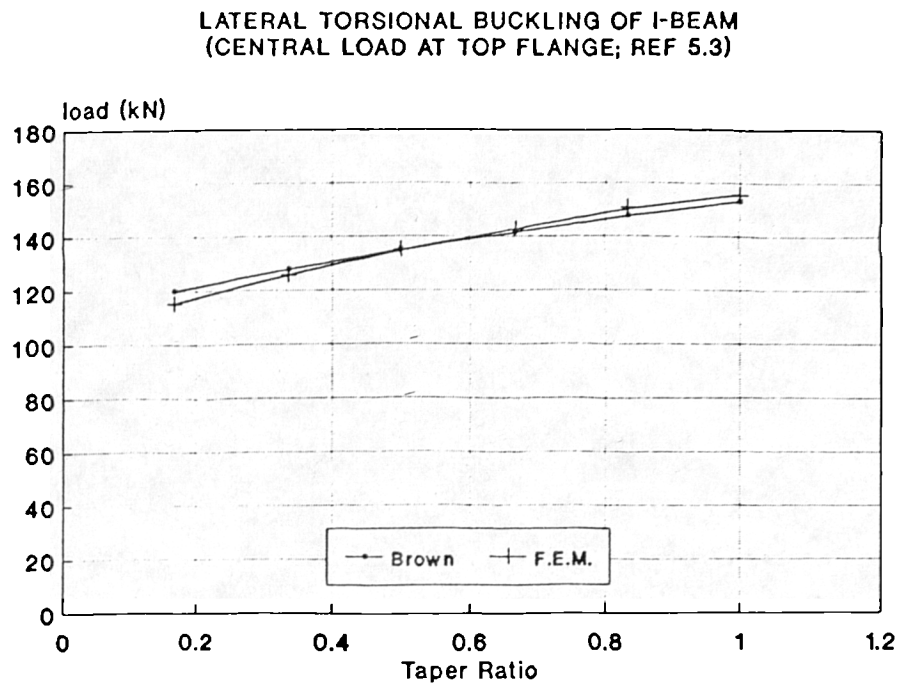


Figure 5.7 Comparison of Brown and Finite Element Method

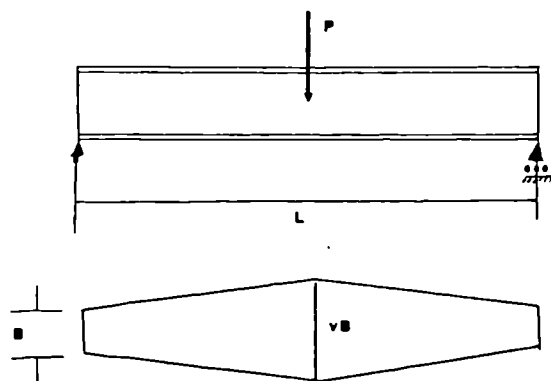


Figure 5.8 Taper Beam with Flange Breadth Curtailed

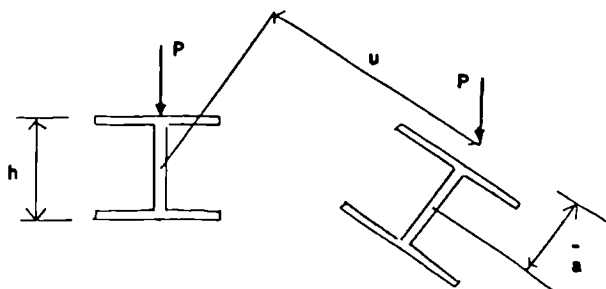


Figure 5.9 Deflected Shape of Buckled Beam
Considered by Kitipornchai & Trahir (5.5)

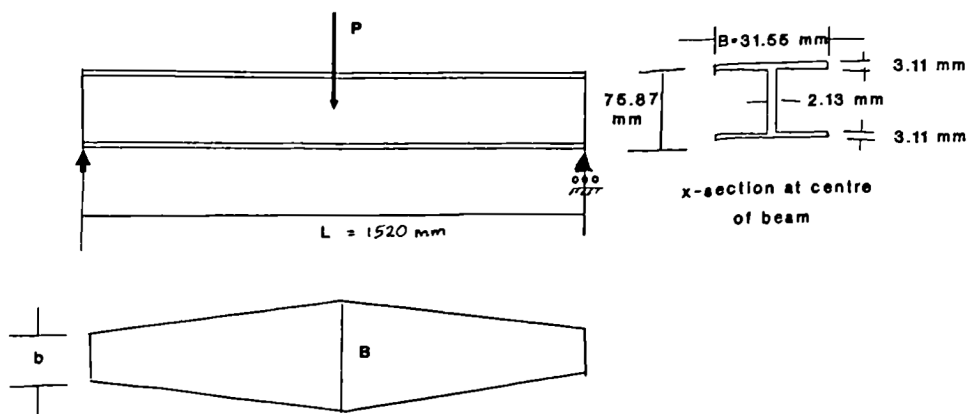


Figure 5.10 Properties of Beam used in the Analysis for P_{cr}

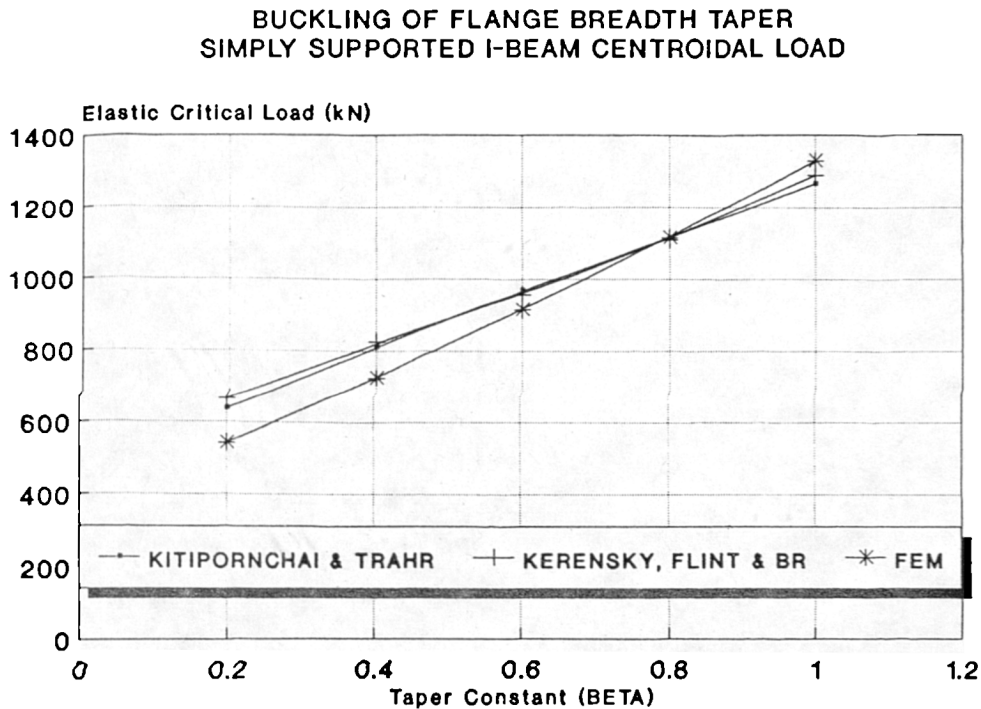


Figure 5.11 Comparison of Results of Analysis Between Kitipornchai's, Kerensky's and Finite Element Method

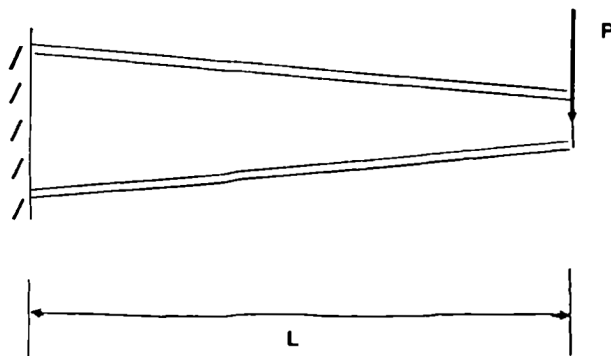


Figure 5.12 Tapered I-Cantilever

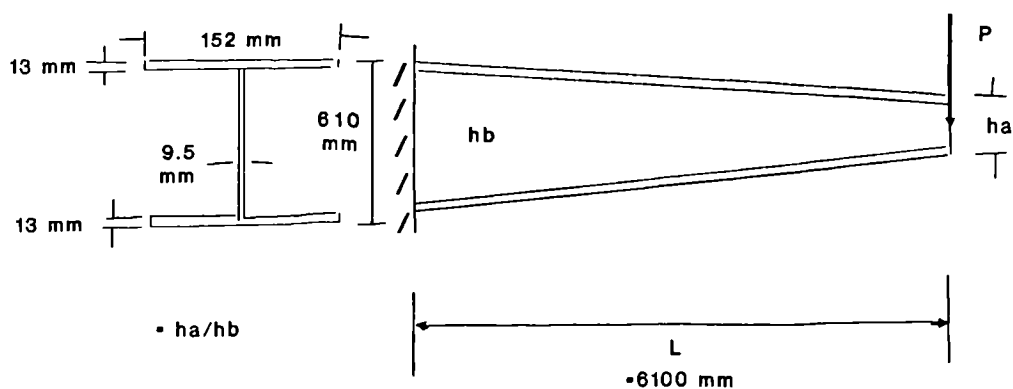


Figure 5.13 Section Properties of Tapered I-Cantilever

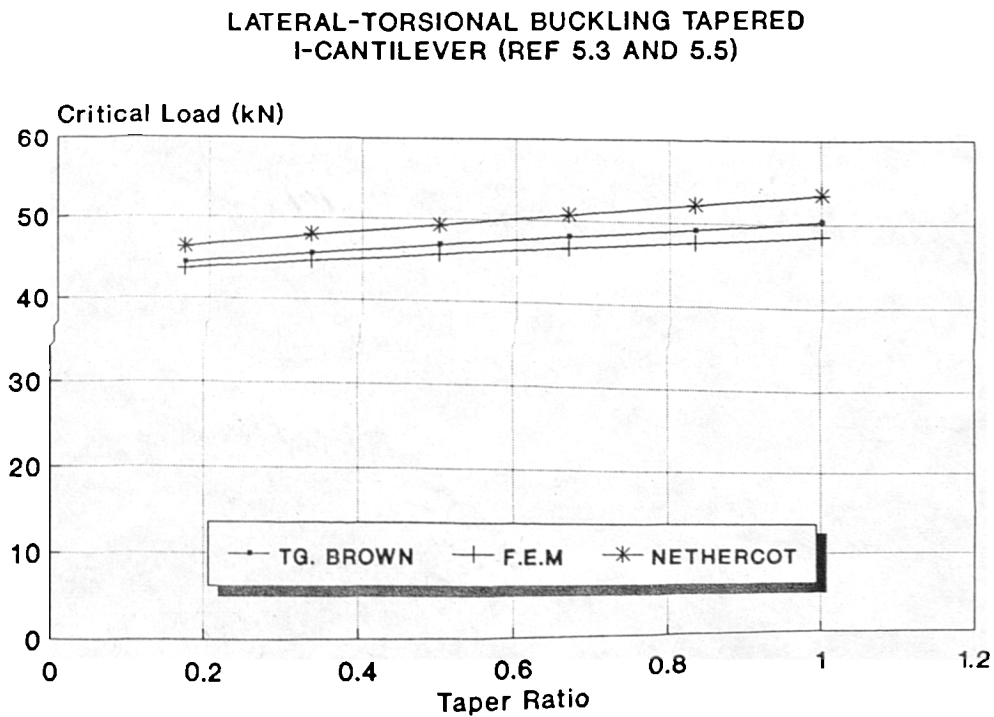


Figure 5.14 Comparison of Results of Analysis by Brown, Nethercot and Finite Element Method

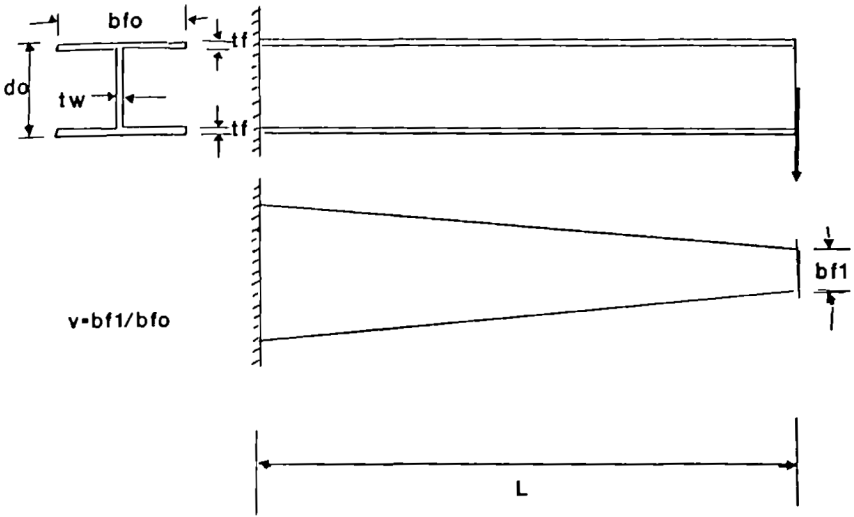


Figure 5.15 I-Cantilever with Flange Breadth Taper

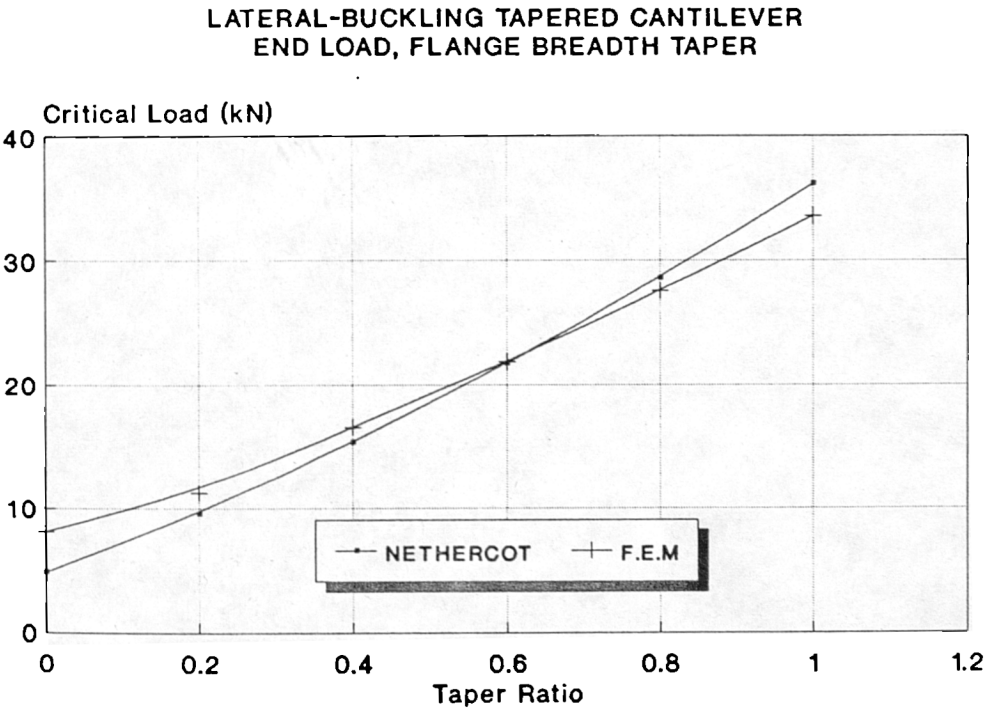


Figure 5.16 Comparison of Results of Analysis by Nethercot and The Finite Element Method

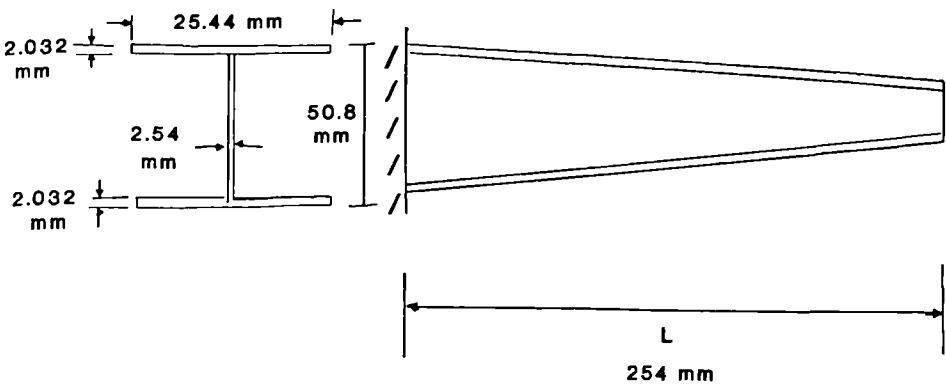


Figure 5.17 Section Properties of Tapered I-Cantilever

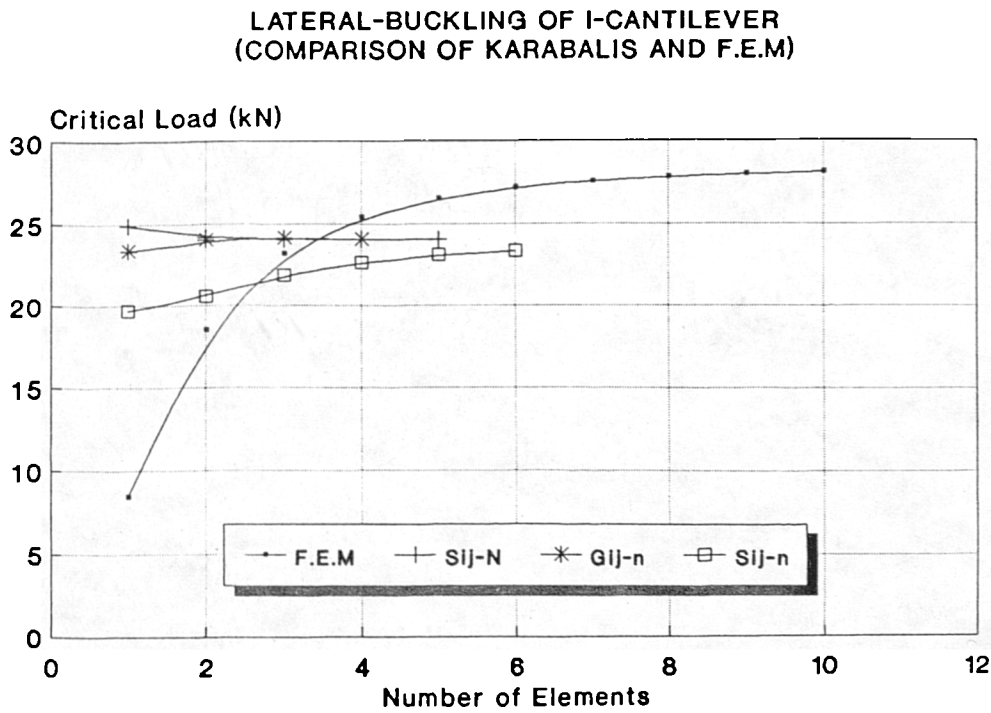


Figure 5.18 Comparison of Results of Analysis by Karabalis and Finite Element Method (case $d_2/d_1=5$)

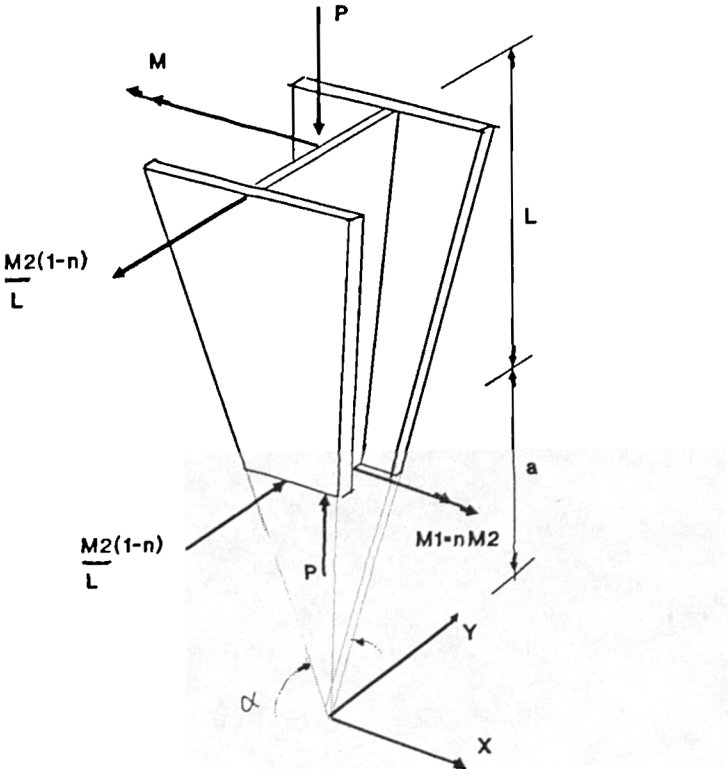


Figure 5.19 Tapered I-Section Beam-Column

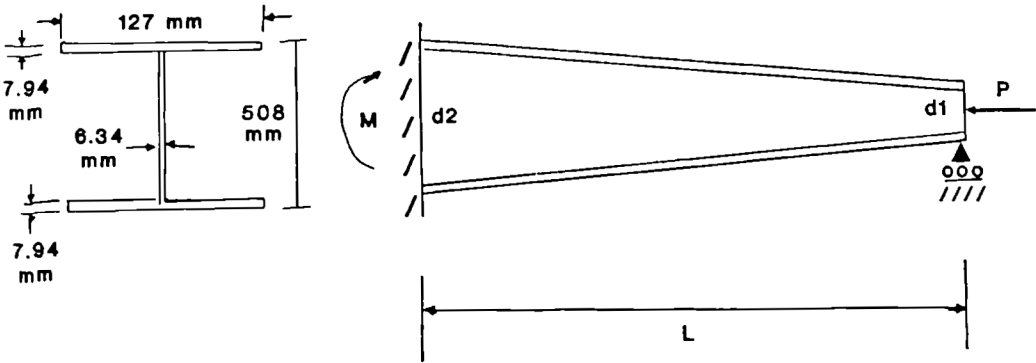


Figure 5.20 Fixed-Pinned Tapered Beam-Column

LATERAL-BUCKLING OF TAPERED BEAM-COLUMN
(Moment Large-end & Axial Load Small-end
Large End Fixed & Small End Pinned)

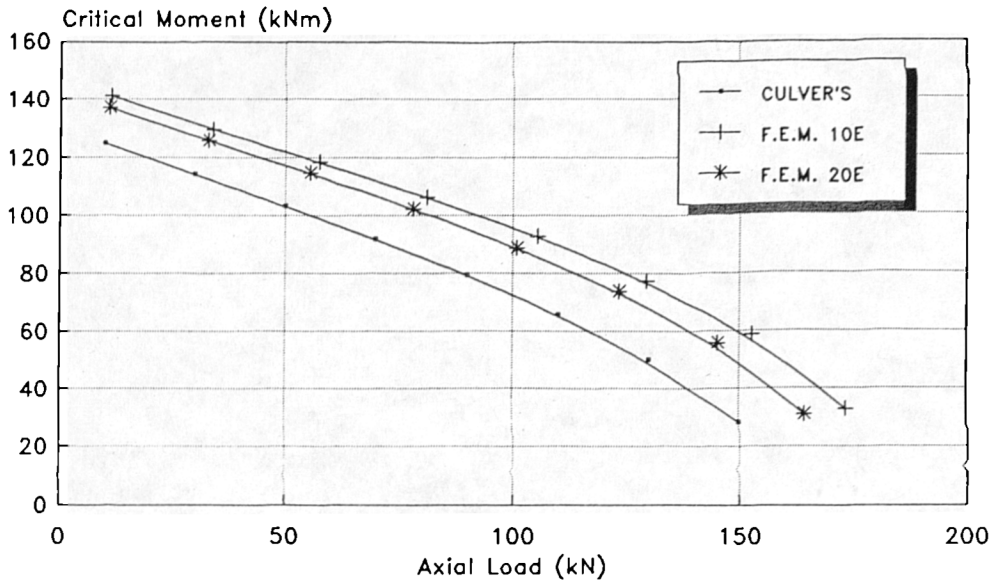


Figure 5.21 Comparison of Results of Culver's Finite Difference (5.7) with Finite Element Method; $d2/d1=2$

LATERAL-BUCKLING TAPERED BEAM-COLUMN
(Moment Large-end & Axial Load Small-end
Small-end Pinned & Large-end Fixed)

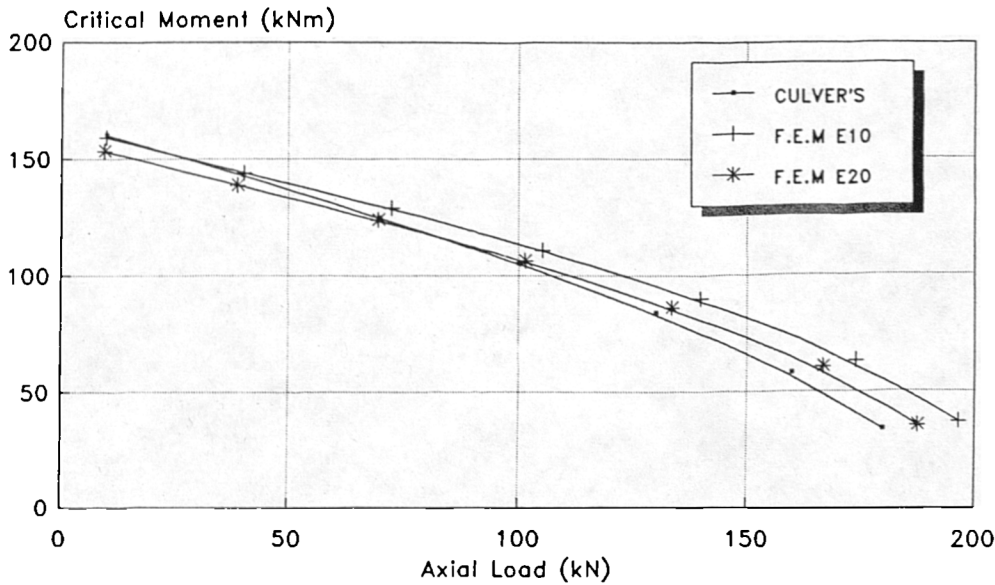


Figure 5.22 Comparison of Results of Culver's Finite Difference (5.7) with Finite Element Method; $d2/d1=1.8$

LATERAL-BUCKLING OF TAPERED BEAM-COLUMN
(Small-end Pinned & Large-end Fixed,
Moment Large-end & Axial Load Small-end)

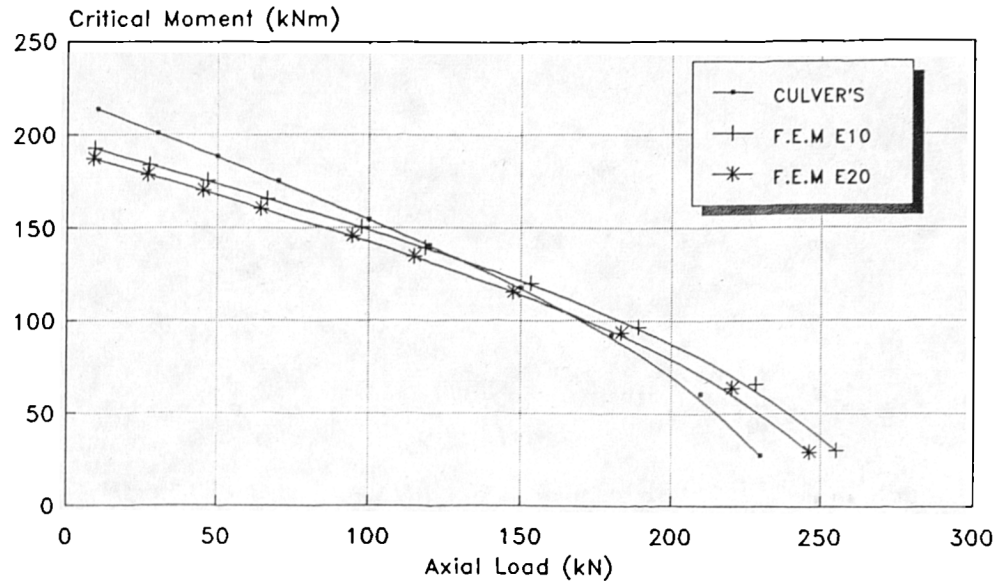


Figure 5.23 Comparison of Results of Culver's Finite Difference (5.7) with Finite Element Method; $d_2/d_1=1.5$

LATERAL-BUCKLING OF TAPERED BEAM-COLUMN
(Small-end Pinned, Large-end Fixed,
Moment-Large end & Axial Load Small-end)

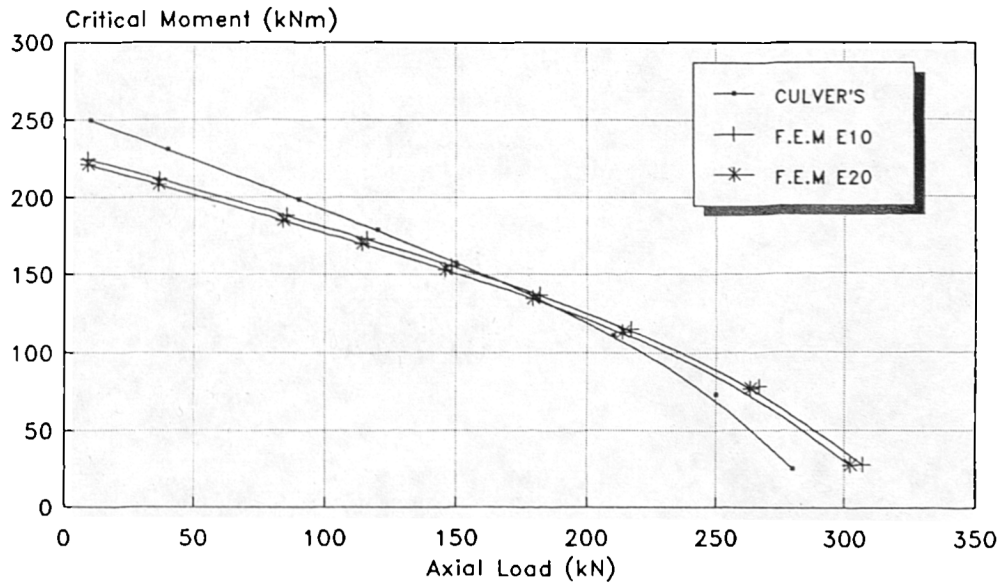


Figure 5.24 Comparison of Results of Culver's Finite Difference (5.7) with Finite Element Method; $d_2/d_1=1.3$

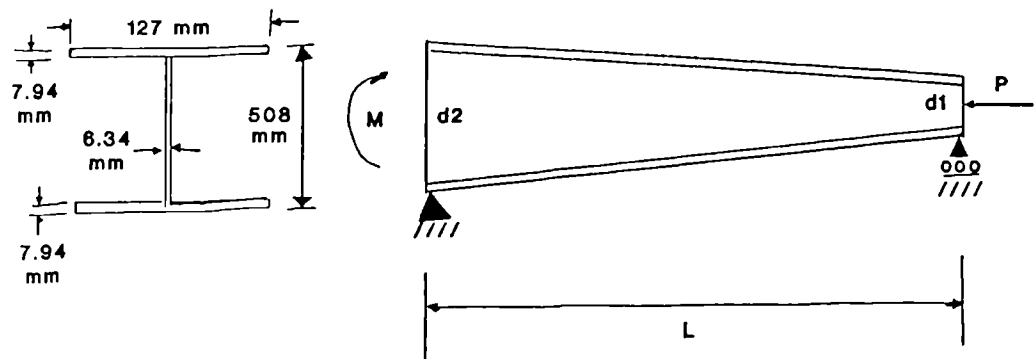


Figure 5.25 Pinned-Pinned Tapered Beam-Column

LATERAL-BUCKLING OF TAPERED BEAM-COLUMN
(Pinned-Pinned Ends ; $d_2/d_1=2$
Moment Large-end & Axial Load Small-end)

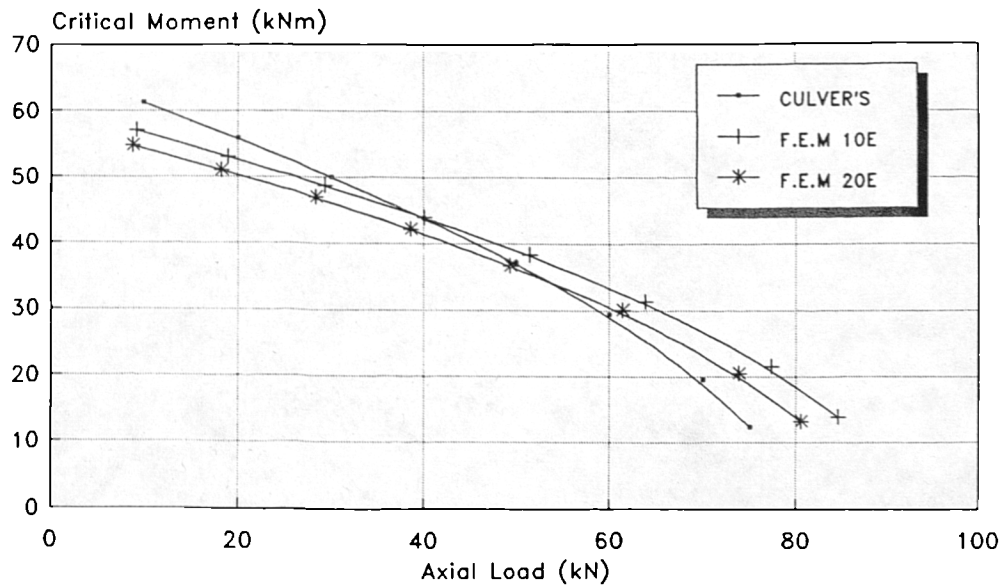


Figure 5.26 Comparison of Results of
Culver's Finite Difference Method (5.7)
With Finite Element Method

LATERAL-BUCKLING OF TAPERED BEAM-COLUMN
(Pinned-Pinned Ends ; $d_2/d_1=1.8$
Moment Large-end & Axial load Small-end)

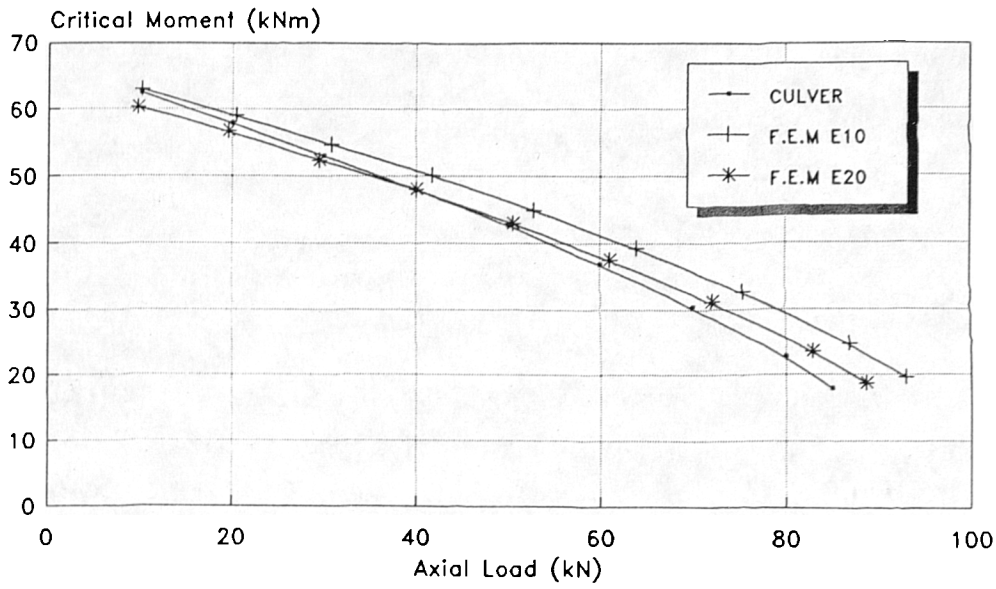


Figure 5.27 Comparison of Results of
Culver's Finite Difference Method (5.7)
With Finite Element Method

LATERAL-BUCKLING OF TAPERED BEAM-COLUMN
(Pinned-Pinned Ends; $d_2/d_1=1.5$
Moment Large-end & Axial Load Small-end)

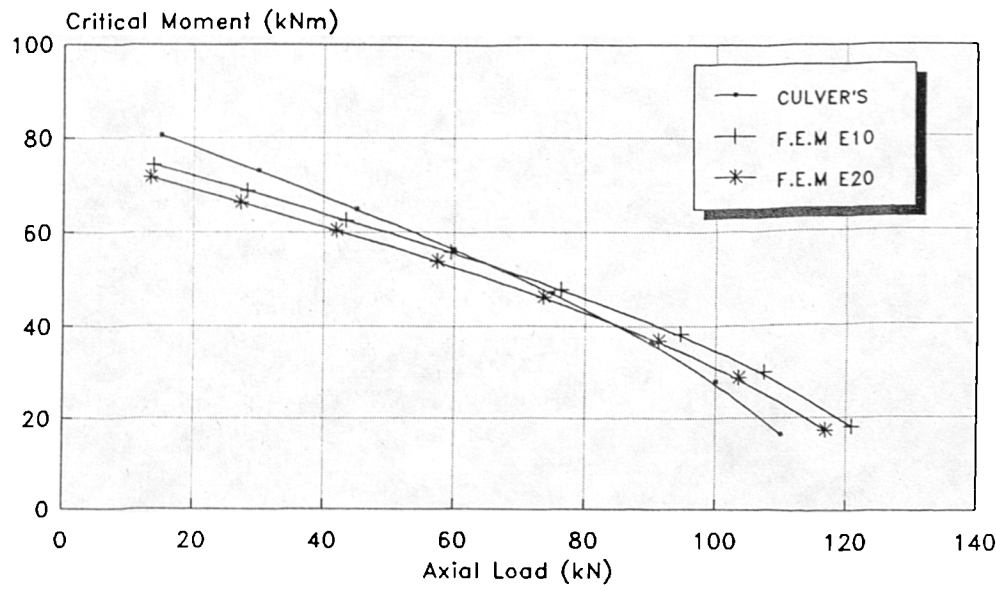


Figure 5.28 Comparison of Results of
Culver's Finite Difference Method (5.7)
With Finite Element Method

LATERAL-BUCKLING OF TAPERED BEAM-COLUMN
(Pinned-Pinned Ends ; $d_2/d_1=1.3$
Moment Large-end & Axial Load Small-end)

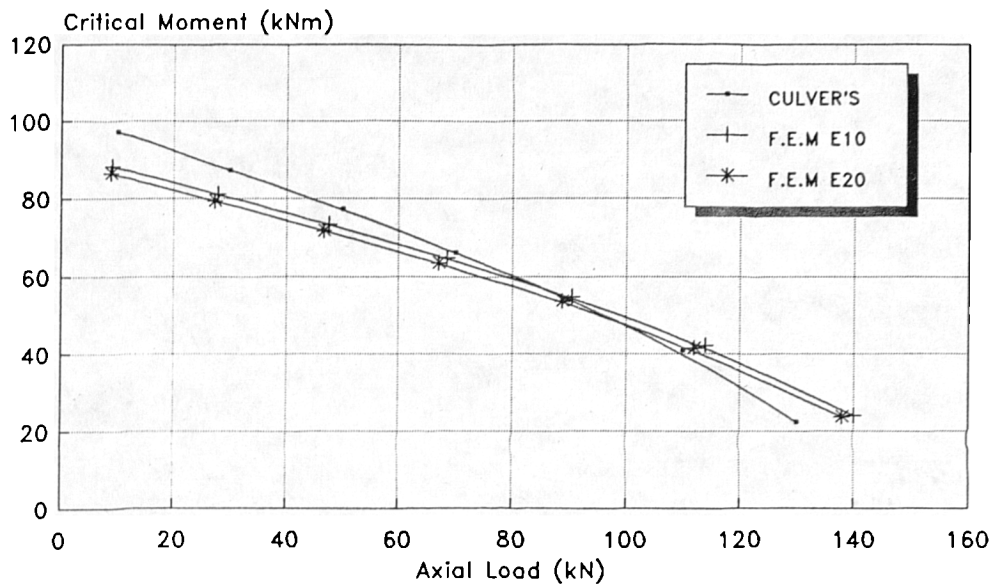


Figure 5.29 Comparison of Results of
Culver's Finite Difference Method (5.7)
With Finite Element Method

TABLE 5.1 RESULTS OF ANALYSIS BY LEE (EQ 1) AND F.E.M

TAPER RATIO γ	LEE (EQUATION 1) kNm	FINITE ELEMENT METHOD	
		kNm	ERROR %
1	76.75	77.41	0.85%
0.8	72.40	70.26	- 2.9%
0.6	67.91	66.22	- 2.48%
0.4	63.24	62.08	- 1.8%
0.2	58.35	57.95	- 0.68%

TABLE 5.2 PROPERTIES OF BEAM AND RESULTS OF ANALYSIS

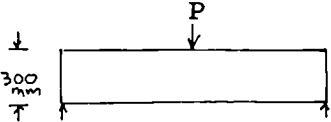
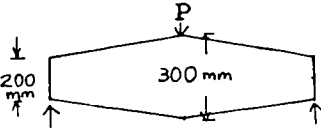
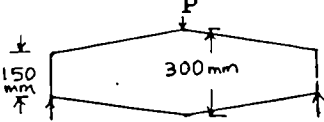
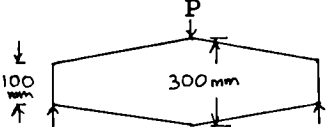
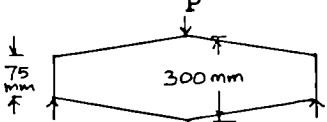
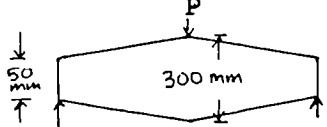
BEAM PROPERTIES (THICKNESS OF BEAM 25 mm)	MASSEY P_{cr} (kN)	F.E.M P_{cr} (kN)	% ERROR
$\alpha=1$ $\beta=1$ 	190.7	195	2.09
$\alpha=1.5$ $\beta=1.5$ 	163	165	1.22
$\alpha=2$ $\beta=2$ 	147	149.5	1.7
$\alpha=3$ $\beta=3$ 	129	131	1.55
$\alpha=4$ $\beta=4$ 	118.7	121	1.93
$\alpha=6$ $\beta=6$ 	106.5	109	2.34

TABLE 5.3 RESULTS OF ANALYSIS OF SIMPLY SUPPORTED DOUBLE TAPER I-BEAM

TAPER RATIO α	T.G BROWN P_{cr} (kN)	F.E.M P_{cr} (kN)	% ERROR
0.167	120.0	115.5	3.75
0.333	127.9	125.8	1.64
0.500	135.1	135.08	0.01
0.667	141.6	142.7	0.77
0.833	147.6	150.7	2.1
1.000	153.2	155.7	1.63

NOTE: $\alpha=h_a/h_b$

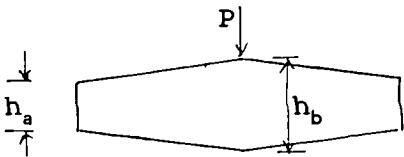


TABLE 5.4 RESULTS OF ANALYSIS OF FLANGE BREADTH TAPER I-BEAM

TAPER RATIO β	KITIPORNCHAI & TRAHIR P_{cr} (N)	KERENSKY, FLINT & BROWN P_{cr} (N)	F.E.M P_{cr} (N)
0.2	638	667	540
0.4	811	825	725
0.6	970	956	916
0.8	1114	1110	1116
1.0	1267	1290	1329

NOTE: $\beta=b/B$

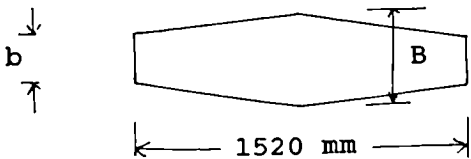


TABLE 5.5 RESULTS OF ANALYSIS OF TAPERED I-CANTILEVER

TAPER RATIO α	T.G BROWN P_{cr} (kN)	NETHERCOT P_{cr} (kN)	F.E.M P_{cr} (kN)
0.167	44.34	48.27	43.64
0.333	45.60	47.90	44.60
0.500	46.80	49.188	45.67
0.667	48.06	50.69	46.65
0.833	49.14	52.10	47.61
1.000	50.28	53.40	48.54

NOTE: $\alpha=h_a/h_b$

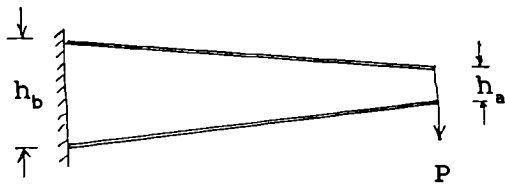


TABLE 5.6 RESULTS OF ANALYSIS OF FLANGE BREADTH TAPER I-CANTILEVER

TAPER RATIO v	NETHERCOT P_{cr} (kN)	F.E.M P_{cr} (kN)	% ERROR
0.2	9.51	11.26	18.4
0.4	15.32	16.54	7.90
0.6	21.69	21.88	0.87
0.8	28.58	27.54	3.60
1.0	36.16	33.60	7.07

NOTE: $v=b_{f1}/b_{fo}$

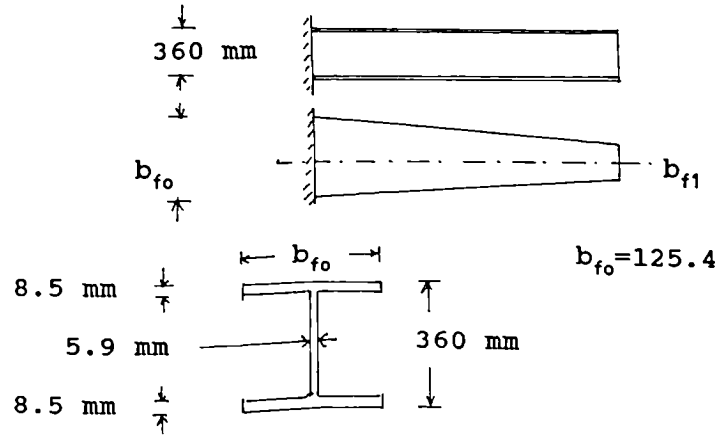
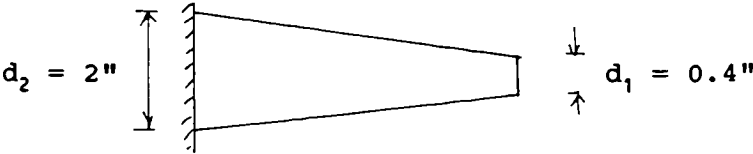


TABLE 5.7 COMPARISON OF RESULTS OF VARIOUS FINITE ELEMENT FORMULATIONS

NO OF ELEMENTS	SPACE F.E.M P_{cr} (kN)	KARABALIS S_{ij}^*-N P_{cr} (kN)	KARABALIS $G_{ij}-N$ P_{cr} (kN)	KARABALIS $S_{ij}-n$ P_{cr} (kN)
1	8.44	24.9	23.39	19.7
2	18.5	24.15	24.02	20.54
3	23.2	24.06	24.14	21.84
4	25.36	24.04	24.03	22.64
5	26.5	24.03	-	23.1
6	27.2	-	-	23.35
7	27.55	-	-	-
8	27.81	-	-	-
9	27.96	-	-	-
10	28.09	-	-	-

NOTE : $d_2/d_1 = 5$



CHAPTER 6

6.0 Design for Lateral-Torsional Buckling to BS 5950:

Part 1

6.1 Introduction

When an unrestrained beam is subjected to inplane bending it will not only suffer inplane deflection but also an out-of-plane deformation and twist about its longitudinal axis. This effect is magnified as the load is increased until the beam buckles at an applied moment which may be less than the moment of resistance of the section. This effect is known as lateral-torsional buckling.

Although the basic theory of lateral-torsional buckling provides an adequate description of the behaviour of the beam under very carefully controlled laboratory conditions, it does not cater for several factors which, affect the lateral stability of the beam in an actual structure. Some of these factors such as the presence of residual stresses or geometrical imperfections, can affect the behaviour of the real beam.

BS 5950 (6.1) is the main British Code of Practice for steel design which superseded BS 449. The design for hot-rolled sections in simple and continuous construction is contained in Part 1 of the code and Part 2 covers the specification

for materials, fabrication and erection.

This chapter deals with the study of the design procedure laid down in BS 5950: Part 1 for the design of members subjected to lateral-buckling. The code specifies two types of length between torsional restraints, which are:

- (1) An Unrestrained Length, i.e., no intermediate restraints are positioned between the lateral-torsional restraints, and
- (2) A Restrained Length, i.e., at least one restraint has been positioned between the lateral-torsional restraints.

From these two basic situations, 8 relevant cases can be identified and these are shown in table 6.1. The following are studies considered for each of those cases, however, the general theoretical basis for design for lateral-torsional buckling is first presented.

6.2 Theoretical Basis of Design for Elastic Lateral-Torsional Buckling of Beams

6.2.1 The Basic Problem of Lateral-Torsional Buckling

The basic problem used to illustrate the theory of lateral-torsional buckling is shown in figure 6.1. in which, the perfect elastic beam is loaded with equal and opposite end moments. The beam's end conditions are simply supported in

the lateral plane with, twist and lateral deflection prevented, and no rotational restraint in plan.

The problem may be regarded as analogous to the basic pin-ended Euler strut. When the beam is placed in a buckled position, the magnitude of the moment necessary to hold it in that position is determined by equating the disturbing effect of the end moments, acting through the buckling deformation, to the internal (bending and torsional) resistance of the section. The elastic critical buckling moment given in standard texts (6.2, 6.3, 6.4) is;

$$M_E = \frac{\pi \sqrt{EI_y GJ}}{L} \sqrt{1 + \frac{\pi^2 EI_w}{GJ L^2}} \dots \dots \dots (6.1)$$

where EI_y is the minor axis flexural rigidity, and EI_w is the warping rigidity of the beam. The presence of the flexural (EI_y) and torsional (GJ and EI_w) stiffness of the member is the direct consequence of the lateral and torsional components of the buckling deformations. The relative importance of the two mechanisms for resisting twisting is reflected by the second square root term. Length is also an important factor, influencing the first term directly and indirectly in the second term via the $\pi^2 EI_w / L^2 GJ$ term.

6.2.2 Extension of the Theory for Application to Other Cases

6.2.2.1 Loading Pattern on Member

The basic solution for lateral-torsional buckling described

in the previous section is the most severe case of loading that can be imposed on the beam. Since the basic terms are the same for other cases or loading, this solution can be conveniently compared with other cases of loading pattern. For example, consider the beam subjected to a central load acting at the level of the centroidal axis shown in figure 6.2. In this case the critical moment, i.e., maximum moment when the beam is on the point of buckling is given in standard texts as;

$$M_{cr} = \frac{4.24}{L} \sqrt{(EI_y \cdot GJ)} \sqrt{\left(1 + \frac{\pi^2 EI_x}{L^2 \cdot GJ}\right)} \dots \dots \dots (6.2)$$

The ratio of the constants of equations 6.1 and 6.2 is $\pi/4.24 = 0.74$ is often termed the 'equivalent uniform moment factor' m , which is a direct measure of the severity of the particular pattern of moments relating to the basic case. Other cases of loading pattern can also be conveniently compared with the basic solution giving different values of m . Some approximate solutions for the maximum moment M_{max} at elastic buckling for simply supported beams are shown in table 6.2.

6.2.2.2 Position of Loading

Figure 6.3. shows a simply supported beam with a central concentrated load P acting at a distance \bar{a} above the shear centre axis of the beam. When the beam buckles by deflecting

laterally and twisting, the line of action of the load moves with the central cross section, but remains vertical. When the load is applied at either the top or the bottom flanges, the solution of equation 6.2 may still be used providing the numerical constant is replaced by a variable, the value of which depends upon the ratio L^2GJ/EI_w shown in figure 6.4

Load which acts above the shear centre is more critical than load applied at the shear centre. This is because additional torque which equals to $P\bar{a}(\phi)_{L/2}$ increases the twisting of the beam and decreases the resistance to buckling. It can be seen that the condition becomes more significant as the depth of the section increases and/or the span reduces, i.e., as L^2GJ/EI_w becomes smaller.

6.2.3 Conditions of Lateral Support

Lateral stability of a beam can be improved by an arrangement of lateral support which may inhibit the growth of buckling deformation. Similarly, lateral stability may be reduced by less effective lateral support. Any arrangement of the lateral support can be considered provided the appropriate boundary conditions can be incorporated in the analysis.

6.2.3.1 Rigid Restraints at Support

A practical case of interest is the cantilever. The support conditions of cantilever are different from the simply supported beam described earlier. A cantilever is usually completely fixed at one end and completely free at the other. The elastic buckling solution for a cantilever beam acted upon by a uniform bending moment M applied at the end and centroid of the cross section is given by equation 6.1 for simply supported beams by replacing the beam length L by twice the cantilever length $2L$, whence,

$$M_c = \pi \frac{\sqrt{(EI_y \cdot GJ)}}{2L} \sqrt{\left(1 + \frac{\pi^2 EI_w}{4L^2 GJ}\right)} \dots \dots \dots (6.3)$$

Results of analysis of a case of buckling of a cantilever (6.3) in comparison with a simply supported beam under uniform moment is shown in figure 6.5. It can be seen that the cantilever under end moment is less stable than the similar, simply supported beam.

6.2.3.2 Effective Lengths

In the basic problem of lateral-torsional buckling it was assumed that the beam was supported laterally only at its ends. When the same beam is provided with additional rigid support at its centre, which prevents lateral deflection and twist, then the buckled shape as given in (6.4) is,

$$\frac{\phi}{(\phi)_{L/4}} = \frac{u}{(u)_{L/4}} = \sin \frac{\pi z}{L/2} \dots\dots\dots (6.4)$$

and its elastic critical moment M_c is given by

$$\frac{M_c L/2}{\sqrt{(EI_y \cdot GJ)}} = \pi \sqrt{\left(1 + \frac{\pi^2 EI_w}{GJ \cdot (L/2)^2}\right)} \dots\dots\dots (6.5)$$

In general, the elastic critical moment M_{cu} of a restrained beam with equal and opposite end moments can be expressed as

$$\frac{M_{cu} l}{\sqrt{(EI_y \cdot GJ)}} = \pi \sqrt{\left(1 + \frac{\pi^2 EI_w}{GJ \cdot l^2}\right)} \dots\dots\dots (6.6)$$

in which the effective length l is related to the span L by

$$l = kL \dots\dots\dots (6.7)$$

in which k is the effective length factor.

Thus the critical moment of a simply supported I-beam is substantially increased when a restraint is provided, which prevents the centre of the beam from deflecting laterally and twisting. This restraint however, need not be completely rigid, but may be elastic, provided its translational and rotational stiffness exceeds a certain minimum value as specified by the relevant design code.

6.2.4 Inelastic Beams

Theoretically expression 6.1 for the critical moment is only

valid while the beam remains elastic. In a short span beam, yielding occurs before the ultimate moment is reached, and significant portions of the beam are inelastic when buckling commences. The portions which yield will reduce the rigidity and consequently, the critical moment of the beam is also reduced.

For beams with uniform moment, the distribution of yield across the section does not vary along the beam, and in the absence of residual stresses, the inelastic critical moment can be calculated by modifying equation 6.1. In this case the 'reduced' flexural and torsional rigidity quantities, which are active at buckling are used for the actual ones. Estimates of these rigidities can be obtained by using the tangent moduli of elasticity (6.18), which are appropriate to the varying stress levels throughout the section. This method thus determines the lower bound estimate of the critical moment.

6.2.5 The Behaviour of A Real Beam

The case of a simply supported beam with uniform moment which has an initial curvature and twist is given in (6.4) by

$$\frac{U_0}{\delta_0} = \frac{\theta_0}{\theta_0} = \sin \frac{\pi z}{L} \dots \dots \dots (6.8)$$

in which the central initial lack of straightness δ_0 and

twist θ_0 are related by

$$\frac{\delta_0}{\theta_0} = \frac{M_E}{\pi^2 EI_y / L^2} \dots \dots \dots (6.9)$$

The deformation of the beam is given by;

$$\frac{u}{\delta} = \frac{\theta}{\theta_0} = \sin \frac{\pi z}{L} \dots \dots \dots (6.10)$$

in which

$$\frac{\delta}{\delta_0} = \frac{\theta}{\theta_0} = \frac{M/M_E}{1 - M/M_E} \dots \dots \dots (6.11)$$

The graph of the equation 6.11 plotted non-dimensionally for central deflection δ/δ_0 and twist θ/θ_0 , as in figure 6.6, which shows that deformation begins at the commencement of loading and increases rapidly as the critical moment M_{cr} is approached. The simple load-deformation relationship of equations 6.10 and 6.11 are of the same form as that of an imperfect strut (6.4), i.e., compression members with sinusoidal initial curvature. Therefore the Southwell plot technique for extrapolating the elastic critical loads of compression members from experimental measurements may be used for the beams.

The real beam therefore differs from the ideal beam analysed earlier in much the same way as do real compression members. Its behaviour can be represented by curve A in figure 6.7. For the case of a beam with imperfections such as residual stresses or variations in material properties, the behaviour can be represented by curve B, while the behaviour of a real

beam having both types of imperfection can be represented by curve C. It can be seen that its behaviour shows a transition from the elastic behaviour of a beam with equivalent curvature and twist to the elastic post buckling behaviour of a beam with equivalent residual stresses.

6.3 Design Approach for Lateral-Torsional Buckling

6.3.1 General

The theoretical approach to the problems of lateral-torsional buckling previously discussed could not be directly used for design since significant differences exist between the assumptions, which form the basis of the theory and the characteristics of the real beam. Furthermore the formulae involved are too complex for routine use. A realistic approach therefore is to consider both theory and experiment in deriving a design method.

A comparison (6.4) of a typical set of lateral-torsional buckling test data obtained using an actual hot-rolled section with the theoretical elastic critical moment given by equation 6.1 is shown in figure 6.8. Three distinguished regions of beam behaviour can be observed and they are;

1. Stocky beam; $(M_p/M_E)^{1/2} < 0.4$ for which the moment M_p is attained.

2. Beams of intermediate slenderness;

$0.4 < (M_p/M_E)^{1/2} < 1.2$, which collapse through the combined effect of plasticity and instability moment behaviour M_E or M_p .

3. Slender beam; $(M_p/M_E)^{1/2} > 1.2$, which buckles at moment approaching M_E .

The beams categorised as stocky beams are not prone to lateral-torsional buckling. Beams of intermediate slenderness, which covers much of the practical range of beams without lateral restraint, will either suffer elastic or inelastic buckling. Therefore beams in this category must be designed based on consideration of inelastic buckling suitably modified to allow for imperfections.

Assessment of the buckling test data for hot-rolled sections was carried out by various researchers (6.5, 6.6, 6.7, 6.8) in order to establish approximate lower bound values, which are suitable for design. The work of Fukumoto and Kubo (6.5, 6.6, 6.7) produced satisfactory agreement with test results, however it precludes the use of the full plastic capacity concept. Taylor et al (6.8) have eliminated this deficiency by the formulation of ultimate strength (M_{uo}) relationship for hot-rolled beam as follows;

$$(M_E - M_{uo})(M_p - M_{uo}) = \eta M_E M_{uo} \dots \dots \dots (6.12)$$

in which

$$\eta = 0.007 \pi \sqrt{\left(\frac{E}{F_y}\right)} \left(\sqrt{\left(\frac{M_p}{M_E}\right)} - 0.4 \right) \neq 0 \dots \dots \dots (6.13)$$

This defines the slenderness range of $0 < \sqrt{(M_p/M_E)} < 0.4$.

Equation 6.12 has been adopted as the basis of the design code in BS 5950 : Part 1, for hot-rolled sections in the design of elastic lateral-torsional buckling, in which case $M_{uo} = M_b$. This imperfection parameter η was adopted to produce a reasonable agreement between the values of M_b and the ultimate moment capacity M_u obtained from tests, such as those shown in figure 6.9 for beams in near uniform bending.

In plastic design, account must be taken of the plastic rotation requirements which may affect member stability. An example of this problem is the inelastic deformation due to plasticity in bending about the major axis of an I-section caused the warping resistance to decrease more drastically than St Venant torsional resistance. In regions of low moment gradient, due to its greater elastic rotation capacity, the rotation requirements are less severe than in regions of high moment gradients. Furthermore, the effect of reduction in the full plastic capacity must also be accounted for.

6.3.2 Design for Lateral-Torsional Buckling of Beams With Unrestrained Length in BS 5950: Part 1

Design methods for laterally unrestrained beams should provide a clear relationship between the strength of the beam and the major parameters necessary to describe the

problem. In elastic design, the condition of member stability is assessed simply by reference to the forces and corresponding stresses derived from an elastic analysis of the frame. Before the introduction of BS 5950, the stability of the uniform members or parts of uniform members, not containing plastic hinges, could be readily checked by using conventional allowable stress limitations as given in BS 449 (6.30) or the design charts given in the BCSA publication No 23 (6.31) using factored loading. In BS 5950, the moment capacity M_b as the most appropriate measure of strength is given by;

$$M_b = p_b S_x \dots \dots \dots (6.14)$$

in which p_b = bending strength allowing for susceptibility to lateral-torsional buckling, S_x = plastic section modulus for compact section.

For the case of hot-rolled I-beams subjected to uniform bending, M_b is calculated from the equation;

$$\frac{M_b}{M_p} = \left(\frac{1 + (1 + \eta) M_E / M_p}{2} \right) - \sqrt{\left[\left(\frac{1 + (1 + \eta) M_E / M_p}{2} \right)^2 - \frac{M_E}{M_p} \right]} \dots \dots \dots (6.15)$$

which is a derivative of equation 6.12. The evaluation of equation 6.12 is simplified through the introduction of a lateral slenderness ratio λ_{LT} (6.8, 6.9, 6.10), defined by;

$$\lambda_{LT} = \sqrt{\left(\frac{\pi^2 E}{P_y} \right)} \cdot \bar{\lambda}_{LT} \dots \dots \dots (6.16)$$

where $\bar{\lambda}_{LT} = \sqrt{(M_p / M_E)}$ (see figure 6.10).

In the absence of instability, equation 6.14 permits the full plastic moment capacity, i.e the beam strength is controlled by the development of full plasticity at the most heavily stressed cross-section, thus identifying the limiting condition of the members. However, for slender beams, p_b , is a function of λ_{LT} .

In BS 5950 λ_{LT} , termed as equivalent slenderness may be evaluated from

$$\lambda_{LT} = nuv\lambda \dots \dots \dots (6.17)$$

in which $u = [(4S_x^2\gamma)/(A^2h_s^2)]^{1/4}$ is the buckling parameter, $x = 0.566h_s(A/J)^{1/2}$ is the torsional index, $\gamma = (1 - I_y/I_x)$, $v = [1 + (1/20)(\lambda/x)^2]^{-1/4}$, $\lambda = L/r_y$ and n is the slenderness correction factor. A safe approximation for value of u is 0.9 for hot-rolled sections (UBs, UCs and Channels) and 1 for all other sections. Thus the use of this equivalent slenderness caters for all the variables for loading and restraint conditions.

The elastic buckling moment M_E is related to the design strength M_b by the Perry equation (6.11)

$$M_b = \frac{M_E M_p}{\phi_B + \sqrt{(\phi_B^2 - M_E M_p)}} \dots \dots \dots (6.18)$$

where

$$\phi_B = \frac{M_p + (\eta_{LT} + 1) M_E}{2} \dots \dots \dots (6.19)$$

in which the Perry Coefficient η_{LT} for a rolled section is

given by $\eta=0.007[\lambda_{LT}-0.4/(\pi^2 E/p_y)]$.

Alternatively, the determination of moment capacity M_b of equal flanged hot-rolled beams in uniform bending is given in BS 5950 by tabulations of $p_b=M_b/s_x$ for given values of p_y (yield stress), $\lambda=L/r_y$ and $x=D/T$. These are based on the approximation ;

$$\frac{M_E}{Z_p} \approx \frac{250000000}{(L/r_y)^2} \cdot \sqrt{\left[1 + \frac{1}{20} \left(\frac{L}{r_y} \cdot \frac{T}{D}\right)^2\right]} \dots N/mm^2 \dots (6.20)$$

where Z_p is the plastic section modulus.

BS 5950 also provides guidance on the choice of suitable effective length (l) values as a means of allowing for different lateral support conditions for beams and cantilevers. In cases where beams, or segments of beams between points of lateral support, are subjected to non uniform moments, direct use of the equivalent uniform moment factor, m , described earlier as a means of comparing the relative severity of different moment patterns in elastic lateral-torsional buckling is permitted. This provision is given in Clause 4.3.7.2 of the code in which the lateral stability is checked for an equivalent moment \bar{M} given by:

$$\bar{M} = m M_{\max} \dots (6.21)$$

in which $m = 0.57 + 0.33\beta + 0.10\beta^2 \leq 0.43$ and

$$\beta = M_{\min}/M_{\max} \quad (1.0 \geq \beta \geq -1.0)$$

The design checks for lateral-stability for a beam with

unrestrained length can therefore be carried out in terms of critical lengths of member between restraints. Four cases have been identified to be under this category and they are;

- (1) Uniform member with unrestrained length containing no plastic hinge, (L_e),
- (2) Non-uniform member with unrestrained length containing no plastic hinge, (L_e),
- (3) Uniform member with unrestrained length containing plastic hinge, (L_m) and,
- (4) Non-uniform member with unrestrained length containing plastic hinge, (L_m).

6.3.2.1 Stability of Uniform Member with Unrestrained Length Containing No Plastic Hinge

The design for lateral-torsional buckling of a uniform member with unrestrained length containing no plastic hinges is given in Section 4.3 of BS 5950. The derivation of the formulae within this clause is based on the theoretical consideration just described. The equivalent slenderness given in Section 4.3.7.5 (i.e., equation 6.17) is determined first, and in this case, the value of L_e , which is dependent on the end conditions (table 9 of the code) will affect the results via the relationship $\lambda = L_e / r_y$. Table 11 of the code is used to find the bending strength p_b for a chosen design strength p_y , once the equivalent slenderness λ_{LT} has been calculated. However, the convenient way of calculating λ_{LT}

will sacrifice accuracy as several approximations were made in setting up the table concerned. More accurate calculation of λ_{LT} can be carried out as described earlier and given in Appendix B in BS 5950.

The buckling resistance moment, M_b is then calculated as in equation 6.14 above. The check must ensure that the value of \bar{M} does not exceed M_b .

6.3.2.2 Stability of Non-Uniform Member with Unrestrained Length Containing No Plastic Hinge

A non-uniform or tapered I-beam of doubly-symmetric cross section is designed in BS 5950 by a modification of the rules for uniform members. This provision is given in Section 4.3.7.5 in the code, which also refers to Appendix B. The elastic critical moment M_E given in Appendix B is calculated from

$$M_E = \frac{M_p \pi^2 E}{\lambda_{LT}^2 P_y} \dots \dots \dots (6.22)$$

in which M_p is the full plastic moment of the section at the point where the factored applied moment is the greatest, and where λ_{LT} the familiar 'equivalent slenderness'. In calculating the equivalent slenderness (equation 6.17) for tapered members, the effective length L_E is used for calculating the slenderness λ and n is a coefficient related to the degree of tapering given by

$$n = 1.5 - 0.5 (A_{sm}/A_{lm}) > 1.0 \dots \dots \dots (6.23)$$

in which A_{sm} and A_{lm} are the flange areas at the points of smallest and largest moment.

The elastic buckling moment M_e is related to the design strength M_b of the tapered beam in the similar manner as the uniform member by equation 6.18 and 6.19. The calculation of M_b can also be achieved by the appropriate tables in BS 5950. When tables are used, for a given slenderness ratio λ , only the quantities of λ/x and n need to be calculated.

6.3.2.3 Uniform Member with Unrestrained Length Containing Plastic Hinge

In the case when a design considers moments greater than $M_y = Z_x p_y$, but less than M_p , the plastic moment, lateral buckling is likely to occur. The code of practice BS 5950 inherently requires lateral bracing at locations where plastic hinges are expected to occur in the failure mechanism. Upon reaching a plastic hinge at any section, the extreme fibres will be strained near or into the strain hardening region.

Some of the studies of inelastic lateral buckling reported include those of Galambos (6.12), Lay and Galambos (6.13, 6.14), Massey and Pitman (6.15), Hartmann (6.16), Nethercot and Trahair (6.17) and Trahair (6.18).

Several methods exist by which the stability of members in plastically designed structures may be ensured; and these always result from rather different approaches to the problem. In the US, most researchers approached the problem by assuming that the rigidities EI_y and GJ are taken to include the values in the inelastic range as well as the elastic range, thus the equilibrium equation for pure moment (equation 6.1), may also be used for the plastic range. Since for beams where plastic moments are assumed to develop, the distances between lateral support points will be relatively short, it has been determined (6.13) that the term involving torsional rigidity GJ may be neglected. Thus equation 6.1, neglecting terms with GJ becomes;

$$M_{cr} = \frac{\pi^2 E}{L^2} \sqrt{I_w I_y} \dots \dots \dots (6.24)$$

Since M_{cr} must reach M_p , substitute $M_p = S_x p_y$ for M_{cr} . Also $I_w = I_y h^2/4$ and $I_y = A r_y^2$. Solving equation 6.24 then gives the maximum slenderness ratio,

$$\frac{L}{r_y} = \sqrt{\frac{\pi^2 E}{2 p_y} \left(\frac{h A}{S_x} \right)} \dots \dots \dots (6.25)$$

for uniform plastic moment. The extreme fibre strain will be approaching or already into the strain hardening range; thus the strain hardening modulus should be used instead of modulus of elasticity E in equation 6.25. Furthermore, for situations of non-uniform moment or other variables, the modified equation may be multiplied by some factors. Thus in the US, the AISC requirement for 'compact section' was based on the modified version of equation 6.25.

Prior to the introduction of BS 5950 in the UK, a design procedure for checking the stability of uniform members with plastic hinges at the ends has been available. This design procedure made use of design charts, the basis of which was given by Horne (6.20). In using the charts, the uniform member is assumed to be subjected to end moments that act about the major axis only, the larger moment causing a plastic hinge to form at one end. For such members subjected to a linear moment gradient, the BCSA publication No. 23 (Horne, 6.21) gives a direct checking procedure. To use the charts it is necessary to know the slenderness ratio l/r_y , where l is the length of the member being considered, and the torsion constant T ($=AGK/Z_x^2$) a property of the cross section of the member. The Constrado publication, "Plastic Design" (6.22) also provides values of T , which are given as properties for both the universal sections and the RSJs.

Although BS 5950 does not refer directly to this approach, or indeed to any other methods, it effectively permits the use of any reasonable approach. A formula is given in Clause 5.3.5 of BS 5950 for the expression for the maximum distance between points of restraint L_m as;

$$L_m \leq \frac{38r_y}{\left[\frac{f_c}{130} + \left(\frac{p_y}{275} \right)^2 \left(\frac{x}{36} \right)^2 \right]^{1/2}} \dots \dots \dots (6.26)$$

in which f_c = compressive stress due to axial load (N/mm^2)
 p_y = design strength (N/mm^2)
 x = torsional index

For a beam (i.e., $f_c=0$) of Grade 43 steel having the fairly high value of x of 36, equation 6.26 gives a limit of $38r_y$, which is in line with values specified in several overseas' codes.

The theoretical treatment of equation 6.26 was based on the work of Baker (6.32) in which the maximum unsupported length is given by

$$L_m = \frac{43r_y}{\sqrt{\left[\frac{p}{100} + \left(\frac{p_y}{240}\right)^2 \left(\frac{x}{36}\right)^2\right]}} \dots\dots\dots \{6.27\}$$

Equation 6.27 gives the limiting slenderness curve indicated on design charts, as illustrated by figure 6.11. It was shown that at a slenderness below this limiting curve, full plastic action may be assumed in the member for design purposes, irrespective of the ratio of end moments. Thus equation 6.27 gives the safe permissible spacing of supports to the compression flange whatever the ratio of end moments and the degree of plasticity, provided there is no destabilising force acting on the compression flange between the support.

On the same basis equation 6.26 was derived, however taking into consideration the higher strength of the present day steel being manufactured.

6.3.2.4 Non-Uniform Member with Unrestrained Length Containing Plastic Hinge

It has been shown that for non-uniform members, the equilibrium equation for pure moment is more complicated than for uniform members. Due to the complicated nature of the equation involved, the solution has been mostly numerical (6.17, 6.18).

The approach in BS 5950 is to use the same empirical formula given in Clause 5.3.5 (i.e., equation 6.26) but for non-uniform members the values of r_y and x used are dependent on the following rules;

- (1) Where a member has unequal flanges, r_y should be taken as the lesser of the values for the compression flange only or for the whole section,
- (2) Where the cross section of the member varies within the length L_m the minimum value of r_y and the maximum value of x should be used.

6.3.3 Design for Lateral-Torsional Buckling of Beam With Restrained Length in BS 5950 : Part 1

6.3.3.1 Introduction

In the design of portal frames, conditions by which sheeting rails and purlins are attached to the mainframe members are

always encountered. Purlins attached to the compression flange of a main member would normally be acceptable as providing a full restraint; where purlins are attached to the tension flange they should be capable of providing positional restraint to that flange but are unlikely to be able to prevent twisting. The earlier code of practice BS 449, ignored the effect of the presence of purlins and sheeting rails in providing positional restraints and treated the member as completely unsupported laterally between points of support. Realising the benefit of the presence of the purlins has led to several research projects in the study of buckling of laterally restrained members.

A study on members with lateral restraints provided on one flange was reported by Dooley (6.23, 6.24) in 1967. He studied the buckling of eccentrically loaded columns attached at intervals to sheeting rails that were capable of providing positional restraint. His study showed that it was practical to regard a series of discrete restraints as the same case as continuous restraints. In 1969, Singh (6.25) proposed an empirical method of predicting the elastic critical buckling loads of uniform I-sections restrained at one flange and subjected to inplane loads giving arbitrary bending moment distribution about the major axis. In the same year, Horne and Ajmani (6.26), reported the findings of their study on uniform I-section columns with restraints at intervals along one edge. This work, which gave a treatment of the torsional buckling of columns having the major axis

of bending varying linearly along the length of the member, was then adopted as the basis of a design procedure (6.27). This work was also extended to cover plastic design and in 1971 Horne and Ajmani (6.28) proposed a complete design procedure.

The current code of practice BS 5950: Part 1, gave consideration for members with such restraint conditions and provided clauses for the design of uniform and non-uniform members. The four cases which have been identified earlier come under this category and they are covered in Appendix G in BS 5950. Before details of each case is considered, the theoretical approach of the work mentioned above will first be described.

6.3.3.2. Stability of Uniform Members Restrained Along the Tension Flange

6.3.3.2.1 Elastic Stability of Restrained Uniform Member

Horne and Ajmani (6.26, 6.27) presented an expression for the critical length of a laterally restrained uniform beam under its yield moment M_y , as;

$$M_y = \frac{1}{2a} \left[GJ + \frac{\pi^2 EI_y}{L_{cr}^2} \left(a^2 + \frac{d^2}{4} \right) \right] \dots \dots \dots (6.28)$$

where $a = a_1 + d/2$, the distance between the centroid of the

section and the axis of restraints. The loading condition considered (figure 6.13) was for a symmetrical I-section member ^{ends} supported against lateral deflection in both flanges and subjected to uniform moments. The ends are assumed free to rotate about the minor axis of the section with no restraint against warping. Also the section is assumed to be restrained by the rails at intervals of s along the axis AB and the ratio of a/d is 0.75.

The value of L_{cr} can be derived entirely in terms of non-dimensional geometric constants D/t_f , d/b and t_w/t_f . By taking $G/E=0.4$ and assuming only the economic UB section, i.e $d/b=2.5$ and $t_w/t_f=0.6$, the expression for L_{cr} becomes,

$$\frac{L_{cr}}{r_y} = 3.27 \left[\frac{\left[1 + 0.75 \left(1 - \frac{t_f}{d} \right) \right] \left(1 + \frac{t_f}{d} \right)}{\left(\frac{f_y}{E} \right) \left[1 + 0.25 \left(1 - \frac{t_f}{d} \right) \right] - 0.226 \left(\frac{t_f}{d} \right) \left(1 + \frac{t_f}{d} \right)} \right]^{1/2} \dots\dots (6.29)$$

where r_y is the minor axis of gyration.

The critical slenderness ratios calculated from equation 6.29 for values of D/t_f covering the full range of UB sections for $f_y=250 \text{ N/mm}^2$ and 350 N/mm^2 are given in figure 6.14. Singh (6.25) also obtained a similar curve, however, his results gave slightly higher values since he used a different expression for the torsion constant J . These two sets of curves are shown in figure 6.14.

An empirical expression for the elastic critical slenderness ratio is given by Horne, Shakir-Khalil and Akhtar (6.29) as;

$$\frac{L_{cr}}{r_y} = \frac{8.0 + 150 (f_y/E) (D/t_f)}{[4.4 (f_y/E) (D/t_f)^2 - 1]^{1/2}} \dots \dots \dots (6.30)$$

They stipulated that equation 6.30 is easier to use than equation 6.29 and gives results, which are in close agreement.

An elastic design procedure for design of a restrained column similar to figure 6.13 loaded by axial thrust P and terminal moments M_x' and M_x'' was proposed by Horne and Ajmani (6.27). The design criterion was that the yield stress should not be exceeded in the extreme fibres anywhere in the member. The criterion is satisfactory on condition that

$$\begin{aligned} p + f_x' &\leq p_y \\ p + f_x'' &\leq p_y \end{aligned} \dots \dots \dots (6.31)$$

where p is the mean axial stress, f_x' and f_x'' are the major axis bending stresses at the ends and p_y is the yield stress. In this case, $f_x' = M_x'/Z_x$ and $f_x'' = M_x''/Z_x$, where Z_x is the elastic section modulus about the major axis.

In this design procedure, the applied non-uniform major axis moment is replaced by an 'equivalent' uniform moment $M_x = \mu M_x'$. The value of μ is chosen so that, under a given axial thrust P, the elastic critical load will be reached under unequal terminal moments $\lambda M_x'$ and $\lambda M_x''$ or a uniform major axis moment λM_x where λ is the load factor. It was shown (6.26) that the equivalent uniform moment factor μ depends only on the ratio of terminal moment β and a non-dimensional quantity α , which

expresses the ratio of net torsional rigidity about the axis of restraint. This relationship shows that as α approaches a large value, the member tends to fail by pure torsional buckling in the immediate vicinity of the larger terminal moment and $\mu \approx 1$ for all values of β .

The maximum allowable stress on the member is calculated taking into consideration the effect of magnification of lateral displacements and the bending stress f_o due to initial imperfection. This method of elastic design enables members to be designed with any ratio of end moments, but when a hinge exists at one end, the method fails to give results as the ratio of end moments approaches +1. This is because, as the critical uniform moment is approached, it is impossible to attain full plasticity at or near the end because of the destruction of lateral stiffness due to the spreading of the plastic zone along the member. Therefore, the design method leads to zero permissible slenderness ratio when $0.7 < \beta \leq 1.00$, whatever the axial thrust may be.

The approximate design criterion for uniform moment after considering the typical sections of Universal Beams can be given by

$$(p_y - f_x) \geq \frac{2p_y \left(\frac{1}{100r_y} \right)}{20 - \left[0.065p_y - 3000 \left(\frac{t_f}{D} \right)^2 \right] \left(\frac{1}{100r_y} \right)^2} \dots\dots (6.32)$$

singh (6.25) had developed a satisfactory method of calculating the critical elastic buckling conditions for a restrained uniform member, subjected to non-uniform moment, in the absence of axial load. He considered the elastic extreme fibre stresses f_1, f_2, f_3, f_4 and f_5 due to applied moments M_1, M_2, M_3, M_4 and M_5 respectively at 4 equal intervals as shown in figure 6.15(d), where M_1 and M_5 are the moments at the ends, M_3 is the moment at mid-length and M_2 and M_4 are the quarter point moments. A factor k is calculated where

$$k = \frac{1}{12p_y} [f_1 + 3f_2 + 4f_3 + 3f_4 + f_5 + 2(f_{Smax} - f_{Emax})] \dots (6.33)$$

The elastic stresses f_{Smax} and f_{Emax} are the maximum span and end stresses, respectively. The stresses f_1 to f_5 , and f_{Smax} and f_{Emax} are positive if they correspond to compression in the outstand flange, otherwise they are zero. Similarly, the quantity $(f_{Smax} - f_{Emax})$ is only included if it is positive. In this analysis, if L_{cr} is the critical buckling length of a member subjected to a uniform moment producing extreme fibre stress of p_y , then the critical buckling length for the given moment distribution is L'_{cr} where

$$L'_{cr} = \frac{L_{cr}}{\sqrt{k}} \dots (6.34)$$

6.3.3.2.2 Plastic Stability of Restrained Uniform Member

The design criterion established earlier (6.26, 6.27) was not suitable for plastic design. Horne and Ajmani (6.28), then investigated the elastic plastic post-buckling behaviour of I-section beams and columns, laterally restrained near one flange and subjected to a uniform major axis bending moment, using the concept of a complex plastic hinge situated at mid-height of the column. By considering also the elastic response curve in the presence of initial imperfections, they derived a complete elastic-plastic load deformation relationship.

The relationship between the applied moment M and the angle of twist ϕ of the central section of a beam, provided with lateral restraints at a distance a from the shear centre of the beam is shown in figure 6.16. This is based on the assumption that the material of the beam has an elastic-pure plastic stress-strain relationship and that the beam has an initial central twist of ϕ_{co} . The maximum moment attained in this case is denoted by M_f . Because of strain-hardening, an actual beam would have a moment versus central twist curve AJK , with a peak moment M_j greater than M_f .

Theoretical calculations for curves $AGFH$ and AJK are difficult, but the two curves AGC and DB , intersecting at E are more readily obtained. AGC represents the elastic behaviour of the beam with initial central twist ϕ_{co} , while

DB is the 'plastic mechanism curve' obtained by assuming the formation of a plastic hinge at the central section with no spread of plasticity and no initial twist. The relationship AEB would therefore present the behaviour of an idealised elastic-plastic beam having initial central twist ϕ_{co} in which plasticity was confined to the central section. The moment M_e at E, although should be higher than M_f , is closely related to it and to M_j . The extent to which M_e falls below M_p is a good measure of the importance of instability. It was then established that a suitable criterion to be used for a beam in a plastically designed structure is that M_e at intersection point E should not be more than 4% short of M_p .

Using the same type of analyses presented by Horne and Ajmani (6.28) for the derivation of both the plastic mechanism and elastic response curves for a restrained I-section member subjected to uniform moment and axial load, and with some approximations, the limiting slenderness ratio L/r_y at the point E such that $M_e = 0.96M_p$, can be established.

Lower limiting slenderness curves applicable to loading in the plastic range with any ratio of end moments β are also derived by considering post-buckling behaviour. In producing design charts it is again assumed that a/d is 0.75. Using this value, then the limiting slenderness between restraints to the compression flange while allowing plastic action is given by

$$\frac{L_m}{r_y} = \frac{\left[5.4 + 0.7 \left(\frac{P_y}{240} \right) \right] x}{\sqrt{\left[\left(\frac{x}{12.3} \right)^2 \left(\frac{P_y}{240} \right) - 1 \right]}} \dots\dots (6.35)$$

Assuming grade 43 steel, then equation 6.35 becomes

$$\frac{L_m}{r_y} = \frac{6.1x}{\sqrt{\left[\left(\frac{x}{12.3} \right)^2 - 1 \right]}} \dots\dots\dots (6.36)$$

A typical example of the resulting design chart is shown in figure 6.17.

6.3.3.3. Stability of Non-Uniform Members Restrained Along the Tension Flange

6.3.3.3.1 Elastic Stability of Non-Uniform Members Restrained Along the Tension Flange

The theoretical approach in the study of stability of non-uniform members restrained along one flange has been mainly concentrated on the tapered and haunched members of portal frames. The haunch member in a portal frame is normally three-flanged (figure 6.12), and Horne and Morris (6.33) studied the stability of these types of haunched members and the two flanged member as shown in figure 6.18. It was shown that treatment for a three-flanged haunched member is more complicated and that it was safe to assume two-flanged members in the design.

In their study of the two-flanged case, it is assumed that restraint is provided at intervals along the flange AB in figure 6.18 and the outstand flange is laterally restrained at points C and D, or point E. They assumed the design condition in equation 6.32, and referred to the deepest section of the haunch rafter for the relevant geometrical properties and k is calculated from equation 6.33, based on the induced compression stresses in the outstand flange. This approach involves many assumptions, especially in using equation 6.33 to calculate for the value of k and equation 6.34 to obtain the elastic critical length L'_{cr} .

Horne, Shakir-Khalil and Akhtar (6.29) considered the elastic critical behaviour of tapered and haunched I-beams with the restraints as shown in figure 6.15(a). The beam has a length L , of which a uniform depth d_1 extends over the length $q'L$. The depth of the beam increases uniformly to d_2 over the haunch length qL . The ratio of the deeper depth to the shallower depth is defined as r (i.e $r=d_2/d_1$). For tapered beam as shown in figure 6.15(c), the same notation is used but $q'=0$ and $q=1$.

A moment varying uniformly from M at the shallower end to βM at the deeper end was applied to the beam. It was assumed that the beam was free from imperfection and that the cross section of the original shape is retained during buckling. Another assumption made was that the value of I_x was much greater than I_y enabling the effect of curvature about the

major axis to be neglected. The end conditions of the beam prevented lateral displacement and rotation about the longitudinal axis, but allowing freedom to warp and rotate about the minor axis.

The beam is restrained at intervals along the length against lateral displacement, with the axis of restraints being at a distance a_1 from the tension flange. It was also assumed that for a non-uniform member under non-uniform load, the effect of discrete lateral support is the same as for uniform member under uniform moment. This is with the provision that the supports are placed at sufficiently close intervals to prevent unrestrained lateral torsional buckling between supports.

From the assumptions and the approximations made, terms and expressions (6.29) for the buckled state of the beam were presented. The governing differential equation for twisting about the restraint axis was established by equating the internal resistance of the section of the beam to the torque due to the applied forces. By further differentiation and arrangement, the differential equation in equation 6.37 was arrived at.

$$\begin{aligned} &\frac{B}{2}[a_1^2 + [b_1 + (z - q'L) \tan \alpha]^2] \frac{d^4 \phi}{dz^4} + [B[b_1 + (z - q'L) \tan \alpha] \tan \alpha] \frac{d^2 \phi}{dz^2} \\ &\quad + \left[M \left(1 + \frac{B-1}{L} z \right) [f_1 + (z - q'L) \tan \alpha] - [C_1 + k_w (z - q'L)] \right] \frac{d^2 \phi}{dz^2} \\ &\quad + \left[M \left(1 + \frac{B-1}{L} z \right) \tan \alpha + M \left(\frac{B-1}{L} \right) [f_1 + (z - q'L) \tan \alpha] - k_w \right] \frac{d \phi}{dz} + k_1 \phi = 0 \\ &\hspace{10em} \dots\dots\dots (6.37) \end{aligned}$$

Horne et al (6.29) solved equation 6.37 by the finite difference method and they checked the results for validity with results obtained from energy solution using fourier sine series. It was shown that the greatest difference between the results was 1.3% and hence they concluded that manner in which the finite difference procedure was applied was regarded as satisfactory.

By using this finite difference procedure, Horne, Shakir-Khalil and Akhtar presented a semi-empirical method to calculate the permissible length of the restrained tapered and haunched beam.

In the semi-empirical method presented, the maximum stable length L_s' of a haunched beam can be expressed as:

$$L_s' = \frac{L_s}{c\sqrt{k}} \dots\dots\dots (6.38)$$

where L_s is the reference length, equal to the maximum stable length of a uniform beam subjected to a uniform moment with a section equal to the base section. It represents either the length for elastic critical buckling or the limiting length for plastic action. The factor c

allows for the variable section of a tapered or haunched member and the factor k allows for arbitrary distribution of bending moments.

In using equation 6.38 for checking against lateral instability, the length L_s is made equal to the critical buckling length L_{cr} and in this instance, equation 6.30 can be used.

The shape factor c is a ratio of the elastic critical length of a haunched or tapered member, subjected to a moment just sufficient to cause yield in the extreme fibres at each cross-section, to the critical length L_{cr} of a uniform member of the base section subjected to a uniform moment just sufficient to cause yield at its extreme fibres. Horne, Shakir-Khalil and Akhtar solved the differential equation for torsional buckling of a haunched beam by the finite difference method. After successive approximations, the value of c can be expressed by an empirical equation;

$$c = 1 + \frac{3}{(D/t_f) - 9} (r-1)^{2/3} \sqrt{q} \dots \dots \dots (6.39)$$

The coefficient k in equation 6.38 depends on the bending moment diagram of the beam concerned. The expression to obtain the value of k , which was used by Horne, Shakir-Khalil and Akhtar (6.29) was adopted from the empirical method used by Singh (6.25) for uniform members discussed earlier. The expression for uniform members can

also be written in the form;

$$k = \frac{1}{12M_d} [M_1 + 3M_2 + 4M_3 + 3M_4 + M_5 + 2(Ms_{\max} - Me_{\max})] \dots \dots (6.40)$$

where, M_1 , M_2 , M_3 , M_4 and M_5 are values of bending moments at the ends, quarter points and midspan, Ms_{\max} is the maximum of the span moment M_2 , M_3 , and M_4 and Me_{\max} is the greater of the end moments M_1 and M_5 . For elastic critical loads, M_d is the yield moment M_y and when considering plastic design M_d is the plastic moment M_p . In evaluating k from equation 6.41 only moments producing compression in the outstanding flange are included, with the rest taken as zero. Furthermore the term $(Ms_{\max} - Me_{\max})$ is only considered when $Ms_{\max} > Me_{\max}$.

For haunched and tapered beams, equation 6.40 was modified to allow for the variation of M_d along the beam. Hence the expression for k for a tapered or haunched beam is written as;

$$k = \frac{1}{12} \left[\frac{M_1}{M_{d1}} + \frac{3M_2}{M_{d2}} + \frac{4M_3}{M_{d3}} + \frac{3M_4}{M_{d4}} + \frac{M_5}{M_{d5}} + 2 \left[\left(\frac{M_s}{M_{ds}} \right)_{\max} - \left(\frac{M_e}{M_{de}} \right)_{\max} \right] \right] \dots \dots (6.41)$$

where M_{d1} , M_{d2} , M_{d3} , M_{d4} , and M_{d5} are the values of M_y or M_p at the section corresponding to the moment M_1 , M_2 etc.

6.3.3.3.2 Plastic Stability of Non-Uniform Members Restrained Along the Tension Flange

In the case of maximum permissible length L'_m of a haunched

beam for plastic design, Horne et al (6.29) suggested the following equation

$$L'_m = \frac{L_m}{c\sqrt{k}} \dots\dots\dots (6.42)$$

The value of L_m is obtained from the limiting slenderness ratio they proposed and is given by

$$\frac{L_m}{r_y} = \frac{(5.4 + 600 F_y/E) (D/t_f)}{[5.4 (f_y/E) (D/t_f)^2 - 1]^{1/2}} \dots\dots\dots (6.43)$$

In the evaluation of k, equation 6.41 can be used. The factor c is determined from equation 6.39.

Experimental confirmation of equation 6.43 was limited to cases where plastic hinges formed at the haunch/rafter intersection while the moment at the springing of the haunch does not exceed the yield value. If a plastic hinge is allowed to form within the taper, it is difficult to ensure satisfactory plastic rotation capacity because of sensitivity to instability of deepened I-sections. In order to develop a plastic hinge at the haunch/rafter intersection, full depth web stiffeners are required in that position. This was confirmed by Morris and Nakane (6.34).

6.3.3.4 Design of Members with Restrained Length in
Accordance with BS 5950: Part 1

6.3.3.4.1 Design of Uniform Member with Restrained Length
Containing No Plastic Hinge in BS 5950: Part 1

The elastic design of laterally restrained Universal Beams is given in Clause 5.5.3.5 in BS 5950 : Part 1. This clause, which deals with rafter stability considers restraints provided by the purlins. The clause states that where the tension flange is restrained at intervals, the maximum length between restraints to the compression flange L_t (as shown in figure 6.19) may be conservatively taken as

$$\frac{K_1 r_y x}{(72x^2 - 10^4)^{1/2}} \dots\dots\dots (6.44)$$

for grade 43 steel, or

$$\frac{K_2 r_y x}{(94x^2 - 10^4)^{1/2}} \dots\dots\dots (6.45)$$

for grade 50 steel.

In equation 6.44 and 6.45;

r_y is the minimum radius of gyration of the rafter section,

x is the torsional index of the rafter section, and

K_1 and K_2 have the following values;

Depth of haunch/depth of rafter

= 1;	$K_1 = 620,$	$K_2 = 645$
= 2;	$K_1 = 495,$	$K_2 = 515$
= 3;	$K_1 = 445,$	$K_2 = 465$

This clause however is valid only for the following conditions;

- (1) the rafter is a UB section,
- (2) the haunch flange is not smaller than the rafter flange,
- (3) the depth of haunch is not greater than 3 times the depth of the rafter,
- (4) the buckling resistance is satisfactory when checked by clause 4.3 using an effective length L_e equal to the spacing of the tension flange restraints.

However, where conditions of equation 6.44 or 6.45 are not met, or where conditions provided other than those mentioned in the clause, then Appendix G in BS 5950 should be referred to.

The provision of clause 5.5.3.5, specifically the derivation of the empirical equations 6.44 and 6.45, was based on the work of Horne and Ajmani (6.26, 6.27) based on inelastic stability, as given in equation 6.35. In the case of grade 43 steel, equation 6.36 was simplified and made more conservative.

When reference is made to Appendix G in BS 5950, the code specifies for elastic stability of uniform members

$$\frac{F}{P_c} + \frac{\bar{M}}{M_b} \leq 1 \dots \dots \dots (6.46)$$

In the absence of axial load, the condition of elastic

stability becomes $\bar{M} \leq M_b$. This condition is then similar to the basic condition laid down in clause 4.3.7.7. However, in this case the equivalent uniform moment is $\bar{M} = m_t M_A$ where, m_t is the equivalent uniform moment factor (clause G.3.4) and M_A is the maximum moment on the member or portion of the member under consideration. The value of m_t which is a measure of severity of the loading is taken as 1.0 when intermediate loads are applied between the effective torsional restraints, otherwise it must be obtained from table 39 of the code. This value of m_t is different from the value m given in clause 4.3.7.6 for unrestrained members.

The determination of buckling resistance M_b is based on $M_b = p_b S_x$ which is also general to the problems of lateral-torsional buckling covered by the code. However, due to the effect of the lateral restraint on the tension flange, the calculation of the bending strength p_b is also determined in accordance with clause 4.3.7 except that the equivalent slenderness should be taken as λ_{TB} and this is given in clause G.3.3. The expression for values of λ_{TB} is as follows;

$$\lambda_{TB} = n_t u v_t c \lambda \dots \dots \dots (6.47)$$

where the factors;

n_t is the slenderness correction factor taken as 1.0 where there are no intermediate loads, or given by Clause G.3.6

u is a buckling parameter, taken as 0.9 for U.Bs and 1 for tapered members;

v_t is a slenderness factor given in equation 6.42

c is the shape factor which is taken as 1 for uniform members

λ is the slenderness L/r_y between the member's effective torsional restraints.

The expression for v_t is as follows;

$$v_t = \left[\frac{4a/hs}{1 + (2a/hs)^2 + 1/20 (\lambda/x)^2} \right]^{1/2} \dots\dots\dots (6.48)$$

where, x is the torsional index for the section, the value of which is obtained from section B.2.5.1 of the code or from published tables. The value is close to D/t_f (i.e D is equal to overall depth of the section and t_f is the thickness of the flange),

a is the distance between reference axis to restraint axis, and

h_s is the distance between the shear centres of the flanges.

Thus it can be said that the provision of Appendix G for design of uniform members with restrained tension flange containing no plastic hinge is to a large extent based on the design criterion in the theoretical treatment by Horne and Ajmani (6.26, 6.27).

6.3.3.4.2 Design of Non-Uniform Member with Restrained Length Containing No Plastic Hinge in BS 5950 : Part 1

The elastic design of tapered members with restrained length

is covered in Clause G(a)(2). The condition at any section of the beam given in the clause is

$$\frac{F}{A} + \frac{M}{S_x} \leq p_b \dots \dots \dots (6.49)$$

where, F is the applied axial load where present

M is the applied moment at the section considered

A is the cross sectional area under consideration

S_x is the plastic modulus at the section considered

p_b is the lateral-torsional buckling resistance

A similar method is used for the calculation of the factors for calculating p_b as for uniform members, however, in this case the tapering effect is considered. The subsequent computation for the values of p_b , which consider the variation in the value of yield moment due to the tapering shape, made use of expressions which have been based on the work of Horne et al (6.26, 6.27, 6.28, 6.29) and Singh (6.25).

A haunched member with ratio of depth of haunch/depth of rafter equal 2 or 3 can also be designed using clause 5.5.3.5 discussed earlier. The relevant values of K_1 and K_2 are used in equations 6.44 or 6.45 in accordance with the code.

6.3.3.4.3 Design of Uniform Member with Restrained Length Containing Plastic Hinge in BS 5950 : Part 1

The conditions for plastic stability covered in Appendix G

in clause G.2(b) apply to restrained members which contain plastic hinge locations. For uniform members, clause G.2(b)(1) or (2) are applied. Thus for lengths without lateral loads clause G.2(b)(1) specifies;

$$L_t = \frac{L_k}{\sqrt{m_t}} \left(\frac{M_p}{M_{pr} + aF} \right)^{1/2} \dots\dots\dots (6.50)$$

where; L_k is the limiting length,

m_t is the equivalent uniform moment factor,

$M_p = p_y S_x$

$M_{pr} = p_y S_{rx}$ (S_{rx} is the reduced plastic modulus due to axial load)

F applied axial load where present

a distance between reference axis and restraint axis

The expression for L_k is the same as equation 6.43 proposed by Horne et al (6.29). They also suggested that the effect of an axial force on the stability of the member may be allowed for by adding $P(a_1 + d/2)$ to the moments $M_1, M_2 \dots M_5$ in equation 6.40. It is quite difficult to pinpoint exactly where the equation in clause G.2(b)(1) originated from. However, it is mainly based on the theoretical treatment by Horne et al mentioned earlier.

For lengths with lateral loads clause G.2(b)(2) specifies;

$$L_t = \frac{L_k}{C \cdot n_t} \dots\dots\dots (6.51)$$

where; L_t is the maximum permissible length

L_k is the limiting length calculated for the

smaller section (i.e., given in equation 6.43)

c is the taper parameter or the shape factor

n_t is the slenderness correction factor

It can be seen that this clause is entirely based on the work of Horne et al (6.29). Equation 6.51 is the same semi-empirical approach they suggested (equation 6.42), while the taper parameter c is given in equation 6.39. The slenderness correction factor n_t is the same as the square root of equation 6.41 which they proposed.

6.3.3.4.4 Design of Non-Uniform Member with Restrained Length Containing Plastic Hinge in BS 5950:Part 1

Appendix G of BS 5950 specifies that plastic stability for a tapered member with restraint along the tension flange is to be designed by clause G.2.(b)(2). The way in which this clause is applied and its origin was described in the previous section.

6.3.4 Conclusion

An assessment of the clauses related to lateral-torsional buckling found in BS 5950: Part 1, is made. The approach to the generalised method of design for lateral-torsional buckling was discussed on the basis of a real beam. Clauses related to unrestrained members were discussed in the light of the generalised method of design. Particular attention is

given to Appendix G in which the stability of members restrained along the tension flange is treated. It was shown that the contribution of Horne et al (6.26, 6.27, 6.28, 6.29) in the development of the clauses in Appendix G is tremendous.

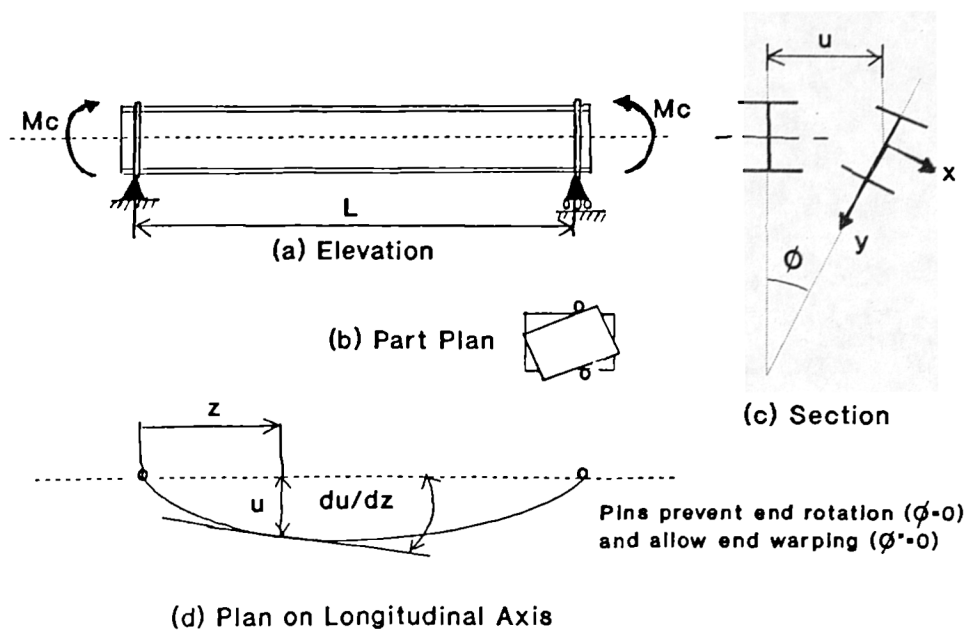


Fig 6.1 Buckling of a Simply Supported I-Beam

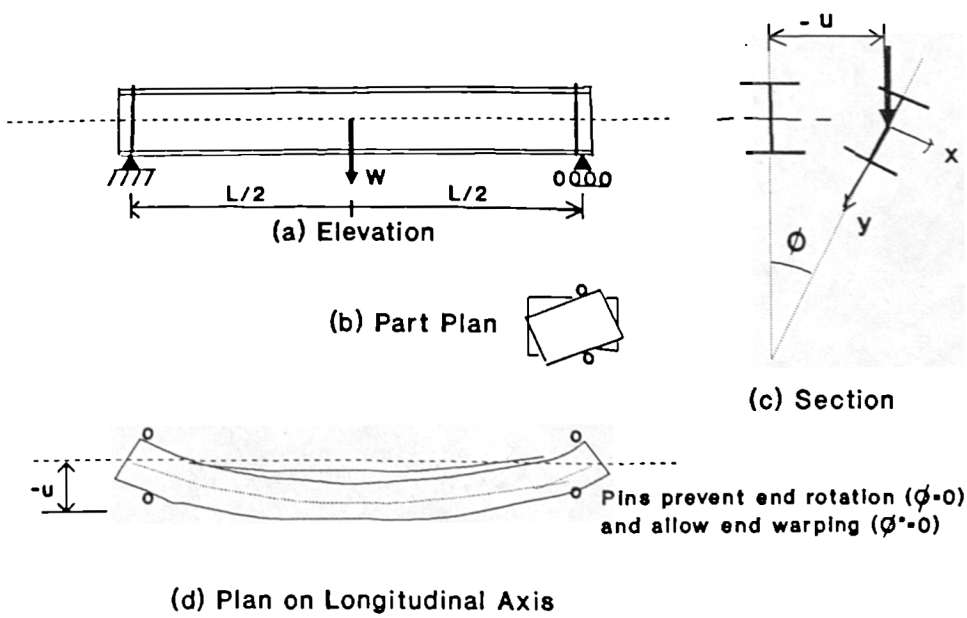


Figure 6.2 Buckling of a Beam with a Central Transverse Load

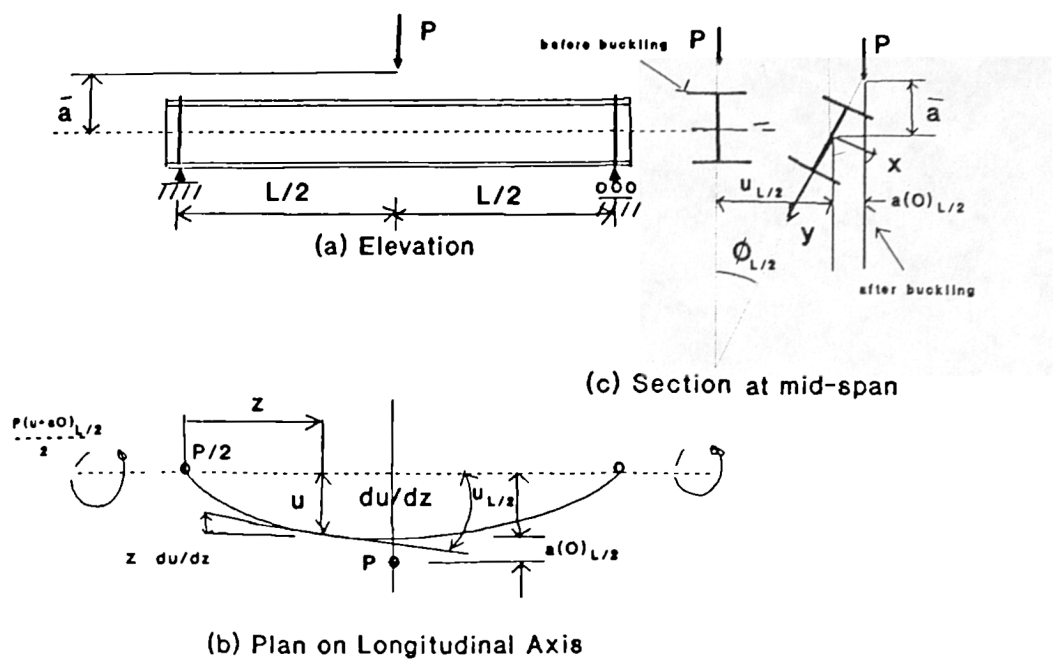


Figure 6.3 I-beam with Central Concentrated Load

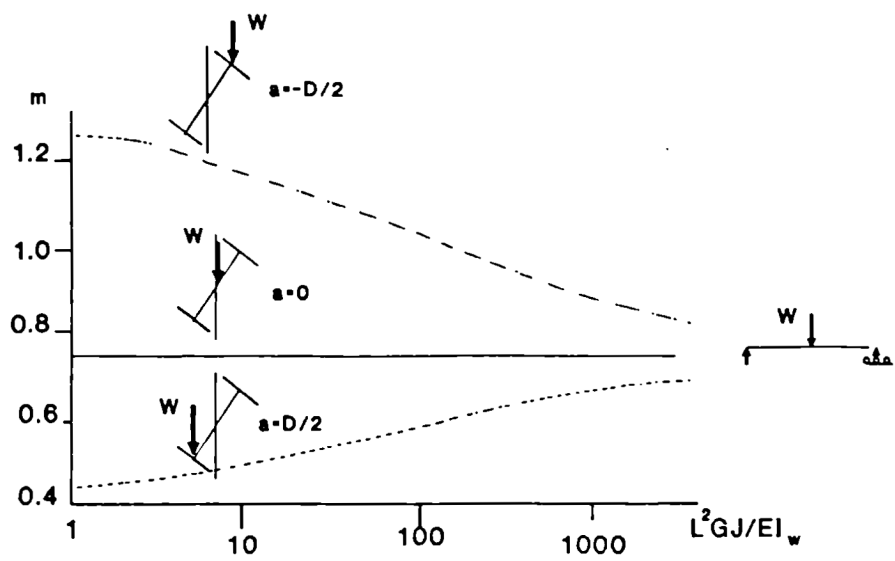


Figure 6.4 Effect of Level of Loading on Beam Stability

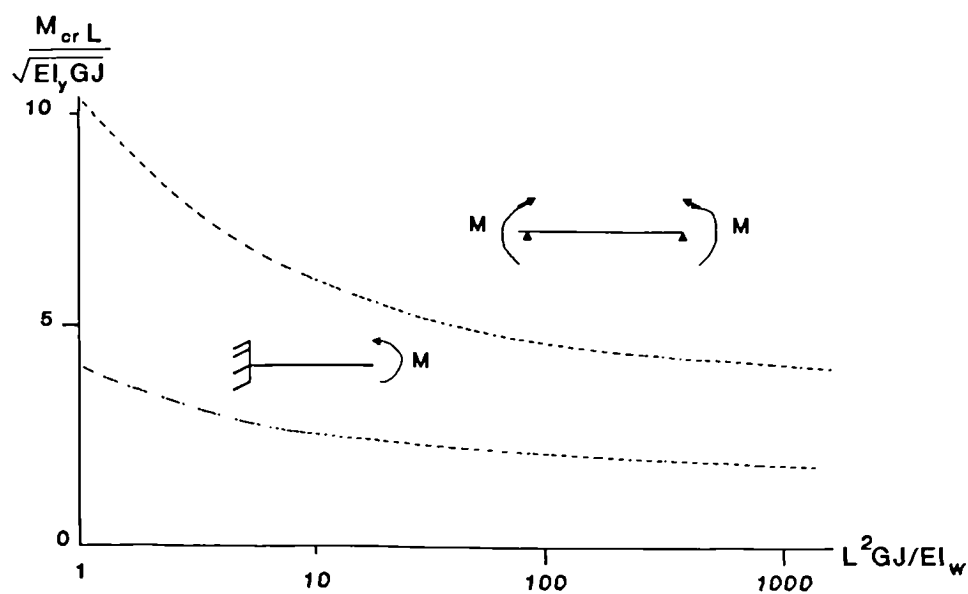


Figure 6.5 Buckling of Cantilever and Simply Supported Beams Under Uniform Moment

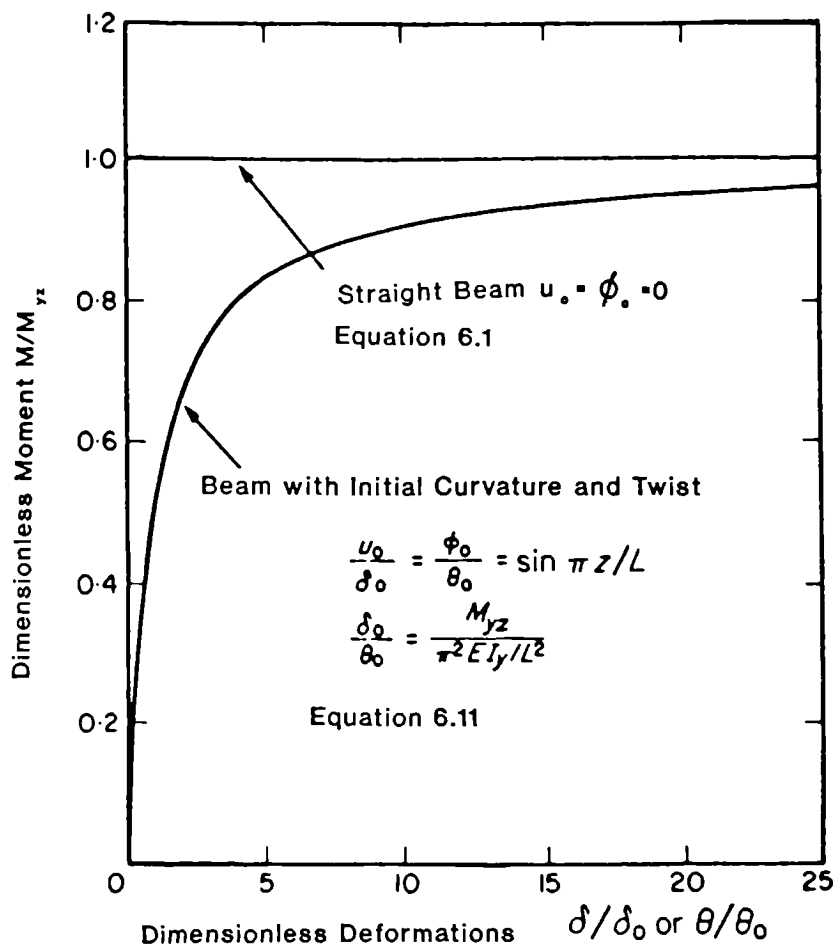


Figure 6.6 Lateral Deflection and Twist of a Beam with Equal End Moments

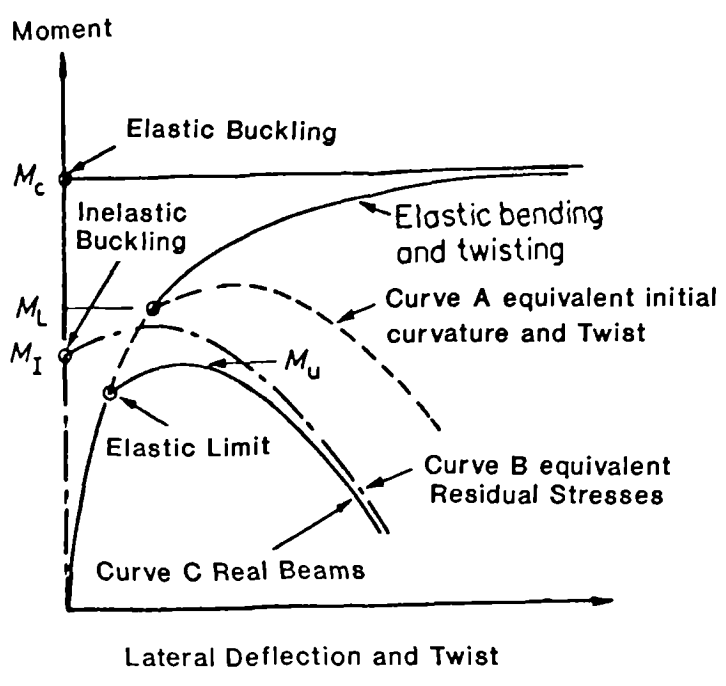


Figure 6.7 Behaviour of Real Beams

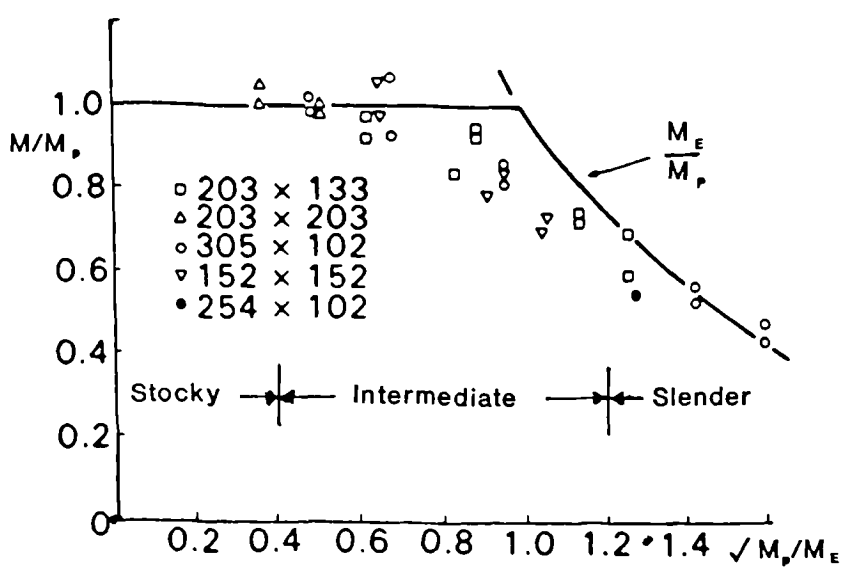


Figure 6.8 Lateral Torsional Buckling Strength of Grade 55 Steel

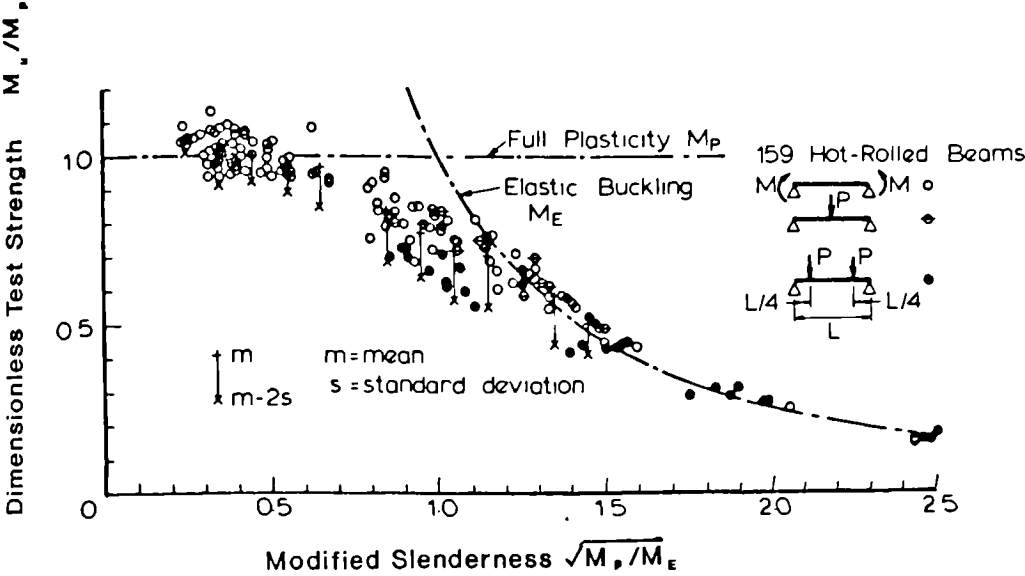


Figure 6.9 Test Results for Hot-Rolled Beams

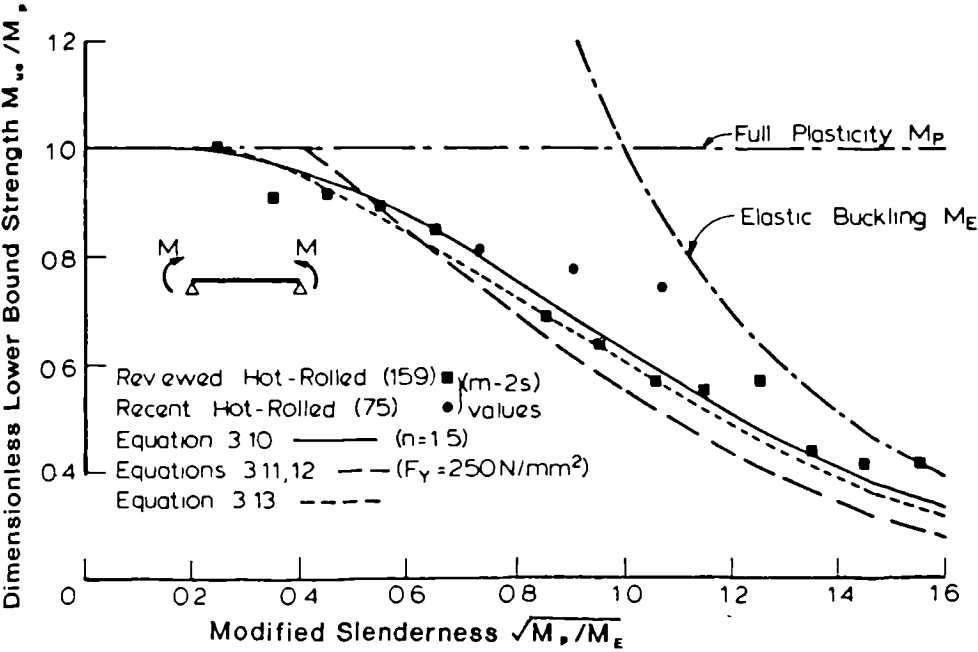


Figure 6.10 Comparison of Lower Bound Strength Approximations for Uniform Bending

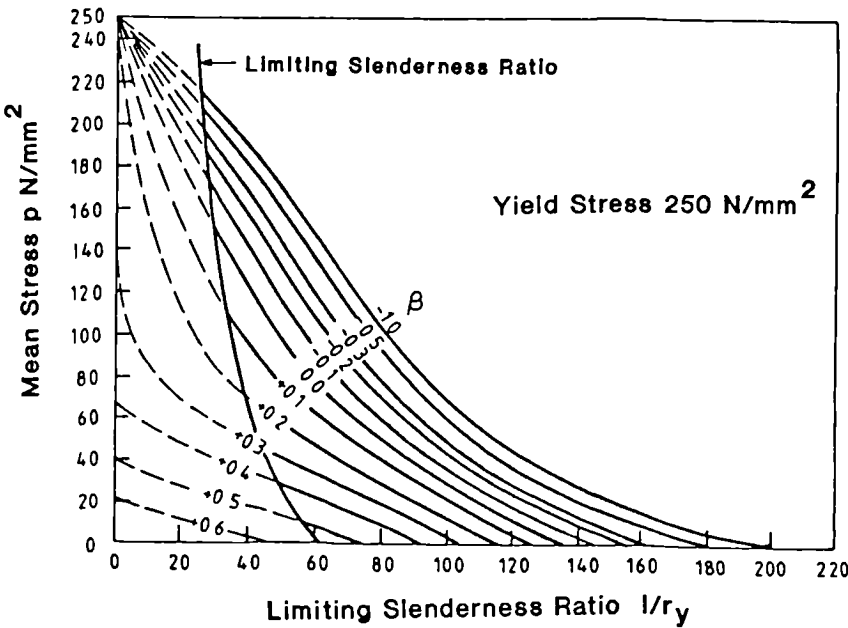


Figure 6.11 Typical Stability Curve - Unrestrained Member.

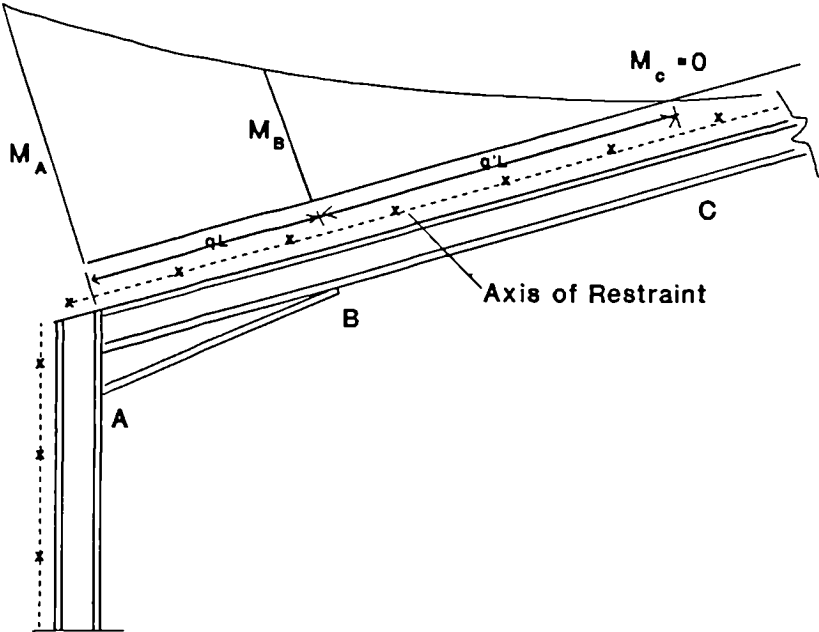


Figure 6.12 Bending Moment Distribution in A Portal Frame (A Typical Example with Haunch)

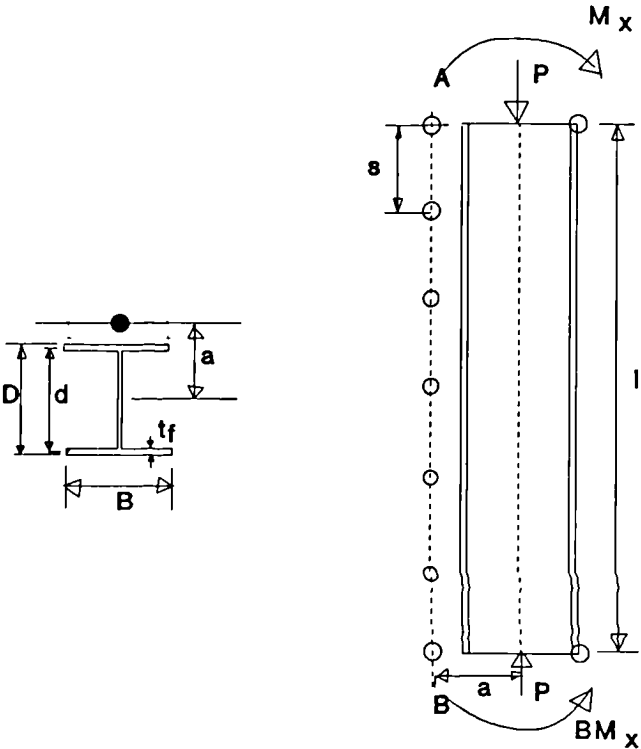


Figure 6.13 Restrained Member Subject to Linear Moment Gradient

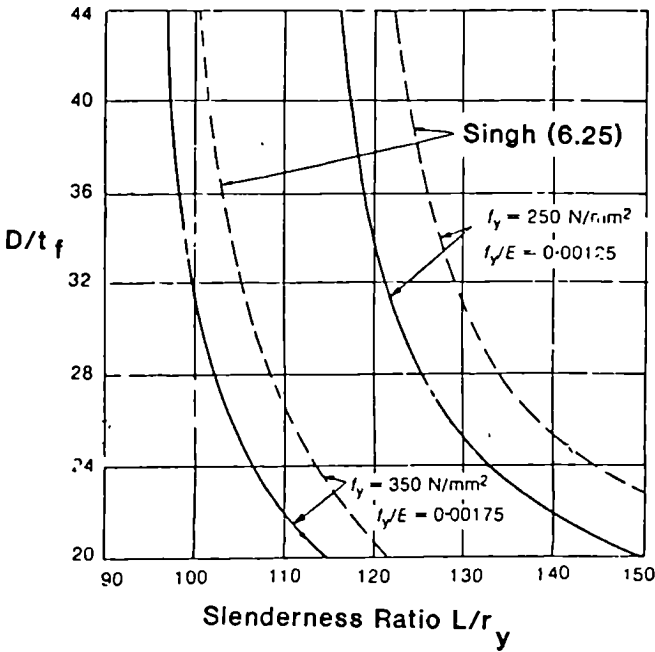


Figure 6.14 Critical Slenderness Ratio of Restrained Universal Beams Sections

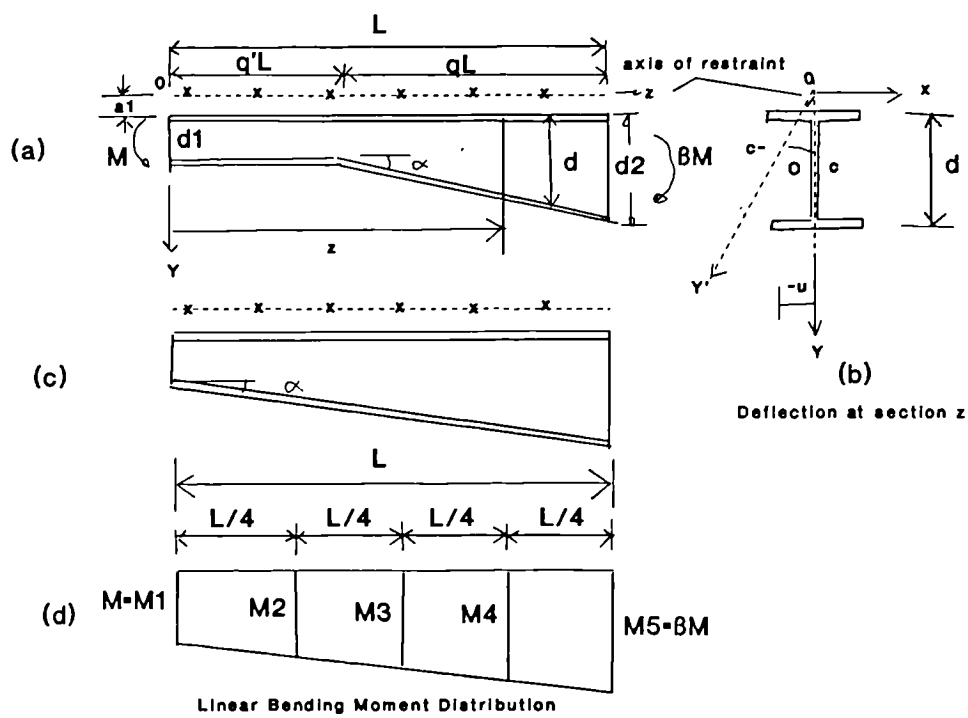


Figure 6.15 Lateral Buckling of Tapered and Haunch Beam

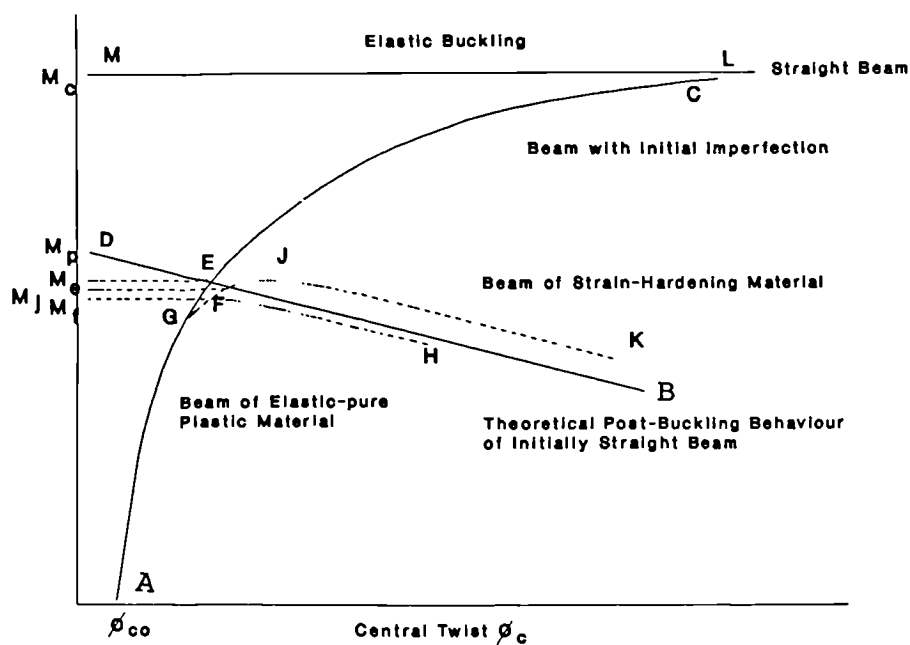


Figure 6.16 Out of Plane Behaviour of Restrained I-Beam Under Uniform Moment

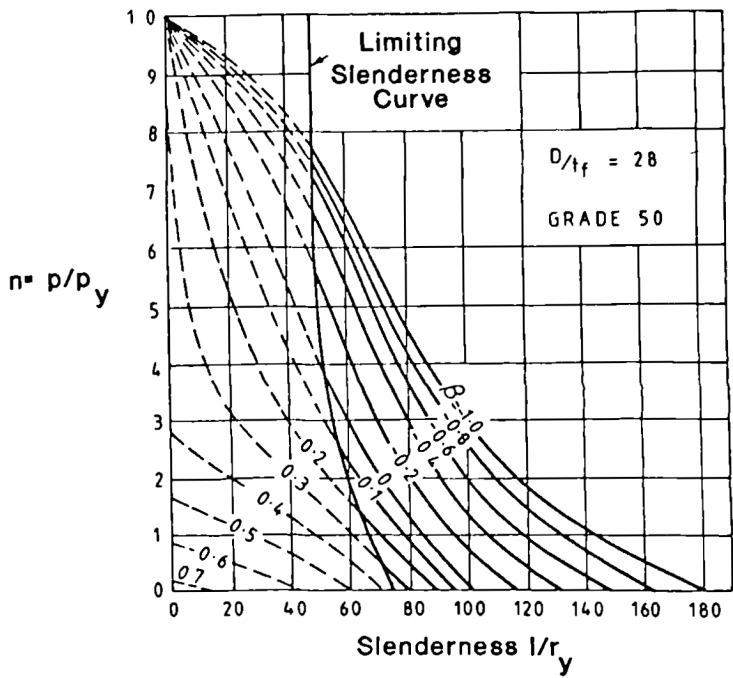


Figure 6.17 Typical Stability Curve - Restrained Member

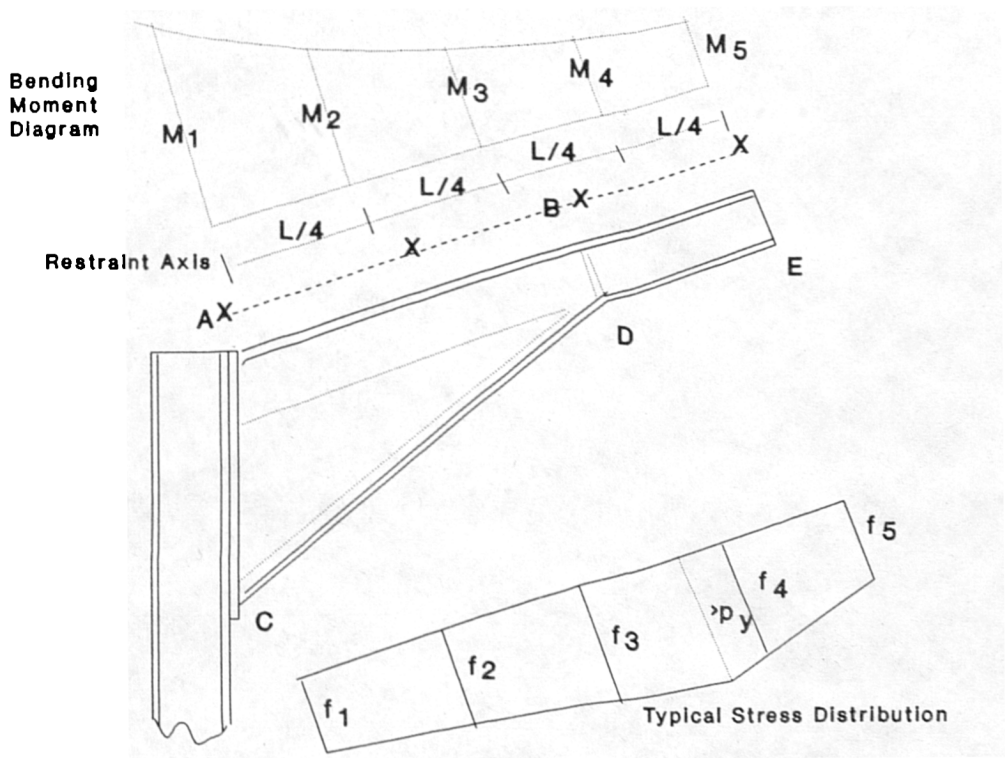


Figure 6.18 Two-flanged Haunched Rafter

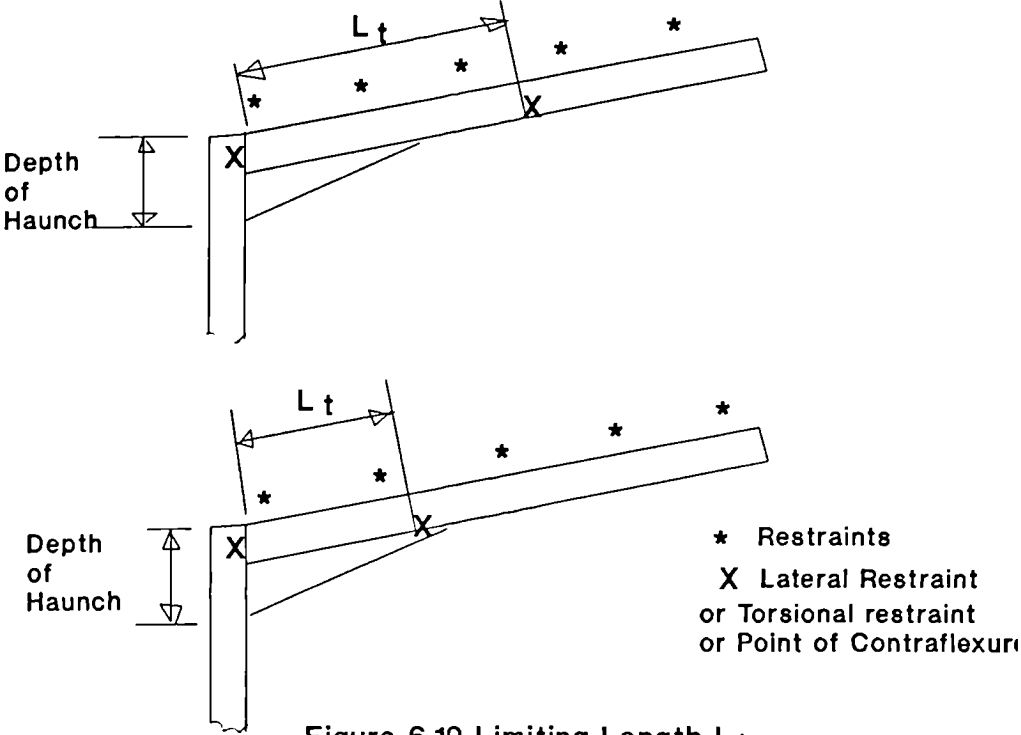


Figure 6.19 Limiting Length L_t

Table 6.1 Various cases for member between restraints in
BS 5950 : Part 1



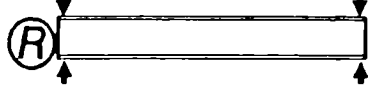

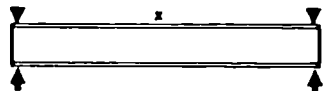
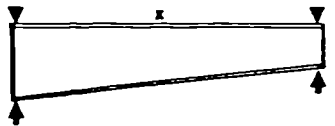
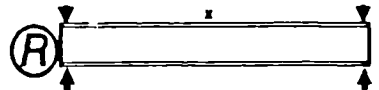

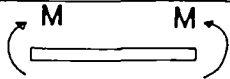
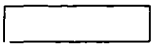
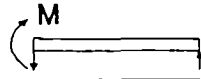
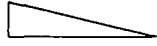
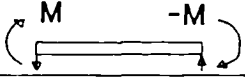
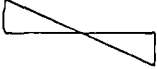
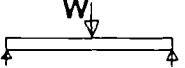
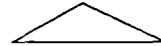


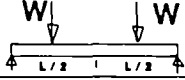
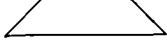
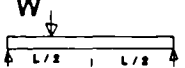
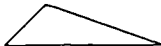
	UNIFORM	TAPERED
UNRESTRAINED LENGTH NO PLASTIC HINGE	 BS 5950 : PART 1 SECTION 4	 BS 5950 : PART 1 SECTION 4
	 BS 5950 : PART 1 CLAUSE 5.3.5 (L_m)	 BS 5950 : PART 1 CLAUSE 5.3.5 (L_m)
RESTRAINED LENGTH NO PLASTIC HINGE	 BS 5950 : PART 1 CLAUSE 5.5.3.5 OR APPENDIX G - G2(a)(1) (L_t)	 BS 5950 : PART 1 APPENDIX G - G2(a)(2) OR CLAUSE 5.5.3.5 ON SPECIAL CASES (L_t)
	 BS 5950 : PART 1 APPENDIX G - G2(b)(1) OR G2(b)(2) (L_t)	 BS 5950 : PART 1 APPENDIX G - G2(b)(2) (L_t)

Table 6.2 Equivalent Uniform Moment Factors, m,
for Simply Supported Beams

$M_{cr} = \frac{1}{m} \frac{\pi}{L} \sqrt{EI_y GJ} \sqrt{1 + \frac{\pi^2 EI_w}{L^2 GJ}}$			
Beam and Load	Bending Moment	M_{max}	m
		M	1.00
		M	0.6
		M	0.4
		WL/4	0.74
		WL ² /8	0.89
		WL/4	0.94
		3WL/16	0.68

CHAPTER 7

7.0 Assessment of the Lateral Stability Clauses in BS 5950

7.1 Introduction

The basic design principles and the clauses for lateral stability in BS 5950 have been presented in chapter 6. In this chapter those stability clauses discussed earlier are assessed by the Finite Element "SPACE" computer programme, described in chapter 4.

The assessment is divided into three parts. The first part, deals with the design for lateral stability of prismatic sections. In this part, five different types of universal beam were chosen for the analysis and the details of the properties of the sections selected are given in table 7.1.

The second part of the assessment, deals with the design for tapering members. In this case, beam specimens shown in table 7.2 were investigated by considering a linear moment distribution with zero moment at one end.

The third part of the assessment, considers the design clauses for beams with restrained tension flanges and unrestrained compression flanges as given in Appendix G. In this assessment, both the cases of prismatic sections and haunched sections were considered. The section properties of

the beam specimens considered is as shown in table 7.2.

In the assessment by Finite Element Method, a 10-element model was used for the analysis of uniform members, while a 20-element model was used for the analysis of tapered and haunched members. The design strength of $P_y=275 \text{ N/mm}^2$ was used in all the calculations.

7.2 Assessment 1: General Clause for Lateral Buckling of Prismatic Members

In this section the design of five unrestrained prismatic members consisting of selected universal beams with properties shown in table 7.1 was considered. The following design cases were studied;

- (1) simply supported beam with uniform bending moment,
- (2) simply supported beam with moment gradient,
- (3) simply supported beam with destabilising concentrated load at the centre,
- (4) cantilever with destabilising load at the free end.

7.2.1 Design of Simply Supported Beams with Uniform Moment

A simply supported beam with uniform moment was used for the basis of design in BS 5950 for lateral stability of a beam with other loading conditions. It has been shown in the

previous chapter that the beam moment capacity M_b is calculated in BS 5950 using the relationship between the elastic critical moment, M_{cr} and the full plastic moment M_p . Imperfections were considered in the design formulation by the introduction of an imperfection parameter η , which was adopted so as to produce reasonable agreement between the values of M_b and the ultimate moment capacities M_u obtained from tests. Assessment in this section will therefore be used only to prove that point.

Analyses were conducted for the universal beam section shown in table 7.1. by BS 5950 and the Finite Element Method. Details of the calculation are given in Appendix 3.1. and the graphs of strength against slenderness ratio L/r_y for all the beams considered are presented as shown in figures 7.1. to 7.5.

The curves in figures 7.1. to 7.5. follow a similar pattern indicating the consistency of the results obtained by both methods. Since the Finite Element curve gave the basic formula for lateral torsional buckling, it shows that the design curve gave more conservative results due to the consideration of material imperfection and residual stresses in the design expressions.

7.2.2 Design of Simply Supported Beam with Moment Gradient

For a simply supported beam with moment gradient, BS 5950

gives a condition that the equivalent uniform moment M must be less than the buckling resistance moment M_b . The value of M was obtained by multiplying m , equivalent uniform moment factor to the value of the maximum moment on the beam under consideration.

For each of the beams shown in table 7.1., the moment capacity and buckling moment for different lengths were calculated for beams with moment gradients in accordance to BS 5950. The moment ratios $\beta=0.5$ and $\beta=-0.5$ were considered in the calculations. An example of these calculations are shown in Appendix 3.2.

The beams were also analysed by using the Finite Element computer programme. For moment ratio $\beta=0.5$, modelling for this effect was achieved by applying an initial moment of 10 kN.cm at one end and -5 kN.cm at the other. Modelling for moment ratio $\beta=-0.5$ was done by applying the initial moments of 10 kN.cm at one end and 5 kN.cm at the other end.

The results of the critical moments in the analyses by both methods are shown in figures 7.6 to 7.10. Figures 7.6 to 7.10 show similar a pattern of behaviour for all the beams under consideration. Based on the moment ratio given in table 18 of BS 5950, it can be seen that the results of the design curve with $\beta=-0.5$ gave a generally higher strength capacity. This is due to the smaller value of m (i.e., 0.43) given in table 18 of the code that resulted in a higher

value of modified slenderness. The whole curve seems to have been shifted due to this factor. In the case of $\beta=0.5$ the design curve adopted the value of $m=0.76$, however the reciprocal of this gave a smaller value for the modified slenderness.

Comparing the Finite Element curves with that of the design curve when $\beta=0.5$, it shows that the design curve gave a lower strength than the F.E.M. However, for $\beta=-0.5$, the values of the modified slenderness more than 1.2, the design curve gave a higher strength when compared with that of the F.E.M.

It can be concluded that for all the cases of beams with moment gradient $\beta=0.5$, analysis by BS 5950 gave safer results for short beams but as the beam gets longer the results seem to be the same as F.E.M. In $\beta=-0.5$, analysis by BS 5950 gave a safer design for shorter beams but as the beam gets longer F.E.M. gave safer results.

7.2.3 Simply Supported Beam with Destabilising Concentrated Load at the Centre

Calculations of the buckling moment capacity for the case of a simply supported beam subjected to destabilising transverse load at the top flange were carried out for different lengths of beam shown in table 7.1.

Clause 4.3.5. of the code stated that the length L used in the calculation of the moment capacity was to be increased by 20%. Clause 4.3.7. stated that for a member subjected to destabilising load, both the values of the factors m and n used in the calculation must be equal to 1. An example of the calculation is shown in Appendix 3.3.

The beams were also analysed by Finite Element computer programme. The models for the analysis use the same boundary conditions as the above cases. In this case, the load was applied at the top flange of the beam model.

Results of the analysis by method of the code and that of Finite Element are presented in figures 7.11 to 7.15. The strengths of the beams were presented by dimensionless moment M_b/M_p and M_e/M_p in the Y axis and against the modified slenderness $\sqrt{M_p/M_e}$ in the X axis.

It can be seen in all the cases considered that the BS 5950 curves for M_e/M_p are in exact agreement with that of the Finite Element curves for M_e/M_p . The design curves for M_b/M_p showed lower moment capacity than that of the Finite Element Method thus providing allowances for the effect of yield and geometrical imperfection of the strength of the real beam.

7.2.4 Cantilever with Destabilising Load at Free End

Calculation for the buckling capacity for a cantilever beam subjected to destabilising load at the free end were carried out for different lengths of beam sections shown in table 7.1 by the method of BS 5950 and by the Finite Element Method.

Cantilevers which are free to deflect laterally and twist at the unsupported end are treated by clause 4.3.6.2 BS 5950 as *equivalent beam with transverse loads*. However, the length used in the calculation for the moment capacity is increased by 150%. Further, as given in clause 4.3.7.6. the values of the factors m and n used in the calculation must be equal to 1. An example of the calculation by the code is given in Appendix 3.4.

The Cantilevers are also analysed by the Finite Element *computer programme*. The boundary conditions used for the model were that the fixed end was completely fixed (i.e., zero displacement, rotation and warping) and the free end was free to displace and rotate in the x , y , and z directions, and was free to warp. An initial load of 10 kN was applied at the top of the flange at the free end.

Results of the analysis by the method of BS 5950 and that of the Finite Element are presented in figures 7.16 to 7.20. The strengths of the beams are presented by dimensionless

moment ratios M_b/M_p and M_e/M_p on the vertical axis and against the modified slenderness $\sqrt{M_p/M_e}$ on the horizontal axis.

It can be seen that the results are similar to the previous case. The BS 5950 curves for M_e/M_p are in exact agreement with the Finite Element curves for M_e/M_p . The design curves for M_b/M_p showed lower moment capacity than that of the Finite Element Method thus providing allowances for the effect of yield and geometrical imperfection on the strength of the real beam.

7.3 Assessment 2: The General Clauses for Lateral Stability of Unrestrained Non-Uniform Member

In this section, the design of haunched beams without restraints, in accordance with BS 5950 was assessed by the Finite Element computer programme. The geometry of the haunched beams considered in this analysis are shown in table 7.2.

A total of 30 haunched beam specimens from 5 different base universal beams were analysed by method of BS 5950 for lateral stability. Calculations were made for different lengths of haunched beams for each beam specimen with major axis bending moment acting at the larger end and zero moment at the smaller end.

In the BS 5950 rules, only the geometries of the large end and the small end of the beam are considered. Therefore, results in the graphs can only be produced one for each case of ratio of depth of large end to shallow end, r (i.e., $r=3$ and 2). Furthermore the rules in BS 5950 do not differentiate the values of q , the ratio of the tapered length to the total length. An example of the calculation by the method of the code is shown in Appendix 3.5.

In the assessment by the Finite Element method, the different lengths of the haunched beam shown in table 7.2 were analysed. This analysis required the use of a 20-element model in order to obtain accurate results since the beam model contained two parts, namely the uniform section and the tapered section. The beam was assumed to be simply supported with its ends restrained from rotation about the X axis but free to warp. An initial bending moment of 100 kN.cm was applied at the larger end only.

The results of both analyses are presented in the form of the graphs of critical moment against length shown in figures 7.21 (A and B) to 7.25 (A and B). It can be seen that all the design curves gave lower buckling moments compared to those given by the Finite Element Method. This was due to the considerations of materials and beam imperfections in the design formulae.

The design and the F.E.M. curves were used to find the

critical length of the haunched beam. This was done when the critical bending moment to cause yield at the point of intersection of the tapered part and the uniform part were known. Based on a linear distribution of moment (figure 7.26), the moment at the larger end to cause buckling can be calculated by simple geometry. It shows that by this method, for the same type of base section (i.e., same yield stress) the factor of q will control the critical moment. This is shown in table 7.3 where the buckling moments are highest when $q=0.6$ and lowest when $q=0.3$.

The values of the critical lengths for all of the beam specimens considered are given in table 7.3. This shows that, for all the cases considered, the cases when $r=3$ gave a percentage error between 30% to 40%. Whereas for the cases when $r=2$, the error is in the lower region of 16 to 20%.

The results show that there is a linear decrease in percentage error with decrease value of q (the ratio length of tapered section to the total length) for the same value of r . In simple terms it can be said that longer critical length can be achieved if the value of q is small for haunched beams with the same value of r . On the other hand the results show that beams with the same value of q but with smaller value of r give a longer critical length for the analysis by BS 5950 while the Finite Element results show otherwise.

7.4 Assessment 3: The Assessment of Appendix G

In this section the design of both prismatic and tapered sections with restraints to the tension flange designed in accordance with Appendix G of BS 5950: Part 1 were assessed by the results of the Finite Element methods.

The first part of this section deals with 12 different types of universal beams subjected to moment gradient, with $\beta=0.5$ and with restraints on the tension flange.

The second part deals with 30 haunched specimens with restraints to the tension flange which were designed in accordance with Appendix G of BS 5950 and whose results were compared with F.E.M..

The third part deals with the assessment of Appendix G by comparison with clause 5.5.3.5. of BS 5950.

7.4.1 Analysis of Prismatic Sections in Accordance with Appendix G and F.E.M.

Twelve different universal beams with properties shown in table 7.4 were analysed by Appendix G for the cases of loading shown in figure 7.26. In the analyses the beams are assumed to be restrained laterally at both ends but free to warp. The tension flanges are restrained laterally by the

presence of the purlins. The beams are subjected to bending moment gradient with the moment ratio of the smaller moment to the greater moment at the ends, $\beta=0.5$. An example of the calculation with the help of a mathematical software package (7.1) for the critical length for elastic and plastic stability is shown in Appendix 3.6. A similar analysis was also carried out by a computer programme "APG8" that was written by Engel (7.2) specifically for design by Appendix G.

The beams are also analysed by the Finite Element computer programme. In this case the boundary conditions used for each model were that the ends were restrained from rotation but free to warp. The tension flange was restrained by "restraint elements" spaced at regular intervals. Different lengths of beam specimens were analysed for which the results are presented graphically showing the predicted critical moment against length of the specimen. From these graphs the critical length at a moment equal to the yield moment of the beam can be obtained.

Results of the critical length by the methods mentioned above are given in table 7.5. In table 7.5, it is shown that both the results of calculation by computer programme APG8 and by the mathematical software (i.e., appendix 3.6) gave similar results and are consistent. This finding verified the programme "APG8". Comparing the results of the elastic stability analysis by Appendix G with that of Finite Element

Method, the error is between 39 to 53% for all the cases considered. There is also no correlation between torsional index D/t with that of the percentage error.

Figure 7.27 shows the second moment of area about the minor axis, (I_y), plotted against the critical length at which buckling occurred, for both the results of Appendix G and Finite Element method. It shows that there is a good relationship between I_y and the critical length for the values of I_y greater than 1000 cm^4 . For values of I_y less than this, the relationship was not so good.

7.4.2 Analysis of Restrained Haunch Members by Appendix G and the Finite Element Method.

7.4.2.1 General

Five universal beam base sections with six different taper parameters making a total of 30 haunch beam specimens were analysed in this section. Details of the beam properties are shown in table 7.2. In the analysis values of $f_y=250 \text{ N/mm}^2$ and $E=200 \times 10^3 \text{ N/mm}^2$ were used.

The beams were analysed by the method of Appendix G and the Finite Element method. Results of analysis by Finite difference method obtained by Horne et al (7.3) on similar types of haunch specimen are presented for comparison.

Analysis of an alternative method to Appendix G i.e., clause 5.5.3.5 was also conducted and results were compared with those given by the Finite Element method.

7.4.2.2 Analysis of Haunched Beams by the Method of Appendix G

Based on the provision of Appendix G of BS 5950: Part 1, critical lengths of the beam were calculated using the computer program "APG8" and by the calculations shown in Appendix 3.7. In the calculations the haunched beam specimens were divided into 29 sections and the stresses at each section of the haunched beam were calculated. A critical length was met when the applied stress at one section exceeded the allowable buckling stress at that particular section. The method of calculation for the applied stress and the allowable buckling stress is given in the previous chapter. In the calculation, the applied moment at the larger end of the haunched beam was known. This loading condition was represented by considering the haunched member to be subjected to moment varying uniformly from zero at the small end. A common design situation was one in which the yield moment M_y of the base section was just reached at the junction of the uniform and tapered parts. By simple geometry, the values of the bending moment at the larger end of the beam can be calculated when the yield moment was known.

The results of the analysis by method of Appendix G for the haunched beams for elastic stability are given in table 7.6.

7.4.2.3 Analysis of Haunched Beams by the Finite Element Method

Finite Element analysis was also carried out on the beam specimen by using the SPACE Finite Element computer programme. The beam was modelled with restraints provided at intervals along the top flange A.B. shown in figure 7.28. The effective point of resistance is $a=0.75 \times D_{\min}$. Points G and E of the outstand flange were also restrained from lateral displacement. The minimum number of elements used in the modelling was 20 and, depending on the value of q , the number of equal lengths of element allocated for the tapered parts were at least 12. The sectional properties of the elements were based on two flanges, ignoring the presence of middle flange in the tapered region. An initial moment of 100 kNcm was applied at the first node at the larger end of the specimen. This caused tension at the top flange and compression at the bottom flange.

The results of the analysis by Finite Elements are shown in figures 7.29 (A & B) in which the critical moments predicted by computer were plotted against the lengths. It shows that all the graphs plotted gave smooth curves indicating consistency of the results obtained.

Based on a linear distribution of moment shown in figure 7.28, the critical bending moment for a particular beam can be obtained. This was "controlled" by the yield moment of the base section at the point of intersection of the tapered and the uniform section. The curves in figures 7.29 (A & B) to 7.33 (A & B) then can be used to obtain the critical length when the critical bending moment was known. The critical lengths of the haunched beam obtained by this method are shown in table 7.6.

Table 7.6 also gave results of analysis of the same haunched beams by the finite difference method. The critical lengths of the beam were established in the same manner as the finite element cases mentioned earlier. It can be seen that the results of analysis by finite difference method are in close agreement with that of the finite element method. This proved that the the finite element formulations and modelling of the haunched beams were valid.

7.4.2.4 Assessment of Clause 5.5.3.5

Clause 5.5.3.5. of BS 5950 is an alternative to that of Appendix G for checking the limiting length of members with restraints on the tension flange but unrestrained on the compression flange. Details of clause 5.5.3.5. are given in chapter 6. For all the haunched beams under consideration, the conditions for the validity of using clause 5.5.3.5. are

met. This clause is simple to use and quick results can be obtained without the need for extensive computation. Details of the data used in the calculation and the results of analysis by clause 5.5.3.5 are given in table 7.7.

In table 7.7 it is shown that the results of analysis by clause 5.5.3.5. were less conservative than those of Appendix G. Furthermore the expression in the clause does not include the taper length parameter q , although it considers the depth parameter r . Therefore, when using the expression in this clause for the same type of beam, different values of r gave different results. In all the cases considered, the results of the critical lengths obtained by method of clause 5.5.3.5. were larger than that of Appendix G. However, when compared to results by Finite Element method, the values obtained by clause 5.5.3.5 can give a rough estimate of the results of Appendix G.

7.4.3 Assessment of Appendix G for Plastic Stability of Haunch Beam

Besides the assessment for elastic stability, the haunch beam specimens given in table 7.2 were also assessed for plastic stability. The beams were calculated for plastic stability in accordance with the clauses in Appendix G. An example of the calculation is given in Appendix 3.8. Results of the analysis are given in table 7.8. The finite element

results are provided to give an idea of the difference in the results obtained.

The result shows that the values of the Limiting length L_t are always lower than the results of analysis by finite element method. The finite element results however, are for elastic buckling only and therefore direct comparison between the two results are not appropriate.

In table 7.8, it is shown that the values of L_t are controlled by the factors c and n_t . The values of L_k are the same for one base section. In all the cases considered it is shown that, for the same ratio of tapered length to the total length q , higher values of critical length were obtained for specimens with smaller ratios of depths r .

The results of the finite element method and the elastic stability analysis of the same beam specimen appear to be similar and it was found that they gave more conservative results than the analysis for plastic stability by Appendix G.

7.4.4 Summary of the Assessment

The assessment of the general clauses for lateral stability of BS 5950 gave very satisfactory results compared with the results of analysis by the Finite Element Method. The

same, is true for unrestrained non-uniform members in which the results are acceptable. However it seems that the analysis by Appendix G gave some interesting findings. For uniform members, Appendix G gave deleberately oversafe results in the region of 39% to 53% as compared to the results by Finite Element methods. This large percentage error when using the design code, even after taking consideration of imperfections and residual stresses is unacceptable. Modification of the design formulation should be aimed at reducing this percentage error based on the F.E.M. results to a more acceptable value.

In non-uniform members, it is shown that the results of analysis by Finite Element method gave very close agreement to that of Finite difference method. However, the results obtained by Appendix G gave a much lower critical length. The percentage error when compared to F.E.M. is in the region of 70%. It can therefore be said that Appendix G gave an oversafe design. Clause 5.5.3.5, is less conservative than Appendix G, with the percentage error in the region of 65%.

Therefore modification to clauses in Appendix G and clauses 5.5.3.5. must be aimed at reducing the percentage error to the lower values of (say) 30% to 40%.

7.5 Conclusion

From the analysis and comparison of the results obtained within this chapter, it shows that the general aspects of design for lateral buckling as assessed in section 7.2. agrees with analysis by Finite Element method. The result shows that some aspects of the real beam properties such as imperfections and residual stresses that were considered in the formulation of the design equation are acceptable.

From the analysis and comparison of the general clause on elastic stability for non-uniform members, it has been shown that (table 7.3) the code gave lower values of critical length compared to the Finite Element results. Indeed a larger percentage error was observed for cases of $r = 3$ than that for $r = 2$. However for all the cases considered, the largest percentage error observed was only 40% indicating that the provision for imperfections and residual stresses in the design equations are sufficient and that the design equations are acceptable.

In Appendix G, the comparison made on the results of Finite Elements and Finite Difference method shows clearly that the clauses of Appendix G gave an oversafe design. However, it must be stressed that the provisions in Appendix G were based on analyses that assumed several approximations and therefore the results were approximate. In the same manner the results of design by an alternative method to Appendix

G i.e., clause 5.5.3.5. show that the provision for the design for both prismatic and non-uniform beams with tension flanges restrained, produce oversafe designs, however, it was less conservative than Appendix G.

From these findings it is thought that some modifications to Appendix G can be made in order to make the results more acceptable. The next chapter is devoted to the study of approaches to modifying Appendix G and Clause 5.5.3.5. and proposals for the ammendments are forwarded.

The assessment of the lateral torsional buckling clauses of BS 5950 using the finite element analysis described in chapter 4 involves the comparision of the elastic critical buckling capacity with the actual design capacity predicted by BS 5950 which incorporates yield, residual stresses and geometric imperfections in addition to buckling effects.

Some difference between the two methods is therefore inevitable. In order to progress the work and make the comparison, the author has judged that a difference of 30 - 40% is more acceptable than the present discrepancy.

Chapter 7 demonstrates this difference in analysis, and chapter 8 and 9 follow from the above judgement.

STRENGTH OF BEAM IN UNIFORM BENDING
IN ACCORDANCE WITH BS 5950 AND
COMPARISON WITH F.E.M

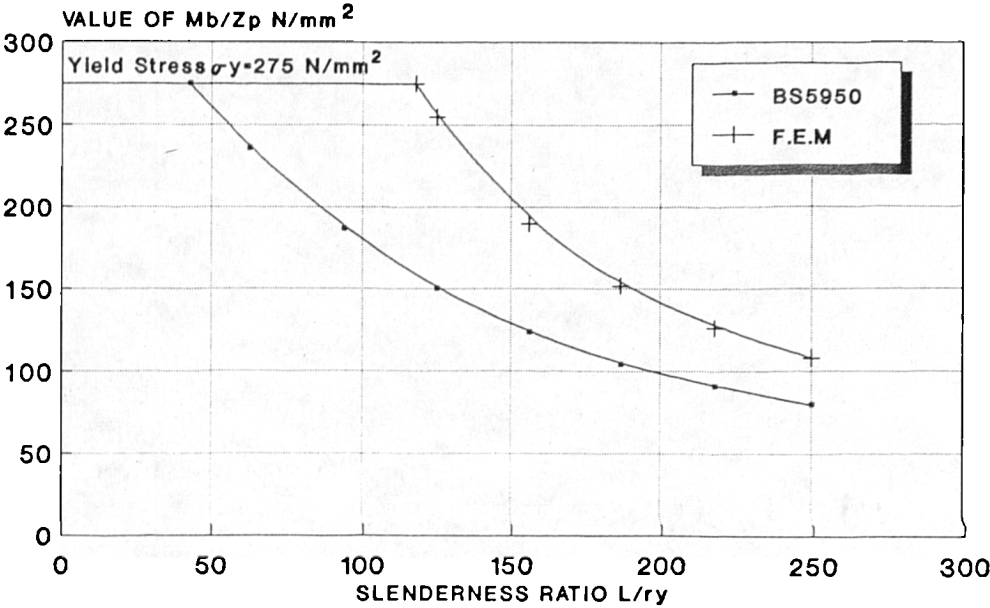


Figure 7.1 Graph for Universal Beam
size 203x133xUB30 (D/T=21)

STRENGTH OF BEAM IN UNIFORM BENDING
IN ACCORDANCE WITH BS 5950 AND
COMPARISON WITH F.E.M

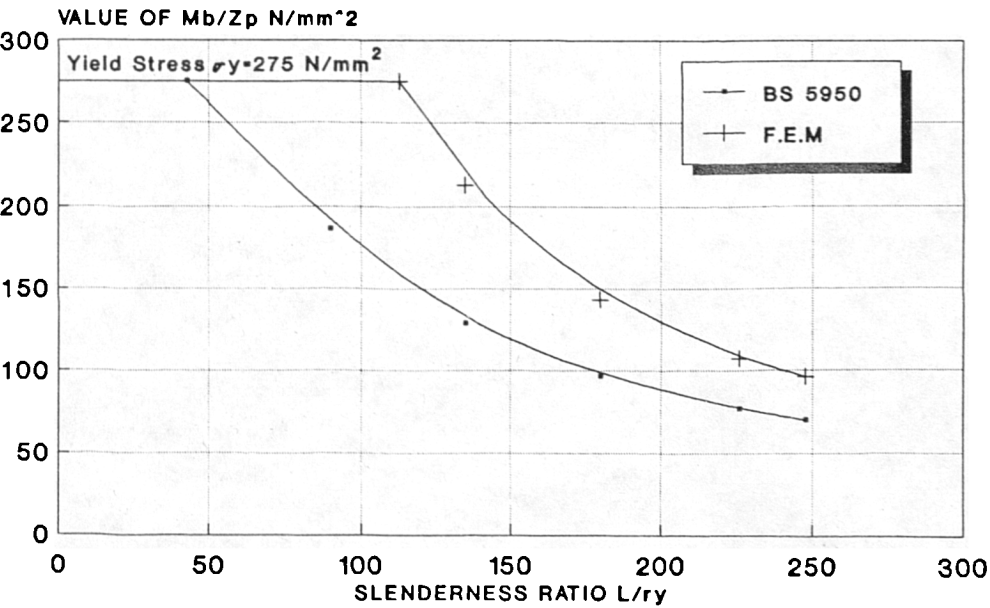


Figure 7.2 Graph for Universal Beam size
254x102xUB28 (D/T=26)

STRENGTH OF BEAM IN UNIFORM BENDING
IN ACCORDANCE WITH BS 5950 AND
COMPARISON WITH F.E.M

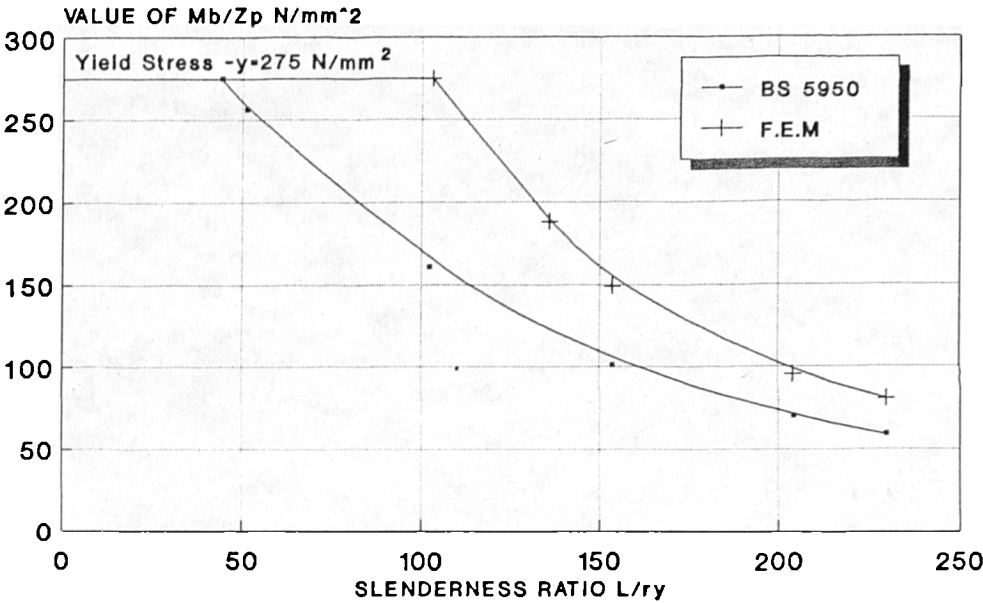


Figure 7.3 Graph for Universal Beam size
305x102xUB25 (D/T = 45)

STRENGTH OF BEAM IN UNIFORM BENDING
IN ACCORDANCE WITH BS 5950 AND
COMPARISON WITH F.E.M

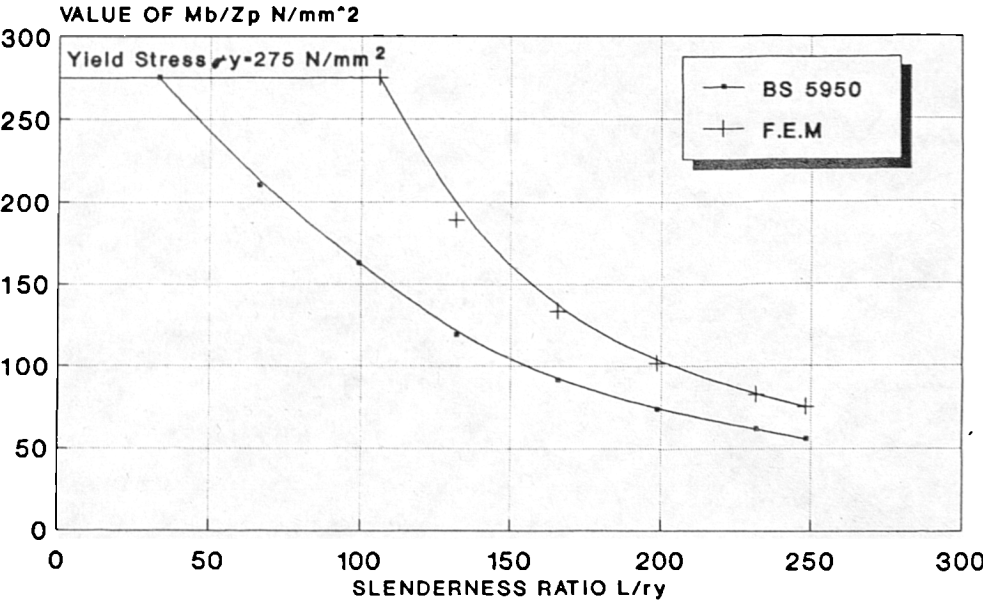


Figure 7.4 Graph for Universal Beam size
406x140xUB46 (D/T = 36)

STRENGTH OF BEAM IN UNIFORM BENDING
IN ACCORDANCE WITH BS 5950 AND
COMPARISON WITH F.E.M

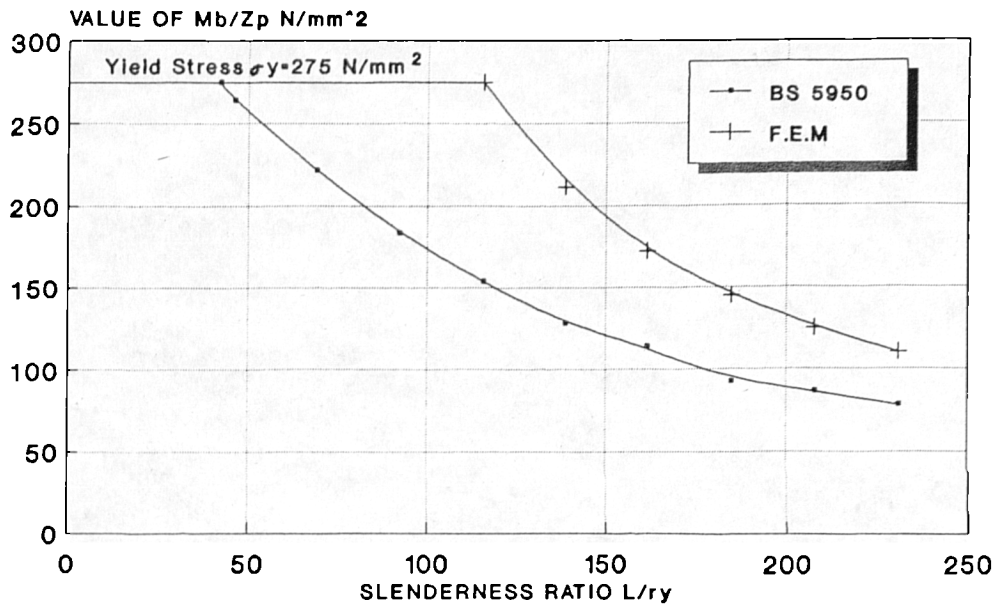


Figure 7.5 Graph for Universal Beam size 457x191xUB98 (D/T=24)

STRENGTH OF BEAM UNDER MOMENT GRADIENT
IN ACCORDANCE WITH BS 5950 AND
COMPARISON WITH F.E.M

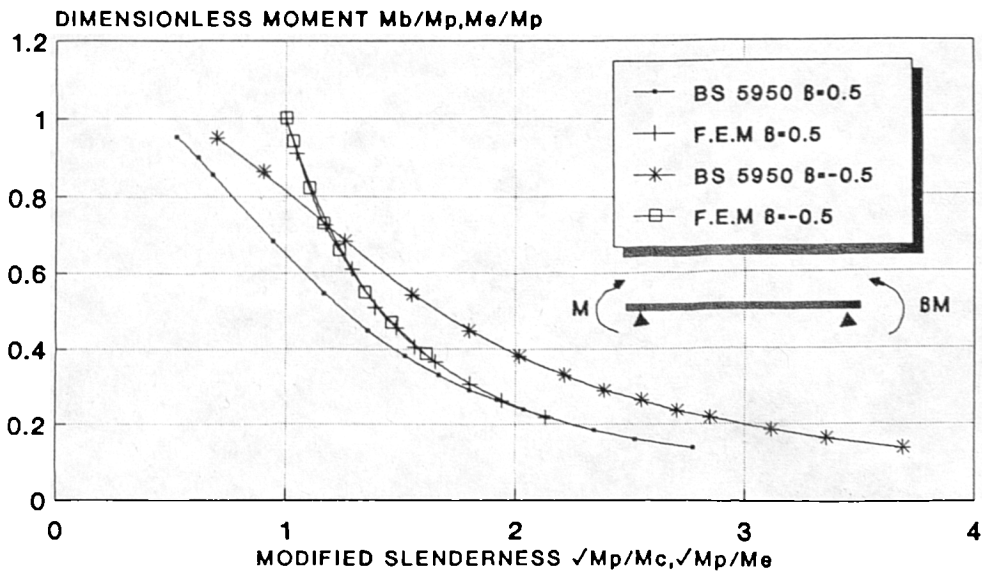


Figure 7.6 Graphs for Beam 203x133xUB30 (D/T=21). Results of Analysis for Moment Ratio $B=0.5$ and $B=-0.5$

STRENGTH OF BEAM UNDER MOMENT GRADIENT
IN ACCORDANCE WITH BS 5950 AND
COMPARISON WITH F.E.M

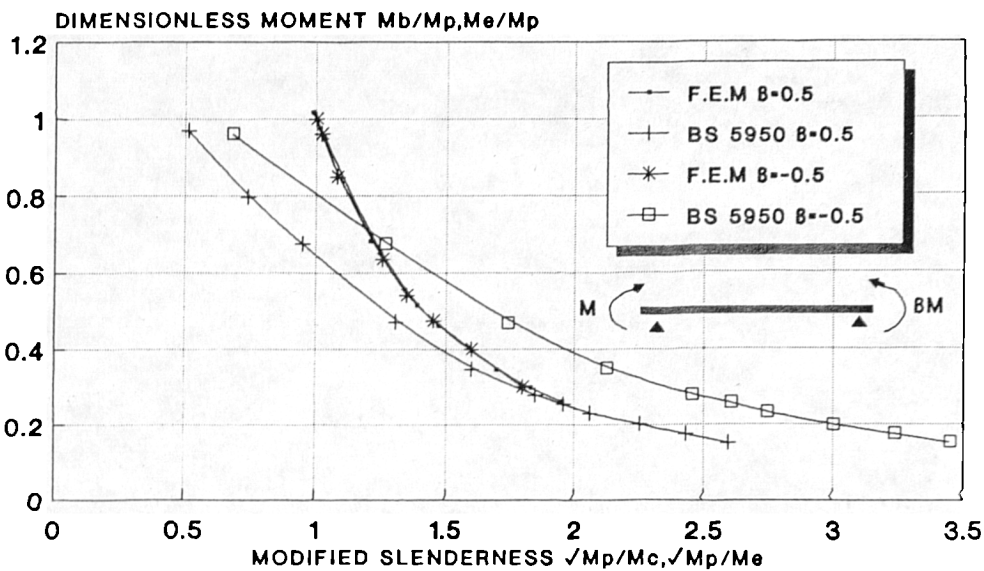


Figure 7.7 Graphs for Beam 254x102xUB28
(D/T=26). Results of Analysis for Moment
Ratio $\beta=0.5$ and $\beta=-0.5$

STRENGTH OF BEAM UNDER MOMENT GRADIENT
IN ACCORDANCE WITH BS 5950 AND
COMPARISON WITH F.E.M

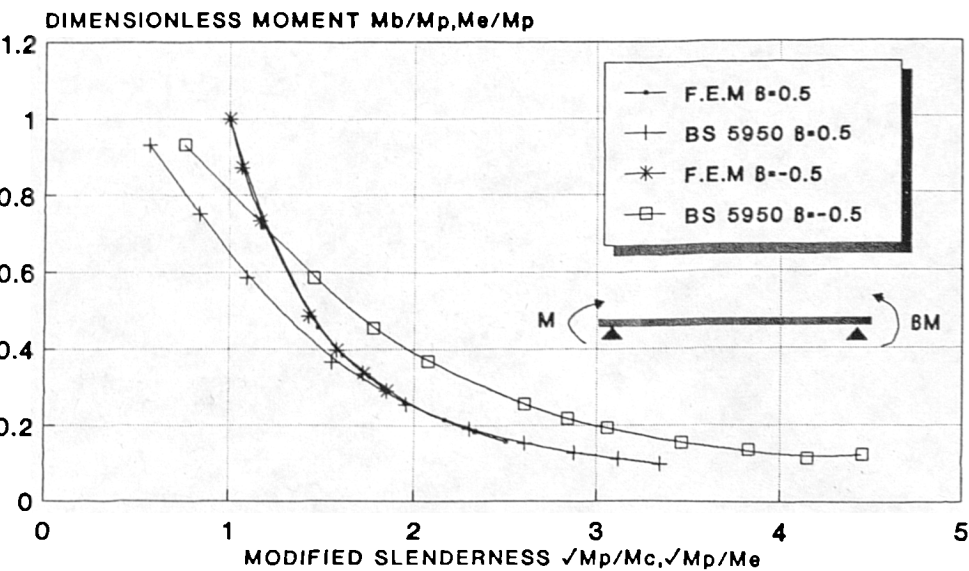


Figure 7.8 Graphs for Beam 305x102xUB25
(D/T=45). Results of Analysis for Moment
Ratio $\beta=0.5$ and $\beta=-0.5$

STRENGTH OF BEAM UNDER MOMENT GRADIENT
IN ACCORDANCE WITH BS 5950 AND
COMPARISON WITH F.E.M

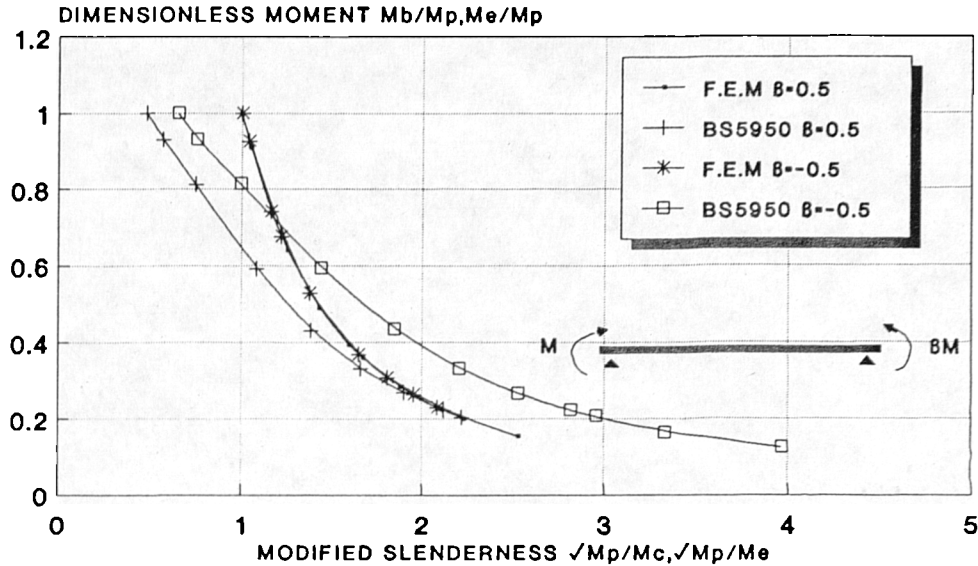


Figure 7.9 Graphs for Beam 406x140xUB46
(D/T=35.9). Results of Analysis for
Moment Ratio $\beta=0.5$ and $\beta=-0.5$

STRENGTH OF BEAM UNDER MOMENT GRADIENT
IN ACCORDANCE WITH BS 5950 AND
COMPARISON WITH F.E.M

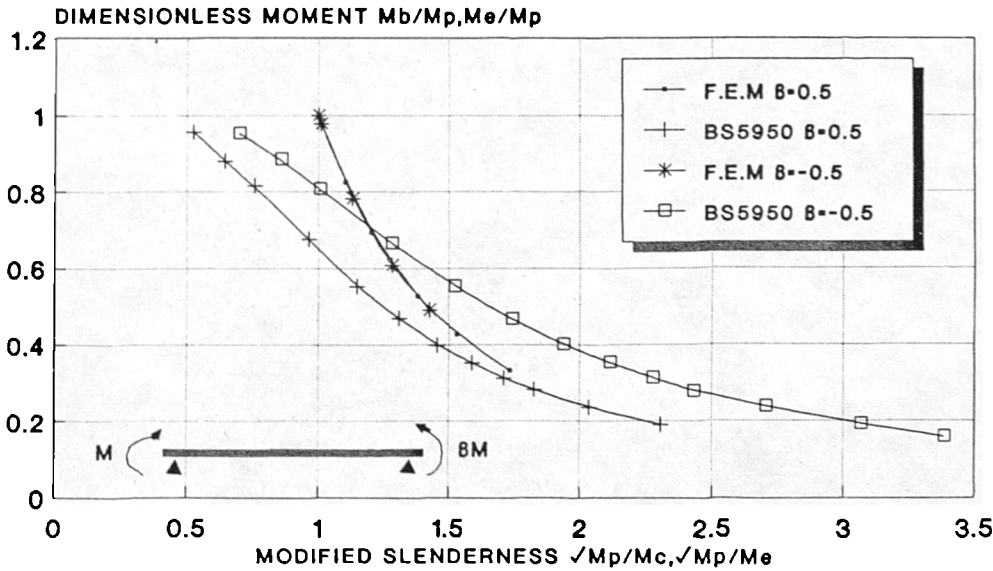


Figure 7.10 Graphs for Beam 457x191xUB98
(D/T=24). Results of Analysis for Moment
Ratio $\beta=0.5$ and $\beta=-0.5$

STRENGTH OF BEAM SUBJECTED TO
DESTABILISING TRANSVERSE LOAD ACCORDING
TO BS 5950 AND COMPARISON WITH F.E.M.

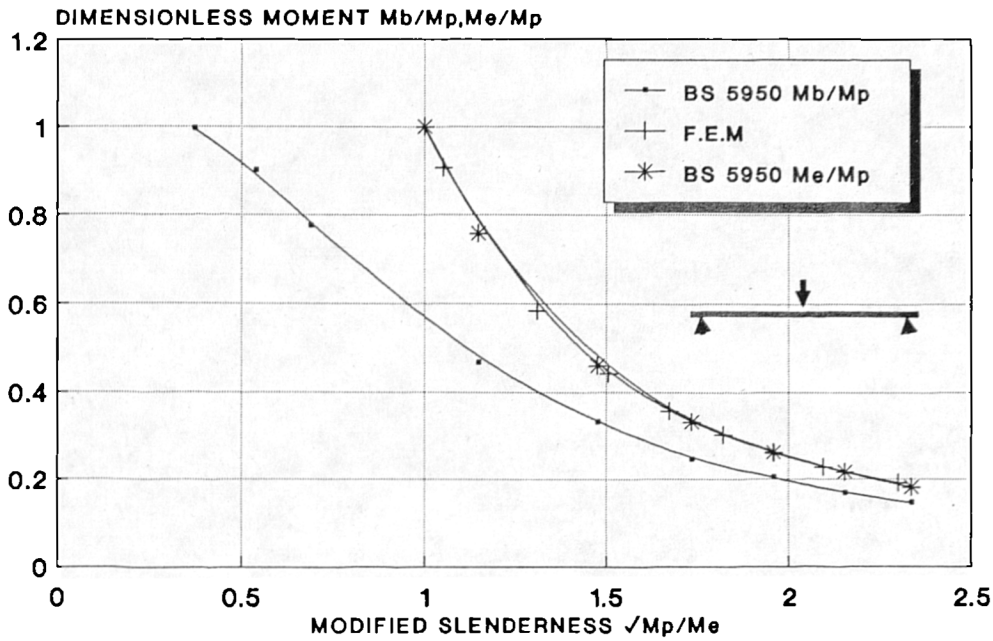


Figure 7.11 Graphs for Beam 203x133xUB30

STRENGTH OF BEAM SUBJECTED TO
DESTABILISING TRANSVERSE LOAD ACCORDING
TO BS 5950 AND COMPARISON WITH F.E.M.

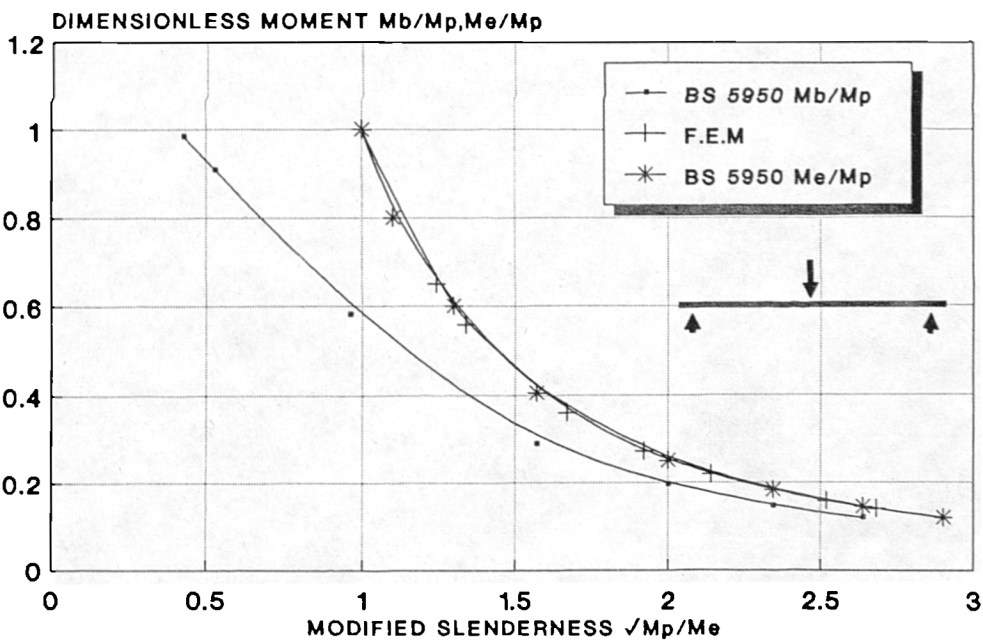


Figure 7.12 Graphs for Beam 254x102xUB28

STRENGTH OF BEAM SUBJECTED TO
DESTABILISING TRANSVERSE LOAD ACCORDING
TO BS 5950 AND COMPARISON WITH F.E.M.

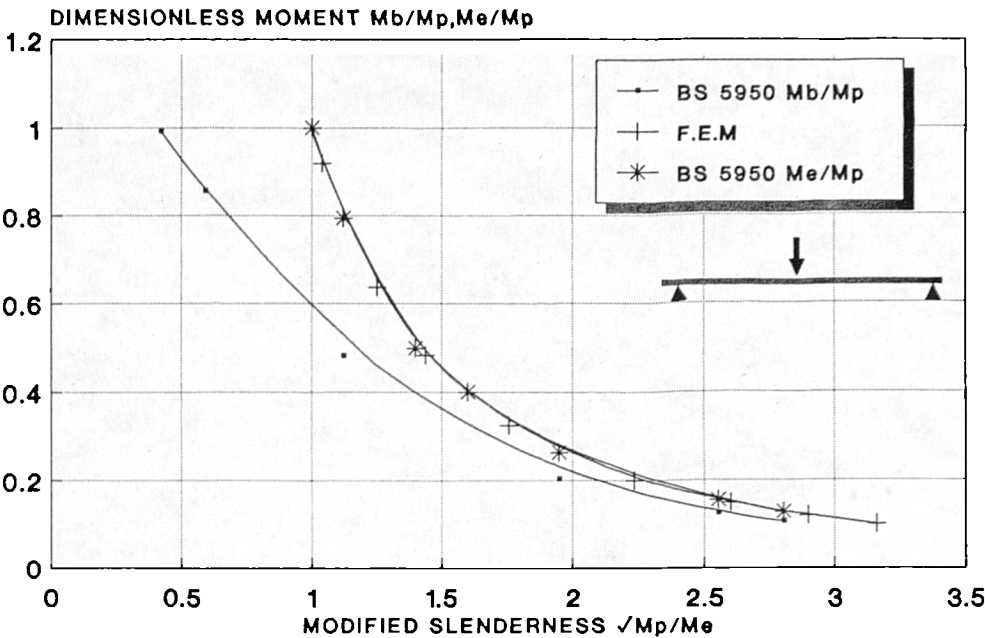


Figure 7.13 Graphs for Beam 305x102xUB25

STRENGTH OF BEAM SUBJECTED TO
DESTABILISING TRANSVERSE LOAD ACCORDING
TO BS 5950 AND COMPARISON WITH F.E.M.

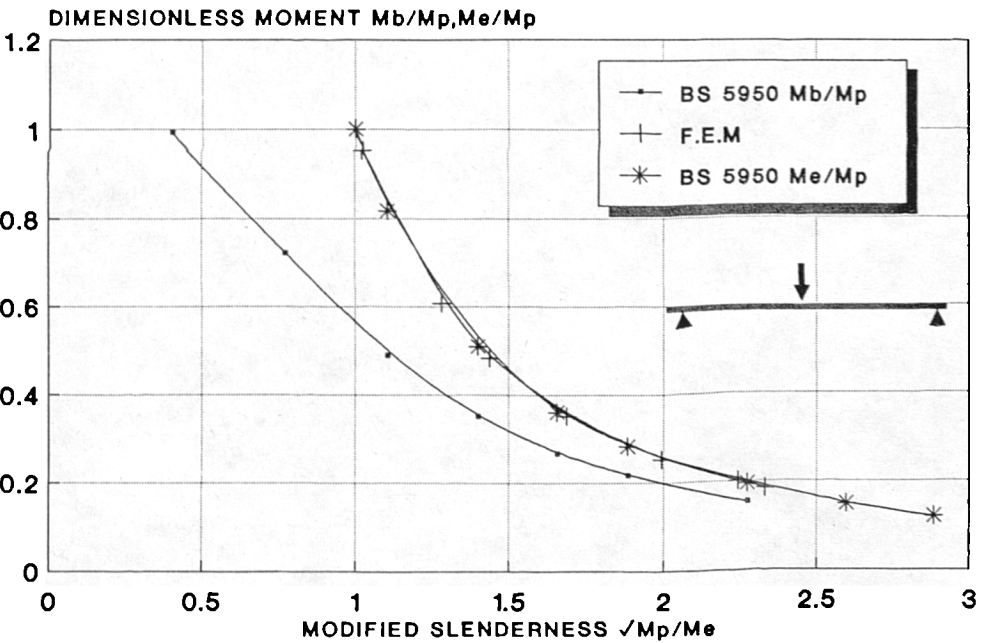


Figure 7.14 Graphs for Beam 406x140xUB46

STRENGTH OF BEAM SUBJECTED TO
DESTABILISING TRANSVERSE LOAD ACCORDING
TO BS 5950 AND COMPARISON WITH F.E.M.

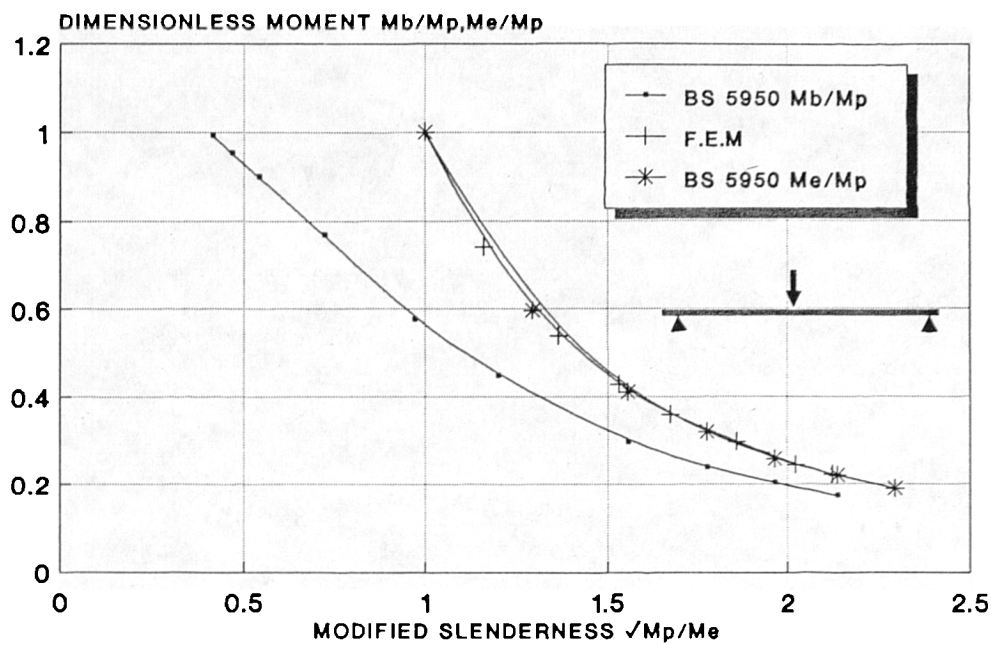


Figure 7.15 Graphs for Beam 457x191xUB98

STRENGTH OF CANTILEVER SUBJECTED TO
DESTABILISING LOAD AT THE FREE END IN
ACCORDANCE WITH BS 5950 AND F.E.M

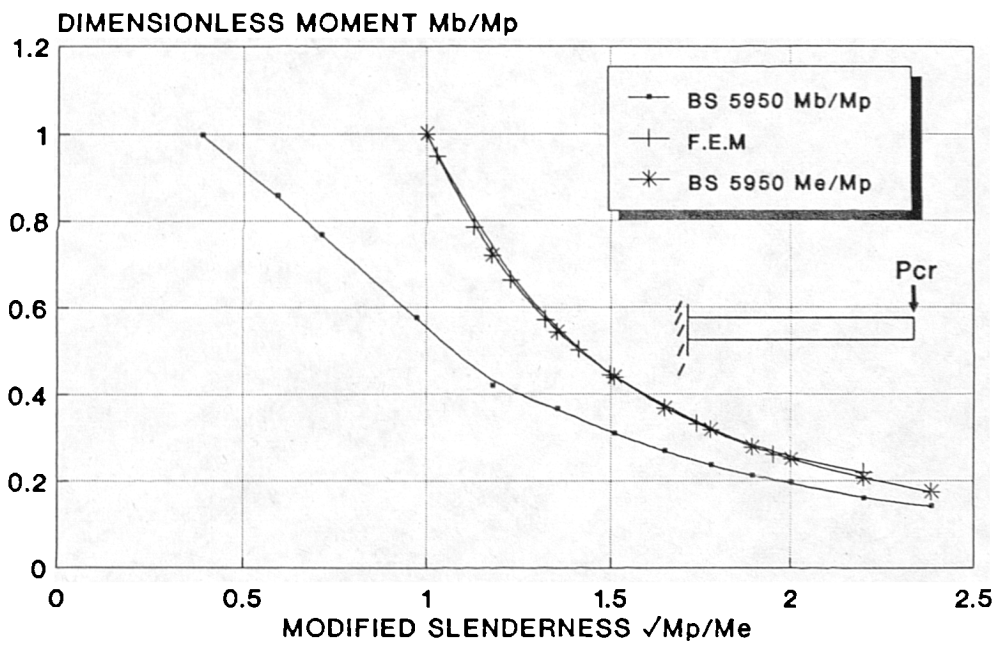


Figure 7.16 Graphs for Beam 203x133xUB30

STRENGTH OF CANTILEVER SUBJECTED TO
DESTABILISING LOAD AT THE FREE END IN
ACCORDANCE WITH BS 5950 AND F.E.M

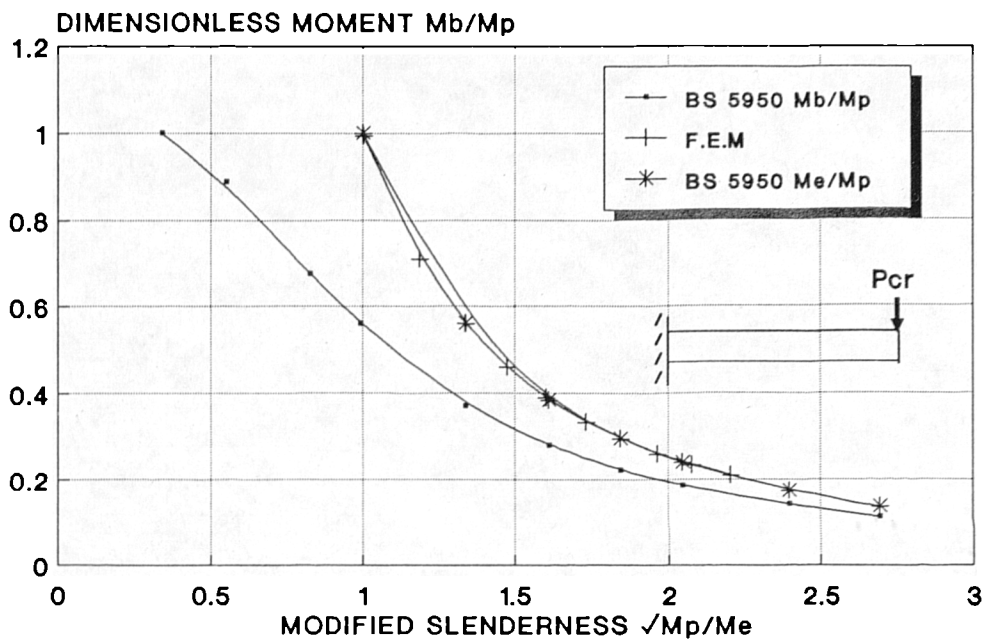


Figure 7.17 Graphs for Beam 254x102xUB28

STRENGTH OF CANTILEVER SUBJECTED TO
DESTABILISING LOAD AT THE FREE END IN
ACCORDANCE WITH BS 5950 AND F.E.M

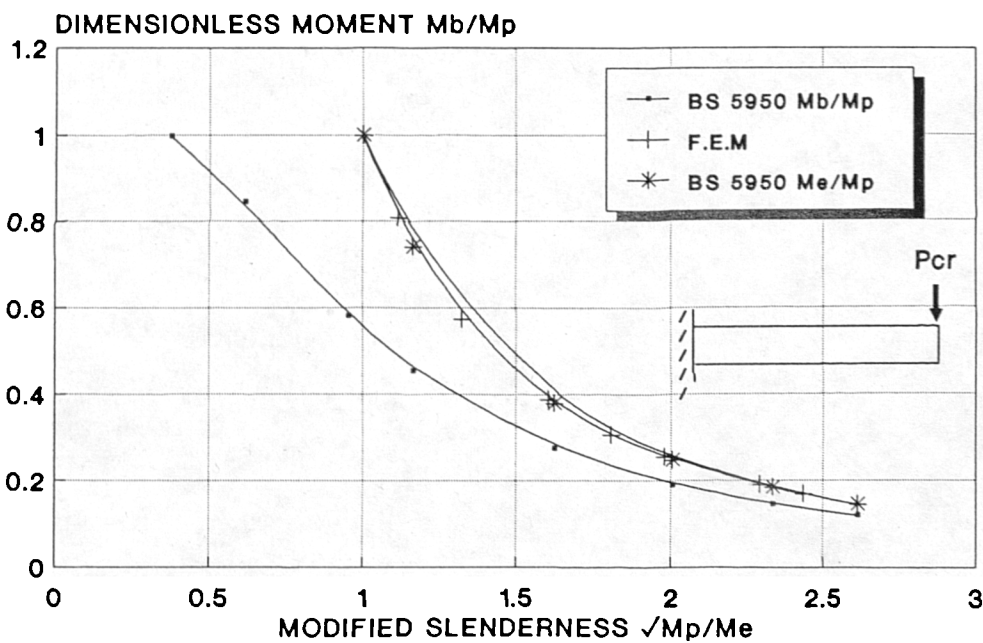


Figure 7.18 Graphs for Beam 305x102xUB25

STRENGTH OF CANTILEVER SUBJECTED TO
DESTABILISING LOAD AT THE FREE END IN
ACCORDANCE WITH BS 5950 AND F.E.M

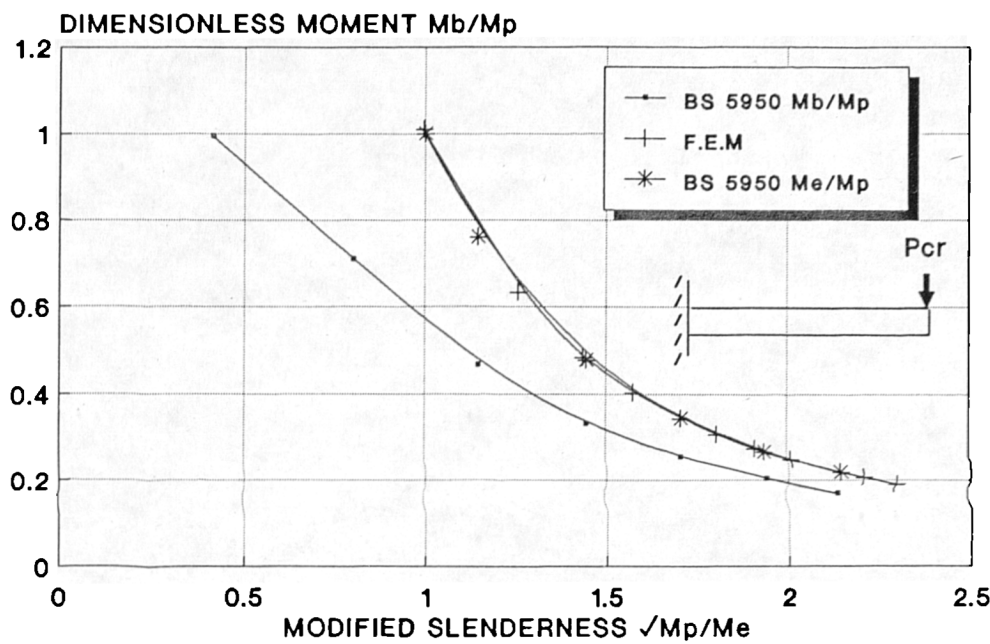


Figure 7.19 Graphs for Beam 406x140xUB46

STRENGTH OF CANTILEVER SUBJECTED TO
DESTABILISING LOAD AT THE FREE END IN
ACCORDANCE WITH BS 5950 AND F.E.M

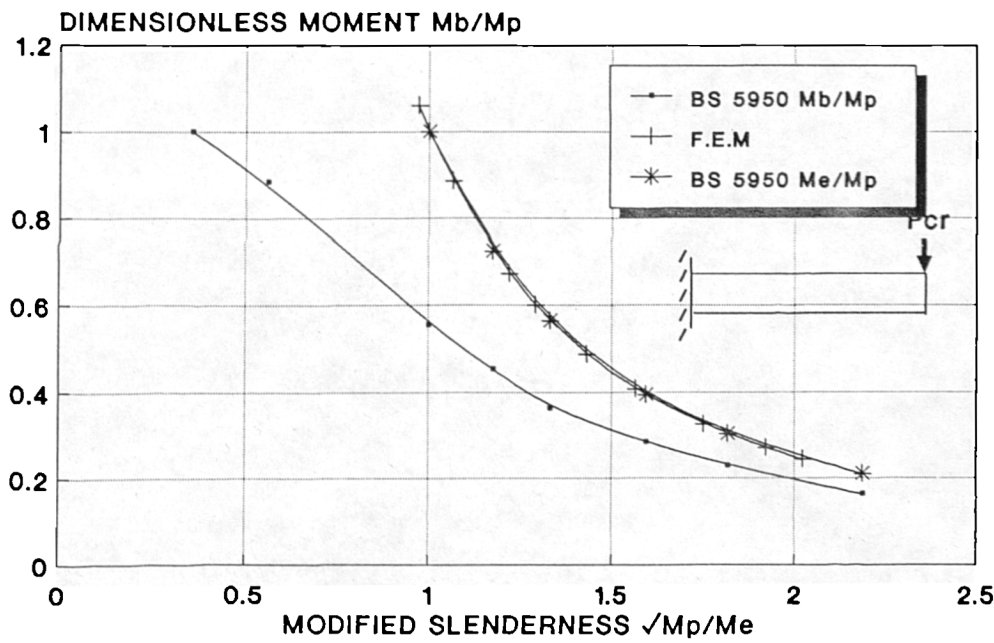


Figure 7.20 Graphs for Beam 457x191xUB98

NOTE: HON1, HON2, HIN4 & HON6 Have Ratio
of Tapered Length to Total Length $q =$
0.6, 0.5, 0.4 and 0.3 Respectively

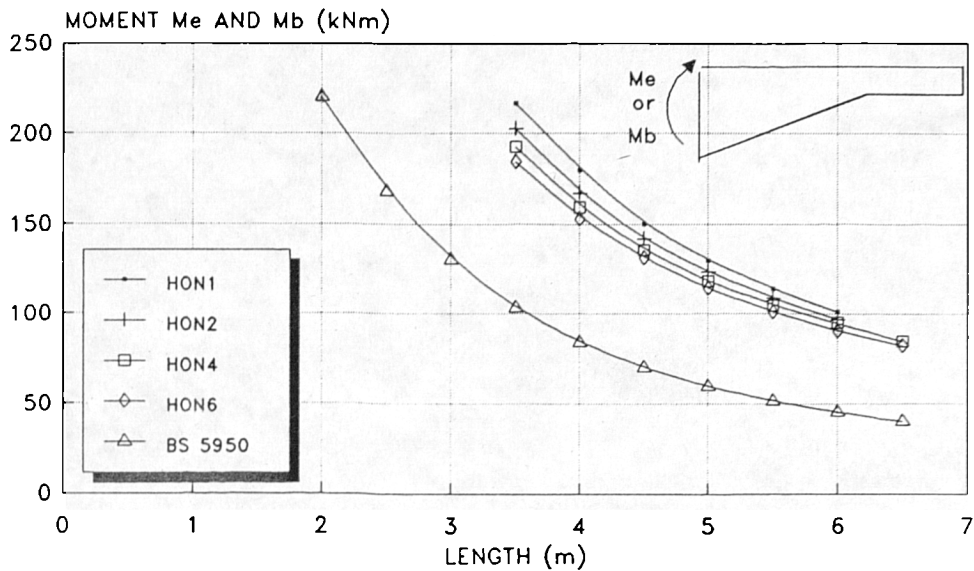


Figure 7.21A Results of Analysis of
Tapered Beam, Base Section 203x133xUB30
 $r=(D2/D1)=3$

NOTE: HON3 and HON5 Have ratio of
Tapered Length to the Total Length
 $q = 0.4$ and 0.3 Respectively

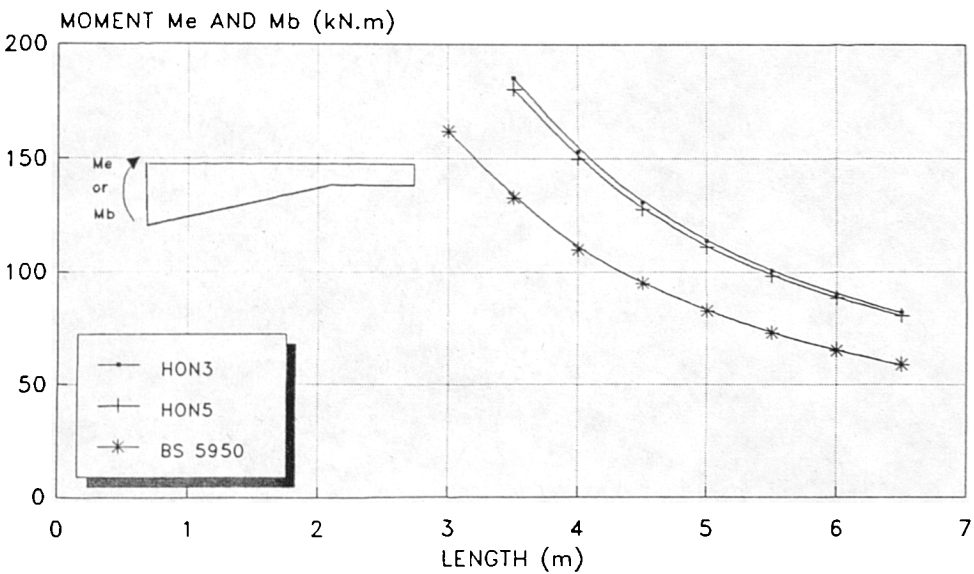


Figure 7.21B Results of Analysis Tapered
Beam, Base Section 203x133xUB30
 $r=(D2/D1)=2$

NOTE: HON7, HON8, HON10 & HON12 Have
Ratio of Tapered Length to Total Length
 $q = 0.6, 0.5, 0.4 \text{ \& } 0.3$ Respectively

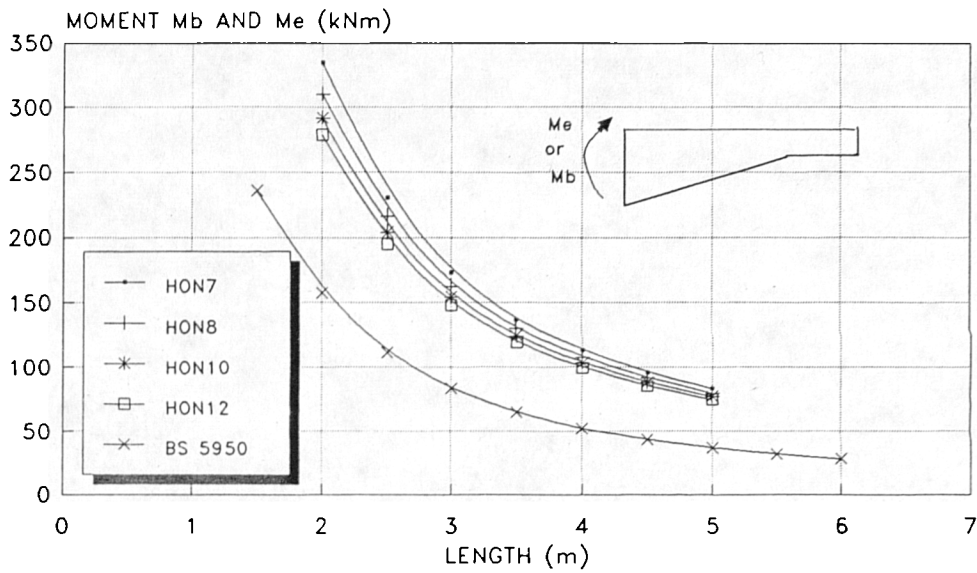


Figure 7.22A Results of Analysis of
Tapered Beam, Base Section 254x102xUB28
 $r=(D2/D1)=3$

NOTE: HON9 and HON11 Have the Ratio of
Tapered Length to Total Length,
 $q = 0.4 \text{ \& } 0.3$ Respectively

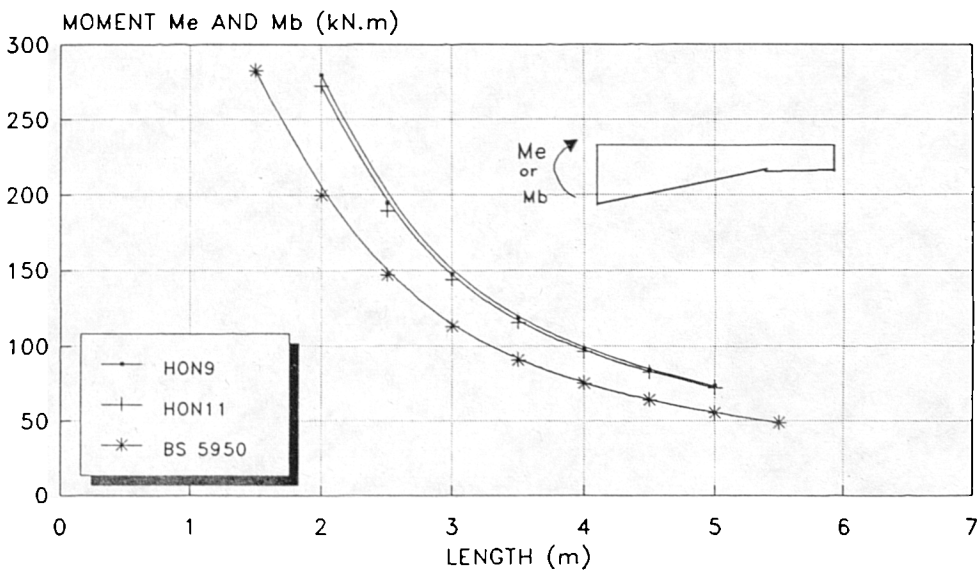


Figure 7.22B Results of Analysis of
Tapered Beam, Base Section 254x102xUB28
 $r=(D2/D1)=2$

NOTE: HON13, HON14, HON16 & HON18 Have
Ratio of Tapered Length to Total Length
 $q = 0.6, 0.5, 0.4 \text{ \& } 0.3$ Respectively

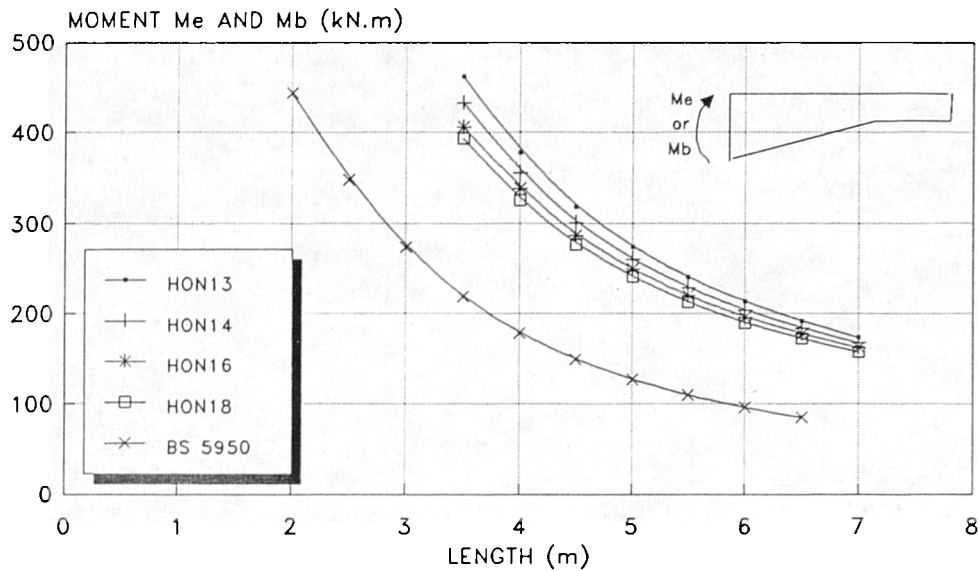


Figure 7.23A Results of Analysis of
Tapered Beam, Base Section 254x146xUB43
 $r=(D2/D1)=3$

NOTE: HON15 And HON17 Have the Ratio of
Tapered Length to Total Length
 $q = 0.4 \text{ \& } 0.3$ Respectively

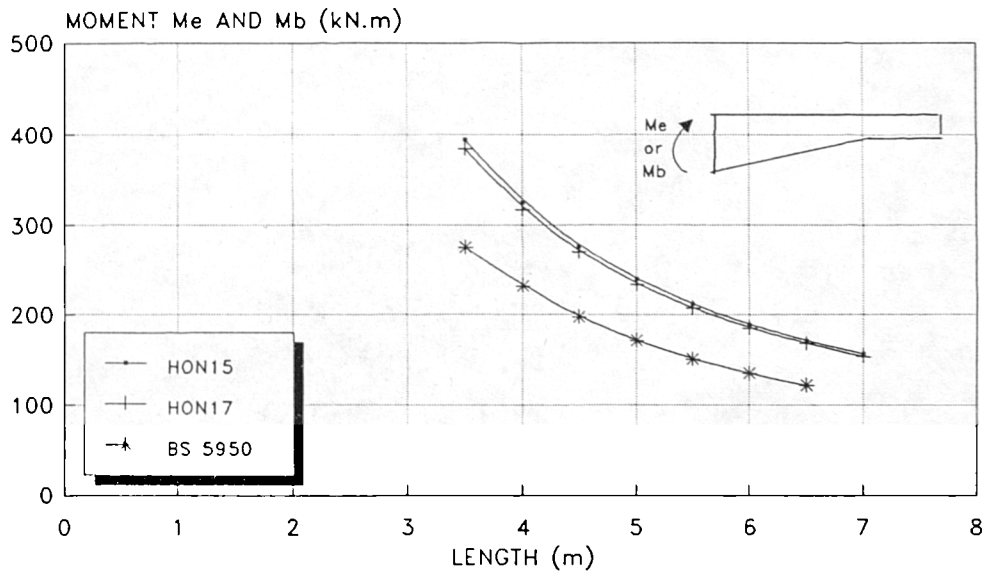


Figure 7.23B Results of Analysis of
Tapered Beam, Base Section 254x146xUB43
 $r=(D2/D1)=2$

NOTE: HON19, HON22 & HON24 Have the
Ratio of Tapered Length to Total Length
 $q = 0.6, 0.5, 0.4$ and 0.3 Respectively

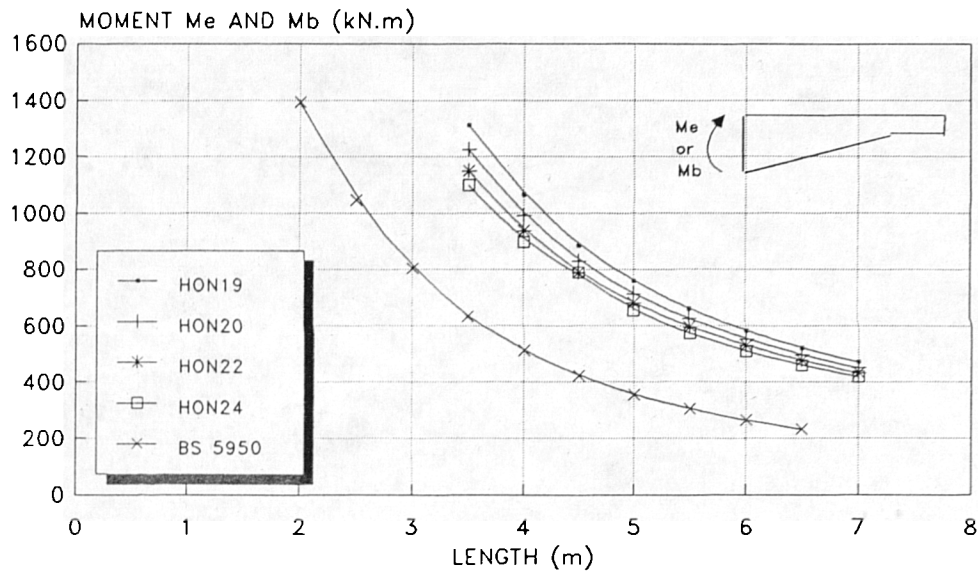


Figure 7.24A Results of Analysis of
Tapered Beam, Base Section 457x152xUB82
 $r = (D2/D1) = 3$

NOTE: HON21 And HON23 Have the Ratio
of Tapered Length to Total Length
 $q = 0.4$ and 0.3 Respectively

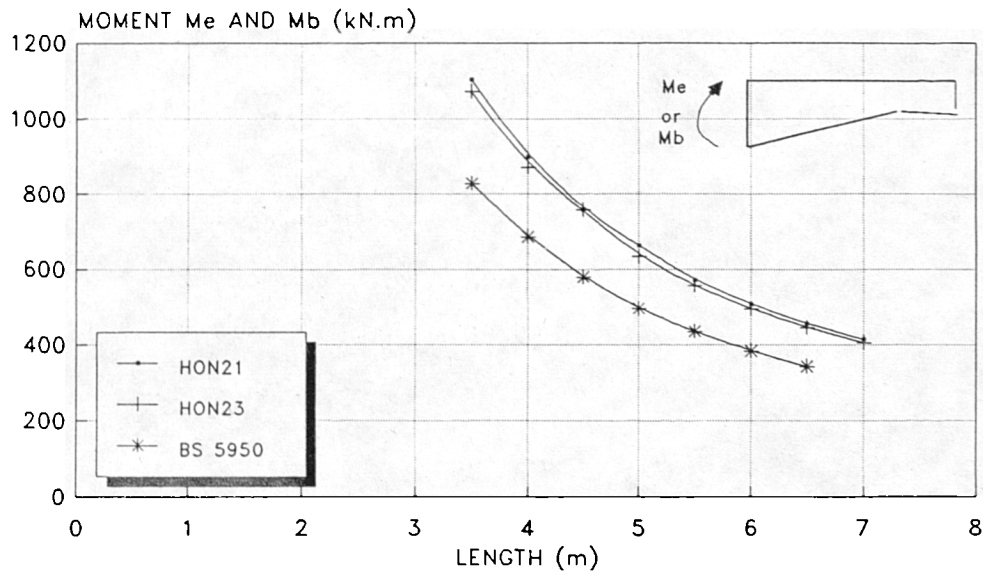


Figure 7.24B Results of Analysis of
Tapered Beam, Base Section 457x152xUB82
 $r = (D2/D1) = 2$

NOTE: HON25, HON26, HON28 & HON30 Have
Ratio of Tapered Length to Total Length
 $q = 0.6, 0.5, 0.4 \text{ \& } 0.3$ Respectively

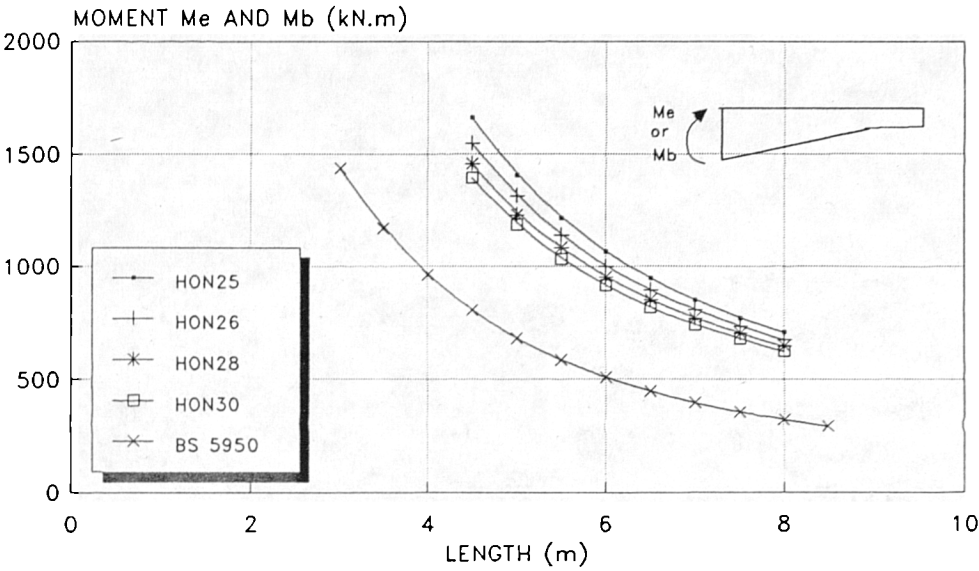


Figure 7.25A Results of Analysis of
Tapered Beam, Base Section 457x191xUB98
 $r = (D2/D1) = 3$

NOTE: HON27 And HON29 Have the Ratio of
Tapered Length to Total Length
 $q = 0.4 \text{ and } 0.3$ Respectively

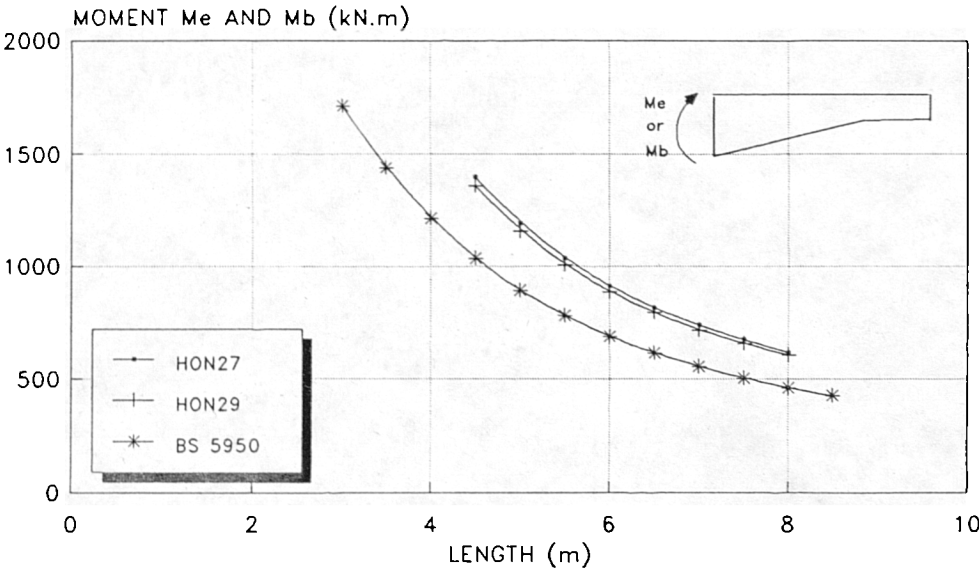


Figure 7.25B Results of Analysis of
Tapered Beam, Base Section 457x191xUB98
 $r = (D2/D1) = 2$

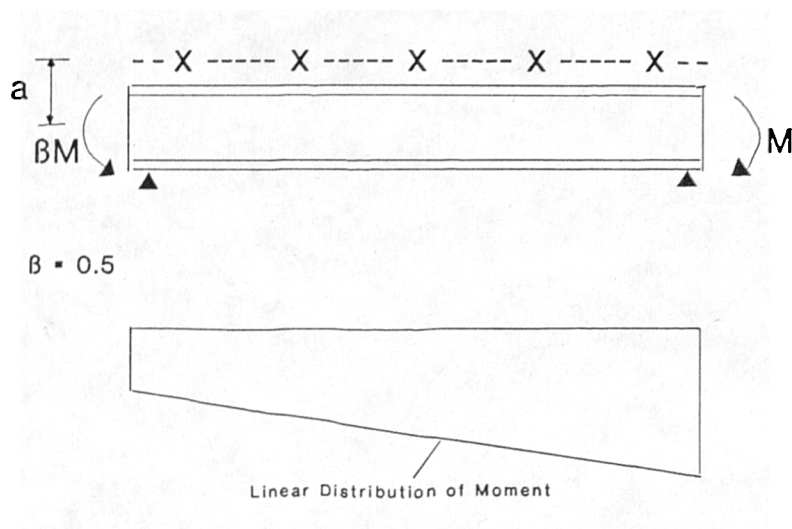


Figure 7.26 Beam With Tension Flange Restrained

THE RELATIONSHIP BETWEEN CRITICAL
LENGTH AND SECOND MOMENT OF AREA I_y
(COMPARISON OF APPENDIX G AND F.E.M)

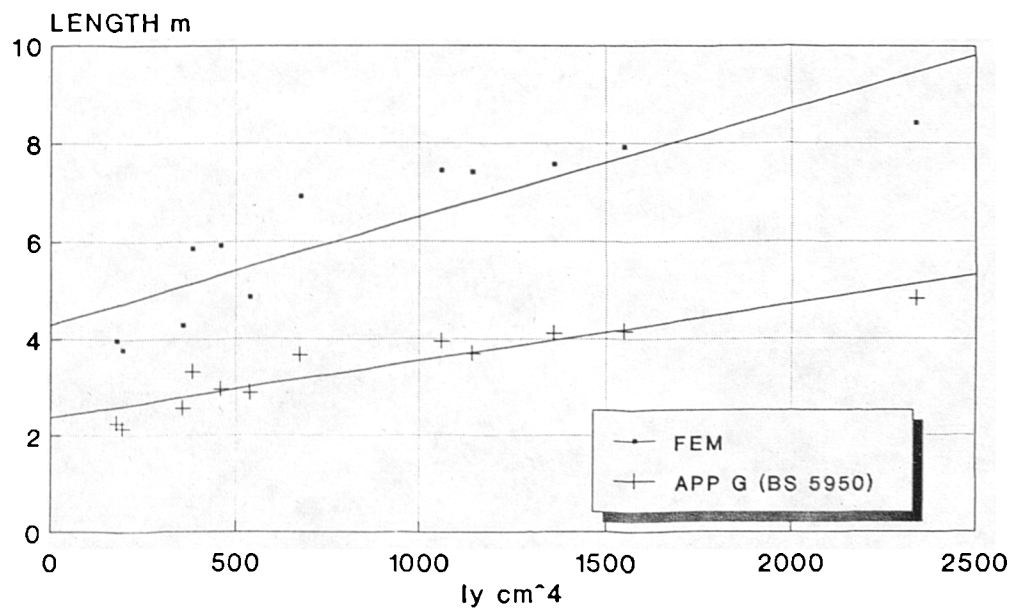


Figure 7.27 Results of Prismatic Member
with Moment Gradient ($\beta=0.5$)

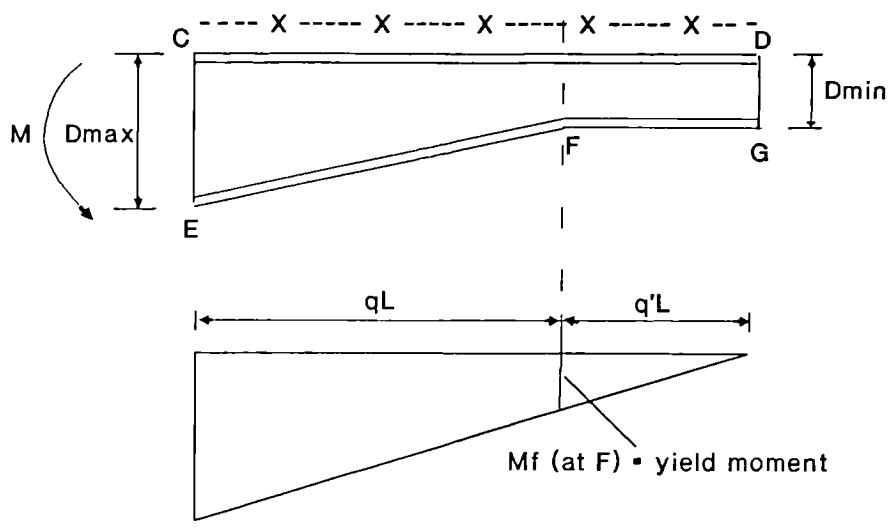


Figure 7.28 A Model of Haunch Beam
and the Bending Moment Diagram

NOTE: H1, H2, H3 And H6 Have the Ratio
of Tapered Length to Total Length
 $q = 0.6, 0.5, 0.4 \text{ \& } 0.3$ Respectively

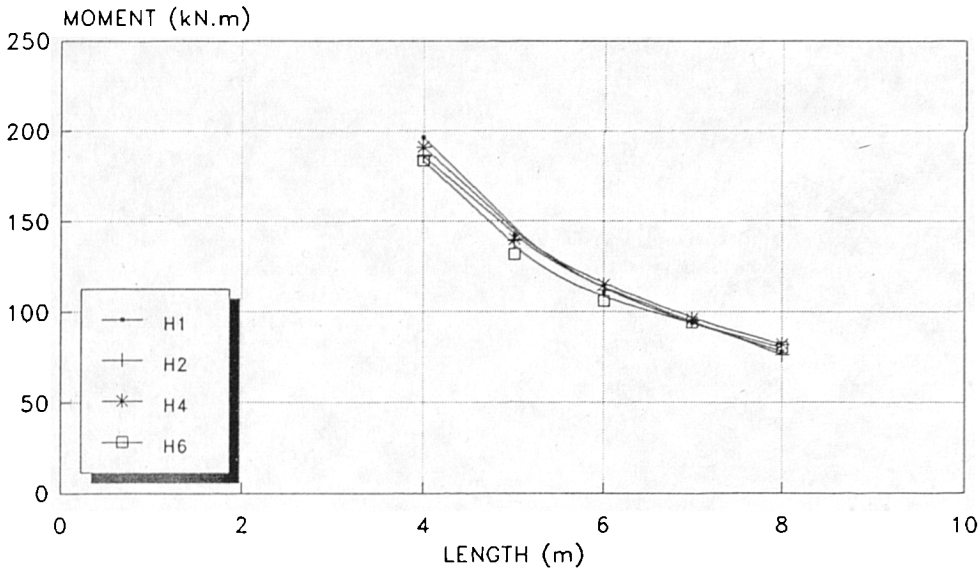


Figure 7.29A Results of Analysis of
Tapered Beam, (Top Flange Restrained)
Base Section 203x133xUB30, $r=(D2/D1)=3$

NOTE: H3 And H5 Have the Ratio of
Tapered Length to the Total Length
 $q = 0.4 \text{ and } 0.3$ Respectively

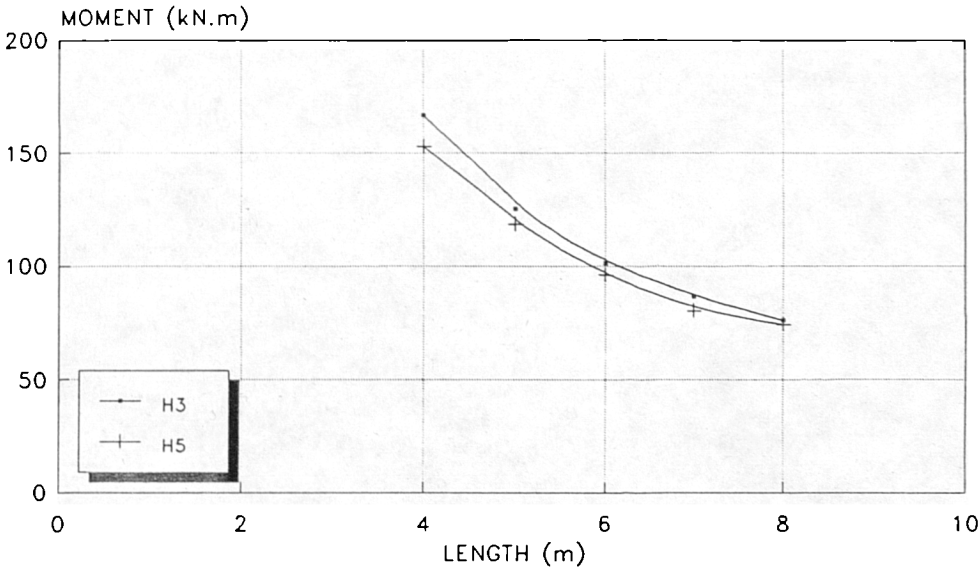


Figure 7.29B Results of Analysis of
Tapered Beam, (Top Flange Restrained)
Base Section 203x133xUB30, $r=(D2/D1)=2$.

NOTE: H7, H8, H10 & H12 Have the
Ratio of Tapered Length to Total Length
 $q = 0.6, 0.5, 0.4 \text{ \& } 0.3$ Respectively

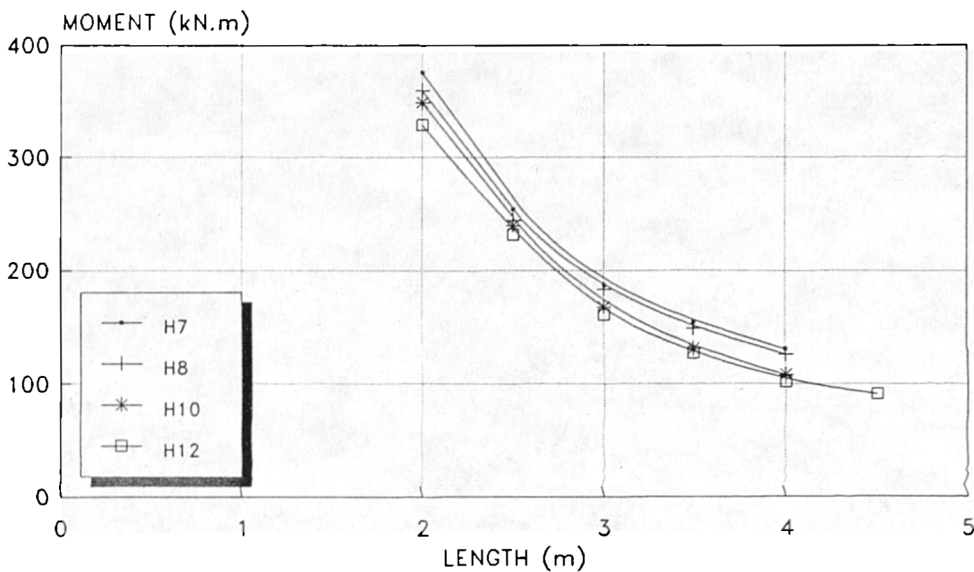


Figure 7.30A Results of Analysis of
Tapered Beam, (Top Flange Restrained)
Base Section 254x102xUB28, $r=(D2/D1)=3$

NOTE: H9 And H11 Have the Ratio of
Tapered Length to the Total Length
 $q = 0.4 \text{ \& } 0.3$ Respectively

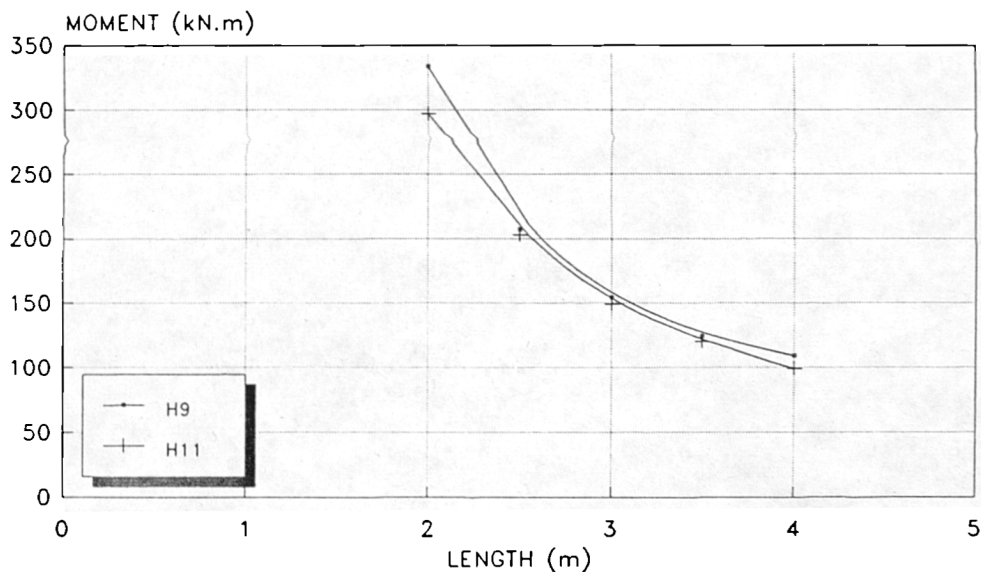


Figure 7.30B Results of Analysis of
Tapered Beam, (Top Flange Restrained)
Base Section 254x102xUB28, $r=(D2/D1)=2$

NOTE: H13, H14, H16 And H18 Have the
Ratio of Tapered Length to Total Length
 $q = 0.6, 0.5, 0.4$ and 0.3 Respectively

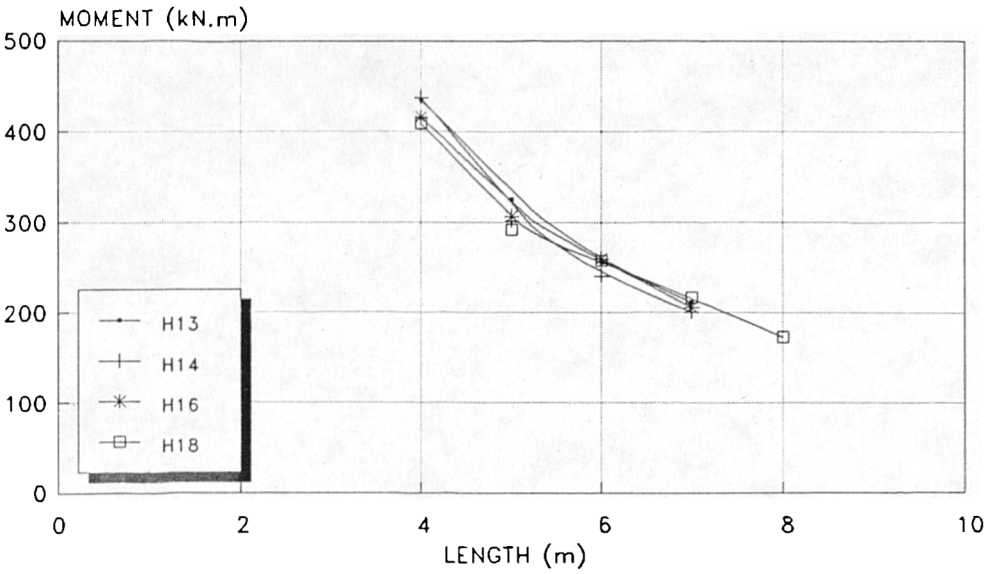


Figure 7.31A Results of Analysis of
Tapered Beam, (Top Flange Restrained)
Base Section 254x146xUB43, $r=(D2/D1)=3$

NOTE: H15 And H17 Have the Ratio of
Tapered Length to the Total Length
 $q = 0.4$ and 0.3 Respectively

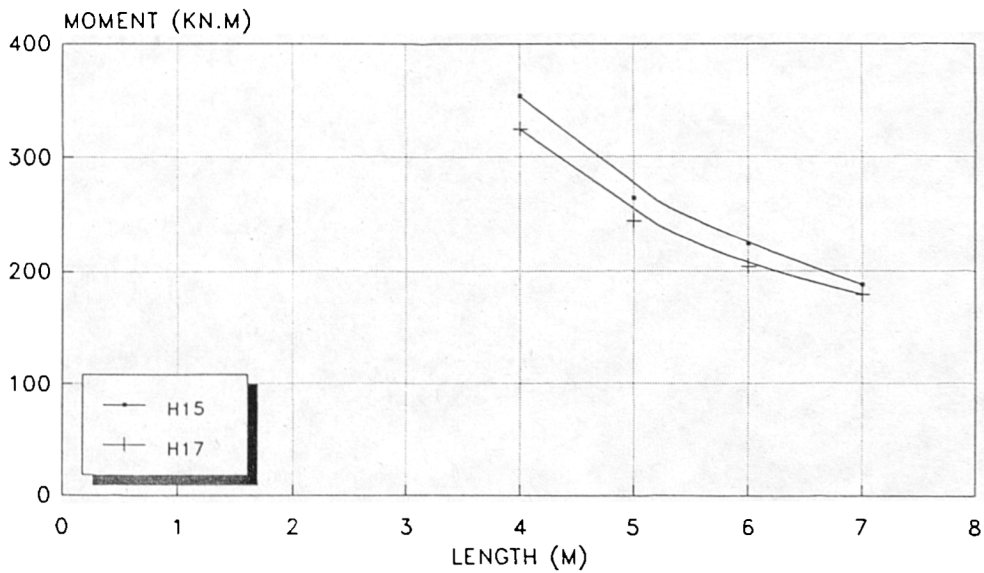


Figure 7.31B Results of Analysis of
Tapered Beam (Top Flange Restrained)
Base section 254x146xUB43, $r=(D2/D1)=2$

NOTE: H19, H20, H22 & H24 Have the
Ratio of Tapered Length to Total Length
 $q = 0.6, 0.5, 0.4$ and 0.3 Respectively

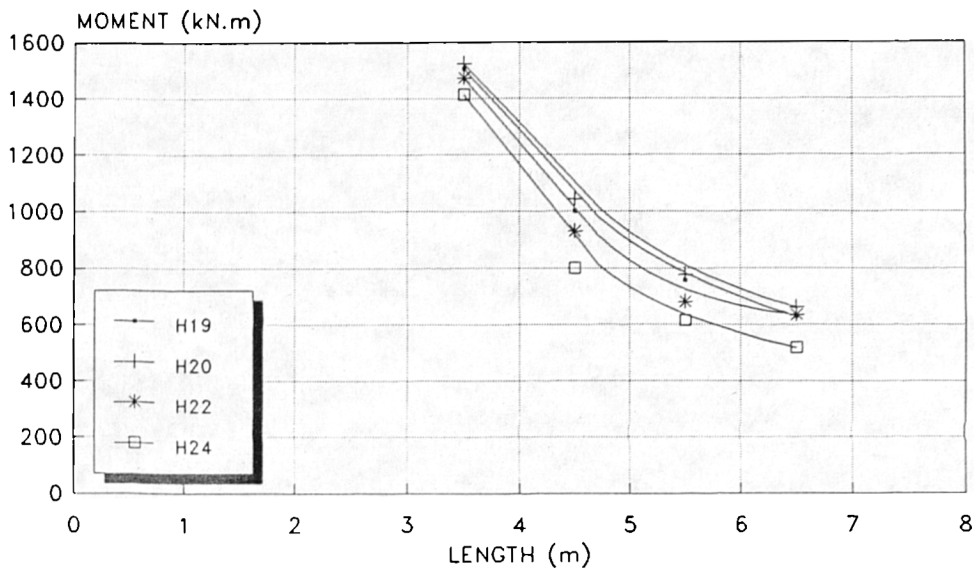


Figure 7.32A Results of Analysis of
Tapered Beam, (Top Flange Restrained)
Base Section 457x152xUB82, $r=(D2/D1)=3$

NOTE: H21 And H23 Have the Ratio of
Tapered Length to Total Length
 $q = 0.4$ and 0.3 Respectively

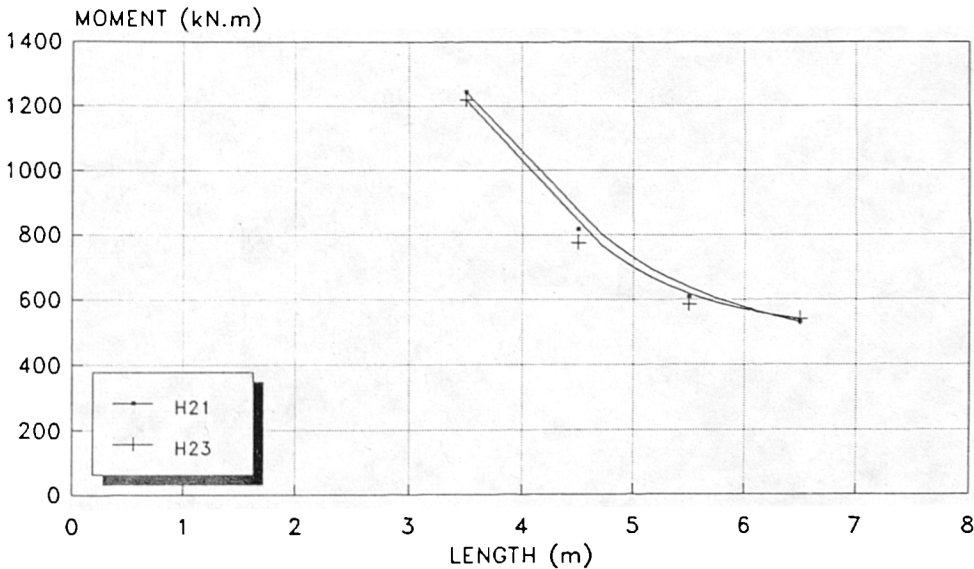


Figure 7.32B Results of Analysis of
Tapered Beam, (Top Flange Restrained)
Base Section 457x152xUB82, $r=(D2/D1)=2$

NOTE: H25, H26, H28 And H30 Have the Ratio of Tapered Length to Total Length $q = 0.6, 0.5, 0.4$ and 0.3 Respectively

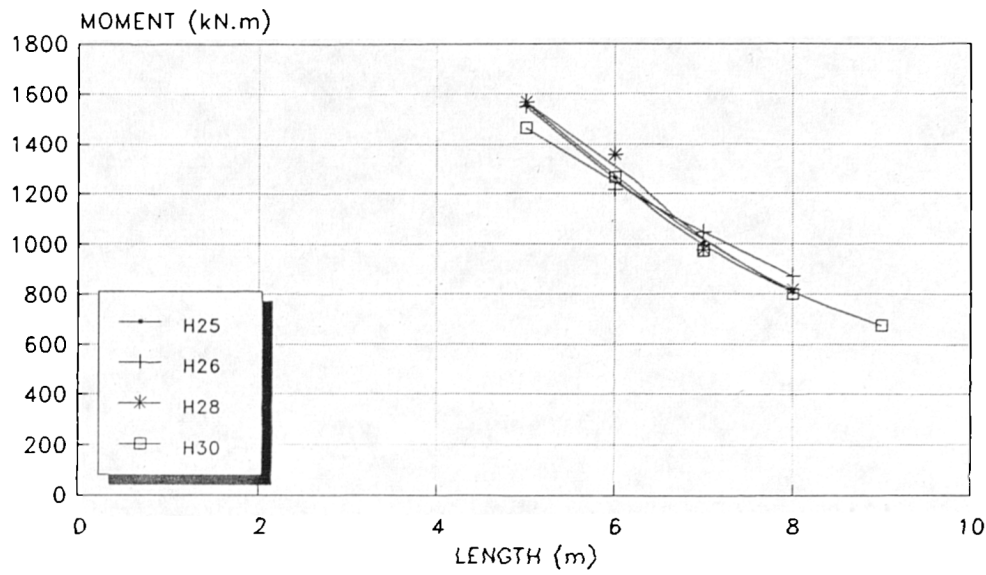


Figure 7.33A Results of Analysis of Tapered Beam (Top Flange Restrained)
Base Section 457x191xUB98, $r=(D2/D1)=3$

NOTE: H27 And H29 Have the Ratio of Tapered Length to the Total Length $q = 0.4$ and 0.3 Respectively

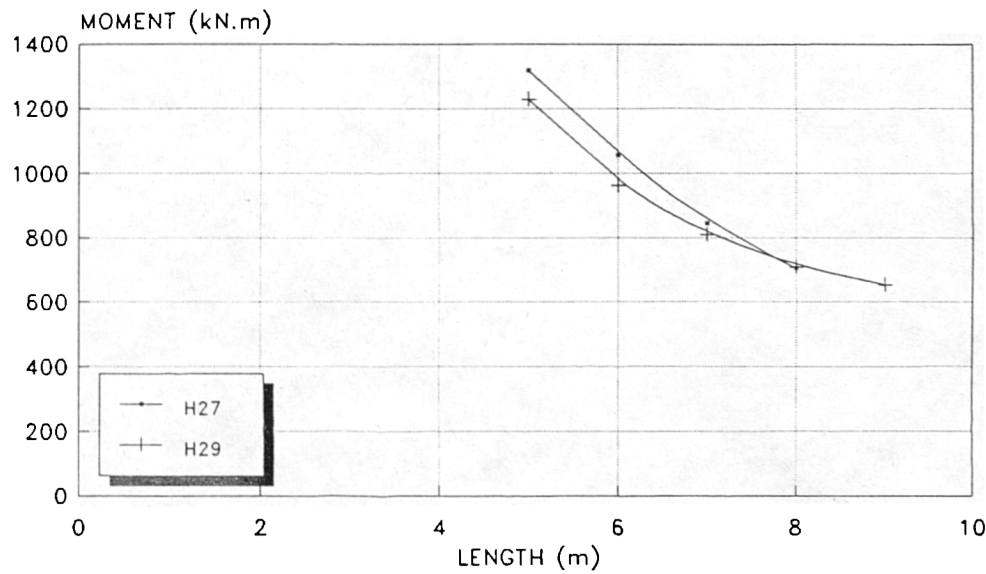


Figure 7.33B Results of Analysis of Tapered Beam, (Top Flange Restrained)
Base Section 457x191xUB98, $r=(D2/D1)=2$

Table 7.1 Properties of universal beams used in the assessment for the general clause in the design for elastic stability for prismatic member.

	UB1 203X133 XUB30	UB2 254X102 XUB28	UB3 305X102 XUB25	UB4 406X140 XUB46	UB5 457X191 UB98
D (mm)	206.8	260.4	304.8	402.3	467.4
b (mm)	133.8	102.1	101.6	142.4	192.8
tw (mm)	6.3	6.4	5.8	6.9	11.4
tf (mm)	9.6	10	6.8	11.2	19.6
A (cm ²)	38.1	36.2	31.4	59.0	125.3
r (mm)	7.6	7.6	7.6	10.2	10.2
I _x (cm ⁴)	2900	4008	4387	15647	45717
I _y (cm ⁴)	383.3	178	120	539	2343
Z _x (cm ³)	279	307.9	287.9	777.8	1956
Z _y (cm ³)	57.4	34.9	23.6	75.7	243
S _x (cm ³)	313	353.4	337.8	888.4	2232
S _y (cm ³)	88.05	54.84	37.98	118.3	378.3
r _{yy} (cm)	3.2	2.22	1.96	3.02	4.33
J	9.455	8.9	4.024	17.49	117.92
H	37260	27800	26390	206100	1174000
E (kN/cm ²)	20500	20500	20500	20500	20500
G	8000	8000	8000	8000	8000
D/tf	21.5	26	45	35.9	24

TABLE 7.2 GEOMETRY OF HAUNCHED MEMBER

	q	r	Dmax (mm)	Dmin (mm)	tf (mm)	tw (mm)	b (mm)	BASE SECT
HON1	0.6	3.0	620.4	206.8	9.6	6.3	133.8	203
HON2	0.5	3.0	620.4	206.8	9.6	6.3	133.8	X
HON3	0.4	2.0	413.6	206.8	9.6	6.3	133.8	133
HON4	0.4	3.0	620.4	206.8	9.6	6.3	133.8	X
HON5	0.3	2.0	413.6	206.8	9.6	6.3	133.8	UB30
HON6	0.3	3.0	620.4	206.8	9.6	6.3	133.8	
HON7	0.6	3.0	781.2	260.4	10.0	6.4	102.1	254
HON8	0.5	3.0	781.2	260.4	10.0	6.4	102.1	X
HON9	0.4	2.0	520.8	260.4	10.0	6.4	102.1	102
HON10	0.4	3.0	781.2	260.4	10.0	6.4	102.1	X
HON11	0.3	2.0	520.8	260.4	10.0	6.4	102.1	UB28
HON12	0.3	3.0	781.2	260.4	10.0	6.4	102.1	
HON13	0.6	3.0	778.8	259.6	12.7	7.3	147.3	254
HON14	0.5	3.0	778.8	259.6	12.7	7.3	147.3	X
HON15	0.4	2.0	519.2	259.6	12.7	7.3	147.3	146
HON16	0.4	3.0	778.8	259.6	12.7	7.3	147.3	X
HON17	0.3	2.0	519.2	259.6	12.7	7.3	147.3	UB43
HON18	0.3	3.0	778.8	259.6	12.7	7.3	147.3	
HON19	0.6	3.0	1395.3	465.1	18.9	10.7	153.5	457
HON20	0.5	3.0	1395.3	465.1	18.9	10.7	153.5	X
HON21	0.4	2.0	930.2	465.1	18.9	10.7	153.5	152
HON22	0.4	3.0	1395.3	465.1	18.9	10.7	153.5	X
HON23	0.3	2.0	930.2	465.1	18.9	10.7	153.5	UB82
HON24	0.3	3.0	1395.3	465.1	18.9	10.7	153.5	
HON25	0.6	3.0	1402.2	467.4	19.6	11.4	192.8	457
HON26	0.5	3.0	1402.2	467.4	19.6	11.4	192.8	X
HON27	0.4	2.0	934.8	467.4	19.6	11.4	192.8	191
HON28	0.4	3.0	1402.2	467.4	19.6	11.4	192.8	X
HON29	0.3	2.0	934.8	467.4	19.6	11.4	192.8	UB98
HON30	0.3	3.0	1402.2	467.4	19.6	11.4	192.8	

TABLE 7.3 RESULTS OF ANALYSIS FOR LATERAL STABILITY OF HAUNCHED MEMBER

	q	r	YIELD MOMENT AT F (kNm)	BUCKLING MOMENT MB (kNm)	BS5950 CRIT LENGTH L (m)	F.E.M CRIT LENGTH L (m)	% ERROR
HON1	0.6	3.0	77	192	2.27	3.85	40%
HON2	0.5	3.0	77	153.6	2.7	4.3	37%
HON3	0.4	2.0	77	128	3.6	4.55	20.8%
HON4	0.4	3.0	77	128	3.05	4.82	36%
HON5	0.3	2.0	77	110	3.97	4.91	19%
HON6	0.3	3.0	77	110	3.29	5.08	35%
HON7	0.6	3.0	85	212	1.67	2.72	38%
HON8	0.5	3.0	85	169.3	1.94	2.92	34%
HON9	0.4	2.0	85	141.1	2.61	3.14	17%
HON10	0.4	3.0	85	141.1	2.2	3.3	33%
HON11	0.3	2.0	85	121	2.93	3.45	16%
HON12	0.3	3.0	85	121	2.47	3.53	30%
HON13	0.6	3.0	139	347.5	2.51	4.24	40%
HON14	0.5	3.0	139	278	2.97	4.80	38%
HON15	0.4	2.0	139	231.6	3.93	5.08	23%
HON16	0.4	3.0	139	231.6	3.38	5.3	36%
HON17	0.3	2.0	139	198.6	4.58	5.73	20%
HON18	0.3	3.0	139	198.6	3.79	5.87	35%
HON19	0.6	3.0	428	1070	2.6	4.17	37%
HON20	0.5	3.0	428	856	3.03	4.57	34%
HON21	0.4	2.0	428	714	3.9	4.73	17%
HON22	0.4	3.0	428	714	3.27	4.86	33%
HON23	0.3	2.0	428	612	4.36	5.18	16%
HON24	0.3	3.0	428	612	3.64	5.3	31%
HON25	0.6	3.0	538	1345	3.16	5.2	39%
HON26	0.5	3.0	538	1076	3.82	5.84	34%
HON27	0.4	2.0	538	897	5.0	6.13	18%
HON28	0.4	3.0	538	897	4.18	6.18	32%
HON29	0.3	2.0	538	769	5.4	6.4	16%
HON30	0.3	3.0	538	769	4.7	6.8	31%

NOTE: THE YIELD STRESS USED IN THE ABOVE CALCULATIONS IS
 $P_y = 27.5 \text{ kN/cm}^2$.

TABLE 7.4 DATA FOR PRISMATIC MEMBERS USED IN THE CALCULATION
FOR APPENDIX G

	UMB-1 203X133 XUB30	UMB-2 254X102 XUB28	UMB-3 254X146 XUB43	UMB-4 305X102 XUB33	UMB-5 305X127 XUB48	UMB-6 305X 165X UB54
D cm	20.68	26.04	25.96	31.27	31.04	31.09
a cm	18	19	19	19	19	19
A cm ²	38.1	36.4	55.4	42	61.4	68.6
tf cm	0.96	1.0	1.27	1.08	1.4	1.37
b cm	13.38	10.21	14.73	10.24	12.52	16.68
tw cm	0.63	0.64	0.73	0.66	0.89	0.77
Iy cm ⁴	383.3	177.4	676.5	193.3	457.9	1059.6
Ix cm ⁴	2900.1	4038.2	6617.5	6553.3	9630.7	11777
hw cm	18.76	24.04	23.42	29.11	28.24	28.85
hs cm	19.72	25.04	24.69	30.19	29.64	30.22
py kN/cm ²	25	25	25	25	25	25
E kN/cm ²	21000	21000	21000	21000	21000	21000
Sx1 cm ³	314.5	356	573.1	484.3	715	849.2
ry cm	3.2	2.2	3.5	2.1	2.73	3.93
Ma kNcm	6982	7697	12632	10375	15310	18832
β	0.5	0.5	0.5	0.5	0.5	0.5
Zx cm ³	279.3	307.9	505.3	415	612.4	753.3

Ma Yield moment

TABLE 7.4 DATA FOR PRISMATIC MEMBERS USED IN THE CALCULATION
FOR APPENDIX G
(CONTINUE)

	UMB-7 356X127 XUB39	UMB-8 356X171 XUB67	UMB-9 406X140 XUB46	UMB10 406X178 XUB74	UMB11 457X152 XUB82	UMB12 457X 191X UB98
D cm	35.28	36.4	40.23	41.28	46.51	46.74
a cm	18	19	19	19	19	19
A cm ²	49.2	86.1	58.9	96	105.8	126.6
tf cm	1.07	1.57	1.12	1.60	1.89	1.96
b cm	12.64	17.32	14.24	17.97	15.35	19.28
tw cm	0.65	0.91	0.69	0.97	1.07	1.14
Iy cm ⁴	356.7	1359.5	539	1547.4	1139.3	2341.1
Ix cm ⁴	10057.8	19698.2	15637.4	27685.2	36801.3	46418.
hw cm	33.14	33.26	37.99	38.08	42.73	42.82
hs cm	34.21	34.83	39.11	39.68	44.62	44.78
py kN/cm ²	25	25	25	25	25	25
E kN/cm ²	21000	21000	21000	21000	21000	21000
Sx1 cm ³	651.4	1223.1	887.6	1552.7	1827.1	2263.7
ry cm	2.69	4.0	3.0	4.0	3.3	4.30
Ma kNcm	14295	26825	19445	33100	38925	48900
B	0.5	0.5	0.5	0.5	0.5	0.5
Zx cm ³	571.8	1073	777.8	1324	1557	1956

Ma Yield moment

TABLE 7.5 RESULTS OF ANALYSIS OF PRISMATIC MEMBER
BY APPENDIX G AND FINITE ELEMENT METHOD

(1) BEAM	(2) TOR INDX D/tf	(3) PLAST. STABIL APG8 Lt (cm)	(4) PLAST. STABIL MCAD Lt (cm)	(5) ELAST. STABIL APG8 L (cm)	(6) ELAST. STABIL MCAD L (cm)	(7) FINITE ELEMEN METHOD L (cm)
UMB-1	21.54	339 (42%)	341.5 (42%)	332.5 (43%)	332.5 (43%)	585
UMB-2	26.04	211.7 (46%)	216.6 (45%)	225.2 (43%)	223 (43%)	396
UMB-3	20.4	379.7 (45%)	379.8 (45%)	367.2 (47%)	367.2 (47%)	690
UMB-4	28.95	205.6 (45%)	201.2 (46%)	215.5 (43%)	211.0 (44%)	377
UMB-5	22.17	283 (52%)	282.4 (52%)	296.2 (50%)	293.5 (50%)	591
UMB-6	22.69	406.5 (45%)	408 (45%)	395 (47%)	395 (47%)	743
UMB-7	32.97	253.5 (41%)	253.2 (41%)	256.5 (40%)	256.5 (40%)	428
UMB-8	23.18	406.4 (46%)	408.5 (46%)	411.5 (46%)	405 (46%)	756
UMB-9	35.92	281.9 (42%)	279.4 (42%)	288.5 (41%)	283.7 (41%)	485
UMB10	25.8	397 (50%)	395.1 (50%)	416.5 (47%)	405 (48%)	790
UMB11	24.60	325.6 (58%)	326.5 (58%)	369.5 (52%)	344.5 (55%)	776
UMB12	23.84	433.6 (48%)	433.1 (48%)	482.5 (43%)	441.5 (47%)	840

TABLE 7.6 RESULTS OF ANALYSIS OF HAUNCHED MEMBER BY THE METHOD OF APPENDIX G. (ELASTIC STABILITY)

	q	r	Dmax	Dmin	BS 5950 APP-G (cm)	FINITE ELEM. METHOD (cm)	FINITE DIFF. METHOD (cm)
H1	0.6	3.0	620.4	206.8	148.5	447.0	450.0
H2	0.5	3.0	620.4	206.8	141.5	507.0	520.0
H3	0.4	2.0	413.6	206.8	149.5	545.0	529.0
H4	0.4	3.0	620.4	206.8	155.0	595.0	588.0
H5	0.3	2.0	413.6	206.8	159.0	588.0	593.0
H6	0.3	3.0	620.4	206.8	158.0	648.0	648.0
H7	0.6	3.0	781.2	260.4	113.5	308.0	316.0
H8	0.5	3.0	781.2	260.4	111.0	340.0	359.0
H9	0.4	2.0	520.8	260.4	112.0	347.0	356.0
H10	0.4	3.0	781.2	260.4	120.0	358.0	396.0
H11	0.3	2.0	520.8	260.4	118.0	378.0	389.0
H12	0.3	3.0	781.2	260.4	121.5	382.0	423.0
H13	0.6	3.0	778.8	259.5	160.5	520.0	500.0
H14	0.5	3.0	778.8	259.6	157.5	582.0	580.0
H15	0.4	2.0	519.2	259.6	166.0	625.0	594.0
H16	0.4	3.0	778.8	259.6	173.0	678.0	659.0
H17	0.3	2.0	519.2	259.6	175.5	692.0	672.0
H18	0.3	3.0	778.8	259.6	175.0	770.0	733.0
H19	0.6	3.0	1395.3	465.1	170.5	475.0	476.0
H20	0.5	3.0	1395.3	465.1	167.5	551.0	542.0
H21	0.4	2.0	930.2	465.1	171.0	540.0	539.0
H22	0.4	3.0	1395.3	465.1	180.5	603.0	600.0
H23	0.3	2.0	930.2	465.1	180.0	600.0	591.0
H24	0.3	3.0	1395.3	465.1	183.0	630.0	643.0
H25	0.6	3.0	1402.2	467.4	215.0	618.0	613.0
H26	0.5	3.0	1402.2	467.4	211.0	730.0	700.0
H27	0.4	2.0	934.8	467.4	218.0	725.0	699.0
H28	0.4	3.0	1402.2	467.4	228.0	785.0	777.0
H29	0.3	2.0	934.8	467.4	230.0	810.0	769.0
H30	0.3	3.0	1402.2	467.4	232.0	865.0	838.0

TABLE 7.7 RESULTS OF ANALYSIS OF HAUNCHED MEMBER BY THE METHOD
OF CLAUSE 5.5.3.5 OF BS5950 (ELASTIC STABILITY)

	q	r	K1	X	ry	CLAUSE 5.5.3.5 Lt (cm)	BS 5950 APP-G (cm)	FINITE ELEM. METHOD (cm)
H1	0.6	3	445	22.35	3.2	197.5	148.5	447.0
H2	0.5	3	445	22.35	3.2	197.5	141.5	507.0
H3	0.4	2	495	22.35	3.2	219.7	149.5	545.0
H4	0.4	3	445	22.35	3.2	197.5	155.0	595.0
H5	0.3	2	495	22.35	3.2	219.7	159.0	588.0
H6	0.3	3	445	22.35	3.2	197.5	158.0	648.0
H7	0.6	3	445	28.5	2.2	126.7	113.5	308.0
H8	0.5	3	445	28.5	2.2	126.7	111.0	340.0
H9	0.4	2	495	28.5	2.2	140.9	112.0	347.0
H10	0.4	3	445	28.5	2.2	126.7	120.0	358.0
H11	0.3	2	495	28.5	2.2	140.9	118.0	378.0
H12	0.3	3	445	28.5	2.2	126.7	121.5	393.0
H13	0.6	3	445	21.55	3.5	219.2	160.5	520.0
H14	0.5	3	445	21.55	3.5	219.2	157.5	582.0
H15	0.4	2	495	21.55	3.5	243.8	166.0	625.0
H16	0.4	3	445	21.55	3.5	219.2	173.0	678.0
H17	0.3	2	495	21.55	3.5	243.8	175.5	692.0
H18	0.3	3	445	21.55	3.5	219.2	175.0	740.0
H19	0.6	3	445	27.80	3.3	191.1	170.5	475.0
H20	0.5	3	445	27.80	3.3	191.1	167.5	551.0
H21	0.4	2	495	27.80	3.3	212.6	171.0	540.0
H22	0.4	3	445	27.80	3.3	191.1	180.5	603.0
H23	0.3	2	495	27.80	3.3	212.6	180.0	600.0
H24	0.3	3	445	27.80	3.3	191.1	183.0	630.0
H25	0.6	3	445	26.15	4.3	252.6	215.0	618.0
H26	0.5	3	445	26.15	4.3	252.6	211.0	730.0
H27	0.4	2	495	26.15	4.3	281.0	218.0	725.0
H28	0.4	3	445	26.15	4.3	252.6	228.0	785.0
H29	0.3	2	495	26.15	4.3	281.0	230.0	810.0
H30	0.3	3	445	26.15	4.3	252.6	232.0	865.0

TABLE 7.8 RESULTS OF ANALYSIS FOR PLASTIC STABILITY FOR HAUNCHED MEMBERS TO APPENDIX G:BS5950 PART 1.

	q	r	nt	c	Lk (cm)	APP G PLAST STAB. Lt (cm)	F.E.M (cm)
H1	0.6	3.0	0.825	1.281	285	269	447
H2	0.5	3.0	0.811	1.256	285	279	507
H3	0.4	2.0	0.774	1.145	285	321	545
H4	0.4	3.0	0.756	1.229	285	306	595
H5	0.3	2.0	0.759	1.125	285	333	588
H6	0.3	3.0	0.737	1.199	285	322	648
H7	0.6	3.0	0.818	1.192	184	189	308
H8	0.5	3.0	0.798	1.175	184	196	340
H9	0.4	2.0	0.764	1.099	184	219	347
H10	0.4	3.0	0.744	1.157	184	214	358
H11	0.3	2.0	0.749	1.085	184	226	378
H12	0.3	3.0	0.725	1.136	184	223	393
H13	0.6	3.0	0.824	1.298	318	297	520
H14	0.5	3.0	0.81	1.272	318	309	582
H15	0.4	2.0	0.774	1.154	318	357	625
H16	0.4	3.0	0.755	1.244	318	339	678
H17	0.3	2.0	0.758	1.133	318	371	692
H18	0.3	3.0	0.736	1.211	318	357	740
H19	0.6	3.0	0.815	1.20	275	281	475
H20	0.5	3.0	0.795	1.182	275	293	551
H21	0.4	2.0	0.761	1.103	275	328	540
H22	0.4	3.0	0.741	1.163	275	319	603
H23	0.3	2.0	0.747	1.089	275	339	600
H24	0.3	3.0	0.723	1.141	275	334	630
H25	0.6	3.0	0.82	1.218	364	365	618
H26	0.5	3.0	0.802	1.199	364	379	730
H27	0.4	2.0	0.767	1.112	364	427	725
H28	0.4	3.0	0.748	1.178	364	414	785
H29	0.3	2.0	0.752	1.097	364	441	810
H30	0.3	3.0	0.729	1.154	364	433	865

CHAPTER 8

8.0 Amendments to Appendix G and Clause 5.5.3.5 BS 5950: Part 1.

8.1 Introduction

In the previous chapter it has been shown that the general provisions of BS 5950 for the lateral torsional buckling of both prismatic and non-uniform members were satisfactory and within acceptable practical limits. However, Appendix G, which is for the design of members, or portions of members between effective torsional restraints, provided with intermediate restraints in the tension flange but leaving the compression flange unrestrained are shown to be over-safe. For that reason a more detailed study of the clauses of Appendix G and clause 5.5.3.5. was conducted in order to investigate the deficiencies in those clauses and how to improve them.

In this chapter some possible amendments to the clauses in Appendix G and clause 5.5.3.5. are investigated and analysed in the light of the prismatic and non-uniform members already discussed in chapter 7. Results given by these amended or modified expressions of Appendix G and clause 5.5.3.5. are compared with those of Appendix G and the Finite Element method. Analyses were also made based on the results of the full-scale test on Frame 3 to further check

the validity of these amended expressions. Based on these analyses some recommendations are proposed.

8.2 Elastic and Plastic Stability of Prismatic Members

8.2.1 General

The analysis according to Appendix G of twelve prismatic members with properties as shown in table 7.4. was given in chapter 7. The results for beams with and without plastic hinges loaded with moment gradient $\beta=0.5$ as shown in table 7.5, indicated that there was little difference in the results. When compared with the results of the Finite Element Method, it was shown that the clauses in Appendix G for elastic and plastic stability are safe. The results produced indicated an error in the critical buckling length of 40% to 50%. In this section a study is conducted to look into the possibility of amending the clause so that this percentage error is reduced while ensuring that the beam remains safe.

8.2.2 Amendment to Appendix G for Elastic Stability of Prismatic Member

In dealing with the lateral-torsional buckling of unrestrained members, BS 5950 gives consideration to the

effective length of the member concerned and this is given in clauses 4.3.5. and 4.3.6. The effective length is dependent upon the conditions at the support and the loading conditions. In simply supported beams with a normal loading condition and various conditions at the supports, the effective length varies from $0.7L$ to $1.2(L+2D)$ in which L is the length of the beam between restraints and D is the depth of the beam. For the same beam with a destabilising load condition the effective length ranges from $0.85L$ to $1.4(L+2D)$.

Based on the results of Finite Element analysis, it has been shown that restraining the tension flange will contribute an improvement to the lateral stability of the beam. This is because lateral buckling involves two deformation components, lateral deflection and twist and restraints against either action may be used to increase a beam's stability.

In the design of prismatic beams with restraints on the tension flange, Appendix G considers the effect of the restraints by modifying the slenderness of the beam using equation 8.1.

$$\lambda_{TB} = n_t u v_t c \lambda \dots\dots\dots (8.1)$$

in which;

u is a buckling parameter and conservatively taken as 0.9.

c is equal to 1 for prismatic members

v_t is a slenderness factor given in clause G.3.3.

In the expression for v_t the restraining effect of the tension flange is considered. The limiting condition for elastic stability in a prismatic member given in Appendix G is;

$$\frac{F}{P_C} + \frac{M}{M_b} < 1 \dots \dots \dots (8.2)$$

M is equal to the actual moment M_A acting on the beam multiplied by the equivalent uniform member factor, m_t . The manner in which m_t is obtained is given in clause G.3.4. It is a factor that is dependent on the loading condition and the slenderness factor Y . Table 39 of BS 5950 contains the values of m_t with reference to the slenderness factor Y and load ratio β .

M_b , the buckling moment is calculated from the product of plastic modulus S_x and the buckling stress p_b . p_b is obtained from table 11 of BS 5950 when λ_{TB} has been calculated from equation 8.1. Results of the analysis of prismatic members by Appendix G are shown in table 7.5, which indicate a 40 - 50% error when compared to the results obtained from the Finite Element method.

The above discussion shows that to increase the critical length of the beam, while maintaining the ratio of M and M_b in expression 8.2 equal to 1, is to modify λ_{TB} of equation

8.1. This is because the value of M_b depends on p_b that in turn depends on λ_{TB} . Looking into the detailed derivation of λ_{TB} it is found that most of the relevant factors have been considered except the factor for the full end restraint.

Therefore it is proposed in this section to include a new factor k_l , to be called the "effective length with full restraint" (ELR) factor in the calculation for slenderness λ , in the form;

$$\lambda = k_l \cdot \frac{L}{r_y} \dots \dots \dots (8.3)$$

The introduction of the ELR factor into λ is to consider the full restraints provided at the end supports. This new value of λ (with the ELR factor) is used in all the calculations to find other factors such as v_t and m_t . In this study the values of $k_l=0.9, 0.8, 0.7$ and 0.6 were used in the calculations. The calculations then followed exactly the procedure laid down in Appendix G.

A detailed example of calculation for this case with zero axial load is shown in Appendix 4. The analysis shows that, by adopting this procedure, the value of λ_{TB} achieved has a similar value to Appendix G (see Appendix 3.6.) and that the buckling stress p_b still has the same value and yet an increased buckling length is achieved.

Results of analysis by this method for the ELR value of

$k_l=0.9, 0.8, 0.7$ and 0.6 for the prismatic beams shown in table 7.4 are shown in table 8.1. This shows that by adopting $k_l=0.9, 0.8, 0.7$ and 0.6 , the error has been reduced to (38-47%), (28-36%), (19-32%) and (7-21%) respectively. Figure 8.1 shows the relationship between critical length and the second moment of area I_y , for all the beams under consideration. It shows that results of analysis by Appendix G formed the lower bound and the F.E.M. is the upper bound limit. It is therefore proposed that the ELR factor to be used in the calculation is $k_l=0.8$ which gives results consistent with reasonable safety.

8.2.3 Amendment to Appendix G for the Case of the Plastic Stability of a Prismatic Member

The condition for the plastic stability of a prismatic member without lateral loads is given in Appendix G of BS 5950 by the expression,

$$L_t \leq \frac{L_k}{\sqrt{m_t}} \left(\frac{M_p}{M_{pr} + aF} \right)^{1/2} \dots\dots\dots (8.4)$$

where L_k is the limiting length, M_p is the plastic moment, M_{pr} is the reduced plastic moment in the presence of axial load, F is the axial load, a is the distance between the shear centre of the beam and the axis of restraint and m_t is the equivalent uniform moment factor. In the absence of axial load the value of L_t is dependent on L_k and m_t .

The value of m_t is calculated in the same manner as in the analysis for elastic stability. The value of the limiting length L_k is given by clause G.3.5. as,

$$L_k = \frac{(5.4 + 600 \frac{Py}{E}) r_y x}{(5.4 \frac{Py}{E} x^2 - 1)^{1/2}} \dots \dots \dots (8.5)$$

The results of analysis for plastic stability of the beams under consideration are shown in table 7.5. In this section, the ELR factor discussed earlier was introduced into λ , the slenderness of the beam, and the rest of the calculations follow the method as given by Appendix G. The prismatic beams shown in table 7.4 are analysed by this method.

The results of analysis for plastic stability by the introduction of the ELR factor are shown in table 8.2. The analysis according to Appendix G gave a buckling length with errors between 41 - 52%. Table 8.2 shows that there is no effect on the critical length for plastic stability by the introduction of ELR factors of 0.9, 0.8, 0.7 and 0.6 to the slenderness of the beam. This is because L_t is dependent on the value of L_k and m_t and the ELR factors introduced do not affect the L_k and m_t values. A sample of this calculation is shown in Appendix 4.

It is now clear that the value of L_t can only be increased by introducing another factor into the expression for L_k . However the empirical expression for L_k in equation 8.5. was

developed by Horne (42) based on analysis of both the plastic mechanism and elastic response curve for a restrained I-shaped member. Horne's work showed that the ratio of the limiting slenderness L_m/r_y to the elastic critical slenderness L_{cr}/r_y was found to vary between 0.63 and 0.71. In his treatment of the corresponding problems for unrestrained beams, he proposed a ratio of 0.6 between the limiting slenderness and the elastic critical slenderness given by ignoring the warping rigidity, so resulting in the effective ratio less than 0.6. The higher ratio obtained for restrained beams occurred because of the relative importance for this case of St. Venant torsion as compared with warping torsional resistance.

The basic approach adopted by the author is to reduce the error in the results of analysis by Appendix G from 41-52% to about 30-40%. To do this a factor must be included in the expression for L_k . Since the expression for L_k is based on the limiting slenderness equation, the most appropriate form of amendment is to include the ELR factor in the expression for L_k as follows ;

$$L_k = \frac{(5.4 + 600 \frac{Py}{E}) r_y x}{k_l \sqrt{5.4 (\frac{Py}{E}) x^2 - 1}} \dots\dots\dots (8.6)$$

Analyses were conducted for values of L_k with ELR factors $k_l = 0.9, 0.8, 0.7$ and 0.6 and the values L_k were calculated using equation 8.4. The results of this analysis are shown

in table 8.3. The results show that there is an increase in the critical length with decreasing values of k_1 . By using values of $k_1=0.9, 0.8, 0.7$ and 0.6 , the error or the safety reserve compared to F.E.M. is in the region of 35-45%, 30-38%, 18-29% and 5-20% respectively. It therefore can be safely said if a recommendation were to be made for an amendment to the plastic stability clause, then the most appropriate thing to do, is to include an ELR factor of 0.9 in the calculation of the limiting length. Otherwise the clause should be maintained as it is.

8.3 Elastic and Plastic Stability of Non-uniform Members

8.3.1 General

The way in which Appendix G deals with haunched members is to define the buckling stress at all sections such that all the stresses (combined stresses in the presence of an axial load) due to the applied load must not exceed the value of the buckling stress at each section. This necessary condition is given by clause G.2.a (2) in Appendix G as;

$$\frac{F}{A} + \frac{M}{S_x} \leq P_b \dots \dots \dots (8.7)$$

The results of analyses conducted previously for haunched members are shown in table 7.6. The details of the calculation for the example of beam case H1 are given in

Appendix 3.7. The results show that, by comparison with results of analysis by the Finite Element method and Finite Difference method described in chapter 6, analysis using Appendix G gives an oversafe design.

In the calculation of the critical length of a haunched beam, the loading conditions considered were represented by considering the moment to be varying uniformly from zero at the point of contraflexure. A common design situation is one in which the yield moment M_y of the base section is just reached at the junction of the uniform and tapered parts. Based on this situation the moment at the larger end of the haunched beam was calculated. The results in table 7.5. were obtained after a series of lengths were tried.

The calculation in Appendix 3.7. was done for beams which were divided into 29 sections. The section at the point of intersection of the tapered and the uniform part was always the most critical. Since the values of the maximum applied moments on the beam were fixed, it follows that the stress due to the applied load (M/S_x) will remain the same irrespective of the length being either increased or decreased. The behaviour of the buckling stress p_b during the analysis however, showed that it will increase if the beam length is decreased and decrease when the beam length is increased. Therefore the critical length for each beam was obtained when the most critical section reached almost the same stresses (i.e, $p_b = M/S_x$).

Observations of the results of computer analysis compared with those given by Appendix G shows that the reason it gave an "oversafe" design was due to the low value of allowable buckling strength p_b at the region of the critical section (i.e., at the point of intersection of the uniform to tapered part). Further increase in length would only reduce the value of p_b further. Since the criteria for stability in this case was that of stress, it therefore follows that the critical length of the haunched beam can only be increased by increasing the allowable buckling stress p_b . The following methods were investigated to increase the allowable buckling stress p_b .

8.3.2 Increasing Allowable Buckling Stress to the Average of Buckling and Yield Stress

The results of the calculations in accordance with Appendix G for the haunched members under consideration showed the presence of a critical section of the beam where buckling was likely to occur. This section of the beam, where the stress due to the applied load tended to exceed the allowable buckling stress, was located at the point of intersection of the uniform and the tapered parts of the beam. It can also be seen that the allowable buckling stress at that point will always be less than the yield stress. Assuming the actual buckling stress lies between the yield stress and the allowable buckling stress, a possible

estimate of the actual buckling stress will be the average of these two stresses. An analysis is carried out to check the possibility of increasing the critical length of the haunched beam by this method.

This new condition for elastic stability is therefore;

$$\frac{F}{A} + \frac{M}{S_x} \leq \left(\frac{P_b + P_y}{2} \right) \dots \dots \dots (8.8)$$

A Computer programme "APG8" mentioned earlier was modified to include these proposed changes and was used in the analysis. It was observed that when beams with lengths equal to those given by earlier analysis according to Appendix G were used, the allowable stress at the critical section was increased to the value of $p_{av} = (p_b + p_y)/2$. When the length of the specimen was increased, this value of the p_{av} was reduced, however, the actual stress due to the applied load remained the same.

Different lengths of specimens were analysed, and the critical lengths were obtained when the stresses at the critical point were almost identical. There was no problem with the rest of the member because the actual stress will always be lower than the allowable stress p_{av} . Since increasing the length will reduce the allowable buckling stress at each section the analysis shows that by this method the critical length of the haunched beam can be increased. Results of the analysis shown in table 8.4. and

table 8.6. showed the details of the actual stresses.

8.3.3 Increasing the Allowable Buckling Stress by A Stress Factor

Related to the idea that the allowable buckling stress p_b should be increased to the average of the buckling stress and yield stress, (p_{av}), a similar effect can be obtained by employing an allowable buckling stress factor. In this study, three stress factors of the values 1.11, 1.25 and 1.66 were employed, these being based on the reciprocals of 0.9, 0.8 and 0.6 respectively.

By including these stress factors, the stability conditions become;

$$\frac{F}{A} + \frac{M}{S_x} \leq 1.11 \cdot p_b \dots \dots \dots (8.9a)$$

$$\frac{F}{A} + \frac{M}{S_x} \leq 1.25 \cdot p_b \dots \dots \dots (8.9b)$$

$$\frac{F}{A} + \frac{M}{S_x} \leq 1.66 \cdot p_b \dots \dots \dots (8.9c)$$

For these analyses, the computer programme APG8 was again used, after first modifying it to suit these new conditions. In the calculation of the buckling stress for different lengths of beam, it was observed that the pattern of stress behaviour was the same as in the earlier case in which, by increasing the length the allowable stress was reduced and vice versa. By employing the same technique as before, the

critical lengths of the beams under consideration were obtained. Results of the analysis for the different stress factors are shown in table 8.4, and the details of the stresses are shown in tables 8.6 to table 8.9.

8.3.4 Analysis of Results

Table 8.4. shows the results of analysis by the methods described above. It shows that the methods employed were able to increase the critical length of the haunched beam under consideration.

Comparing all the results of critical length obtained, clearly the critical lengths have been most effectively increased by equation 8.9c. and followed by equation 8.9b and equation 8.8. Equation 8.9a appears to give the least increase in the critical length in all the cases considered. Indeed the results of analysis by equation 8.8. and 8.9b appear to be quite close to each other. Table 8.5. shows the percentage error or percentage safety reserve for all the cases considered. It showed that using equation 8.9c gave the most effective results in reducing the percentage error from the region 65-75% to 35-50%.

Tables 8.6. to 8.9. show details of the stresses at the critical sections of the beams under consideration. They show that in all the cases considered, the maximum actual

stress and allowable stress reached was 22.2 kN/cm^2 ; however, in most cases the stresses are in the region of 21 kN/cm^2 . These values were about 84% to 89% of the yield stress (i.e., 25 kN/cm^2).

Regarding percentage increase, from that of the results of analysis by Appendix G it was found that by employing equation 8.8, the increase was between 26 and 40%. In equations 8.9a, 8.9b and 8.9c, the increase was 16-21%, 36-44% and 76-100% respectively.

Figures 8.2(a) to 8.2(e) shows the relationships of the ratio q of the tapered part to the total length of the haunched beam, to the critical length for the analysis by equations 8.8, to 8.9(a), 8.9(b) and 8.9(c). These graphs show that Appendix G does not give significantly different values of critical length for different values of q . The Finite Element Method, however, gave significant differences to the results for different values of q . Modifying Appendix G by including the stress factors will increase the critical lengths. This graph helps to explain why the results of percentage error in table 8.5 are always highest for $q=0.3$ and $q=0.4$, whereas they are always lower for $q=0.6$ and 0.5 .

As mentioned earlier, when employing equation 8.9c, the safety reserve was reduced to 35-50% and this appears to be within the acceptable safety limit. Therefore it is recommended that equation 8.9c be used for the amendment to

the elastic stability clauses for non-uniform members in Appendix G of BS 5950.

8.3.5 Amendments to Plastic Stability Clauses in Appendix G

Plastic stability conditions for non-uniform members are given by Appendix G in the form:

$$L_t \leq \frac{L_k}{C \cdot n_t} \dots \dots \dots (8.10)$$

where L_k is the limiting length (equation 8.5), c is the shape factor and n_t is the slenderness correction factor.

Results of analysis by this method for the haunched beam under consideration are given in table 7.7. A study was carried out to include the ELR factor in the expression for L_k to investigate its effect on the critical length of the beam. The expression given by equation 8.6 was used, however only values of $k_1=0.9$ and 0.8 were considered.

The results of analysis using expressions 8.6 and 8.10 with $k_1=0.9$ and 0.8 are shown in table 8.13. In the table these results are compared to the results given by Appendix G. Table 8.14 shows the percentage error or the safety reserve for the treatment given. It shows that the original method of Appendix G gave a safety reserve of 40-50%, whereas when using $k_1=0.9$ and 0.8 , the reserve in safety is 35-45% and 25-40% respectively. This shows that the method of Appendix

G, will result in a safe design. Introducing an ELR value equal to 0.9 will reduce the safety reserve slightly but it will remain on the safe side. It is therefore recommended that an ELR value of 0.9 be used in equation 8.6.

8.3.6 The Application of the Amended Expressions to the Haunch of Portal Frame 3

It has been shown that analysis according to Appendix G correctly predicted the failure by lateral-torsional buckling at the haunch of Portal Frame 3. In this study it has been shown that Appendix G provides an over-safe design. Further checking of the details of the analysis and the experimental results of frame 3 showed that Appendix G predicted the haunch to fail at a much lower load factor. Indeed, at the design load (i.e., at load 1.5 kN/m^2) the actual stress was about $1.75 \times$ the allowable buckling stress. This therefore confirms the finding that Appendix G gives an over-safe design. In this section the amended expressions studied earlier are applied to the haunch of Portal Frame 3 to "test" the validity of the amended expressions.

In order that the expressions 8.8, 8.9a, 8.9b and 8.9c can be examined in detail with regard to the haunch of frame 3, different types of analysis were carried out. These are;

- (i) Analysis at the Ultimate load (1.5 kN/m^2) with

values of Young's Modulus $E=205 \times 10^3 \text{ N/mm}^2$ and Yield Stress $P_y=275 \text{ N/mm}^2$.

- (ii) Analysis at the Ultimate load with the actual measured value of E and P_y .
- (iii) Analysis at the Actual Collapse load with actual measured Value of E and P_y .

8.3.6.1 Analysis of the Haunch of Frame 3 at the Design Load with Nominal Values of E and P_y

The haunch of frame 3 was analysed at the design load by the method of Appendix G and the amended expressions. The computer programme "APG8" was used in the analysis of Appendix G and the modified versions of the programme were used for the analysis with the amended expressions. The results of the analyses are shown in row number 1 of table 8.17. This shows that for all the cases considered, Appendix G gave the highest ratio of the bending stress to the allowable buckling stress. All the methods predicted that the haunch would fail. However, Appendix G predicted that failure would occur at a much lower load than the rest.

8.3.6.2 Analysis of Haunch of Frame 3 at the Ultimate Load with Actual Measured Values of E and P_y

The haunch of frame 3 was analysed at the ultimate load by

the method of Appendix G and the amended expressions. The computer programme "APG8" was used in the analysis of Appendix G and the modified versions of the programme were used for the analysis with the amended expressions. The actual measured values of E and P_y used in the calculation were $206 \times 10^3 \text{ N/mm}^2$ and 295 N/mm^2 . The results of the analyses are shown in row number 2 of table 8.17. This shows that analysis by Appendix G gave the highest ratio of bending stress to the allowable buckling stress, indicating its estimation of elastic buckling to occur at a much lower load. Although all the results indicate failure at the haunch at that load, the analysis by expression 8.9c gave very satisfactory design criteria. Therefore it can be said that there is a tendency for expression 8.9c to give slightly overestimated values of allowable buckling stress.

8.3.6.3 Analysis of Haunch of Frame 3 at the Collapse Load with Actual Measured Values of E and P_y

The same procedures were conducted as in the previous section with the values of E and P_y used equal to $206 \times 10^3 \text{ N/mm}^2$ and 295 N/mm^2 respectively. The results of the analyses are shown in row number 4 of table 8.17. The results here are very interesting because they show the validity of the expressions used in the analysis. The analysis according to Appendix G showed the highest ratio of bending stress to the allowable buckling stress and therefore predicted elastic

buckling to occur at a much lower load when compared to the other expressions. It is interesting to see that expressions 8.8 and 8.9c did not predict elastic buckling in the haunch at the collapse load. However, expressions 8.9a and 8.9b predicted elastic buckling to occur at a higher load than predicted by Appendix G. Expression 8.9b gave the closest prediction of the failure. It predicted buckling failure at a stress of 18.4 N/mm^2 and the actual bending stress at collapse was 18.8 N/mm^2 .

8.3.6.4 Recommendations for the Modification of Appendix G

The analyses therefore showed that in all the cases of loading, Appendix G gave the highest ratio of bending stress to the allowable buckling stress at the most critical part of the haunch. This ratio can be taken as an indicator of buckling occurrence. When the ratio is less than unity elastic buckling will not occur at the haunch at that particular load. This ratio must be more than unity for the prediction of elastic buckling. In section 8.3.6.3., Appendix G and all the other amended expressions were "tested" against the collapse conditions of the haunch of Frame 3. The results showed that only Appendix G, Expression 8.9a and Expression 8.9b were valid. However, Expression 8.9b provides the most accurate prediction of failure at collapse. It can therefore be said that Appendix G gave a lower-bound solution and Expression 8.9b gave an upper-bound

solution.

It is recommended that both Expressions 8.9a and 8.9b should be included in Appendix G. Whereas the original expressions in Appendix G can be used to calculate the requirement for restraints, the inclusion of these modified expressions can give a more accurate prediction of buckling failure.

8.4. Amendment to Clause 5.5.3.5

8.4.1 General

The Code BS 5950 allows an alternative to Appendix G in dealing with elastic stability for members with the tension flange restrained at intervals. This is by clause 5.5.3.5.

This clause was discussed in detail in chapter 6 in section 6.7. In chapter 7 the results of analysis of haunched beams by this clause were discussed in the light of Appendix G and the Finite Element Method. In this section, a method to amend this clause is studied in detail. However, only expressions for grade 43 steel in Clause 5.5.3.5 are considered since a similar effect is expected for grade 50 steel. The expressions obtained can be applied to the haunch of frame 3. By comparing them with the test results for frame 3, an amendment to Clause 5.5.3.5 is proposed.

8.4.2 The Effect of the Factor q

It is evident from table 7.8 that the expression used for the limiting length L_t in clause 5.5.3.5. does not adequately consider the effect of the taper parameter q . From F.E.M. analysis it was clear that the effect of q is significant, therefore, it was decided that the factor q must be included in the expression in this clause. The amended expression, for grade 43 steel that includes the factor for q is as follows;

$$L_t = \frac{K_1 r_y x}{\sqrt{q(72x^2 - 10^4)}} \dots\dots\dots (8.11)$$

where q is the ratio of the length of the tapered part to the total length of the beam and all other variables are as given by clause 5.5.3.5. of BS 5950.

Equation 8.11 was used to analyse the haunched beam under consideration and the results are as shown in table 8.10. This shows that by employing equation 8.11 the limiting length L_t was increased, thus reducing the percentage error or the safety reserve when compared to the Finite Element Method.

8.4.3 The Inclusion a Factor f in Equation 8.11

To study the effect of the relationships of q to the critical length in more detail, expression 8.11. was further

modified. The factor f that has a similar effect as an "effective length" is included in the expression as shown in equation 8.12.

$$L_t = \frac{fK_1 r_y x}{\sqrt{q(72x^2 - 10^4)}} \dots \dots \dots (8.12)$$

Expression 8.12 was evaluated for values of $f=1.1, 1.15, 1.2$ and 1.25 . Table 8.11 shows the results obtained when expression 8.12 is used to analyse the haunched beam under consideration.

Figures 8.3A to 8.3E show the results for the limiting length as a function of the different values of q used in the equation. They show that the curve for clause 5.5.3.5. is a horizontal straight line indicating no difference for different values of q . However the curves given by equations 8.11 and 8.12 show how the value of q effects the critical length of the haunched beam.

Considering the results obtained by using equation 8.11 and that obtained by using equation 8.9c, shows that in all the cases considered, values of critical length obtained for $q=0.6$ were higher for equation 8.9c. However, the results from equation 8.11 gradually get higher than those given by equation 8.9c, at the value of $q=0.3$ all the cases considered show values of the limiting length or the critical length to be higher for equation 8.10. Figures 8.3 (A to E) show that the graphs obtained from equations 8.11

and 8.12 gave almost parallel lines to the graph of the results of the Finite Element analysis whereas figures 8.2 (A to E) show that the graph for equation 8.9c is parallel to the graph of Appendix G.

It can therefore be said that equation 8.11 gave a more realistic account of the behaviour of the haunched beam than the other clauses. Therefore it is recommended that clause 5.5.3.5. should be amended to include the effect of q .

8.4.4 Comparison of Results of Frame 3 with the Amended Expressions 8.11 and 8.12

Expressions 8.11 and 8.12 are used to analyse the haunch of Frame 3. This is done so that the expressions can be tested for the real case and therefore realistic design expressions can be proposed. However in the case of the haunch of Frame 3, the analysis was for a value of $q=1$. Therefore, results of analysis by clause 5.5.3.5 and that of expression 8.11 will be the same.

Nevertheless, comparison can be made between the results of Clause 5.5.3.5 and expression 8.12 with values of $f=1.1$, 1.15, 1.2 and 1.25. Table 8.18 compares the results of the analyses with the actual length of haunch of Frame 3. Table 8.18 shows that the critical length by these two methods gave the same critical length of 1574 mm (i.e., 67% of

actual length). In Expression 8.12, increasing the value of f led to an increase in the critical length. At a value of $f=1.25$ the critical length is 1968 mm i.e., 83% of the actual length. Therefore it can be said that Expression 8.12 is valid for the haunch of Frame 3.

8.5 Conclusions

In this chapter, some possible amendments to Appendix G and Clause 5.5.3.5 were investigated and analysed. Results given by these modified expressions were compared with the results given by the original clauses and by finite element analyses for both prismatic and non-uniform members.

In the case of the elastic and plastic stability of prismatic members, it was shown in chapter 7 that the methods of Appendix G provide safe designs. Detailed study of these design methods indicate safety reserves of 40%-50% of the actual buckling load. In section 6.2.2 amendment to the clauses in Appendix G relating to the elastic stability of prismatic members were proposed to reduce this safety reserve or increase the critical length. A new factor, with values less than unity, called the ELR or "Effective length with full restraint" factor in the calculation of the slenderness λ was introduced. However, the method of calculation used in Appendix G was maintained. The results of analysis considering this new factor achieved the desired

reduction in the safety reserve. Based on the analysis of selected beams it was proposed that an ELR factor $k_l=0.8$ can be introduced in the manner described, in this clause of Appendix G.

In section 8.2.3., a slightly different treatment was given to the plastic stability of prismatic members. The ELR factor was also introduced but in this case into the expression for the limiting length, L_k . Analysis of this amended clause showed that, the introduction of the ELR factor achieved the desired reduction in the safety reserve when compared with the results of analysis by Finite Element Method. Subsequently, an ELR factor of $k_l=0.9$ was proposed for introduction into this clause of Appendix G, but otherwise it should remain as it is.

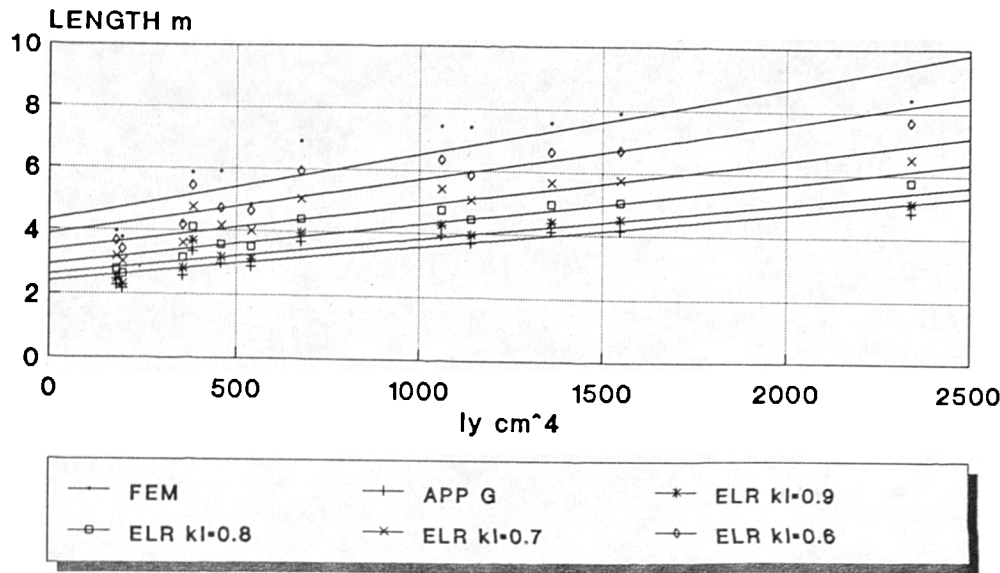
In the earlier chapter, it was also shown that Appendix G provided oversafe designs for tapered or haunched members. In elastic stability, the bending stresses produced and the buckling stresses allowed by the design were analysed thoroughly to reduce these oversafe conditions. Based on this analysis, it was found that the critical length could be increased by increasing the allowable buckling stress. Thus four alternative methods were proposed and analysed. Comparing the results with analysis by the Finite Element Method showed considerable improvement to the situation. These amended expressions were then tested against the results of the full-scale test conducted on Frame 3 to check

their validity. From this analysis, recommendations for amendments to the clauses for the elastic buckling of non-uniform members in Appendix G of BS 5950 were made.

In the case of the plastic stability of non-uniform members, the analysis in section 8.3.5. showed that by the introduction of an ELR factor $k_l=0.9$ into the expression for limiting length reduced the safety reserve slightly but maintained it on the safe side. Hence, it was recommended that this value of ELR factor be introduced in the relevant clause in Appendix G.

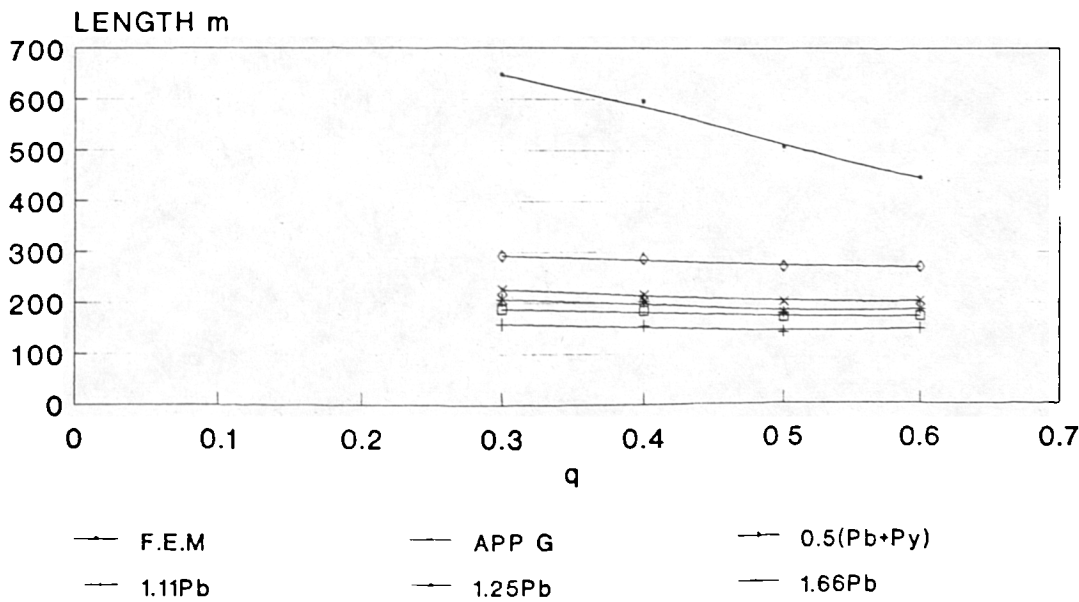
Finally amendments to clause 5.5.3.5., of BS 5950 were addressed in section 8.4. In the treatment of this clause, two approaches were studied namely the introduction of q , the ratio of the tapered length to the total length and in addition, the introduction of a factor f . Results given by the modified expressions were compared with those given by the Finite Element Method. It was shown that inclusion of the factor q in the original expressions made the behaviour of the beam more realistic. The inclusion of a factor f increased the critical length. A check with the actual case of Frame 3 had shown that the amended expressions were valid and on the safe side. Therefore, the expressions were proposed to be introduced into Clause 5.5.3.5.

FIG 8.1 THE RELATIONSHIP BETWEEN
CRITICAL LENGTH AND SECOND MOMENT
OF AREA OF MINOR AXIS I_y



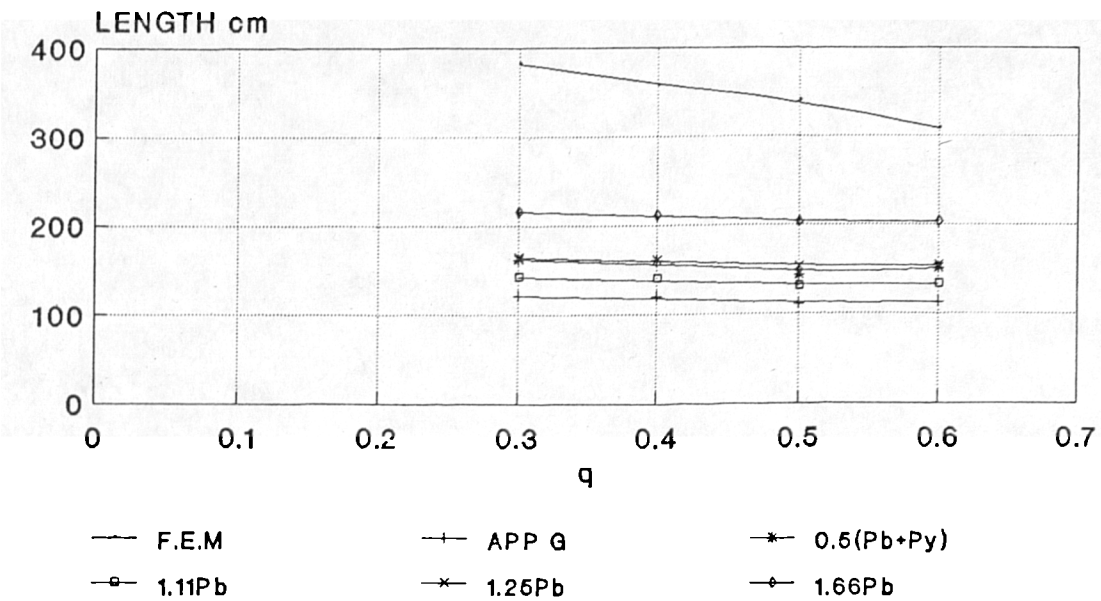
BASED ON RESULTS FOR A PRISMATIC MEMBER
WITH MOMENT GRADIENT ($\beta=0.5$)

FIG 8.2(A) GRAPH OF RELATIONSHIP OF
 q TO CRITICAL LENGTH APP G AND THE
MODIFIED CLAUSES OF APP G.



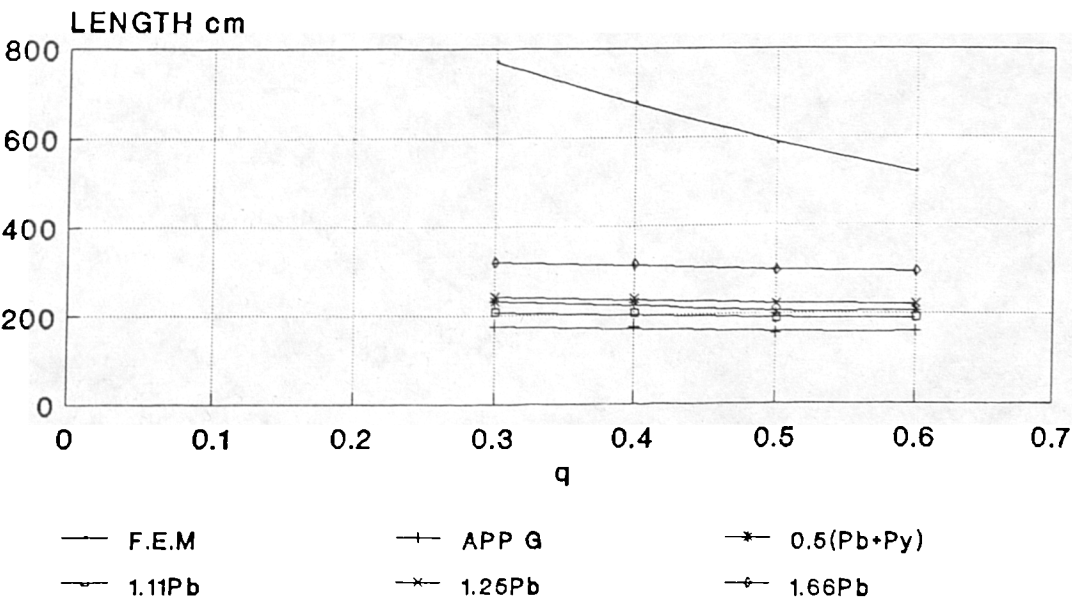
CASE OF HAUNCHED BEAM 203x133xUB30.
 q IS THE RATIO OF TAPERED LENGTH TO
TOTAL LENGTH OF THE HAUNCHED BEAM.

FIG 8.2(B) GRAPH OF RELATIONSHIP OF q TO CRITICAL LENGTH FOR APP G AND THE MODIFIED CLAUSE OF APP G.



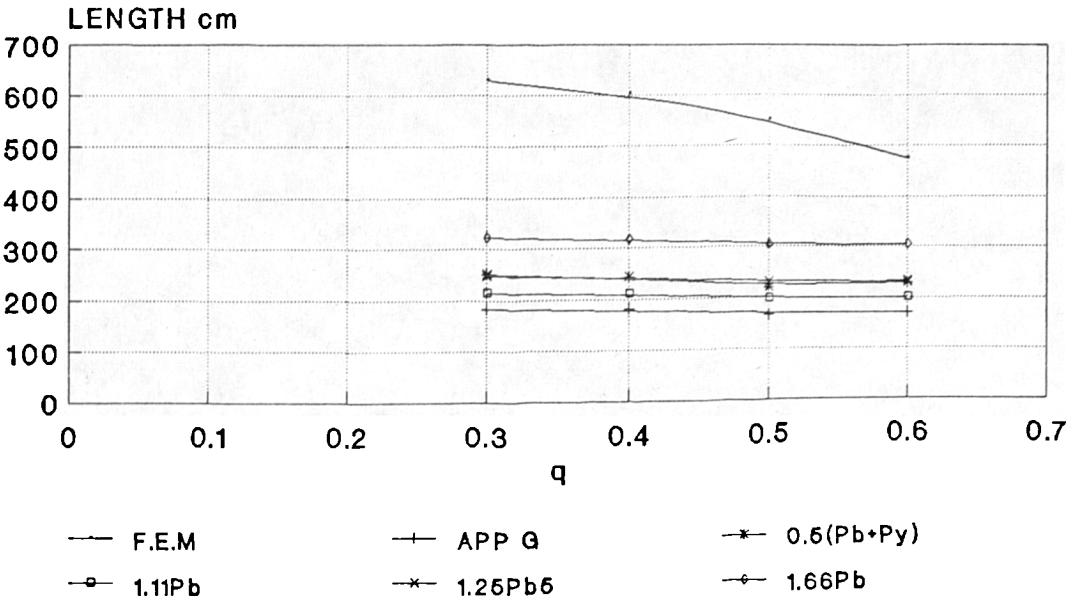
CASE OF HAUCHED BEAM 264x102xUB28.
 q IS THE RATIO OF TAPERED LENGTH TO
TOTAL LENGTH OF THE HAUCHED BEAM.

FIG 8.2(C) GRAPH OF RELATIONSHIP OF q TO CRITICAL LENGTH FOR APP G AND THE MODIFIED CLAUSE OF APP G.



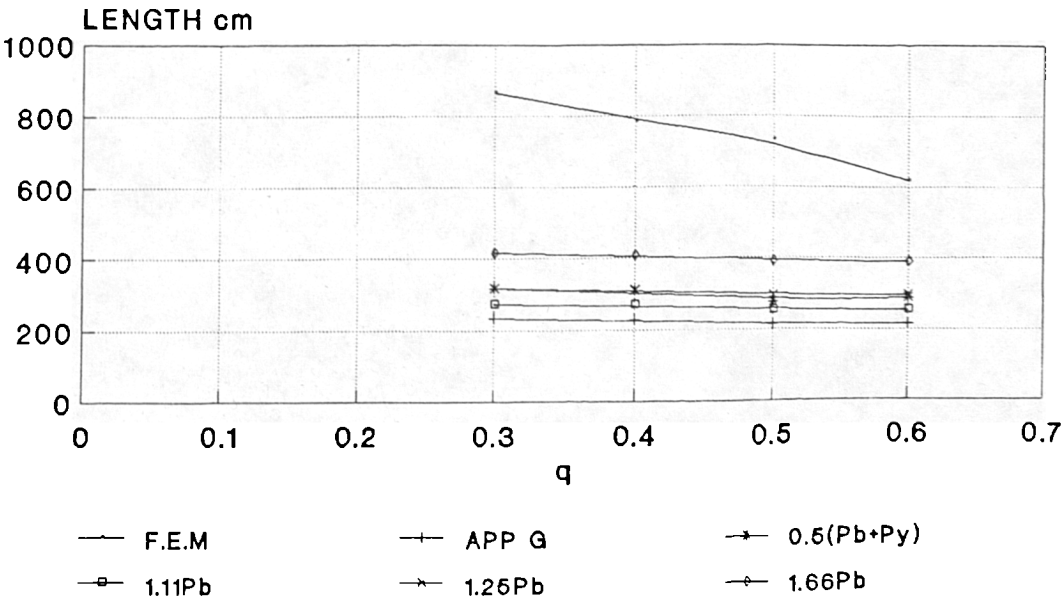
CASE OF HAUCHED BEAM 264x146xUB43.
 q IS THE RATIO OF TAPERED LENGTH TO
TOTAL LENGTH OF THE HAUCHED BEAM.

FIG 8.2(D) GRAPH OF RELATIONSHIP OF q TO CRITICAL LENGTH FOR APPENDIX G AND THE MODIFIED CLAUSE OF APP G.



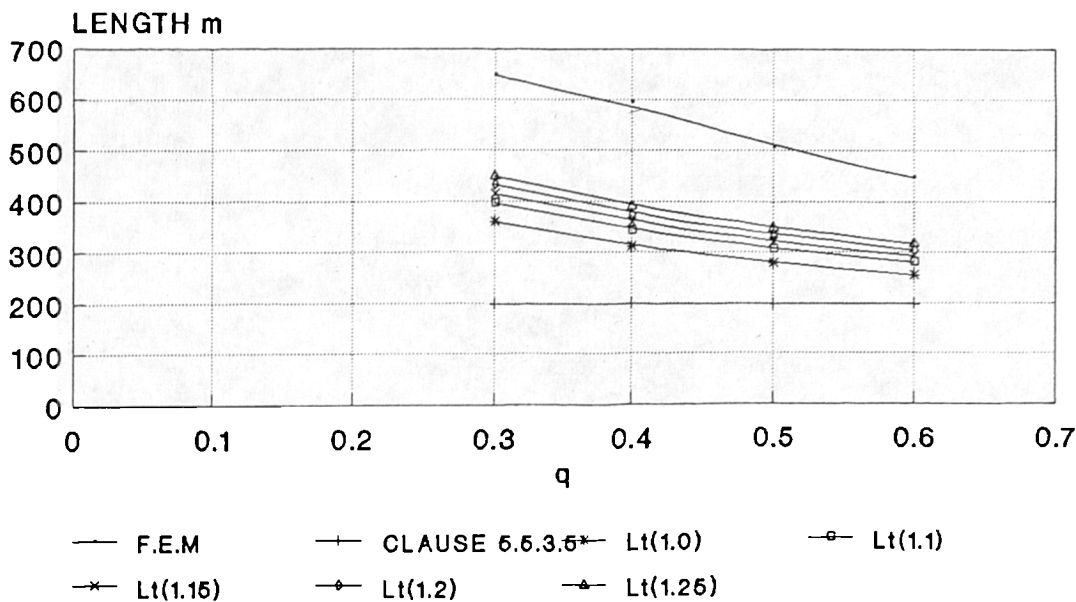
CASE OF HAUNCHED BEAM 457x162xUB82.
q IS THE RATIO OF TAPERED LENGTH TO
TOTAL LENGTH OF THE HAUNCHED BEAM.

FIG 8.2(E) GRAPH OF RELATIONSHIP OF q TO CRITICAL LENGTH FOR APPENDIX G AND THE MODIFIED CLAUSE OF APP G.



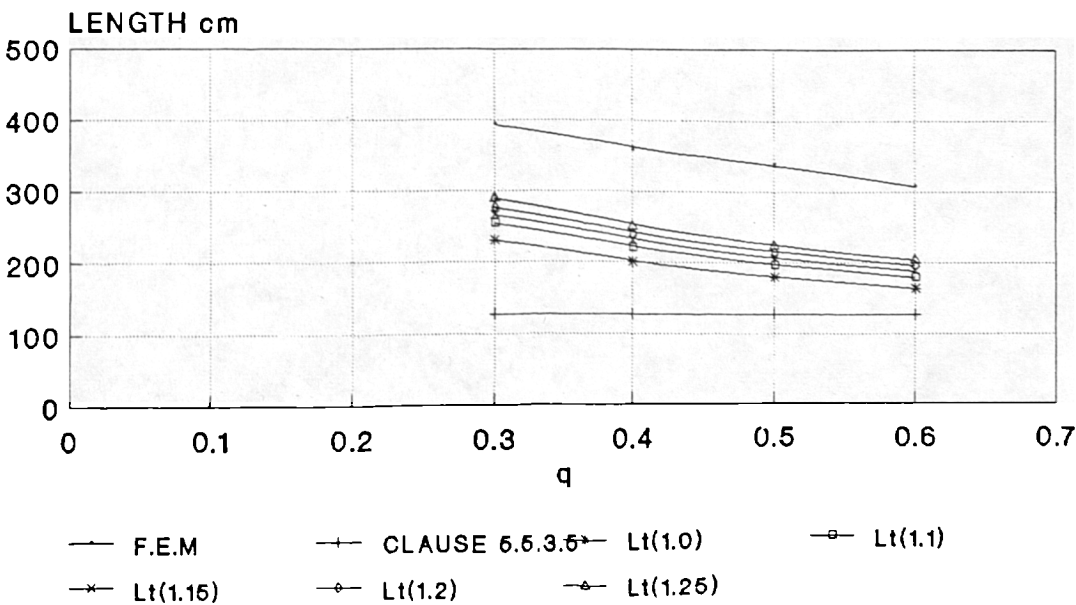
CASE OF HAUNCHED BEAM 457x191xUB98.
q IS THE RATIO OF TAPERED LENGTH TO
TOTAL LENGTH OF THE HAUNCHED BEAM.

FIG 8.3(A) GRAPH OF RELATIONSHIP OF q TO CRITICAL LENGTH FOR CLAUSE 5.5.3.5 AND THE MODIFIED CLAUSE.



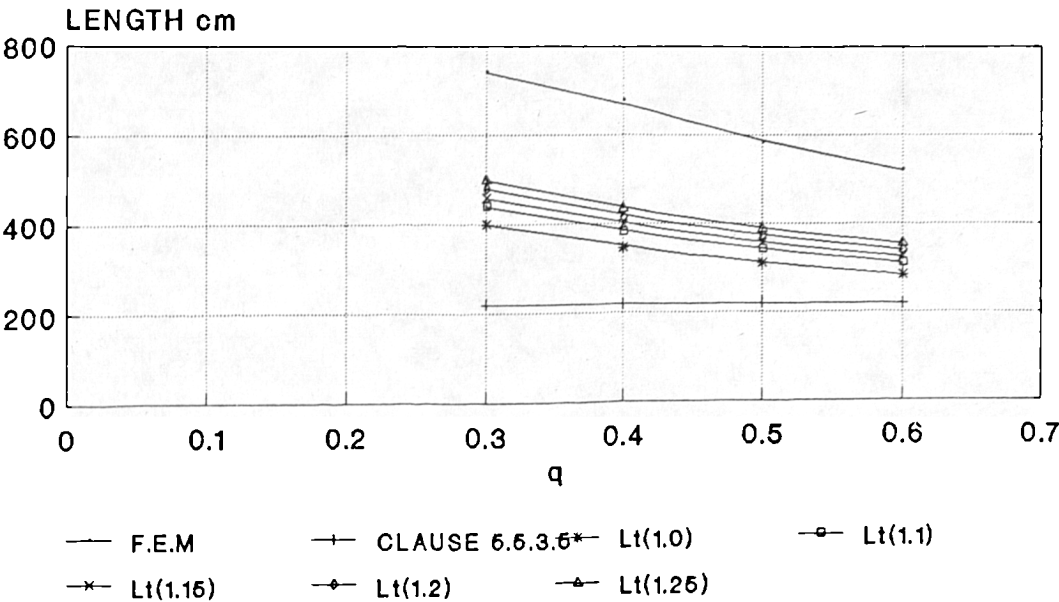
CASE OF HAUNCHED BEAM 203x133xUB30.
 q IS THE RATIO OF TAPERED LENGTH TO
TOTAL LENGTH OF THE HAUNCHED BEAM.

FIG 8.3(B) GRAPH OF RELATIONSHIP OF q TO CRITICAL LENGTH FOR CLAUSE 5.5.3.5 AND THE MODIFIED CLAUSE.



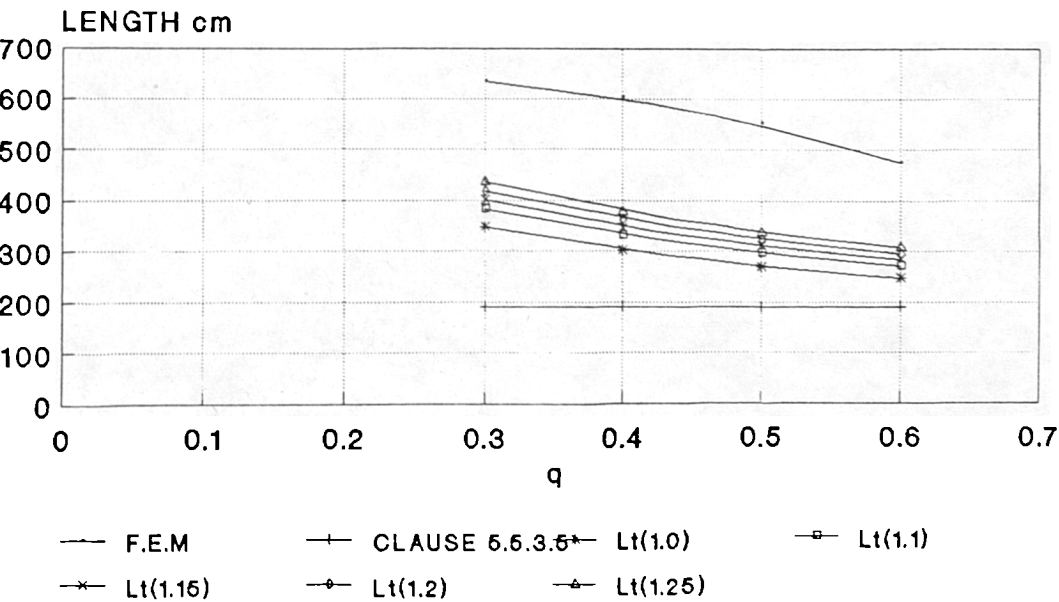
CASE OF HAUNCHED BEAM 254x102xUB28.
 q IS THE RATIO OF TAPERED LENGTH TO
TOTAL LENGTH OF THE HAUNCHED BEAM.

FIG 8.3(C) GRAPH OF RELATIONSHIP OF q TO CRITICAL LENGTH FOR CLAUSE 5.5.3.5 AND THE MODIFIED CLAUSE.



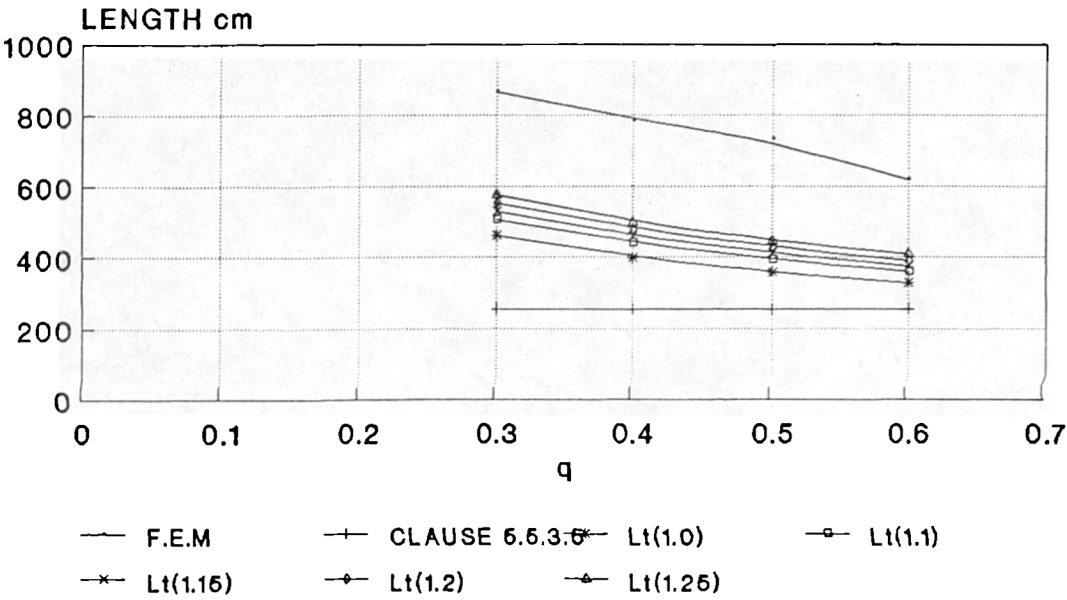
CASE OF HAUNCHED BEAM 254x146xUB43.
 q IS THE RATIO OF TAPERED LENGTH TO
TOTAL LENGTH OF THE HAUNCHED BEAM.

FIG 8.3(D) GRAPH OF RELATIONSHIP OF q TO CRITICAL LENGTH FOR CLAUSE 5.5.3.5 AND THE MODIFIED CLAUSE.



CASE OF HAUNCHED BEAM 467x152xUB82.
 q IS THE RATIO OF TAPERED LENGTH TO
TOTAL LENGTH OF THE HAUNCHED BEAM.

FIG 8.3(E) GRAPH OF RELATIONSHIP OF
 q TO CRITICAL LENGTH FOR CLAUSE 5.5.3.5
AND THE MODIFIED CLAUSE.



CASE OF HAUNCHED BEAM 457x191xUB98.
 q IS THE RATIO OF TAPERED LENGTH TO
TOTAL LENGTH OF THE HAUNCHED BEAM.

TABLE 8.1 RESULTS OF NUMERICAL ANALYSIS FOR ELASTIC STABILITY OF PRISMATIC MEMBER; BY AMMENDMENT TO APPENDIX G (BY INTRODUCING THE ELR FACTOR k_1 , IN CALCULATING FOR THE SLENDERNESS λ OF THE MEMBER BETWEEN EFFECTIVE TORSIONAL RESTRAINTS TO BOTH FLANGES).

	APP G. ELAST. STABL. L (cm)	ELAST. STABL. $k_1=0.9$ L (cm)	ELAST. STABL. $k_1=0.8$ L (cm)	ELAST. STABL. $k_1=0.7$ L (cm)	ELAST. STABL. $k_1=0.6$ L (cm)	FINITE ELEMENT METHOD L (cm)
UMB-1	332.5 (43%)	365 (38%)	410 (30%)	475 (19%)	545 (7%)	585
UMB-2	225.5 (43%)	245 (38%)	275 (31%)	315 (20%)	365 (8%)	396
UMB-3	367.2 (47%)	395 (43%)	440 (36%)	503 (27%)	595 (14%)	690
UMB-4	215.5 (43%)	229 (39%)	260 (31%)	298 (21%)	340 (10%)	377
UMB-5	296.2 (50%)	314 (47%)	355 (39%)	415 (29%)	472 (20%)	591
UMB-6	395 (47%)	428 (42%)	475 (36%)	540 (27%)	635 (15%)	743
UMB-7	256.5 (41%)	278 (35%)	313 (27%)	358 (16%)	418 (3%)	428
UMB-8	411.5 (46%)	440 (42%)	497 (34%)	565 (25%)	665 (12%)	756
UMB-9	288.5 (41%)	310 (36%)	349 (28%)	398 (18%)	465 (4%)	485
UMB-10	416.5 (47%)	450 (43%)	505 (36%)	575 (27%)	670 (15%)	790
UMB-11	369.5 (52%)	395 (46%)	445 (40%)	505 (32%)	585 (21%)	740
UMB-12	482.5 (43%)	510 (39%)	576 (31%)	650 (23%)	768 (9%)	840

TABLE 8.2 RESULTS OF NUMERICAL ANALYSIS OF PRISMATIC BEAM FOR PLASTIC STABILITY BY AMMENDMENT TO APPENDIX G (i.e BY INCLUDING THE ELR FACTOR k_1 , IN THE CALCULATION FOR SLENDERNESS λ THE MEMBER BETWEEN EFFECTIVE TORSIONAL RESTRAINTS TO BOTH FLANGES)

	APP G. PLAST. STAB. Lt (cm)	PLAST. STAB. $k_1=0.9$ Lt (cm)	PLAST. STAB. $k_1=0.8$ Lt (cm)	PLAST. STAB. $k_1=0.7$ Lt (cm)	PLAST. STAB. $k_1=0.6$ Lt (cm)	F.E.M ELAST STAB. L (cm)
UMB-1	341.5 (42%)	341.5 (42%)	341.5 (42%)	341.5 (42%)	341.5 (42%)	585
UMB-2	216.6 (45%)	216.6 (45%)	216.6 (45%)	216.6 (45%)	216.6 (45%)	396
UMB-3	379.8 (45%)	379.8 (45%)	379.8 (45%)	379.8 (45%)	379.8 (45%)	690
UMB-4	201.2 (46%)	201.2 (46%)	201.2 (46%)	201.2 (46%)	201.2 (46%)	377
UMB-5	282.4 (52%)	282.4 (52%)	282.4 (52%)	282.4 (52%)	282.4 (52%)	590
UMB-6	408.0 (45%)	408.0 (45%)	408.0 (45%)	408.0 (45%)	408.0 (45%)	743
UMB-7	253.2 (41%)	253.2 (41%)	253.2 (41%)	253.2 (41%)	253.2 (41%)	428
UMB-8	408.5 (46%)	408.5 (46%)	408.5 (46%)	408.5 (46%)	408.5 (46%)	756
UMB-9	279.4 (42%)	279.4 (42%)	279.4 (42%)	279.4 (42%)	279.4 (42%)	485
UMB-10	395.1 (50%)	395.1 (50%)	395.1 (50%)	395.1 (50%)	395.1 (50%)	790
UMB-11	326.5 (56%)	326.5 (56%)	326.5 (56%)	326.5 (56%)	326.5 (56%)	740
UMB-12	433.1 (48%)	433.1 (48%)	433.1 (48%)	433.1 (48%)	433.1 (48%)	840

NOTE: RESULTS SHOWS NO EFFECT TO THE CRITICAL LENGTH.

TABLE 8.3 RESULTS OF NUMERICAL ANALYSIS OF PRISMATIC BEAM FOR PLASTIC STABILITY BY AMMENDMENT TO APPENDIX G (i.e BY INCLUDING THE ELR FACTOR k_l , IN THE CALCULATION FOR LIMITING LENGTH L_k ;

$$L_k = \frac{(5.4 + 600 \frac{P_y}{E}) r_{yx}}{k_l \sqrt{5.4 (\frac{P_y}{E}) x^2 - 1}}$$

	APP G. PLAST. STAB. Lt (cm)	PLAST. STAB. $k_l=0.9$ Lt (cm)	PLAST. STAB. $k_l=0.8$ Lt (cm)	PLAST. STAB. $k_l=0.7$ Lt (cm)	PLAST. STAB. $k_l=0.6$ Lt (cm)	F.E.M ELAST STAB. L (cm)
UMB-1	341.5 (42%)	379.0 (35%)	427.0 (27%)	487.0 (17%)	569.0 (3%)	585
UMB-2	216.6 (45%)	240.0 (39%)	271.0 (32%)	309.0 (22%)	361.0 (9%)	396
UMB-3	379.8 (45%)	422.0 (39%)	475.0 (31%)	543.0 (21%)	633.0 (8%)	690
UMB-4	201.2 (46%)	223.0 (41%)	251.0 (33%)	288.0 (24%)	336.0 (11%)	377
UMB-5	282.4 (52%)	313.0 (47%)	353.0 (40%)	404.0 (32%)	471.0 (20%)	590
UMB-6	408.0 (45%)	453.0 (39%)	510.0 (31%)	583.0 (22%)	680.0 (8%)	743
UMB-7	253.2 (41%)	281.0 (34%)	316.0 (26%)	362.0 (16%)	422.0 (1%)	428
UMB-8	408.5 (46%)	454.0 (40%)	511.0 (32%)	584.0 (23%)	681.0 (10%)	756
UMB-9	279.4 (42%)	310.0 (36%)	349.0 (28%)	399.0 (18%)	466.0 (4%)	485
UMB-10	395.1 (50%)	439.0 (44%)	494.0 (38%)	565.0 (29%)	659.0 (17%)	790
UMB-11	326.5 (56%)	363.0 (51%)	409.0 (45%)	467.0 (37%)	545.0 (26%)	740
UMB-12	433.1 (48%)	481.0 (43%)	541.0 (36%)	619.0 (26%)	722.0 (14%)	840

TABLE 8.4 RESULTS OF ANALYSIS BY INCREASING THE ALLOWABLE BUCKLING STRESS IN EXPRESSION G.2.(a).2 OF APPENDIX G. THE CASE OF ELASTIC STABILITY OF HAUNCHED BEAMS.

	α	r	MOMENT AT END (kNcm)	APP G ELAST STAB. L(cm)	F/A+ M/Sx < 0.5Pb +0.5Py L (cm)	F/A+ M/Sx < 1.11Pb L (cm)	F/A+ M/Sx < 1.25Pb L (cm)	F/A+ M/Sx < 1.66Pb L (cm)
H1	0.6	3	17455	148.5	187.0	173.0	203.0	270.5
H2	0.5	3	13964	141.5	179.5	171.5	202.0	271.5
H3	0.4	2	11636	149.5	195.0	182.0	216.0	298.0
H4	0.4	3	11636	155.0	203.0	184.5	215.5	286.5
H5	0.3	2	9970	159.0	212.0	191.5	226.0	311.0
H6	0.3	3	9970	158.0	207.0	188.0	226.0	292.5
H7	0.6	3	19200	113.5	150.5	133.0	154.5	203.5
H8	0.5	3	15394	111.0	143.5	131.0	153.0	203.0
H9	0.4	2	12830	112.0	150.5	134.5	157.5	212.0
H10	0.4	3	12830	120.0	161.0	140.0	161.5	212.0
H11	0.3	2	10990	118.0	162.0	140.5	163.5	219.0
H12	0.3	3	10990	121.5	162.5	142.0	164.5	216.0
H13	0.6	3	31580	160.5	208.0	190.5	222.5	296.0
H14	0.5	3	25264	157.5	200.5	189.0	222.0	297.5
H15	0.4	2	21050	166.0	219.5	202.0	240.0	332.0
H16	0.4	3	21050	173.0	228.0	203.5	237.5	315.0
H17	0.3	2	18045	175.5	239.0	212.5	251.0	346.0
H18	0.3	3	18045	175.0	231.5	207.5	242.0	321.0
H19	0.6	3	97313	170.5	230.0	200.5	232.0	304.0
H20	0.5	3	77850	167.5	220.0	198.0	230.5	304.0
H21	0.4	2	64875	171.0	234.0	204.5	238.5	320.0
H22	0.4	3	64875	180.5	244.0	211.0	243.5	318.0
H23	0.3	2	55607	180.0	251.5	213.0	247.5	330.0
H24	0.3	3	55607	183.0	250.5	214.0	247.0	323.0
H25	0.6	3	122250	215.0	287.0	254.5	295.5	389.5
H26	0.5	3	97800	211.0	276.0	252.0	294.0	390.0
H27	0.4	2	81500	218.0	292.5	261.0	306.5	414.0
H28	0.4	3	81500	228.0	310.0	269.0	311.5	408.5
H29	0.3	2	69850	230.0	315.5	273.0	318.5	429.0
H30	0.3	3	69850	232.0	315.5	273.0	316.5	416.0

TABLE 8.5 COMPARISON OF PERCENTAGE ERROR/PERCENTAGE SAFETY RESERVE FOR VARIOUS AMMENDMENTS TO APPENDIX G, THE CASE FOR ELASTIC BUCKLING. (PERCENTAGE WITH REFERENCE TO RESULTS OF FINITE ELEMENT METHOD).

	FINITE ELEMENT METHOD	APP G ELAST STAB.	F/A+ M/Sx < 0.5Pb +0.5Py	F/A+ M/Sx < 1.11Pb	F/A+ M/Sx < 1.25Pb	F/A+ M/Sx < 1.66Pb
	L(cm)	%	%	%	%	%
H1	447.0	67%	58%	61%	55%	39%
H2	507.0	73%	64%	66%	60%	46%
H3	545.0	73%	64%	67%	60%	45%
H4	595.0	74%	66%	69%	64%	52%
H5	588.0	73%	64%	67%	62%	47%
H6	648.0	75%	68%	71%	66%	55%
H7	308.0	63%	51%	57%	50%	34%
H8	340.0	67%	58%	61%	55%	40%
H9	347.0	68%	57%	61%	55%	39%
H10	358.0	67%	55%	61%	55%	41%
H11	378.0	69%	57%	63%	57%	42%
H12	393.0	69%	59%	64%	58%	45%
H13	520.0	69%	60%	63%	57%	43%
H14	582.0	73%	65%	68%	62%	49%
H15	625.0	73%	65%	68%	62%	47%
H16	678.0	74%	66%	70%	65%	54%
H17	692.0	75%	65%	70%	64%	50%
H18	740.0	76%	69%	72%	67%	57%
H19	475.0	64%	52%	58%	51%	36%
H20	551.0	70%	61%	65%	59%	46%
H21	540.0	68%	57%	62%	56%	41%
H22	603.0	71%	60%	66%	60%	48%
H23	600.0	71%	60%	66%	61%	47%
H24	630.0	70%	59%	65%	60%	47%
H25	618.0	65%	54%	59%	52%	37%
H26	730.0	71%	62%	65%	60%	47%
H27	725.0	70%	60%	64%	58%	43%
H28	785.0	71%	61%	66%	60%	48%
H29	810.0	72%	61%	66%	61%	47%
H30	865.0	73%	64%	68%	63%	52%

TABLE 8.6 STRESSES AT THE CRITICAL SECTION WHEN ANALYSED BY INCREASING THE ALLOWABLE BUCKLING STRESS IN EXPRESSION G.2.(a).2 OF APPENDIX G BY EXPRESSION $F/A + M/S_x < (P_b + P_y)/2$.

	MOMENT AT END (kNcm)	$F/A + M/S_x$ <0.5(P _b) +0.5(P _y) L (cm)	LENGTH INCR. OVER APP G %	CRIT. SECTION ON THE BEAM	STRESS DUE TO APPLIED MOMENT kN/cm ²	ALLOW- ABLE BUCKL. STRESS kN/cm ²
H1	17455	187.0	26%	12	21.8	21.8
H2	13964	179.5	27%	15	22.2	22.2
H3	11636	195.0	30%	18	22.0	22.0
H4	11636	203.0	31%	18	21.5	21.5
H5	9970	212.0	33%	20	21.5	21.5
H6	9970	207.0	31%	20	21.5	21.5
H7	19200	150.5	32%	12	21.2	21.2
H8	15394	143.5	29%	15	21.6	21.6
H9	12830	150.5	34%	18	21.4	21.4
H10	12830	161.0	34%	18	20.9	20.9
H11	10990	162.0	37%	20	20.9	21.0
H12	10990	162.5	34%	20	20.9	21.0
H13	31580	208.0	29%	12	21.6	21.7
H14	25264	200.5	27%	15	22.0	22.0
H15	21050	219.5	32%	18	21.8	21.8
H16	21050	228.0	32%	18	21.8	21.8
H17	18045	239.0	36%	20	21.4	21.4
H18	18045	231.5	32%	20	21.4	21.4
H19	97313	230.0	35%	12	20.9	20.9
H20	77850	220.0	31%	15	21.3	21.3
H21	64875	234.0	27%	18	21.1	21.1
H22	64875	244.0	35%	18	20.6	20.7
H23	55607	251.5	40%	20	20.7	20.7
H24	55607	250.5	37%	20	20.7	20.7
H25	122250	287.0	33%	12	21.2	21.2
H26	97800	276.0	31%	15	21.6	21.6
H27	81500	292.5	34%	18	21.4	21.4
H28	81500	310.0	36%	18	20.9	20.9
H29	69850	315.5	37%	20	20.9	20.9
H30	69850	315.5	36%	20	20.9	20.9

TABLE 8.7 STRESSES AT THE CRITICAL SECTION WHEN ANALYSED BY INCREASING THE ALLOWABLE BUCKLING STRESS IN EXPRESSION G.2.(a).2 OF APPENDIX G BY EXPRESSION $F/A + M/Sx < 1.11 P_b$

	MOMENT AT END (kNcm)	$F/A + M/Sx$ <1.11 P_b L (cm)	LENGTH INCR. OVER APP G %	CRIT. SECTION ON THE BEAM	STRESS DUE TO APPLIED MOMENT kN/cm ²	ALLOW- ABLE BUCKL. STRESS kN/cm ²
H1	17455	173.0	16%	12	21.8	21.8
H2	13964	171.5	21%	15	22.2	22.2
H3	11636	182.0	22%	18	22.2	22.2
H4	11636	184.5	19%	18	21.5	21.5
H5	9970	191.5	20%	20	21.5	21.5
H6	9970	188.0	19%	20	21.5	21.5
H7	19200	133.0	17%	12	21.2	21.2
H8	15394	131.0	18%	15	21.6	21.7
H9	12830	134.5	20%	18	21.4	21.4
H10	12830	140.0	17%	18	20.9	20.9
H11	10990	140.5	19%	20	20.9	21.0
H12	10990	142.0	17%	20	20.9	21.0
H13	31580	190.5	19%	12	21.6	21.7
H14	25264	189.0	20%	15	22.0	22.0
H15	21050	202.0	21%	18	21.8	21.8
H16	21050	203.5	18%	18	21.3	21.4
H17	18045	212.5	21%	20	21.4	21.4
H18	18045	207.5	19%	20	21.4	21.4
H19	97313	200.5	17%	12	20.9	20.9
H20	77850	198.0	18%	15	21.3	21.3
H21	64875	204.5	20%	18	21.1	21.1
H22	64875	211.0	17%	18	20.6	20.6
H23	55607	213.0	18%	20	20.7	20.7
H24	55607	214.0	17%	20	20.7	20.7
H25	122250	254.5	18%	12	21.2	21.2
H26	97800	252.0	19%	15	21.6	21.6
H27	81500	261.0	20%	18	21.4	21.4
H28	81500	269.0	18%	18	20.9	20.9
H29	69850	273.0	19%	20	20.9	20.9
H30	69850	273.0	18%	20	20.9	21.0

TABLE 8.8 STRESSES AT THE CRITICAL SECTION WHEN ANALYSED BY INCREASING THE ALLOWABLE BUCKLING STRESS IN EXPRESSION G.2.(a).2 OF APPENDIX G BY EXPRESSION $F/A + M/S_x < 1.25 P_b$

	MOMENT AT END (kNcm)	$F/A + M/S_x$ <1.25 P_b L (cm)	LENGTH INCR. OVER APP G %	CRIT. SECTION ON THE BEAM	STRESS DUE TO APPLIED MOMENT kN/cm ²	ALLOW- ABLE BUCKL. STRESS kN/cm ²
H1	17455	203.0	37%	12	21.8	21.8
H2	13964	202.0	43%	15	22.2	22.2
H3	11636	216.0	44%	18	22.0	22.0
H4	11636	215.5	39%	18	21.5	21.5
H5	9970	226.0	42%	20	21.5	21.5
H6	9970	220.0	43%	20	21.5	21.5
H7	19200	154.5	36%	12	21.2	21.2
H8	15394	153.0	38%	15	21.6	21.7
H9	12830	157.5	41%	18	21.4	21.4
H10	12830	161.5	35%	18	20.9	20.9
H11	10990	163.5	39%	20	20.9	21.0
H12	10990	164.5	35%	20	20.9	21.0
H13	31580	222.5	39%	12	21.6	21.7
H14	25264	222.0	41%	15	22.0	22.1
H15	21050	240.0	44%	18	21.8	21.8
H16	21050	237.5	37%	18	21.3	21.3
H17	18045	251.0	43%	20	21.4	21.4
H18	18045	242.0	38%	20	21.4	21.4
H19	97313	232.0	36%	12	20.9	20.9
H20	77850	230.5	38%	15	21.3	21.3
H21	64875	238.5	39%	18	21.1	21.1
H22	64875	243.5	35%	18	20.6	20.6
H23	55607	247.5	38%	20	20.7	20.7
H24	55607	247.0	35%	20	20.7	20.7
H25	122250	295.5	37%	12	21.2	21.2
H26	97800	294.0	39%	15	21.6	21.6
H27	81500	306.5	40%	18	21.4	21.4
H28	81500	311.5	37%	18	20.9	20.9
H29	69850	318.5	38%	20	20.9	21.0
H30	69850	316.5	36%	20	20.9	20.9

TABLE 8.9 STRESSES AT THE CRITICAL SECTION WHEN ANALYSED BY INCREASING THE ALLOWABLE BUCKLING STRESS IN EXPRESSION G.2.(a).2 OF APPENDIX G BY EXPRESSION $F/A + M/S_x < 1.66 P_b$

	MOMENT AT END (kNcm)	$F/A + M/S_x$ < 1.66 P_b L (cm)	LENGTH INCR. OVER APP G %	CRITICAL SECTION ON THE BEAM	STRESS DUE TO APPLIED MOMENT kN/cm ²	ALLOW- ABLE BUCKL. STRESS kN/cm ²
H1	17455	270.5	82%	12	21.8	21.8
H2	13964	271.5	92%	15	22.2	22.2
H3	11636	298.0	99%	18	22.0	22.0
H4	11636	286.5	85%	18	21.5	21.5
H5	9970	311.0	95%	20	21.5	21.5
H6	9970	292.5	85%	20	21.5	21.5
H7	19200	203.5	79%	12	21.2	21.2
H8	15394	203.0	83%	15	21.6	21.7
H9	12830	212.0	89%	18	21.4	21.4
H10	12830	212.0	77%	18	20.9	20.9
H11	10990	219.0	86%	20	20.9	21.0
H12	10990	216.0	78%	20	20.9	21.0
H13	31580	296.0	84%	12	21.6	21.7
H14	25264	297.5	89%	15	22.0	22.1
H15	21050	332.0	100%	18	21.8	21.8
H16	21050	315.0	82%	18	21.3	21.3
H17	18045	346.0	97%	20	21.4	21.4
H18	18045	321.0	83%	20	21.4	21.4
H19	97313	304.0	78%	12	20.9	21.0
H20	77850	304.0	81%	15	21.3	21.3
H21	64875	320.0	87%	18	21.1	21.1
H22	64875	318.0	76%	18	20.6	20.6
H23	55607	330.0	83%	20	20.7	20.7
H24	55607	323.0	76%	20	20.7	20.7
H25	122250	389.5	81%	12	21.2	21.2
H26	97800	390.0	85%	15	21.6	21.6
H27	81500	414.0	90%	18	21.4	21.4
H28	81500	408.5	82%	18	20.9	20.9
H29	69850	429.0	87%	20	20.9	21.0
H30	69850	416.0	79%	20	20.9	21.0

TABLE 8-10 RESULTS OF ANALYSIS OF HAUNCHED MEMBER BY MODIFICATION
OF THE LIMITING LENGTH EXPRESSION IN CLAUSE 5.5.3.5
OF BS5950. THE NEW EXPRESSION IS;
 $L_t = (K_1 r_y X) / \sqrt{q(72 X^2 - 10^4)}$

	q	r	K ₁	X	r _y	CLAUSE 5.5.3.5 L _t (cm)	NEW EXPRES L _t (cm)	FINITE ELEM. METHOD (cm)
H1	0.6	3	445	22.35	3.2	197.5	255	447.0
H2	0.5	3	445	22.35	3.2	197.5	279	507.0
H3	0.4	2	495	22.35	3.2	219.7	347	545.0
H4	0.4	3	445	22.35	3.2	197.5	312	595.0
H5	0.3	2	495	22.35	3.2	219.7	401	588.0
H6	0.3	3	445	22.35	3.2	197.5	360	648.0
H7	0.6	3	445	28.5	2.2	126.7	164	308.0
H8	0.5	3	445	28.5	2.2	126.7	179	340.0
H9	0.4	2	495	28.5	2.2	140.9	223	347.0
H10	0.4	3	445	28.5	2.2	126.7	200	358.0
H11	0.3	2	495	28.5	2.2	140.9	257	378.0
H12	0.3	3	445	28.5	2.2	126.7	231	393.0
H13	0.6	3	445	21.55	3.5	219.2	283	520.0
H14	0.5	3	445	21.55	3.5	219.2	310	582.0
H15	0.4	2	495	21.55	3.5	243.8	385	625.0
H16	0.4	3	445	21.55	3.5	219.2	346	678.0
H17	0.3	2	495	21.55	3.5	243.8	445	692.0
H18	0.3	3	445	21.55	3.5	219.2	400	740.0
H19	0.6	3	445	27.80	3.3	191.1	247	475.0
H20	0.5	3	445	27.80	3.3	191.1	270	551.0
H21	0.4	2	495	27.80	3.3	212.6	336	540.0
H22	0.4	3	445	27.80	3.3	191.1	302	603.0
H23	0.3	2	495	27.80	3.3	212.6	388	600.0
H24	0.3	3	445	27.80	3.3	191.1	349	630.0
H25	0.6	3	445	26.15	4.3	252.6	326	618.0
H26	0.5	3	445	26.15	4.3	252.6	357	730.0
H27	0.4	2	495	26.15	4.3	281.0	444	725.0
H28	0.4	3	445	26.15	4.3	252.6	399	785.0
H29	0.3	2	495	26.15	4.3	281.0	513	810.0
H30	0.3	3	445	26.15	4.3	252.6	461	865.0

TABLE 8-11 RESULTS OF ANALYSIS OF HAUNCHED MEMBER BY MODIFICATION OF THE LIMITING LENGTH EXPRESSION IN CLAUSE 5.5.3.5 OF BS5950. THE NEW EXPRESSION IS;
 $Lt_{(f)} = f\{Kl \text{ ry } X\} / \sqrt{\{q(72 X^2 - 10^4)\}}$
 WHERE $f = 1, 1.1, 1.15, 1.2, \text{ AND } 1.25$

	CLAUSE 5535 Lt (cm)	NEW EXPR Lt ₁ (cm)	NEW EXPR Lt _{1.1} (cm)	NEW EXPR Lt _{1.15} (cm)	NEW EXPR Lt _{1.2} (cm)	NEW EXPR Lt _{1.25} (cm)	FINITE ELEM. METHOD (cm)
H1	197.5	255	280	293	305	318	447.0
H2	197.5	279	307	321	335	349	507.0
H3	219.7	347	382	399	416	434	545.0
H4	197.5	312	343	359	374	390	595.0
H5	219.7	401	441	461	481	501	588.0
H6	197.5	360	396	414	432	450	648.0
H7	126.7	164	180	188	196	204	308.0
H8	126.7	179	197	206	215	224	340.0
H9	140.9	223	245	256	267	278	347.0
H10	126.7	200	220	230	240	250	358.0
H11	140.9	257	283	296	309	322	378.0
H12	126.7	231	254	266	277	289	393.0
H13	219.2	283	311	325	340	354	520.0
H14	219.2	310	341	356	372	388	582.0
H15	243.8	385	424	443	463	482	625.0
H16	219.2	346	381	398	416	433	678.0
H17	243.8	445	490	512	534	557	692.0
H18	219.2	400	440	460	480	500	740.0
H19	191.1	247	271	284	296	308	475.0
H20	191.1	270	297	311	324	338	551.0
H21	212.6	336	370	386	403	420	540.0
H22	191.1	302	332	347	363	378	603.0
H23	212.6	388	427	446	466	485	600.0
H24	191.1	349	384	401	419	436	630.0
H25	252.6	326	359	375	391	408	618.0
H26	252.6	357	393	411	429	446	730.0
H27	281.0	444	489	511	533	555	725.0
H28	252.6	399	439	459	479	499	785.0
H29	281.0	513	564	590	616	641	810.0
H30	252.6	461	507	530	553	576	865.0

TABLE 8.12 PERCENTAGE ERROR/SAFETY RESERVE TO THE RESULTS OF ANALYSIS OF HAUNCHED MEMBER BY MODIFICATION OF THE LIMITING LENGTH EXPRESSION IN CLAUSE 5.5.3.5 OF BS5950 TO RESULTS OF ANALYSIS BY FINITE ELEMENT METHOD. THE NEW EXPRESSION IS;

$$L_{t_{(f)}} = f(K_1 r_y X) / \sqrt{\{q(72 X^2 - 10^4)\}}$$

WHERE $f = 1, 1.1, 1.15, 1.2, \text{ AND } 1.25$

	CLAUSE 5535 % ERR	NEW EXPR L_{t_1} %ERR	NEW EXPR $L_{t_{1.1}}$ %ERR	NEW EXPR $L_{t_{1.15}}$ %ERR	NEW EXPR $L_{t_{1.2}}$ %ERR	NEW EXPR $L_{t_{1.25}}$ %ERR	FINITE ELEM. METHOD (cm)
H1	56%	43%	37%	34%	32%	29%	447.0
H2	51%	45%	39%	37%	34%	31%	507.0
H3	60%	36%	30%	29%	24%	20%	545.0
H4	67%	48%	42%	40%	37%	34%	595.0
H5	63%	32%	25%	22%	18%	15%	588.0
H6	70%	44%	39%	36%	33%	31%	648.0
H7	59%	47%	42%	39%	36%	34%	308.0
H8	63%	47%	42%	39%	37%	34%	340.0
H9	59%	36%	29%	26%	23%	20%	347.0
H10	65%	44%	39%	36%	33%	30%	358.0
H11	63%	32%	25%	22%	18%	15%	378.0
H12	68%	41%	35%	32%	30%	26%	393.0
H13	58%	46%	40%	38%	35%	32%	520.0
H14	62%	47%	41%	39%	36%	33%	582.0
H15	61%	38%	32%	31%	26%	23%	625.0
H16	68%	49%	44%	41%	39%	36%	678.0
H17	65%	36%	29%	26%	23%	20%	692.0
H18	70%	46%	41%	38%	35%	32%	740.0
H19	60%	48%	43%	40%	38%	35%	475.0
H20	65%	51%	46%	43%	41%	39%	551.0
H21	61%	38%	31%	29%	25%	22%	540.0
H22	68%	50%	45%	42%	40%	37%	603.0
H23	64%	35%	29%	26%	22%	19%	600.0
H24	70%	45%	39%	36%	33%	31%	630.0
H25	59%	47%	42%	39%	37%	34%	618.0
H26	65%	51%	46%	44%	41%	39%	730.0
H27	61%	39%	33%	30%	26%	24%	725.0
H28	68%	49%	44%	42%	39%	36%	785.0
H29	65%	37%	30%	27%	24%	21%	810.0
H30	71%	47%	41%	39%	36%	33%	865.0

TABLE 8.13 RESULTS OF ANALYSIS FOR PLASTIC STABILITY FOR HAUNCHED MEMBERS BY INCLUDING ELR FACTOR IN EXPRESSION FOR L_k . IN APPENDIX G. COMPARISON ARE MADE FOR RESULTS OF $L_{t(0.8)}$, $L_{t(0.9)}$ AND APPENDIX G).

	nt	c	APP G Lk (cm)	APP G Lt (cm)	$L_{k0.8}$ (cm)	$L_{t0.8}$ (cm)	$L_{k0.9}$ (cm)	$L_{t0.9}$ (cm)
H1	0.825	1.281	285	269	356	337	317	300
H2	0.811	1.256	285	279	356	349.5	317	311
H3	0.774	1.145	285	321	356	402	317	358
H4	0.756	1.229	285	306	356	383	317	341
H5	0.759	1.125	285	333	356	417	317	371
H6	0.737	1.199	285	322	356	403	317	358
H7	0.818	1.192	184	189	230	236	202	207
H8	0.798	1.175	184	196	230	245	202	216
H9	0.764	1.099	184	219	230	274	202	241
H10	0.744	1.157	184	214	230	267	202	235
H11	0.749	1.085	184	226	230	283	202	249
H12	0.725	1.136	184	223	230	279	202	246
H13	0.824	1.298	318	297	398	372	352	330
H14	0.81	1.272	318	309	398	386	352	342
H15	0.774	1.154	318	357	398	446	352	395
H16	0.755	1.244	318	339	398	424	352	375
H17	0.758	1.133	318	371	398	464	352	411
H18	0.736	1.211	318	357	398	447	352	396
H19	0.815	1.20	275	281	344	352	305	311
H20	0.795	1.182	275	293	344	366	305	325
H21	0.761	1.103	275	328	344	410	305	364
H22	0.741	1.163	275	319	344	399	305	354
H23	0.747	1.089	275	339	344	423	305	375
H24	0.723	1.141	275	334	344	417	305	370
H25	0.82	1.218	364	365	455	456	404	404
H26	0.802	1.199	364	379	455	474	404	420
H27	0.767	1.112	364	427	455	534	404	474
H28	0.748	1.178	364	414	455	517	404	458
H29	0.752	1.097	364	441	455	552	404	489
H30	0.729	1.154	364	433	455	541	404	480

TABLE 8.14 PERCENTAGE ERROR/RESERVE OF SAFETY FOR PLASTIC STABILITY FOR HAUNCHED MEMBERS BY INCLUDING ELR FACTOR IN EXPRESSION FOR L_k IN APPENDIX G. PERCENTAGE ARE BASED ON THE RESULTS OF RESULTS FOR ELASTIC STABILITY BY FINITE ELEMENT ANALYSIS

	FINITE ELEMENT METHOD (ELASTIC STABIL.) L (cm)	APP G (PLASTIC STABILITY Lt % (cm) ERR	Lt _{0.8}		Lt _{0.9}	
			Lt (cm)	% ERR	Lt (cm)	% ERR
H1	447	269 (40%)	337	(25%)	300	(33%)
H2	507	279 (44%)	349	(31%)	311	(39%)
H3	545	321 (41%)	402	(26%)	358	(34%)
H4	595	306 (49%)	383	(36%)	341	(43%)
H5	588	333 (43%)	417	(29%)	371	(37%)
H6	648	322 (50%)	403	(38%)	358	(45%)
H7	308	189 (39%)	236	(23%)	207	(33%)
H8	340	196 (42%)	245	(28%)	216	(36%)
H9	347	219 (37%)	274	(21%)	241	(31%)
H10	358	214 (40%)	267	(25%)	235	(34%)
H11	378	226 (40%)	283	(25%)	249	(34%)
H12	393	223 (43%)	279	(29%)	246	(37%)
H13	520	297 (43%)	372	(29%)	330	(37%)
H14	582	309 (47%)	386	(34%)	342	(41%)
H15	625	357 (43%)	446	(29%)	395	(37%)
H16	678	339 (50%)	424	(37%)	375	(45%)
H17	692	371 (46%)	464	(33%)	411	(41%)
H18	740	357 (51%)	447	(40%)	396	(46%)
H19	475	281 (41%)	352	(26%)	311	(35%)
H20	551	293 (47%)	366	(34%)	325	(41%)
H21	540	328 (39%)	410	(24%)	364	(33%)
H22	603	319 (47%)	399	(34%)	354	(41%)
H23	600	339 (44%)	423	(30%)	375	(38%)
H24	630	334 (47%)	417	(34%)	370	(41%)
H25	618	365 (41%)	456	(26%)	404	(35%)
H26	730	379 (48%)	474	(35%)	420	(42%)
H27	725	427 (41%)	534	(26%)	474	(35%)
H28	785	414 (47%)	517	(34%)	458	(42%)
H29	810	441 (46%)	552	(32%)	489	(40%)
H30	865	433 (50%)	541	(37%)	480	(45%)

TABLE 8.15 RESULTS OF ANALYSIS FOR ELASTIC STABILITY FOR HAUNCHED MEMBERS BY USING Lk VALUE FROM HORNE'S EQUATION (HORNE, SHAKIR-KHALIL AND AJMANI, 1979)
NOTE; THE REST OF THE PROCEDURE FOLLOWS APP. G.

$$Lk = ([8.0 + (150 Py/E)] r y x) / (\sqrt{[4.4 (Py x^2/E) - 1]})$$

$$Lt \leq Lk / (c nt)$$

	q	r	nt	c	Lk cm	APP G (HORNE'S EQU. Lk)		APPENDIX G BS5950.		F E M L cm
						Lt (cm)	% ERR	LENGTH L (cm)	% ERR	
H1	0.6	3.0	0.825	1.281	443	419	6%	148.5	67%	447
H2	0.5	3.0	0.811	1.256	443	435	14%	141.5	73%	507
H3	0.4	2.0	0.774	1.145	443	500	8%	149.5	73%	545
H4	0.4	3.0	0.756	1.229	443	477	20%	155.0	74%	595
H5	0.3	2.0	0.759	1.125	443	519	12%	159.0	73%	588
H6	0.3	3.0	0.737	1.199	443	501	23%	158.0	75%	648
H7	0.6	3.0	0.818	1.192	276	282	8%	113.5	63%	308
H8	0.5	3.0	0.798	1.175	276	294	14%	111.0	67%	340
H9	0.4	2.0	0.764	1.099	276	328	5%	112.0	68%	347
H10	0.4	3.0	0.744	1.157	276	320	11%	120.0	67%	358
H11	0.3	2.0	0.749	1.085	276	339	10%	118.0	69%	378
H12	0.3	3.0	0.725	1.136	276	335	15%	121.5	69%	393
H13	0.6	3.0	0.824	1.298	495	463	11%	160.5	69%	520
H14	0.5	3.0	0.81	1.272	495	481	17%	157.5	73%	582
H15	0.4	2.0	0.774	1.154	495	555	11%	166.0	73%	625
H16	0.4	3.0	0.755	1.244	495	527	22%	173.0	74%	678
H17	0.3	2.0	0.758	1.133	495	577	17%	175.5	75%	692
H18	0.3	3.0	0.736	1.211	495	556	25%	175.0	76%	740
H19	0.6	3.0	0.815	1.20	417	426	10%	170.5	64%	475
H20	0.5	3.0	0.795	1.182	417	443	20%	167.5	70%	551
H21	0.4	2.0	0.761	1.103	417	496	8%	171.0	68%	540
H22	0.4	3.0	0.741	1.163	417	483	20%	180.5	70%	603
H23	0.3	2.0	0.747	1.089	417	512	15%	180.0	70%	600
H24	0.3	3.0	0.723	1.141	417	505	20%	183.0	71%	630
H25	0.6	3.0	0.82	1.218	554	555	10%	215.0	65%	618
H26	0.5	3.0	0.802	1.199	554	576	21%	211.0	71%	730
H27	0.4	2.0	0.767	1.112	554	650	10%	218.0	70%	725
H28	0.4	3.0	0.748	1.178	554	629	20%	228.0	71%	785
H29	0.3	2.0	0.752	1.097	554	672	17%	230.0	72%	810
H30	0.3	3.0	0.729	1.154	554	659	24%	232.0	73%	865

TABLE 8.16 RESULTS OF ANALYSIS FOR ELASTIC STABILITY
FOR HAUNCHED MEMBERS BY HORNE'S METHOD (HORNE,
SHAKIR-KHALIL AND AJMANI, 1979)

$$Lk = \{[8.0 + (150 Py/E)] r_y x\} / \{\sqrt{[4.4 (Py x^2/E) - 1]}\}$$

$$Lt \leq Lk / (c \cdot nt)$$

	q	r	nt	c	Lk cm	HORNE'S ELASTIC STAB.		APPENDIX G BS5950 CRIT.		F E M L cm
						Lt (cm)	% ERR	LENGTH L(cm)	% ERR	
H1	0.6	3.0	0.847	1.294	453	413	8%	148.5	67%	447
H2	0.5	3.0	0.861	1.268	453	415	18%	141.5	73%	507
H3	0.4	2.0	0.821	1.151	453	479	12%	149.5	73%	545
H4	0.4	3.0	0.801	1.240	453	456	23%	155.0	74%	595
H5	0.3	2.0	0.804	1.131	453	498	15%	159.0	73%	588
H6	0.3	3.0	0.781	1.208	453	480	26%	158.0	75%	648
H7	0.6	3.0	0.839	1.216	284	278	10%	113.5	63%	308
H8	0.5	3.0	0.858	1.198	284	276	19%	111.0	67%	340
H9	0.4	2.0	0.820	1.111	284	311	10%	112.0	68%	347
H10	0.4	3.0	0.799	1.177	284	302	16%	120.0	67%	358
H11	0.3	2.0	0.803	1.096	284	322	15%	118.0	69%	378
H12	0.3	3.0	0.779	1.153	284	316	20%	121.5	69%	393
H13	0.6	3.0	0.847	1.322	514	453	13%	160.5	69%	520
H14	0.5	3.0	0.860	1.294	514	462	21%	157.5	73%	582
H15	0.4	2.0	0.821	1.166	514	537	14%	166.0	73%	625
H16	0.4	3.0	0.801	1.263	514	508	25%	173.0	74%	678
H17	0.3	2.0	0.804	1.144	514	559	19%	175.5	75%	692
H18	0.3	3.0	0.781	1.228	514	536	27%	175.0	76%	740
H19	0.6	3.0	0.837	1.236	435	421	11%	170.5	64%	475
H20	0.5	3.0	0.857	1.216	435	418	24%	167.5	70%	551
H21	0.4	2.0	0.819	1.122	435	474	12%	171.0	68%	540
H22	0.4	3.0	0.799	1.193	435	457	24%	180.5	70%	603
H23	0.3	2.0	0.803	1.105	435	491	18%	180.0	70%	600
H24	0.3	3.0	0.779	1.167	435	479	24%	183.0	71%	630
H25	0.6	3.0	0.841	1.248	575	548	11%	215.0	65%	618
H26	0.5	3.0	0.859	1.227	575	546	25%	211.0	71%	730
H27	0.4	2.0	0.820	1.128	575	623	14%	218.0	70%	725
H28	0.4	3.0	0.800	1.203	575	598	24%	228.0	71%	785
H29	0.3	2.0	0.804	1.111	575	645	20%	230.0	72%	810
H30	0.3	3.0	0.780	1.176	575	628	27%	232.0	73%	865

Table 8.17 Results of Analysis of Haunch of Frame 3 by modified expressions

	APP-G	EXP (8.8)	EXP (8.9a)	EXP (8.9b)	EXP (8.9c)
ULTIMATE LOAD (NOMINAL DESIGN VALUES)					
1) BENDING STRESS Mb	25.2	25.2	25.2	25.2	25.2
2) BUCKLING STRESS Pb	14.2	20.8	15.8	17.7	23.6
3) DESIGN CRITERIA	NOT OK	NOT OK	NOT OK	NOT OK	NOT OK
4) Mb/Pb	1.77	1.21	1.59	1.42	1.06
ULTIMATE LOAD (ACTUAL MEASURED VALUES)					
1) BENDING STRESS Mb	25.2	25.2	25.2	25.2	25.2
2) BUCKLING STRESS Pb	15.18	22.1	16.4	18.4	24.5
3) DESIGN CRITERIA	NOT OK	NOT OK	NOT OK	NOT OK	NOT OK
4) Mb/Pb	1.66	1.14	1.54	1.37	1.03
WORKING LOAD (ACTUAL MEASURED VALUES)					
1) BENDING STRESS Mb	12.6	12.6	12.6	12.6	12.6
2) BUCKLING STRESS Pb	15.19	22.2	16.4	18.5	24.6
3) DESIGN CRITERIA	OK	OK	OK	OK	OK
4) Mb/Pb	0.83	0.56	0.77	0.68	0.51
COLLAPSE LOAD (ACTUAL MEASURED VALUES)					
1) BENDING STRESS Mb	18.8	18.8	18.8	18.8	18.8
2) BUCKLING STRESS Pb	14.7	22.2	16.4	18.4	24.6
3) DESIGN CRITERIA	NOT OK	OK	NOT OK	NOT OK	OK
4) Mb/Pb	1.27	0.85	1.15	1.02	0.76

NOTE: (i) Value of stress; N/mm². (ii) OK - buckling is not predicted. (iii) NOT OK - buckling is predicted.

Table 8.18 Results of Analysis of Haunch of Frame 3 by Clause 5.5.3.5 and the Expressions 8.11 and 8.12.

		f=1.1	f=1.15	f=1.2	f=1.25
CLAUSE 5.5.3.5	1577 (mm)	-	-	-	-
EXPRESSION 8.11	1577 (mm)	-	-	-	-
EXPRESSION 8.12	-	1735 (mm)	1813 (mm)	1892 (mm)	1971 (mm)
ACTUAL LENGTH	2364 (mm)	-	-	-	-

CHAPTER 9

9.0 Conclusions

9.1 Summary of Research

A full scale test on a 24 m span industrial portal frame was conducted. The method of testing described in this thesis is completely new. The set up of the test was essentially to allow the realistic behaviour of the frame to be observed. The effects of the secondary members such as the purlins and sheeting that enhanced the stability of the frame were considered. This was done by a special test rig that was designed with articulated gable frames. The test was meticulously planned so that all aspects of the behaviour of the frame, its secondary members and connections were monitored and recorded. Sophisticated instrumentation and data logging devices were used during the test. The simulation of snow + self load was by using a total of 96 hangers connected to timber frames spreading the load over an array of 576 points on the roof and loaded using six hydraulic jacks.

Checks on the design of the frame showed some aspects of poor design which could be eliminated by proper use of the design code BS 5950. Of these, the stability of the haunch attracted attention. The checks by Appendix G and Clause 5.5.3.5 showed that it was not stable at the collapse load.

During the test, the frame failed by lateral-torsional buckling at one of the haunches at a load factor 1.668.

The important aspect of this research was that initially it was thought that Appendix G and Clause 5.5.3.5 had predicted correctly the failure of the frame. Superficially, this prediction was proved correct, however calculation checks showed that Appendix G predicted failure at a much lower load. This led to the conclusion that Appendix G provides an over-safe design. Thus the research was then directed to the study of lateral-torsional buckling with particular attention to the effect of tapered members.

A literature review on the previous studies of tapered members was carried out. In the study of the elastic stability of tapered members, in particular with I-sections, some experimental research was reported but most of the research was theoretical and numerical in nature. The available methods of analysis for lateral-torsional buckling of tapered members were also reviewed. The finite element method that proved to be accurate and versatile appears to be the most suitable method of analysis for the research undertaken in this thesis.

A finite element formulation based on a beam element that can reproduce the structural behaviour of a three dimensional I-beam, was described in chapter 4 of this thesis. This element has two nodes and seven global

displacement fields namely three translational displacements, three rotations and one warping displacement. A computer programme called the "SPACE" finite element computer programme which employed this finite element formulation was also described. This formulation, that is valid for many cross-section shapes of prismatic members, is also valid for non-uniform members.

In the early stages of using this finite element program, some computational difficulties were encountered. These were due to the changes to the program made by previous workers. After these problems were resolved it was then decided that the program must be verified again for prismatic members. Further, before accepting the results of this finite element model in simulating the behaviour of tapered members, additional verification exercises were conducted. The theoretical models were calibrated against various published experimental and theoretical evidence from different sources. Although some of the data had been obtained over thirty years ago, the comparison between the theoretical simulations by the finite element formulation and the published evidence proved to be very satisfactory.

Earlier, it has been suspected that the provisions in Appendix G of BS 5950 gave over-safe design. Therefore a detailed study of the design approach to the problem of lateral-torsional buckling according to BS 5950 was conducted. In this study, the theoretical basis of design

for elastic lateral-torsional buckling of beams was first considered. Different cases of design for prismatic and non-uniform members with different loading conditions were then given. This was followed by the detailed investigation of the clauses related to lateral-torsional buckling in BS 5950. Particular interest on this section was the detailed study of the clauses in Appendix G.

An assessment of the clauses for lateral stability in BS 5950 was then conducted. This assessment was conducted by the finite element computer program verified earlier. The assessment was divided into three parts in which design for lateral stability of a prismatic section was considered first. This was followed by the assessment of the design for tapering members. The third part of the assessment was concerning Appendix G and clause 5.5.3.5. Selected Universal Beam sections were used in this assessment.

The results of this assessment showed that the behavioral aspects of design for lateral buckling provided by BS 5950 agreed well with the finite element method. Some aspects of the real beam properties that were considered in the formulation of the design equations were acceptable. However, the assessment of the clauses in Appendix G confirmed the suspicion that it gave an over-safe design. Contrary to most thought, in this assessment Clause 5.5.3.5 was less conservative than Appendix G although it had other set-backs.

Subsequently, a more detailed study of the clauses of Appendix G and Clause 5.5.3.5 was conducted in order to investigate the deficiencies of the clauses and to find ways to improve them. Some amendments to the clauses were investigated and the results of the analyses using these amended expressions were compared with the original clauses and the finite element method. The results showed some improvement compared to the original clauses and gave safe values when compared with the finite element method. These amended expressions were then tested against the results of the full-scale test on frame 3 to check the validity of these amended expressions. Recommendations were made to include the validated expressions into the code BS 5950.

This research has proved that theoretical development must always be quantified with experimental verification. Although an experimental exercise of this nature is expensive, the large amount of results it generated will be very useful in years to come. Furthermore, it has also proved that it is possible to model most aspects of the behaviour of pitched roof portal frames at low cost compared with solutions using commercial finite element packages.

9.2 Suggested Further Studies

The recorded realistic behaviour of Frame 3 during the test can certainly help to calibrate any sophisticated

mathematical models of portal frame behaviour. This should provide stimulus for further development in the software side.

The conditions in the haunch region and column head of a portal frame offer some interesting problems. From analysis of the frame and the test results it was shown that this region is susceptible to instability. In principle fly braces can be provided by connection through the other subsidiary members such as the purlins and the sheeting rails. However, with the large spacing of purlins in modern construction this becomes difficult. Further research into the provision of fly braces in the haunch region whether by connection through purlins or another means must be carried out.

The finite element formulation used was based on a beam element. Perhaps, a further study on solving elastic stability problems of tapered members by different finite element formulations will reveal some interesting results.

Attention is drawn to the author's assumption of an acceptable difference of 30 - 40% between his theoretical analysis and the design method. The empirical corrections proposed in chapter 8 are based on this assumption, which needs further justification.

REFERENCES

Chapter 1

- 1.1 Hans Straub. " A History of Civil Engineering." Cambridge M.A. MIT Press 1964.(pp. 173-180)
- 1.2 Maier-Librtiz H. " Test Results, Their Interpretation and Application." Second Congress IABSE, Berlin 1936
- 1.3 Baker J.F. and Roderick J.W. "An Experimental Investigation of the Strength of Seven Portal Frames", Trans. Inst. Welding, Vol 1, (1938)
- 1.4 Baker J.F., Horne M.R. and Heyman J. "The Steel Skeleton" Vol 2. Cambridge University Press 1956.
- 1.5 Schilling C.G., Schutz F.W and Beedle L.S. "Behaviour of Welded Single Span Frames Under Combined Loadings" The Welding Journal Vol. 35. No 5 pp 234, 1956
- 1.6 Discroll G.C. and Beedle L.S. " The Plastic Behaviour of Structural Member and Frames, Progress Report No 21, Welded Continue Frames and their Components" The Welding Journal of Research Supplement, June 1957
- 1.7 Greenberg H. and Prager W. "On Limited Design of Beams and Frame." Transactions of the American Society of Civil Engineers. Vol 117, 1952
- 1.8 Baker J.F. and Eickhoff K.G. "The Behaviour of Saw-tooth Portal frames." Conference on the Corelation of Stresses and Displacements." Institute of Civil Engineers, 1955
- 1.9 Baker J.F., Eickhoff K.G. and Roscoe K.H. "Tests on Two Worth-Light Portals" British Welding Research Association. Report No FE1/49, 1956
- 1.10 Vickery R.J. "The Influence of Deformations and Strain-hardening on Collapse Load of Rigid Frame Steel Structures." Research Report No R 22, University of Sydney, Sept. 1960
- 1.11 Charlton T.M. "A Test on a Pitched Portal Structure with Short Stanchions." Welding Journal No 7 1960
- 1.12 Vickery R.J. "The Behaviour at Collapse of Simple Steel Frames with Tapered Members." The Structural Engineer 1982
- 1.13 Bates W., Bryan E.R and El-Dakhakhni W.M. "Full Scale Tests on a Portal Frame Shed." The Structural Engineer 1965

- 1.14 Horne M.R and Chin M.W. "Full Scale Tests on Portal Frame of High Tensile Steel." Welding Journal, August 1967
- 1.15 Davies J.M. "Stability of Plane Framework Under Static and Repeated Loading." Ph.D Thesis, University of Manchester, 1965
- 1.16 Chin M.W. Ph.D Thesis, University of Manchester, 1965.
- 1.17 Horne M.R. and Chin M.W. "Plastic Design of Portal Frame in Steel to BS 968." BCSA Publication No 29 1966
- 1.18 Shepherd R. "Strains in a Steel Portal Frame Structure." Proceedings of Institution of Civil Engineers, March 1966
- 1.19 Halasz O. and Ivyani M. "Elastic Plastic Frames" Department of Steel Structures, Technical University, Budapest, Hingary (1978)
- 1.20 Dowling P.J., Mears T.F., Owen G.W. and Raven G.K. "A Development in the Automated Design and Fabrication of Portal Framed Industrial Building." The Structural Engineer, Vol. 60A No 10 Oct. 1982
- 1.21 Dowling P.J., Mears T.F. and Owen G.W. "A Development in the Automated Design and Fabrication of Portal Framed Industrial Building ." (Discussion). The Structural Engineers, No 12, Vol 61A, December 1983
- 1.22 Owen G.w. and Dowling P.J. "Full Scale Testing of Tapered Portal Frame." Structural Assessment - Joint Institution of Structural Engineers / B.R.E. Building Research Station, Garston, Watford, England.
- 1.23 Elvidge M. "The Plastic Analysis of Pitched Roof Portal Frames." Ph.D Thesis submitted to Bradford University, Dec.1986
- 1.24 British Standard Institution, Structural Use of Steelwork in Building, BS 5950: Part 1. 1985 London BSI.
- 1.25 Nemir M.T.M "Finite Element Stability Analysis of Thin-Walled Structures." Ph.D Thesis submitted to University of Salford, 1985
- 1.26 Barsoum R.S. and Gallagher R.H. "Finite Element Analysis of Torsional and Torsional-flexural Stability Problem." International Journal for Numerical Method in Engineering, Vol. 1, 1970

Chapter 2

- 2.1 Engel, P. "The Full-scale Testing and the Analysis of a 12 Metre Span Pitched Roof Portal Frame." Internal Report, Department of Civil Engineering, University of Salford, 1987**
- 2.2 Engel, P. "The Full-scale Testing and the Analysis of a 12 Metre Span Agricultural Pitched Roof Portal Frame." Internal Report, Department of Civil Engineering, University of Salford, 1987**
- 2.3 Davies J.M., Morris L.J., Liu T.T.C. and Engel P. "Realistic Modelling of Steel Portal Frame behaviour." The Structural Engineers, Vol 68 No 1 1990**
- 2.4 Engel P. "The Testing and Analysis of Pitched Roof Portal Frames." Ph.D Thesis Submitted to University of Salford, 1990**
- 2.5 British Standard Institution, Structural Use of Steelwork in Building, BS 5950: Part 1. 1985 London BSI.**
- 2.6 Andrade S.A.L. and Morris L.J. "Assessment of Parametre Affecting the Behaviour of Haunch Rafters." Pacific Structural Steel Conference, New Zealand, August 1986. Vol. 2.**
- 2.7 Davies J.M and Bryan E.R. "Manual of Stressed-skin Diaphragm Design." Granada 1982**
- 2.8 Davies J.M. "The Plastic Collapse of Frame Structures Clad with Corrugated Steel Sheeting." The Institution of Civil Engineers, 1973**
- 2.9 Lawson R.M. "The Flexibility and Strength of Corrugated Diaphragm." Ph.D Thesis Submitted to University of Salford, 1976**
- 2.10 Horne M.R. and Medland I.C. "The Collapse of Loads of Steel Framework Allowing for the Effect of Strain-hardening." Proceedings of the Institution of Civil Engineers, Vol. 33, March 1966**
- 2.11 Davies J.M. "A Computer Programme for the Elastic and Plastic Analysis and Design of Plane Frame." Programme User's Manual, Sept. 1982. Department of Civil Engineering, University of Salford**
- 2.12 Davies J.M. "Frame Instability and Strain-hardening in Plastic Theory." A.S.C.E. Journal of Structural Division, Vol. 92, No ST3 June 1966**
- 2.13 Davies J.M. "False Mechanism in Elastic-Plastic Analysis." The Structural Engineers, Vol 66 No 16**

August 1988

Chapter 3

- 3.1 Timoshenko S.P. "Buckling of bars of Variable cross-section", Bulletin Polytechnic Institute, Kiev, USSR, 1908.
- 3.2 Hartmann A.J. "Elastic Lateral Buckling of Continuous Beams", Journal of Strutural Division, ASCE, Vol. 93, No. ST4. Proc. Paper 5363, August, 1967, pp 11-26.
- 3.3 Trahair N.S. "Elastic Stability of Continuous Beams", Journal of Structural Division, ASCE, Vol. 95, No. ST6 June 1969, pp 1295-1312.
- 3.4 Bleich F. "Buckling Strength of Metal Structures", McGraw-Hill Book Co., Inc. New York, 1952.
- 3.5 Column Research Council, Guide to Design Criteria for Metal Compression Members, 2nd. ed., Ed. B.G Johnston, John Wiley and Sons, New York, 1966.
- 3.6 Galambos T.V. "Structural Members and Frames", Prantice-Hall. Inc. Englewood Cliffs, New Jersey, 1968.
- 3.7 Timoshenko S.P and Gere J.M., "Theory of Elastic Stability", Second Edition, McGraw-Hill Book Co. Inc. New York, 1970.
- 3.8 Morley A. "Critical Loads for Long Tapering Struts", Engineering, London, England, 104, 295 (1951)
- 3.9 Dinnik A.N. "Design of Columns of Varying Cross-Sections", Transactions ASME, 51, (1929). Applied Mechanical Division. (Also published in 1932)
- 3.10 Nakagawa H. "Buckling of Columns with Tapering Part", Trans. ASME, 3(ii) 111 (1937)
- 3.11 Boley B.A. and Zimnoch V.P. "Lateral Buckling of Non-Uniform Beams", journal of Aeronautical Sciences, Vol 19, No. 8, 1952, pp 567.
- 3.12 Lee L.H.N. "Non-Uniform Torsion of Tapered I-Beams", Journal of Franklin Institute, Vol 262, July 1956, pp37.
- 3.13 Krefeld W.J., Butler D.J. and Anderson G.B. "Welded Cantilever Wedge Beams", Welding Journal. Vol. 38, No. 3, 1959, pp97.
- 3.14 Lee L.H.N. "On the Lateral-Buckling of Tapered Narrow Rectangular Beam", Journal of Applied Mechanics, Sept 1959, pp457.

- 3.15 Venkayya V.P. "Lateral Stability of Non-Prismatic Continuous Beams", PhD thesis presented to the University of Illinois, at Urbana, Ill., Dec 1961.
- 3.16 Austin W.J., Yegian S. and Tung T.P. "Lateral-Buckling of Elastically End-Restrained I-Beams", Journal of Structural Division, ASCE, Vol 81, Sep. No 673 April 1955.
- 3.17 Butler D.J. "Elastic Buckling Tests on Laterally and Torsionally Braced I-Beams", Welding Journal, Vol 45, No 1, 1966.
- 3.18 Lee G.C. and Szabo B.A. "Torsional Response of Tapered I-Girders", Journal of Structural Division, ASCE, Vol 93, No ST5, Proc. Paper 5505, October 1967, pp 233-252.
- 3.19 Kittipornchai S. and Trahair N.S. "Elastic Stability of Tapered I-Beams", Journal of Structural Division, ASCE, 98 No. ST3 (1972) pp 713-728.
- 3.20 Lee G.C., Morrell M.L. and Ketter R.L. "Design of Tapered Members", Welding Research Council Bulletin 173, 1972.
- 3.21 Lee G.C., Morrell M.L. and Ketter R.L. "Allowable Stress for Web Tapered Beams", Bulletin No. 192, Welding Research Council, 1974
- 3.22 Horne M.R., Shakir-Khalil H. and Akhtar S. "The Stability of Tapered and Haunched Beams", Proc. Institute of Civil Engineers, 67, Part 2 (Sept 1979) pp 677-694
- 3.23 Horne M.R., Shakir-Khalil H. and Akhtar S. "Tests on Tapered and Haunched Beams", Proc. Institute of Civil Engineers, 67, Part 2 (Sept 1979) pp 845-850
- 3.24 Brown T.G. "Lateral-Torsional Buckling of Tapered I-Beams", Journal of Structural Division, ASCE, 107, No ST4 (1981) pp 689-697
- 3.25 Bradford M.A. "Stability of Tapered I-Beams" Journal of Constructional Steel Research, 9 (1988) pp 195-216
- 3.26 Bradford M.A. and Cuk P.E. "Elastic Buckling of Tapered Monosymmetric I-Beams", Journal of Structural Engineering, ASCE, Vol. 114, No 5, May, 1988
- 3.27 Gatewood B.E. "Buckling Loads for Beams of Variable Cross-Section Under Combined Loads", Journal of Aeronautical Sciences, Vol. 22, No 4, April 1955, pp 281
- 3.28 Gere J.M. and Carter W.O. "Critical Buckling Loads for Tapered Columns", Journal of Structural Division, ASCE,

Vol. 88, No ST1, Feb 1962

- 3.29 **Butler D.J. and Anderson G.B.** "The Elastic Buckling of Tapered Beam-Columns", *Welding Journal*, Vol. 42, No 1, Jan, 1963, pp 29
- 3.30 **Olowokere O.** "On the Design of Web-Tapered, Unequal-Flanged Structural Steel Columns", *Journal of Constructional Steel Research*, 4 (1984) pp 81-116
- 3.31 **Emorpoulos J.C.** "Buckling of Tapered Bars under Stepped Axial Loads", *Journal of Structural Engineering*, Vol. 112, No 6, June, 1986
- 3.32 **William F.W. and Aston G.** "Exact or Lower Bound Tapered Columns Buckling Loads", *Journal of Structural Engineering*, ASCE, Vol 115, No 5, May, 1989
- 3.33 **American Institute of Steel Construction (AISC)** "Specification for the Design, Fabrication and Erection of Structural Steel for Buildings, New York, U.S.A, 1978
- 3.34 **Culver C.G. and Preg S.M.** "Elastic Stability of Tapered Beam-Columns", *Journal of Structural Division*, ASCE, Vol. 94, No ST2, Proc. Paper 5796, Feb, 1968 pp 455-470
- 3.35 **Prawel S.P., Morrell M.L and Lee G.C.** "Bending and Buckling Strength of Tapered Structural Members", *Welding Journal* 53, No 2, 1974, pp 75-84
- 3.36 **Salter J.B., Anderson D. and May I.D.** "Tests on Tapered Steel Columns", *The Structural Engineer*, 58A, No 6, (1980) pp 189-193
- 3.37 **Salter J.B.** "Column Behaviour and Deflection Control in Steel Frames", Ph.D Thesis, Warwick University, August 1976
- 3.38 **Shiomi, H. and Kurata M.** "Strength Formula for Tapered Beam-Columns", *Journal of Structural Engineering*, ASCE, 110, No 7 (1984) pp 1630-1643
- 3.39 **Leeming J.J. and Redshaw S.C.** "The Testing of Two Portal Frames Girders", *The Structural Engineer*, Feb. 1939
- 3.40 **Baker J.F.** "Tests on Miniature Portal Frames", *The Structural Engineer*, June 1950
- 3.41 **Baker J.F. and Roderick J.W.** "An Experimental Investigation of the Strength of Seven Portal Frames", (First Interim Report, Research Committee of the Institute of Welding) *Transactions of Institute of Welding*, Vol. 1 No 4 1939

- 3.42 Baker J.F. and Roderick J.W. "Further Tests on Beams and Portals", (Second Interim Report, Research Committee of the Institute of Welding, Vol. 3, No 2, 1940
- 3.43 Just D.J. "Plane Frameworks of Tapering Box and I-Section", Journal of Structural Division, ASCE, Vol. 103, No. ST1 Jan. 1977
- 3.44 Al-Saraff S.Z. "Elastic Instability of Frames with Uniformly Tapered Members", The Structural Engineer, Vol. 57B, No 1, March 1979
- 3.45 Fraser D.J. "Design of Tapered Member Portal Frames", Journal of Constructional Steel Research, Vol. 3, 1983
- 3.46 Nethercot D.A. "Lateral Buckling of Tapered Beams", International Association for Bridge and Structural Engineering Vol. 33 Part 11, 1973, pp. 173-192.
- 3.47 Karabalis D.L. and Beskos D.E. "Static, Dynamic and Stability Analysis of Structures composed of Tapered Beams", Computers and Structures, Vol. 16, No. 6, pp. 731-748, 1983.
- 3.48 Nemir M.T.M. "Finite Element Stability Analysis of Thin-Walled Steel Structures", Ph.D Thesis presented to the University of Salford, 1985.
- 3.49 Barsoum R.S. and Gallagher R.H. "FiniteElement Analysis of Torsional and Torsional-Flexural Stability Problems", International Journal for Numerical Methods in Engineering, 2(1970) pp 335-52.
- 3.50 Vlasov V.Z. "Thin-Walled Elastic Beams", 2nd. ed. Isreal Program for Scientific Translations, Jurusalem, 1961.
- 3.51 Ghali A. and Neville A.M. "Structural Analysis - A Unified Classical and Matrix Approach", Intex Paperback Press, Scarton, Pa. 1972.

Chapter 4

- 4.1 Zienkiewicz O.C. "The Finite Element Method" Third Edition. McGraw.Hill, 1979
- 4.2 Rockey K.C., Evans H.R., Griffiths D.W. and Nethercot D.A. "The Finite Element Method, A Basic Introduction for Engineers." Second Edition, Collins, 1983
- 4.3 Fron B.M ans Ahmad S. "Techniques of Finite Elements." Ellis Howard Series, England, 1980
- 4.4 Barsoum R.S. and Gallagher R.H. "Finite Element

Analysis of Torsional and Torsional-flexural Stability Problem." International Journal for Numerical Method in Engineering, Vol 1, 1970

- 4.5 Powell G. and Klinger R. "Elastic Lateral Buckling of Steel Beams." Journal of Structural Division, ASCE, 96 No ST 9, 1976 (pp 1630-1643)
- 4.6 Tebedge N. and Tall L. "Linear Stability Analysis of beam Column." Journal of Structural Division ASCE> 90 No ST 9, 1970
- 4.7 Alwis W.A.M and Usmi T. "Lateral-Torsional Buckling of Unbraced and Braced Plane Frames." Journal of Computer and Structures, Vol 10, 1979 (pp 517-529)
- 4.8 Nethercot D.A. and Rockey K.L. "Finite Element Solution for the Building of Columns and Steel Beams." International Journal of Mechanical Science Vol 13, 1971 (pp945-949)
- 4.9 Nemir M.T.M. "Finite Element Stability Analysis of Thin-Walled Structures." Ph.D Thesis submitted to University of Salford, 1985
- 4.10 Vlasov V.Z. "The Walled Elastic Beam." Second Edition, National Science Foundation, Washington 1961
- 4.11 Davies J.M. "A Computer Program For the Elastic and Plastic Analysis and Design of Plane Frames", Dept. of Civil Engineering, Unoversity of Salford, 1982.
- 4.12 Jennings A. and Majid K.I. "The Computer Analysis of Space Frames Using Sparse Matrix Technique." International Conference on Space Structures 1966. Department of Civil Engineering, University of Surrey.

Chapter 5

- 5.1 Lee L.H.N. "On the Lateral-Buckling of Tapered Narrow Rectangular Beam", Journal of Applied Mechanics, Sept 1959, pp457.
- 5.2 Massey P.C. "The Lateral Stability of A Non-Prismatic Beam", Building Science, Vol.2, 1967, pp 273.
- 5.3 Brown T.G. "Lateral Torsional Buckling of Tapered I-Beams", Journal of Structural Division, ASCE, 107, No ST4, 1981, pp 689-93.
- 5.4 Kerensky O.A., Flint A.R. and Brown W.C. "The Basis for Design of Beams and Plate Girders In the Revised British Standard 153", Proc. I.C.E. Part 111, Vol. 5 August 1956, pp396.

- 5.5 Kittipornchai S. and Trahair N.S. "Elastic Stability of Tapered I-Beams", Journal of Structural Division, ASCE, 98 No. ST3 (1972) pp 713-728.
- 5.6 Nethercot D.A. "Lateral Buckling of Tapered Beams", International Association for Bridge and Structural Engineering Vol. 33 Part 11, 1973, pp. 173-192.
- 5.7 Karabalis D.L. and Beskos D.E. "Static, Dynamic and Stability Analysis of Structures composed of Tapered Beams", Computers and Structures, Vol. 16, No. 6, pp. 731-748, 1983.
- 5.8 Culver C.G. and Preg S.M. "Elastic Stability of Tapered Beam-Columns", Journal of Structural Division, ASCE, Vol. 94, No ST2, Proc. Paper 5796, Feb, 1968 pp 455-470
- 5.9 Vlasov V.Z. "Thin-Walled Elastic Beams", 2nd. ed. Isreal Program for Scientific Translations, Jurusalem, 1961.
- 5.10 Lee L.H.N. "Non-Uniform Torsion of Tapered I-Beams", Journal of Franklin Institute, Vol 262, July 1956, pp37.

Chapter 6

- 6.1 British Standard Institution, Structural Use of Steelwork in Building, BS 5950: Part 1. 1985 London BSI.
- 6.2 Timoshenko S.P and Gere J.M., "Theory of Elastic Stability", Second Edition, McGraw-Hill Book Co. Inc. New York, 1970.
- 6.3 Dowling P.J., Knowles P. and Owen G.W. "The Structural Steel Design", Butterworths, 1988.
- 6.4 Trahair N.S and Bradford M.A. "The Behaviour and Design of Steel Structures", 2nd. ed. Chapman and Hall, 1988.
- 6.5 Fukumoto Y. and Kubo M. "A Survey of Tests on Lateral Buckling Strength of Beams, Preliminary Report, 2nd International Colloquium on Stability of Steel Structures, ECCS-IABSE, Leige, 1977, pp 233-240.
- 6.6 Fukumoto Y. and Kubo M. "A Supplement to a Survey of Test on Lateral Buckling Strength of Beams", Final Report, 2nd Colloquium on Stability of Steel Structures, ECCS-IABSE, Leige, 1977, pp 115-117.
- 6.7 Fukumoto Y. and Kubo M. "An Experimental Review of Lateral Buckling of Beam and Girder", Proc. International Colloquium on Stability of Steel

Structures under Static and Dynamic Loads, SSRC-ASCE, Washington, 1977, pp 541-62.

- 6.8 Taylor J.C., Dwight J.B. and Nethercot D.A. "Buckling of Beams and Strut", A new British Code - Proc. Conference on Metal Structures and the Practising Engineers, Institute of Engineers Australia, Melbourne, Nov 1974, pp 27-31.
- 6.9 Nethercot D.A. and Taylor J.C. "Use of A Modified Slenderness in the Design of Unsupported Beams", Proc. Report 2nd. International Colloquium on Stability of Steel Structures, ECCS - IABSE, Leige, 1977, pp 197-202.
- 6.10 Nethercot D.A. "Design of Beams and Plate Girder; Treatment of Overall and Local Flange Buckling", In the Design of Steel Bridge ed. Rockey K.C. and Evans H.R, Granada Publishing, St. Albans, pp 243-262.
- 6.11 Trahair N.S. "The Behaviour and Design of Steel Structures", Chapman and Hall, London, 1977.
- 6.12 Galambos T.V. "Inelastic Lateral Buckling of Beams", Journal of Structural Division, ASCE 89, ST5 (Oct 1963) pp 217-242.
- 6.13 Lay M.G and Galambos T.V. "Inelastic Steel Beams Under Uniform Moments", Journal of Structural Division, ASCE 91 (Dec 1965) pp 67-93.
- 6.14 Lay M.G and Galambos T.V. "Inelastic Beams Under Moment Gradient", Journal of Structural Division, ASCE 93, ST1 (Feb 1967) pp 381-399.
- 6.15 Massey C. and Pitman F.S. "Inelastic Lateral Stability Under a Moment Gradient", Journal of structural Division, ASCE 95, ST6 (June 1969) pp 1173-1188.
- 6.16 Hartmann A.J. "Inelastic Flexural-Torsional Buckling", Journal of Engineering Mechanics Division, ASCE 97, EM4 (August 1971) pp 1103-1119.
- 6.17 Nethercot D.A. and Trahair N.S. "Inelastic Lateral Buckling of Determinate Beams", Journal of structural Division, ASCE 102(ST4) Proc. Paper 12020, 1976, pp 701-17.
- 6.18 Trahair N.S. "Inelastic Lateral Buckling Beam and Beam-Column", Stability and Strength, Applied Science Publisher, 1983.
- 6.19 Horne M.R. "The Stanchion Problem in Frame Structure Designed According To Ultimate Carrying Capacity", Proc. Institute of Civil Engineers, 5(1), Part 111, April 1956, pp 105-60.

- 6.20 Horne M.R. "Safe Loads on I-Section Column in Structures Designed by Plastic Theory", Proc. Institute of Civil Engineers, Sept. 1964, pp 137-50.
- 6.21 Horne M.R. "The Plastic Design of Column", BCSA Publication No 23, 1964.
- 6.22 Morris L.J. and Randall A.L. "Plastic Design", Constrado Publication, 1979.
- 6.23 Dooley J.F. "On the Torsional Buckling of Columns of I-Section Restrained at Finite Intervals", Int. Journal of Mech. Sci., 1967, 9, Jan., 1.
- 6.24 Dooley J.F. "The Torsional Deformations of Columns of Monosymmetric I-Section, with Restrained Axis of Twist, Under Doubly Eccentric Load", Int. Journal of Mech. Sci., 1967, 9, Sept., pp 585.
- 6.25 Singh K.P. "Ultimate Behaviour of Laterally Supported Beams", Ph.D thesis, University of Manchester, 1969.
- 6.26 Horne M.R. and Ajmani J.L. "Stability of Columns Supported Laterally by Side-Rails", Int. Journal of Mech. Sci., 1969, 11, Feb., pp 159.
- 6.27 Horne M.R. and Ajmani J.L. "Design of Columns Restrained by Side-Rails. Strut. Engr, 1971, 49, No.8 Aug., pp 339.
- 6.28 Horne M.R. and Ajmani J.L. "The Post Buckling Behaviour of Laterally Restrained Columns", The Structural Engineer, 1971, 49, No. 8 Aug. pp 346.
- 6.29 Horne M.R., Shakir-Khalil and Akhtar S. "Stability of Tapered and Haunched Beams", Proc. Inst. Civil Engineers, Part 2, 1979, 67, Sept., pp 677-694.
- 6.30 British Standard Institution, "Use of Structural Steel in Building, BS 449: 1969, London, BSI.
- 6.31 Horne M.R. "Safe Loads on I-Section Columns in Structures Designed by Plastic Theory", Proc. Instn. Civil Engineers, 1964, 29, Sept., pp 137-150.
- 6.32 Baker J.F, Horne M.R and Heyman J. "The Steel Skeleton" Vol 2. Cambridge University Press, 1956.
- 6.33 Horne M.R. and Morris L.J. "The Design Against Instability of Haunched Members Restrained at Intervals Along the Tension Flange", Preliminary Report, 3rd. International Colloquium on Stability and Dynamics of Steel Structures, Washington, ASCE, pp 618-29.
- 6.34 Morris L.J. and Nakane K. "Experimental Behaviour of Haunched Members", International Conference on

Instability and Plastic Collapse of Steel Structures,
Granada Publishing, London, pp 547-59.

Chapter 7

- 7.1 MathCAD Software Manual, Mathsoft Inc., One Kendall Square, Cambridge, MA 02139, USA.
- 7.2 Engel P. "The Testing and Analysis of Pitched Roof Portal Frames", Ph.D Thesis, University of Salford, 1990.
- 7.3 Horne M.R., Shakir-Khalil and Akhtar S. "Stability of Tapered and Haunched Beams", Proc. Inst. Civil Engineers, Part 2, 1979, 67, Sept., pp 677-694.

APPENDIX 1 DESIGN OF FRAME 3

Frame Dimension

Span	24.00 m
Centers	5.00 m
Height to eaves	4.00 m
Height to underside of haunch	3.50 m

Loading on Plan Area

Dead load

Charateristic

Cladding (Cold-formed sheet)	0.06 kN/m ²
Lining (say polyurethane liner)	0.01 kN/m ²
Purlin (Zed purlin)	0.030 kN/m ²
Rafter and Services	1.170 kN/m ²
Total dead load	<u>0.217 kN/m²</u>

Snow load

0.750 kN/m²

Charateristic design load:

Ultimate design load

$$[1.4 \times 0.217] + [1.6 \times 0.75] \quad 1.5038 \text{ kN/m}^2$$

Total Ultimate load on frame

$$[150 \times 24 \times 5] \quad 180.46 \text{ kN}$$

Rafter/Column (Mp) Ratio (S_x ratio) 0.515

Base Mp (pinned base) 0.000

Plastic Analysis:

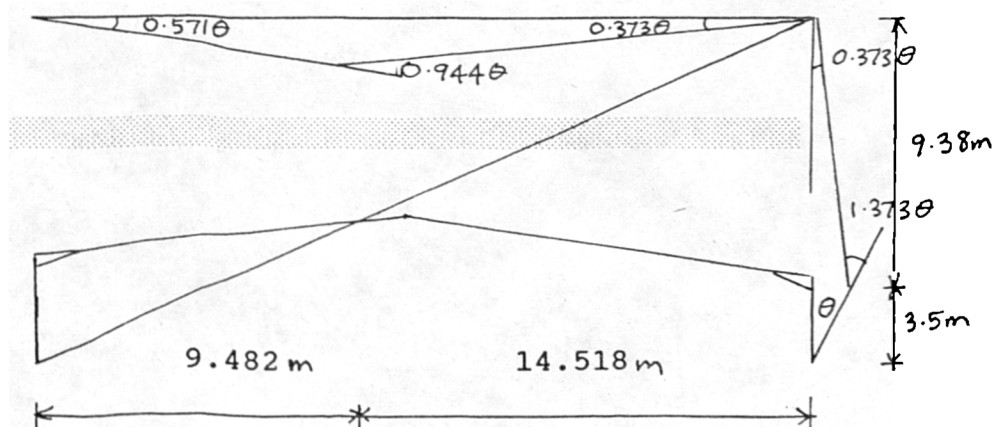


fig A.1

<u>Internal work done</u>	<u>External work done</u>
$0.515 \times M_p \times 0.944\theta = 0.486\theta$	$180.46 \times (9.482/2) \times 0.571\theta$
$M_p \times 1.373\theta = 1.373\theta$	
$= 1.859M_p\theta$	$= 488.52\theta$

Therefore M_p required $M_p = 488.52\theta / 1.859\theta = 262.76 \text{ kNm}$

Sections

Rafter

Plastic Modulus Required

$$= 0.515 \times 262.76 \times 10^3 / 275 = 492 \text{ cm}^3$$

Therefore try 356 x 127 x 33 UB ($S_x = 539.8 \text{ cm}^3$)

Column

Plastic Modulus Required

$$= 262.76 \times 10^3 / 275 = 955.5 \text{ cm}^3$$

Therefore try 406 x 178 x 54 UB ($S_x = 1048 \text{ cm}^3$)

The Bending Moment Diagram

Assuming gravitational load only the bending moment distribution in the frame is calculated. Figure A1.2 shows the bending moment diagram for frame 3 subjected to Uniformly distributed load of 180.46 kN/m.

Checking Sway Stability of Frame (Clause 5.5.3.2)

Stanchion Inertia	I_c	$= 18626$	cm^4
Rafter Inertia	I_r	$= 8200$	cm^4
Design strength of Rafter	P_{yr}	$= 275$	N/mm^2
Span	L	$= 24.00$	m
Stanchion height	h	$= 4.00$	m
$\rho = (2 I_c / I_r) (L/h) = (2 \times 18626 / 8200) (24/4) = 27.25$			
$W_r = \text{Factored vertical load on rafter} = 180.46 \text{ kN}$			
$W_o = \text{Max value of } W_r \text{ which could cause}$			
plastic failure of the rafter treated			

as a fixed ended beam of span L

$$\text{i.e., } W_o = (S_x \times P_{yr} \times 16)/L$$

$$= (539.8 \times 275 \times 16)/(24 \times 10^3) = 98.96$$

$$\text{Arching Ratio } \Omega = W_r/W_o = 180.46/98.96 = 1.82$$

$$L/D = 24/0.3485 = 68.866$$

L_r = Developed length of rafter

$$= (L/\cos 6.56^\circ) = 24.158$$

$$[44/\Omega] \cdot [L/h] \cdot \{\rho/(4+\rho L_r/L)\} \cdot [275/P_{yr}]$$

$$[44/1.82][24/4]\{27.25/(4+27.25(24.158/24))\}[275/275]$$

$$24.175 \times 6 \times 0.867 \times 1 = 125.76$$

$$\text{i.e., } 68.866 < 125.76$$

Therefore section is satisfactory for sway stability

Member Stability

Checking Column Member Buckling

From bending moment calculation the adequacy ratio $\alpha=1.082$. Using clause 5.3.5 the plastic stability for the length is checked.

$$L_m \leq \frac{38r_y}{\sqrt{\left[\frac{f_c}{130} + \left(\frac{P_y}{275}\right)^2 \left(\frac{x}{36}\right)^2\right]}}$$

where $p_y = 275 \text{ N/mm}^2$

$$f_c = \alpha \times 180.46/(2 \times 68.4) = 14.27 \text{ N/mm}^2$$

$$x = \text{torsion index} = D/T = 36.93$$

$$\text{therefore the value of } L_m = 1.357 \text{ m}$$

Clause 5.3.5 stated that within the member containing plastic hinge, L_m is the maximum distance from the hinge restraint to the adjacent restraint. The design assumed that the hinge form here is the last hinge in the mechanism therefore clause 5.5.3.1 can be applied, in which case no

restraint is required. (See figure A1.3)

Checking Buckling Capacity Between Stay Position 1 and 2

From clause 4.8.3.3.1 and Adopting simplified approach)

$$\frac{F}{A_g \cdot P_c} + \frac{m \cdot M_x}{M_b} + \frac{m \cdot M_y}{P_y \cdot Z_y} \leq 1$$

where $A_g = 6840 \text{ mm}^2$

$P_c = \{ \text{for } L_e = L \text{ therefore } \lambda = L_e / r_y = 33.7$

from table 27c of BS 5950 } $P_c = 265 \text{ N/mm}^2$

from tables 13 and 18 $m \cdot M_x = 0.57 \times 164 = 93.48 \text{ kN.m}$

$M_b = P_b \times S_x$ { P_b is obtained for $\lambda_{LT} = \text{nuv}\lambda$

for $n=1$ $v=0.99$ and $u=0.9$ -(table 14)

therefore $\lambda_{LT} = 30$. From table 13 $P_b = 275 \text{ N/mm}^2$ }

$M_b = 287 \text{ kNm}$

Therefore ;

$$(180.46) / (2 \times 6840 \times 265) + (0.57 \times 164) / (287) = 0.375$$

i.e $0.375 < 1$. Therefore, the section is OK for buckling capacity between stay 1 and 2.

Check for Column Stability by Clause 5.5.3.5

$$L_t = \frac{K_1 \cdot r_y \cdot x}{[72 \cdot x^2 - 10^4]^{1/2}}$$

where, $K_1 = 620$

$r_y = 38.5$

$x = D/T = 36.93$

$$\therefore L_t = \frac{620 \times 38.5 \times 36.93}{\sqrt{72 \times 36.93^2 - 10^4}} = 2968 \text{ mm}$$

Since the maximum length between the lateral restraint in column is 2.00 m the member should remain stable.

Checking for Rafter Stability

Assumption; Rotational properties are required of the hinge at the first purlin point along the ridge.

(Clause 5.3.5. Stay is provided at the first purlin position from the apex.)

Checking Rafter Stability at the Apex

From Clause 4.3.7.5; $\lambda_{LT} = nuv\lambda$

for values of $n=1$, $u=0.9$, $v=0.97$, and

$\lambda = 1795/25.9 = 69$, therefore

$\lambda_{LT} = 60$. From table 11 of BS 5950 $P_b = 213 \text{ N/mm}^2$

$M_b = P_b S_x = 213 \times 0.5398 \text{ kNm} = 115 \text{ kNm}$.

However, moment at the first purlin is 148 kNm therefore the region at the apex is unstable. By considering span between purlins equal 1.795 m it can be seen that the stress is reduced by about 22%. Therefore moment resistance at the vicinity of the rafter is in the region of 118 kNm.

Checking Rafter Buckling at the Eaves Region

(1) The haunch section was checked for elastic stability by the clauses in Appendix G:BS 5950 Part 1.

Results of the analysis as shown in the computer output at the end of this appendix. The results shows that the conditions of Appendix G was not satisfied.

(2) Check by Clause 5.5.3.5

$$L_t = \{K_1 r_y x\} / \{\sqrt{(72x^2 - 10^4)}\}$$

$$= \{495 \times 25.9 \times 41\} / \{\sqrt{(72 \times 41^2 - 10^4)}\}$$

= 1577 mm. Since the length of the haunch provided was 2408 mm lateral-torsional buckling at the

haunch is not satisfied.

Conclusion

The calculations show that at factored load of 180.46 it is possible that the frame will collapse. The frame may fail by lateral torsional buckling at the haunch region.

APPENDIX 2

VERIFICATION OF FINITE ELEMENT FORMULATION AND CORRESPONDING COMPUTER PROGRAMME FOR ANALYSIS OF PRISMATIC MEMBERS

A2.1 GENERAL

The derivation of the finite element formulation for the elastic torsional-flexural buckling of thin walled structures is given in chapter 4. This section proves the validity and accuracy of the finite element formulation by comparing solutions for a variety of problems for prismatic members against exact or highly accurate solutions by alternative methods. The computer program (1) described in chapter 4 was used to predict the buckling loads.

The verification begins by presenting solutions to some conventional stability problems to illustrate the validity of the modified "Southwell technique". This technique is employed in the computer program for evaluating the critical buckling loads. It then proceeds to establish the accuracy of the formulation when used to analyse the elastic buckling behaviour of the prismatic section.

A2.2 Conventional Stability Problems

Several separate examples are discussed in this section. These include the cases for buckling of I-beams, cantilevers, columns, lipped and unlipped channel beams and pure torsional buckling of members.

A2.2.1 Lateral Buckling of I-Beam

Three cases are dealt with in this section. They are:

- (i) simply supported beams in pure bending
- (ii) simply supported beams with a central concentrated load, and
- (iii) Cantilever I-beams.

In all the cases considered, two different beam specimens of commercial I-section are selected for the numerical calculation using the exact solution by Timoshenko (2). The results of this analysis are compared with the prediction by the finite element computer program. The details of these beam specimens are given in table A2.1. In the computer analysis, results were obtained for 4,8,16,20 and 24-element models.

A2.2.1.1 Lateral Buckling of Simply Supported I-Beam in Pure Bending

Figure A2.1 shows a simply supported I-beam specimen of 400cm length loaded by a uniform bending moment M_z . Assuming that the ends of the beam cannot rotate about the x axis, but are free to warp. The exact solution for this case as given by Timoshenko (2) is:

$$M_{cr} = \frac{\pi}{L} \sqrt{EI_n C \left(1 + \frac{C_1 \pi^2}{CL^2}\right)} \dots\dots\dots (A2.1)$$

where, I_n is the minor axis second moment of area, $C=GJ$ is the torsional rigidity and $C_1=EI_w$ is the warping rigidity.

Table A2.2 shows the results of analysis of specimen B1 and B2. The convergence graphs are shown in figure A2.2. For specimen B1, it can be seen that the 2-element solution differs by 8.4% from the exact solution while the 4, 8, 10, 16, 20 and 24-elements, are 0.09, 0.12, 0.12, 0.13, 0.13 and 0.05% in error respectively. It can be said that all the cases considered gave excellent agreement with the exact solution, however the results are slightly underestimated.

For Specimen B2, the 2-element solution gave a result that differs by 7.3% from the exact solution while the 4, 8, 10, 16, 20 and 24-elements are 0.11, 0.08, 0.08, 0.075, 0.05, and 0.13% in error respectively. The cases of 16 and

20-element models gave the closest agreement with the exact solution and all the solutions gave over-estimated values of buckling load. For both cases the convergence graph (figure A2.2) showed that by using only a 4-element model accurate results can be obtained.

A2.2.1.2 Lateral Buckling of a Simply Supported I-Beam

A2.2.1.2.1 Central Concentrated Load

Figure A2.3(a) shows a simply supported I-beam specimen of 400cm length loaded by a central concentrated load P acting at the shear centre. It is assumed that during deformation the ends of the beam can rotate freely about the principal axes of inertia parallel to the y and z axes. The rotation with respect to the x axis is prevented by some constraint. The exact solution given Timoshenko (2) is;

$$P_{cr} = \frac{\gamma_2 \sqrt{EI_n C}}{L^2} \dots \dots \dots (A2.2)$$

in which I_n is the second moment of area in the minor axis, C is the torsional rigidity (GJ) and, γ_2 is a dimensionless factor which depends upon the ratio $(L^2 GJ/EI_n)$. The values of γ_2 are tabulated in table 6.5 of reference 5.

Table A2.1 shows the data for specimen C1 and C2, and the results of the analysis by exact solutions and the computer predictions are shown in table A2.3. For specimen C1, the finite element solutions gave overestimated values of

buckling load for 4 and 8-element cases. It can be seen that the 8-element solutions differ by 1.59% from the exact solution, while the 10, 16, 20 and 24-element, finite element solutions are 0.82, 0.59, 0.53 and 0.17% in error respectively. In this case, the 24-element gave the closest agreement with the exact solution.

For specimen C2, it can be seen that the finite element computer program gave over-estimated value of buckling load for the 4-element solution which differs by 7.09% from the exact solution. The 8, 10, 16, 20 and 24-element finite element solution however, gave underestimated values which are 0.28, 0.29, 2.72, 2.09 and 2.6% in error respectively. The 8-element model gave the closest results to the exact solution.

The convergence curve shown in figure A2.4 for both the cases presently considered showed that accurate results can be obtained with a 4-element model.

A2.2.1.2.2 Central Concentrated Load at Top Flange

Figure A2.3(b) shows a simply supported I-beam specimen of 400cm length loaded by a central concentrated load acting on the top flange. Assuming the same boundary conditions applied as in section A2.2.1.2.1, the exact solution given by Timoshenko (2) is the same as equation A2.2.

Using the same data of specimen shown in table A2.1 the case of load acting on the top flange was analysed by exact solution and by the Finite Element computer programme. For the Finite Element computer programme, the specimens were modelled with a load applied a certain height above the centroid of the beams. In this case the beam was modelled for 4, 8, 10, 16 and 20 elements along the length of the beam. One perpendicular element with length equal to the height above the centroid was positioned vertically from the centroid of the beam. This vertical element was made stiffer than the rest of the elements and the load was applied on the top end of this perpendicular element.

The results for both cases of specimens C1 and C2 are shown in table A2.4. For specimen C1 the Finite Element gave overestimated values of buckling load for 4 and 8-element models, while the 10, 16 and 20-element models gave slightly underestimated values. The 8-element model gave the closest agreement with the theoretical values. All the cases considered giving less than 1% error, with the exception of the 4-element case.

For specimen C2, it can be seen that only the 4-element model gave over-estimated results whereas the other cases considered giving underestimated results. The 8-element model gave the closest agreement with the theoretical value.

It can be said that exact correlation between the theoretical and the Finite Element formulation were obtained by using 8 elements and more.

A2.2.1.2.3 Central Concentrated Load at Lower Flange

Figure A2.3(c) shows a simply supported I-beam specimen loaded by a central concentrated load acting at the bottom flange. Assuming the same boundary conditions applied as in section A2.2.1.2.1 the exact solution given by Timoshenko (2) is also the same as equation A2.2.

Using the same data of specimen as C1 and C2, the case of concentrated load acting at the bottom flange was analysed by exact solution and by the Finite Element computer programme. The same approach of modelling by the Finite Element method was carried out as in section A2.2.1.2.2. However, the perpendicular element is positioned below the centroid. The load is applied at the bottom tip of that element.

The results for the cases of specimens C1 and C2 are shown in table A2.5. For specimen C1 it can be seen that all the cases gave overestimated results, however, the case of 4-elements gave a grossly overestimated result of 12.3%. The 16 elements gave the closest agreement with the theoretical with only 0.22% error.

For specimen C2, the 4-element case gave overestimated results of 10.24% and the 8 element case gave 0.59% error. The other cases of 10, 16 and 20 elements gave underestimated results of 0.35%, 1.42% and 1.66%. The 10 elements gave the closest agreement with the theoretical.

It can be seen that the Finite Element formulation gave accurate results with 8 elements and more.

A2.2.1.3 Lateral Buckling of Cantilever Beam by Concentrated Load at the Free End

A2.2.1.3.1 Load at the Centre of the Web Free End

Two types of specimens are dealt with in this section. The specimens have the same properties as the beams discussed earlier. Figure A2.5(a) shows a cantilever beam of 400cm length with a concentrated load at the centroid of the free end. The exact solution of this case was presented by Timoshenko (2) and is similar to equation A2.2, however the values of γ is obtained from table 6.3 of reference 2.

Table A2.1 shows the data for specimen D1 and D2, and the results of the analyses by Timoshenko and the predictions by the Finite Element Computer Programme are given in table A2.6. Concerning specimen D1, it can be seen that the Finite Element solutions gave overestimated values of buckling load when a 4-element model was used, but gave

underestimated values for models with a higher number of elements. The 4-element solution differs by 9.35% from the exact solution while the 8, 10, 16, 20 and 24 elements are 3.80, 2.84, 1.70, 1.41 and 1.18% in error, respectively. In this case, the 24-element model gave the closest agreement of buckling load with the exact solution.

For specimen D2, it can be seen that the finite element solution gave over-estimated values of buckling load. The 4-element solution differs by 9.67% from the exact solution, while the 8, 10, 16, 20 and 24-element solutions are 2.7, 1.82, 0.85, 0.61 and 0.61% in error respectively. The 20 and 24-element models gave the closest agreement of buckling load compared with that of the exact solution.

A2.2.1.3.2 Load at Top Flange at the Free End

The effect of load applied at the point of application above or below the end cross section is given by;

$$P_{cr} = \frac{\gamma_2 \sqrt{EI_n C}}{L^2} \left(1 - \frac{a}{L} \sqrt{\frac{EI_n}{C}} \right) \dots (A2.3)$$

in which, I_n is the second moment of area in the minor axis, C is the torsional rigidity (GJ) and γ_2 is a dimensionless factor that depends on the ratio $L^2 GJ / EI_n$. The values of γ_2 are given in table 6.3 in reference 2. In equation A2.3, "a" denotes the distance of the point of application of the load vertically above the centroid (figure A2.5(b)).

Specimens D1 and D2 are used for the analysis by using equation A2.3 and by the finite element method. Modelling for the finite element method was done so that the load can be applied at a height above the centroid. A similar number of element models were used in the analysis as in the previous cases.

The results of the analyses are shown in table A2.7. Concerning specimen D1, it can be seen that the finite element solution gave underestimated results for the 4 and 8-element models, while the 16 and 20-element models gave overestimated results. Except the 4-element model, all other models gave results with errors less than 1%.

Similar types of results are obtained for specimen D2. The 4 and 8-element models gave underestimated results while the 16 and 20-element models gave over-estimated results. Again, except the 4-element model all other models gave less than 1% error when compared to the results of equation A2.3.

In both cases the results of analysis by a 10-element model gave very accurate results with 0% error.

A2.2.1.3.3 Load at the Bottom Flange

Equation A2.3 can also be used when the load is applied

below the centroid of the free end. In this case, it is only necessary to change the displacement "a" to "-a". Figure A2.5(c) shows a cantilever subjected to a concentrated load at the bottom of the flange of the free end.

Specimens D1 and D2 are used again in this section for the analysis by using equation A2.3 and by finite element method. Modelling for the specimens is similar to the previous section, but the loads are applied at the bottom of the flange.

The results of the analyses are shown in table A2.8. For both the specimens D1 and D2, the 4-element model gave underestimated values while the others gave slightly overestimated values when compared to results of equation A2.3. In both the cases the 8-element model gave the closest correlation with the theoretical values. Judging from the results of this section and the previous section, the method of modelling for the effect of the load employed appear to be acceptable.

A2.2.2 Pure Torsional-Buckling

Concerning how an axial compressive load may cause torsional buckling was shown by Timoshenko (2). In his analysis, he considered a doubly symmetric bar of cruciform section (figure A2.6(a)) with four identical

flanges. It was shown that under such load the strut exhibits angular displacements only. The exact solution presented by Timoshenko (2) is given by,

$$P_{cr} = \frac{A}{I_o} \left(\frac{\pi^2 EI_w}{L^2} + GJ \right) \dots \dots \dots (A2.4)$$

The cruciform section used in this analysis is shown in figure A2.6(b) with a length equal to 400cm. The results of the finite element solution with two numbers of elements are compared with the closed form solution. It was found that the results were consistent as reported by Nemir (1). When considering $C_w=0$, the theoretical results based on equation 6, gave a value of 3518.7 kN. Whereas the finite element formulation gave a result of 3518.0 kN.

The general shape of the displacement as obtained from the results was observed to be correct. Therefore the computer program produced results that are consistent with the theoretical values for the specimen considered.

A2.2.3 The Elastic Buckling of Column

The study reported in this section was undertaken to examine the validity and accuracy of the finite element computer program for stability analysis to evaluate the critical load of two cases of column problems for which the exact theoretical solutions are already established (2). The problems considered are; (1) column with built-in base, and (2) column with hinged ends.

A2.2.3.1 Column with Built-in Base

Figure A2.7 shows a slender, ideal column built-in vertically at the base, free at the upper end and subjected to an axial force P . The column is assumed to be perfectly elastic, and the stresses do not exceed the proportional limit.

The equilibrium equation that describes the buckling behaviour of the column known as the Euler equation is presented (2) as follows:

$$P_{cr} = \frac{\pi^2 EI_y}{4L^2} \dots \dots \dots (A2.5)$$

This is the smallest critical load for the column in figure A2.7, that is, the smallest axial force that can maintain the bar in a slightly bent shape. I_y is the minimum value of the second moment of area.

The results of the analysis are shown in table A2.9. It shows an excellent correlation between the Euler equation and that of the finite element method. For specimen CL1 almost accurate results were obtained even using only a 2-element model giving over-estimated results of 0.84% error. The 4-element model gave exact results as the theoretical whilst the 8, 10, 16, 20 and 24-element models gave results in the margin of 0.06-0.07% error.

Similarly for for specimen CL2, the 2-element model gave an

almost accurate result, but underestimated with an error of 0.72%. The 4-element model gave 0.01% error, whilst the 8, 10, 16, and 20-element models also gave over-estimated results with 0.15, 0.28, 0.45, and 0.25% respectively. The 24-element model gave an underestimated result with an error of 1.96%.

A2.2.3.2 Column with Hinged Ends

The critical load for a column with hinged ends, shown in Figure A2.8, is obtained by substituting $L/2$ for L in the Euler equation to give:

$$P_{cr} = \frac{\pi^2 EI}{L^2} \dots\dots\dots (A2.6)$$

The case of a bar with hinged ends is probably assumed in practice more frequently than any other, and it is called the fundamental case of buckling of a prismatic bar.

The results of the finite element analysis shown in Table A2.10 gave an excellent agreement with that of the theoretical values of the critical buckling load. In both cases of specimens CL3 and CL4 almost accurate results can be obtained by using a 2-element model, in which they gave over-estimated results of 0.83 and 0.74% in error respectively. More accurate results were obtained by using models with a larger number of elements.

A2.2.4 Buckling Behaviour of Cold-Formed Channel Subject to Stress Gradient

The study reported in this section was undertaken to examine the validity and accuracy of the finite element formulation for stability analysis of light gauge steel beams subjected to a major axis bending moment applied to one end. The loading on the beam produce a linearly varying distribution of bending moment along the length of the beam.

Leach (3) conducted tests on four different sections over various lengths to compare the results with that of the Generalised Beam Theory. In the tests conducted, the load deflection characteristics of the beams were measured, as were the failure loads. The end conditions of the beam were simply supported but restrained against warping and cross section distortion. Buckling was considered to have occurred when the central rotation of the beam exceeded 0.06 radians, or overall buckling failure had occurred. The results of the tests conducted by Leach (3) are compared with the results of the finite element analysis.

Table A2.11 shows the dimensions of the four sections tested and figure A2.9 shows the cross-section of a lipped and an unlipped channel. The results obtained are shown in figures A2.10, A2.11, A2.12 and A2.13. It can be seen that for Series B and E, there is a close agreement between the

tests, the Generalised Beam Theory and the finite element method especially when the beams are longer than 350cm in both cases. For series G and H, it can be seen that the results of the tests and the two theoretical methods agreed well for long beams, however, they appear to disperse as the beams get shorter.

It can be said from this observation, that accurate results of elastic buckling of cold-formed channels can be obtained using the finite element formulation when the beam specimens are long enough. Grossly over-estimated results are obtained with short beam specimens. The graphs show convergence of the three methods with increase in the length of the beam specimens.

A2.2.5 Torsional-Flexural Buckling of Cold-formed Channel Columns

This section presents a study undertaken to examine the validity and accuracy of the finite element formulation in analysing lateral-torsional buckling of cold-formed channel columns.

For open thin-walled section columns, three modes of failure are possible in the analysis of overall instability. They are flexural-buckling, torsional-buckling and torsional-flexural buckling. During the torsional-flexural buckling mode, bending and twisting of the cross-

section occurs simultaneously. The equation for buckling of thin-walled columns are given (4) as;

$$P_x = \frac{\pi^2 EI_x}{(KL)^2} \dots \dots \dots (A2.7)$$

$$P_y = \frac{\pi^2 EI_y}{(KL)^2} \dots \dots \dots (A2.8)$$

$$P_z = \left[\frac{\pi^2 EC_w}{(KL)^2} + GJ \right] \left(\frac{1}{r_o^2} \right) \dots \dots \dots (A2.9)$$

in which, KL is the effective length of the column. For hinged ends, K=1; for fixed ends, K=0.5. C_w is the warping constant and r_o is the polar radius of gyration of the cross section about the shear centre. Equations A2.7 and A2.8 describe the Euler flexural-buckling load about the x-axis and the y-axis respectively. Equation A2.9 describes torsional buckling about the z axis.

For monosymmetric shape, such as angles, channels, hat sections, T-sections and I-sections with unequal flanges (figure A2.14), the equation for the critical torsional-flexural buckling load can be given (4) as;

$$P_{cr} = \frac{1}{2\beta} \left[(P_x + P_z) - \sqrt{(P_x + P_z)^2 - 4\beta P_x P_z} \right] \dots \dots \dots (A2.10)$$

where $\beta = 1 - (x_o/r_o)^2$, and x_o is the x coordinate of the shear centre. The values of P_x , P_y and P_z are given in equations A2.7, A2.8 and A2.9 respectively.

In the analysis for flexural-torsional buckling of thin-walled sections two types of channel profiles were

considered. These are for both the cases of lipped and unlipped channels. For the lipped channel specimen series B from table A2.11 was used while for unlipped channel specimen H was used. Equations A2.7 to A2.10 were used in the analysis for lengths of specimen B and H equal to 200 cm, 250 cm, 300 cm, 350 cm and 400 cm.

The specimens were also analysed using the finite element method and were modelled with 10-elements each. The results are shown in tables A2.12 and A2.13, and figure A2.15. For both the cases of lipped and unlipped channels, the shorter length of specimens gave better accuracy of results compared to the longer lengths. This is because when the length was increased the critical loads decreased. The percentage error tends to increase when compared to the smaller critical load. Nevertheless the results as shown in figure A2.15 are in closely agreement and within the acceptable limit.

A2.2.6 Elastic Buckling of Beam-Column

Beam-columns are structural members which combine the beam function of transmitting transverse forces or moments with the compression (or tension) member function of transmitting axial forces. In this section only isolated beam-column cases are considered and then only limited to members in axial compression. An example of a beam-column is shown in figure A2.16.

When an unrestrained beam-column is bent about its major axis, it may buckle by deflecting laterally and twisting at a load which is significantly less than the maximum load predicted by an inplane analysis. The flexural-torsional buckling may occur while the member is still elastic, or after some yielding due to inplane bending and compression had occurred.

A2.2.6.1 Beam-Column with Equal and Opposite End Moments

Consider a perfectly straight, elastic beam-column bent about its major axis by equal and opposite end moments M (so that $\beta=-1$), and loaded by an axial force P (figure A2.16). The beam-column, is made of an I-section and therefore doubly symmetrical. The ends of the beams are assumed to be simply supported and free to warp, but end twisting is prevented.

When the applied load and moments reached the critical values P_{oc} , and M_c a deflected and twisted equilibrium position is possible. The elastic buckling combination P_{oc} and M_c is given (5) by,

$$\frac{M_c^2}{r_o^2 P_y P_z} = \left(1 - \frac{P_{oc}}{P_y}\right) \left(1 - \frac{P_{oc}}{P_z}\right) \dots (A2.11)$$

$$P_y = \frac{\pi^2 EI_y}{L^2} \dots \dots \dots (A2.12)$$

$$P_z = \left(\frac{GJ}{r_o^2}\right) \left(1 + \frac{\pi^2 EI_w}{GJL^2}\right) \dots \dots \dots (A2.13)$$

in which r_o is the polar radius of gyration, and P_y and P_z are the minor axis and torsional buckling loads respectively.

Specimen B1 which is shown in table A2.1 was analysed using equations A2.11 to A2.13 with values of $P_{oc}/P_y = 0.2, 0.4, 0.5, 0.6, 0.7$ and 0.8 . The same specimen of beam-column was analysed by the finite element method. The specimens were modelled with 10-elements each and boundary conditions as stated above.

The results of the analysis are shown in table A2.14. It can be seen that there is a close agreement between the results of analysis by equations A2.11-A2.13, and that of the finite element method. However the results of the analysis by the finite element method appear to give a slightly lower value. This is also shown in figure A2.17 in which the finite element results are more conservative. The average error in this analysis is 1-2%.

Therefore it can be said that this finite element formulation is able to predict, accurately, the behaviour

of beam-columns with equal and opposite moments at the ends.

A2.2.6.2 Beam-Column with Unequal End Moments

The elastic flexural-torsional buckling of simply supported beam-columns with unequal major axis end moments M and βM has been investigated numerically (5). Horne (6) proposed a conservative interaction equation which gave the approximate equation for elastic buckling of beam-columns in a form;

$$\frac{(M_c/\sqrt{F})^2}{M_{yz}^2} = \left(1 - \frac{P_{oc}}{P_y}\right) \cdot \left(1 - \frac{P_{oc}}{P_z}\right) \dots\dots (A2.14)$$

Cuk and Trahir (7) however, gave a more accurate prediction of elastic buckling of beam-columns with unequal end moments by the following equations;

$$\left(\frac{M_c}{C_{bc}M_{yz}}\right)^2 = \left(1 - \frac{P_{oc}}{P_y}\right) \cdot \left(1 - \frac{P_{oc}}{P_z}\right) \dots\dots (A2.15)$$

where;

$$\frac{1}{C_{bc}} = \left(\frac{1-\beta}{2}\right) + \left(\frac{1+\beta}{2}\right)^3 \left(0.40 - 0.23 \frac{P}{P_y} \dots\dots (A2.16)\right)$$

$$M_{yz} = \frac{\pi\sqrt{(EI_y GJ)}}{L} \sqrt{\left(1 + \frac{\Pi^2 e i_w}{GJL^2}\right)} = r_o \sqrt{P_y P_z} \dots\dots (A2.17)$$

Beam-columns with the cross-section properties of specimen

B1 and conditions as shown in figure A2.18 were analysed for the critical moment using equations A2.15, A2.16 and A2.17. The values of P_{oz}/P_y used in the analysis are; 0.2, 0.4, 0.5, 0.6, 0.8 and 0.9. Similarly, the same specimens of beam-columns were analysed by the finite element method using 10-element models. The results of the analysis are shown in table A2.15.

The results in table A2.15 and figure A2.19 show that there is a close agreement between the results of analysis by the equation A2.15 and that of the finite element method. However, the finite element results gave a slightly higher value. This is in contrast to beam-columns with equal and opposite moments considered earlier, in which case the finite element method gave results with lower values.

A2.3 Results of Verification

Tables A2.2 to A2.15 show the results of the computer predictions of the elastic buckling loads of the models mentioned earlier. It can be seen that the Finite Element computer program gave accurate results when compared to the exact solution for all the cases under consideration. The procedure followed to predict the buckling load, which is known as "the modified Southwell plot" has proved to be very efficient and a straight forward technique.

One major advantage of the computer program is that it

calculates the displacement so that the general shape of the buckling mode can be observed.

A2.4 Summary and Conclusion

The finite element method formulation found in Reference (1) was used to analyse varieties of torsional flexural buckling problems using the corresponding 'SPACE' computer program. The cases considered can be summarised as follows:

- (a) Four types of conventional buckling problems were investigated, namely,
 - 1. Lateral buckling of a simply supported I-beam by uniform bending;
 - 2. Lateral buckling of a simply supported I-beam by central concentrated load, for cases of load at the centroid, top flange and bottom flange.
 - 3. Lateral buckling of I-cantilevers by a concentrated load at the free end. The cases of load at the centroid, top flange and bottom flange were considered.
 - 4. Pure torsional buckling of an axially loaded strut.
- (b) Two types of conventional column buckling problems were investigated, namely;
 - 1. Column with built-in base;
 - 2. Column with hinged ends.
- (c) Four types of cold-form channel subject to stress

gradient were investigated. They were;

1. Cold-formed lipped channel series B;
2. Cold-formed lipped channel series E;
3. Cold-formed unlipped channel series G; and
4. Cold-formed unlipped channel series H.

(d) Cold-formed channel section column. And

(e) Elastic buckling of Beam-column.

The results of the analyses by finite element method were compared with the results of solutions by other accurate alternative means or tests results. All the cases considered showed a good convergence of the finite element solutions and in excellent agreement with alternative solutions.

From the above discussion, it can be concluded that the finite element formulation presented by Nemir (1) was valid in solving most of the conventional lateral buckling problems.

A2.5 References

- 1) Nemir M.T.M "The Finite Element Stability Analysis of Thin-walled steel structures" Ph.D Thesis submitted to University of Salford, 1985.
- 2) Timoshenko and Gere "Theory of Elastic Stability " McGraw-Hill Book Co. New York, 1961.
- 3) Leach P "The Generalised Beam Theory with Finite Difference Applications" Ph.D thesis submitted to University of Salford, 1989.

- 4) Wei Wen Yu "Cold formed steel structures- Design and Analysis" Robert E Kneiger Publishing Co. Malabar, Florida 1973.
- 5) Trahair N.S and Bradford M.A "The Behaviour and Design of Structures" Chapman and Hall, 1988. 1988.
- 6) Horne M.R "The flexural Torsional Buckling of members of symmetrical I-section under combined thrust and unequal terminal moments" Quarterly Journal of Mechanics and Applied Mathematics, 7, pp 410-26, 1954.
- 7) Cuk P.E and Trahair N.S "Elastic Buckling of beam-column with unequal end moments" Civil Engineering Transactions, Institute of Engineers Australia. CE 23, no 3, August 1981.

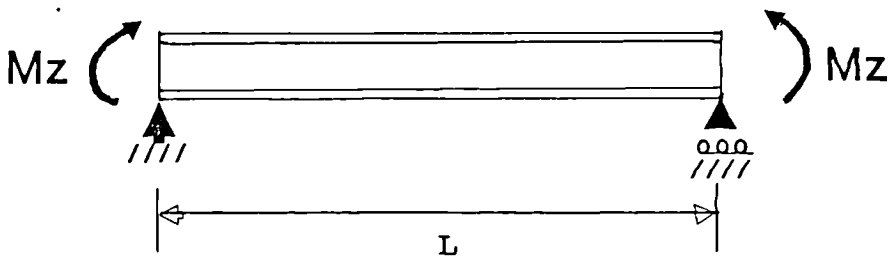


Figure A2.1 Simply Supported I-beam in Pure Bending

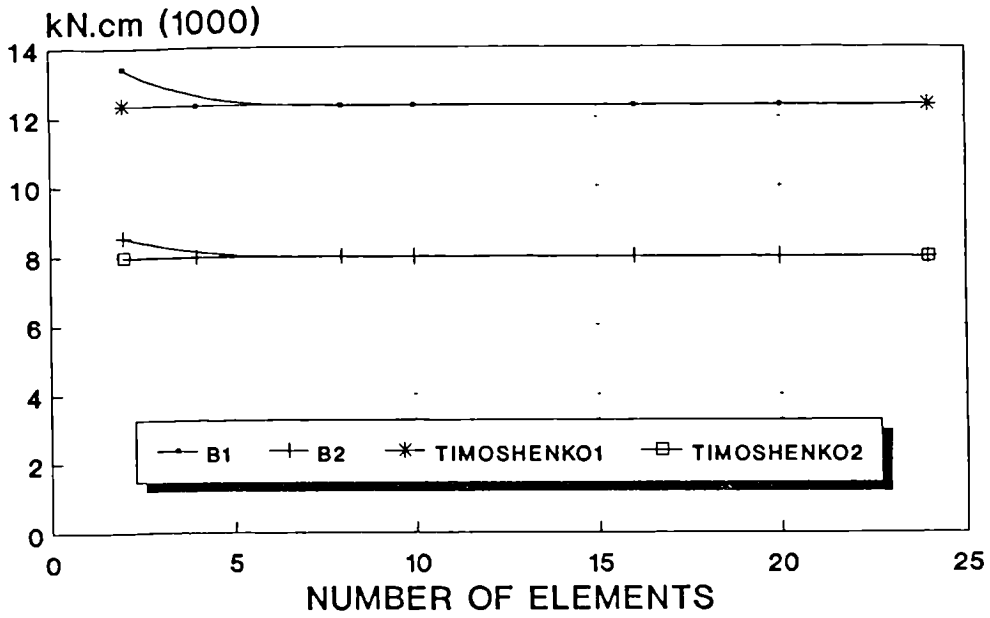


Figure A2.2 Convergence Graphs for Simply Supported I-Beam in Pure Bending

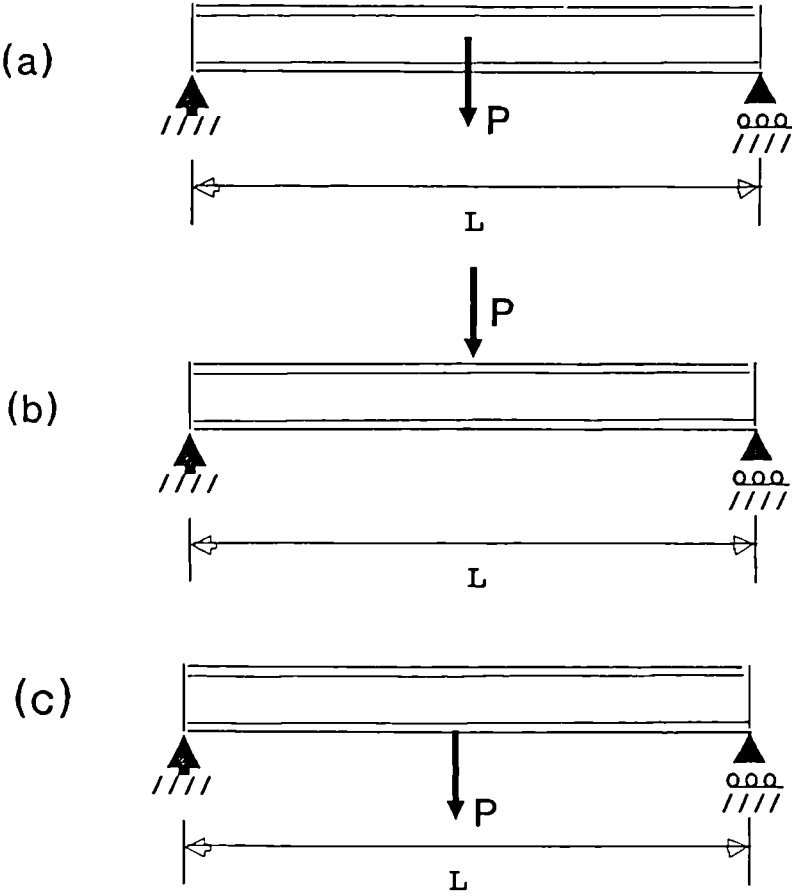


Figure A2.3 Simply Supported I-beam with;
(a) central concentrated load
(b) load at top flange
(c) load at bottom flange

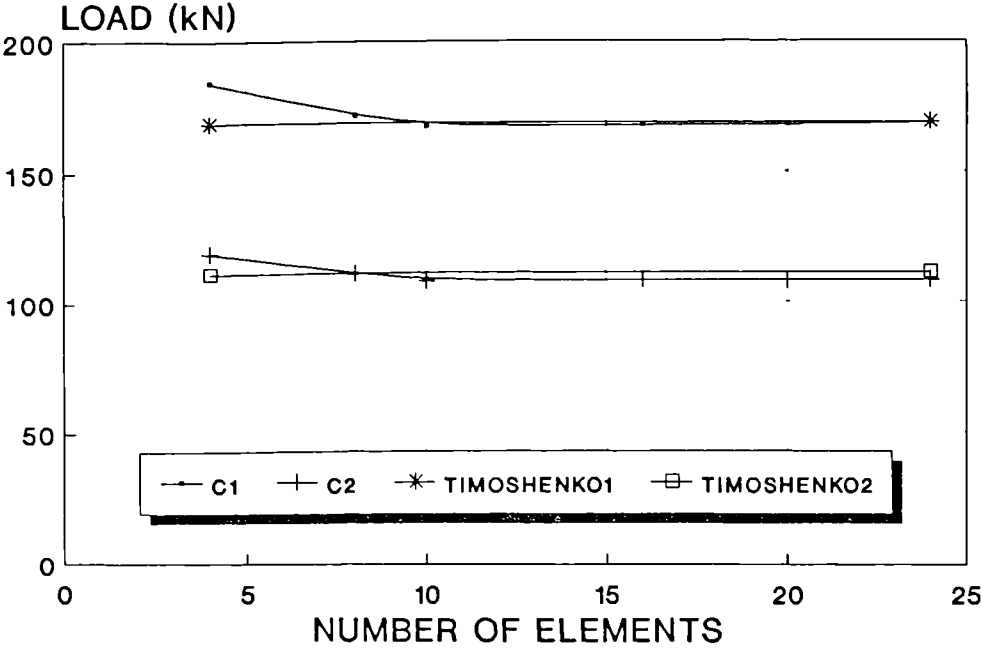


Figure A2.4 Convergence Graphs for Simply Supported I-Beam with Central Concentrated Load

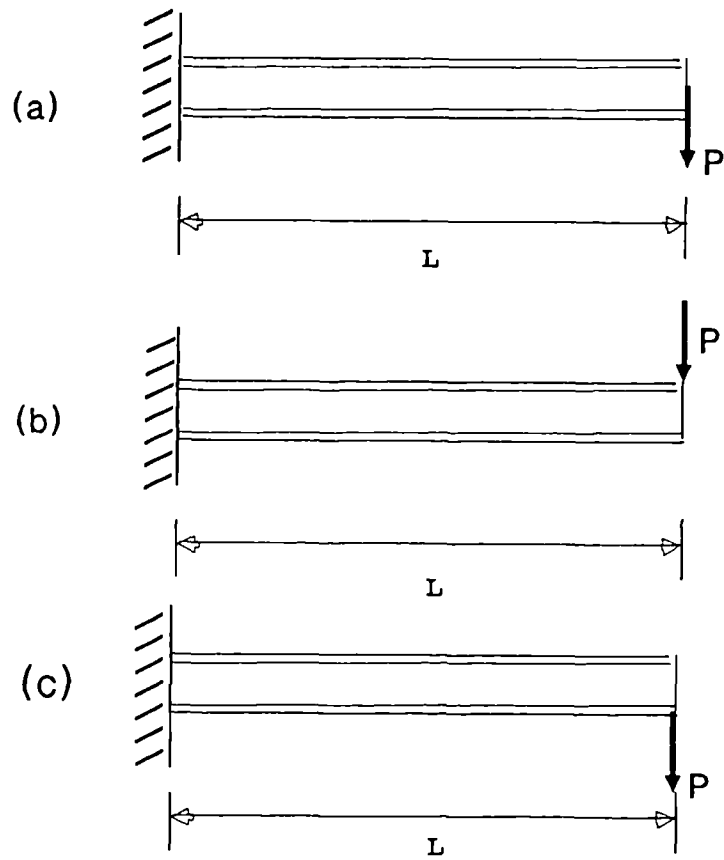


Figure A2.5 Cantilever with concentrated load at free end;
(a) centroid
(b) top flange
(c) bottom flange

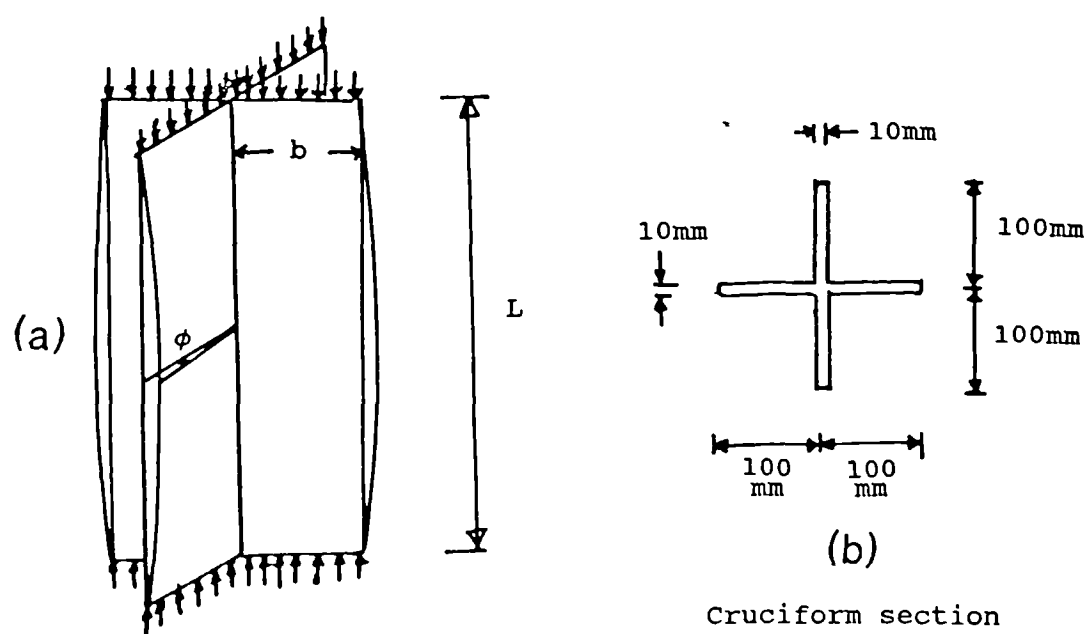


Figure A2.6 Cruciform member; Pure torsional buckling.

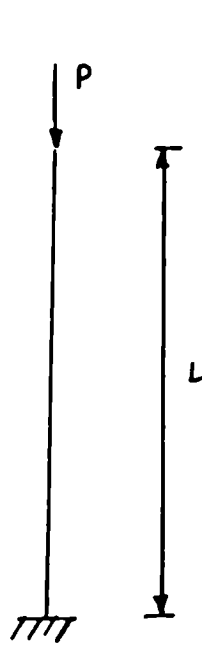


Figure 2.7
Column with Built-in Base

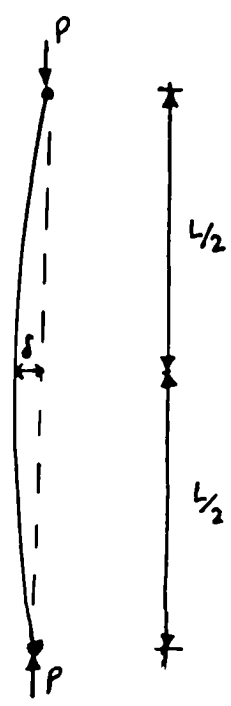
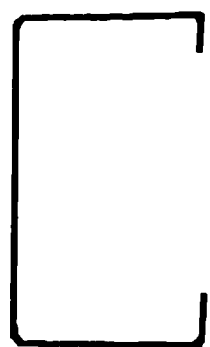


Figure 2.8
Column with hinged-Ends



Lipped Channel



Unlipped Channel

Figure A2.9 Channel Sections used in "Leach" Tests

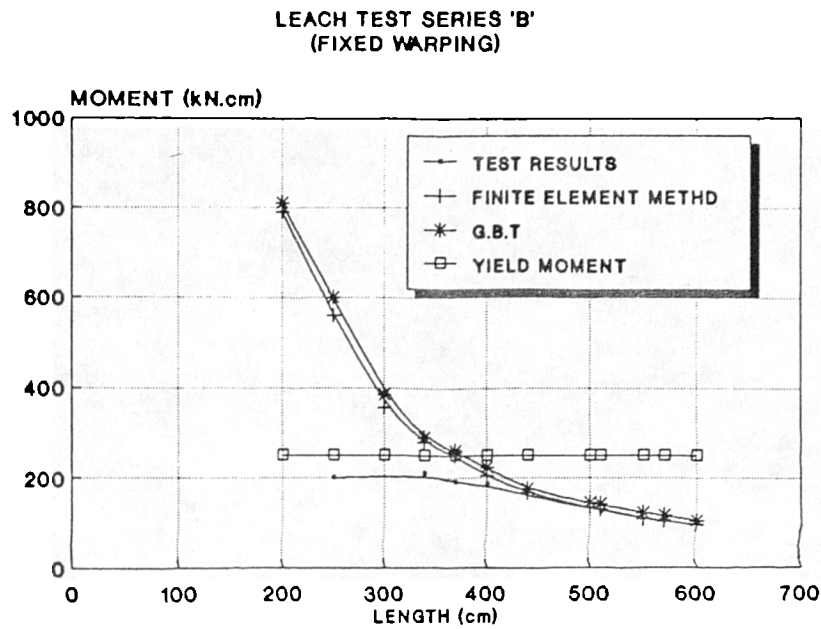


Figure A2.10 Comparison of Results of "Leach" Test, GBT and Finite Element Method (Series B)

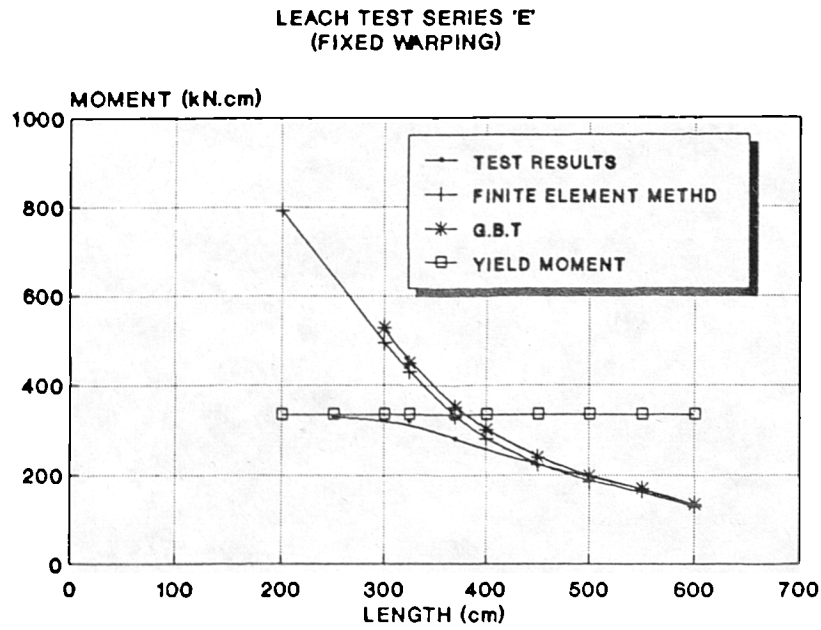


Figure A2.11 Comparison of Results of "Leach" Test, GBT and Finite Element Method (Series E)

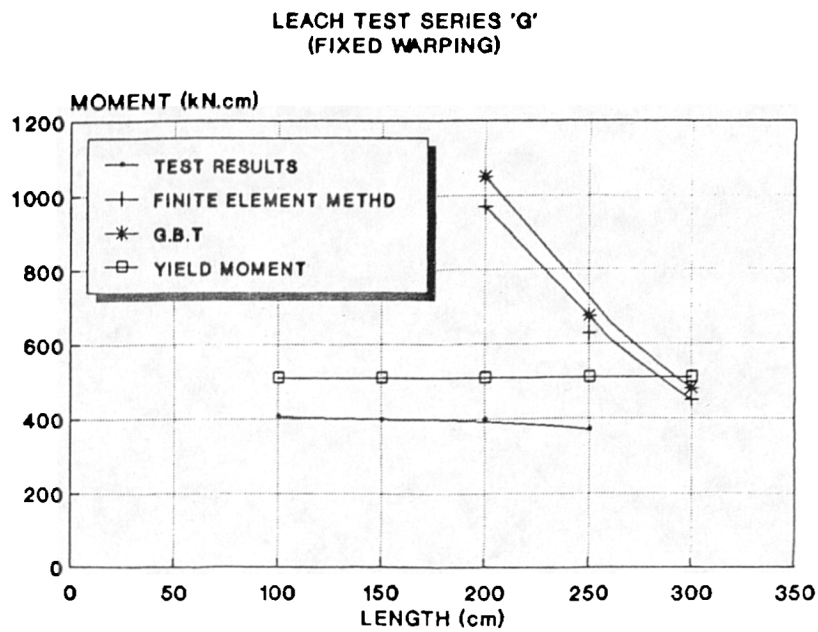


Figure A2.12 Comparison of Results of "Leach" Test, GBT and Finite Element Method (Series G)

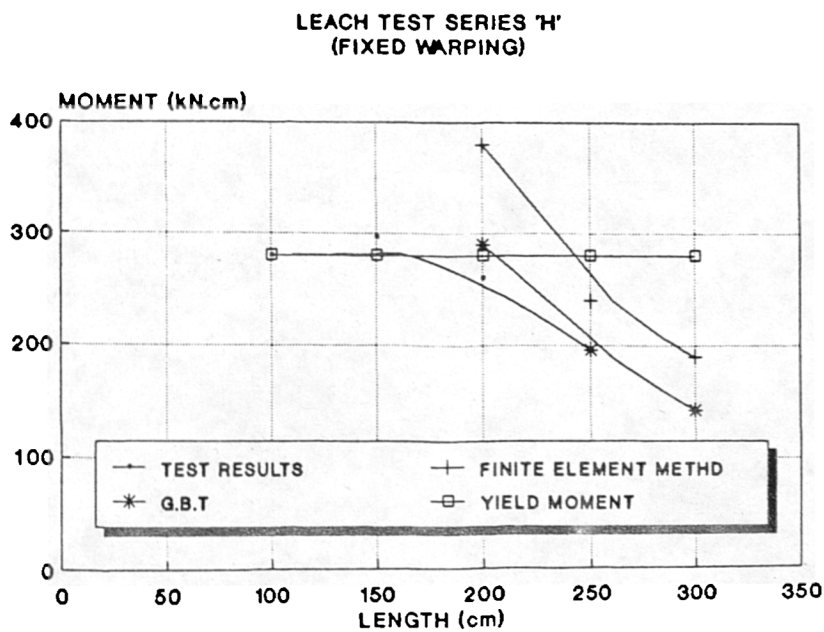


Figure A2.13 Comparison of Results of "Leach" Test, GBT and Finite Element Method (Series H)

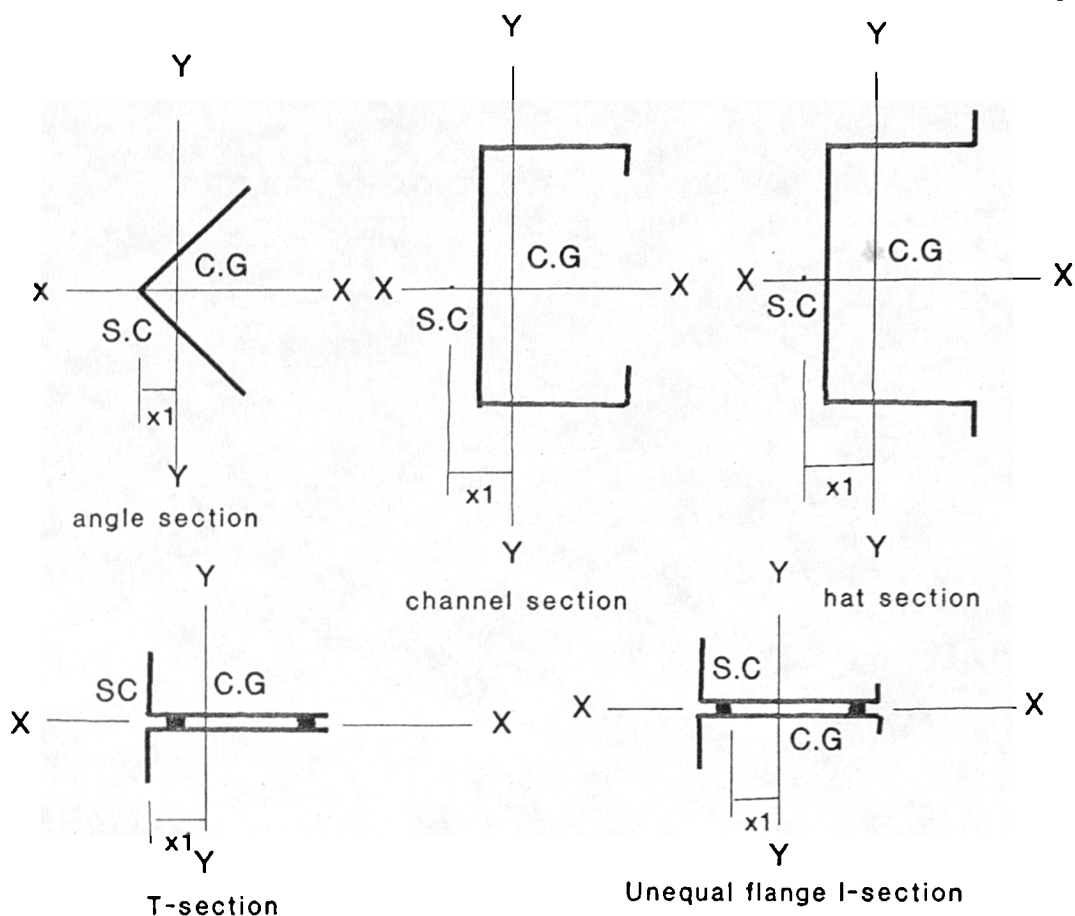


Figure A2.14 Examples of Cold-Formed Section

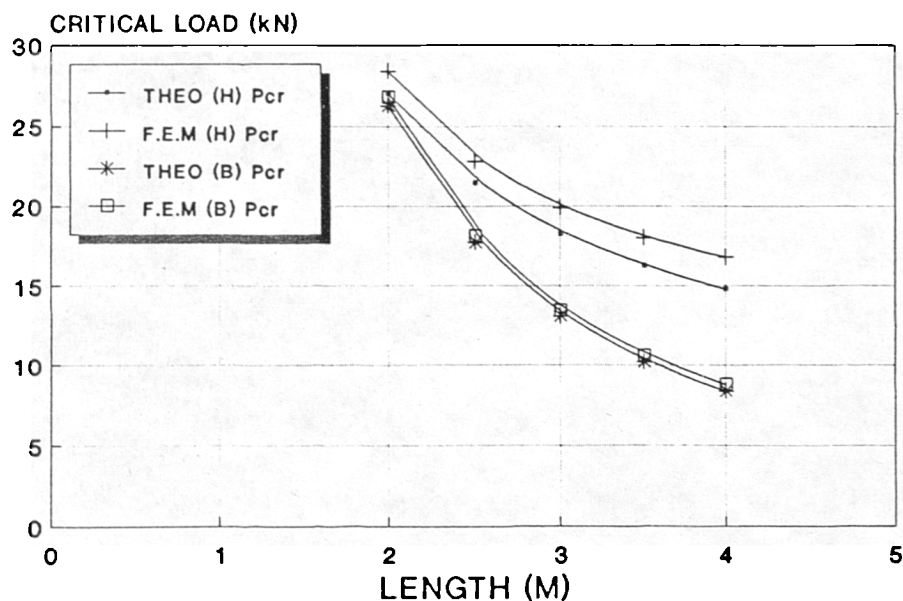


Figure A2.15 Comparison of Theoretical and Finite Element Results for Cold-Formed Column with Hinged Ends (Series B and H)

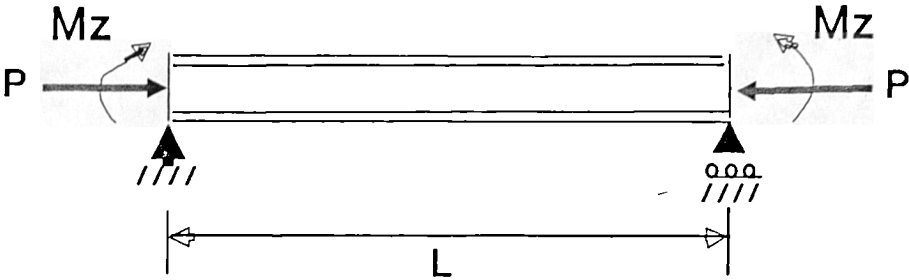


Figure A2.16 Beam-Column with Equal and Opposite End Moment

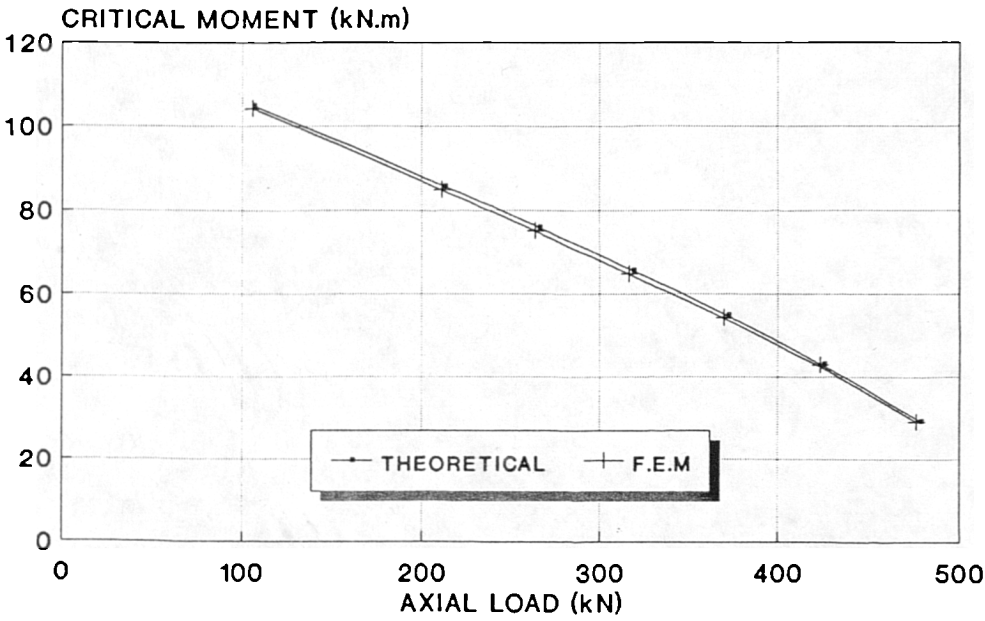


Figure A2.17 Comparison of Theoretical and Finite Element Results for Analysis of Beam-Column with Equal and Opposite End Moments

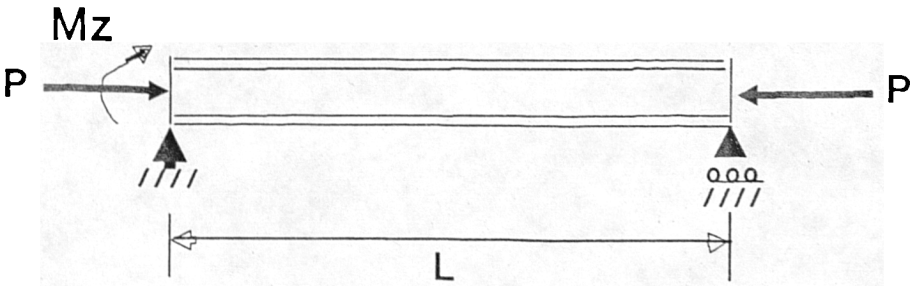


Figure A2.18 Beam-Column with Unequal End Moments

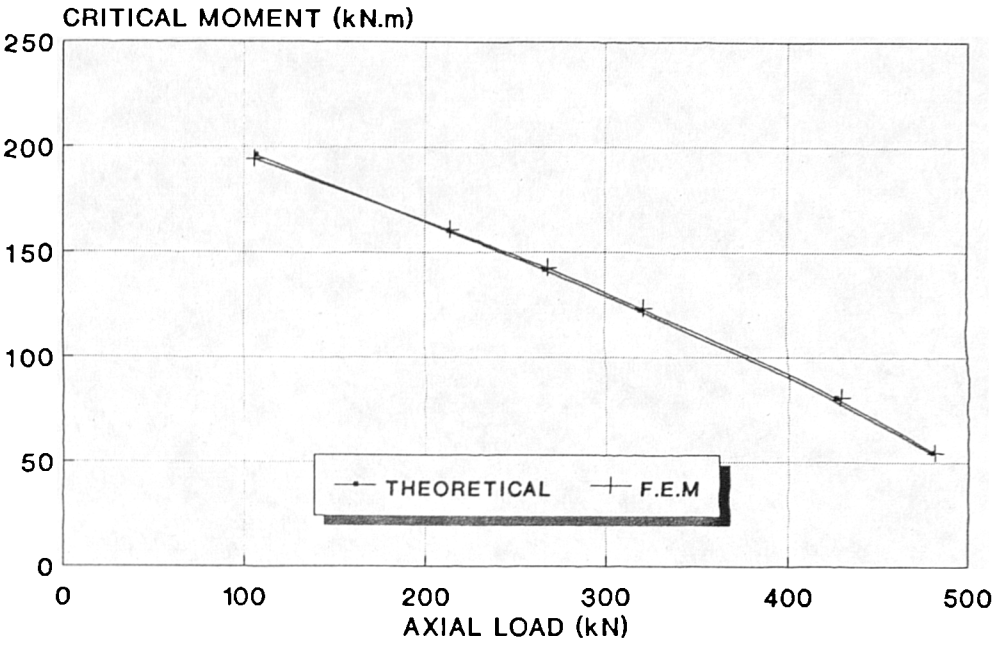
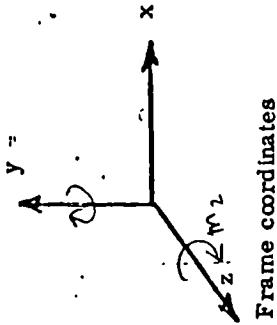


Figure A2.19 Comparison of Theoretical and Finite Element Results for Analysis of Beam-Column with Unequal End Moments

DATA FOR SPACE FRAME ANALYSIS (7 degree of freedom version)



Job No.	Title.....																			

NJS	NMS	NMTS	NBMS	NBMTS	MODE	JCN	JCDF	Tolerance

joint coordinate

Joint	Ja	x			y			z		

Mode ϕ = Single analysis - several load vectors
Mode 1 = Stability analysis at single load level (one vector only)
Mode 2 = Repeated cycles to critical load
Mode 3 = *do - full iteration*

Member properties		Area		I_r		I_2		I_3		C_w		GJ		QS		RS	
E	I_0		I_1		I_2		I_3		I_4		I_5		QZ		QS	AZ	

Member data

Type	JA	JB	JC	QC	RC	PCA	PCB

Load data

NLJS	NILS	NINTS

load vectors

No.	D of F	Load case 1	Load case 2

--	--	--	--	--	--	--	--	--	--	--	--	--	--	--	--	--	--	--	--	--

Note: Identical data applies to 6 degree of freedom version except that (1) JDF has only 6 degrees of freedom
(2) Cw becomes QZR
(3) Second member property card is omitted

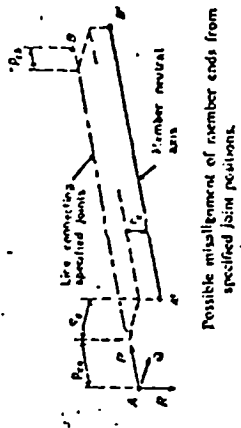


Table A2.1 Properties of Beam Specimen

	SECTION PROPERTIES FOR 406x140x36 UB	SECTION PROPERTIES FOR 356x127x33 UB
FLANGE WIDTH B (cm)	14.18	12.54
OVERALL DEPTH D (cm)	39.73	34.85
WEB THICKNESS t (cm)	0.63	0.59
FLANGE THICKNESS T (cm)	0.86	0.85
AREA A (cm ²)	49.40	41.80
TORSION CONSTANT J (cm ⁴)	10.60	8.68
WARPING CONSTSNT C _w (cm ⁶)	0.155E+6	0.081E+6
2nd MOMENT AREA I _{xx} (cm ⁴)	12500	8200
2nd MOMENT AREA I _{yy} (cm ⁴)	411	280
YOUNG'S MODULUS E (kN/cm ²)	0.210E+5	0.210E+5
TORSIONAL RIGIDITY C (kNcm ²)	84800	69440
WARPING RIGIDITY C ₁ (kNcm ⁴) 0	3.276E+9	1.701E+9

Table A2.2 Results of Analysis of Beam B1 and B2.
(Case of Lateral buckling in pure bending)

RESULTS	SPECIMEN B1 MOMENT kNcm % ERROR	SPECIMEN B2 MOMENT kNcm % ERROR
EXACT SOLUTION (TIMOSHENKO)	12353	7953
F.E.M 2-ELEMENT MODEL	13392 (8.4%)	8536 (7.3%)
F.E.M 4-ELEMENT MODEL	12342 (0.09%)	7962 (0.11%)
F.E.M 8-ELEMENT MODEL	12338 (0.12%)	7960 (0.08%)
F.E.M 10-ELEMENT MODEL	12338 (0.12%)	7960 (0.08%)
F.E.M 16-ELEMENT MODEL	12337 (0.13%)	7959 (0.07%)
F.E.M 20-ELEMENT MODEL	12337 (0.13%)	7959 (0.07%)
F.E.M 24-ELEMENT MODEL	12346 (0.05%)	7964 (0.13%)

Table A2.3 Results of Analysis of Beam C1 and C2. (Case of Lateral buckling by central concentrated load applied at the centroid)

RESULTS	SPECIMEN C1		SPECIMEN C2	
	LOAD	% ERROR	LOAD	% ERROR
	kN		kN	
EXACT SOLUTION (TIMOSHENKO)	168.9		111.4	
F.E.M 4-ELEMENT MODEL	184.5	(9.23%)	119.3	(7.09%)
F.E.M 8-ELEMENT MODEL	171.6	(1.59%)	111.1	(0.28%)
F.E.M 10-ELEMENT MODEL	167.5	(0.82%)	108.1	(2.91%)
F.E.M 16-ELEMENT MODEL	167.9	(0.59%)	108.4	(2.09%)
F.E.M 20-ELEMENT MODEL	168.0	(0.53%)	108.4	(2.09%)

Table A2.4 Results of Analysis of Beam C1 and C2 (Case of Lateral buckling by central concentrated load applied at the top flange)

RESULTS	SPECIMEN C1		SPECIMEN C2	
	LOAD	% ERROR	LOAD	% ERROR
	kN		kN	
EXACT SOLUTION (TIMOSHENKO)	106.7		72.2	
F.E.M 4-ELEMENT MODEL	111.2	(4.20%)	74.28	(2.88%)
F.E.M 8-ELEMENT MODEL	106.8	(0.09%)	71.12	(1.49%)
F.E.M 10-ELEMENT MODEL	106.4	(0.28%)	70.80	(1.93%)
F.E.M 16-ELEMENT MODEL	105.9	(0.75%)	70.40	(2.41%)
F.E.M 20-ELEMENT MODEL	105.8	(0.84%)	70.38	(2.52%)

Table A2.5 Results of Analysis of Beam C1 and C2 (Case of Lateral buckling by central concentrated load applied at the bottom flange)

RESULTS	SPECIMEN C1		SPECIMEN C2	
	LOAD	% ERROR	LOAD	% ERROR
	kN		kN	
EXACT SOLUTION (TIMOSHENKO)	267.3		169.7	
F.E.M 4-ELEMENT MODEL	300.3	(12.3%)	187.1	(10.2%)
F.E.M 8-ELEMENT MODEL	273.5	(2.39%)	120.7	(0.59%)
F.E.M 10-ELEMENT MODEL	270.8	(1.30%)	169.1	(0.35%)
F.E.M 16-ELEMENT MODEL	267.9	(0.22%)	167.3	(1.42%)
F.E.M 20-ELEMENT MODEL	268.6	(0.48%)	166.8	(1.66%)

Table A2.6 Results of Analysis of Beam D1 and D2 (Case of Lateral buckling of cantilever by concentrated load applied at the centroid of the free end)

RESULTS	SPECIMEN D1		SPECIMEN D2	
	LOAD	% ERROR	LOAD	% ERROR
	kN		kN	
EXACT SOLUTION (TIMOSHENKO)	52.15		34.00	
F.E.M 4-ELEMENT MODEL	57.03	(9.35%)	37.29	(9.67%)
F.E.M 8-ELEMENT MODEL	50.14	(3.80%)	34.93	(2.71%)
F.E.M 10-ELEMENT MODEL	50.67	(2.84%)	34.62	(1.82%)
F.E.M 16-ELEMENT MODEL	51.26	(1.70%)	34.29	(0.85%)
F.E.M 20-ELEMENT MODEL	51.41	(1.41%)	34.21	(0.61%)
F.E.M 24-ELEMENT MODEL	51.53	(1.18%)	34.21	(0.61%)

Table A2.7 Results of Analysis of Beam D1 and D2 (Case of Lateral buckling of cantilever by concentrated load applied at the top flange of the free end)

RESULTS	SPECIMEN D1		SPECIMEN D2	
	LOAD	% ERROR	LOAD	% ERROR
	kN		kN	
EXACT SOLUTION (TIMOSHENKO)	26.00		20.37	
F.E.M 4-ELEMENT MODEL	25.10	(3.46%)	19.57	(3.92%)
F.E.M 8-ELEMENT MODEL	25.90	(0.38%)	20.27	(0.49%)
F.E.M 10-ELEMENT MODEL	26.00	(0.00%)	20.37	(0.00%)
F.E.M 16-ELEMENT MODEL	26.11	(0.42%)	20.47	(0.49%)
F.E.M 20-ELEMENT MODEL	26.13	(0.50%)	20.50	(0.63%)

Table A2.8 Results of Analysis of Beam D1 and D2 (Case of Lateral buckling of cantilever by concentrated load applied at the bottom flange of the free end)

RESULTS	SPECIMEN D1		SPECIMEN D2	
	LOAD	% ERROR	LOAD	% ERROR
	kN		kN	
EXACT SOLUTION (TIMOSHENKO)	78.26		47.67	
F.E.M 4-ELEMENT MODEL	73.56	(6.00%)	45.62	(4.15%)
F.E.M 8-ELEMENT MODEL	78.05	(0.28%)	48.48	(1.48%)
F.E.M 10-ELEMENT MODEL	78.63	(0.47%)	48.86	(2.64%)
F.E.M 16-ELEMENT MODEL	79.26	(1.20%)	49.30	(3.57%)
F.E.M 20-ELEMENT MODEL	79.40	(1.45%)	49.40	(3.78%)

Table A2.9 Results of Analysis of Column CL1 and CL2 (Case of column with built-in base)

RESULTS	SPECIMEN CL1		SPECIMEN CL2	
	LOAD	% ERROR	LOAD	% ERROR
	kN		kN	
EXACT SOLUTION (EULER)	133.1		90.67	
F.E.M 2-ELEMENT MODEL	131.98	(0.84%)	90.01	(0.72%)
F.E.M 4-ELEMENT MODEL	133.10	(0.00%)	90.68	(0.01%)
F.E.M 8-ELEMENT MODEL	133.20	(0.07%)	90.81	(0.15%)
F.E.M 10-ELEMENT MODEL	133.20	(0.07%)	90.93	(0.28%)
F.E.M 16-ELEMENT MODEL	133.20	(0.07%)	91.08	(0.45%)
F.E.M 20-ELEMENT MODEL	133.02	(0.06%)	90.90	(0.25%)
F.E.M 24-ELEMENT MODEL	133.18	(0.06%)	88.89	(1.96%)

Table A2.10 Results of Analysis of Column CL3 and CL4 (Case of column with pinned-ends)

RESULTS	SPECIMEN CL3		SPECIMEN CL4	
	LOAD	% ERROR	LOAD	% ERROR
	kN		kN	
EXACT SOLUTION (EULER)	532.00		362.7	
F.E.M 2-ELEMENT MODEL	536.40	(0.83%)	365.4	(0.74%)
F.E.M 4-ELEMENT MODEL	532.79	(0.15%)	362.9	(0.05%)
F.E.M 8-ELEMENT MODEL	532.43	(0.08%)	362.7	(0.00%)
F.E.M 10-ELEMENT MODEL	532.42	(0.08%)	362.7	(0.00%)
F.E.M 16-ELEMENT MODEL	532.41	(0.08%)	362.7	(0.00%)
F.E.M 20-ELEMENT MODEL	532.41	(0.08%)	362.7	(0.00%)
F.E.M 24-ELEMENT MODEL	532.84	(0.16%)	363.0	(0.08%)

Table A2.11 Section properties for "Leach Test"

SERIES	DEPTH (mm)	WIDTH (mm)	LIP SIZE (mm)	THICKNESS (mm)	LENGTH (mm)
B *	90	50	15	1.20	1500-6000
E *	120	50	15	1.20	1500-6000
H #	90	40	0	1.90	800-3000
G #	120	50	0	1.90	800-300

Note ; * Lipped Channels
Unlipped Channels

Table A2.12 Results of Analysis for Torsional-Flexural Buckling of Lipped Channel (Series B)

Length (cm)	Theoretical P_{cr} (kN)	Finite Element Method (kN)
200	26.26	26.79 (2.01%)
250	17.69	18.13 (2.5%)
300	13.13	13.46 (2.51%)
350	10.20	10.62 (4.12%)
400	8.36	8.8 (5.26%)

Table A2.13 Results of Analysis for Torsional-Flexural Buckling of Unlipped Channel (Series H)

Length (cm)	Theoretical P_{cr} (kN)	Finite Element Method (kN)
200	26.99	28.37 (5.10%)
250	21.44	22.83 (6.48%)
300	18.22	19.88 (9.11%)
350	16.26	18.01 (10.7%)
400	14.81	16.81 (13.5%)

Table A2.14 Results of Analysis of Beam-Column with Equal and Opposite End Moments.

P_{oc}/P_y	Theoretical		Finite Element Method	
	P (kN)	M_c (kNcm)	P (kN)	M_c (kNcm)
0.2	106.4	10483	105.8	10421
0.4	213	8575	211.2	8487
0.5	266	7589	263.4	7507
0.6	319.2	6567	316.4	6486
0.7	372.4	5488	369.7	5434
0.8	425.6	4313	423.7	4292
0.9	478.8	2926	476.5	2911

Table A2.15 Results of Analysis of Beam-Column with Unequal End Moments.

P_{oc}/P_y	Theoretical		Finite Element Method	
	P_{ox} (kN)	M_{oc} (kNcm)	P_{oc} (kN)	M_{oc} (kNcm)
0.2	106.4	19592	105.6	19430
0.4	212.8	16028	213.7	16091
0.5	266	14184	267.9	14279
0.6	319.2	12272	321.4	12341
0.8	425.6	8061	429.0	8108
0.9	478.8	5469	481.2	5485

DESIGN OF PRISMATIC MEMBER FOR LATERAL STABILITY IN ACCORDANCE TO BS5950; PART 1.

EXAMPLE OF CALCULATION FOR LATERAL-TORSIONAL BUCKLING FOR THE CASE OF SIMPLY SUPPORTED BEAM SUBJECTED TO EQUAL AND OPPOSITE MOMENT AT BOTH ENDS, (i.e CASE 1). 203x133xUB30.

NOTE; DESIGN CODE BS5950 BASED ITS DESIGN FOR LATERAL BUCKLING FOR OTHER LOADING CONDITIONS ON THE CASE OF SIMPLY SUPPORTED BEAM WITH UNIFORM MOMENT

PROPERTIES OF BEAM

D := 206.8	mm	Sx := 313	cm ³
tf := 9.6	mm	G := 8000	kN/cm ²
Ix := 2900	cm ⁴	E := 20500	kN/cm ²
Zy := 57.4	cm ³	tw := 6.3	mm
ryy := 3.2	cm	r := 7.6	mm
L := 400	cm	Zx := 279	cm ³
a := 0.5 · D · 0.1	cm	Sy := 88.05	cm ³
b := 133.8	mm	py := 275	N/MM ²
A := 38.1	cm ²	Iy := 383.3	cm ⁴

DESIGN CALCULATIONS TO ESTABLISH THE VALUE OF Mp, Mb AND Me

(1) CALCULATION OF TORSION CONSTANT ; CLAUSE B.2.5.1(c)

$$\begin{aligned} t1 &:= tf & t2 &:= tf & b1 &:= b & b2 &:= b \\ hw &:= D - 2 \cdot tf \end{aligned}$$

$$J := \frac{\frac{1}{3} t1^3 \cdot b1 + \frac{1}{3} t2^3 \cdot b2 + \frac{1}{3} tw^3 \cdot hw}{10000} \quad \text{i.e.} \quad J = 9.455 \text{ cm}^4$$

(2) CALCULATION OF WARPING CONSTANT H ; CLAUSE B.2.5.1(c)

$$hs := D - tf$$

$$H := \frac{hs^2 \cdot t1 \cdot t2 \cdot b1 \cdot b2}{12 \cdot \left[t1^3 \cdot b1 + t2^3 \cdot b2 \right] \cdot 10^6} \quad \text{i.e.} \quad H = 3.726 \cdot 10^4$$

(3) BUCKLING PARAMETER u; CLAUSE B.2.5.1(b)

$$\Gamma := 1 - \left[\frac{Iy}{Ix} \right] \quad \text{i.e.} \quad \Gamma = 0.868$$

$$u := \left[\frac{Iy \cdot Sx^2 \cdot \Gamma}{A \cdot H} \right]^{0.25} \quad \text{i.e.} \quad u = 0.881$$

(4) TORSIONAL INDEX x ; CLAUSE B.2.5.1(b)

$$x := 1.132 \cdot \left[\frac{A \cdot H}{I_y \cdot J} \right]^{0.5} \quad \text{i.e.} \quad x = 22.404$$

NOTE ;

" APPROXIMATION OF u GIVEN IN CLAUSE 4.3.7.5 IS $u=0.9$
 APPROXIMATION OF x GIVEN IN CLAUSE 4.3.7.7 IS $x=D/t_f$
 IS 21.542 "

(5) SLENDERNESS FACTOR v . CLAUSE B.2.5.1(d) AND CLAUSE 4.3.5

$$\lambda := \frac{L}{r_{yy}} \quad N := 0.5$$

$$v := \left[\left[4 \cdot N \cdot (1 - N) + \left[\frac{1}{20} \right] \cdot \left[\frac{\lambda}{x} \right]^2 \right]^{0.5} \right]^{-0.5} \quad \text{i.e.} \quad v = 0.791$$

(6) CALCULATION OF BUCKLING RESISTANCE MOMENT

(a) FROM TABLE 6 OF BS5950, $p_y=275 \text{ N/mm}^2$ i.e $t_f < 16$

(b) FROM TABLE 7 OF BS5950,

$b/t_f=6.97$, THEREFORE THE COMPRESSION FLANGE
 IS CLASSIFIED AS PLASTIC

$D/t_w=32.82$, THEREFORE THE WEB WITH A NEUTRAL AXIS AT
 MID DEPTH IS CATEGORISED AS PLASTIC

(7) PLASTIC MOMENT CAPACITY (LOW SHEAR LOAD)

FROM CLAUSE 4.2.5,

$$M_p := p_y \cdot \frac{S_x}{1000} \quad M_p = 86.075 \quad \text{kNm}$$

(8) CALCULATION OF BUCKLING MOMENT M_b

(a) BY CONSERVATIVE APPROACH AS GIVEN IN CLAUSE 4.3.7.7

$$\lambda = 125$$

$$x = 22.404$$

FROM TABLE 19(b); THE BENDING STRENGTH $p_b=146 \text{ N/mm}^2$

THEREFORE $M_b=p_b \cdot S_x/1000= 45.7 \text{ kNm}$

(b) BY MORE ACCURATE APPROACH AS GIVEN IN CLAUSE 4.3.7.3

$$\frac{\lambda}{x} = 5.579 \quad N = 0.5 \quad v = 0.791$$

CLAUSE 4.3.7.5; λ_{LT} THE EQUIVALENT SLENDERNESS IS CALCULATED. FROM TABLE 13 FOR MEMBER SUBJECTED TO DESTABILISING LOAD, $m=1$ AND $n=1$.

$$n := 1$$

$$\lambda_{LT} := n \cdot u \cdot v \cdot \lambda \quad \text{i.e.} \quad \lambda_{LT} = 87.094$$

FROM TABLE 11, THE VALUE OF p_b IS OBTAINED

$$p_b := 150 \quad \text{N/mm}^2$$

$$\text{THEREFORE} \quad M_b := p_b \cdot \frac{S_x}{1000} \quad \text{i.e.} \quad M_b = 46.95 \quad \text{kNm}$$

(9) CALCULATION OF ELASTIC CRITICAL MOMENT M_e

FROM CLAUSE B.2.2

$$M_e := \frac{M_p \cdot \pi^2 \cdot E}{\lambda_{LT}^2 \cdot 27.5} \quad \text{i.e.} \quad M_e = 83.487 \quad \text{kNm}$$

(10) RESULTS

FROM RESULTS OF DESIGN CALCULATIONS FOR BEAMS WITH LENGTHS BETWEEN 100 cm TO 1400 cm, THE VALUES OF $\sqrt{M_p/M_e}$ AND M_b/M_p WERE CALCULATED. RESULTS ARE PLOTTED AS SHOWN IN FIGURE 7.1 IN COMPARISON WITH RESULTS OF ANALYSIS BY FINITE ELEMENT METHOD.

APPENDIX 3.2

DESIGN OF PRISMATIC MEMBER FOR LATERAL STABILITY IN ACCORDANCE TO BS5950; PART 1

EXAMPLE OF CALCULATION FOR LATERAL-TORSIONAL BUCKLING FOR THE CASE OF SIMPLY SUPPORTED BEAM SUBJECTED TO MOMENT GRADIENT WITH $\beta = -0.5$, (i.e CASE 2). UB TYPE 203x133xUB30. THE BEAM LENGTH IN THIS EXAMPLE IS 400 cm.

NOTE; WITH VALUE OF $\beta = -0.5$ TABLE 18 OF BS5950 IS REFERRED FOR THE VALUE OF m

PROPERTIES OF BEAM

D := 206.8	mm	Sx := 313	cm ³
tf := 9.6	mm	G := 8000	kN/cm ²
Ix := 2900	cm ⁴	E := 20500	kN/cm ²
Zy := 57.4	cm ³	tw := 6.3	mm
ryy := 3.2	cm	r := 7.6	mm
L := 400	cm	Zx := 279	cm ³
a := 0.5 · D · 0.1	cm	Sy := 88.05	cm ³
b := 133.8	mm	py := 275	N/MM ²
A := 38.1	cm ²	Iy := 383.3	cm ⁴

DESIGN CALCULATIONS TO ESTABLISH THE VALUE OF M_p , M_b AND M_c

(1) CALCULATION OF TORSION CONSTANT ; CLAUSE B.2.5.1(c)

$$t1 := tf \quad t2 := tf \quad b1 := b \quad b2 := b$$

$$hw := D - 2 \cdot tf$$

$$J := \frac{1}{3} \cdot \frac{t1^3 \cdot b1 + t2^3 \cdot b2 + tw \cdot hw}{10000} \quad \text{i.e} \quad J = 9.455 \text{ cm}^4$$

(2) CALCULATION OF WARPING CONSTANT H ; CLAUSE B.2.5.1(c)

$$hs := D - tf$$

$$H := \frac{hs^2 \cdot t1 \cdot t2 \cdot b1 \cdot b2}{12 \cdot \left[t1^3 \cdot b1 + t2^3 \cdot b2 \right] \cdot 10^6} \quad \text{i.e} \quad H = 3.726 \cdot 10^4$$

(3) BUCKLING PARAMETER u ; CLAUSE B.2.5.1(b)

$$\Gamma := 1 - \left[\frac{Iy}{Ix} \right] \quad \text{i.e} \quad \Gamma = 0.868$$

$$u := \left[\frac{Iy \cdot Sx^2 \cdot \Gamma}{A \cdot H} \right]^{0.25} \quad \text{i.e} \quad u = 0.881$$

(4) TORSIONAL INDEX x ; CLAUSE B.2.5.1(b)

$$x := 1.132 \cdot \left[\frac{A \cdot H}{I_y \cdot J} \right]^{0.5} \quad \text{i.e.} \quad x = 22.404$$

NOTE ;

" APPROXIMATION OF u GIVEN IN CLAUSE 4.3.7.5 IS $u=0.9$
 APPROXIMATION OF x GIVEN IN CLAUSE 4.3.7.7 IS $x=D/t_f$
 IS 21.542 "

(5) SLENDERNESS FACTOR v . CLAUSE B.2.5.1(d) AND CLAUSE 4.3.5

$$\lambda := \frac{L}{r_{yy}} \quad N := 0.5$$

$$v := \left[\left[4 \cdot N \cdot (1 - N) + \left[\frac{1}{20} \right] \cdot \left[\frac{\lambda}{x} \right]^2 \right]^{0.5} \right]^{-0.5} \quad \text{i.e.} \quad v = 0.791$$

(6) PLASTIC MOMENT CAPACITY (LOW SHEAR LOAD)

FROM CLAUSE 4.2.5,

$$M_p := p_y \cdot \frac{S_x}{1000} \quad M_p = 86.075 \quad \text{kNm}$$

(7) CALCULATION OF BUCKLING MOMENT M_b

FROM CLAUSE 4.3.7.3

$$\frac{\lambda}{x} = 5.579 \quad N = 0.5 \quad v = 0.791$$

CLAUSE 4.3.7.5; λ_{LT} THE EQUIVALENT SLENDERNESS IS
 CALCULATED. FROM TABLE 13 FOR MEMBER NOT-SUBJECTED
 TO DESTABILISING LOAD, $m=0.43$ (i.e TABLE 18) AND $n=1$.

$$n := 1$$

$$\lambda_{LT} := n \cdot u \cdot v \cdot \lambda \quad \text{i.e.} \quad \lambda_{LT} = 87.094$$

FROM TABLE 11, THE VALUE OF p_b IS OBTAINED

$$p_b := 150 \quad \text{N/mm}^2$$

THEREFORE

$$M_b := p_b \cdot \frac{S_x}{1000} \quad \text{i.e.} \quad M_b = 46.95 \quad \text{kNm}$$

(8) CALCULATION OF ELASTIC CRITICAL MOMENT M_e

FROM CLAUSE B.2.2

$$M_e := \frac{M_p \cdot \pi^2 \cdot E}{\lambda_{LT}^2 \cdot 27.5} \quad \text{i.e.} \quad M_e = 83.487 \quad \text{kNm}$$

FROM CLAUSE 4.3.7.2 AND FROM TABLE 18 OF BS5950

$m=0.43$. THEREFORE THE CRITICAL MOMENT M_c IS

$$m := 0.43$$

$$M_c := m \cdot M_e \quad M_c = 35.899$$

(10) RESULTS

FROM RESULTS OF DESIGN CALCULATIONS FOR BEAMS WITH LENGTHS BETWEEN 100 cm TO 1400 cm, THE VALUES OF $\sqrt{M_p/M_c}$ AND M_b/M_p WERE CALCULATED. RESULTS ARE PLOTTED AS SHOWN IN FIGURE 7.6 IN COMPARISON WITH RESULTS OF ANALYSIS BY FINITE ELEMENT METHOD.

APPENDIX 3.3

DESIGN OF PRISMATIC MEMBER FOR LATERAL STABILITY IN ACCORDANCE TO BS5950; PART 1.

EXAMPLE OF CALCULATION FOR LATERAL-TORSIONAL BUCKLING FOR THE CASE OF SIMPLY SUPPORTED BEAM SUBJECTED TO DESTABILISING TRANSVERSE LOAD AT TOP FLANGE, i.e (CASE 3). 203x133xUB30.

NOTE; CLAUSE 4.3.5 STATED THAT THE LENGTH L USED IN THE CALCULATION OF THE MOMENT CAPACITY IS INCREASED BY 20%
CLAUSE 4.3.7.6 STATED THAT FOR MEMBER SUBJECTED TO DESTABILISING LOAD; $m=n=1$

PROPERTIES OF BEAM

D := 206.8	mm	Sx := 313	cm ³
tf := 9.6	mm	G := 8000	kN/cm ²
Ix := 2900	cm ⁴	E := 20500	kN/cm ²
Zy := 57.4	cm ³	tw := 6.3	mm
ryy := 3.2	cm	r := 7.6	mm
L := 400	cm	Zx := 279	cm ³
a := 0.5 · D · 0.1	cm	Sy := 88.05	cm ³
b := 133.8	mm	py := 275	N/MM ²
A := 38.1	cm ²	Iy := 383.3	cm ⁴

DESIGN CALCULATIONS TO ESTABLISH THE VALUE OF Mp, Mb AND Me

- (1) CALCULATION OF TORSION CONSTANT ; CLAUSE B.2.5.1(c)

$$t1 := tf \quad t2 := tf \quad b1 := b \quad b2 := b$$

$$hw := D - 2 \cdot tf$$

$$J := \frac{1}{3} \frac{t1^3 \cdot b1 + t2^3 \cdot b2 + tw^3 \cdot hw}{10000} \quad \text{i.e} \quad J = 9.455 \text{ cm}^4$$

- (2) CALCULATION OF WARPING CONSTANT H ; CLAUSE B.2.5.1(c)

$$hs := D - tf$$

$$H := \frac{hs^2 \cdot t1 \cdot t2 \cdot b1 \cdot b2}{12 \cdot [t1^3 \cdot b1 + t2^3 \cdot b2] \cdot 10^6} \quad \text{i.e} \quad H = 3.726 \cdot 10^4$$

- (3) BUCKLING PARAMETER u; CLAUSE B.2.5.1(b)

$$\Gamma := 1 - \frac{Iy}{Ix} \quad \text{i.e} \quad \Gamma = 0.868$$

$$u := \left[\frac{Iy \cdot Sx \cdot \Gamma}{A \cdot H} \right]^{0.25} \quad \text{i.e} \quad u = 0.881$$

(4) TORSIONAL INDEX x ; CLAUSE B.2.5.1(b)

$$x := 1.132 \cdot \left[\frac{A \cdot H}{I_y \cdot J} \right]^{0.5} \quad \text{i.e.} \quad x = 22.404$$

NOTE ;

" APPROXIMATION OF u GIVEN IN CLAUSE 4.3.7.5 IS $u=0.9$
 APPROXIMATION OF x GIVEN IN CLAUSE 4.3.7.7 IS $x=D/t_f$
 IS 21.542 "

(5) SLENDERNESS FACTOR v . CLAUSE B.2.5.1(d) AND CLAUSE 4.3.5

$$\lambda := 1.2 \cdot \frac{L}{r_{yy}} \quad N := 0.5$$

$$v := \left[\left[4 \cdot N \cdot (1 - N) + \left[\frac{1}{20} \right] \cdot \left[\frac{\lambda}{x} \right]^2 \right]^{0.5} \right]^{-0.5} \quad \text{i.e.} \quad v = 0.745$$

(6) CALCULATION OF BUCKLING RESISTANCE MOMENT

(a) FROM TABLE 6 OF BS5950, $p_y=275 \text{ N/mm}^2$ i.e $t_f < 16$

(b) FROM TABLE 7 OF BS5950,

$b/t_f=13.94$, THEREFORE THE COMPRESSION FLANGE
 IS CATEGORISED AS SEMI-COMPACT
 $D/t_w=32.82$, THEREFORE THE WEB GENERALLY IS
 CATEGORISED AS PLASTIC

(7) PLASTIC MOMENT CAPACITY (LOW SHEAR LOAD)

FROM CLAUSE 4.2.5,

$$M_p := p_y \cdot \frac{S_x}{1000} \quad M_p = 86.075 \quad \text{kNm}$$

(8) CALCULATION OF BUCKLING MOMENT M_b

(a) BY CONSERVATIVE APPROACH AS GIVEN IN CLAUSE 4.3.7.7

$$\lambda = 150$$

$$x = 22.404$$

FROM TABLE 19(b); THE BENDING STRENGTH $p_b=124.5 \text{ N/mm}^2$

THEREFORE $M_b=p_b \cdot S_x/1000= 38.97 \text{ kNm}$

(b) BY MORE ACCURATE APPROACH AS GIVEN IN CLAUSE 4.3.7.3

$$\frac{\lambda}{x} = 6.695 \quad N = 0.5 \quad v = 0.745$$

CLAUSE 4.3.7.5; λ_{LT} THE EQUIVALENT SLENDERNESS IS CALCULATED. FROM TABLE 13 FOR MEMBER SUBJECTED TO DESTABILISING LOAD, $m=1$ AND $n=1$.

$$n := 1$$

$$\lambda_{LT} := n \cdot u \cdot v \cdot \lambda \quad \text{i.e.} \quad \lambda_{LT} = 98.492$$

FROM TABLE 11, THE VALUE OF p_b IS OBTAINED

$$p_b := 127.7 \quad \text{N/mm}^2$$

$$\text{THEREFORE} \quad M_b := p_b \cdot \frac{S_x}{1000} \quad \text{i.e.} \quad M_b = 39.97 \quad \text{kNm}$$

(9) CALCULATION OF ELASTIC CRITICAL MOMENT M_e

FROM CLAUSE B.2.2

$$M_e := \frac{M_p \cdot \pi^2 \cdot E}{\lambda_{LT}^2 \cdot 27.5} \quad \text{i.e.} \quad M_e = 65.282 \quad \text{kNm}$$

(10) RESULTS

FROM RESULTS OF DESIGN CALCULATIONS FOR BEAMS WITH LENGTHS BETWEEN 100 cm TO 1400 cm, THE VALUES OF $\sqrt{M_p/M_e}$ AND M_b/M_p WERE CALCULATED. RESULTS ARE PLOTTED AS SHOWN IN FIGURE 7.11 IN COMPARISON WITH RESULTS OF ANALYSIS BY FINITE ELEMENT METHOD.

APPENDIX 3.4

DESIGN OF PRISMATIC MEMBER FOR LATERAL STABILITY IN ACCORDANCE TO BS5950: PART 1

EXAMPLE OF CALCULATION FOR LATERAL TORSIONAL BUCKLING THE CASE OF CANTILEVER BEAM SUBJECT TO DESTABILISING TRANSVERSE LOAD AT TOP FLANGE, i.e case 4. 203x133xUB30. CANTILEVERS WHICH ARE FREE TO DEFLECT Laterally AND TWIST AT THE UNSUPPORTED END ARE TREATED BY BS5950 AS EQUIVALENT BEAMS WITH TRANVERSE LOADS, EXCEPT THAT THE LENGTH USED IN THE CALCULATION OF THE MOMENT CAPACITY IS INCREASED BY 150% WHEN THERE ARE DESTABILISING LOAD.

NOTE; CLAUSE 4.3.6.2 STATED THAT THE EFFECTIVE LENGTH L_e USED IN THE CALCULATION OF THE MOMENT CAPACITY BECOME $2.5L$ (i.e FROM TABLE 10). FROM CLAUSE 4.3.7.6, FOR MEMBER SUBJECTED TO DESTABILISING LOAD; $m=n=1$

PROPERTIES OF SECTION

D := 206.8	mm	Iy := 383.3	cm ⁴
tf := 9.6	mm	Sx := 313	cm ³
Ix := 2900	cm ⁴	G := 8000	kN/cm ²
Zy := 57.4	cm ³	E := 20500	kN/cm ²
ryy := 3.2	cm	tw := 6.3	mm
a := 0.5 · 0.1 · D	mm	r := 7.6	mm
b := 133.8	mm	Zx := 279	cm ³
A := 38.1	cm ²	Sy := 88.05	cm ³
		py := 275	N/mm ²

DESIGN CALCULATIONS

FOR THE CASE OF LENGTH $L := 200$ cm

(1) CALCULATION OF TORSION CONSTANT. CLAUSE B.2.5.1(c)

SAY,

$$t1 := tf \quad t2 := tf \quad b1 := b$$

$$b2 := b \quad hw := D - 2 \cdot tf$$

$$J := \begin{bmatrix} 1 \\ - \\ 3 \end{bmatrix} \cdot \frac{t1^3 \cdot b1 + t2^3 \cdot b2 + tw^3 \cdot hw}{10000}$$

$$J = 9.455 \quad \text{cm}^4$$

(2) CALCULATION OF WARPING CONSTANT H. CLAUSE B.2.5.1(c)

$$\text{SAY,} \quad hs := D - tf$$

$$H := \frac{hs^2 \cdot t1 \cdot t2 \cdot b1 \cdot b2}{12 \cdot \left[t1^3 \cdot b1 + t2^3 \cdot b2 \right] \cdot 10^6}$$

$$H = 3.726 \cdot 10^4$$

(3) CALCULATION OF BUCKLING PARAMETER u . CLAUSE B.2.5.1(b)

$$\Gamma := 1 - \left[\frac{I_y}{I_x} \right] \quad \Gamma = 0.868$$

$$u := \left[\frac{I_y \cdot S_x^2 \cdot \Gamma}{A \cdot H^2} \right]^{0.25} \quad u = 0.881$$

(4) CALCULATION OF TORSIONAL INDEX x . CLAUSE B.2.5.1(b)

$$x := 1.132 \cdot \left[\frac{A \cdot H}{I_y \cdot J} \right]^{0.5} \quad x = 22.404$$

NOTE;

APPROXIMATE VALUE OF u GIVEN IN CLAUSE 4.3.7.5 IS $u=0.9$
 APPROXIMATE VALUE OF x given in clause 4.3.7.7 is $x=D/t_f$
 i.e $x=21.542$

(5) CALCULATION OF SLENDERNESS FACTOR v . CLAUSE B.2.5.1(d), AND CLAUSE 4.3.5

THE EFFECTIVE LENGTH $L_e=2.5L$ (i.e CLAUSE 4.3.6.2 AND TABLE 10)

$$\text{THEREFORE,} \quad \lambda := 2.5 \cdot \frac{L}{r_{yy}} \quad \text{AND} \quad N := 0.5$$

$$v := \left[\left[4 \cdot N \cdot (1 - N) + \left[\frac{1}{20} \right] \cdot \left[\frac{\lambda}{x} \right]^2 \right]^{0.5} \right]^{-0.5} \quad v = 0.735$$

(6) PLASTIC MOMENT CAPACITY (LOW SHEAR LOAD)

$$\text{FROM CLAUSE 4.2.5} \quad M_p := p_y \cdot \frac{S_x}{1000} \quad M_p = 86.075 \quad \text{kNm}$$

(7) CALCULATION OF BUCKLING MOMENT M_b

(a) BY CONSERVATIVE APPROACH, CLAUSE 4.3.7.7

$$\lambda = 156.25$$

$$x = 22.404$$

FROM TABLE 19(b); THE BENDING STRENGTH $p_b=119.8$

$$\text{N/mm}^2, \text{ THEREFORE } M_b = p_b \cdot S_x / 1000 = 37.5 \quad \text{kNm}$$

(b) BY THE MORE ACCURATE APPROACH, CLAUSE 4.3.7.3

$$\frac{\lambda}{x} = 6.974 \quad N = 0.5 \quad v = 0.735$$

FROM CLAUSE 4.3.7.5 THE VALUE OF λ_{LT} IS CALCULATED.
FROM TABLE 13, FOR MEMBER SUBJECTED TO DESTABILISING
LOAD; $m=1$ (REF. IS MADE TO TABLE 18) and $n=1$

$$n := 1$$

$$\lambda_{LT} := n \cdot u \cdot v \cdot \lambda \quad \text{THEREFORE} \quad \lambda_{LT} = 101.14$$

FROM TABLE 11 OF BS5950,

$$p_b := 123 \quad N/mm^2$$

THEREFORE,

$$M_b := p_b \cdot \frac{S_x}{1000} \quad M_b = 38.499 \quad kNm$$

(8) CALCULATION OF ELASTIC CRITICAL MOMENT M_e

FROM CLAUSE B.2.2

$$M_e := \frac{M_p \cdot \pi^2 \cdot E}{\lambda_{LT}^2 \cdot 27.5} \quad M_e = 61.908 \quad kNm$$

(9) RESULTS

THE VALUES OF M_p , M_e AND M_b ARE OBTAINED FOR DIFFERENT
LENGTHS OF CANTILEVERS. A GRAPH OF DIMENSIONLESS
STRENGTH M_p/M_e AGAINST M_b/M_p IS PLOTTED FOR THE
CANTILEVER. THIS IS AS SHOWN IN FIGURE 7.16 TOGETHER
WITH RESULTS OF THE ANALYSIS WITH F.E.M.

APPENDIX 3.5

DESIGN OF HAUNCH MEMBER WITHOUT RESTRAINTS ON THE TENSION FLANGE IN ACCORDANCE TO BS5950; PART 1

THE CASE OF DESIGN FOR BASE SECTION 203X133XUB30 i.e HON1

- NOTES; (i) IN BS5950, DESIGN OF TAPERED I-BEAMS ARE BASED ON MODIFICATION OF RULES FOR PRISMATIC MEMBERS.
(ii) THE CALCULATIONS HEREIN ARE USED TO PLOT A GRAPH OF CRITICAL MOMENT M_b AGAINST LENGTH L .
(iii) ACTUAL CRITICAL LENGTH IS OBTAINED FOR HAUNCHED SECTION FROM THE GRAPH.

DESIGN PARAMETER

(A) TOTAL LENGTH OF THE BEAM	$L := 650$	cm
(B) MOMENT; ASSUMING LINEAR DISTRIBUTION		
MOMENT AT SMALLER END	$M_{se} := 0$	
MOMENT AT LARGER END	$M_e = ?$	KN.cm
(C) AXIAL FORCE	$F := 0$	
(D) PROPERTIES OF SECTION		
DEPTH OF BASIC SECTION	$D := 20.68$	cm
BREADTH OF FLANGE	$b := 13.38$	cm
THICKNESS OF FLANGE	$t_f := 0.96$	cm
THICKNESS OF WEB	$t_w := 0.63$	cm
RATIO OF TAPER/UNI SEC	$q := 0.6$	
RATIO OF DEPTH OF TAPER	$r := 3$	
YIELD STRENGTH	$p_y := 27.5$	KN/cm ²
YOUNG'S MODULUS	$E := 20000$	KN/cm ²

DESIGN CALCULATIONS

(1) CALCULATION OF GEOMETRICAL PROPERTIES

ASSUMING THE WHOLE LENGTH IS TAPERED;
THEREFORE

$$\begin{aligned} L_t &:= 1 \cdot L & L_t &= 650 & \text{cm} \\ L_u &:= L - L_t & L_u &= 0 & \text{cm} \end{aligned}$$

(i) CALCULATION OF I_x AND I_y (SUBSCRIPT 1 FOR SMALL END
SUBSCRIPT 11 FOR LARGER END)

$$\text{SAY, } b_n := b - t_w$$

$$I_{x1} := b \cdot \frac{D^3}{12} - b_n \cdot \frac{(D - 2 \cdot t_f)^3}{12} \quad I_{x1} = 2.846 \cdot 10^3 \quad \text{cm}^3$$

$$I_{x11} := b \cdot \frac{(D \cdot r)^3}{12} - b_n \cdot \frac{(D \cdot r - 2 \cdot t_f)^3}{12} \quad I_{x11} = 3.537 \cdot 10^4 \quad \text{cm}^3$$

$$\text{SAY, } Ay := 2 \cdot tf \cdot \frac{b^3}{12}$$

$$Iy1 := Ay + (D - 2 \cdot tf) \cdot \frac{tw^3}{12} \quad Iy1 = 383.646 \quad \text{cm}^3$$

$$Iy11 := Ay + (D \cdot r - 2 \cdot tf) \cdot \frac{tw^3}{12} \quad Iy11 = 384.508 \quad \text{cm}^3$$

(ii) CALCULATION OF AREA

AREA AT SMALLER END A1 AND AREA AT LARGER END A11

$$\text{SAY, } Af := 2 \cdot b \cdot tf \quad Aw := (D - 2 \cdot tf) \cdot tw$$

THEREFORE,

$$A1 := Af + Aw \quad A11 := Af + (D \cdot r - 2 \cdot tf) \cdot tw$$

$$A1 = 37.508 \quad A11 = 63.56A1 \quad \text{cm}^2$$

(iii) CALCULATION OF ry

$$ry1 := \sqrt{\frac{Iy1}{A1}} \quad ry11 := \sqrt{\frac{Iy11}{A11}}$$

$$ry1 = 3.198 \quad ry11 = 2.459$$

(iv) CALCULATION OF λ FOR TAPERED SECTION

$$\lambda_1 := \frac{Lt}{ry1} \quad \lambda_{11} := \frac{Lt}{ry11}$$

$$\lambda_1 = 203.241 \quad \lambda_{11} = 264.284$$

(2) CALCULATION OF OTHER CONSTANTS FOR TAPERED SECTION

(i) $hs1$ DISTANCE BETWEEN SHEAR CENTRES OF FLANGES

$$hs1 := D - tf \quad hs11 := r \cdot D - tf$$

$$hs1 = 19.72 \quad hs11 = 61.08 \quad (\text{cm})$$

(ii) hw DEPTH OF WEB AT EACH SEGMENT

$$hw1 := D - 2 \cdot tf \quad hw11 := r \cdot D - 2 \cdot tf$$

$$hw1 = 18.76 \quad hw11 = 60.12 \quad (\text{cm})$$

(iii) J TORSION CONSTANT, CLAUSE B.2.5.1

$$J1 := \begin{bmatrix} 1 \\ - \\ 3 \end{bmatrix} \cdot \left[2 \cdot tf^3 \cdot b + tw^3 \cdot hw1 \right]$$

$$\text{SAY,} \quad Jb := 2 \cdot tf^3 \cdot b$$

$$J11 := \begin{bmatrix} 1 \\ - \\ 3 \end{bmatrix} \cdot \left[Jb + tw^3 \cdot hw11 \right]$$

$$J1 = 9.455 \quad J11 = 12.903 \quad (\text{cm}^4)$$

(iv) WARPING CONSTANT H

$$\text{SAY,} \quad Hx := tf \cdot \frac{b^3}{24}$$

$$H1 := \frac{hs1^2 \cdot tf^2 \cdot b^6}{12} \cdot \frac{1}{2 \cdot tf^3 \cdot b}$$

$$H11 := hs11^2 \cdot Hx$$

$$\text{THEREFORE,} \quad H1 = 3.726 \cdot 10^4 \quad \text{cm}^6$$

$$H11 = 3.575 \cdot 10^5 \quad \text{cm}^6$$

(v) THE TORSIONAL INDEX x , CLAUSE B.2.5.1(b)

$$\text{i.e } x = 0.566 \cdot hs \cdot \sqrt{A/J}$$

$$x1 := 0.556 \cdot hs1 \cdot \sqrt{\frac{A1}{J1}} \quad x1 = 21.838$$

$$x11 := 0.566 \cdot hs11 \cdot \sqrt{\frac{A11}{J11}} \quad x11 = 76.733$$

(3) CALCULATION OF PLASTIC MODULUS AT BOTH ENDS

$$Sx1 := 0.25 \cdot tw \cdot hw1^2 + b \cdot tf \cdot (hw1 + tf)$$

$$Sx1 = 308.73 \quad \text{cm}^3$$

$$Sx11 := 0.25 \cdot tw \cdot hw11^2 + b \cdot tf \cdot (hw11 + tf)$$

$$Sx11 = 1.354 \cdot 10^3 \quad \text{cm}^3$$

(4) CALCULATION OF PLASTIC MOMENT M_p

$$\begin{aligned}
 M_{p1} &:= p_y \cdot S_{x1}^3 & M_{p11} &:= p_y \cdot S_{x11}^4 \\
 M_{p1} &= 8.49 \cdot 10^3 & M_{p11} &= 3.723 \cdot 10^4 \quad (\text{kN}\cdot\text{cm})
 \end{aligned}$$

(5) CALCULATION OF EQUIVALENT SLENDERNESS λ_{LT}

$$\lambda_{11} = 264.284$$

$$u := 1 \quad \text{CLAUSE 4.3.7.5 AND G.3.3}$$

$$n := 1 \quad \text{SINCE THERE IS NO FLANGE TAPERING}$$

$$x_{11} = 76.733$$

$$v := \left[1 + \left[\frac{\lambda_{11}}{x_{11}} \right]^2 \cdot \left[\frac{1}{20} \right] \right]^{-0.25}$$

$$\lambda_{LT} := n \cdot v \cdot u \cdot \lambda_{11} \quad \lambda_{LT} = 235.238$$

(6) CALCULATION FOR BUCKLING MOMENT

FROM CLAUSE B.2.4 THE LIMITING EQUIVALENT
SLENDERNESS λ_{LO} ;

$$\lambda_{LO} := 0.4 \cdot \left[\frac{2 \cdot \pi^2 \cdot E}{p_y} \right]^{0.5} \quad \lambda_{LO} = 33.889$$

FROM CLAUSE B.2.3

$$\eta_{LT} := 0.007 \cdot (\lambda_{LT} - \lambda_{LO}) \quad \eta_{LT} = 1.409$$

FROM CLAUSE B.2.2

$$\begin{aligned}
 M_e &:= \left[\frac{M_{p11} \cdot \pi^2 \cdot E}{\lambda_{LT}^2 \cdot p_y} \right] & M_e &= 4.829 \cdot 10^3 \quad \text{kNcm} \\
 \frac{M_e}{100} &= 48.292 \quad \text{kNm}
 \end{aligned}$$

FROM CLAUSE B.2.1

$$\psi_B := \frac{M_{p11} + (\eta_{LT} + 1) \cdot M_e}{2}$$

$$M_b := \frac{M_e \cdot M_{p11}}{\left[\Phi_B^2 - M_e \cdot M_{p11} \right]^{0.5}}$$

$$M_b = 4.008 \cdot 10^3 \text{ kNcm}$$

$$\frac{M_b}{100} = 40.081 \text{ kNm}$$

(7) RESULTS

RESULTS BUCKLING MOMENT M_b AND LENGTH L ARE PLOTTED AS SHOWN IN FIGURE 7.21A AND FOR $r=2$ IN FIGURE 7.21B IN COMPARISON WITH RESULTS OF THE FINITE ELEMENT METHOD. BY GEOMETRY, THE VALUE OF MOMENT AT THE LARGER END CAN CALCULATED WHEN THE YIELD MOMENT AT THE TAPER/UNIFORM SECTION JUNCTION IS KNOWN. FROM THE GRAPH THIS VALUE OF MOMENT IS USED TO FIND THE CRITICAL LENGTH OF THE HAUNCH BEAM.

APPENDIX 3.6

EXAMPLE OF CALCULATION FOR PRISMATIC SECTION IN ACCORDANCE TO
APPENDIX G : BS5950 PART 1

THE CALCULATION HEREIN IS FOR SPECIMEN UMB1 (203X133XUB30).
THE BEAM IS SUBJECTED TO LOADING AS SHOWN IN FIGURE 7.26.
BOTH ENDS OF THE BEAM IS RESTRAINED LONGITUDINALLY AND
TORSIONALLY BUT THE FLANGES ARE FREE TO WARP. THE TENSION
FLANGE OF THE BEAM IS RESTRAINED BY PURLINS. THE VALUE OF β
USED IN THIS CASE IS 0.5

DESIGN CALCULATIONS

BEAM DATA

D := 20.68	cm	PY := 25	kN/cm ²
a := 18.00	cm	E := 21000	kN/cm ²
A := 38.1	cm ²	SX1 := 314.5	cm ⁴
tf := 0.96	cm	L := 332.5	cm
b := 13.38	cm	ry := 3.2	cm
tw := 0.63	cm	L	
IY := 383.3	cm ⁴	$\lambda := \frac{L}{ry}$	
IX := 2900.1	cm ⁴		
hw := D - 2 · tf	cm	F := 0	kN
hs := D - tf	cm	MA := 6982	kN.cm
		MA IS THE YIELD MOMENT	
$\Gamma := 1 - \frac{IY}{IX}$			

(A) CALCULATION FOR ELASTIC STABILITY

APPENDIX SPECIFY THE CRITERIA FOR ELASTIC STABILITY
AS FOLLOWS ;

$$F/P_c + M_{dash}/M_B \leq 1$$

SINCE F=0 THE CALCULATION OF P_c IS IGNORED IN THIS CASE

(i) CALCULATION OF RELEVANT BEAM PROPERTIES

CALCULATION OF H , WARPING CONSTANT. FROM CLAUSE B.2.5.1

$$H := \frac{hs^2 \cdot tf \cdot b^3}{24}$$

$$H = 3.726 \cdot 10^4$$

CALCULATION OF J , THE TORSION CONSTANT. FROM CLAUSE B.2.5.1

$$J := \frac{2 \cdot tf \cdot b^3 + tw \cdot hw^3}{3}$$

$$J = 9.455$$

CALCULATION OF X, THE TORSIONAL INDEX. FROM CLAUSE B.2.5.1

$$X := 1.132 \cdot \frac{\sqrt{A \cdot H}}{\sqrt{IY \cdot J}} \quad X = 22.404$$

CALCULATION OF Y FROM CLAUSE G.3.2

$$Y := \frac{\sqrt{1 + \left[2 \cdot \frac{a}{hs} \right]^2}}{\sqrt{1 + \left[2 \cdot \frac{a}{hs} \right]^2 + \left[\frac{1}{20} \right] \cdot \left[\frac{\lambda}{X} \right]^2}} \quad Y = 0.895$$

FROM THE VALUES OF Y ABOVE AND FROM CLAUSE G.3.4
THE VALUES OF m_t IS OBTAINED FROM TABLE 39 OF THE CODE

$$m_t := 0.74$$

(ii) CALCULATION OF M_{dash}

FROM CLAUSE G.2

$$M_{dash} := M_A \cdot m_t \quad M_{dash} = 5.167 \cdot 10^3 \text{ kN.cm}$$

(iii) CALCULATION OF MINOR AXIS SLENDERNESS RATIO, λ_{TB}

CALCULATION OF BUCKLING PARAMETER u . FROM CLAUSE
4.3.7.5

$$u := \sqrt[2]{\frac{IY \cdot S_{X1}^2 \cdot \Gamma}{A \cdot H}} \quad u = 0.883$$

CALCULATION OF v_t

$$v_t := \left[\frac{4 \cdot \frac{a}{hs}}{1 + \left[2 \cdot \frac{a}{hs} \right]^2 + \left[\frac{1}{20} \right] \cdot \left[\frac{\lambda}{X} \right]^2} \right]^{0.5} \quad v_t = 0.822$$

CALCULATION OF nt

FROM CLAUSE G.3.6.1

$$N1 := 3491 \qquad M1 := 6982.5$$

$$N2 := 4363.8 \qquad M2 := M1$$

$$N3 := 5236.5 \qquad M3 := M1$$

$$N4 := 6109.3 \qquad M4 := M1$$

$$N5 := 6982.5 \qquad M5 := M1$$

$$NMS := \frac{N4}{M4} \qquad NME := \frac{N5}{M5}$$

$$nt := \sqrt{\left[\frac{1}{12} \right] \cdot \left[\frac{N1}{M1} + 3 \cdot \frac{N2}{M2} + 4 \cdot \frac{N3}{M3} + 3 \cdot \frac{N4}{M4} + \frac{N5}{M5} + 2 \cdot (NMS - NME) \right]}$$

WHERE $nt = 0.854$ BUT CLAUSE G.3.3 STATED THAT WHEN THERE IS NO INTERMEDIATE LOAD $nt=1$

THE MINOR AXIS SLENDERNESS RATIO λ_{TB}

$c := 1$ FOR UNIFORM MEMBER (CLAUSE G.3.3)
 $nt := 1$

$$\lambda_{TB} := nt \cdot u \cdot vt \cdot c \cdot \lambda \dots \dots \quad \text{i.e.} \quad \lambda_{TB} = 75.398$$

(iv) CALCULATION OF BENDING STRENGTH p_b , (CLAUSE 4.3.7.4)

FROM TABLE 11 OF BS5950, THE VALUE OF λ_{TB} IS USED IN OBTAINING p_b AND THEREFORE

$$p_b := 16.5 \qquad \text{KN/cm}^2$$

(v) CALCULATION OF BUCKLING RESISTANCE M_B

$$M_B := p_b \cdot S_{X1} \qquad (\text{FROM CLAUSE 4.3.7.3})$$

$$M_B = 5.189 \cdot 10^3 \quad \text{KN.cm} \quad \text{AND} \quad M_{dash} = 5.167 \cdot 10^3 \quad \text{KN.cm}$$

(vi) ELASTIC STABILITY $M_{dash}/M_B < 1$

$$\frac{M_{dash}}{M_B} = 0.996 \qquad \text{CRITICAL LENGTH} \quad L = 332.5 \quad \text{cm}$$

(B) PLASTIC STABILITY OF UNIFORM MEMBER IN ACCORDANCE TO APPENDIX G

THE CONDITION FOR PLASTIC STABILITY FOR BEAM WITHOUT LATERAL LOAD IS

$$L_t = \frac{L_k}{\sqrt{m_t}} \sqrt{\left(\frac{M_P}{M_{pr} + aF} \right)} \quad (\text{CLAUSE G.2(b)})$$

(i) CALCULATION OF M_P

$$M_P := P_Y \cdot S_{X1}$$

(ii) CALCULATION OF LIMITING LENGTH L_k

FROM CLAUSE G.3.5

$$L_k := \frac{\left[5.4 + 600 \cdot \frac{P_Y}{E} \right] \cdot r_y \cdot X}{\sqrt{5.4 \cdot \frac{P_Y^2}{E} \cdot X^2 - 1}}$$

$$\text{i.e.} \quad L_k = 293.757 \quad \text{cm}$$

(iii) CALCULATION OF L_t

$$L_t := \frac{L_k}{\sqrt{m_t}} \cdot \sqrt{\frac{M_P}{M_P + a \cdot F}} \quad L_t = 341.486$$

$$L = 332.5$$

SINCE L_t IS LONGER THAN L , PLASTIC STABILITY IS SATISFIED IN THIS CASE.

THE CRITICAL LENGTH FOR PLASTIC STABILITY IS 341.5 cm

APPENDIX 3.7

DESIGN OF RESTRAINED HAUNCHED MEMBER WITH UNRESTRAINED COMPRESSION FLANGE, IN ACCORDANCE TO APPENDIX G, BS5950: PART 1.

CALCULATIONS FOR HAUNCHED MEMBER H1 AS SHOWN IN FIGURE 7.28. THE BASE SECTION USED IS 203X133XUB30.

THE SPECIMEN IS RESTRAINED Laterally at both ends and the tension flange is restrained by purlins. The bending moment at the smaller end is zero while the bending moment at the larger end BML equals to 17203.4 kNcm. This value of BML is obtained by assuming linear distribution of moment and when moment at point F in figure 7.28 (i.e point of change of cross section area) has just reached yield moment.

PROPERTIES OF BASE SECTION

q := 0.6		(RATIO OF TAPERED SECTION TO TOTAL LENGTH)
r := 3		(RATIO OF GREATER DEPTH TO LESSER DEPTH)
D := 206.8	mm	(DEPTH OF BASE SECTION)
tf := 9.6	mm	(FLANGE THICKNESS)
tw := 6.3	mm	(WEB THICKNESS)
B := 133.8	mm	(BREADTH OF FLANGE)
E := 20000	kN/cm ²	(YOUNG'S MODULUS)
py := 25	kN/cm ²	(YIELD STRESS)
F := 0	kN	(AXIAL LOAD)
L := 148.5	cm	(TOTAL LENGTH OF HAUNCHED BEAM)
Lu := 59.4	cm	(LENGTH OF UNIFORM SECTION)

DESIGN CALCULATIONS

DESIGN FOR ELASTIC STABILITY

NOTE:

THE PERMISSIBLE STRESS OF THE MEMBER WHICH IS EITHER TAPERED OR UNIFORM IS CHECKED BETWEEN THE LATERAL-TORSIONAL RESTRAINTS TO BOTH FLANGES ACCORDING TO THE DESIGN CRITERIA ;

$$F/A + M/S_x \leq p_b \quad \text{AT ANY SECTION} \quad . \quad . \quad (1)$$

WHERE, M = APPLIED LOAD AT THE SECTION CONSIDERED
 S_x = PLASTIC MODULUS AT THE SECTION CONSIDERED
 F = AXIAL FORCE
 A = AREA OF THE SECTION CONSIDERED
 p_b = LATERAL-TORSIONAL BUCKLING RESISTANCE.

IN ORDER TO DO THE CHECK FOR EQUATION (1), THE GEOMETRICAL PROPERTIES OF THE SPECIMEN ALONG THE LENGTH MUST BE KNOWN. THE SPECIMEN IN THIS CASE IS DIVIDED INTO 27 ELEMENTS GIVING 29 CROSS SECTIONS PROPERTIES.

1 SECTIONAL PROPERTIES

(A) CROSS SECTIONAL AREA AT EACH SECTION (cm^2)

A1 := 38.1	A1, A2, A3, A4, A5, A6, A7, A8, A9, A10, A11, AND A12 HAVE SAME VALUE	
A13 := 39.3	A21 := 51.7	A29 := 64.2
A14 := 40.9	A22 := 53.3	
A15 := 42.4	A23 := 54.9	
A16 := 44.0	A24 := 56.4	
A17 := 45.5	A25 := 58.0	
A18 := 47.1	A26 := 59.5	
A19 := 48.6	A27 := 61.1	
A20 := 50.2	A28 := 62.6	

(B) SECOND MOMENT OF AREA Ix AND Iy (cm^4)

Ix1, Ix2, Ix3, Ix4, Ix5, Ix6, Ix7, Ix8, Ix9, Ix10, Ix11, Ix12 HAVE SAME VALUE	Iy1 TO Iy29 HAVE THE SAME VALUE Iy := 383.3
Ix1 := 2900.1	Ix21 := 14703.1
Ix13 := 3541.4	Ix22 := 16756.1
Ix14 := 4469	Ix23 := 18970.9
Ix15 := 5520.8	Ix24 := 21352.4
Ix16 := 6701.5	Ix25 := 23905.2
Ix17 := 8015.8	Ix26 := 26634.0
Ix18 := 9468.3	Ix27 := 29543.6
Ix19 := 11063.9	Ix28 := 32638.7
Ix20 := 12807.3	Ix29 := 35923.9

(C) ELASTIC MODULUS Zx AND Zy (cm^3)

Zx1, Zx2, Zx3, Zx4, Zx5, Zx6, Zx7, Zx8, Zx9, Zx10, Zx11, Zx12 HAVE SAME VALUE	Zy1 TO Zy29 HAVE SAME VALUE Zy1 := 57.3 Zy29 := 57.3
Zx1 := 280.5	Zx21 := 694.8
Zx13 := 313.3	Zx22 := 748.3
Zx14 := 356.5	Zx23 := 803.0
Zx15 := 401.0	Zx24 := 859.0
Zx16 := 446.8	Zx25 := 916.2
Zx17 := 493.8	Zx26 := 974.8
Zx18 := 542.2	Zx27 := 1034.6
Zx19 := 591.8	Zx28 := 1095.7
Zx20 := 642.6	Zx29 := 1158.1

(D) PLASTIC MODULUS S_x AND S_y (cm^4)

$S_{x1}, S_{x2}, S_{x3}, S_{x4},$	S_{y1} TO S_{y29}
$S_{x5}, S_{x6}, S_{x7}, S_{x8},$	HAVE SAME VALUE
$S_{x9}, S_{x10}, S_{x11}, S_{x12}$	$S_{y1} := 85.9$
HAVE SAME VALUE	$S_{y29} := 85.9$

$S_{x1} := 314.5$	$S_{x21} := 800.8$
$S_{x13} := 351.8$	$S_{x22} := 865.5$
$S_{x14} := 401.2$	$S_{x23} := 932.1$
$S_{x15} := 452.6$	$S_{x24} := 1000.7$
$S_{x16} := 505.8$	$S_{x25} := 1071.1$
$S_{x17} := 561.0$	$S_{x26} := 1143.5$
$S_{x18} := 618.1$	$S_{x27} := 1217.8$
$S_{x19} := 677.0$	$S_{x28} := 1294.0$
$S_{x20} := 737.9$	$S_{x29} := 1372.2$

(E) RADII OF GYRATION r_y (cm)

$r_{y1} := 3.2$	$r_{y18} := 2.9$	$r_{y24} := 2.6$
$r_{y13} := 3.1$	$r_{y19} := 2.8$	$r_{y25} := 2.6$
$r_{y14} := 3.1$	$r_{y20} := 2.8$	$r_{y26} := 2.5$
$r_{y15} := 3.0$	$r_{y21} := 2.7$	$r_{y27} := 2.5$
$r_{y16} := 3.0$	$r_{y22} := 2.7$	$r_{y28} := 2.5$
$r_{y17} := 2.9$	$r_{y23} := 2.6$	$r_{y29} := 2.4$

(F) ST. VENANT CONSTANT J (cm^4)

$J_1, J_2, J_3, J_4, J_5, J_6, J_7, J_8, J_9, J_{10}, J_{11}$
AND J_{12} HAVE THE SAME VALUE

$J_1 := 9.5$	$J_{21} := 11.3$
$J_{13} := 9.7$	$J_{22} := 11.5$
$J_{14} := 9.9$	$J_{23} := 11.8$
$J_{15} := 10.1$	$J_{24} := 12.0$
$J_{16} := 10.3$	$J_{25} := 12.2$
$J_{17} := 10.5$	$J_{26} := 12.4$
$J_{18} := 10.7$	$J_{27} := 12.6$
$J_{19} := 10.9$	$J_{28} := 12.8$
$J_{20} := 11.1$	$J_{29} := 13.0$

(G) WARPING CONSTANT H (cm⁶)

H1, H2, H3, H4, H5, H6, H7, H8, H9, H10,
H11 AND H12 HAVE THE SAME VALUE

H1 := 37260	H ₂₁ := 165900
H ₁₃ := 47020	H ₂₂ := 185900
H ₁₄ := 57920	H ₂₃ := 207000
H ₁₅ := 69950	H ₂₄ := 229300
H ₁₆ := 83110	H ₂₅ := 252600
H ₁₇ := 97410	H ₂₆ := 277100
H ₁₈ := 112800	H ₂₇ := 302800
H ₁₉ := 129400	H ₂₈ := 329600
H ₂₀ := 147100	H ₂₉ := 357500

2. CALCULATIONS OF BUCKLING RESISTANCE MOMENT, Mb

IN ORDER THAT EQUATION CAN BE USED, THE VALUE OF THE LATERAL-TORSIONAL BUCKLING STRENGTH p_b MUST FIRST BE OBTAINED FOR EACH SECTION. THE VALUE OF p_b IS DETERMINED IN ACCORDANCE WITH SECTION 4.3.7 EXCEPT THAT THE EQUIVALENT SLENDERNESS SHOULD BE TAKEN AS λ_{TB} .

FROM CLAUSE G.3.3, THE MINOR AXIS SLENDERNESS RATIO, λ_{TB} IS TAKEN AS;

$$\lambda_{TB} = n_t * u * v_t * c * \lambda \quad (2)$$

WHERE ; λ = THE SLENDERNESS L/r_y OF THE MEMBER BETWEEN EFFECTIVE TORSIONAL RESTRAINTS TO BOTH FLANGES.

u = BUCKLING PARAMETER. FOR TAPERED SECTION $u=1$
 n_t = SLENDERNESS CORRECTION FACTOR, SINCE THERE IS NO INTERMEDIATE LOADS BETWEEN RESTRAINTS ($n_t=1$)

$$c = 1 + \frac{2/3}{[3(R-1) \sqrt{q}/(x-9)]} \quad \text{FOR TAPERED MEMBER}$$

$$v_t = \left[\frac{4a/hs}{1 + (2a/hs) + 0.05(\lambda/x)} \right] \quad (3)$$

FOR TAPERED MEMBER v_t IS CALCULATED FOR THE SMALLEST SECTION. (CLAUSE G.3.3)
 IN EQUATION 3 ,

a = DISTANCE BETWEEN REFERENCE AXIS AND RESTRAINT AXIS

hs = DISTANCE BETWEEN THE SHEAR CENTRES OF THE FLANGES.

(i) CALCULATION OF LIMITING EQUIVALENT SLENDERNESS λ_{LO}
FROM CLAUSE B.2.4

$$\lambda_{LO} := 0.4 \cdot \sqrt{\frac{2 \cdot \pi \cdot E}{p_y}} \quad \lambda_{LO} = 35.543$$

(ii) CALCULATION OF v_t

FROM CLAUSE G.3.3

$$a := 15.5 \quad \text{cm} \quad h_s := 19.72 \quad \text{cm}$$

$$\lambda_1 := \frac{L}{r_{y1}} \quad x_1 := 1.132 \cdot \sqrt{\frac{A_1 \cdot H_1}{I_{y1} \cdot J_1}}$$

$$\lambda_1 = 46.406 \quad x_1 = 22.351$$

$$v_t := \sqrt{\frac{4 \cdot \frac{a}{h_s}}{1 + \left[\frac{2 \cdot a}{h_s} \right]^2 + \left[\frac{1}{20} \cdot \left[\frac{\lambda_1}{x_1} \right]^2 \right]}}$$

$$\text{THEREFORE} \quad v_t = 0.923$$

(iii) VALUES OF TORSIONAL INDEX x

$x_1, x_2, x_3, x_4, x_5, x_6, x_7, x_8, x_9, x_{10}$
 x_{11} and x_{12} HAVE THE SAME VALUE i.e 22.351

$$k := 13 \dots 29$$

$$x_k := 1.132 \cdot \sqrt{\frac{A_k \cdot H_k}{I_{y_k} \cdot J_k}}$$

$x_{13} = 25.236$	$x_{19} = 43.919$	$x_{25} = 63.362$
$x_{14} = 28.284$	$x_{20} = 47.16$	$x_{26} = 66.672$
$x_{15} = 31.332$	$x_{21} = 50.374$	$x_{27} = 70.063$
$x_{16} = 34.452$	$x_{22} = 53.67$	$x_{28} = 73.41$
$x_{17} = 37.566$	$x_{23} = 56.742$	$x_{29} = 76.826$
$x_{18} = 40.743$	$x_{24} = 60.024$	

(iv) CALCULATION OF c

$c_1, c_2, c_3, c_4, c_5, c_6, c_7, c_8, c_9, c_{10},$
 c_{11} and c_{12} HAVE SAME VALUE i.e 1.276

$$c_k := 1 + \left[\frac{3}{x_k - 9} \cdot (r - 1)^{\frac{2}{3}} \cdot \sqrt{0.6} \right]$$

$c_{13} = 1.227$	$c_{19} = 1.106$	$c_{25} = 1.068$
$c_{14} = 1.191$	$c_{20} = 1.097$	$c_{26} = 1.064$
$c_{15} = 1.165$	$c_{21} = 1.089$	$c_{27} = 1.06$
$c_{16} = 1.145$	$c_{22} = 1.083$	$c_{28} = 1.057$
$c_{17} = 1.129$	$c_{23} = 1.077$	$c_{29} = 1.054$
$c_{18} = 1.116$	$c_{24} = 1.072$	

(v) VALUES OF λ

VALUES OF λ_1 TO λ_{12} ARE EQUAL TO

$\lambda_1 := 46.406$

$$\lambda_k := \frac{L}{ry_k}$$

$$\lambda_{13} = 47.903$$

$\lambda_{13} = 47.903$	$\lambda_{20} = 53.036$
$\lambda_{14} = 47.903$	$\lambda_{21} = 55$
$\lambda_{15} = 49.5$	$\lambda_{22} = 55$
$\lambda_{16} = 49.5$	$\lambda_{23} = 57.115$
$\lambda_{17} = 51.207$	$\lambda_{24} = 57.115$
$\lambda_{18} = 51.207$	$\lambda_{26} = 59.4$
$\lambda_{19} = 53.036$	$\lambda_{27} = 59.4$
$\lambda_{28} = 59.4$	$\lambda_{29} = 61.875$

(vi) VALUE OF λ_{TB}

THROUGHOUT THE UNIFORM SECTION λ_{TB1} TO λ_{TB12} HAVE EQUAL VALUE

THE VALUES OF n AND u IN THIS CASE ARE 1
 $nt := 1 \qquad u := 1$

$\lambda_{TB1} := nt \cdot u \cdot vt \cdot c1 \cdot \lambda_1 \qquad \lambda_{TB1} = 54.655$

$$\lambda_{TBk} := nt \cdot u \cdot vt \cdot c_k \cdot \lambda_k$$

$\lambda_{TB13} = 54.251$	$\lambda_{TB21} = 55.283$
$\lambda_{TB14} = 52.66$	$\lambda_{TB22} = 54.978$
$\lambda_{TB15} = 53.227$	$\lambda_{TB23} = 56.777$
$\lambda_{TB16} = 52.313$	$\lambda_{TB24} = 56.513$
$\lambda_{TB17} = 53.361$	$\lambda_{TB25} = 56.302$
$\lambda_{TB18} = 52.747$	$\lambda_{TB27} = 58.116$
$\lambda_{TB19} = 54.141$	$\lambda_{TB28} = 57.951$
$\lambda_{TB20} = 53.7$	$\lambda_{TB29} = 60.195$

(vii) PERRY COEFFICIENT η_{LT}

$$\eta_{LT1} := 0.007 \cdot (\lambda_{TB1} - \lambda_{LO}) \quad \eta_{LT1} = 0.134$$

LT1 TO η_{LT12} HAVE SAME VALUE

$$\eta_{LT_k} := 0.007 \cdot [\lambda_{TB_k} - \lambda_{LO}]$$

(viii) THE ELASTIC CRITICAL MOMENT MP AT EACH SECTION

ME1 TO ME12 HAVE SAME VALUE (kNcm)

$$ME1 := \frac{py \cdot Sx1 \cdot \pi^2 \cdot E}{\lambda_{TB1}^2 \cdot py} \quad ME1 = 2.078 \cdot 10^4$$

$$ME_k := \frac{py \cdot Sx_k \cdot \pi^2 \cdot E}{\lambda_{TB_k}^2 \cdot py}$$

(ix) FROM CLAUSE B.2

$$\phi_1 := \frac{py \cdot Sx1 + (\eta_{LT1} + 1) \cdot ME1}{2} \quad \phi_1 = 1.571 \cdot 10^4$$

ϕ_1 TO ϕ_{12} HAVE SAME VALUE

$$\phi_k := \frac{py \cdot Sx_k + [\eta_{LT_k} + 1] \cdot ME_k}{2}$$

(x) CALCULATION OF MB

$$MB1 := \frac{ME1 \cdot py \cdot Sx1}{\phi_1 + \left[\phi_1^2 - (ME1 \cdot py \cdot Sx1) \right]^{0.5}}$$

MB1 TO MB12 HAVE THE SAME VALUE

$$MB1 = 6.576 \cdot 10^3$$

$$MB_k := \frac{ME_k \cdot p_y \cdot Sx_k}{\phi_k + \left[\phi_k^2 - \left[\frac{ME_k \cdot p_y \cdot Sx_k}{k} \right] \right]^{0.5}}$$

(xi) CALCULATION OF pb

$$pb1 := \frac{MB1}{Sx1} \quad pb1 = 20.908 \quad \text{kN/cm}^2$$

THE VALUES OF pb1 TO pb12 ARE THE SAME

$$pb_k := \frac{MB_k}{Sx_k} \quad pb_{13} = 20.997$$

(xiv) ASSUMING LINEAR DISTRIBUTION OF APPLIED LOAD (kNcm)

M ₁ := 0	M ₁₁ := 6140	M ₂₁ := 12290
M ₂ := 610	M ₁₂ := 6760	M ₂₂ := 12900
M ₃ := 1230	M ₁₃ := 7370	M ₂₃ := 13520
M ₄ := 1840	M ₁₄ := 7990	M ₂₄ := 14130
M ₅ := 2460	M ₁₅ := 8600	M ₂₅ := 14750
M ₆ := 3070	M ₁₆ := 9220	M ₂₆ := 15360
M ₇ := 3690	M ₁₇ := 9830	M ₂₇ := 15970
M ₈ := 4300	M ₁₈ := 10440	M ₂₈ := 16590
M ₉ := 4920	M ₁₉ := 11060	M ₂₉ := 17203
M ₁₀ := 5530	M ₂₀ := 11670	

(xiii) CHECK STABILITY CRITERION

M1/Sx1 < OR = pb1 AT SECTION 1 TO 12

$$STR_f := \frac{M_f}{Sx1} \quad STR_k := \frac{M_k}{Sx_k}$$

M/Sx	pb	STATUS
STR = 0	pb := 20.908	OK
1	1	
STR = 1.94	pb := 20.908	OK
2	2	
STR = 3.911	pb := 20.908	OK
3	3	
STR = 5.851	pb := 20.908	OK
4	4	
STR = 7.822	pb := 20.908	OK
5	5	
STR = 9.762	pb := 20.908	OK
6	6	
STR = 11.733	pb := 20.908	OK
7	7	
STR = 13.672	pb := 20.908	OK
8	8	
STR = 15.644	pb := 20.908	OK
9	9	
STR = 17.583	pb := 20.908	OK
10	10	
STR = 19.523	pb := 20.908	OK
11	11	
STR = 21.494	pb := 20.908	NO
12	12	
STR = 20.949	pb = 20.997	OK
13	13	
STR = 19.915	pb = 21.347	OK
14	14	
STR = 19.001	pb = 21.222	OK
15	15	
STR = 18.229	pb = 21.423	OK
16	16	
STR = 17.522	pb = 21.193	OK
17	17	
STR = 16.89	pb = 21.328	OK
18	18	
STR = 16.337	pb = 21.021	OK
19	19	
STR = 15.815	pb = 21.118	OK
20	20	
STR = 15.347	pb = 20.77	OK
21	21	
STR = 14.905	pb = 20.837	OK
22	22	
STR = 14.505	pb = 20.44	OK
23	23	
STR = 14.12	pb = 20.498	OK
24	24	
STR = 13.771	pb = 20.545	OK
25	25	
STR = 13.432	pb = 20.095	OK
26	26	
STR = 13.114	pb = 20.143	OK
27	27	
STR = 12.821	pb = 20.18	OK
28	28	
STR = 12.537	pb = 19.682	OK
29	29	

CALCULATION OF THE CRITICAL LENGTH FOR HAUNCH MEMBER WITH RESTRAINTS IN THE TENSION FLANGE IN ACCORDANCE TO APPENDIX G, BS5950 PART 1. DESIGN FOR PLASTIC STABILITY.

FROM CLAUSE G.2.2(b) FOR PLASTIC STABILITY

$$L_t < \text{or} = L_k / (c \cdot n_t)$$

WHERE;

L_k = LIMITING LENGTH GIVEN IN G.3.5

c = FOR UNIFORM MEMBER IS GIVEN AS

$$i.e \quad c = 1 + (3 \cdot (r-1) \cdot q)^{2/3} / (x-9)$$

n_t = IS THE SLENDERNESS CORRECTION FACTOR
 GIVEN IN G.3.6

THE FOLLOWING PARAMETER ARE USED IN THE DESIGN OF HAUNCH SECTION WITH BASE SECTION 203x133xUB30.

$q := 0.6$ THE RATIO OF TAPERED LENGTH TO TOTAL LENGTH
 (THIS PROGRAM ONLY CALCULATE FOR VALUES OF
 $q < 0.75$)

$R := 3$ THE RATIO OF LARGER TO THE LESSER DEPTHS

$P_y := 25$ (kN/cm²) YIELD STRENGTH

$E := 20000$ kN/cm² THE YOUNG'S MODULUS

(A) SECTION PROPERTIES OF BASIC I-SECTION

$b := 13.38$ cm. BREADTH OF FLANGE

$d := 20.68$ cm. DEPTH OF I-BEAM

$t_w := 0.63$ cm. THICKNESS OF WEB

$t_f := 0.96$ cm. THICKNESS OF FLANGE

$d_w := d - 2 \cdot t_f$ cm. ACTUAL DEPTH OF WEB AT D1

$d_{w1} := d \cdot R - 2 \cdot t_f$ cm. ACTUAL DEPTH OF WEB AT D2

$r_y := 3.18$ cm. RADIUS OF GYRATION

(B) CALCULATION OF MOMENT OF INERTIA I_{xo}

$$I_{xo} := b \cdot \frac{d^3}{12} - (b - tw) \cdot \frac{dw^3}{12}$$

(C) CALCULATION OF MOMENT OF INERTIA I_{yo}

$$I_{yo} := 2 \cdot tf \cdot \frac{b^3}{12} + dw \cdot \frac{tw^3}{12}$$

(D) CALCULATION OF MODULUS OF ELASTICITY OF THE BASE SECTION, Z_o

$$Z_o := I_{xo} \cdot \frac{2}{d}$$

(E) CALCULATION OF PLASTIC MODULUS

$$S_o := 0.25 \cdot tw \cdot dw^2 + b \cdot tf \cdot (dw + tf)$$

(F) CALCULATION OF WARPING CONSTANT OF BASE SECTION, C_{wo}

$$C_{wo} := tf \cdot (d - tf)^2 \cdot \frac{b^3}{24}$$

(G) CALCULATION OF TORSION CONSTANT OF BASE SECTION, J_o

$$J_o := \frac{2 \cdot b \cdot tf^3 + (d - tf) \cdot tw^3}{3}$$

(H) CALCULATION OF THE AREA OF BASE SECTION, A

$$A_o := 2 \cdot b \cdot tf + dw \cdot tw$$

PROPERTIES OF BASE SECTION

AREA	$A_o = 37.508$	cm^2
MOMENT OF INERTIA I_{xo}	$I_{xo} = 2.846 \cdot 10^3$	cm^4
MONENT OF INERTIA I_{yo}	$I_{yo} = 383.646$	cm^4
TORSION CONSTANT J_o	$J_o = 9.535$	cm^4
ELASTIC MODULUS Z_o	$Z_o = 275.254$	cm^3
PLASTIC MODULUS S_o	$S_o = 308.73$	cm^3
WARPING CONSTANT C_{wo}	$C_{wo} = 3.726 \cdot 10^4$	cm^4
RADIUS OF GYRATION MINOR, r_y	$r_y = 3.18$	cm

(I) TAPER PARAMETER x i.e d/t_f

$$x := 1.132 \cdot \sqrt{\frac{A_o \cdot C_{wo}}{I_{yo} \cdot J_o}} \quad x = 22.126$$

COMPARE WITH $\frac{d}{t_f} = 21.542$

(J) TO CALCULATE THE VALUE OF APPLIED MOMENT, N

CLAUSE G.3.6.1,

$$N := P_y \cdot \frac{Z_o}{100} \quad N = 68.814 \quad \text{kNm}$$

$$N_1 := \frac{N}{1 - q} \quad N_1 = 172.034 \quad \text{kNm}$$

$$N_2 := 0.75 \cdot N_1 \quad N_2 = 129.025 \quad \text{kNm}$$

$$N_3 := 0.5 \cdot N_1 \quad N_3 = 86.017 \quad \text{kNm}$$

$$N_4 := 0.25 \cdot N_1 \quad N_4 = 43.008 \quad \text{kNm}$$

$$N_5 := 0.0 \cdot N_1 \quad N_5 = 0 \quad \text{kNm}$$

(K) CALCULATION OF THE VALUE OF MOMENT CAPACITIES,

M1, M2, M3, M4 AND M5. FROM CLAUSE G.3.6.1

(i) THE VALUE OF M1

THE MOMENT OF INERTIA AT POINT 1 (cm⁴)

$$I_{x1} := b \cdot \frac{(d \cdot R)^3}{12} - (b - tw) \cdot \frac{dw1^3}{12} \quad I_{x1} = 3.537 \cdot 10^4$$

THE PLASTIC MODULUS Sx1 (cm³)

$$S_{x1} := 0.25 \cdot tw \cdot dw1^2 + b \cdot tf \cdot (dw1 + tf) \quad S_{x1} = 1.354 \cdot 10^3$$

THE MOMENT CAPACITY M1 (kNm)

$$M1 := Py \cdot \frac{S_{x1}}{10^2} \quad M1 = 338.458$$

(ii) THE VALUE OF M2

$$d2 := d + \left[(R - 1) \cdot d \cdot \frac{q - 0.25}{q} \right] \quad d2 = 44.807$$

$$dw2 := d2 - 2 \cdot tf$$

MOMENT OF INERTIA AT POINT 2 (cm⁴)

$$I_{x2} := b \cdot \frac{d2^3}{12} - (b - tw) \cdot \frac{dw2^3}{12} \quad I_{x2} = 1.649 \cdot 10^4$$

$$S_{x2} := 0.25 \cdot tw \cdot dw2^2 + b \cdot tf \cdot (dw2 + tf)$$

$$S_{x2} = 852.886$$

MOMENT CAPACITY M2

$$M2 := Py \cdot \frac{S_{x2}}{10^2} \quad M2 = 213.222$$

(iii) THE VALUE OF M3

if $q < 0.5$, $M3 = M3a$

$$M3a := Py \cdot \frac{So}{\frac{2}{10}}$$

if $q > 0.5$, $M3 = M3b$

$$d3 := d + \left[(R - 1) \cdot d \cdot \frac{q - 0.5}{q} \right]$$

$$dw3 := d3 - 2 \cdot tf$$

MOMENT OF INERTIA AT POINT 3 (cm⁴)

$$Ix3 := b \cdot \frac{d3^3}{12} - (b - tw) \cdot \frac{dw3^3}{12}$$

PLASTIC MODULUS AT POINT 3 (cm³)

$$Sx3 := 0.25 \cdot tw \cdot dw^2 + b \cdot tf \cdot (dw3 + tf)$$

$$Sx3 = 397.273$$

$$M3b := Py \cdot \frac{Sx3}{\frac{2}{10}}$$

$$M3 := \text{if}(q > 0.5, M3b, M3a)$$

$$M3 = 99.318$$

(iv) THE VALUE OF M4 (kNm)

$$M4 := Py \cdot \frac{So}{\frac{2}{10}}$$

$$M4 = 77.182$$

(v) THE VALUE OF M5 (kNm)

$$M5 := Py \cdot \frac{So}{\frac{2}{10}}$$

$$M5 = 77.182$$

(L) CALCULATION OF CRITICAL LENGTH OF TAPERED MEMBER TO
THE REQUIREMENT OF APPENDIX G OF BS5950: PART 1
FROM CLAUSE G.3.6

(i) GENERAL

$$\frac{N1}{M1} = 0.508 \quad \frac{N2}{M2} = 0.605 \quad \frac{N3}{M3} = 0.866 \quad \frac{N4}{M4} = 0.557 \quad \frac{N5}{M5} = 0$$

$$Nu := \text{if} \left[\frac{N1}{M1} > \frac{N5}{M5}, \frac{N1}{M1}, \frac{N5}{M5} \right]$$

$$Ns := \text{if} \left[\frac{N2}{M2} > \frac{N3}{M3}, \frac{N2}{M2}, \frac{N3}{M3} \right]$$

$$Ns := \text{if} \left[\frac{N4}{M4} > Ns, \frac{N4}{M4}, Ns \right]$$

$$Ns = 0.866$$

$$Nu = 0.508$$

(ii) CALCULATING THE SLENDERNESS RATIO Lk,
FROM CLAUSE G.3.5;

$$Lk := \frac{\left[5.4 + \left[600 \cdot \frac{Py}{E} \right] \right] \cdot ry \cdot x}{\sqrt{\left[5.4 \cdot \left[\frac{x^2}{Py \cdot E} \right] - 1 \right]}}$$

$$Lk = 285.048 \quad \text{cm}$$

(iii) CALCULATION FOR VALUE OF c. FROM CLAUSE G.3.3;"

$$c := 1 + \left[\frac{3}{x - 9} \right] \cdot (R - 1)^{0.666} \cdot \sqrt{q}$$

$$c = 1.281$$

THE SLENDERNESS CORRECTION FACTOR, nt
 FROM CLAUSE G.3.6.1 , AND SECTION L.(i)"

$$nt := \sqrt{\left[\frac{1}{12} \right] \cdot \left[\frac{N1}{M1} + 3 \cdot \frac{N2}{M2} + 4 \cdot \frac{N3}{M3} + 3 \cdot \frac{N4}{M4} + \frac{N5}{M5} + 2 \cdot (Ns - Nu) \right]}$$

nt = 0.825

(M) RESULTS.

THEREFORE THE LIMITING LENGTH Lt. FROM CLAUSE G.2.(b).(2)

$$Lt := \frac{Lk}{c \cdot nt} \qquad Lt = 269.613 \quad cm$$

Lk = 285.048 c = 1.281 nt = 0.825

APPENDIX 4

PROPOSAL FOR CHANGE IN APPENDIX G : BS5950 PART 1, FOR PRISMATIC SECTION.

EXAMPLE OF CALCULATION FOR PRISMATIC SECTION IN BASED ON APPENDIX G : BS5950 PART 1, WITH THE PROPOSED CHANGES.

THE CALCULATION HEREIN IS FOR SPECIMEN UMB1 (203X133XUB30). THE BEAM IS SUBJECTED TO LOADING AS SHOWN IN FIGURE 7.26. BOTH ENDS OF THE BEAM IS RESTRAINED LONGITUDINALLY AND TORSIONALLY BUT THE FLANGES ARE FREE TO WARP. THE TENSION FLANGE OF THE BEAM IS RESTRAINED BY PURLINS. THE VALUE OF β USED IN THIS CASE IS 0.5

THE CHANGES PROPOSED;

(A) ELASTIC STABILITY;

A FACTOR TO BE CALLED 'EFFECTIVE LENGTH RESTRAINT FACTOR' OR ELR FACTOR ' k_1 ', IS INTRODUCED. THIS ELR FACTOR WHICH HAS A VALUE OF $k_1=0.9$ IS USED NORMALLY SUCH AS IN THE CALCULATIONS OF λ BY,

$$\lambda = k_1 * L / r_y.$$

THIS VALUE OF λ IS THEN APPLIED IN ACCORDANCE TO THE REST OF THE CLAUSES FOR THIS CASE.

(B) PLASTIC STABILITY;

THE SAME EFFECTIVE LENGTH RESTRAINT FACTOR k_1 IS INTRODUCED IN THE CALCULATION OF λ . THIS VALUE OF λ IS THEN APPLIED IN ACCORDANCE TO THE REST OF THE CLAUSES FOR THIS CASE.

DESIGN CALCULATIONS

BEAM DATA

D := 20.68	cm	PY := 25	kN/cm ²
a := 18.00	cm	E := 21000	kN/cm ²
A := 38.1	cm ²	SX1 := 314.5	cm ⁴
tf := 0.96	cm	L := 365	cm
b := 13.38	cm	ry := 3.2	cm
tw := 0.63	cm	kl := 0.9	
IY := 383.3	cm ⁴	F := 0	kN
IX := 2900.1	cm ⁴	MA := 6982	kN.cm
hw := D - 2 · tf	cm	MA IS THE YIELD MOMENT	
hs := D - tf	cm		
	IY		kl · L
Γ := 1 - $\frac{IY}{IX}$		λ := $\frac{kl \cdot L}{ry}$	

(C) CALCULATION FOR ELASTIC STABILITY

APPENDIX SPECIFY THE CRITERIA FOR ELASTIC STABILITY

AS FOLLOWS ;

$$F/P_c + M_{dash}/M_B \leq 1$$

SINCE F=0 THE CALCULATION OF P_c IS IGNORED IN THIS CASE

(i) CALCULATION OF RELEVANT BEAM PROPERTIES

(a) CALCULATION OF WARPING CONSTANT. FROM CLAUSE B.2.5.1

$$H := \frac{hs^2 \cdot tf \cdot b^3}{24} \quad H = 3.726 \cdot 10^4$$

(b) CALCULATION OF TORSION CONSTANT. FROM CLAUSE B.2.5.1

$$J := \frac{2 \cdot tf^3 \cdot b + tw^3 \cdot hw}{3} \quad J = 9.455$$

(c) CALCULATION OF TORSIONAL INDEX. FROM CLAUSE B.2.5.1

$$X := 1.132 \cdot \frac{\sqrt{A \cdot H}}{\sqrt{IY \cdot J}} \quad X = 22.404$$

(d) CALCULATION OF Y FROM CLAUSE G.3.2

$$Y := \frac{\sqrt{1 + \left[2 \cdot \frac{a}{hs}\right]^2}}{\sqrt{1 + \left[2 \cdot \frac{a}{hs}\right]^2 + \left[\frac{1}{20}\right] \cdot \left[\frac{\lambda}{X}\right]^2}} \quad Y = 0.897$$

FROM THE VALUES OF Y ABOVE AND FROM CLAUSE G.3.4
 THE VALUES OF m_t IS OBTAINED FROM TABLE 39 OF THE CODE
 $m_t := 0.74$

(ii) CALCULATION OF M_{dash} , FROM CLAUSE G.2

$$M_{dash} := M_A \cdot m_t \quad M_{dash} = 5.167 \cdot 10^3 \quad \text{kN.cm}$$

(iii) CALCULATION OF MINOR AXIS SLENDERNESS RATIO, λ_{TB}

(a) CALCULATION OF BUCKLING PARAMETER u . CLAUSE 4.3.7.5

$$u := \sqrt{\frac{IY \cdot SX1 \cdot \frac{2}{A \cdot H}}{\Gamma}} \quad u = 0.883$$

(b) CALCULATION OF v_t

$$v_t := \left[\frac{4 \cdot \frac{a}{hs}}{1 + \left[2 \cdot \frac{a}{hs}\right]^2 + \left[\frac{1}{20}\right] \cdot \left[\frac{\lambda}{X}\right]^2} \right]^{0.5} \quad v_t = 0.824$$

(c) CALCULATION OF n_t

FROM CLAUSE G.3.6.1, WHERE,

$$N1 := 3491$$

$$M1 := 6982.5$$

$$N2 := 4363.8$$

$$M2 := M1$$

$$N3 := 5236.5$$

$$M3 := M1$$

$$N4 := 6109.3$$

$$M4 := M1$$

$$N5 := 6982.5$$

$$M5 := M1$$

$$NMS := \frac{N4}{M4}$$

$$NME := \frac{N5}{M5}$$

$$n_t := \sqrt{\left[\frac{1}{12} \right] \cdot \left[\frac{N1}{M1} + 3 \cdot \frac{N2}{M2} + 4 \cdot \frac{N3}{M3} + 3 \cdot \frac{N4}{M4} + \frac{N5}{M5} + 2 \cdot (NMS - NME) \right]}$$

i.e. $n_t = 0.854$ BUT CLAUSE G.3.3 STATED THAT WHEN
THERE IS NO INTERMEDIATE LOAD, $n_t=1$

(d) THE MINOR AXIS SLENDERNESS RATIO λ_{TB}

$$c := 1$$

$$n_t := 1$$

FOR UNIFORM MEMBER (CLAUSE G.3.3)

$$\lambda_{TB} := n_t \cdot u \cdot v_t \cdot c \cdot \lambda \dots \dots \dots \text{i.e. } \lambda_{TB} = 74.669$$

(iv) CALCULATION OF BENDING STRENGTH p_b , (CLAUSE 4.3.7.4)FROM TABLE 11 OF BS5950, THE VALUE OF λ_{TB} IS USEDIN OBTAINING p_b AND THEREFORE

$$p_b := 16.5 \quad \text{KN/cm}^2$$

(v) CALCULATION OF BUCKLING RESISTANCE M_B

$$M_B := p_b \cdot S_{X1} \quad (\text{FROM CLAUSE 4.3.7.3})$$

$$M_B = 5.189 \cdot 10^3 \quad \text{KN.cm} \quad \text{AND} \quad M_{dash} = 5.167 \cdot 10^3 \quad \text{KN.cm}$$

(vi) ELASTIC STABILITY $M_{dash}/M_B < 1$

$$\frac{M_{dash}}{M_B} = 0.996 \quad \text{CRITICAL LENGTH} \quad L = 365 \quad \text{cm}$$

(D) PLASTIC STABILITY OF UNIFORM MEMBER IN ACCORDANCE TO
APPENDIX G.

THE CONDITION FOR PLASTIC STABILITY FOR BEAM WITHOUT
LATERAL LOAD IS

$$L_t \leq \frac{L_k}{\sqrt{m_t}} \sqrt{\left(\frac{M_P}{M_{pr} + aF} \right)} \quad (\text{CLAUSE G.2(b)})$$

(i) CALCULATION OF M_P

$$M_P := P_Y \cdot S_{X1}$$

(ii) CALCULATION OF LIMITING LENGTH L_k

FROM CLAUSE G.3.5 AND BY INCLUDING THE AMMENDMENT

FOR k_1 ;

$$L_k := \frac{\left[5.4 + 600 \cdot \frac{P_Y}{E} \right] \cdot r_y \cdot X}{\sqrt{5.4 \cdot \frac{P_Y^2}{E} \cdot X^2 - 1}}$$

$$\text{i.e.} \quad L_k = 293.757 \quad \text{cm}$$

(iii) CALCULATION OF L_t

$$L_t := \frac{L_k}{\sqrt{m_t}} \cdot \sqrt{\frac{M_P}{M_P + a \cdot F}} \quad \begin{array}{l} L_t = 341.486 \\ L = 365 \end{array}$$

SINCE L_t IS SHORTER THAN L , PLASTIC STABILITY
IS NOT SATISFIED IN THIS CASE.

THE CRITICAL LENGTH FOR PLASTIC STABILITY IS 341.5 cm

Appendix 5

Details of the expressions in the geometric metrix given in chapter 4.

$$d_{22} = \frac{1.2P_x}{l} \dots \dots \dots f_{22} = d_{22} \dots \dots \dots e_{22} = -d_{22}$$

$$d_{33} = \frac{1.2P_x}{l} \dots \dots \dots f_{33} = d_{33} \dots \dots \dots e_{33} = -d_{33}$$

$$d_{44} = \frac{1.2C_oP_x}{l} + 0.3 \left[\frac{2(M_{y1} - M_{y2})}{l} + Q_{z1} + Q_{z2} \right] \beta_y$$

$$+ 0.3 \left[\frac{2(M_{z1} - M_{z2})}{l} + Q_{y1} + Q_{y2} \right] \beta_z + \left[\frac{K_{b1}(B_1 - B_2)}{l} + K_{t1}M_x \right] \beta_\omega$$

$$e_{44} = -d_{44} \dots \dots \dots f_{44} = d_{44}$$

$$d_{55} = \frac{2P_x l}{15} \dots \dots \dots e_{55} = -P_x l 30 \dots \dots \dots f_{55} = d_{55}$$

$$d_{66} = \frac{2P_x l}{15} \dots \dots \dots e_{66} = -\frac{P_x l}{30} \dots \dots \dots f_{66} = d_{66}$$

$$d_{77} = \frac{2P_x C_o l}{15} + \left[\frac{(M_{y1} - M_{y2}) l}{15} + \frac{Q_{z1} l^2}{60} + \frac{Q_{z2} l^2}{20} \right] \beta_y$$

$$+ \left[\frac{(M_{z1} - M_{z2}) l}{15} + \frac{Q_{y1} l^2}{60} + \frac{Q_{y2} l^2}{20} \right] \beta_z + [K_{b2}(B_1 - B_2) l + K_{t2}M_x l^2] \beta_\omega$$

$$e_{77} = \frac{-P_x C_o l}{30} - \left[\frac{(M_{y1} - M_{y2}) l}{60} + \frac{(Q_{z1} + Q_{z2}) l^2}{120} \right] \beta_y$$

$$- \left[\frac{(M_{z1} - M_{z2}) l}{60} + \frac{(Q_{y1} + Q_{y2}) l^2}{120} \right] \beta_z - [K_{b4}(B_1 - B_2) l + K_{t4}M_x l^2] \beta_\omega$$

$$f_{77} = \frac{2P_x C_o l}{15} + \left[\frac{(M_{y1} - M_{y2}) l}{15} + \frac{Q_{z1} l^2}{20} + \frac{Q_{z2} l^2}{60} \right] \beta_y$$

$$+ \left[\frac{(M_{z1} - M_{z2}) l}{15} + \frac{Q_{z1} l^2}{20} + \frac{Q_{z2} l^2}{60} \right] \beta_z + [K_{b1}(B_1 - B_2) l + K_{t1}M_x l^2] \beta_\omega$$

$$\begin{aligned}
d_{42} &= \frac{1.2 P_x C_z}{l} + \frac{0.6 (M_{y1} - M_{y2})}{l} + 0.05 Q_{z1} + 0.55 Q_{z2} \\
e_{42} &= \frac{-1.2 P_x C_z}{l} - \frac{0.6 (M_{y1} - M_{y2})}{l} - 0.55 Q_{z1} - 0.05 Q_{z2} \\
d_{43} &= \frac{-1.2 P_x C_y}{l} - \frac{0.6 (M_{z1} - M_{z2})}{l} - 0.05 Q_{y1} - 0.55 Q_{y2} \\
e_{43} &= \frac{1.2 P_x C_y}{l} + \frac{0.6 (M_{z1} - M_{z2})}{l} + 0.55 Q_{y1} + 0.05 Q_{y2} \\
f_{42} &= -e_{42} \dots \dots \dots e_{24} = -d_{42} \\
f_{43} &= -e_{43} \dots \dots \dots e_{34} = -d_{43} \\
d_{62} &= -0.10 P_x \dots \dots e_{62} = d_{62} \dots \dots f_{62} = -d_{62} \dots \dots e_{26} = -d_{62} \\
d_{53} &= -0.10 P_x \dots \dots e_{53} = d_{53} \dots \dots f_{53} = -d_{53} \dots \dots e_{35} = -d_{53} \\
d_{72} &= -0.10 P_x C_z - 0.05 (M_{y1} - M_{y2}) - 0.05 Q_{z2} l \\
e_{72} &= -0.10 P_x C_z - 0.05 (M_{y1} - M_{y2}) - 0.05 Q_{z1} l \\
f_{72} &= -C_{72} \dots \dots \dots e_{27} = -d_{72} \\
d_{73} &= 0.10 P_x C_y + 0.05 (M_{z1} - M_{z2}) + 0.05 Q_{y2} l \\
e_{73} &= 0.10 P_x C_y + 0.05 (M_{z1} - M_{z2}) + 0.05 Q_{y1} l \\
f_{73} &= -e_{73} \dots \dots \dots e_{37} = -d_{73} \\
d_{54} &= 1.10 P_x C_y + 0.55 (M_{z1} - M_{z2}) + 0.10 Q_{y1} l + 0.45 Q_{y2} l \\
e_{54} &= 0.10 P_x C_y + 0.05 (M_{z1} - M_{z2}) - 0.05 Q_{y1} l + 0.10 Q_{y2} l \\
f_{54} &= -1.10 P_x C_y - 0.55 (M_{z1} - M_{z2}) - 0.45 Q_{y1} l - 0.10 Q_{y2} l \\
e_{45} &= -0.10 P_x C_y - 0.05 (M_{z1} - M_{z2}) - 0.10 Q_{y1} l + 0.05 Q_{y2} l \\
d_{64} &= -1.10 P_x C_z - 0.55 (M_{y1} - M_{y2}) - 0.10 Q_{z1} l - 0.45 Q_{z2} l \\
e_{64} &= -0.10 P_x C_z - 0.05 (M_{y1} - M_{y2}) + 0.05 Q_{z1} l - 0.10 Q_{z2} l \\
f_{64} &= 1.10 P_x C_z + 0.55 (M_{y1} - M_{y2}) + 0.45 Q_{z1} l + 0.10 Q_{z2} l \\
e_{46} &= 0.10 P_x C_z + 0.05 (M_{y1} - M_{y2}) + 0.10 Q_{z1} l - 0.05 Q_{z2} l \\
d_{74} &= -0.10 P_x C_o - [0.05 (M_{y1} - M_{y2}) + 0.05 Q_{z1} l] \beta_y \\
&\quad - [0.05 (M_{z1} - M_{z2}) + 0.05 Q_{y1} l] \beta_z - [K_{b3} (B_1 - B_2) + K_{t3} M_x l] \beta_\omega
\end{aligned}$$

$$e_{74} = -0.10 P_x C_o - [0.05 (M_{y1} - M_{y2} + 0.05 Q_{z2} l)] \beta_y \\ - [0.05 (M_{z1} - M_{z2}) + 0.05 Q_{y2} l] \beta_z - [K_{b3} (B_1 - B_2) + K_{t3} M_x l] \beta_\omega$$

$$f_{74} = -e_{74} \dots \dots \dots e_{47} = d_{74}$$

$$d_{75} = \frac{-2 P_x C_y l}{15} - \frac{(M_{z1} - M_{z2}) l}{15} - \frac{Q_{y1} l^2}{60} - 0.05 Q_{y2} l^2$$

$$e_{75} = \frac{P_x C_y l}{30} + \frac{(M_{z1} - M_{z2}) l}{60} + \frac{Q_{y2} l^2}{60}$$

$$f_{75} = \frac{2 P_x C_y l}{15} - \frac{(M_{z1} - M_{z2}) l}{15} - 0.05 Q_{y1} l^2 - \frac{Q_{y2} l^2}{60}$$

$$e_{57} = \frac{P_x C_y l}{30} + \frac{(M_{z1} - M_{z2}) l}{60} + \frac{Q_{y1} l^2}{60}$$

$$d_{76} = \frac{2 P_x C_z l}{15} + \frac{(M_{y1} - M_{y2}) l}{15} + \frac{Q_{z1} l^2}{60} + 0.05 Q_{z2} l^2$$

$$e_{76} = \frac{-P_x C_z l}{30} - \frac{(M_{y1} - M_{y2}) l}{60} - \frac{Q_{z2} l^2}{60}$$

$$f_{76} = \frac{2 P_x C_z l}{15} + \frac{(M_{y1} - M_{y2}) l}{15} + 0.05 Q_{z1} l^2 + \frac{Q_{z2} l^2}{60}$$

$$e_{67} = \frac{-P_x C_z l}{30} - \frac{(M_{y1} - M_{y2}) l}{60} - \frac{Q_{z1} l^2}{60}$$

in which, K_{b1} , K_{b2} , K_{b3} , K_{b4} , K_{t1} , K_{t2} , K_{t3} and K_{t4} are the coefficients resulting from the numerical integration of potential energy equation of bimoment (reference 4.9).